

DEPARTMENT OF THE INTERIOR  
U.S. GEOLOGICAL SURVEY

MINUTES OF THE  
NATIONAL EARTHQUAKE PREDICTION EVALUATION COUNCIL  
April 2 and 3, 1987

edited and compiled by  
Clement F. Shearer<sup>1</sup>

Open File Report 88-37

REPRODUCED FROM BEST AVAILABLE COPY

This report is preliminary and has not been edited or reviewed for conformity with U.S. Geological Survey publication standards and stratigraphic nomenclature.

<sup>1</sup>U.S. Geological Survey, 106 National Center  
Reston, Virginia 22092

## TABLE OF CONTENTS

	<u>Page</u>
Preface	iv.
List of Members, National Earthquake Prediction Evaluation Council (NEPEC)	v.
Minutes of April 1987 meeting	1
Appendices:	
A. Summaries of presentations and papers	13
1. Introduction and overview - Tom Heaton	14
a. "Seismic potential associated with subduction in the northwestern United States"	15
b. "Possible tsunami along the northwestern coast of the United States inferred from Indian traditions"	24
c. "Source characteristics of hypothetical subduction earthquakes in the northwestern United States"	30
d. "Earthquake hazards on the Cascadia Subduction zone"	64
2. Plate motion and seismicity - Hiroo Kanamori	71
3. Seismicity and structure of the Cascadia subduction zone - R. S. Crosson	91
4. "Geometry of the Juan de Fuca plate from seismicity and segmentation of the Cascadia Range based on the distribution of volcanic vents - Craig Weaver	111
a. "Geometry of the Juan de Fuca plate beneath Washington and northern Oregon from seismicity"	113
b. "Distribution of Late Cenozoic volcanic vents in the Cascade Range (USA): volcanic arc segmentation and regional tectonic considerations"	142
5. The initial deformation front along the Oregon-Washington subduction zone - LaVerne Kulm	184
a. "Nature of the deformation front along the Oregon- Washington subduction zone"	185
b. "Oregon subduction zone: venting, fauna, and carbonates"	196

	<u>Page</u>
6. Holocene subsidence deposits in Alaskan earthquakes - Susan Bartsch-Winkle	203
a. "Post-earthquake sedimentation in Upper Cook Inlet, Alaska"	204
b. "Earthquake-caused sedimentary couplets in the Upper Cooke Inlet region"	206
c. "The Placer River silt - an intertidal deposit caused by the 1964 Alaska earthquake"	210
7. Coastal lowland evidence of great Holocene earthquakes in the Cascadia subduction zone - Brian Atwater	222
a. "Evidence for great Holocene earthquakes along the outer coast of Washington State"	223
b. "Summary, as of 2 April 1987, of radiocarbon ages on episodes of rapid coastal subsidence in westernmost Washington State"	228
8. Geodetic deformation measured in Washington and British Columbia - J. C. Savage	229
9. Pleistocene raised marine terraces along the Washington-Oregon coastline and implications to Cascadia subduction zone tectonics - Donald West	239
B. Additional papers	258
1. Estimating seismic potential of subduction zones using the seismic front and forearc morphology - D. E. Byrne, L. R. Sykes and D. M. Davis	259
2. Algorithm of Long-Term Earthquakes' Prediction - A. M. Gabrielor, et al.	267
3. Summary of Parkfield alerts, June 1985 to March 1987	293
4. Map - Segments of Major Faults Recommended for Intensified Monitoring and Study, NEPEC	296
C. Council Correspondence	298
1. General	299
a. Letter from Director, USGS, to Chairman, NEPEC requesting review of southern California earthquake probabilities - March 30, 1987	300

	<u>Page</u>
b. Letter from Chairman, NEPEC, to Director, USGS, summarizing meeting - April 23, 1987	301
2. Soviet prediction	304
a. Chairman, NEPEC, to Leon Knopoff regarding Council's review of Gabrielor paper - April 23, 1987	305
b. Chairman, NEPEC, to Dr. Keilis Borok regarding Council review of predictions - November 2, 1987	306
c. Dr. Keilis-Borok to Chairman, NEPEC - October 1987	308
d. Leon Knopoff to Chairman, NEPEC - August 6, 1987	309
e. Leon Knopoff to Chairman, NEPEC - December 16, 1987	316
3. Central California	318
a. Memorandum to Chief, Office of Earthquakes, Volcanoes, and Engineering, USGS, regarding Cholame field trip - March 24, 1987	319
b. John Filson, NEPEC, to Carl Kisslinger regarding Council review of Adak earthquake prediction - March 24, 1987	326
c. Carl Kisslinger, National Research Council, to Chief Geologist, USGS regarding review of southern California earthquake probabilities - February 24, 1987	327
d. Richard Andrews, California Office of Emergency Services, to William Ellsworth, Chief, Branch of Seismology, USGS, February 19, 1987	329
e. William Bakun, USGS Parkfield Coordinator to John Filson, Chief, Office of Earthquakes, Volcanoes, and Engineering, USGS	330



## PREFACE

The National Earthquake Prediction Evaluation Council (NEPEC) was established in 1979 pursuant to the Earthquake Hazards Reduction Act of 1977 to advise the Director of the U.S. Geological Survey (USGS) in issuing any formal predictions or other information pertinent to the potential for the occurrence of a significant earthquake. It is the Director of the USGS who is responsible for the decision whether and when to issue such a prediction or information.

NEPEC, also referred to in this document as the Council, according to its charter, is comprised of a Chairman, Vice Chairman, and from 8 to 12 other members appointed by the Director of the USGS. The Chairman shall not be a USGS employee, and at least one-half of the membership shall be other than USGS employees.

**NATIONAL EARTHQUAKE PREDICTION EVALUATION COUNCIL**

**Dr. Lynn R. Sykes**  
**CHAIRMAN**

Higgins Professor of Geological Sciences  
Lamont-Doherty Geological Observatory  
of Columbia University  
Palisades, New York 10964  
Office: 914/359-2900  
Home: 914/359-7428

**Dr. John R. Filson**  
**VICE CHAIRMAN**

Chief, Office of Earthquakes, Volcanoes,  
and Engineering  
U.S. Geological Survey  
National Center, MS 905  
Reston, Virginia 22092  
Office: 703/648-6714  
Home: 703/648-2807

**Dr. Clement F. Shearer**  
**EXECUTIVE SECRETARY**

Deputy Assistant Director, Engineering Geology  
Office of the Director  
U.S. Geological Survey  
National Center, MS 106  
Reston, Virginia 22092  
Office: 703/648-4425  
Home: 703/620-9422

**Dr. Keiiti Aki**

Department of Geological Sciences  
University of Southern California  
Los Angeles, California 90007  
Office: 213/743/3510  
Home: 213/559-1350

**Dr. John N. Davies**

State Seismologist, Alaska Department of  
Natural Resources, Division of Geological  
and Geophysical Surveys, and,  
Adjunct Associate Professor, Geophysical  
Institute, University of Alaska  
794 University Avenue, Basement  
Fairbanks, Alaska 99701  
Office: 907/474-7190  
Home: 907/455/6311

**Dr. James F. Davis**

State Geologist, California  
Department of Conservation  
California Division of Mines and Geology  
1416 Ninth Street, Room 1341  
Sacramento, California 95814  
Office: 916/445-1923  
Home: 916/487-6125

Dr. James H. Dieterich	Research Geophysicist Branch of Tectonophysics U.S. Geological Survey 345 Middlefield Road, MS 977 Menlo Park, California 94025 Office: 415/323-8111, ext. 2573 Home: 415/856-2025
Dr. William L. Ellsworth	Chief, Branch of Seismology U.S. Geological Survey 345 Middlefield Road, MS 977 Menlo Park, California 94025 Office: 415/323-8111, ext. 2782 Home: 415/322-9452
Dr. Hiroo Kanamori	Division of Geological & Planetary Science California Institute of Technology Pasadena, California 91125 Office: 818/356-6914 Home: 818/796-8452
Dr. Thomas V. McEvilly	Department of Geology and Geophysics University of California, Berkeley Berkeley, California 94720 Office: 415/642-4494 Home: 415/549-0967
Dr. I. Selwyn Sacks	Department of Terrestrial Magnetism Carnegie Institution of Washington 5241 Broad Branch Road, N.W. Washington, D.C. 20015 Office: 202/966-0863 Home: 301/657-3271
Dr. Wayne Thatcher	Chief, Branch of Tectonophysics U.S. Geological Survey 345 Middlefield Road, MS 977 Menlo Park, California 94025 Office: 415/323-8111, ext. 2120 Home: 415/326-4680
Dr. Robert E. Wallace	Chief Scientist, Office of Earthquakes, Volcanoes, and Engineering U.S. Geological Survey 345 Middlefield Road, MS 977 Menlo Park, California 94025 Office: 415/323-8111, ext. 2751 Home: 415/851-0249

Dr. Robert L. Wesson

Research Geophysicist  
Branch of Seismology  
U.S. Geological Survey  
National Center, MS 922  
Reston, Virginia 22092  
Office: 703/648-6785  
Home: 703/476-8815

Dr. Mark D. Zoback

Professor of Geophysics  
Department of Geophysics  
Stanford University  
Stanford, California 94305  
Office: 415/497-9438  
Home: 415/322-9570

National Earthquake Prediction Evaluation Council  
Minutes of the Meeting  
April 2 & 3, 1987  
Seattle, Washington

Council Members Present

Dr. Lynn Sykes, Chairman, Lamont Doherty Geological Observatory  
Dr. John R. Filson, Vice Chairman, U.S. Geological Survey (USGS)  
Dr. Clement F. Shearer, Executive Secretary, USGS  
Dr. John N. Davies, Alaska Department of Natural Resources  
Dr. James F. Davis, California Department of Conservation  
Dr. James H. Dieterich, USGS  
Dr. William L. Ellsworth, USGS  
Dr. Hiroo Kanamori, California Institute of Technology  
Dr. Thomas V. McEvilly, University of California, Berkeley  
Dr. I. Selwyn Sacks, Carnegie Institution of Washington  
Dr. Wayne Thatcher, USGS  
Dr. Robert E. Wallace, USGS  
Dr. Robert L. Wesson, USGS

Invited Speakers

Dr. Brian Atwater, USGS  
Mrs. Susan Bartsch-Winkler, USGS  
Dr. Kevin Coppersmith, Geomatrix Consultants  
Dr. Robert Crosson, University of Washington  
Dr. Thomas Heaton, USGS  
Dr. James C. Savage, USGS  
Dr. Craig Weaver, USGS  
Mr. Donald O. West, Golder Associates  
Dr. LaVerne Kulm, Oregon State University  
Dr. Charles Sammis, University of Southern California  
Dr. Garry Rogers, Pacific Geoscience Centre

Chairman Sykes opened the meeting with a brief statement on the Council's agenda for the past 2 1/2 years, its plans for the next year, and its missions and responsibilities to the Director of the U.S. Geological Survey (USGS). This meeting is to review the long-term earthquake potential of the subduction zone off the coast of Washington and Oregon and to report to the Director of the USGS on its findings.

Prior to the meeting, on April 1, Brian Atwater led a field trip to inspect evidence for great Cascade earthquakes of Holocene age. This trip is referenced in the report on the Council's Executive Session (pp. 14-17). Council members Davies, Ellsworth, Thatcher, Wallace, and Wesson and speakers Bartsch-Winkler, Heaton, Rogers, Weaver, and West participated in the field trip.

**Tom Heaton** presented an overview of the Cascadia subduction zone. It has long been recognized that the Pacific Northwest is a subduction zone with an active spreading zone off the West Coast and a spreading rate of approximately 6 cm. per year, and convergence rates ranging from 2 cm. to 4 1/2 cm. per year. There are three subducting plates - the Gorda Plate, the Juan de Fuca Plate, and the Explorer Plate. It appears that the Gorda Plate is subducting, but there may be some change in the subduction rate along the zone due to internal deformation within the Gorda plate. There is also some evidence of complications with the Explorer Plate. Nevertheless, it seems that the North America Plate is overriding the whole system at about 2 cm. per year. The total length of the zone, including all three plates, is about 1200 km. Large historic subduction earthquakes haven't been observed in this region and the question remains, does that mean that there never have been any large earthquakes or that we have not waited long enough. A map of the historic seismicity in the area shows that all the transform faults are active and are moving at a rate appropriate for the assumed plate motion. Heaton referred to the subduction zone as unusual - there is no deep ocean trench, no large gravity anomaly, no large mountain chain, and no subduction earthquakes. Sometimes it is called an aseismic subduction zone. However, if it is an aseismic subduction zone, it is not in the same sense or class as the Marianas in that a young ocean floor is being subducted. In referring to the region's seismicity, specifically a lack of large or intermediate subduction earthquakes, Heaton questioned whether any other of the world's subduction zones behaved similarly. From his analysis, Heaton concluded that the subduction zones with M 8 earthquakes are moderately coupled with fairly high rates of background seismicity, and aseismic subduction zones have low but steady rates of seismicity. In contrast, the Washington-Oregon subduction zone has virtually no activity, even in the magnitude 5 to 6 range. Although he questioned applicability of San Andreas seismic models to subduction zones, Heaton did note that those locked areas of the San Andreas fault that did have great earthquakes, such as the 1906 San Francisco earthquake and the 1857 Ft. Tejon earthquake, have been fairly well devoid of continuous seismic activity during the past several decades.

**Hiroo Kanamori** presented a global perspective on plate motion and seismicity. Noting that seismicity should correlate with several parameters, Kanamori described several analyses of such a correlation. He made two assumptions. First, the computed plate velocity is about the same as the present plate velocity, and, second, the modified seismicity,  $M_W'$ , best represents the overall seismicity of the subduction zones. Some positive correlation was found between convergence rate and the magnitude of the largest earthquake in a subduction zone, although it wasn't very satisfactory, suggesting that some other factor is responsible for the generation of large earthquakes. A second plate parameter, the age of the subducting plate, was discussed. The relationship between  $M_W'$  and the age,  $T$ , of the subducting plate is negatively correlated, as was expected. However, the large scatter suggests that plate age alone does not control seismicity. In fact, individual parameters don't lead to a convincing relationship. Next, Kanamori combined three parameters -  $T$ , velocity, and  $M_W'$  - and found a considerably improved correlation. He concluded his discussions by applying this analysis to the Juan de Fuca subduction zone (see paper by Kanamori in this volume).

**Robert Crosson** described the seismicity and structure of the Cascadia subduction zone. His interpretation of refraction and deep reflection data suggests a subducted slab dip of 16 degrees, in contrast to earlier interpretations which placed the dip at about 10 degrees. A selected subset of approximately 5,000 earthquakes was further analyzed. Of the subset, all the earthquakes were intraplate and no earthquakes of any appreciable size were located that could be identified with slip in the subduction zone separating the Juan de Fuca and North America plates. This suggests that the megathrust is between two distinct earthquake zones. Analysis of cross sections and models of the slab's shape and strain requirements indicate an upward arch to the slab in northwestern Washington. Both the slab seismicity and adjacent continental seismicity are concentrated at the slab arch suggesting a structural control for earthquakes near the arch. The structure may be of major significance to earthquake hazard estimation.

**Craig Weaver** discussed variations in volcanic vent and earthquake distributions as evidence for segmentation of the Juan de Fuca plate. His hypothesis is that recent dates of Holocene earthquakes should correlate with volcanic arc segmentation. There is no evidence of Cascade volcanism in the period from 10 to 16 million years ago. The volcanism of that period is concentrated in southeastern Oregon and northwest Nevada and is basically basaltic and associated rhyolites and is commonly interpreted as the initiation of Basin and Range volcanism. In the period of 5 to 10-million years ago, the vents, still predominantly basaltic, were impinging on the modern position of the Cascade volcanic arc. In contrast, though, in the past 5 million years volcanism in the Basin and Range of southeastern Oregon ended; basaltic vents were concentrated along the Brothers Fault Zone, thought to be the northern boundary of the Basin and Range in Oregon. In this same period there was a long, linear distribution of andesitic vents from Mt. Hood down through Oregon, a concentration of basaltic vents in the Mt. Shasta-Medicine Lake region as well as a concentration at Lassen Peak. In the northern section the andesitic boundary seems to have stepped to the west, and in the south the andesites have been slowly contracting. The spread of the vents in the southwest Washington/Oregon portion of the Cascades comes from the basaltic vents. There are few basaltic vents south of Newberry Crater and the distribution begins to change near the California-Oregon border where there is a heavy concentration of basaltic vents. Weaver then made some speculations on the relation between the volcanic arc segmentation and the known structural elements of the Juan de Fuca Plate. If there is any relationship between the shallow geometry of the Juan de Fuca Plate and the volcanic arc segmentation, Weaver and his colleagues expect to see five segments to the shallow subduction zone. He suggested that this segmentation would define the lateral extent of great subduction zone earthquakes on the Juan de Fuca and North American Plate interface.

**Garry Rogers** reviewed the tectonics of Northwest United States and Southwest Canada and commented on the seismic potential of the area. Many of the features of the Cascade seismic zone, such as volcanoes, continue from the United States into Canada. Other features, both offshore and

onshore, stop at the U.S.-Canadian border. One obvious change at the border is the change in direction of the plate boundary. To understand the zone, however, one must treat the boundary in its entirety. The change in subduction zone direction accomplishes two things: 1) It requires that the plate has some kind of folded or buckled structure near the change in strike. 2) It changes an oblique subduction scheme to a direct (perpendicular) subduction zone with almost no oblique component. There are four obvious segments along the zone - the Juan de Fuca segment, the Gorda segment, the Explorer segment, and the Winowna Block. The Explorer segment is defined mainly on the basis of magnetic anomalies and seismicity. Rogers infers from the seismicity analyses that the Explorer segment is being deformed much like the Gorda plate and that the inference of rapid Explorer-North America plate interaction based on rigid plate analysis probably is not valid. Results of a 10-year geodetic study show contraction in the direction of plate convergence along southern Vancouver Island. Also, relative uplift rates and strain appear to have changed in the region of the 1946 Vancouver Island earthquake. And, there is some evidence of seaward tilting in central Vancouver Island. There is evidence of uplift along the coast of Vancouver Island, and inland there are some examples of down-drop. Considering the area that could rupture and the area to moment magnitude relationship, the seismic potential is sizeable and the analysis of repeat times yields recurrence intervals on the order of 400 years, depending on an estimated factor. If this factor is smaller, repeat times would be longer.

Verne Kulm's presentation was on the initial deformation front along the Oregon-Washington subduction zone. Kulm described analyses of abundant turbidites on the Juan de Fuca plate that consistently gave repeat times of about 400 years. He noted, however, that there is no basis for using these data to indicate repeat times for large earthquakes on the Oregon-Washington continental margin. Kulm next discussed fold, fault, and fluid structures and mud volcanoes on the sea floor. He postulated that these features are evidence of nuclear plate movement. Seafloor mapping and seismic reflection surveys reveal an 18-km.-long sediment ridge on the Nitinat Fan dipping toward the oceanic plate and prominent faults and folds striking perpendicular to the convergence direction of the Juan de Fuca plate and oblique to the initial deformation front of the accretionary prism. Further, mud volcanoes are associated with these faults. The rapidly deposited fan sediments and mud volcanoes suggest overpressured abyssal and fan sediments. The lower continental slope has both seaward and landward verging sedimentary ridges of heights up to 1,000 meters above the abyssal plain. The landward verging sequences are in the upper portion of the scraped-off deposits and may represent thin skin overthrusting. About half of the layered sediments are carried beneath the accretionary prism and half are forming the youngest part of the prism. In response to subduction induced compression, the overlying sediments are also faulted and folded. Offsets on the order of several meters can be seen. Active



fluid venting sites exist on a Pleistocene marginal ridge and a Pliocene ridge off the coast of central Oregon. Communities of white clams and worms and concentrations of authigenic carbonates occur along the crest of the marginal ridge. And very high concentrations of methane at the vent sites indicate pore fluids derived from the accretionary complex. Similar communities of clams were found atop a mud volcano off the coast of central Oregon indicating active fluid venting. Carbonate chimneys recently dragged from the sea floor on the Outer Continental Shelf at Cape Falcon suggest fluid venting in the oldest and youngest portions of the accretionary prism. Although the Cascadia subduction zone has many features and processes similar to Circum-Pacific subduction zones, neither the relationship between them and coupling or decoupling of the Juan de Fuca and North American plates nor how they can be used to estimate seismic potential has been determined.

**Susan Bartsch-Winkler** reported on Holocene subsidence deposits and Alaskan earthquakes. She noted three prevailing conditions favorable to post earthquake sedimentation in the Cook Inlet: 1) abundant earthquakes; 2) plenty of readily transportable sediment; and 3) a dynamic tidal regime to provide the energy for rapid sediment deposition. These factors provide an instantaneous sedimentological picture of the effects of subsidence after a major earthquake. Bartsch-Winkler paid particular attention to sedimentation changes after the 1964 Great Alaskan Earthquake. Regional uplift and regional as well as local subsidence caused by the earthquake affected intertidal and near-tidal sediment in southcentral Alaska and initiated intertidal aggradation in Upper Cook Inlet. From 1964 to 1974 about  $22 \times 10^6$  cubic meters of Placer River Silt, the post-earthquake intertidal deposit, were deposited over 18 square km. at the head of the Portage Arm. Bartsch-Winkler cited earlier reports indicating that organic layers were present at various shore lines in south Alaska and attributable to relative sea level changes. Searches for evidence of recurrent earthquakes in Upper Cook Inlet were begun by looking for peat layers interbedded with intertidal silt. The hypothesis that earthquake related events occurred throughout the late Holocene is being tested by radiocarbon dating of these layers. Additional evidence, however, includes sequences of contorted and undisturbed beds, anomalous sand layers atop peat layers, sand blows, and rapid changes in the base level of stratigraphic sections.

**Brian Atwater** discussed his work on rapid coastal-lowland subsidence as evidence of great Holocene earthquakes in the Cascadia subduction zone. Atwater described the stratigraphy and results of radiocarbon dating of plant remains from four episodes of inferred rapid coastal subsidence in southwest Washington. His results suggest rapid subsidence at about 300, 1700, 2700, and 3000-3400 years ago, times of great earthquakes in the region. Studies in northwest Washington suggests an age of about 1000 sidereal years ago for the most recent episode of coast subsidence near Neah Bay.

**Charles Sammis** discussed fault zone rheological considerations in the area. He noted that the Juan de Fuca plate being subducted is particularly young and fairly unique in that it is covered by thick sediments. In addition to having a high volume of sediment, it is unique in that the sediment exists all the way out to the Juan de Fuca ridge. This is important because the sediment shuts off hydrothermal circulation and puts the plate in a conductive cooling regime. Based on considerations of possible ages of the plate and thermal models, Sammis hypothesized that the plate is so young that it is not in a stick-slip earthquake regime but may be in a stable-sliding regime. Sammis considered several other factors - fluid pressure, age of the subducting plate, strain rate, and ductility - on whether the plate is in a stick-slip or stable-sliding regime. The only factor that would suggest that the plate boundary is in a stick-slip regime is systems stiffness. He concludes: 1) that the Juan de Fuca plate is thermally unique; with a thick cover of sediment extending out to the ridge that cools through its history in a conductive regime; 2) from a stick-slip/stable-sliding point of view it is not obvious that stable-sliding could be accomplished.

**Kevin Coppersmith** presented the results of an experts study on the probability of exceeding design seismicity at a site in western Washington. The purpose of the study was to represent the range of scientific opinion on the issue. Coppersmith emphasized the study's methodology and not the preliminary results. The uncertainties associated with the probability estimates concern the seismogenic potential of major tectonic elements in the subduction zone. The seismic sources of interest are those associated with the plate interface itself and those earthquakes that can occur within the oceanic slab. The experts were questioned on the crustal geometry, potential seismic sources, probability of activity and tectonically significant earthquakes, location of rupture, maximum magnitudes, convergence rates, seismic coupling, recurrence of earthquakes, and earthquake distribution. Some of the expert assessments of the factors were discussed and the results briefly summarized. The favored crustal geometry places the hypocenters of recorded earthquakes near the upper part of the downgoing oceanic slab. Many of the experts felt that the interface is not segmented. There was no consensus on the probability of activity. Favored convergence rates are on the order of 30-40 mm. per year. The maximum magnitudes, when given, were in the range of  $M \geq 7.5$  for interslab earthquakes to  $M \geq 8.5$ . Nearly all experts answered questions regarding coupling but the answers exhibited a very broad distribution of estimates.

**Jim Savage** presented results of geodetic deformation measurements made in Washington and British Columbia. Savage reported that the measurements of a geodetic network near Seattle in 1981 indicated compression in the direction of plate convergence and suggested that this can be attributed to strain across the Cascadia subduction zone. This interpretation was tested further at several sites and confirmed that the direction of greatest compression was east northeast on the order of 0.1 microstrain

per year. Savage cited work by others on vertical deformation based on leveling and tide gauge records. It appears that the Seattle and Puget Sound region is subsiding where the Pacific coast of Washington is being raised. More recent work presents a somewhat more complicated picture. The entire coast along the Cascadia subduction zone may not have been uplifted; in particular, coastal uplift may not have occurred along the Pacific coast at Vancouver Island and central Washington. Based on strain accumulation rates in other areas of subduction, Savage argued that the observed accumulated strain is elastic. Savage further argues that the strain accumulation measurement gives strong evidence that major megathrust earthquakes will eventually occur along the Cascadia subduction zone.

**Don West** discussed the geology of Pleistocene raised marine terraces along the Pacific northwest coastline. West's presentation emphasized the uplift observed along the Oregon-Washington coastline. The presentation began with a discussion of the coastal deformation associated with other seismically active subduction zones. Next, West attempted to characterize long-term uplift in these other subduction zones and then to compare the long-term deformation of the Cascadia subduction zone to determine its seismic potential. West noted from a study of 14 earthquakes along nine subduction zones, that as earthquake magnitude increases so does the length of the deformation zone. And, there is a weak relationship of increasing vertical deformation with increased magnitude. Further, the distance from the trench at which vertical coastline deformation occurs is roughly related to earthquake magnitude; more specifically, he noted that for  $M > 8.0$  coseismic subsidence generally does not occur closer than about 110 to 120 km. from the trench and coseismic uplift no further than 150 km. from the trench. From his reviews of coseismic and long-term vertical deformation of coastlines at near plate boundaries, West suggested that virtually all of the Oregon coast is in a zone of expected coseismic and long-term uplift and that the Washington coast could experience either uplift or subsidence. Further, apparent differences with other subduction zones, particularly the lack of Holocene terraces and low overall rate of late Quaternary uplift, suggest a significantly longer recurrence time for large magnitude thrust events. (See paper by West in this volume.)

#### EXECUTIVE SESSION, APRIL 3, 1987

Sykes presented the following agenda. First, a review of yesterday's meeting to be followed by discussions of the Parkfield experiment, southern California strategy, the Keilis-Borok earthquake prediction, and last, discussion of future Council meetings.

#### Review of Meeting - Subduction Earthquakes in the Pacific Northwest

**Sykes** asked each member to give his assessment of the meeting, particularly his opinion on whether the subduction zone moves aseismically or in great earthquakes; and whether the work performed to date is adequate.

**Davies** strongest impressions were of the field trip led by Brian Atwater and the argument that the buried peat horizons can be explained easiest by earthquake activity. The burden of proof, however, falls to those arguing

against subduction-type earthquakes to explain the occurrence of the sequences of peat layers. He suggests the possibility of large earthquakes with recurrence intervals of 500-800 years. He also feels that the questions raised yesterday regarding heat flow and mechanics are important and need to be resolved.

**Ellsworth's** impressions are also largely driven by the field trip. He noted that Brian Atwater has found these features over a large area, up and down the coasts of Washington and Oregon. Further, it is obvious that we are at an early stage of determining what these features mean, although the large earthquake hypothesis is most likely. He feels that the meeting reaffirmed the USGS decision to shift more of its regional hazards assessment work (element III in the National Earthquake Hazards Reduction Program) to the Pacific Northwest. He feels that the chances of large earthquakes are high, with recurrence intervals on the order of 1000 years.

**Dieterich** added that arguments can be made on both sides of the issue - seismic slip or aseismic subsidence. The strain accumulation data presented by Savage causes him to lean strongly toward the seismic-slip hypothesis. He noted that there are many opportunities for expanded geological investigations. The argument for aseismic slip, in his opinion, hinges on the uniqueness of this plate and subduction zone. Dieterich appreciated the approach and analysis of Sammis regarding thermal arguments but offers a different conclusion. He believes that to follow the analysis of stiffness controlling instability requires experimental data that aren't available and what is available is contradictory.

**Kanamori** feels that the evidence for large seismic events in the past is very good, but our knowledge of the past 50 years is very limited and maybe they represent very unusual events. He emphasized the need for basic research to resolve this problem and noted that the discussions were a very good example of the integration of basic research from different disciplines - rheology, seismology, subduction zone studies - into a focussed study. He did find Savage's strain data analysis to be strong but noted that alternative interpretations do exist. Kanamori is still puzzled by both the absence of earthquakes of magnitude > 6 or 6.5 for the past 50 years and the unique combination of a young sea floor and thick sediments and therefore still is undecided regarding seismic subduction.

**Sachs** is impressed by the absence of thrust earthquakes in the region and feels that this region must be unusual in some manner. He noted that it is somewhat younger than other regions, it has high heat flows, thick sediments, and ongoing subduction, but that this does not necessarily mean that there will be seismic release. He finds Brian Atwater's work important in that his observations do indicate uplift, but it may be over periods of years, which could be interpreted as slow uplift, rather than the instantaneous uplift associated with earthquakes.

**Filson** is still skeptical about the subduction zone generating large earthquakes. He was impressed by Vern Kulm's presentation of underwater scans of accretionary wedges as direct evidence of plate convergence. He also found Savage's data on elastic strain accumulation in the continental

plate very good but agrees with Sachs that we don't know whether that argues for slow strain release or an earthquake with instantaneous release of strain. He also feels that those arguing for the potential for large subduction earthquakes have to both address Sammis' questions, and explain the absence of Holocene terraces. He also offered that the turbidity currents and undersea landslides could occur regularly due to sediment loading and do not require a seismic genesis.

**McEvilly** added that the accumulation of evidence - seismic, strain, and oceanographic - speaks convincingly in favor of plate convergence, but the anomalous seismic behavior is not that of a region capable of large earthquakes.

**Thatcher** believes that Atwater's data are critical to all of the arguments on this topic. Therefore, this issue needs more attention by people experienced in this type of research. The important issues remaining to be resolved include; if the subduction is seismic, how frequently does it occur and what are the characteristics of the source regions. He noted that whether the zone ruptures in a series of earthquakes of M 7.5, as in the southern part of the Japan Trough, or as a single earthquake of M 9 or greater is very important from the standpoint of hazards. Thatcher favors the former.

**Wallace** is impressed by the suggestion of seismogenic subduction provided by the series of sudden subsidence events described by Brian Atwater and shown to the Council on a field trip. He is also intrigued by Savage's strain data which is consistent with convergence, but he wonders if it is too small a sample from which to base a model. More evidence of sudden prehistoric uplift and subsidence should be sought in the geologic record, and more precise dating of known young displacements in the seabed should be pursued.

**Sykes** believes that a lot more work needs to be done on the Quaternary geology of the region. He is evenly split on the debate between the aseismic hypothesis versus seismogenic hypothesis. He feels, though, that the chances that the zone will rupture in a truly great earthquake, M 9, is remote and that more work is needed to define the zone of coupling. Sykes believes that the coupled zone would not extend far to sea and that the crucial area to look at is essentially from the coastline to about Puget Sound, i.e., the plate boundary beneath the Olympics. He is uncomfortable about extrapolating from other regions using the Ruff and Kanamori idea of coupling. The presence of large amounts of young, highly porous sediments may promote a seismic slip along a greater part of the plate boundary in a downdip direction.

**Wesson** sees good agreement on plate convergence and subduction. He is impressed with Atwater's work but, noting three competing factors, feels that good research is needed on the fundamental Quaternary geology of the coastline. The first factor is eustatic sea level changes, the second is 70,000 year-old elevated terraces, and the third factor is episodes of submergence.

**Thatcher** stressed that Savage was measuring evidence of elastic coupling across the interface of the Juan de Fuca and the North America plates. The unresolved issue is the intensity of the coupling. In other words, is  $\alpha$  equal to 1 or 0.1? The crucial point, as noted by **Dieterich**, is that the contraction may represent inelastic deformation rather than elastic strain accumulation. **Ellsworth**, noting the seismicity patterns of sections of the San Andreas Fault, cautioned against assuming that because there have been few earthquakes the area is not capable of large earthquakes.

### Parkfield, California

Based on the Council's recommendations of November 1986, the USGS revised the open-file report "Parkfield Earthquake Prediction Scenarios and Response Plans." Additional features of the report include a list and the coordinates of all the instruments in the field and sample warning messages.

**Filson** reported that the USGS participated in a California Office of Emergency Services tabletop exercise and field trip on the public service response to the issuance of a short-term prediction for Parkfield.

**Filson** also reported that during the first week of February an unambiguous strain change clearly preceded a M 2.7 earthquake at Parkfield and constituted a level C alert. Specifically, on February 1, there was a minor earthquake, M 1.5, in the Middle Mountain alert zone. A few hours later there was a 10 cm. drop in a water well above the Middle Mountain zone. Later that day there was a 0.2 mm. right-lateral creep event at the Middle Mountain creep meter and then later in the day other minor earthquakes occurred. Early the next morning the M 2.7 earthquake occurred. These events indicate that the Parkfield recording system is in place and successfully recorded some kind of premonitory event on separate instruments, which is the intent of the experiment.

**Wallace** reported on a field review of the geomorphic interpretations of Sieh and Jahns, which led to the interpretation that the predicted Parkfield M 6 earthquake might instead be, or might be followed closely by, a larger, M 7, earthquake. Although the geomorphic features clearly record strike slip on the fault, the amount and timing of individual prehistoric slip events is uncertain; even the amount of slip that seems likely to have accompanied the great 1857 earthquake. The postulated M 7 earthquake is considered possible, based on general rates and distribution of strain, but the geomorphic evidence neither strongly supports the M 7 theory nor rules it out. A report by the review team, including Sieh, was distributed to the panel, and recommends: 1) a study of long-term slip rate based on geologic and geomorphic evidence, 2) trenching of selected sites, 3) further detailed study of offsets of a few gulches. The Council suggested that of the three, additional trenching might be most productive.

**Thatcher** and **Davis** both reported that the Parkfield response plan is working well. **Ellsworth** reported that the open-file document has been extremely useful; it has helped to focus attention on the details of the system, increased the ability to accurately and efficiently communicate with the State of California, and helped to debug the system. **Thatcher**

noted that despite some initial reservations about designing response plans without more data on the region, this method has been working, is essentially being conducted in areas such as Tokai, Japan, and could be adopted wherever researchers are monitoring instrumented areas, such as in Southern California.

### Southern California Strategy

**Sykes** reviewed the Council's deliberations on Southern California. The Council's letter of May 9, 1986, to the Director, USGS, summarized its review of its first 2 years of meetings on California and Alaska. As suggested in the last two meetings, Sykes discussed their findings and recommendations for intensified studies at briefings for the National Academy of Sciences subcommittee that is advisory to the USGS. At a meeting with Frank Press, the head of the National Academy of Sciences, Sykes and Kisslinger discussed the widely quoted estimate, in FEMA and other documents, that there is about a 50 percent chance of a large and damaging earthquake in Southern California within the next 30 years. Frank Press recommended that NEPEC officially review that forecast, and depending on that review, he would consider asking the National Academy of Sciences to consider the situation further. The National Academy of Sciences subsequently sent a letter to the Chief Geologist of the USGS suggesting a review of Southern California earthquakes. Sykes then met with USGS officials on March 24, 1987, with an agenda similar to the National Academy of Sciences meeting. At this meeting Sykes noted the difficulty in tracing the scientific evidence for this prediction and that more recent field work suggests a need to review the original probability statement. He suggested to the USGS that a working group be established to derive one or more probability maps and to prepare a report for NEPEC's review.

**Dieterich** likes the idea of convening a working group on this topic. **Kanamori's** principal question is what methodology will be used in a probabilistic approach, particularly in light of the small amount of data. He asked whether it would be prudent to have a group consider the implications of this probabilistic methodology. **Ellsworth** pointed out that there is a distinction between risk analysis for specific fault segments and risk for a large region, e.g., the Los Angeles basin. Therefore, it is important to decide what the working group should do - either focus on a few segments of the San Andreas and address the problem of a large to great or to address the Los Angeles Basin hazard issue and develop some probabilistic estimate of what may happen in the next 30 years. He feels that the latter is the more important aspect of the issue. The Council discussed whether it could or should assess the risk for various magnitude earthquakes associated with particular faults, both associated with and distinct from the San Andreas.

The Council also discussed some of the published probability estimates and methods used for the Southern California region. The Council agreed to form a working group to respond to the charge by the Director of the USGS

to assess by the end of the year the likelihood of a great earthquake in the Southern California region during the next few decades. Further, the working group would develop a short document on the consensus and divergence of opinion on these issues for the Council's review. The Council also agreed to ask the working group to consider M 7.5 or greater earthquakes, and, to the extent possible, also consider the likelihood of smaller events, that could have major consequences. Delivery of the draft report will be requested for October 1987.

#### Future Meetings

The Council decided not to meet until the October 1987 Southern California earthquake data review.

#### Keilis-Borok Prediction

**Sykes** briefed the Council on how the Keilis-Borok prediction of a large earthquake in California came to the Council's attention by way of a letter from Leon Knopoff. Knopoff was on sabbatical in England and promised to send further information regarding the prediction to Sykes.

**Filson** and several other Council members viewed this prediction as basic research, as opposed to an operational prediction capability. The Council noted its interest in this line of research but is concerned about the very large area involved in the prediction. It did conclude, however, that the present data and documentation were not specific enough to permit a useful review by the Council.

The Council was of the opinion that further consideration could be delayed until fall 1987 when a Soviet delegation is expected to be in the United States for discussions of the bilateral earthquake program. The Keilis-Borok prediction would be included in the agenda and NEPEC members invited to attend that presentation.

Sykes will send a letter to Knopoff expressing the Council's views.



## APPENDIX A

### Summaries of Presentations and Papers

Articles reprinted with the permission of the Seismological Society of America and the American Association for the Advancement of Science.

**APPENDIX A. 1.**

**Introduction and Overview**

**by**

**Tom Heaton**

## SEISMIC POTENTIAL ASSOCIATED WITH SUBDUCTION IN THE NORTHWESTERN UNITED STATES

BY THOMAS H. HEATON AND HIROO KANAMORI

### ABSTRACT

Despite good evidence of present-day convergence of the Juan de Fuca and North American plates, there has been remarkably little historical seismic activity along the shallow part of the Juan de Fuca subduction zone. Although we cannot completely rule out the possibility that the plate motion is being accommodated by aseismic creep, we find that the Juan de Fuca subduction zone shares many features with other subduction zones that have experienced great earthquakes.

### INTRODUCTION

In this paper, we compare the mode of subduction of the Juan de Fuca plate beneath the North American plate with that of other subduction zones. We show that the Juan de Fuca subduction zone shares many features with other subduction zones that experience great earthquakes, while several features indicative of aseismic subduction are absent. General reviews of characteristics of the subduction process are given by Kanamori (1977a), Uyeda and Kanamori (1979), Ruff and Kanamori (1980), and Lay *et al.* (1982). They demonstrate the existence of striking correlations between the nature of seismic energy release and the physical characteristics of subduction zones. In general, they find that total seismic energy release rates are highest along subduction zones where young oceanic crust is subducted rapidly. They interpret this result to be a systematic variation in seismic coupling which is related to buoyancy of the subducted lithosphere.

We begin by summarizing the results of the studies mentioned above. We then discuss the physical characteristics of the Juan de Fuca subduction zone, describe some of the similarities between it and other subduction zones, and make some inferences about the expected seismic potential of the area.

### SEISMIC COUPLING AND EARTHQUAKE SIZE

Kanamori (1977a) points out that the seismic energy release rate along subduction zones is not a simple linear function of convergence rates. Ruff and Kanamori (1980) show that the seismic energy release rate is closely related to the size of the maximum observed earthquake along any subduction zone. That is, the cumulative energy release from small events is usually negligible compared to the energy released by the largest events in a region. Kanamori (1977b) shows that, on a world-wide basis, the cumulative seismic energy release rate is closely related to the occurrence of very large earthquakes. It follows that the seismic energy release rate along individual subduction zones is closely related to the size of the maximum earthquake observed along that zone. In general, shallow low-angle thrust events are the dominant factor in determining seismic energy release rates.

Kanamori (1977a) concludes that variations in the seismic energy release rates (i.e., size of maximum earthquake) for differing subduction zones are caused by differences in seismic coupling. Strong seismic coupling implies that slip occurs only during earthquakes, whereas weak seismic coupling implies that slip occurs mainly in the form of aseismic creep.

## SEISMIC COUPLING AND SUBDUCTION ZONES

We now summarize the results of Kanamori (1977a), Uyeda and Kanamori (1979), Ruff and Kanamori (1980), and Lay *et al.* (1982), who correlated physical characteristics of the subduction process with the maximum earthquake size for most of the major subduction zones. As was just discussed, this correlation is interpreted in terms of seismic coupling, which is related to the buoyancy of the subducted lithosphere. The following features seem well correlated with observed maximum earthquake size.

*Convergence rate and age of subducted lithosphere.* In Figure 1, we show the

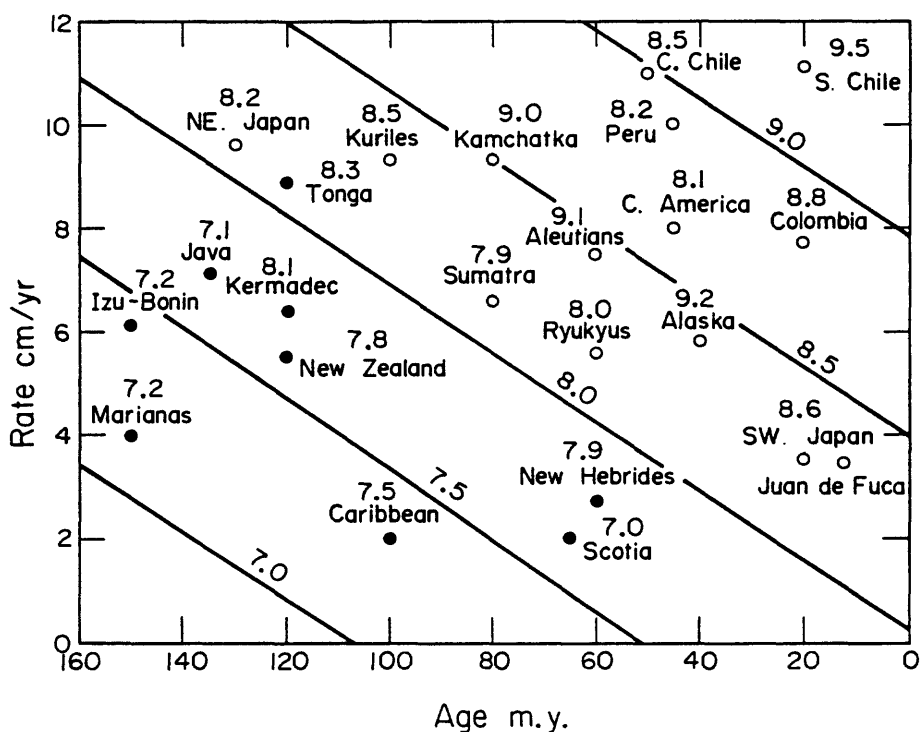


FIG. 1. Relation of maximum energy magnitude,  $M_w$ , to convergence rate and age of subducted lithosphere for major subduction zones. The contours of  $M_w$  are the predicted maximum earthquake magnitudes resulting from linear regression of observed maximum earthquake magnitude against the other two variables. Dots and circles are subduction zones with and without active back-arc basins, respectively (modified from Ruff and Kanamori, 1980).

relation between the maximum observed energy magnitude,  $M_w$ , and the convergence rate and age of subducted lithosphere for the major subduction zones. Ruff and Kanamori (1980) performed a linear regression of convergence rate and lithospheric age against the maximum observed moment magnitude, and the solid diagonal lines represent the best linear least-squares fit. It is clear that the maximum observed earthquake size increases with increasing convergence rate and decreasing lithospheric age. In Figure 2, we show this same correlation. In this figure, however, the observed maximum energy magnitude is plotted against the energy magnitude predicted from the regression analysis and convergence rate and lithospheric age. Ruff and Kanamori's analysis indicates that the maximum energy magnitude is well fit by the following relationship.

$$M_w = -0.00889T + 0.134V + 7.96, \quad (1)$$

# SEISMIC POTENTIAL: SUBDUCTION IN THE NW U.S.

where  $T$  is the age of the subducting plate in millions of years,  $V$  is the convergence rate in centimeters/year, and the standard deviation of the observed  $M_w$  around the predicted value is 0.4.

*Presence of active back-arc basins.* In Figures 1 and 2, subduction zones with and without active back-arc basins are plotted as dots and circles, respectively. Subduction zones without active back-arc basins are clearly associated with the occurrence of large shallow subduction earthquakes. Thus, the absence of an active back-arc basin seems to be a good indication of relatively strong seismic coupling.

*Depth of seismicity.* Ruff and Kanamori (1980) show a good inverse correlation between the maximum depth of observed seismicity and the age of the subducted

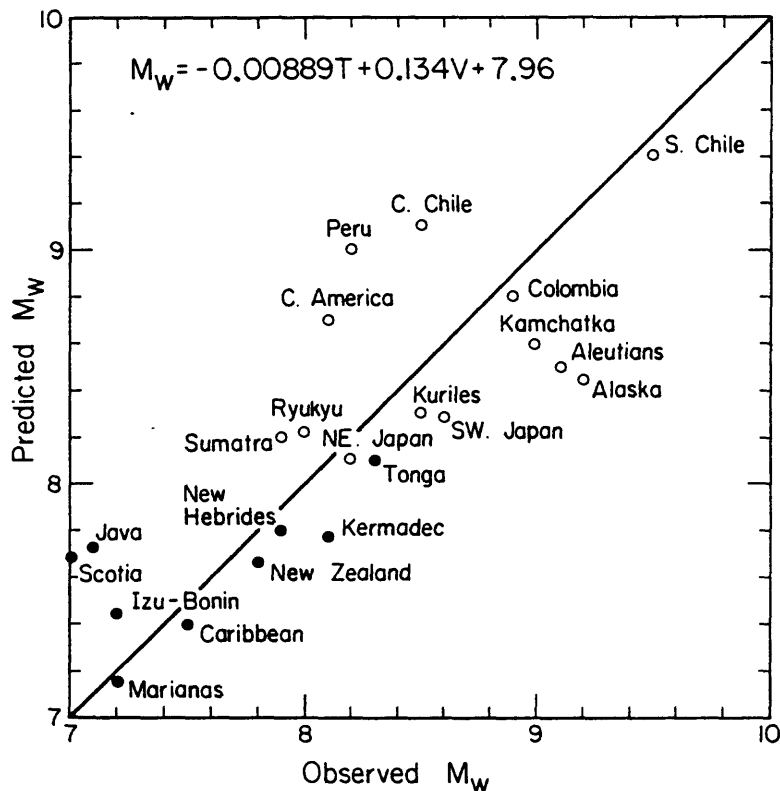


FIG. 2. Maximum observed energy magnitudes plotted against maximum energy magnitudes predicted from regression analysis shown in Figure 1.  $T$  is the age of the subducted plate in million years, and  $V$  is the convergence rate in centimeters/year. Dots and circles are subduction zones with and without active back-arc basins (modified from Kanamori, 1983).

plate, but the corresponding correlation between depth of seismicity and convergence rate is poor. Consequently, there is a weak correlation between the maximum depth of seismicity and the maximum observed earthquake size. However, 3 of the 4 subduction zones that have produced earthquakes of  $M_w \geq 9.0$  have maximum depths of seismicity of less than 200 km.

*Depth of oceanic trench.* Uyeda and Kanamori (1979) suggest that strongly coupled subduction zones are accompanied by shallow oceanic trenches, whereas weakly coupled subduction zones are accompanied by very deep oceanic trenches. Similarly, they conclude that free-air gravity anomalies tend to be larger for those trenches with weak seismic coupling.

*Dip of Benioff-Wadati zone.* Uyeda and Kanamori (1979) conclude that strong

seismic coupling is usually associated with subduction zones having relatively gently dipping Benioff-Wadati zones. The uppermost part of strongly coupled subduction zones generally dips between  $10^\circ$  and  $20^\circ$ . They also conclude that strongly coupled subduction zones are characterized by the presence of well-developed fore-arc basins, which are believed to be accretionary prisms of sediments that develop on the landward wall of trenches. Furthermore, they note that this style of subduction is often accompanied by crustal uplift and compression in the overriding plate. These features are schematically shown in Figure 3.

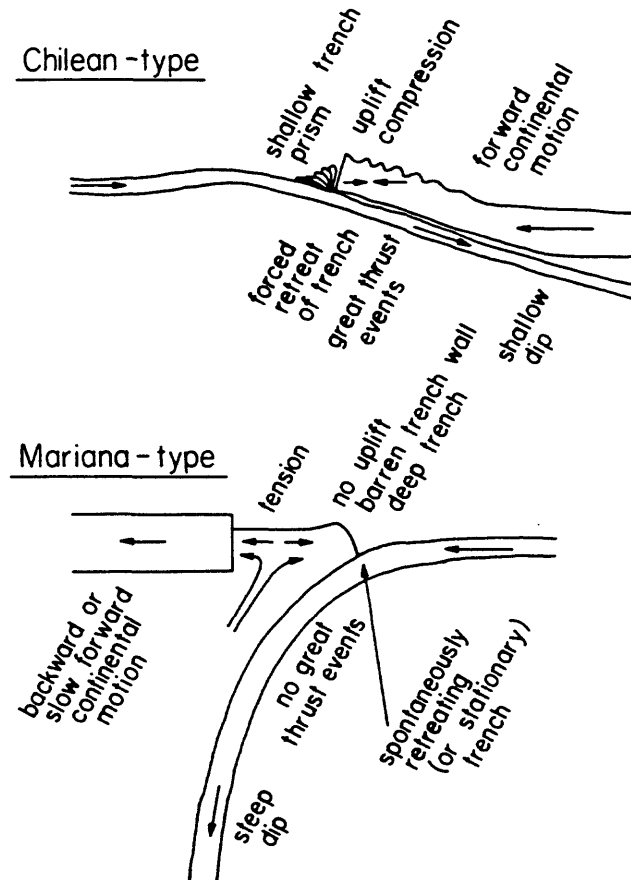


FIG. 3. Diagrams showing characteristics of strongly coupled (Chilean type) and weakly coupled (Mariana type) subduction zones (modified from Uyeda and Kanamori, 1979).

*Topography of the subducted slab.* Kelleher and McCann (1977) and Lay *et al.* (1982) both note that very large subduction earthquakes are more likely to occur in regions where the subducted plate has smooth topography. That is, the subduction of plates with transforms, ridges, or numerous seamounts is rarely associated with great earthquakes. Lay *et al.* (1982) suggest that the subduction of irregular topography results in heterogeneous strength distributions along the subduction zone and thereby inhibits the occurrence of earthquakes of large dimension.

*Seismic quiescence.* Although weakly coupled subduction zones may display a total absence of major earthquakes, they still have relatively high seismic activity at small magnitudes. Benioff-Wadati zones capable of truly great earthquakes, however, often show significant periods of extremely low seismicity (Lay *et al.*,

1982). This pattern may be somewhat analogous to the seismicity observed along the San Andreas fault in California. The central creeping portion of the fault is characterized by relatively high seismicity, but no large earthquakes. However, the portions of the fault that are capable of great earthquakes (1857 and 1906 breaks) are almost devoid of present-day seismicity.

#### THE JUAN DE FUCA SUBDUCTION ZONE

We have seen that there are systematic differences between subduction zones that are capable of great earthquakes and those that are not. The Juan de Fuca subduction zone has been ignored in the studies that established these differences. The Juan de Fuca subduction zone has been considered somewhat anomalous because there has been virtually no shallow thrust seismicity of the type we usually associate with active subduction zones. There are several possible explanations for this low level of seismicity: (1) the North American and Juan de Fuca plates are no longer converging; (2) the plates are converging but slip is accommodated aseismically; and (3) the northwestern United States is a major seismic gap that is locked and presently seismically quiescent, but that will fail in great earthquakes in the future. Each of these possibilities is discussed below.

*Present-day convergence.* The geometry of important plate boundaries and the seismicity in the Pacific Northwest are shown in Figure 4. Delaney *et al.* (1981) note that there appears to be 43 km of new oceanic crust formed on the Juan de Fuca ridge since the 700,000-yr-old Brunhes-Matuyama magnetic reversal, yielding a half-spreading-rate of about 3 cm/yr. The fact that the oldest crust found in the Juan de Fuca plate is on the order of 10 m.y. old (Atwater, 1970) indicates that subduction has occurred in the past. The average convergence rate for the past 5 m.y. has been estimated from magnetic reversal data to be 3.5 cm/yr by Riddihough (1977), 4.2 cm/yr by Chase *et al.* (1975), and 3.0 cm/yr by Nishimura *et al.* (1984).

Hyndman and Weichert (1983) show that historic seismicity can account for slip rates expected from magnetic reversal data on all plate boundaries between the Pacific plate and the North American plate except on the Juan de Fuca subduction zone. Furthermore, it seems difficult to concoct a model of plate motions which has 3.5 cm/yr slip rates on faults both north and south of the Juan de Fuca subduction zone, but with no convergence on the subduction zone itself. It thus appears that presently available evidence supports present-day plate convergence of 3 to 4 cm/yr across the Juan de Fuca subduction zone.

*Physical features of the Juan de Fuca subduction zone and seismic coupling.* The subducted part of the Juan de Fuca plate appears to be very young, probably between 10 and 15 m.y. old. We earlier said that subduction of young oceanic crust usually is associated with strong coupling. The subduction rate, 3 to 4 cm/yr, however, is not particularly high, and this rate does not in itself indicate particularly strong coupling. If we insert these values into equation (1), then we predict a maximum moment magnitude of  $8.3 \pm .5$ . This high value is supported by inspecting Figure 1. We see that strong coupling is associated with every subduction zone where the subducted plate is less than 40 m.y. old. The notion of strong seismic coupling along the Juan de Fuca subduction zone is further supported by the fact that there is clearly no active back-arc basin in the northwestern United States.

A cross section of seismicity in the Puget Sound region is shown in Figure 5. Although a clear Benioff-Wadati zone can be seen, seismicity deeper than 100 km has not been observed. The dip of the Benioff-Wadati zone, as defined by the axis of the trench and the pattern of seismicity beneath Puget Sound, is between  $10^\circ$

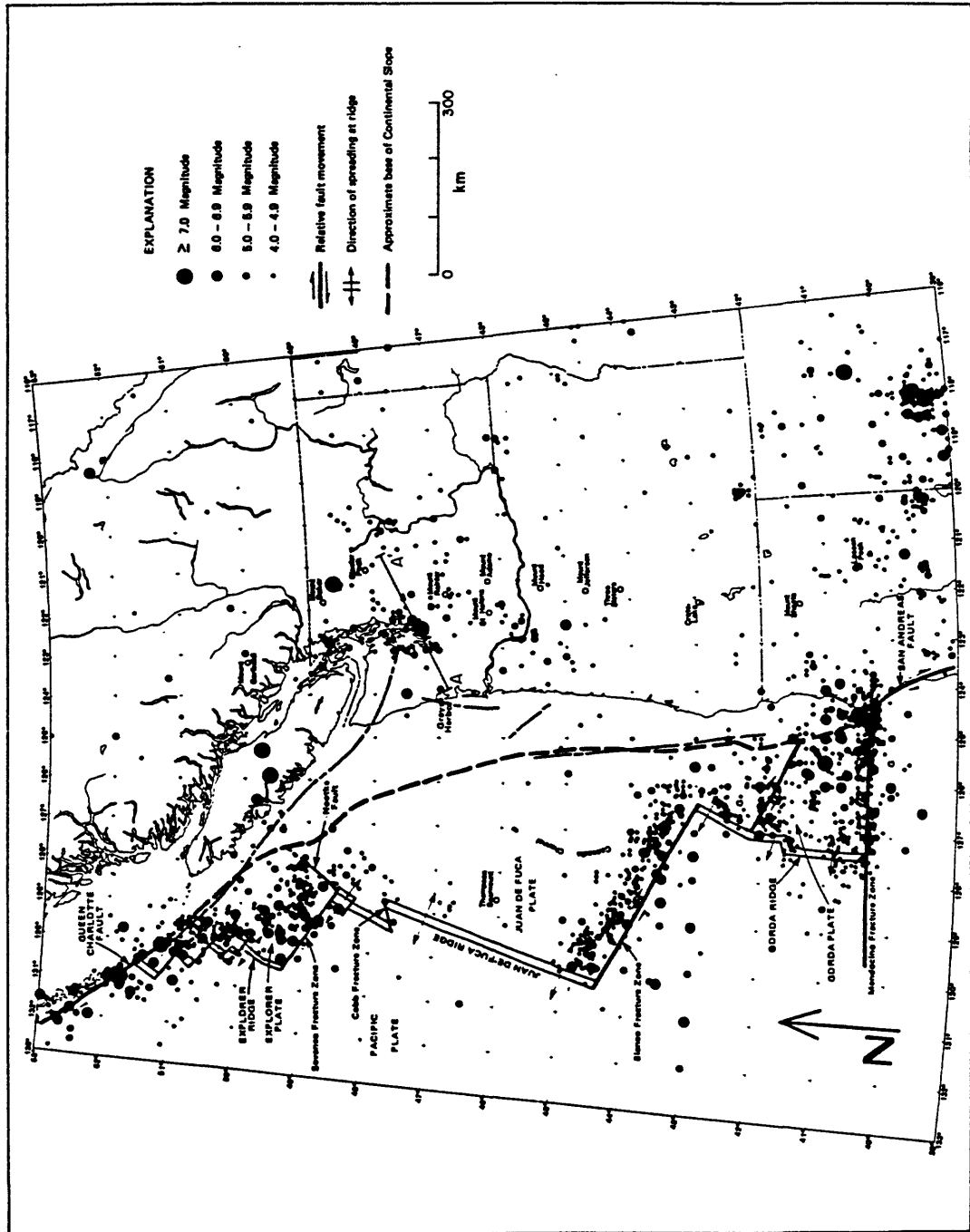


FIG. 4. Major tectonic features and associated seismicity of the Pacific Northwest (modified from Washington Public Power Supply System, 1983).



and  $15^\circ$ . Both of these features are characteristic of subduction zones with strong seismic coupling.

The oceanic trench off the coast of the Pacific Northwest is topographically a relatively subtle feature. Free-air gravity anomalies over the trench are also small compared to most other subduction-zone trenches (Riddihough, 1979) and much of the trench appears to be buried under a thick wedge of sediment (Scholl, 1974). Furthermore, the Juan de Fuca plate is topographically characterized as a smooth, featureless plain. All of these features further corroborate the interpretation that the Juan de Fuca subduction zone is strongly coupled and capable of large, shallow, thrust earthquakes.

One of the most striking features of the Juan de Fuca subduction zone is its present-day very low level of seismicity. There have been moderate events at depths of about 60 km under the Puget Sound in 1949 ( $M$  7.2) and 1965 ( $M$  6.5). However, these events appear to be on high-angle normal faults that occur within the

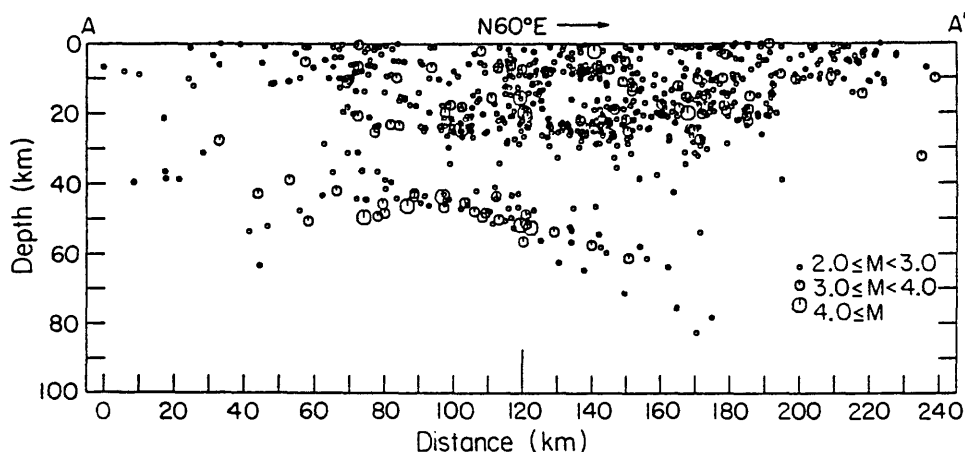


FIG. 5. Cross-section of seismic activity in the Puget Sound region from 1970 through 1978 (see Figure 4 for location of A – A'). Earthquakes with epicenters whose perpendicular distances from A – A' is less than 150 km are included (modified from Crosson, 1980).

subducted slab (Wickens and Hodgson, 1967; Langston and Blum, 1977). The shallowest parts of the subduction zone are presently quiescent with respect to earthquakes of magnitude 4 or greater, and there is no historical record of a large shallow thrust earthquake anywhere along the subduction zone within the past 150 yr (Washington Public Power Supply System, 1983). This 500-km gap in seismic activity is one of the most remarkable to be found anywhere in the circum-Pacific seismic belt. As we noted earlier, the best examples of seismically quiescent plate boundaries are ones that have experienced great earthquakes but that could be considered as otherwise locked. If slip is occurring aseismically on the shallow part of the subduction zone, then this particular example would have to be considered unique.

Ando and Balazs (1979) discuss crustal uplift in the Pacific Northwest as inferred from leveling surveys in the period 1904 to 1974. They interpret crustal-uplift rates of about 2 mm/yr within 50 km of the coastline as being due to aseismic slip along the entire subduction plate boundary. However, this conclusion is contradictory to an interpretation by Savage *et al.* (1981) of horizontal strain as measured by laser ranging in the period 1972 to 1979. They report horizontal compression of 0.13

( $\pm 0.02$ ) microstrain/yr along a principal axis of compression directed N71°E. Weaver and Smith (1983) report northeast-southwest compression axes for earthquakes in the continental crust in southwestern Washington. Both Savage *et al.* (1981) and Weaver and Smith (1983) conclude that these observations are best modeled by coupling between the North American and Juan de Fuca plates which causes compressive strains oriented perpendicular to the subduction zone.

### CONCLUSIONS

The Juan de Fuca and North American plates appear to be converging at a rate of between 3 and 4 cm/yr. The Juan de Fuca subduction zone shares many features with other subduction zones that are strongly coupled and capable of producing very large earthquakes. Although the shallow part of this subduction zone shows little present-day seismicity and no significant historical activity, we feel that there is sufficient evidence to warrant further study of the possibility of a great subduction zone earthquake in the Pacific Northwest.

### ACKNOWLEDGMENTS

We thank Clarence Allen, Don Anderson, Bill Ellsworth, Tom Hanks, Paul Somerville, and Wayne Thatcher for critical reviews of the manuscript. This research was partially supported by NSF Grant EAR 811-6023.

### REFERENCES

- Ando, M. and E. I. Balazs (1979). Geodetic evidence for aseismic subduction of the Juan de Fuca plate, *J. Geophys. Res.* **84**, 3023-3028.
- Atwater, T. (1970). Implications of plate tectonics for the Cenozoic tectonic evolution of western North America, *Geol. Soc. Am. Bull.* **81**, 3513-3535.
- Chase, R. L., D. L. Tiffin, and J. W. Murray (1975). The western Canadian continental margin, in *Canada's Continental Margins and Offshore Petroleum Exploration*, Canadian Society of Petroleum Geologists in association with the Geological Association of Canada, Calgary, Alberta, Canada, 701-721.
- Crosson, R. S. (1980). Review of seismicity in the Puget Sound region from 1970 through 1978, in *Proceedings of Workshop XIV, Earthquake Hazards of the Puget Sound Region, Washington, U.S. Geol. Surv., Open-File Rept.* 83-19, 6-18.
- Delaney, J. R., H. P. Johnson, and J. L. Karsten (1981). The Juan de Fuca hotspot-propagating rift system: new tectonic, geochemical and magnetic data, *J. Geophys. Res.* **86**, 11747-11750.
- Hyndman, R. D. and D. H. Wiechert (1983). Seismicity and rates of relative motion on the plate boundaries of western North America, *Geophys. J. R. Astr. Soc.* **72**, 59-82.
- Kanamori, H. (1977a). Seismic and aseismic slip along subduction zones and their tectonic implications, in *Island Arcs, Deep Sea Trenches and Back-Arc Basins*, Maurice Ewing Series, M. Talwani and W. C. Pittman, Editors, Am. Geophys. Union, Washington, D.C., 173-174.
- Kanamori, H. (1977b). The energy release in great earthquakes, *J. Geophys. Res.* **82**, 2981-2987.
- Kanamori, H. (1983). Global seismicity, in *Earthquakes: Observation, Theory, and Interpretation*, Soc. Italiana di Fisica, Bologna, Italy, 596-608.
- Kelleher, J. and W. McCann (1977). Bathymetric highs and the development of convergent plate boundaries, in *Island Arcs, Deep Sea Trenches, and Back-Arc Basins*, Maurice Ewing Series I, M. Talwani and W. C. Pittman, Editors, Am. Geophys. Union, Washington, D.C., 115-122.
- Langston, C. and D. Blum (1977). The April 20, 1965 Puget Sound earthquake and the crustal and upper mantle structure of western Washington, *Bull. Seism. Soc. Am.* **67**, 693-711.
- Lay, T., H. Kanamori, and L. Ruff (1982). The asperity model and the nature of large subduction zone earthquakes, in *Earthquake Prediction Research*, 1, Terra Scientific Publishing Co., Tokyo, Japan, 3-71.
- Nishimura, C., D. S. Wilson, R. N. Hey (1984). Pole of rotation analysis of present-day Juan de Fuca motion, *J. Geophys. Res.* (in press).
- Riddiough, R. P. (1977). A model for recent interactions off Canada's west coast, *Can. J. Earth Sciences* **14**, 384-396.

## SEISMIC POTENTIAL: SUBDUCTION IN THE NW U.S.

- Riddihough, R. P. (1979). Gravity and structure of an active margin: British Columbia and Washington, *Can. J. Earth Sciences* **16**, 350-362.
- Ruff, L. and H. Kanamori (1980). Seismicity and the subduction process, *Phys. Earth Planet. Interiors* **23**, 240-252.
- Savage, J. C., M. Lisowski, and W. H. Prescott (1981). Geodetic strain measurements in Washington, *J. Geophys. Res.* **86**, 4929-4940.
- Scholl, D. W. (1974). Sedimentary sequences in the North Pacific Trenches, in the *Geology of Continental Margins*, C. Burk and L. Drake, Editors, Springer-Verlag, New York, 493-504.
- Uyeda, S. and H. Kanamori (1979). Back-arc opening and the mode of subduction, *J. Geophys. Res.* **84**, 1049-1061.
- Washington Public Power Supply System (1983). Final safety analysis report, Supply System Nuclear Project No. 3, vol 4.
- Weaver, C. S. and S. W. Smith (1983). Regional tectonic and earthquake hazard implications of a crustal fault zone in southwestern Washington, *J. Geophys. Res.* (in press).
- Wickens, A. J. and J. H. Hodgson (1967). Computer re-evaluation of earthquake mechanism solutions, 1922-1962, Dominion Observatory, Ottawa, Publications, 33, vol. 1, 560 pp.

U.S. GEOLOGICAL SURVEY  
CALIFORNIA INSTITUTE OF TECHNOLOGY  
PASADENA, CALIFORNIA 91125

SEISMOLOGICAL LABORATORY  
CALIFORNIA INSTITUTE OF TECHNOLOGY  
PASADENA, CALIFORNIA 91125  
CONTRIBUTION No. 4070

Manuscript received 16 August 1983

## POSSIBLE TSUNAMI ALONG THE NORTHWESTERN COAST OF THE UNITED STATES INFERRED FROM INDIAN TRADITIONS

BY THOMAS H. HEATON AND PARKE D. SNAVELY, JR.

Subduction of the Juan de Fuca and Gorda plates beneath western North America presents a paradox; despite the fact that there is good evidence of 3 to 4 cm/yr of ongoing convergence, there is a remarkable paucity of either historic or instrumentally recorded shallow subduction earthquakes. Steady aseismic slip along the entire Cascadia subduction zone provides one explanation for this seismic quiescence. However, the Cascadia subduction zone shares many features, including temporal quiescence, with other subduction zones that have experienced very large shallow subduction earthquakes (Heaton and Kanamori, 1984). Yet, there is no direct geologic or historical evidence presently available to confirm that great shallow subduction earthquakes have occurred along the coast of Washington, Oregon, and northern California. However, there are reports describing Indian legends of great sea-level disturbances that may be related to large nearby earthquakes. In this letter, we briefly review the history of exploration and settlement of this region by nonnative people and then discuss legends from Indians in northern Washington and northern California.

The coastline of Washington was first explored by Captain Bruno Heceta of Spain in 1775, and a Spanish settlement was briefly occupied (5 months) in 1792 at Neah Bay (see Figure 2). This coastline was also explored by Captain James Cook (England) in 1778 and Captain Robert Gray (United States) in 1792. Fur trading settlements were established by Canadians in 1810 and 1811 at Spokane, Astoria, and Fort Okanogan. Permanent, but sparse, settlement of the region persisted until the 1850's when a major wave of immigration occurred.

It seems certain that great coastal subduction earthquakes have not occurred since the 1850's and highly probable that they have not occurred since the 1790's. However, Judge James Swan has reported curious Indian "traditions" that suggest effects that could have resulted from a great shallow subduction earthquake. Swan was a renowned student of Indian lore, writing several fascinating accounts of his experiences with coastal Indians from Washington, Oregon, and British Columbia during the 1850's through 1870's (Swan, 1857, 1868, 1874).

The following excerpts are from Swan's 1868 publication, "The Indians of Cape Flattery." Although it is useful to study a large quantity of Swan's writings in order to better understand the context of the "traditions" of a large sea-level disturbance, the first excerpt indicates Swan's impressions of the reliability of Indian legends.

History, Traditions, Etc.—The history of this tribe (Makah), as far as their knowledge extends, is a confused mass of fables, legends, myths, and allegories. Nothing that they can state prior to the existence of a few generations back is clear or wholly to be relied upon. There are a few prominent events that have been remembered as having occurred; but the detail is confused, and it is very rare that two Indians tell the same story alike, unless it may be some wild and improbable legend, like the fairy tales related in nurseries, which are remembered in after life. A notable instance of this unreliability is in their version of the account of the

Spanish settlement attempted at Neeah Bay by Lieut. Quimper, in 1792 by order of the commandant of the Spanish forces at Nootka. All they really know about it, is that they have been told by their fathers that the Spaniards were here, and they can point out the locality where yet may be found pieces of tile used by the Spaniards in building. But although that occurrence was only seventy-three years ago, there is but one man living in the tribe who remembers the circumstances, and he is in his dotage. Almost every Indian I have questioned upon the subject gives a different version of the detail. Now, as they cannot relate correctly matters given in our history, and of a comparatively recent date, but little dependence can be placed upon the tales of their origin, which are interesting only for their fabulous and superstitious nature.

More recent events, such as the murder of the crews of the ship *Boston*, in 1803, and of the *Tonquin*, in 1811, and the captivity of Jewett among the Nootkans, they remember hearing about, and relate with tolerable accuracy. As events recede in years, however, they become obscured with legends and fables, so that the truth is exceedingly difficult to discover.

Keeping these strong caveats in mind, we now reprint Swan's (1868) account of Indian "traditions" of a great sea level disturbance along the coast of Washington. Geographic locations of tribes and places mentioned in this account are shown in Figures 1 and 2 (modern spelling of some words may differ from that in the account). In addition, the word, *Makah*, is used by eastern inland Indians and nonnative people; the word, *Classet*, is used by northern Coastal Indians, and the word *Kwenaitchechat* is used by Cape Flattery Indians (*Makahs*). All of these words have the same meaning: "people who live on a point of land projecting into the sea (i.e. Cape Flattery)."

The only tradition that I have heard respecting any migratory movement among the *Makahs*, is relative to a deluge or flood which occurred many years ago, but seems to have been local, and to have had no connection with the Noachic deluge which they know nothing about, as a casual visitor might suppose they did, on hearing them relate the story of their flood. This I give as stated to me by an intelligent chief; and the statement was repeated on different occasions by several others, with a slight variation in detail.

"A long time ago," said by informant, "but not at a very remote period, the water of the Pacific flowed through what is now the swamp and prairie between Waatch village and Neeah Bay, making an island of Cape Flattery. The water suddenly receded leaving Neeah Bay perfectly dry. It was four days reaching its lowest ebb, and then rose again without any waves or breakers, till it had submerged the Cape, and in fact the whole country, excepting the tops of the mountains at *Clyoquot*. The water on its rise became very warm, and as it came up to the houses, those who had canoes put their effects into them, and floated off with the current, which set very strongly to the north. Some drifted one way, some another; and when the waters assumed their accustomed level, a portion of the tribe found themselves beyond Nootka, where their descendants now reside, and are known by the same name as the *Makahs* in *Classett*, or *Kwenaitchechat*. Many canoes came down in the trees and were destroyed, and numerous lives were lost. The water was four days regaining its accustomed level."

# LETTERS TO THE EDITOR

The same tradition was related to be by the Kwilleuyutes, who stated that a portion of that tribe made their way to the region in the vicinity of Port Townsend, where their descendants are known as the Chemakum tribe. I have also received the same tradition from the Chemakum Indians, who claim to have originally sprung from the Kwilleuyutes. There is no doubt in my mind of the truth of this tradition. The Waatch prairie shows conclusively that the water of the Pacific once flowed through it; and on cutting through the turf at any place between Neeah Bay and Waatch, the whole

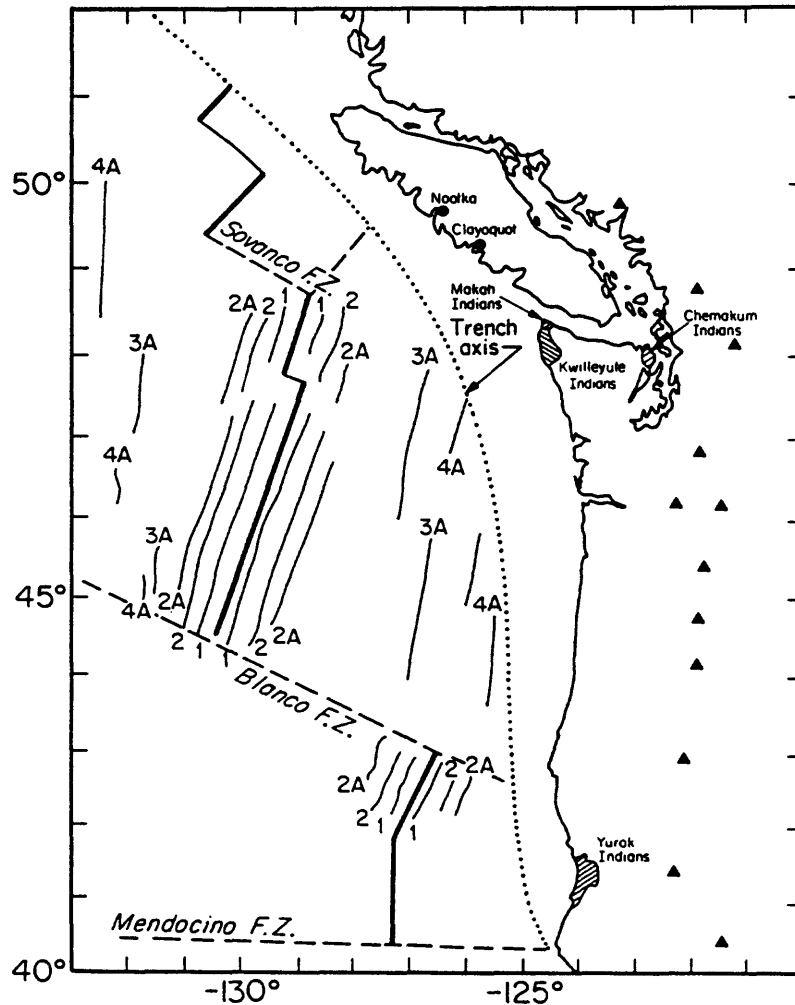


FIG. 1. Approximate location of Indian tribes and place names mentioned in this report. Approximate locations of sea-floor magnetic lineations and Quaternary volcanoes (triangles) are also shown.

substratum is found to be pure beach sand. In some places the turf is not more than a foot thick; at others the alluvial deposit is two or three feet.

As this portion of the country shows conclusive evidence of volcanic action, there is every reason to believe that there was a gradual depression and subsequent upheaval of the earth's crust, which made the waters rise and recede as the Indians stated. Fossil remains of whales are said by the Indians to be found around a lake near Clayoquot, which were possibly deposited at the time of this flood. I have not seen these remains, but I

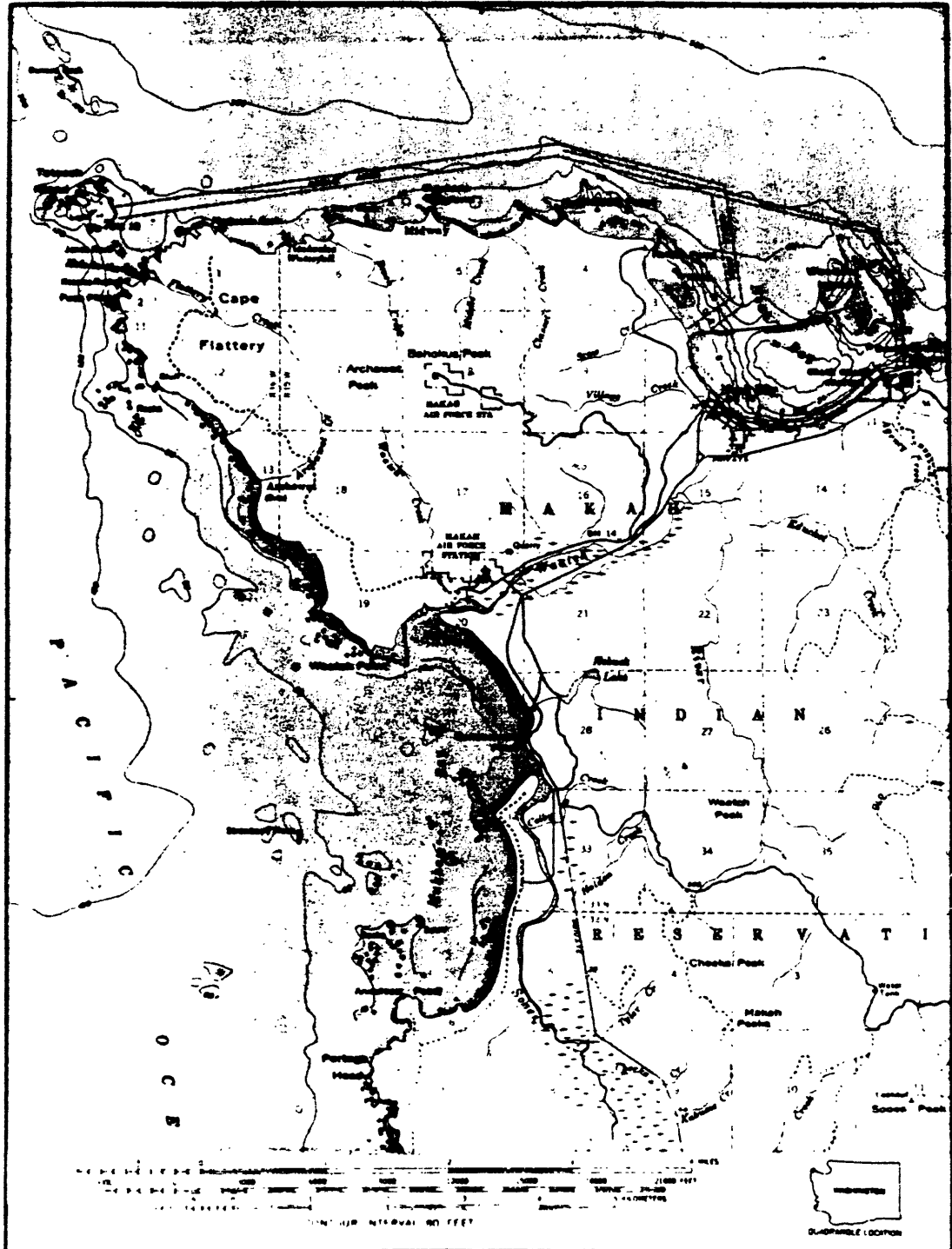


FIG. 2. Topographic map of the Cape Flattery region (U.S. Geological Survey Cape Flattery Quadrangle, 15-min series).

have been told of their existence by so many different Indians who professed to have seen them, that I think the story probably correct. The Indians do not think they got there by means of the flood, but that, as before stated, they are the remains of the feasts of the T'hlukloots, or thunder bird, who carried the whales there in his claws, and devoured them

## LETTERS TO THE EDITOR

at his leisure. With the single exception of this legend of the flood, I have never learned from them that they have any tradition respecting the tribe coming to or going from the place where they now reside, and this is the only one which they relate of ancient times that is corroborated by geological or other evidence.

Could this be an account of a great tsunami? Although there are many features of this report that seem exaggerated, apparently Swan was convinced that some remarkable sea-level disturbance had occurred. He clearly segregates this report from the majority of legends which he feels are of a more mythical nature. The words, "a long time ago, but not at a very remote period," indicate that the alleged disturbance predates the lifetimes of the reporting Indians, but was not to be confused with an ancient time which was associated with the great majority of their mythical legends.

If this is an account of an ancient tsunami, then what can be deduced about its nature and origin? Great tsunamis may have periods of tens of minutes to hours, but 4 days is without precedent. If we are to believe that this is an account of a through the years. If the event is real, then it is apparent that the effects must have been substantial. However, it seems incredulous that any tsunami could have overtopped the entire Cape Flattery region since the highest elevation of the cape exceeds 400 m. Furthermore, one is hard pressed to explain why the water would become warm. Nevertheless, the description of water receding from Neah Bay and then returning in a strong current is clearly suggestive of a tsunami.

If this is a tsunami description, could the sea wave have originated from a great earthquake at a distant location? Since there is no mention of any ground shaking, this might be a logical conclusion. However, large historical earthquakes along the Pacific rim have not generated large tsunamis at Neah Bay. The  $M_w$  9.2 Alaskan earthquake in 1964 caused a tsunami of only about 1.3 m at Neah Bay (Cloud and Scott, 1972). Furthermore, the story indicates that Cape Flattery was an island before this legendary event. This may be plausible since a low marshy area between Waatch and Neah Bay is the only thing that currently prevents Cape Flattery from being an island. If there was permanent uplift of the Waatch lowland associated with the event described in the legend, then crustal deformation associated with a nearby subduction earthquake could explain the uplift. However, this and any other conjectures about the significance of this legend are purely speculative. There are enough inconsistencies in the legend that one must seriously consider the interpretation that this Indian tradition may be entirely fictional. Nevertheless, it is noteworthy that such a report exists for a region for which there is growing concern that large subduction earthquakes and subsequent tsunamis may be a real possibility.

We have mentioned this report by Swan to several colleagues and this resulted in the rediscovery of other Indian legends of earthquake activity along the northwestern coastal United States. Gary Carver (Department of Geology, Humboldt State University, Arcata, California) informed us of myths of the Yurok Indians in which earthquakes seem to play a prominent role. These myths were recorded by A. L. Kroeber (1976) between 1900 and 1907. Yurok Indians inhabited the region that roughly coincides with Redwood National Park in northernmost coastal California (see Figure 1). According to Yurok mythology, the god, Earthquake, was a very powerful being that ran over the earth, shaking and tearing the ground, breaking trees, and disturbing the rivers and ocean. However, the Yurok stories are very



## LETTERS TO THE EDITOR

allegorical and seem to be correctly classified as myths. We do not reproduce these myths here since they are somewhat lengthy, difficult to interpret, and their factual basis is unknown.

## CONCLUSIONS

We thank Gary Carver for generously providing materials relating to Yurok Indian mythology. We also thank Joseph Ziony and Robert Wallace for thoughtful reviews of the manuscript. This work is supported, in part, by the U.S. Nuclear Regulatory Commission.

## REFERENCES

- Cloud, W. K. and N. H. Scott (1982). Distribution of intensity, in *The Great Alaska Earthquake of 1964, Seismology and Geodesy*, National Academy of Sciences, Washington, D.C., 65-108.
- Heaton, T. H. and H. Kanamori (1984). Seismic potential associated with subduction in the northwestern United States, *Bull. Seism. Soc. Am.* **74**, 933-941.
- Kroeber, A. L. (1976). *Yurok Myths*, University of California Press, Berkeley, California, 488 pp.
- Swan, J. G. (1857). *The Northwest Coast*, Harper and Brothers, Publishers, New York, 435 pp.
- Swan, J. G. (1868). The Indians of Cape Flattery, at the entrance to the straight of Juan de Fuca, Washington Territory, *Smithsonian Contributions To Knowledge*, **220**, 108 pp.
- Swan, J. G. (1874). The Haidah Indians, of the Queen Charlotte Islands, British Colombia, *Smithsonian Contributions To Knowledge*, **267**, 25 pp.

U.S. GEOLOGICAL SURVEY  
SEISMOLOGICAL LABORATORY  
CALIFORNIA INSTITUTE OF TECHNOLOGY  
PASADENA, CALIFORNIA 91125 (T.H.)

U.S. GEOLOGICAL SURVEY  
345 MIDDLEFIELD ROAD  
MENLO PARK, CALIFORNIA 94025 (P.S.)

Manuscript received 8 May 1985

## SOURCE CHARACTERISTICS OF HYPOTHETICAL SUBDUCTION EARTHQUAKES IN THE NORTHWESTERN UNITED STATES

BY THOMAS H. HEATON AND STEPHEN H. HARTZELL

### ABSTRACT

Historic earthquake sequences on subduction zones that are similar to the Cascadia subduction zone are used to hypothesize the nature of shallow subduction earthquakes that might occur in the northwestern United States. Based on systematic comparisons of several physical characteristics, including physiography and seismicity, subduction zones that are deemed most similar to the Cascadia subduction zone are those in southern Chile, southwestern Japan, and Colombia. These zones have all experienced very large earthquake sequences, and if the Cascadia subduction zone is also capable of storing elastic strain energy along its greater than 1000 km length, then earthquakes of very large size ( $M_w > 8\frac{1}{2}$ ) must be considered. Circumstantial evidence is presented that suggests (but does not prove) that large subduction earthquakes along the Cascadia subduction zone may have an average repeat time of 400 to 500 yr.

### INTRODUCTION

This is the third in a series of four papers that lead to an estimation of the seismic hazard associated with the subduction of the Juan de Fuca and Gorda plates beneath North America. In the first paper, Heaton and Kanamori (1984) compared physical characteristics of the Cascadia subduction zone (also referred to as the Juan de Fuca subduction zone) with those of other subduction zones and concluded that the Cascadia subduction zone is similar to other subduction zones with strong seismic coupling, and thus may be capable of producing great shallow subduction earthquakes. In the second paper, Hartzell and Heaton (1985) compared the nature of the time history of seismic energy release for 60 of the largest subduction earthquakes to occur in the past 50 yr. In this paper, we extend the results of the previous studies to estimate the nature of shallow subduction earthquakes that could be postulated if the Cascadia subduction zone is assumed to have strong seismic coupling. In the fourth paper, Heaton and Hartzell (1986) estimate the nature of strong ground motions that may result from earthquakes hypothesized in this study.

Key issues addressed here are: (1) the dimensions and geometry of hypothetical Cascadia subduction earthquakes; (2) plausible repeat time; (3) identification of analogous historic earthquakes; and (4) estimation of possible tsunami amplitudes.

Subduction of the Juan de Fuca and Gorda plates has presented earth scientists with a dilemma. Despite compelling evidence of active plate convergence (Riddihough, 1977; Snively *et al.*, 1980; Hyndman and Wiechert, 1983; Adams, 1984a; Nishimura *et al.*, 1985), subduction on the Cascadia zone has often been viewed as a relatively benign tectonic process (Riddihough, 1978; Ando and Balazs, 1979; Acharya, 1981, 1985). There is no deep oceanic trench off the coast; there is no extensive Benioff-Wadati seismicity zone; and most puzzling of all, there have not been any historic low-angle thrust earthquakes between the continental and subducted plates. The two simplest interpretations of these observations are: (1) the Cascadia subduction zone is completely decoupled and subduction is occurring aseismically, or (2) the Cascadia subduction zone is uniformly locked and storing elastic energy to be released in future great earthquakes. Full resolution of this issue

may prove elusive. Although it is somewhat surprising that no shallow subduction earthquakes have been documented in this region, the duration of written history is relatively short. It seems certain that great shallow subduction earthquakes have not occurred in this region since the 1850's and highly probable that they have not occurred since the 1790's. If large shallow subduction earthquakes do occur on the Cascadia subduction zone, we can infer their characteristics only by studying the nature of subduction earthquakes that have occurred on other subduction zones that can be considered as analogous. Unfortunately, no subduction zone is exactly the same as the Cascadia subduction zone, and thus, the search for analogs will always lead to fundamental ambiguities.

Systematic variations in the nature of seismic energy release with physical characteristics of subduction zones have been discussed by Kelleher *et al.* (1974), Kanamori (1977), Uyeda and Kanamori (1979), Ruff and Kanamori (1980), Lay *et al.* (1982), Peterson and Seno (1984), and Uyeda (1984). Many types of correlations have been suggested, but since quantification of the physical characteristics of subduction zones and their earthquakes is often rather subjective, not all of these studies seem to reach compatible conclusions. Perhaps the most consistent observation is that subduction of young lithosphere is associated with strong seismic coupling whereas subduction of old lithosphere is associated with weak seismic coupling. Ruff and Kanamori (1980) demonstrate that the seismic coupling is well-correlated with a simple linear function of subducted plate age and convergence velocity in which decreasing age and increasing convergence velocity imply stronger seismic coupling. Heaton and Kanamori (1984) show that the Cascadia subduction zone is clearly different from the class of aseismic subduction zones that is characterized by the subduction of old lithosphere. They further show that it shares many characteristics with subduction zones that have experienced very large shallow subduction earthquakes. In this report, we do not restate all of the arguments given by Heaton and Kanamori (1984), but instead we extend that study by systematically comparing trench bathymetry and shallow seismicity for a world-wide sampling of subduction zones.

#### TRENCH BATHYMETRY AND GRAVITY

Uyeda and Kanamori (1979) suggest that strongly coupled subduction zones are accompanied by relatively shallow trenches, whereas weakly coupled subduction zones are accompanied by deep oceanic trenches. Similarly, they conclude that free-air gravity anomalies tend to be larger for those trenches with weak seismic coupling. The Cascadia subduction zone is somewhat unusual in that it has virtually no bathymetric trench. In order to assess just how anomalous this is, we have constructed profiles of bathymetry and free-air gravity for many circum-Pacific convergent boundaries. Figure 1 shows shiptrack segments that were used to construct the profiles shown in Figure 2. The shiptrack data were obtained in digital form from NOAA (1981). All data are plotted on a common scale, and the subducted plate is always on the right-hand side of the profile. Bathymetry and free-air gravity are plotted together. Unfortunately, gravity data were not available for all the shiptracks selected, and thus, only bathymetry is plotted for some of the profiles.

Comparing the profiles from differing subduction zones, we see that the Cascadia subduction zone (profiles 38–43) is indeed remarkable for its lack of a bathymetric trench, very shallow ocean floor, and very small gravity anomalies. However, there are several factors that may help to explain these characteristics. The shallow 3 km depth of the Juan de Fuca plate before subduction is near the average depth of very

# SUBDUCTION EARTHQUAKES IN THE NORTHWESTERN U.S.

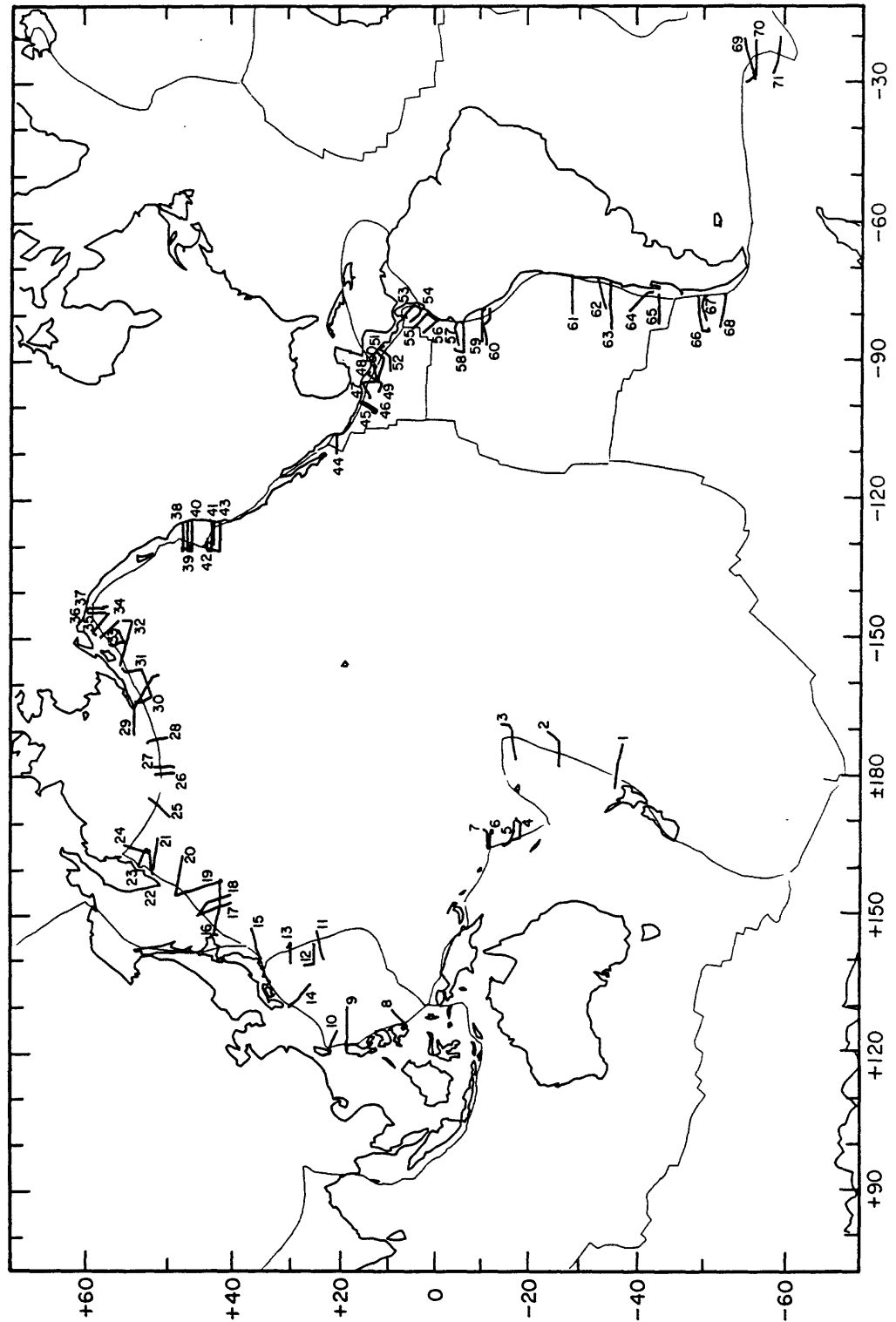


FIG. 1. Shiptracks used to construct profiles of bathymetry and free-air gravity for world-wide subduction zones shown in Figure 2.

young oceanic lithosphere (Parsons and Sclater, 1977). Furthermore, reflection profiles (Snively *et al.*, 1980; Kulm *et al.*, 1984) reveal the presence of a shallow trench that has been completely inundated by approximately 2 km of sediments. Grellet and Dubois (1982) show that there is a good correlation between the age of subducted plate and both the absolute trench depth and the trench depth relative

a

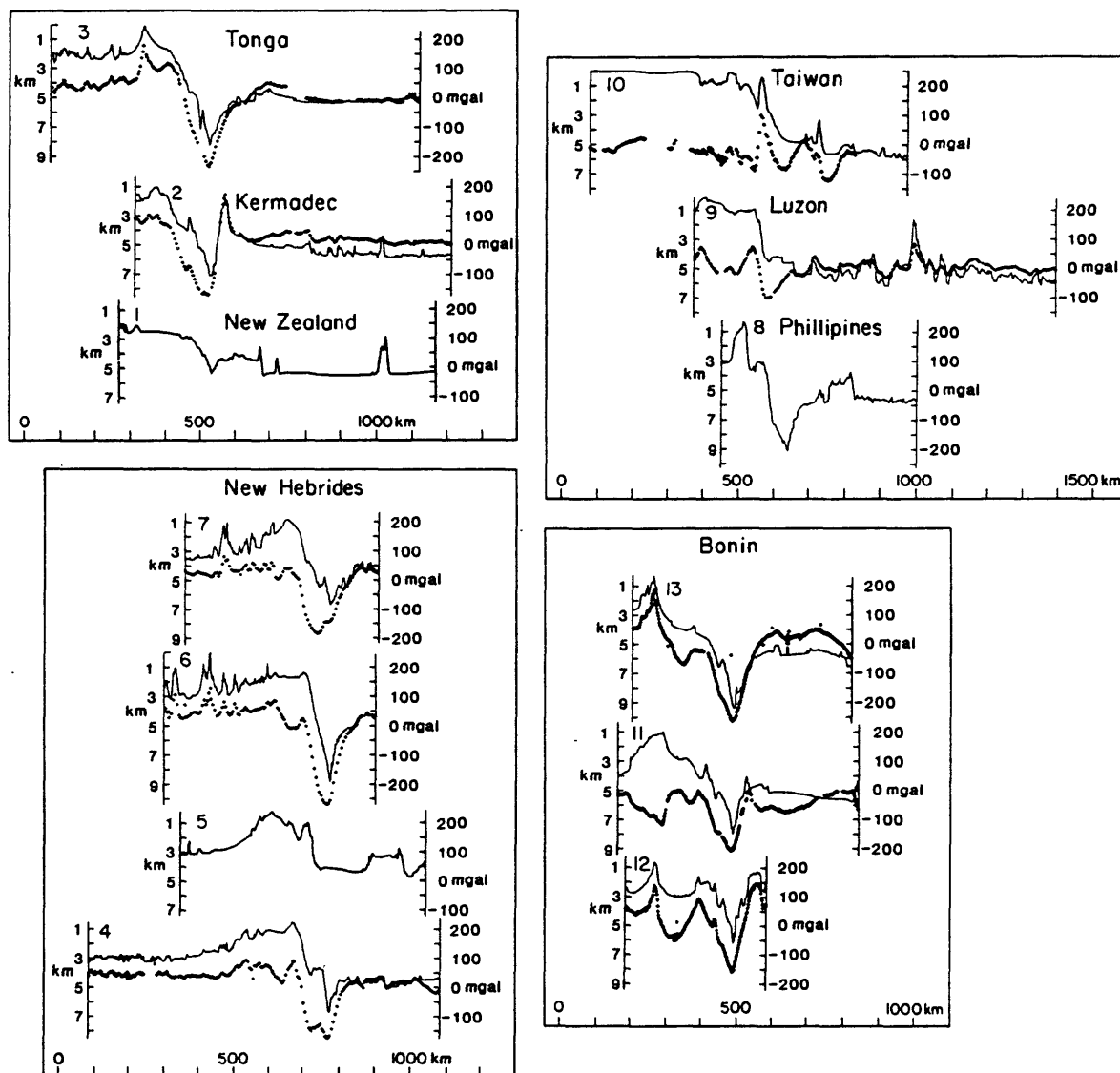


FIG. 2. (a) to (g) Profiles of bathymetry (light solid line) and free-air gravity (dotted heavy line) for shiptracks shown in Figure 1. All profiles are plotted on a common scale and are aligned approximately perpendicular to the trench axes. The subducting ocean plate is always on the *right-hand side* of each profile. The number in the *upper left* corner of each profile corresponds to the shiptrack numbers in Figure 1.

to the adjacent abyssal plain. Once again, the very shallow depth of the Cascadia trench is consistent with the subduction of very young oceanic lithosphere.

Searching through the profiles in Figure 2, we see that there are other subduction zones that have features similar to those observed for the Cascadia subduction zone. New Zealand, Nankai Trough, Alaska, Colombia, and southern Chile are all notable

## SUBDUCTION EARTHQUAKES IN THE NORTHWESTERN U.S.

for the absence of a well-developed bathymetric trench. Hilde (1984) reports extensive trench sediments for all of these areas, and with the possible exception of New Zealand, these trenches have experienced very large shallow subduction earthquakes. We particularly note striking similarities in both bathymetry and gravity profiles between the Cascadia subduction zone, Colombia, and southern Chile.

### SEISMICITY

One of the most striking features of the Cascadia subduction zone is the remarkable paucity of shallow earthquake activity between the trench axis and the coastal

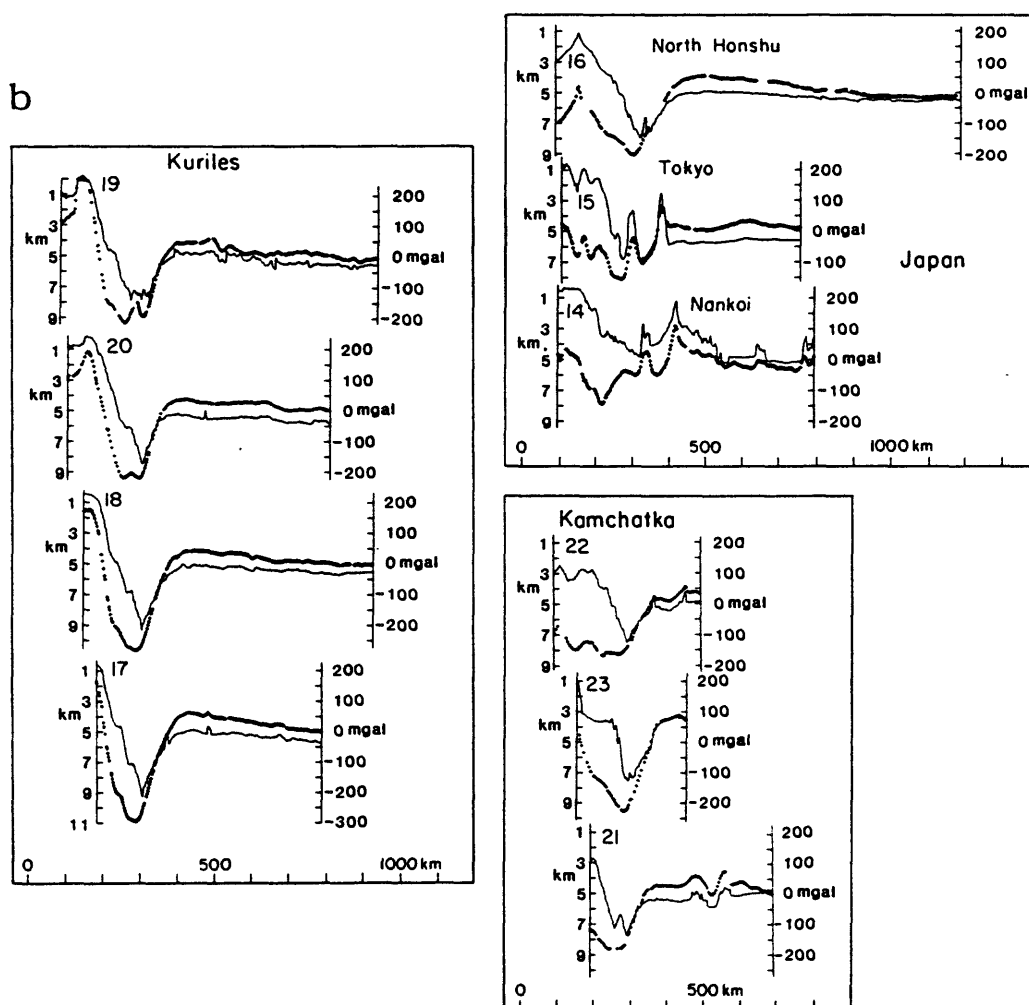


FIG. 2. Continued.

mountain ranges (Taber and Smith, 1985). Despite the continuous monitoring of this region with a local seismometer network since 1970, very few earthquakes of any size have been observed in the coastal regions of Washington and Oregon. This seems somewhat puzzling for a major plate boundary that is undergoing 3 to 4 cm/yr of convergence. Heaton and Kanamori (1984) suggest that this behavior may be analogous to that observed on the San Andreas fault in California. That is, while the central section of the San Andreas fault, which appears to slip principally through aseismic creep, experiences numerous small earthquakes, the sections of

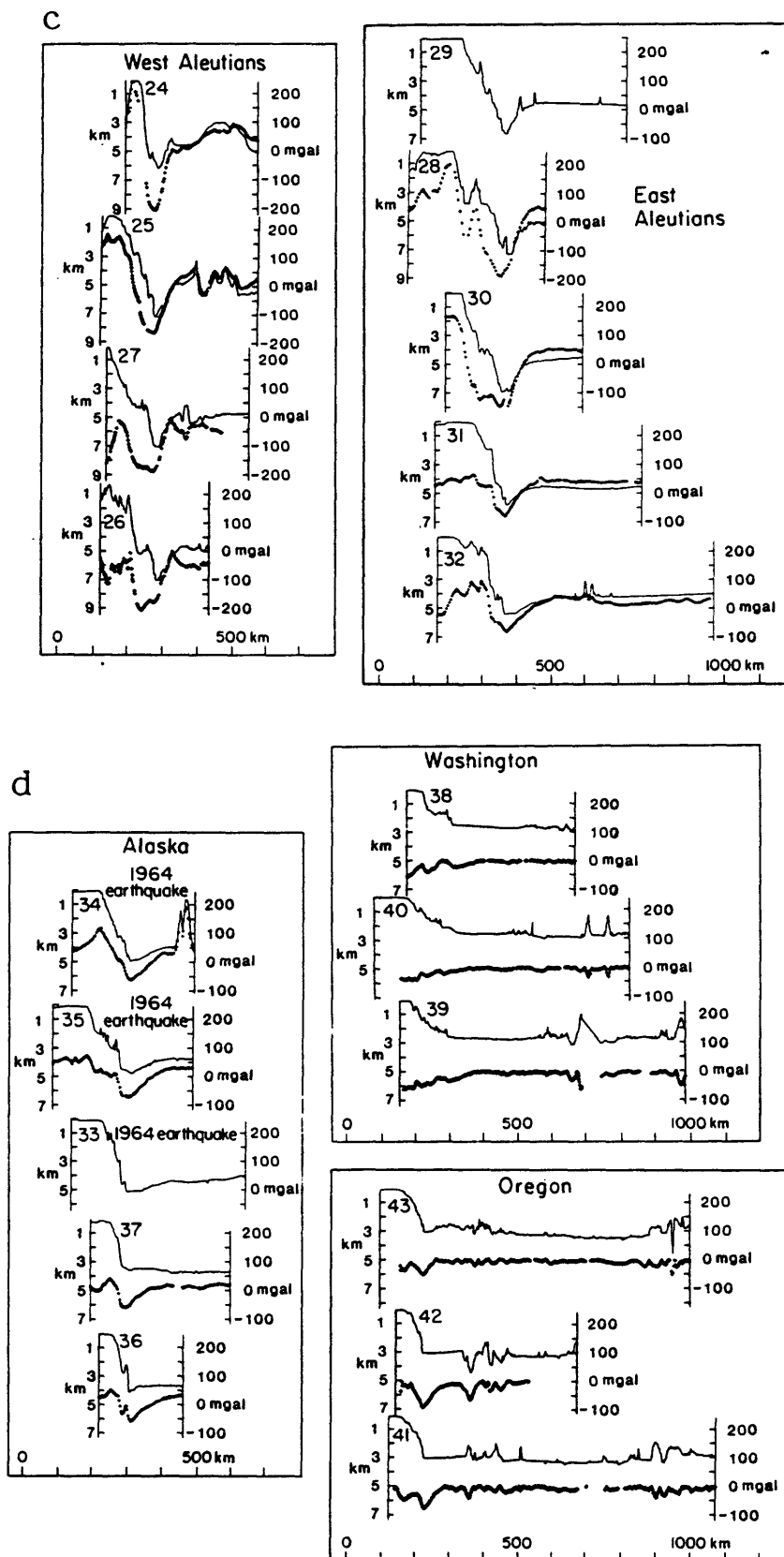
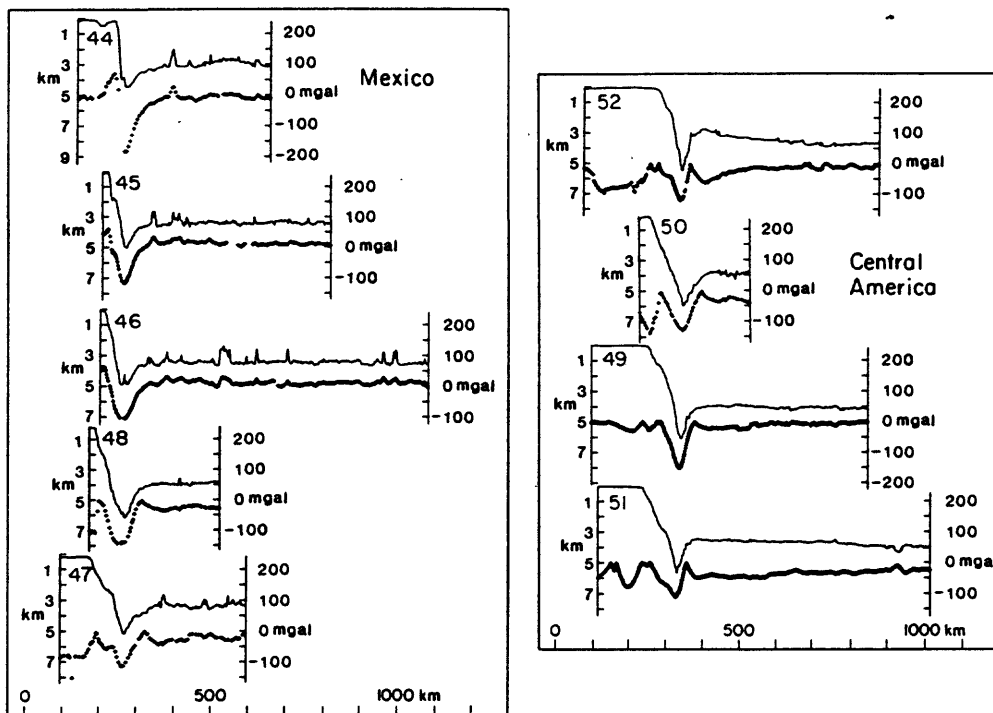


FIG. 2. Continued.

# SUBDUCTION EARTHQUAKES IN THE NORTHWESTERN U.S.

e



f

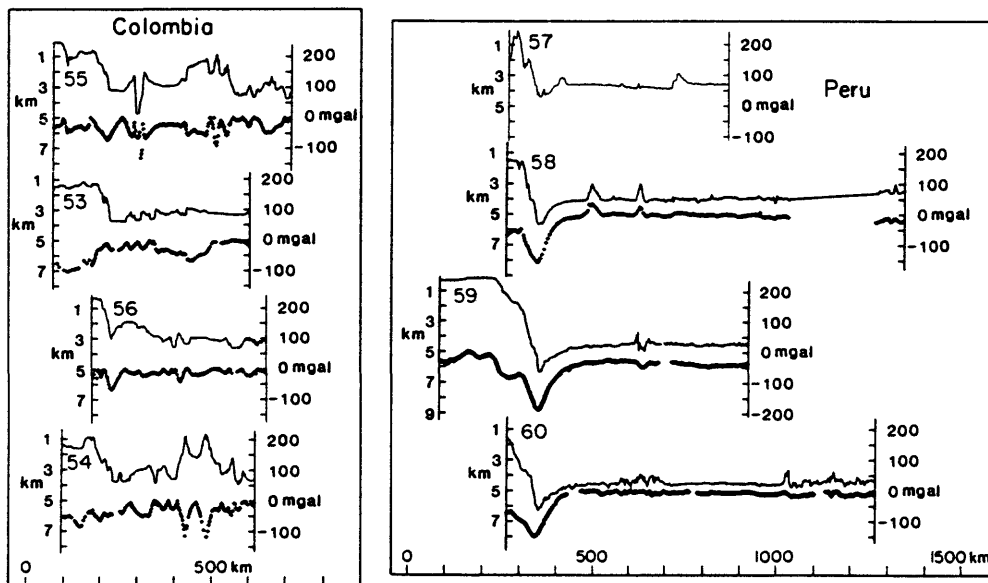


FIG. 2. Continued.

the fault that experienced great earthquakes in 1857 and 1906 are almost totally devoid of present-day seismicity. One hypothesis is that stress increases smoothly and uniformly on fault zones that are strongly coupled over large areas, whereas numerous local stress concentrations occur on faults having large areas that undergo aseismic slip. Although this model may help to explain the paucity of shallow



activity along the Cascadia subduction zone, it has not yet been demonstrated that it generally applies to subduction zones.

Unfortunately, catalogs of local seismicity are not available for many subduction zones that are thought to be strongly coupled. However, there is remarkably little shallow seismicity in the Nankai Trough (Takagi, 1982), a well-instrumented subduction zone having many similarities to the Cascadia subduction zone. In particular, seismicity is very low in the region offshore of the Tokai district (Japan Meteorological Agency, 1984), an area that is often considered as the potential source of a large, shallow subduction earthquake.

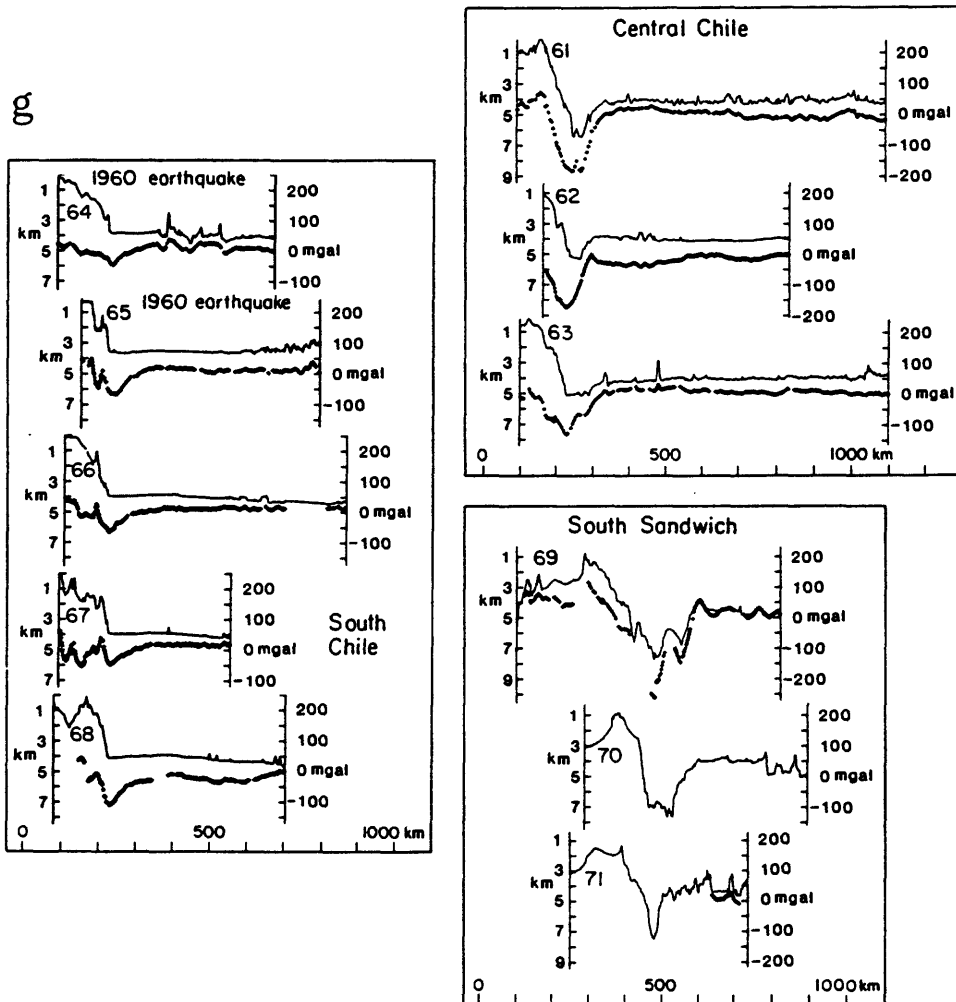


FIG. 2. Continued.

Lacking local seismicity catalogs for most subduction zones, we have systematically compared shallow seismicity from different subduction zones as reported by the NOAA catalog. We wish to identify those zones that have experienced significant time periods of very low seismicity. To this end, we have selected earthquakes with hypocentral depths of less than 50 km from the regions shown in Figure 3. We then plotted the cumulative number of earthquakes in each region as a function of time for the period from 1930 to 1979 (Figure 4). The number of earthquakes in each

# SUBDUCTION EARTHQUAKES IN THE NORTHWESTERN U.S.

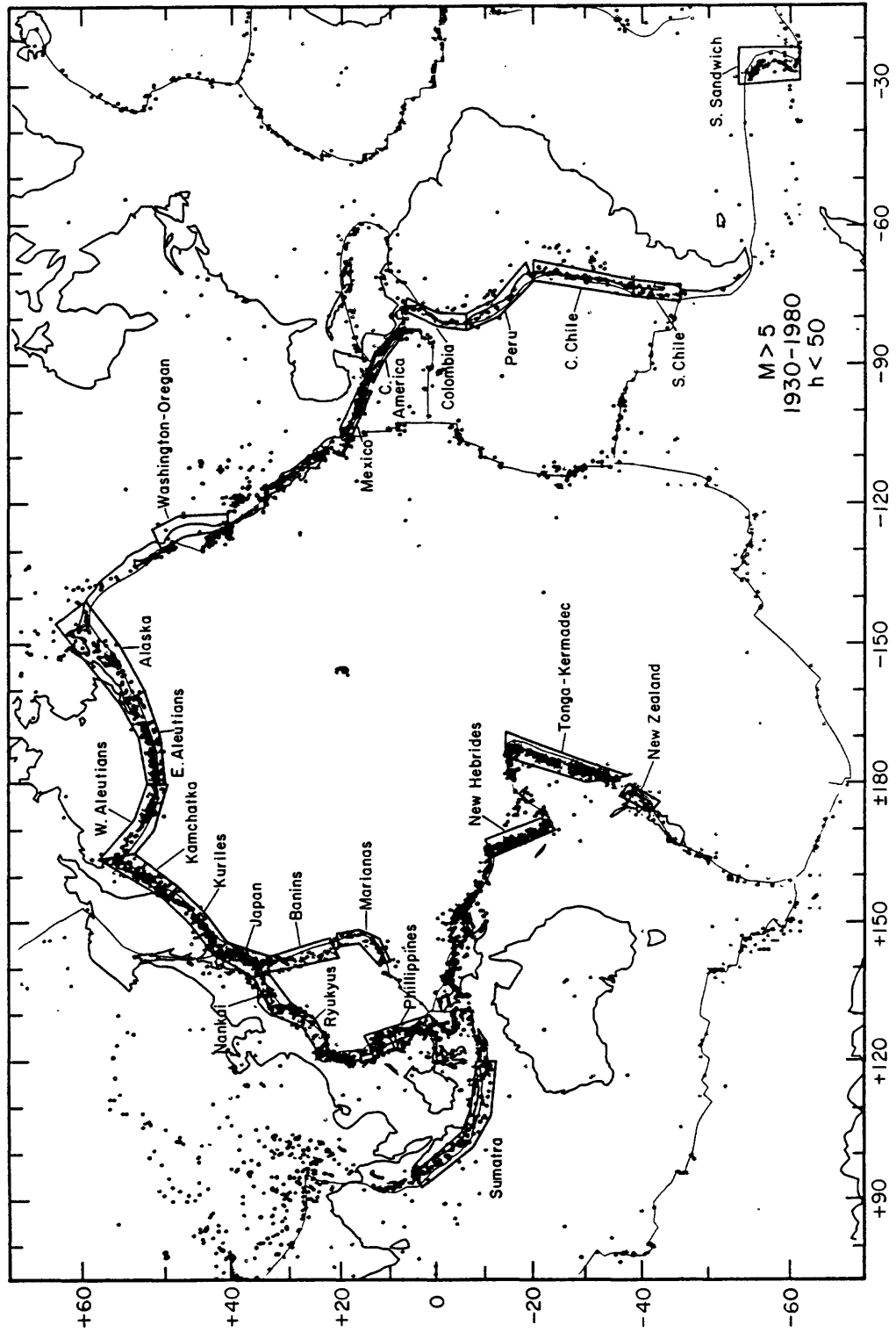


Fig. 3. World-wide map of shallow (depth < 50 km) earthquakes of  $M > 5$  taken from the NOAA catalog for the period from 1930 to 1980. Boxes outline the regions for which cumulative seismicity plots (shown in Figure 4) were constructed.

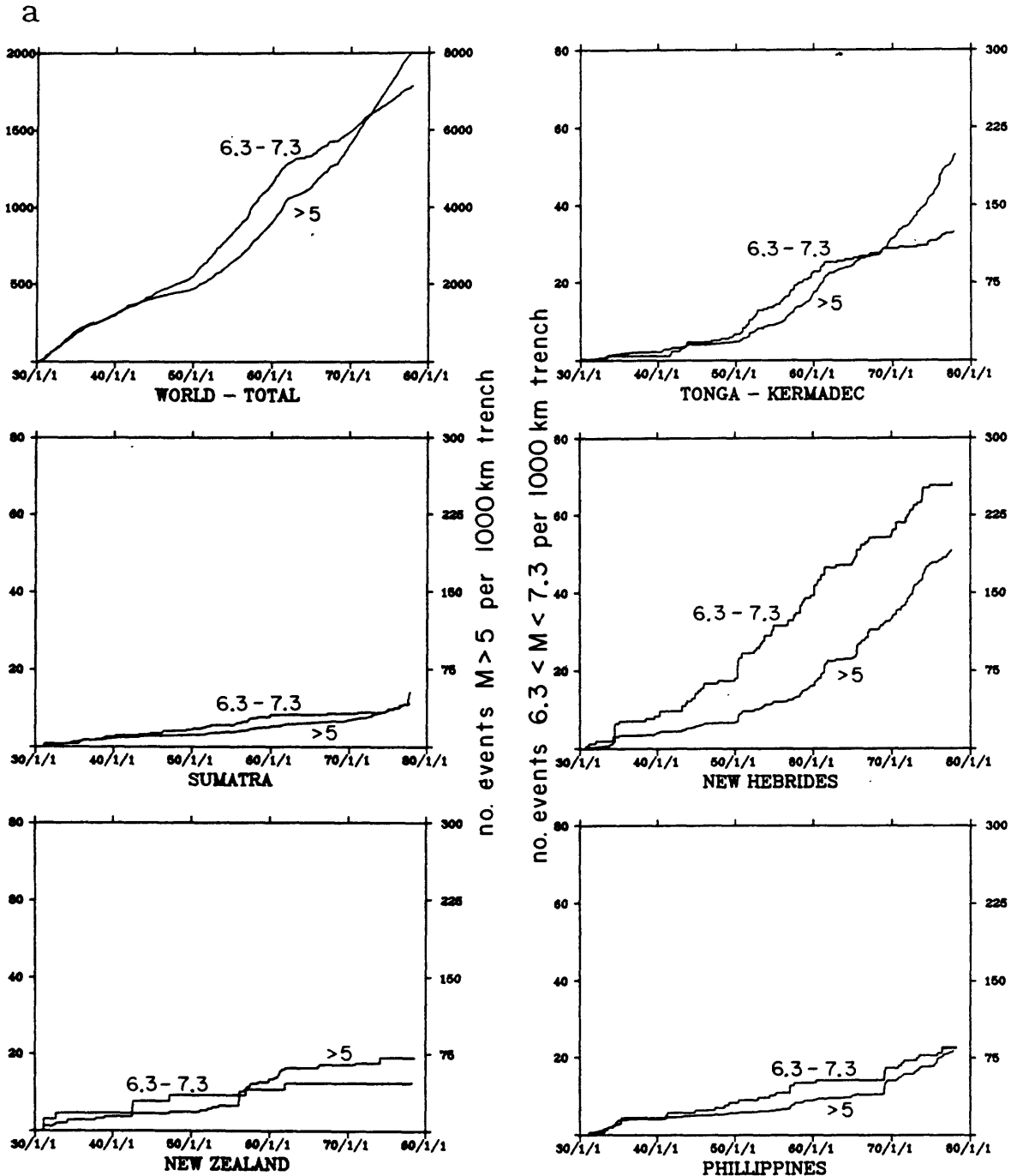


FIG. 4. (a) to (d) Cumulative number of earthquakes shown as a function of time for the regions defined in Figure 3. Both the cumulative number of earthquakes above  $M$  5 (right-hand scale) and the cumulative number of earthquakes between  $M$  6.3 and  $M$  7.3 (left-hand scale) are plotted for the period from 1930 to 1980. The NOAA catalog is probably incomplete for  $M > 5$  earthquakes, but should be complete for  $M$  6.3 to  $M$  7.3 earthquakes. Plots have been scaled for the length of the trench section used, but have not been scaled for convergence rates.

region has been normalized by the trench length, but has not been normalized by convergence rate. Unfortunately, there are almost certainly important spatial and temporal variations in the completeness of the NOAA catalog. Thus, we have selected two magnitude windows: (1) all events between  $M$  6.3 and  $M$  7.3 (amplitude

# SUBDUCTION EARTHQUAKES IN THE NORTHWESTERN U.S.

scale on the left axis of each plot), and (2) all events larger than  $M$  5 (amplitude scale on the right axis of each plot). We believe that the catalog detection is approximately homogeneous with respect to differing regions for earthquakes larger

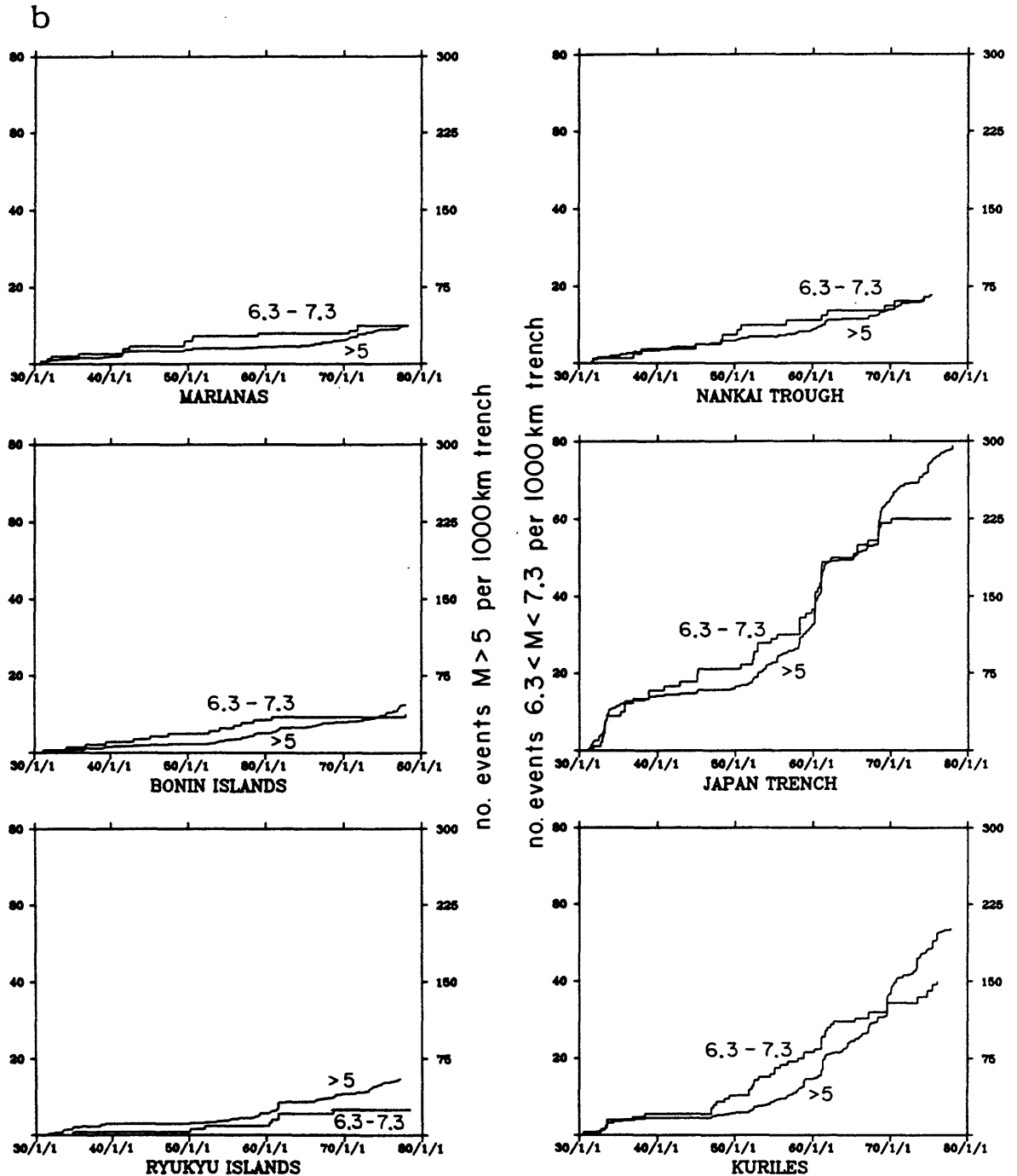


FIG. 4. Continued.

than  $M$  6.3. However, the fact that there are significant temporal variations in the world-wide rate of occurrence of  $M$  6.3 to  $M$  7.3 earthquakes suggests that there may be systematic temporal variations in the calculation of magnitude. Although

the completeness of the NOAA catalog for  $M$  5 earthquakes almost certainly varies with time and region, it is useful to recognize that these earthquakes have occurred in some regions, even if completeness problems will not allow us to prove that they

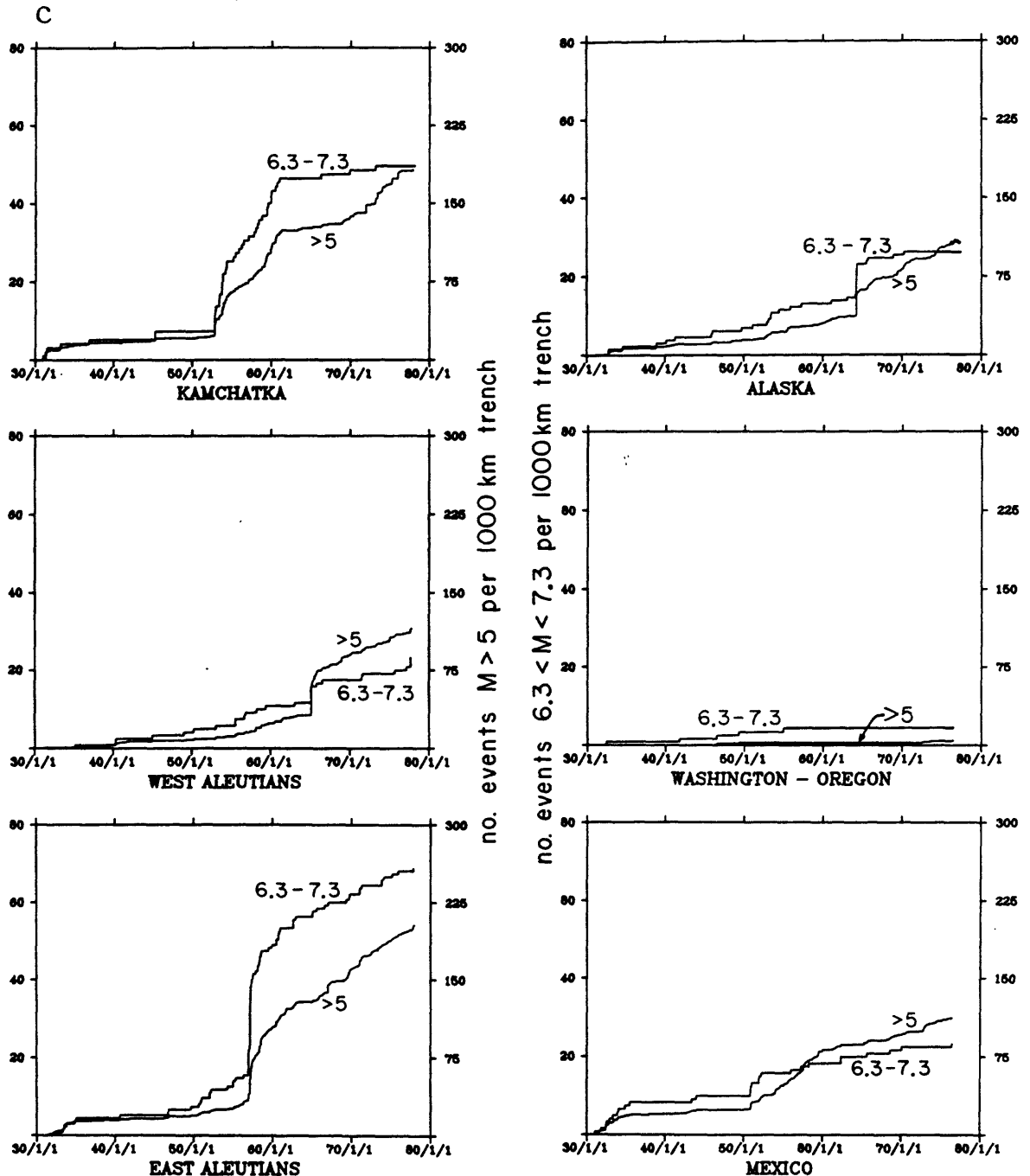


FIG. 4. Continued.

have not occurred in other regions. That is, regions for which there are numerous  $M$  5 earthquakes reported must certainly have a higher level of seismicity than the Cascadia subduction zone, whereas those regions for which few  $M$  5 earthquakes

# SUBDUCTION EARTHQUAKES IN THE NORTHWESTERN U.S.

are reported may or may not have seismicity levels comparable to the Cascadia subduction zone.

A careful study of Figure 4 reveals that coastal Washington and Oregon are

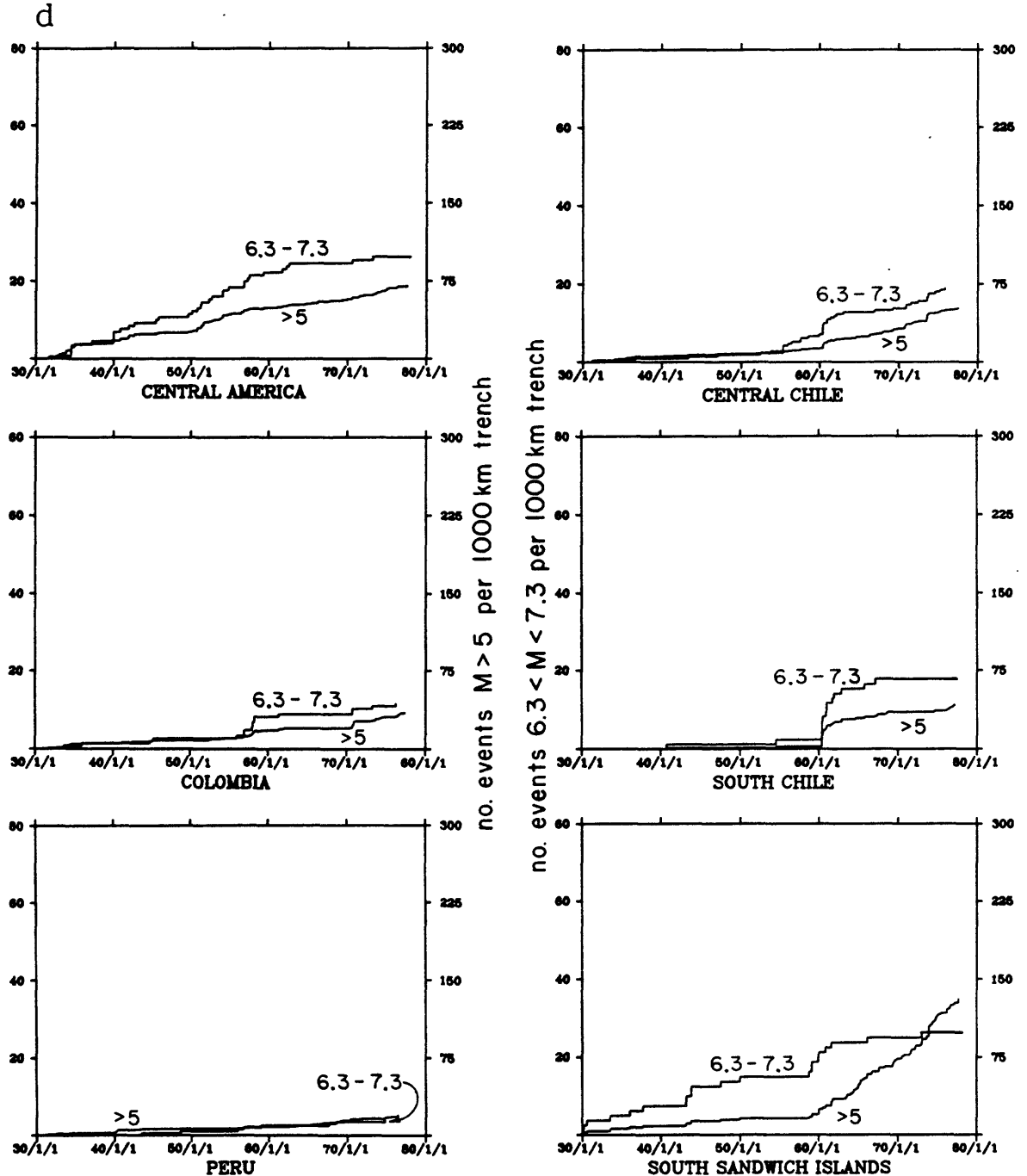


FIG. 4. Continued.

indeed remarkable for their very low levels of earthquake activity. In particular, the Marianas and Bonin Island regions, which are representative of the aseismic subduction of very old lithosphere, have experienced low, but continuous, seismicity.

Regions experiencing high levels of seismicity (Tonga-Kermadec, New Hebrides, Japan Trench, Kurils, and Aleutians) can all be classified as moderately to strongly coupled. Despite high convergence rates and the occurrence of very large earthquakes, South American subduction zones have a relatively low seismicity level. The seismicity in southern Chile prior to the 1960  $M_w$  9.5 earthquake is particularly noteworthy. Most of the earthquakes shown for this region are aftershocks of the 1960 earthquake, and Duda (1963) reports that earthquake activity was very slight for the region south of 37°S latitude for a period of at least 17 yr before the earthquake. Although questions about the completeness of seismicity catalogs prevents us from concluding that the area of the 1960 Chilean earthquake experienced a seismic quiescence as profound as that observed in Washington and Oregon, it does seem clear that seismicity in the southern Chilean region was very low relative to most other subduction zones.

### SPECIFIC EXAMPLES

In Figures 5, 7, and 9, we show selected subduction zones where relatively young oceanic crust is subducted. These regions are all plotted on the same scale and show the relative geometry of these subduction zones. Approximate locations of seafloor magnetic lineations, Quaternary volcanoes, and the rupture extent of the largest shallow subduction earthquakes are also shown.

*Southern Chile.* Figure 5 (a and b) shows southern Chile and the northwestern United States, respectively, and represent subduction zones where very young oceanic crust is presently subducting. The coseismic vertical deformation from the 1960 Chilean earthquake (Plafker and Savage, 1970) is contoured and illustrates several key points. The epicenter of the 1960 earthquake is at the northern end of the zone, which extends nearly 1000 km southward to the point at which the South Chile rise is subducted beneath South America. The rupture propagated across several major fracture zones, with the age of subducted oceanic lithosphere varying between 30 and 5 m.y. The magnetic anomaly time scale is shown in Figure 6. Seismicity prior to the 1960 earthquake appears to have been very low in the region south of 41° where the youngest oceanic lithosphere is subducting (Duda, 1963). The predominant onland coseismic vertical deformation was subsidence; uplift was only observed along the northern coastal region and along southern islands located relatively near to the trench axis. Significant subsidence and uplift of up to 6 m were observed in the south where the youngest oceanic crust is presently subducting. Thus, it appears that large earthquakes in southern Chile involve the subduction of very young oceanic crust.

Several features of subduction in southern Chile are also observed for the Cascadia subduction zone. We have already noted similarities in trench bathymetry as well as the suggestion that both zones may experience significant periods of seismic quiescence. The lengths of the two zones are roughly comparable and the distance between the trench axis and the volcanic arc is slightly greater in the northwestern United States. One to two kilometers of clastic sediments overlie the oceanic plates in both trenches (Schweller *et al.*, 1981; Herron *et al.*, 1981; Kulm *et al.*, 1984), and relatively high heat flows of 1 to 2 HFU have been reported in both areas (Herron *et al.*, 1981; Kulm *et al.*, 1984). Although much of the South American subducting margin is characterized by the juxtaposition of the great heights of the massive Andes Mountains and the great depths of the Peru-Chile Trench, the region of the 1960 earthquake is better characterized (from west to east) by a broad continental margin, low coastal ranges, a central valley that grades southward into an inland

# SUBDUCTION EARTHQUAKES IN THE NORTHWESTERN U.S.

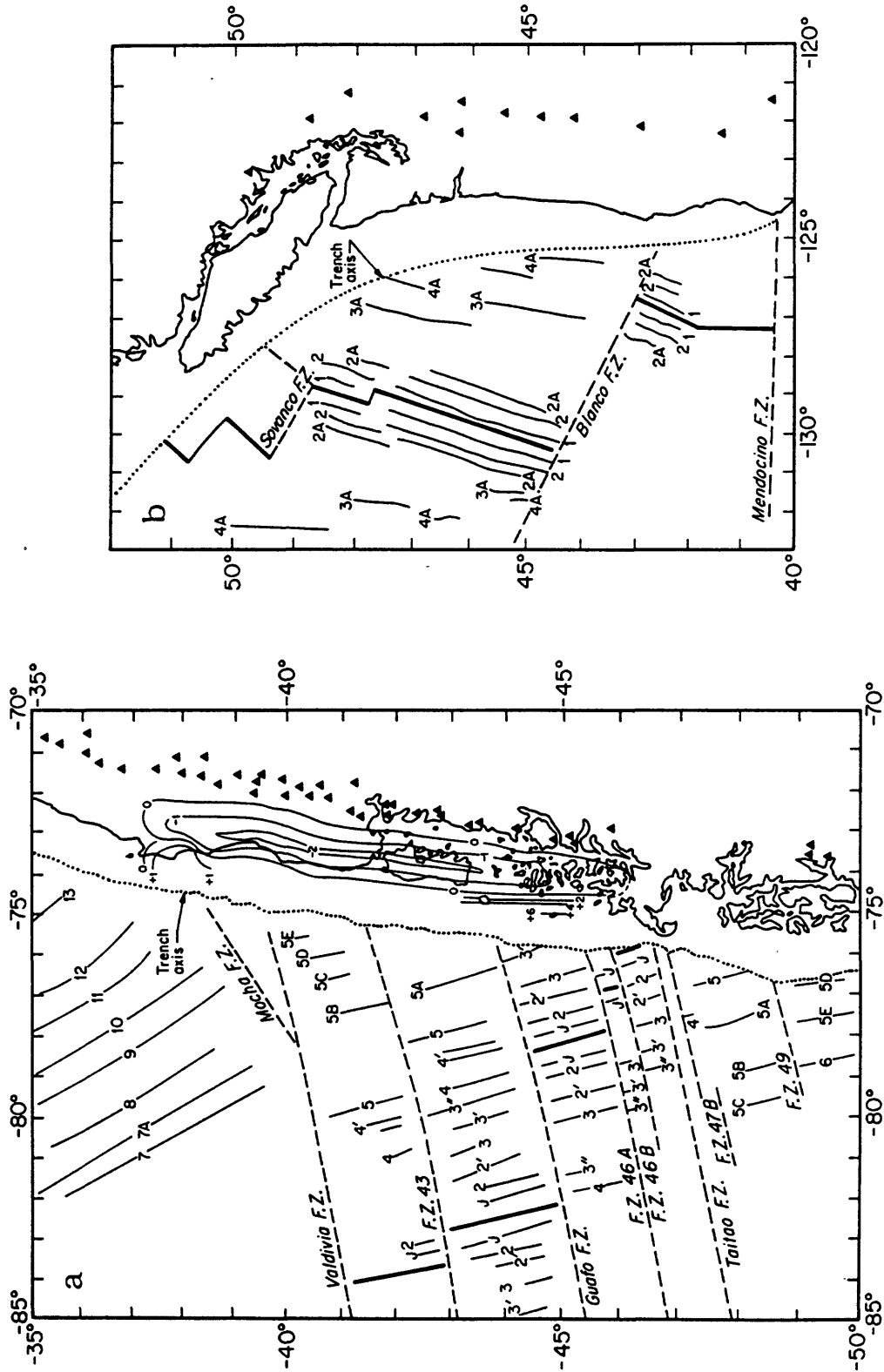


FIG. 5. Comparison of subduction in southern Chile (a) and the northwestern United States (b). All maps shown in Figures 5, 7, and 9 are plotted on approximately the same scale. Active spreading centers (heavy solid lines), seafloor magnetic lineations, and Quaternary volcanoes (solid triangles) are shown. Contours (meters) of the coseismic vertical deformation associated with the 23 May 1960 Chilean earthquake ( $M_w$  9.5) are also shown (Pflafer and Savage, 1970).



sea, and finally a chain of strato-volcanoes (Lowrie and Hey, 1981). These landforms are very similar to those encountered in the northwestern United States.

Lomnitz (1970) reports that earthquakes similar to that in 1960 may have occurred in 1575, 1737, and 1837, thus giving an average repeat time of 128 yr. However, Plafker and Savage (1970) estimate the average dislocation of the 1960 earthquake to be in excess of 20 m, and Minster and Jordan (1978) estimate that the convergence rate is about 9.0 cm/yr. Thus, we might expect the recurrence interval for 1960-sized events to exceed 200 yr. Nishenko (1985) suggests that the events in 1737 and 1837 were somewhat smaller than the one in 1960. In particular, the teleseismic tsunami from the 1837 Chilean earthquake was 57 per cent of the size of the 1960

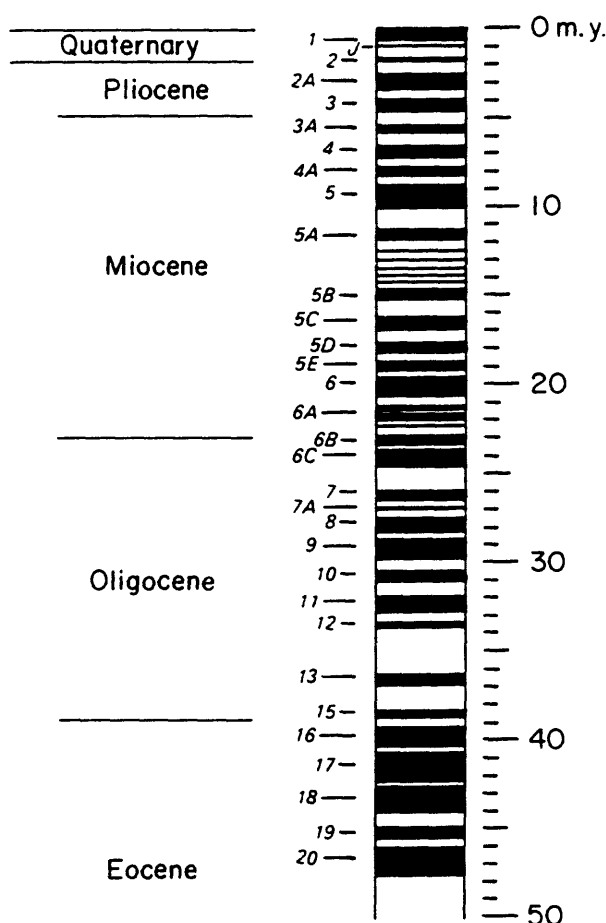


FIG. 6. The geomagnetic time scale.

tsunami as measured at Hilo, Hawaii (Nishenko, 1985). Furthermore, the tsunami from the 1960 earthquake is considered to be the largest teleseismic tsunami in Japanese history (Yoshikawa *et al.*, 1981). Plafker (written communication, 1985) also suggests that the 1960 earthquake was significantly larger than previous events since the type of inundation damage from widespread coastal subsidence that was reported in 1960 was not reported for earlier events. Kanamori and Cipar (1974) report that the 1960 sequence was accompanied by anomalous long-period seismic radiation. They show long-period strain records from Pasadena, California, on which very large 300- to 600-sec waves arrive shortly after the times expected for major seismic phases from the  $M_S$  6.8 foreshock that occurred about 15 min prior

to the main shock. At periods of greater than 300 sec, the foreshock may have been larger than the main shock, and the moment of the entire sequence may have exceeded  $6 \times 10^{30}$  dyne-cm ( $M_w$  9.8). Since it is difficult to explain the observed coseismic coastal deformation with such a large moment, Kanamori and Cipar (1974) speculate that a large-scale, deep-seated deformation was associated with this earthquake. In any case, it appears as though most of the interplate motion in southern Chile occurs during great earthquake sequences.

If the Cascadia subduction zone is analogous to that in southern Chile, then what might we infer about the recurrence time of Cascadia subduction zone earthquakes? Nishimura *et al.* (1984) report convergence rates along the Cascadia subduction zone that range from  $3.3 \pm 0.9$  cm/yr in the south to  $4.3 \pm 0.9$  cm/yr in the north. A simple scaling of convergence rates between the northwestern United States and southern Chile would lead us to postulate great earthquakes along the Cascadia subduction zone with average dislocations in excess of 10 m and recurrence times of 250 to 500 yr. Furthermore, if an earthquake similar to the 1960 Chilean earthquake were to occur, then we might expect the hinge line for coseismic vertical deformation to lie near the coastline, with much of the coast experiencing coseismic subsidence.

*Nankai Trough.* As can be seen in Figure 7a, there are many geometric similarities between the Nankai Trough and the Cascadia subduction zone. As is the case in southern Chile and the northwestern United States, there are 1 to 2 km of clastic sediments filling a shallow structural trench (Hilde, 1984; Shephard and Bryant, 1983), a broad continental margin, and coast ranges that bound an inland sea or central valley. Unlike southern Chile or the northwestern United States, southwestern Japan does not have a zone of Quaternary strato-volcanoes. Although the oceanic lithosphere subducted beneath southwestern Japan is very young (about 20 m.y.; Kobayashi and Nokada, 1978), it is about twice as old as the lithosphere subducting beneath the northwestern United States. This young age is consistent with the relatively high heat flows (1 to 2 HFU) that are observed in the Philippine seaplate off southwestern Japan (Uyeda, 1984). One unusual feature of this subduction zone is the fact that its seafloor magnetic lineations are oriented perpendicular to the trench axis.

Southwestern Japan is of particular significance because the convergence rate of 3.3 to 4.3 cm/yr (Seno, 1977) is very close to that in the northwestern United States and also because there is an extensive historical earthquake record for this region. This historical record was used by Imamura to anticipate the great earthquakes of 1944 and 1946 (Usami, 1982) despite the fact that, in the words of Richter (1958), they occurred "in a part of the Pacific seismic belt which had been almost completely quiet during the rise of international seismology." More recently, Ando (1975) proposed that coseismic geodetic data from the 1944 and 1946 earthquakes, historical earthquake data, and coastal geomorphic features can be explained by a model that segments the subduction zone into the four semi-independent patches shown in Figure 8. According to Ando's model, these four patches have each ruptured eight times in the last 1300 yr. The patches rupture either simultaneously or individually, but in most instances, failure of the four segments occurred within a time period of less than 3 yr. This pattern has apparently been broken by the absence of rupture in the Tokai region during the sequence of 1944 through 1946.

Although the Nankai Trough is remarkable for its pattern of clusters of great earthquakes that extend the length of the interface with an average repeat of 180 yr, there is apparently still considerable variation in the character and timing of

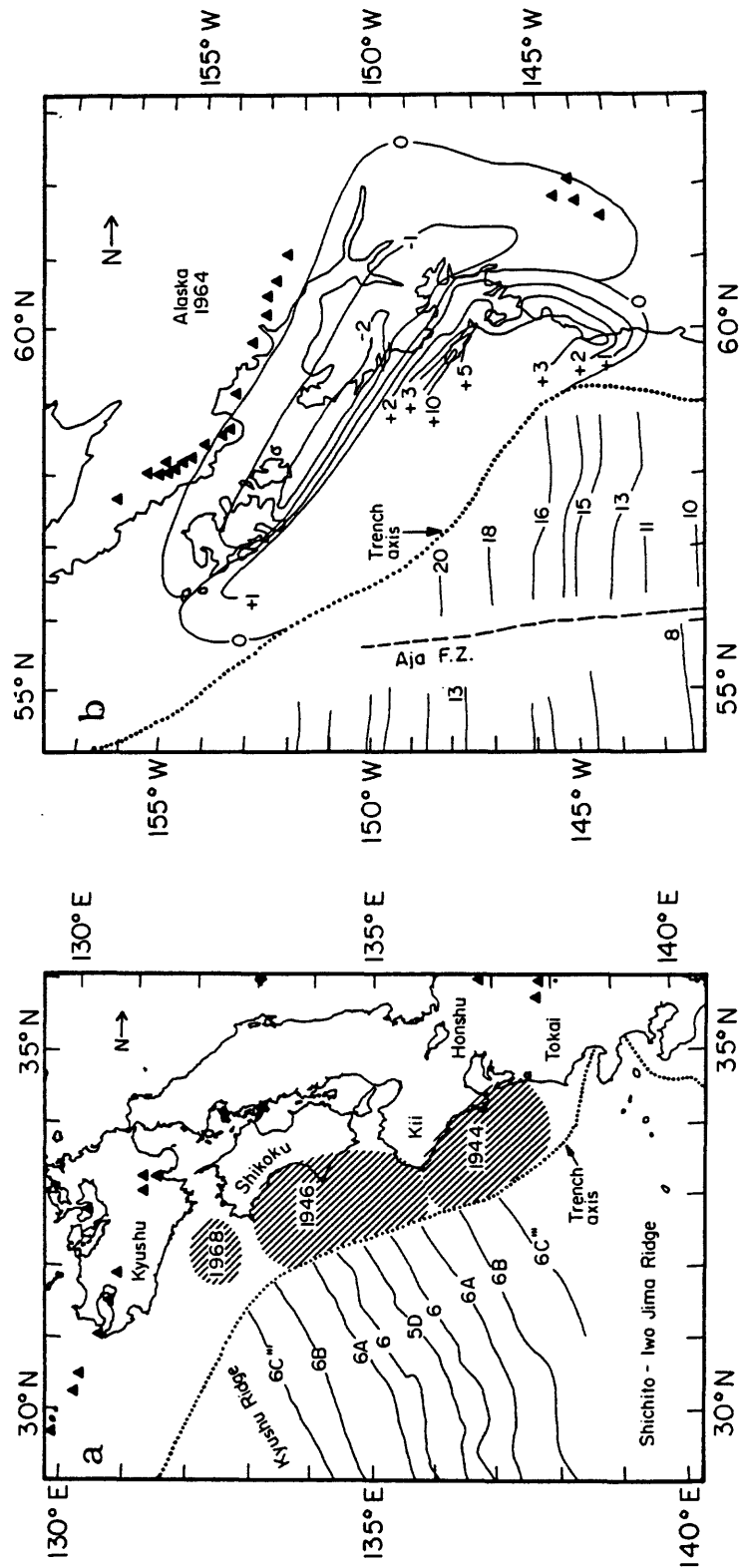


FIG. 7. Similar to Figure 5, but for the Nankai Trough of southwestern Japan (a) and Alaska (b). The approximate rupture areas are indicated for the largest earthquakes in the Nankai Trough in this century (1944 Tonankai earthquake,  $M_w$  8.1; 1946 Nankaido earthquake,  $M_w$  8.1; 1968 Hyuganada earthquake,  $M_s$  7.5). Contours (meters) of the coseismic deformation associated with the 28 March 1964 Alaska earthquake ( $M_w$  9.2) are also shown (Plafker, 1972).

# SUBDUCTION EARTHQUAKES IN THE NORTHWESTERN U.S.

these sequences. Although there is some uncertainty about the completeness of this record prior to 1707, the apparent time interval between sequences has been as little as 90 yr and as much as 260 yr. Shimazaki and Nakata (1980) have studied uplifts on the Muroto peninsula (large peninsula on Shikoku near the middle of the 1946 rupture) from the earthquakes in 1707, 1854, and 1946, and they report uplifts of 1.8, 1.2, and 1.15 m, respectively. From this, they infer that a larger dislocation was associated with the 1707 earthquake than for events in 1854 and 1946. They interpret this data as evidence for the "time-predictable" recurrence model in which

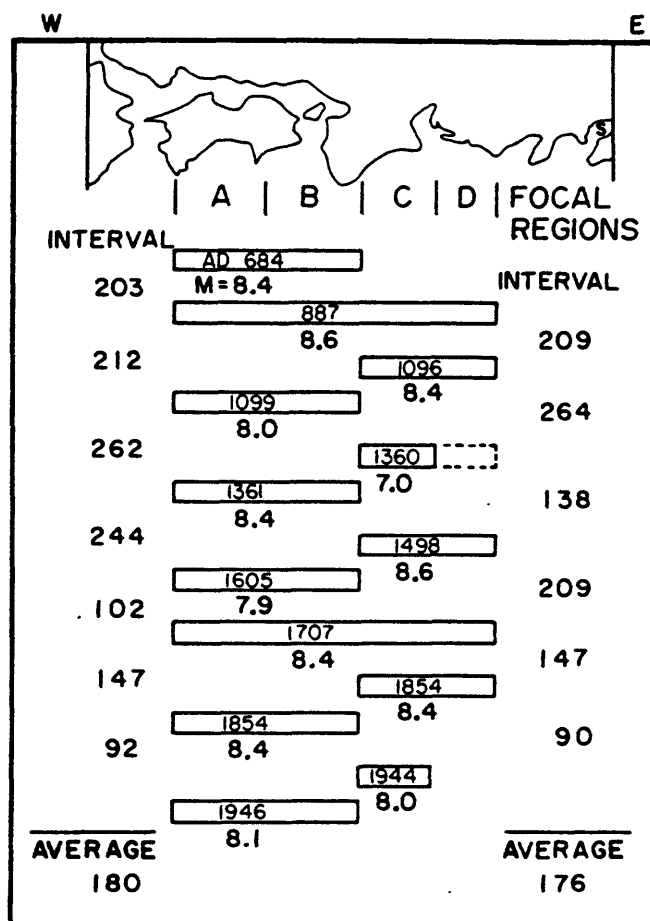


FIG. 8. Ando's (1975) model of historic ruptures along the Nankai Trough in southwestern Japan (from Sieh, 1981). The Tokai seismic gap is indicated by region D.

the time between two earthquakes is determined by the dislocation from the first. However, if the "time-predictable" model is appropriate here and if the historic record is complete, then one must wonder about the nature of earlier events with repeat times in excess of 200 yr.

Estimating the size of the largest Nankai Trough events is somewhat problematic. Kanamori (1972) studied long-period surface waves, and Hartzell and Heaton (1985) studied teleseismic body waves and they both report that the 1944 and 1946 earthquakes have comparable moments of about  $1.5 \times 10^{28}$  dyne-cm ( $M_w$  8.05). Kanamori (1972) estimates a seismic slip of about 3 m for each event. However, Ando (1975) modeled geodetic data from these earthquakes and infers a moment of

$6.6 \times 10^{28}$  dyne-cm ( $M_w$  8.5) and  $1.8 \times 10^{28}$  dyne-cm ( $M_w$  8.1) for the 1946 and 1944 earthquakes, respectively. The 1944 and 1946 earthquakes are clearly not the largest historic events in southwestern Japan. It appears that the 1707 Hiei earthquake ruptured most of the 700 km length of the Nankai Trough (Ando, 1975) and was one of the largest earthquakes in Japanese history. Historic uplift data is scarce, but uplifts in central Shikoku were at least 50 per cent larger in 1707 than in later earthquakes, and Ando's estimates of rupture parameters for this event would indicate a moment of about  $1.5 \times 10^{29}$  dyne-cm ( $M_w$  8.7). Although the scarcity of data makes it difficult to confirm this large moment estimate, it does appear that the estimated rupture length alone, suggests an energy magnitude of at least  $M_w$  8.5 for the 1707 Hiei earthquake.

The subduction zones in southwestern Japan and the northwestern United States are similar in their dimensions, convergence rates, and overall physical characteristics. Although this in no way proves that they experience similar earthquakes, it does suggest that we should consider the possibility that the Cascadia subduction zone may experience sequences of several great earthquakes ( $M_w > 8.0$ ) with repeat times of the sequences from 100 to 250 yr.

*Alaska.* Although the oceanic crust that is subducting at a rate of 5.7 cm/yr beneath Alaska is relatively young (40 to 50 m.y., Figure 7b), it is considerably older than the oceanic lithosphere in the Cascadia or any other subduction zone considered in this study. One of the most remarkable features of the Alaskan subduction zone is its extensive accretionary wedge; the width of the Alaskan continental margin is about twice that of other subduction zones considered in this study. Although there is a bathymetric trench, it is a relatively subtle feature, and it is filled with 2 km of clastic sediments (Von Huene *et al.*, 1978) having properties similar to those found in the Nankai Trough and the Cascadia subduction zone (Shephard and Bryant, 1983).

Contours of the coseismic vertical uplift associated with the  $M_w$  9.2 1964 Alaskan earthquake are shown in Figure 7b (Plafker, 1972a). Localized uplifts of up to 12 m appear to be associated with activation of high-angle imbricate faults on Montague Island. Coseismic horizontal motions were even more impressive than the vertical deformations; much of the coastline moved oceanward by more than 10 m, and the maximum horizontal displacement was 20 m (Plafker, 1972a). Alewine (1974) modeled these vertical and horizontal deformations and concluded that the fault dislocation exceeded 10 m over a rupture width of greater than 200 km with dislocations of nearly 30 m over the central 70 km of the rupture zone.

Unfortunately, the period of recorded history is very short in Alaska, and the timing and sizes of previous earthquakes must be inferred from geologic evidence. Middleton Island lies far out on the continental margin near the trench axis and displays a sequence of six marine terraces, the oldest of which has a maximum elevation of 46 m and a radiocarbon age of 4500 y.b.p. and the youngest of which was formed during the 1964 earthquake and has an elevation of  $3\frac{1}{2}$  m (Plafker, 1972b). Detailed analyses of these terraces indicate time separations of as little as 500 yr for the older terraces and as much as 1350 yr for the most recent terrace, which is also the smallest terrace observed (Plafker and Rubin, 1978). If each terrace can be associated with a great subduction earthquake, then the Middleton Island record implies an average recurrence time of 800 yr, an exceedingly long time when compared with the recurrence time of great historic earthquakes in southern Chile. However, permanent uplifts of Middleton Island are most likely due to slippage along imbricate faults in the accretionary wedge, and there may not be a one-to-

## SUBDUCTION EARTHQUAKES IN THE NORTHWESTERN U.S.

one correspondence between slippage on the main thrust plane and slippage on individual imbricate faults. Although the terrace sequence on Middleton Island may yield an incomplete record of great earthquakes, Plafker (1972b) notes that there is evidence for gradual widespread subsidence of many shorelines for a period of at least 930 yr prior to the 1964 earthquakes. This may be corroborating evidence for a very long repeat time for great Alaskan subduction earthquakes. It is interesting to note, though, that the recurrence times for great earthquakes in the other sections of the Aleutian Trench lying to the west are generally less than 100 yr (Sykes *et al.*, 1981). Although there is evidence suggesting that repeat times of great Alaskan earthquakes may be very long, further corroborating evidence must be found before this result can be considered to be compelling.

We have noted differences in the age of the subducted lithosphere and in the dimensions of the accretionary wedge between the Alaskan and the Cascadia subduction zones. On the other hand, there are similarities in the convergence rate, trench bathymetry, and sedimentation processes. Furthermore, the length of the Cascadia subduction zone is comparable to the rupture length of the 1964 earthquake. If similar earthquakes occur on the Cascadia subduction zone, then it may be that repeat times exceed 1000 yr.

*Colombia.* The oceanic lithosphere that is subducted at a rate of 8 cm/yr (Minster and Jordan, 1978) beneath southwestern Colombia and northern Ecuador is very young, ranging in age from 10 to 15 m.y. (Figure 9a). As is the case in other regions of young lithosphere subduction, thick sediments fill a shallow structural trench in this region (Hilde, 1984). Colombia has an extensive western continental margin that is somewhat wider, on average, than that encountered in the northwestern United States. A low coastal plain, ranging in width from 30 to 100 km and consisting of several large river deltas, is bounded on the east by three separate mountain chains separated by narrow linear valleys. The central mountain range has peak elevations from 4000 to 6000 m and contains a chain of Quaternary volcanoes. Although some of these landforms are found in other subduction zones, the presence of large river deltas is somewhat unusual and may indicate relative stability or slow subsidence of the coastal region.

Although large earthquakes along Colombia's western coast have been relatively infrequent this century, there have been large subduction earthquakes in 1906, 1942, 1958, and 1979. The area of the rupture zone of the largest of these events, the 1906 earthquake, has been estimated by Kelleher (1972) and is shown in Figure 9a. Seismic radiation from all of these events has been studied by Kanamori and McNally (1982), and they report that despite the fact that the combined rupture areas of the 1942, 1958, and 1979 earthquakes seem to cover the rupture surface of the 1906 earthquakes, the combined moment of these later events is only about one-fifth of that of the 1906 event. They estimate that the 1906 earthquake had a seismic moment of  $2 \times 10^{29}$  dyne-cm ( $M_w$  8.8) with an average dislocation of 5 m over a rupture area of  $1.1 \times 10^5$  km<sup>2</sup>. The 1979 earthquake is the second largest earthquake having a seismic moment of about  $2.9 \times 10^{28}$  dyne-cm ( $M_w$  8.2) with an average dislocation of 2.7 m over a rupture area of about  $2.8 \times 10^4$  km<sup>2</sup> (Kanamori and McNally, 1982).

Unfortunately, historical earthquake records in this region are very sketchy. Ramirez (1933) compiled records of earthquakes during the period from 1575 to 1915, but there is not enough information to clearly identify other great coastal earthquakes. Ramirez does report a great earthquake in 1797 that caused extensive damage in a region extending more than 400 km from southwestern Colombia to

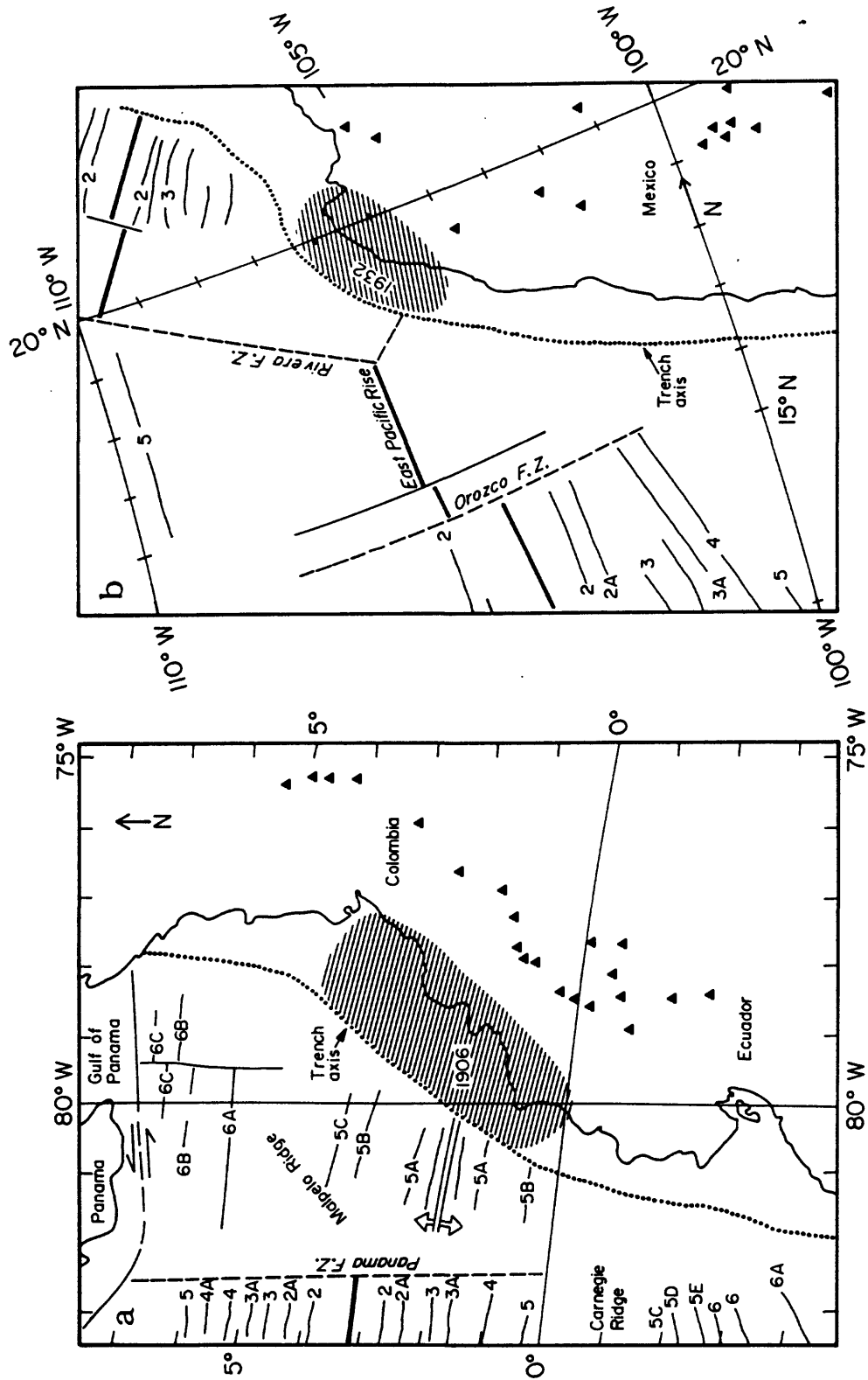


FIG. 9. Similar to Figure 5, but for Colombia (a) and western Mexico (b). The approximate rupture areas of the largest events of this century for each region are also shown.

## SUBDUCTION EARTHQUAKES IN THE NORTHWESTERN U.S.

central Ecuador. There are no known tsunami reports from this shock, and the source region of this earthquake is unknown. However, the region of high damage seems to extend several hundred kilometers south of that of the 1906 earthquake.

As is apparently the case in the Nankai Trough, it appears that the Colombian subduction zone may rupture either during single very large earthquakes or during a sequence of smaller ones.

*Mexico.* Subduction of the Rivera plate beneath the North American plate in the region of Jalisco, Mexico, is of considerable interest to us since it represents the slow subduction of a very young and small plate (Figure 9b). Klitgord and Mammerickx (1982) suggest that the subducting Rivera lithosphere is younger than 10 m.y., while the northernmost part of the Cocos plate subducting beneath Colima, Mexico, may be younger than 5 m.y. Eissler and McNally (1984) estimate that in the region of the Rivera fracture zone, the Rivera and Cocos plates are subducting at rates of about 2.3 and 5.5 cm/yr, respectively. Unlike the other areas considered in this report, the continental margin of central Mexico is relatively narrow. Furthermore, there is a shallow bathymetric trench with relatively little clastic sediment (0.6 km; Shepard and Bryant, 1983).

The historic rate of seismicity is relatively high along most of the Middle American Trench with many events in the magnitude 7 to 8 range. Singh *et al.* (1981) and Astiz and Kanamori (1984) suggest that the average repeat times for individual segments of the zone vary between 30 and 60 yr. The largest earthquake sequence documented along the Middle American Trench occurred in 1932 in the Jalisco region of Mexico and the approximate aftershock area as estimated by Singh *et al.* (1985) is shown in Figure 9b. The 1932 earthquake sequence contained two large shocks, a  $M_S$  8.2 (Abe, 1981) event on 3 June that has an estimated moment of  $10^{28}$  dyne-cm (Singh *et al.*, 1985) and a  $M_S$  7.8 (Abe, 1981) event on 18 June with an estimated moment of  $7.3 \times 10^{27}$  dyne-cm (Singh *et al.*, 1985). The average dislocation for the 1932 sequence is estimated to be 1.9 m over an area of 230 km by 80 km. Both events were accompanied by local and teleseismic tsunamis (Abe, 1979), and there is little doubt that these events represent thrusting of the Rivera plate beneath the North American continental margin.

Singh *et al.* (1981) identify other large earthquakes in the Jalisco region in 1837 ( $M_S$  7.7), 1875 ( $M_S$  7.5), 1900 ( $M_S$  7.9), and 1911 ( $M_S$  7.7). However, none of these events appears to be as large as the 1932 sequence. Furthermore, seismicity in the Jalisco region has been remarkably low since the 1932 earthquakes (Astiz and Kanamori, 1984; LeFevre and McNally, 1985).

Although there are clear differences in the physiographic features and the frequency of moderately large coastal earthquakes between subduction of the Rivera and Juan de Fuca plates, the earthquake history of the Jalisco region clearly demonstrates that the slow subduction of a small, very young plate does not necessarily imply aseismic slip.

## CASCADIA SUBDUCTION ZONE: LOCKED OR UNLOCKED?

We have noted that there is a large variation in the size and recurrence interval of shallow subduction earthquakes in subduction zones that share physical characteristics with the Cascadia subduction zone. However, it does seem clear that the subduction of very young oceanic lithosphere is often, if not usually, associated with the occurrence of very large shallow earthquakes. Although this does not prove that great earthquakes will occur on the Cascadia subduction zone, it does suggest that



it is inappropriate to assume that great earthquakes will not occur based on observations of bathymetry, lithospheric age, trench sediments, heat flow, convergence rate, physiography, overall size of the subducted plate, Quaternary volcanism, or the rate of background seismicity. A summary of the comparison of physical characteristics of the subduction zones just discussed is found in Table 1.

*Geodetic strain.* The observation and interpretation of geodetic strain may eventually lead to a fairly clear picture of the subduction process along the Cascadia subduction zone. Savage *et al.* (1981) and later Lisowski and Savage (1986) discuss Geodolite surveys in the Seattle region from 1972 to 1984 and triangulation surveys in the Strait of Juan de Fuca from 1892 to 1954. Their analyses indicate that both regions show maximum contraction in a direction nearly parallel to the proposed east-northeast plate convergence direction. Lisowski and Savage (1986) report shortening at a rate of  $0.05 \pm 0.02 \mu\text{strain/yr}$  in the Seattle region and shortening at a rate of  $0.22 \pm 0.07 \mu\text{strain/yr}$  in the Strait of Juan de Fuca. Repeated leveling surveys along much of the coastline adjacent to the Juan de Fuca plate (Ando and Balazs, 1979; Reilinger and Adams, 1982; Riddihough, 1982) show steady uplift of the coastal region at a rate of up to 3 mm/yr and subsidence of the inner coastal areas at a rate of about 1 mm/yr. Although Ando and Balazs (1979) interpret the uplift data as evidence of aseismic slip, Lisowski and Savage (1986) show that the combined geodolite, triangulation, and uplift data may be better explained by a model in which the shallow thrust zone is locked between the trench axis and the coastal region. It is interesting to note that the coseismic extension in the central valley of southern Chile ranged from 25 to 50  $\mu\text{strain}$  for the 1960 earthquake (Plafker and Savage, 1970). Furthermore, coseismic extensions from the 1964 Alaskan earthquake ranged from about 15  $\mu\text{strain}$  in the inland coastal areas to over 50  $\mu\text{strain}$  in the outer coastal areas (Plafker, 1972). At the current strain rate, it would take several hundred to 1000 yr for comparable horizontal strains to accumulate along the Cascadia subduction zone. Weaver and Smith (1983) interpret focal mechanisms in southwestern Washington as evidence for crustal compression parallel to the plate convergence direction, and they suggest that these observations are best explained by a model in which the Cascadia subduction zone is locked.

*Geomorphology.* Holocene geomorphic and depositional features often record the occurrence of great subduction earthquakes. These features vary from region to region and are usually recognized only after a modern earthquake creates features that are repeated in the geologic record. Sequences of uplifted Holocene marine terraces are some of the more easily recognizable features. However, such features are relatively rare since their preservation requires the right combination of high, long-term uplift rates, large coseismic uplifts, and moderate to low coastal erosion rates. Adams (1984a, b) discusses long-term coastal uplift rates along the Cascadia subduction zone and reports relatively slow emergence and probably submergence for most of Washington and northern Oregon. He further reports uplift rates of as high as 1.5 mm/yr in southern Oregon. However, coastal erosion is very strong along this coastline and few, if any, Holocene strand lines have been identified in this region. Curiously, large tree stumps in apparent growth position are found in the intertidal zone at Sunset Bay in southern Oregon. This indicates either short-term or short-wavelength subsidence in a region that has risen at a rate of about 0.6 mm/yr for the last several hundred thousand years (Adams, 1984a, b).

The highest geologic uplift rates documented anywhere along the Cascadia subduction zone occur near Cape Mendocino, California, in the region of the Gorda-

SUBDUCTION EARTHQUAKES IN THE NORTHWESTERN U.S.

TABLE 1  
SUMMARY OF SUBDUCTION ZONE CHARACTERISTICS

	Cascadia	Southern Chile	Nankai Trough	Alaska	Colombia	Mexico (Riviera Plate)
Age (m.y.) of subducted plate	10	5 to 30	18 to 24	40 to 50	10 to 15	10?
Convergence rate (cm/yr)	3.3 to 4.3	9	3.3 to 4.3	5.7	8	2.3
Character of trench	Shallow, sediment-filled	Shallow, sediment-filled	Shallow, sediment-filled	Shallow, sediment-filled	Shallow, sediment-filled	Shallow, few sediments
Free-air gravity anomaly	Small (50 mgal)	Small (50 mgal)	Moderate (100 mgal)	Moderate (100 mgal)	Small (50 mgal)	Moderate (100 mgal)
Background seismicity	Very low	Very low	Low	Moderate	Low	?Moderate?
Heat flow	High (1-2 HFU)	High (1-2 HFU)	High (1-2 HFU)			
Quaternary volcanism	Yes	Yes	No	Varies along the trench	Yes	Yes
Inland sea or valley	Yes	Yes	Yes	Yes	?No?	No
Width of continental margin	30-120 km	100 km	110 km	180 km	130 km	80 km
Largest historic earthquakes ( $M_w$ )	None in 150 yr	9.5 (1960)	8.1 (1944, 1946) ?8.5? (1707)	9.2 (1964)	8.8 (1906)	8.2 (1932)
Average repeat time	?400 yr?	128 yr	180 yr	?800 yr?	Unknown	?50 yr?

Pacific-North America triple junction. Lajoie *et al.* (1983) report Holocene terraces along a 40 km stretch that runs southward from Cape Mendocino. A flight of nine emergent terraces and beachridges, uplifted as much as 16.8 m, have been reported in the Cape Mendocino region and  $^{14}\text{C}$  dates indicate a maximum uplift rate of 3.6 mm/yr (Lajoie *et al.*, 1983). This would indicate an average repeat time of about 500 yr. However, the relationship between these beach terraces that lie near the structurally complex triple junction and large subduction earthquakes along the length of the subduction zone is unclear.

*Turbidites.* Adams (1984a) has suggested that extensive Holocene turbidites studied by Griggs and Kulm (1970) may have been triggered by large earthquakes along the continental shelf. Since the deposition of Mazama Ash 6,600 yr ago, there have been approximately 16 major turbidites in the Cascadia channel, indicating an average repeat time of 410 yr. Furthermore, there are hemipelagic layers of relatively uniform thickness between the turbidites, indicating a relatively uniform repeat time. Griggs and Kulm (1970) suggest that this time interval is controlled by the sedimentation rate, with turbidity currents occurring spontaneously due to gravitational instability. However, Adams (1984b) points out that several channels that feed the main Cascadia channel have turbidity sequences comparable to that in the main channel. He suggests this indicates the turbidites were synchronously triggered in several independent channels and may be evidence for the recurrence of great earthquakes every 400 to 500 yr. However, these channels lie within 50 km of each other, and simultaneous turbidity currents may have been triggered by moderate-size earthquakes in the continental margin.

*Other evidence.* Snavely (1986) reviews evidence of Cenozoic folding and faulting in the continental margin of Washington and Oregon and concludes that several major and numerous minor faults have been active in the Late Pleistocene and Holocene. Upper Pleistocene abyssal sediments have been uplifted by as much as 1100 m along anticlinal ridges that are bounded by thrust faults in the outer continental margin (Snavely *et al.*, 1980). Snavely (1986) interprets the combination of geologically active faults in the accretionary wedge together with a lack of historic earthquakes as evidence for episodic activity of the main thrust zone. However, Adams (1984a) suggests that these deformations may also be occurring through steady aseismic creep.

Snavely (1986) also suggests that major coastal earthquakes may have triggered major landslides. He cites archaeological evidence (Mauger and Daughert, 1979; Samuels, 1983) that mudflows buried Indian structures at Ozette on the northwest Olympic Coast about 800 y.b.p. and again about 350 y.b.p. Snavely (1986) also suggests that multiple landslides at Lake Crescent adjacent to the Strait of Juan de Fuca in northern Washington may have been triggered by subduction earthquakes. A submerged tree that was probably transported by the youngest slide has a  $^{14}\text{C}$  date of 350 y.b.p. Unfortunately, the significance of these observations is unknown. While it is highly probable that the occurrence of great subduction earthquakes would trigger major landslides, it is also likely that major landslides would occur even if major earthquakes never occur in this region.

Heaton and Snavely (1985) discuss legends of Washington coastal Indians that were recorded in the 1860's and that suggest the occurrence of a large tsunami along the northwestern Washington coast. They suggest that a large prehistoric subduction earthquake could be responsible for these legends.

Much of the evidence that we have presented is compatible with a simple model in which the Cascadia subduction zone fails during great earthquakes with a repeat

## SUBDUCTION EARTHQUAKES IN THE NORTHWESTERN U.S.

time of 400 to 500 yr. However, it is important to recognize that the logical structure behind this hypothesis is quite weak, consisting of many poorly constrained inferences and conjectures. Does this evidence clearly demonstrate that the Cascadia subduction zone is locked? We don't think so. Furthermore, this issue may remain ambiguous for quite some time. Proving that the subduction process is aseismic seems even more difficult since it requires that one prove that great earthquakes have not occurred. While the 150-yr paucity of historic earthquakes supports this alternative explanation, it may be very difficult to prove that prehistoric earthquakes have not occurred.

### HYPOTHETICAL CASCADIAN EARTHQUAKES

If the Cascadia subduction zone is locked, then what is the nature of the earthquakes that may occur there? This question must be answered if we are to provide estimates of the shaking and tsunami hazard from Cascadian subduction earthquakes. However, we address this question under duress; the question is of central importance, but our answers are clearly speculative. We present several hypothetical earthquake sequences that may be plausible for the Cascadia subduction zone.

*Completely aseismic zone with no interplate earthquakes.* In this case, we assume that slip along the entire boundary between the accretionary wedge and the oceanic lithosphere occurs as aseismic creep. Although we need not worry about great low-angle thrust earthquakes if this condition exists, we must still ask whether the geologically recent faulting and folding observed within the accretionary wedge (Snively, 1985) has been associated with major earthquakes. Deformation of the accretionary wedge often occurs simultaneously with great interplate earthquakes, and there are not many clear examples where independent large earthquakes are due to subsidiary faults in the accretionary wedge. The  $M$  7.1 Mikawa earthquake (1945) of southwestern Japan may be an example. This earthquake was locally very damaging and occurred along a high-angle thrust fault in the near-coastal region adjacent to the 1944 Tonankai earthquake (Richter, 1958).

Large-scale submarine landsliding or slumping along the continental slope may also present a significant tsunami hazard even if large interplate earthquakes are absent. Kanamori (1985) has suggested that the 1929 Grand Banks, Canada, earthquake ( $M_S$  7.2) and the 1946 Aleutian Islands earthquake ( $M_S$  7.4) may be best described as large landslides in the continental shelf. Despite its small surface wave magnitude, the 1946 Aleutian Islands event generated one of the largest local and teleseismic tsunamis in recent history (Abe, 1979). However, such events are rare and poorly understood.

*Mainly aseismic slip with isolated earthquakes of  $M < 8$ .* This is thought to be the situation for what is traditionally called "aseismic" subduction zones such as the Bonins or Marianas. However, there are clearly many physical differences between the Cascadia subduction zone and those of the Marianas' type. If several earthquakes of magnitudes less than 8 were the ultimate culmination of at least 150 yr of plate convergence, then the Cascadia subduction zone would still be considered to be a weakly coupled zone. If isolated moderate-size interplate events do occur here, then one must wonder why isolated earthquakes of  $M$  4, 5, or 6 have not already been observed. Although there is no compelling reason to believe that this is the failure mode of this subduction zone, our present understanding is too limited to allow us to rule out a moderate-size ( $8 > M > 7$ ) interplate earthquake anywhere beneath the continental margin of the northwestern United States.

*Moderately coupled with earthquakes of  $M < 8\frac{1}{4}$ .* This is the situation that seems to exist for many world-wide subduction zones; northern Japan and central America may be examples. However, the Cascadia subduction zone does not seem to fit into this category. That is, a moderately high level of seismicity with earthquakes up to  $M 8\frac{1}{4}$  is the distinguishing feature of these zones. Thus, the Cascadia subduction zone's historic quiescence seems to eliminate this category.

*Strongly coupled with earthquakes of  $M > 8$ .* We have seen that the Cascadia subduction zone shares many features with other zones that are strongly coupled and have experienced very large earthquakes. In this hypothetical situation, we assume that interplate slip occurs only during great earthquakes. Based on our observations of the Nankai Trough, Colombia, and southern Chile, we hypothesize that the Cascadia subduction zone may experience either a sequence of several great earthquakes, or alternatively, a single giant earthquake that ruptures the entire zone. As proposed by Adams (1984a), the average recurrence time of 410 yr for Cascadia basin turbidity currents suggests that the average repeat time for great earthquakes is at least this long.

We can somewhat arbitrarily subdivide the Cascadia subduction zone into three segments: the southern 250 km segment along which the Gorda plate is subducting; the central 800 km segment from the Blanco fracture zone to the middle of Vancouver Island along which the Juan de Fuca plate is subducting; and the northern segment (250 km?) along which the Explorer plate may be subducting. There is little dispute that the central segment is subducting, probably at about 4 cm/yr, but the kinematics of the northern and southern segments are less certain. In the model of Nishimura *et al.* (1984), the Gorda plate is subducted at a rate of 3.3 cm/yr. However, models by Riddihough (1980) and Knapp (1982) suggest that there may be significant complications introduced by internal deformation of the Gorda plate. Riddihough (1984) suggests that the Explorer plate may have a hot-spot rotation pole that is located within the plate itself. Nevertheless, according to Riddihough's model, the North American plate is overriding the Explorer plate at a rate of 2 to 3 cm/yr.

The width of the hypothetical locked zone is another important parameter about which there is considerable uncertainty. The models of Lisowski *et al.* (1985) suggest that, in northern Washington, the plate boundary may be locked from the coastal region to the trench axis, a distance of about 120 km. This may be comparable to the width of the locked zone encountered in southwestern Japan, southern Chile, and Colombia. However, it is probably considerably less than that encountered in Alaska and considerably greater than that encountered in Mexico.

The width of the locked zone may not correspond with the width of the rupture zone of great subduction earthquakes. That is, coseismic rupture may extend beyond the locked zone into the regions that experience aseismic slip (Kanamori and McNally, 1982). The width of the rupture zone may be a function of the length of the rupture zone as well as the width of the locked zone. For the present, we will sidestep the issue of just how wide the rupture zone may be for Cascadia earthquakes. Instead, we will consider the types of sequences that would cover the length of the Cascadia subduction zone.

We begin by proposing that earthquakes on the Cascadia subduction zone are analogous to those in the Nankai Trough. We have seen that the Nankai Trough has repeatedly experienced sequences of great earthquakes that cover the 700 km length of this subduction zone. Four or five earthquakes similar to the 1944 or 1946

## SUBDUCTION EARTHQUAKES IN THE NORTHWESTERN U.S.

Nankai earthquakes ( $M_w$  8.1) would probably cover the length of the Cascadia subduction zone. Such earthquakes may be closely spaced in time as has been the case for many sequences in southwestern Japan. Larger earthquakes, such as the 1707 Hōei earthquake that apparently ruptured over a 700 km length of the Nankai Trough, should also be considered as a possibility. As we have already discussed, it is difficult to estimate the true size of the 1707 earthquake, but it seems likely that it was at least in the  $M_w$  8.5 range. Convergence rates in southwestern Japan are similar to those along the Cascadia subduction zone, and thus we might expect the average repeat time of such sequences to be between 100 and 250 yr in the Cascadia subduction zone.

Several earthquakes of the size of the 1906 Colombian earthquake ( $M_w$  8.8) could also cover the length of the Cascadia subduction zone. Such earthquakes may have rupture lengths of about 500 km.

Finally, the overall dimensions of the Cascadia subduction zone are similar to the zone that ruptured during the 1960 Chilean earthquake ( $M_w$  9.5). This is the largest event recorded in this century, and thus, we consider it to be a reasonable upper bound for hypothetical Cascadia subduction earthquake. Dislocations in an event of this nature may exceed 20 m, and the repeat time would probably be at least 400 yr.

## TSUNAMI POTENTIAL

If a great subduction earthquake were to occur along the Cascadia subduction zone, then it is very likely that it would generate a large local tsunami. It is beyond the scope of this study to attempt to predict tsunami run-up heights from specific models of the source and coastal physiography. However, we can make several general observations of tsunami run-up heights for great world-wide subduction earthquakes. Figure 10, modified from a figure prepared by Abe (1979), shows the maximum observed local run-up heights of various world-wide earthquakes for which Abe calculated a tsunami magnitude,  $M_t$ . Abe (1979) defines the  $M_t$  scale to be the logarithm of tsunami amplitude as measured at calibrated sites at great distances. Abe (1979) shows that there is a close correspondence between  $M_t$  and energy magnitude  $M_w$ . Thus, Figure 10 is similar to a plot of maximum local run-up height as a function of energy magnitude,  $M_w$ . As is obvious from this plot, maximum run-up height is not simply a function of earthquake size. Local tsunami run-up heights often vary considerably along the shoreline adjacent to major earthquakes, and the maximum run-up height may be several times the average run-up height.

All of the regions that we considered to be possible analogs for the Cascadia subduction zone have experienced large local tsunamis. The 1944 and 1946 Nankai Trough earthquakes generated tsunamis that had maximum local run-up heights of 7.5 and 6.0 m, respectively, and the 1707 Hōei probably generated an even larger tsunami (Lockridge and Smith, 1984). The 1906 Colombian earthquake also generated a large local tsunami that extensively damaged much of the coastal regions of southwestern Colombia and northern Ecuador (Lockridge and Smith, 1984). The 1960 Chilean earthquake generated one of the largest well-documented tsunamis in recent times with heavy damage occurring both locally (Sievers *et al.*, 1963) and also in Hawaii (Cox and Mink, 1963) and Japan (Yoshikawa *et al.*, 1981). Although the maximum local run-up may have been over 20 m (Lockridge and Smith, 1984),

it seems likely that most coastal regions adjacent to the earthquake experienced local run-up heights of less than 10 m (Sievers *et al.*, 1963).

It is very difficult at this point to provide reliable estimates of the tsunami run-up heights that may occur following any large subduction earthquakes along the Cascadia subduction zone. However, run-up heights ranging from several meters to several tens of meters have been observed along other subducting boundaries after events of the type that we consider to be plausible for the Cascadia subduction zone.

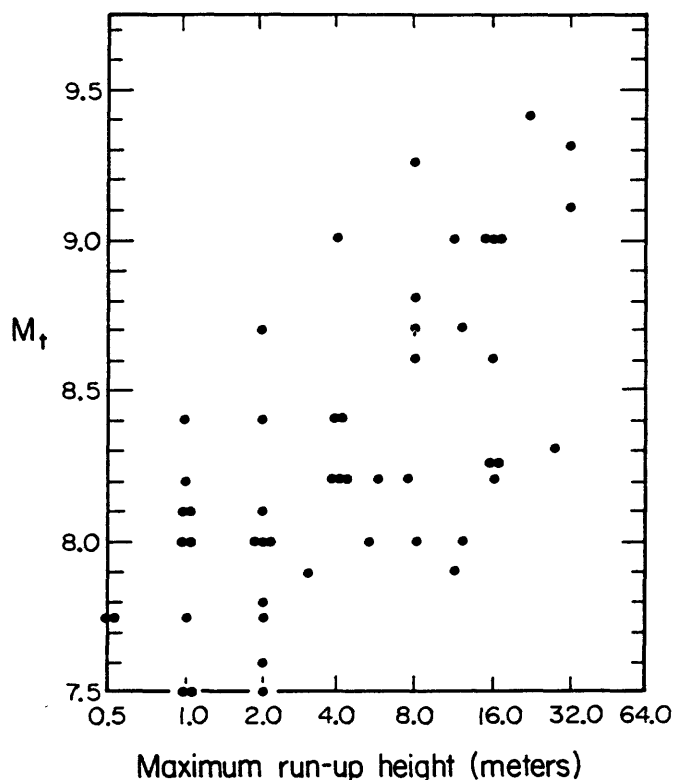


FIG. 10. Maximum local tsunami run-up heights as a function of Abe's (1979) tsunami magnitude which corresponds closely to energy magnitude  $M_w$  (modified from Abe, 1979).

### CONCLUSIONS

Is slip along the Cascadia subduction zone a benign process, occurring slowly as aseismic creep? Or alternatively, is elastic strain energy accumulating along this zone, and if it is, what is the nature of earthquakes that may result? Unfortunately, this study has not satisfactorily resolved these important issues. However, of other world-wide subduction zones, the Cascadia subduction zone seems most similar to southern Chile, the Nankai Trough, and Colombia, each of which have experienced very large historic earthquake sequences. The length of the subducting margin along the Cascadia subduction zone probably exceeds 1000 km, and if the zone is locked, then earthquakes of very large size must be considered. Several observations seem compatible with a model in which great earthquake sequences occur with an average repeat time of 400 to 500 yr, but because of the nature of this data, we consider this hypothesis to be highly speculative.

# SUBDUCTION EARTHQUAKES IN THE NORTHWESTERN U.S.

## ACKNOWLEDGMENTS

This research was supported by the U.S. Nuclear Regulatory Commission. The authors benefited from discussions with Hiroo Kanamori, Greg Davis, Parke Snavely, Jr., John Adams, Larry Ruff, Craig Weaver, Yoko Ota, Atsumasa Okada, Kerry Sieh, George Plafker, and Mike Lisowski. We thank Jim Savage and Peter Ward for reviewing the manuscript.

## REFERENCES

- Abe, K. (1979). Size of great earthquakes of 1837-1974 inferred from tsunami data, *J. Geophys. Res.* **84**, 1561-1568.
- Abe, K. (1981). Magnitude of large shallow earthquakes from 1904 to 1980, *Phys. Earth Planet. Interiors* **27**, 72-92.
- Acharya, H. (1981). Juan de Fuca Plate—Aseismic subduction at 1.8 cm/yr, *Geophys. Res. Letters* **8**, 1123-1125.
- Acharya, H. (1985). Comment on seismic potential associated with subduction in the northwestern United States by T. H. Heaton and H. Kanamori, *Bull. Seism. Soc. Am.* **75**, 889-890.
- Adams, J. (1984a). Active deformation of the Pacific Northwest continental margin, *Tectonics* **3**, 449-472.
- Adams, J. (1984b). Vertical crustal deformation of the Pacific Northwest continental margin: some enigmas with bearing on great-earthquake risk, *Proceedings of Chapman Conference on Vertical Crustal Motion*.
- Alewine, R. W., III (1974). Application of linear inversion theory toward the estimation of seismic source parameters, *Ph.D. Thesis*, California Institute of Technology, Pasadena, California, 303 pp.
- Ando, M. (1975). Source mechanisms and tectonic significance of historical earthquakes along the Nankai Trough, Japan, *Tectonophysics* **27**, 119-140.
- Ando, M. and E. I. Balazs (1979). Geodetic evidence for aseismic subduction of the Juan de Fuca plate, *J. Geophys. Res.* **84**, 3023-3028.
- Astiz, L. and H. Kanamori (1984). An earthquake doublet in Ometepec, Guerrero, Mexico, *Phys. Earth Planet. Interiors* **34**, 24-45.
- Cox, D. C. and J. F. Mink (1963). The tsunami of 23 May 1960 in the Hawaiian Islands, *Bull. Seism. Soc. Am.* **53**, 1191-1210.
- Duda, S. J. (1963). Strain release in the Circum-Pacific belt, Chile: 1960, *J. Geophys. Res.* **68**, 5531-5544.
- Eissler, H. K. and K. C. McNally (1984). Seismicity and tectonics of the Rivera plate and implications for the 1932 Jalisco, Mexico, earthquake, *J. Geophys. Res.* **89**, 4520-4530.
- Grellet, C. and J. Dubois (1982). The depth of trenches as a function of the subduction rate and age of the lithosphere, *Tectonophysics* **82**, 45-56.
- Griggs, G. B. and L. D. Kulm (1970). Sedimentation in Cascadia deep-sea channel, *Geol. Soc. Am. Bull.* **81**, 1361-1384.
- Hartzell, S. H. and T. H. Heaton (1985). Teleseismic time functions for large shallow subduction zone earthquakes, *Bull. Seism. Soc. Am.* **75**, 965-1004.
- Heaton, T. H. and H. Kanamori (1984). Seismic potential associated with subduction in the northwestern United States, *Bull. Seism. Soc. Am.* **74**, 933-941.
- Heaton, T. H. and P. D. Snavely, Jr. (1985). Possible tsunami along the northwestern coast of the United States inferred from Indian traditions, *Bull. Seism. Soc. Am.* **75**, 1455-1460.
- Heaton, T. H. and S. H. Hartzell (1986). Estimation of strong ground motions from hypothetical earthquakes on the Cascadia subduction zone (manuscript in preparation).
- Herron, E. M., S. C. Camde, and B. R. Hall (1981). An active spreading center collides with a subduction zone: a geophysical survey of the Chile margin triple junction, *Geol. Soc. Am. Memoir* **154**, 683-701.
- Hilde, T. W. C. (1984). Sediment subduction versus accretion around the Pacific, *Tectonophysics* **99**, 381-397.
- Hyndman, R. D. and D. H. Wiechert (1983). Seismicity and rates of relative motion on the plate boundaries of western North America, *Geophys. J. R. Astr. Soc.* **72**, 59-82.
- Japan Meteorological Agency (1984). Hypocentral distribution in the Tokai and southern Kanto districts, 1963-1983, *Report of the Coordinating Committee for Earthquake Prediction* **32**, 212-215.
- Kanamori, H. (1972). Tectonic implications of the 1944 Tonankai and 1946 Nankaido earthquakes, *Phys. Earth Planet. Interiors* **5**, 129-139.
- Kanamori, H. (1977). Seismic and aseismic slip along subduction zones and their tectonic implications,



- in *Island Arcs, Deep Sea Trenches and Back-Arc Basins*, Maurice Ewing Series, M. Talwani and W. C. Pitman, Editors, American Geophysical Union, Washington, D.C., 163-174.
- Kanamori, H. (1985). Non-double couple seismic source, 23rd General Assembly of IASPEI, Tokyo, Japan.
- Kanamori, H. and J. J. Cipar (1974). Focal process of the great Chilean earthquake of May 22, 1960, *Phys. Earth Planet. Interiors* **9**, 128-136.
- Kanamori, H. and K. C. McNally (1982). Variable rupture mode of the subduction zone along the Ecuador-Colombia Coast, *Bull. Seism. Soc. Am.* **72**, 1241-1253.
- Kelleher, J. A. (1972). Rupture zones of large South American earthquakes and some predictions, *J. Geophys. Res.* **77**, 2087-2103.
- Kelleher, J., J. Savino, H. Rowlett, and W. McCann (1974). Why and where great thrust earthquakes occur along island arcs, *J. Geophys. Res.* **79**, 4889-4899.
- Klitgord, K. D. and J. Mammerrickx (1982). Northeast Pacific Rise: magnetic anomaly and bathymetric framework, *J. Geophys. Res.* **87**, 6725-2750.
- Knapp, J. S., Jr. (1982). Seismicity, crustal structure, and tectonics near the northern termination of the San Andreas fault, *Ph.D. Thesis*, University of Washington, Seattle, Washington.
- Kobayashi, K. and M. Nakada (1978). Magnetic anomalies and tectonic evolution of the Shikoku Inter-arc Basin, *J. Phys. Earth* **26** (Supplement), 391-402.
- Kulm, L. D., et al. (1984). Western North American continental margin and adjacent ocean floor off Oregon and Washington, Atlas 1 Ocean Margin Drilling Program, Regional Atlas Series: Marine Science International, Woods Hole, Massachusetts, 32 sheets.
- Lajoie, J. R., G. L. Kennedy, S. A. Mathieson, A. M. Sarna-Wojcicki, S. A. Morrison, and M. K. Tobish (1983). Emergent Holocene marine terraces at Cape Mendocino and Ventura, California, U.S.A., *Proc. International Symposium on Development of Holocene Shorelines*, Tokyo, Japan.
- Lay, T., H. Kanamori, and L. Ruff (1982). The asperity model and the nature of large subduction zone earthquakes, in *Earthquake Prediction Research*, Terra Scientific Publishing Co., Tokyo, Japan, 3-71.
- LeFevre, L. V. and K. C. McNally (1985). Stress distribution and subduction of aseismic ridges in the Middle America subduction zone, *J. Geophys. Res.* **90**, 4495-4510.
- Lisowski, M. and J. C. Savage (1986). Geodetic strain in northwestern Washington (manuscript in preparation).
- Lockridge, P. A. and R. H. Smith (1984). *Tsunamis in the Pacific Basin*, map published by the National Geophysical Data Center, NOAA, Boulder, Colorado.
- Lomnitz, C. (1970). Major earthquakes and tsunamis in Chile during the period 1535-1955, *Geol. Rundsh.* **59**, 938-960.
- Lowrie, A. and R. Hey (1981). Geological and geophysical variations along the western margin of Chile near lat 33° to 36°S and their relation to Nazca plate subduction, *Geol. Soc. Am. Memoir* **154**, 741-754.
- Mauger, J. E. and R. D. Daugherty (1979). Ozette Archaeological Project, Interim Final Report, Phase XI, Project Report No. 68, Washington Archaeological Research Center, Washington State University, Pullman, Washington.
- Minster, J. B. and T. H. Jordan (1978). Present-day plate motions, *J. Geophys. Res.* **83**, 5331-5354.
- Nishenko, S. P. (1985). Seismic potential for large and great interplate earthquakes along the Chilean and southern Peruvian Margins of South America: a quantitative reappraisal, *J. Geophys. Res.* **90**, 3589-3615.
- Nishimura, C., D. S. Wilson, and R. N. Hey (1984). Pole of rotation analysis of present-day Juan de Fuca plate motion, *J. Geophys. Res.* **89**, 10283-10290.
- NOAA (1981). The marine geophysical data exchange format 'MGD77', Key to Geophysical Records Documentation No. 10, National Geophysical and Solar-Terrestrial Data Center, Boulder, Colorado, 17 pp.
- Parsons, B. and J. G. Sclater (1977). An analysis of the variation of the ocean floor bathymetry and heat flow with age, *J. Geophys. Res.* **82**, 803-827.
- Peterson, E. T. and T. Seno (1984). Factors affecting seismic moment release rates in subduction zones, *J. Geophys. Res.* **89**, 10,233-10,248.
- Plafker, G. (1972a). Tectonics, in *The Great Alaska Earthquake of 1964, Seismology and Geodesy*, National Academy of Sciences, Washington, D.C.
- Plafker, G. (1972b). Alaskan earthquake of 1964 and Chilean earthquake of 1960, implications for arc tectonics, *J. Geophys. Res.* **77**, 901-925.
- Plafker, G. and J. Savage (1970). Mechanism of the Chilean earthquakes of May 21 and 22, 1960, *Geol. Soc. Am. Bull.* **81**, 1001-1030.

# SUBDUCTION EARTHQUAKES IN THE NORTHWESTERN U.S.

- Plafker, G. and M. Rubin (1978). Uplift history and earthquake recurrence as deduced from marine terraces on Middleton Island, Alaska, *Proc. Conf. VI: Methodology for Identifying Seismic Gaps and Soon-to-Break Gaps*, U.S. Geol. Surv., Open-File Rept. 78-943, 687-722.
- Ramirez, J. E. (1933). Earthquake history of Colombia, *Bull. Seism. Soc. Am.* **23**, 13-22.
- Reilinger, R. E. and J. Adams (1982). Geodetic evidence for active landward tilting of the Oregon and Washington coastal ranges, *Geophys. Res. Letters* **9**, 401-403.
- Richter, C. F. (1958). *Elementary Seismology*, W. H. Freeman and Company, San Francisco, California, 768 pp.
- Riddihough, R. P. (1977). A model for recent interactions off Canada's west coast, *Can. J. Earth Sci.* **14**, 384-396.
- Riddihough, R. P. (1978). The Juan de Fuca plate, *EOS* **59**, 836-842.
- Riddihough, R. P. (1980). Gorda plate motions from magnetic anomaly analysis, *Earth Planet. Sci. Letters* **51**, 163-170.
- Riddihough, R. P. (1982). Contemporary vertical movements and tectonics on Canada's west coast: a discussion, *Tectonophysics* **86**, 319-341.
- Riddihough, R. P. (1984). Recent movements of the Juan de Fuca plate systems, *J. Geophys. Res.* **89**, 6980-6984.
- Ruff, L. and H. Kanamori (1980). Seismicity and the subduction process, *Phys. Earth Planet. Interiors* **23**, 240-252.
- Samuels, S. M. (1983). Spatial patterns and cultural processes in three Northwest Coast longhouse floor middens from Ozette, *Ph.D. Thesis*, Washington State University, Pullman, Washington.
- Savage, J. C., M. Lisowski, and W. H. Prescott (1981). Geodetic strain measurements in Washington, *J. Geophys. Res.* **86**, 4929-4940.
- Schweller, W. D., L. D. Kulm, and R. A. Prince (1981). Tectonics structure, and sedimentary framework of the Peru-Chile Trench, *Geol. Soc. Am. Memoir* **154**, 323-349.
- Seno, T. (1977). The instantaneous rotation vectors of the Philippine Sea plate relative to the Eurasian plate, *Tectonophysics* **42**, 209-226.
- Shephard, L. E. and W. R. Bryant (1983). Geotechnical properties of lower trench inner-slope sediments, *Tectonophysics* **99**, 279-312.
- Shimazaki, K. and T. Nakata (1980). Time-predictable recurrence model for large earthquakes, *Geophys. Res. Letters* **1**, 279-282.
- Sieh, K. E. (1981). A review of geological evidence for recurrence times of large earthquakes, in *Earthquake Prediction an International Review*, Maurice Ewing Series 4, American Geophysical Union, 181-207.
- Sievers, H. A., G. Villegas, and G. Barros (1963). The seismic sea wave of 22 May 1960 along the Chilean Coast, *Bull. Seism. Soc. Am.* **53**, 1125-1190.
- Singh, S. K., L. Astiz, and J. Havskov (1981). Seismic gaps and recurrence periods of large earthquakes along the Mexican subduction zone: a reexamination, *Bull. Seism. Soc. Am.* **71**, 827-843.
- Singh, S. K., L. Ponce, and S. P. Nishenko (1985). The great Jalisco Mexico earthquakes of 1932 and the Rivera subduction zone, *Bull. Seism. Soc. Am.* **75**, 1301-1313.
- Snively, P. D., Jr. (1986). Tertiary geology and petroleum potential of the western Oregon and Washington continental margin, in *Geology and Resource Potential of the Continental Margin of Western North America and Adjacent Ocean Basins—Beaufort Sea to Baja California*, D. W. Scholl, A. Grantz, and J. G. Vedder, Editors, American Association of Petroleum Geologists Memoir Series (in press).
- Snively, P. D., Jr., H. C. Wagner, and D. L. Lander (1980). Interpretation of the Cenozoic geologic history, central Oregon continental margin: cross-section summary, *Geol. Soc. Am. Bull. (Part I)*, **91**, 143-146.
- Sykes, L. R., J. B. Kisslinger, L. S. House, J. N. Davies, and K. H. Jacob (1981). Rupture zones and repeat times of great earthquakes along the Alaska-Aleutian Arc, in *Earthquake Prediction*, D. W. Simpson and P. G. Richards, Editors, American Geophysical Union, Washington, D.C., 73-80.
- Taber, J. J. and S. W. Smith (1985). Seismicity and focal mechanisms associated with the subduction of the Juan de Fuca plate beneath the Olympic Peninsula, Washington, *Bull. Seism. Soc. Am.* **75**, 237-249.
- Takagi, A. (1982). How small earthquakes occur, in *Earthquake Prediction Techniques*, T. Asada, Editor, University of Tokyo press, Tokyo, Japan, 63-88.
- Usami, T. (1982). Great earthquakes of the past, in *Earthquake Prediction Techniques*, T. Asada, Editor, University of Tokyo Press, Tokyo, Japan, 11-29.
- Uyeda, S. (1984). Subduction zones: their diversity, mechanism, and human impacts, *Geol. J.* **8.4**, 381-406.

THOMAS H. HEATON AND STEPHEN H. HARTZELL

- Uyeda, S. and H. Kanamori (1979). Back-arc opening and the mode of subduction, *J. Geophys. Res.* **84**, 1049-1061.
- Von Huene, R., J. C. Moore, and G. W. Moore (1978). Cross section of Alaska Peninsula-Kodiak Island-Aleutian Trench, Geological Society of America, MC-28A.
- Weaver, C. S. and S. W. Smith (1983). Regional tectonic hazard implications of a crustal fault zone in southwestern Washington, *J. Geophys. Res.* **88**, 10371-10383.
- Yoshikawa, T., S. Kaizuka, and Y. Ota (1981). *The Landforms of Japan*, University of Tokyo Press, Tokyo, Japan, 222 pp.

U.S. GEOLOGICAL SURVEY  
CALIFORNIA INSTITUTE OF TECHNOLOGY  
PASADENA, CALIFORNIA 91125

Manuscript received 22 September 1985

# Earthquake Hazards on the Cascadia Subduction Zone

THOMAS H. HEATON AND STEPHEN H. HARTZELL

Large subduction earthquakes on the Cascadia subduction zone pose a potential seismic hazard. Very young oceanic lithosphere (10 million years old) is being subducted beneath North America at a rate of approximately 4 centimeters per year. The Cascadia subduction zone shares many characteristics with subduction zones in southern Chile, southwestern Japan, and Colombia, where comparably young oceanic lithosphere is also subducting. Very large subduction earthquakes, ranging in energy magnitude ( $M_w$ ) between 8 and 9.5, have occurred along these other subduction zones. If the Cascadia subduction zone is also storing elastic energy, a sequence of several great earthquakes ( $M_w$  8) or a giant earthquake ( $M_w$  9) would be necessary to fill this 1200-kilometer gap. The nature of strong ground motions recorded during subduction earthquakes of  $M_w$  less than 8.2 is discussed. Strong ground motions from even larger earthquakes ( $M_w$  up to 9.5) are estimated by simple simulations. If large subduction earthquakes occur in the Pacific Northwest, relatively strong shaking can be expected over a large region. Such earthquakes may also be accompanied by large local tsunamis.

**D**ESPITE COMPELLING EVIDENCE THAT THE GORDA, JUAN de Fuca, and Explorer plates are actively subducting along the 1200-km-long Cascadia subduction zone in the Pacific Northwest, there have been no large historic shallow subduction earthquakes of the type experienced at most other subducting plate boundaries. Is the Cascadia subduction process benign, with the differential plate motion occurring through aseismic creep, or is the zone storing elastic strain energy to be released in future great subduction earthquakes? If the Cascadia subduction zone is storing strain energy, how large might the earthquakes be, how often might they occur, and what might the ground motions be? These are all difficult, but vital, questions whose answers dramatically affect the estimation of seismic risk in the Pacific Northwest.

## Active Subduction in the Pacific Northwest

The geometry of the major plate boundaries and seismicity in the Pacific Northwest is shown in Fig. 1. A half-spreading rate of 3 cm/year was inferred for the Juan de Fuca ridge by Delaney *et al.* (1) who reported that 43 km of new oceanic crust has formed since the

700,000-year-old Brunhes-Matuyama magnetic reversal. Nishimura *et al.* (2) calculated a convergence rate of 3.5 to 4.5 cm/year across the Cascadia subduction zone from sea-floor magnetic lineation data. The suitability of this kinematic model to present-day plate motions is supported by work of Hyndman and Weichert (3) who showed that historic seismicity is compatible with slip rates expected from magnetic lineation data on all the plate boundaries of the Pacific Northwest except on the Cascadia subduction zone. It seems difficult to construct a model of plate motions that slips 5 cm/year on plate boundaries both north and south of the Cascadia subduction zone, but with no convergence on the subduction zone.

## Subduction of Young Lithosphere

The oceanic lithosphere that is subducting beneath the Pacific Northwest is very young, about 10 million years old (4). Several characteristics of the Cascadia subduction zone distinguish it from most other worldwide subduction zones, and most of these can be attributed to the youthfulness of the subducted oceanic lithosphere. More specifically, there is no significant bathymetric trench or large gravity anomaly for the Cascadia subduction zone. The sea floor adjacent to the continental margin is only about 3 km deep, and the average heat flow is relatively high (5); both of these features are directly attributable to the youth of the oceanic lithosphere (6). Furthermore, although there is a distinct Benioff-Wadati seismicity zone in the Pacific Northwest (7), it stops at a much shallower depth than in most other subduction zones, extending to a depth of less than 80 km.

Uyeda and Kanamori (8) suggested that the seismic coupling of subducting plate boundaries (the fraction of plate slip that occurs during earthquakes) is related to the physical characteristics of the plate boundary. Ruff and Kanamori (9) demonstrated that weakly coupled zones tend to have slow subduction of very old oceanic crust, whereas strongly coupled zones tend to have fast subduction of young crust. They suggested that old lithosphere is dense and subducts spontaneously with oceanward retreat of the trench and subsequent opening of back-arc basins (Marianas type, weakly coupled). Young, buoyant lithosphere tends to subduct only when it is overridden by continental lithosphere, as is the case along much of the western coast of North and South America (Chilean type, strongly coupled).

## Comparison of Cascadia with Other Subduction Zones

Heaton and Kanamori (10) pointed out that the Cascadia subduction zone has physical characteristics very different from those of the traditional "aseismic" subduction zone (weakly coupled, Marianas type). Furthermore, they reported that the Cascadia

The authors are geophysicists associated with the Pasadena field office of the U.S. Geological Survey, 525 South Wilson Avenue, Pasadena, CA 91106, and with the California Institute of Technology, Pasadena, CA 91125.

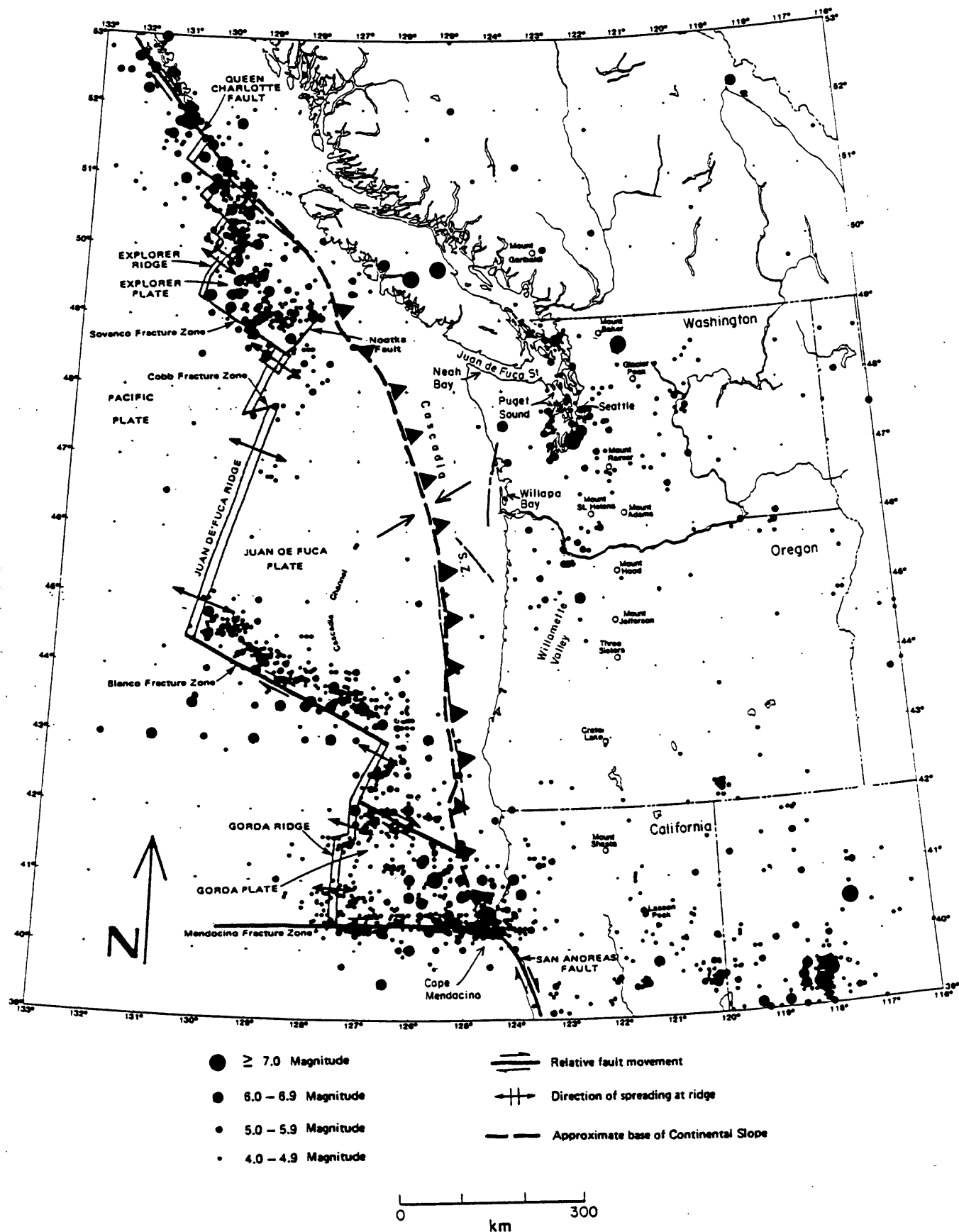


Fig. 1. Seismicity and plate tectonics of the Pacific Northwest.

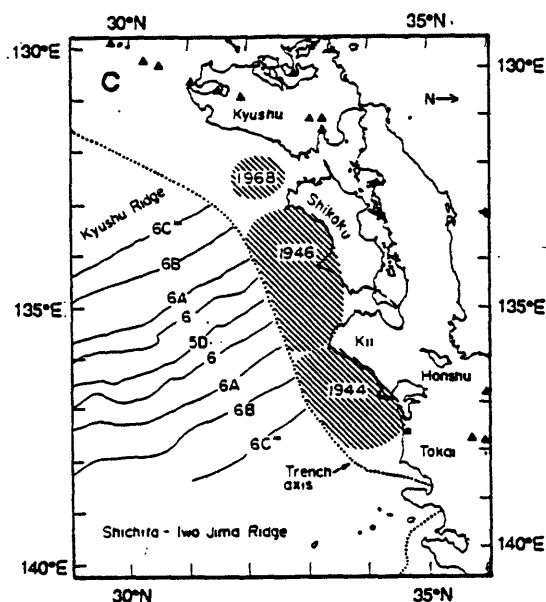
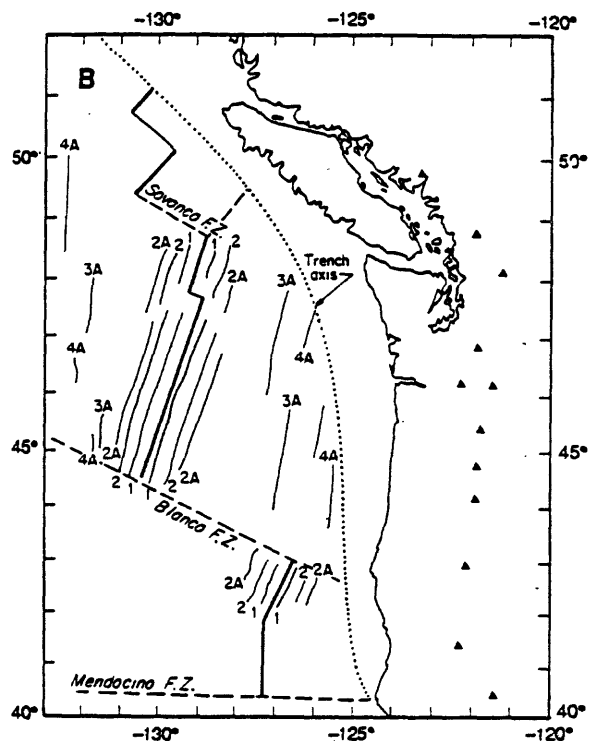
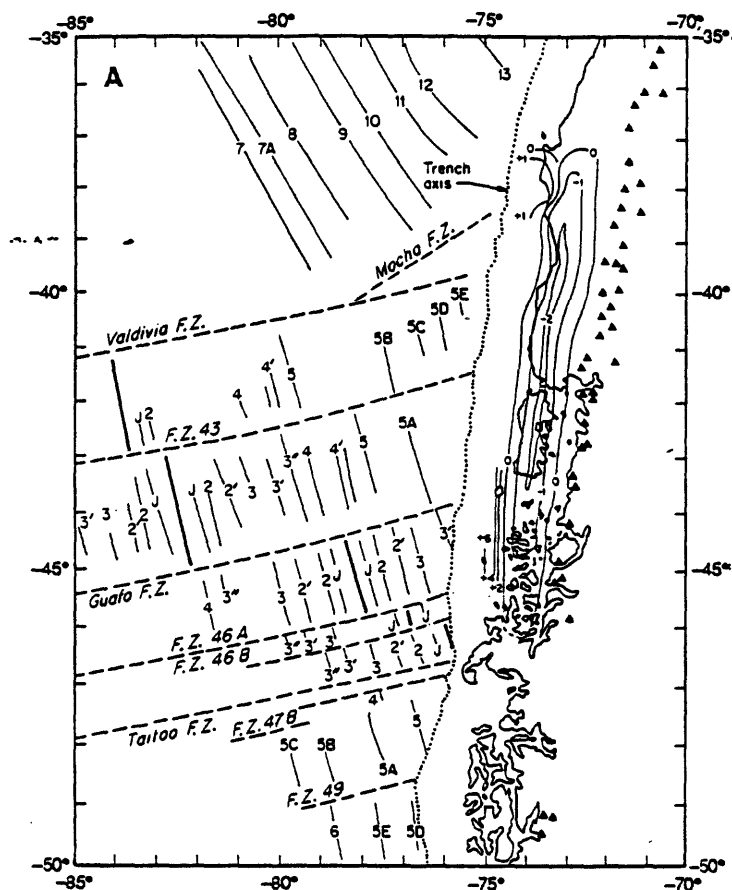


Fig. 2. Comparison of subduction in southern Chile (A), Pacific Northwest (B), and southwestern Japan (C). All maps are plotted on approximately the same scale. Active spreading centers (heavy solid lines), sea-floor magnetic lineations (light solid lines), Quaternary volcanoes (solid triangles), and fracture zones (F.Z.) are shown. Symbols on the magnetic lineations refer to the geomagnetic time scale; lineation 1 is about 1 million years, 5 about 10 million years, 6 about 20 million years, and 10 about 30 million years. The approximate rupture areas of large Japanese earthquakes and contours (meters) of vertical deformation associated with the 22 May 1960 Chilean earthquake are also shown (15).

subduction zone has many similarities to other strongly coupled subduction zones (Chilean type). Heaton and Hartzell (11) concluded that of all worldwide subduction zones, the Cascadia subduction zone seems most similar to those in southern Chile, southwestern Japan, and Colombia. Very young oceanic lithosphere is subducting in each of these locations, and very large, shallow, thrust earthquakes have occurred at each of these other zones. Maps comparing the geometries of the subduction zones in the Pacific Northwest, southern Chile, and southwestern Japan are shown on

the same scale in Fig. 2, which shows the similarity of the overall dimensions of these plate boundaries.

Kanamori and Astiz (12) have suggested that as the age of the subducted plate approaches 0 years, we may expect increasing aseismic slip to result from high temperatures at the subducting boundary. Perhaps the Cascadia subduction zone is so hot that slip along this boundary is occurring as aseismic creep. Unfortunately we do not know the age at which this mechanism may become important. However, at other locations where the youngest oceanic

lithosphere is subducting (less than 5 million years in southern Chile) (Fig. 2), major slip has occurred during great earthquakes (11).

One of the most remarkable features of the Cascadia subduction zone is the striking paucity of historic shallow coastal seismicity. Although this may indicate aseismic slip along the plate boundary, the sections of the San Andreas fault that are currently creeping have a relatively high level of small earthquake seismicity, whereas the sections of the fault that experienced great earthquakes in 1857 and 1906 are currently devoid of any measurable activity. One explanation for this behavior is that stress increases smoothly and uniformly on fault zones that are coupled over large areas, whereas numerous stress concentrations occur on faults having large areas that undergo aseismic slip. Heaton and Hartzell (11) noted that significant periods of low seismicity have been observed at subduction zones similar to the Cascadia subduction zone, whereas subduction zones of the Marianas type (mainly aseismic slip) show a low, but steady, rate of seismicity. Heaton and Hartzell (11, pp. 697–698) stated that “although [the comparison study] does not prove that great earthquakes will occur on the Cascadia subduction zone, it does suggest that it is inappropriate to assume that great earthquakes will not occur based on observations of bathymetry, lithospheric age, trench sediments, heat flow, convergence rate, physiography, overall size of the subducted plate, Quaternary volcanism, or the rate of background seismicity.”

## Cascadia Subduction Zone—Locked or Unlocked?

Although comparison of the Cascadia subduction zone with other subduction zones leads us to believe that there may be a potential for large subduction earthquakes, it would be far more satisfying to have both direct evidence that elastic strain is accumulating and evidence for prehistoric large earthquakes. Since the question of large subduction earthquakes has been asked only recently, the search for direct evidence is still in a very early stage.

**Geodetic strain.** Savage *et al.* (13) and later Lisowski and Savage (14) discussed Geodolite surveys made in the Seattle region from 1972 to 1986 and triangulation surveys along the Strait of Juan de Fuca from 1892 to 1954. Their analyses indicate that both regions show a maximum contraction in a direction that is nearly parallel to the east-northeast plate convergence directions at rates of  $0.03 \pm 0.01$  and  $0.2 \pm 0.07$  microstrain per year for the Seattle and Strait of Juan de Fuca regions, respectively. Unfortunately, ambiguity exists in the interpretation of the strains from the Seattle Geodolite network, at least partly because of a poor signal-to-noise ratio (15). Repeated leveling surveys along much of the coastline adjacent to the Juan de Fuca plate show uplift of the coast regions at a rate of up to 3 mm/year and subsidence of the inner coastal areas at a rate of about 1 mm/year (16). Lisowski and Savage (14) showed that the combined Geodolite, triangulation, and leveling data can be explained by a model in which the shallow thrust zone is locked between the trench axis and the coastal region. Coseismic extensions ranging from 25 to 50 microstrain were observed in the central valley of southern Chile for the 22 May 1960 Chilean earthquake (17), and coseismic extensions from the 28 March 1964 Alaskan earthquake ranged from about 15 microstrain in the inner coastal areas to more than 50 microstrain in the outer coastal areas (18). At the current strain rates, it would take several hundred to a thousand years for comparable strains to accumulate along the Cascadia subduction zone.

**Holocene shorelines.** Holocene geomorphic and depositional features often record the occurrence of great subduction earthquakes.

However, such features are relatively rare since they are preserved only when there are high, long-term uplift rates, large coseismic uplifts, and moderate to low coastal erosion rates. From reviews of the sparse literature on Pleistocene marine terraces, Adams (19) reported relatively slow emergence and possible submergence for most of the coastline of Washington and northern Oregon. He further reported moderate uplift rates of less than 1.5 mm/year in southern Oregon. Coastal erosion rates are high, and few, if any, uplifted Holocene strand lines have been identified along the coast of Washington and Oregon. The highest geologic uplift rate (3.6 cm/year) documented along the Cascadia subduction zone occurs near Cape Mendocino, California, in the region of the Gorda-Pacific-North America triple junction (20). A flight of nine emergent terraces and beach ridges has formed during the past 5000 years at Cape Mendocino (20), but it is uncertain whether these terraces have any bearing on the problem of large subduction earthquakes in the Pacific Northwest.

The lack of raised Holocene terrace in Oregon and Washington may be due to coseismic coastal subsidence, a commonly observed by-product of great subduction earthquakes. Most of the coastal areas adjacent to the 22 May 1960 Chilean earthquakes subsided by 1 to 2 m, whereas uplift occurred only at the outer islands and at the northern end of the rupture zone (Fig. 2). In a reconnaissance study of Holocene relative sea levels on the Washington coast, Atwater (21) found evidence that a tidal marsh subsided suddenly near Neah Bay (northwesternmost tip of Washington) approximately 1100 years ago. He also found similar evidence for multiple jerks of subsidence in the Willapa Bay region 200 km to the south. Atwater (21) proposed that each jerk of subsidence may mark a great prehistoric earthquake on the Cascadia subduction zone.

**Holocene turbidites.** Adams (4, 22) has suggested that extensive Holocene turbidites studied by Griggs and Kulm (23) may have been triggered by large earthquakes along the continental shelf. Since the deposition of Mazama ash 6600 years ago, there have been approximately 16 major turbidites in the Cascadia Channel, which is consistent with an average earthquake repeat time of 410 years. Adams (22) pointed out that two separate channels separated by 50 km, and that also feed the main Cascadia Channel, have turbidite sequences comparable in number to those seen in the main channel. This seems to be evidence that turbidity currents were simultaneously triggered in separate channels, perhaps by great subduction earthquakes.

**Historical records.** Although first explored by Europeans in the late 1700s, coastal Washington had no permanent Caucasian settlements until 1810. There being no known written accounts of any event that can be interpreted as a great subduction earthquake, it seems unlikely that any such events have occurred for at least 200 years. However, a few legends of Washington coastal Indians suggest the occurrence of a large tsunami along the northwestern Washington coast (24). There are also legends of large earthquakes and disturbances of the coastal waters from coastal Indians in northernmost California (24). Unfortunately, these legends are too vague to constitute proof that large subduction earthquakes have occurred.

## Hypothetical Subduction Earthquakes

If the Cascadia subduction zone is locked, what sort of earthquakes may occur there? Although this question is central to the assessment of seismic hazards, at this point our answers are speculative. For simplicity, we assume that earthquakes on the Cascadia subduction zone may resemble earthquakes on the subduction zones that seem to be the most similar to the Cascadia zone—namely, southern Chile, southwestern Japan, and Colombia. Heaton and

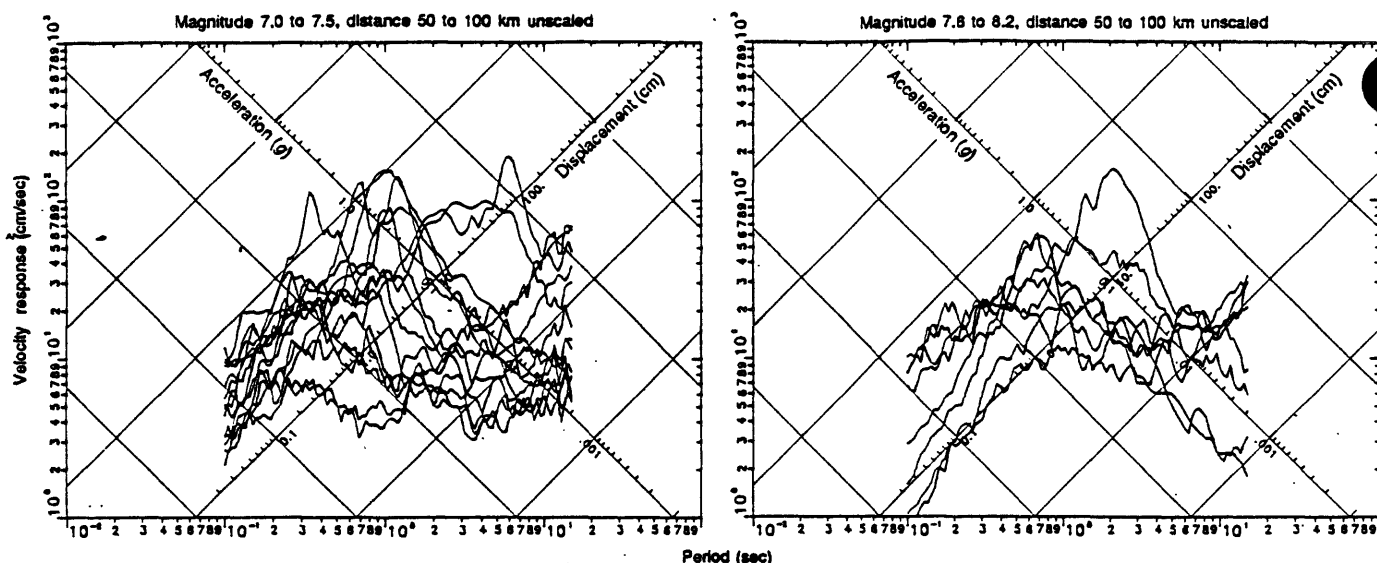


Fig. 3. Pseudovelocity response spectra (5% damped) of horizontal components of ground motion for sites at distances between 50 and 100 km for large subduction earthquakes.

Hartzell (11) summarized historic earthquake activity for these subduction zones and chose several historic earthquake sequences that they considered to be plausible for the Pacific Northwest if, in fact, the subduction zone is locked. In the first scenario, a sequence of four or five earthquakes similar to the 1944 and 1946 energy magnitude ( $M_w$ ) 8.1 southwestern Japan earthquakes (Fig. 2) would be sufficient to cover the length of the Cascadia subduction zone. Such earthquakes might be closely spaced in time, as has been the case for many sequences in southwestern Japan. Plate convergence rates in southwestern Japan are comparable to those in the Pacific Northwest. The average earthquake recurrence interval in southwestern Japan is about 180 years (25).

Another scenario calls for an earthquake similar to the 1906  $M_w$  8.8 Colombian earthquake. An average dislocation of about 5 m over a rupture length of about 500 km has been estimated for this event (26). The section of the zone that ruptured in 1906 seems to have ruptured again in a sequence of smaller earthquakes (1942, 1948, and 1979) whose moment sum is only one-fifth that of the 1906 event (26). The convergence rate at Colombia is about 8 cm/year, but the historic records are insufficient to allow an estimation of the recurrence interval of great Colombian earthquakes.

The 22 May 1960 Chilean earthquake is the largest documented earthquake of this century ( $M_w$  9.5). The rupture covered a length of about 1000 km and ruptured through many different segments of

the South Chile subduction zone (Fig. 2). The dimensions of the 1960 rupture zone are comparable to those of the entire Cascadia subduction zone (Fig. 2), and thus we consider the 1960 earthquake to represent the largest earthquake feasible in the Pacific Northwest. The convergence rate in southern Chile is about 9 cm/year, and large earthquakes also occurred in this region in 1575, 1737, 1837, and 1960—an average recurrence time of about 128 years. However, there is strong evidence that average dislocations of greater than 20 m accompanied the 1960 earthquake (17), and thus a recurrence interval of 128 years seems inconsistently short with respect to the long-term convergence rate. There is evidence that the 1960 earthquake may have been significantly larger than previous historic events in this area (11). If earthquakes similar to the 1960 Chilean earthquake do occur on the Cascadia subduction zone, their average recurrence interval would probably exceed 500 years.

## Rupture Process for Large Subduction Earthquakes

We have argued that the very young age of the subducted lithosphere in the Pacific Northwest may determine the seismic coupling of the plate boundary. Is there a systematic difference with the age of the subducted plate in the nature of seismic energy release during large subduction earthquakes? Hartzell and Heaton (27) studied broad-band teleseismic  $P$ -waves from 63 of the largest shallow earthquakes in the last 45 years. The earthquakes studied occurred in 15 subduction zones with a wide range in the ages of subducted lithosphere and represent a wide range of convergence rates and maximum size of earthquakes. Hartzell and Heaton derived teleseismic time functions in the period band from 2 to 50 seconds and characterized those functions in terms of roughness, overall duration, multiplicity of sources, spectral slopes, and duration of individual pulses. These measures varied widely from one earthquake to another, although earthquakes within the same subduction zone seem to be similar. Comparing the time functions with age, rate, and maximum  $M_w$  of the subduction zones does not yield obvious global trends. These observations indicate that important differences are not expected in the nature of energy release from earthquakes at subduction zones that are similar to the Cascadia subduction zone.

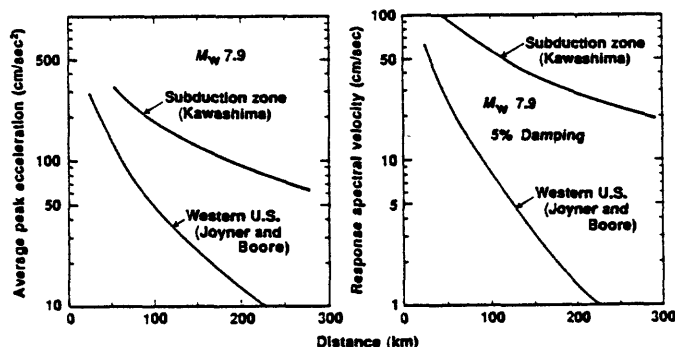


Fig. 4. Comparison of predictions of average peak ground motions obtained by regression analysis of data from the southwestern United States (29) and from Japan (31). Soil sites and 5% damping are assumed for the response spectra.



## Strong Ground Motions Observed During Large Subduction Earthquakes

Heaton and Hartzell (28) discussed the nature of strong ground motions that might be expected if large subduction earthquakes occur in the Pacific Northwest. They assumed that gap-filling earthquake sequences that are similar to those already observed in southern Chile, southwestern Japan, and Colombia may also occur in the Pacific Northwest. The largest earthquakes in these sequences range in size from  $M_w$  8 to  $M_w$  9.5. Strong motion records are available for shallow subduction earthquakes as large as  $M_w$  8.2, but strong ground motions have not yet been recorded for larger earthquakes. Heaton and Hartzell assumed that ground motions from  $M_w$  8 earthquakes on the Cascadia subduction zone would not be systematically different from the motions recorded during  $M_w$  8 earthquakes on other subduction zones. For earthquakes of  $M_w$  less than 8.2, their approach is to simply construct suites of ground motions that were recorded under conditions similar to those existing at sites for which ground motion estimates are desired.

Heaton and Hartzell (28) collected 56 recordings of strong ground motion from 25 shallow subduction earthquakes of  $M_w \geq 7.0$  for their study. Pseudovelocity response spectra for ground motions recorded in the distance range from 50 to 100 km are shown in Fig. 3. They also prepared similar figures for other distance ranges out to 300 km. One of the most striking features is the large degree of scatter in the spectra for ground motions observed at similar distances and from similar sized earthquakes. This scatter is troublesome when it is necessary to estimate the ground motion that a particular site will experience. Even if the earthquake magnitude and distance are known, the resulting ground motions are still uncertain by a factor of 10. Much of this scatter can be attributed to differences in the response characteristics of individual recording sites (28). Thus, refined estimates of ground motion should be obtained by determining the site response from the ground motions of small earthquakes.

Another feature of ground motions recorded during large subduction zone earthquakes is their large size at very large distances. In Fig. 4, we compare ground motion levels for  $M_w$  7.9 earthquakes predicted from regression analysis of earthquakes in the western United States (29, 30) with those predicted from regression analysis of large subduction earthquakes in Japan (31). At distances of more than 50 km, ground motions from large subduction earthquakes are expected to be far larger than those from large crustal earthquakes in the southwestern United States. As can be seen in the response spectral velocities at 1 second, this effect is pronounced at periods of concern to large structures. Unfortunately, the western United States curves are uncertain since there have been no strong motion recordings from earthquakes of this size in the western United States and these curves are extrapolations outside the data. Peak ground accelerations and velocities for earthquakes of magnitude less than 7 are not dramatically different for Japanese and western United States earthquakes (32). The origin of the difference between ground motion estimates at large distances for large subduction earthquakes and large crustal earthquakes in the southwestern United States is not yet fully understood.

## Simulating Ground Motions for Giant Earthquakes

If the Cascadia subduction zone is strongly coupled, earthquakes far larger than any of the events for which we have strong motion records can be postulated. What might the ground motions look like from a giant earthquake such as the 1960 Chilean earthquake? Its

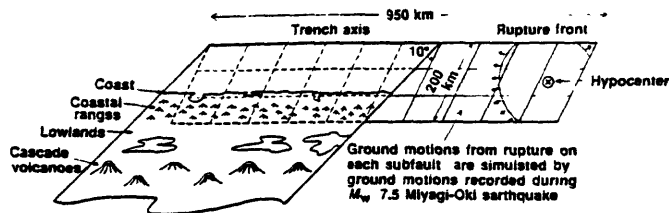


Fig. 5. Schematic drawing of the simulation of an earthquake similar to the 22 May 1960 Chilean earthquake ( $M_w$  9.5) by the superposition of 1978 Miyagi-Oki earthquakes ( $M_w$  7.5).

seismic moment is at least 100 times that of the largest earthquake for which we have strong motion data (33). Heaton and Hartzell (28) simulated the ground motions from giant earthquakes ( $M_w > 8.5$ ) by summing records from smaller earthquakes in such a way that they simulate the occurrence of larger earthquakes. That is, the records from smaller earthquakes are used as Green's functions, and this technique is often referred to as the empirical Green's functions technique. A schematic diagram of a model in which the 22 May 1960 Chilean earthquake is simulated by a collection of smaller earthquakes, in this case the 12 May 1978  $M_w$  7.5 Miyagi-Oki earthquake, is shown in Fig. 5. In this example, the 1960 Chilean earthquake is simulated by the superposition of 120 Miyagi-Oki earthquakes. Models of this type can be used to simulate teleseismic P-waveform data as well as strong ground motions. Although there are no strong motion records from giant earthquakes, there are records of teleseismic P-waves (27, 28) that are used to constrain the modeling parameters used in the empirical Green's function technique. The teleseismic data suggest that a large part of the seismic energy associated with giant earthquakes is of very long period. This very long period energy is outside the frequency band of earthquake engineering interest. Heaton and Hartzell (28) concluded that summing 120 Miyagi-Oki records simulates short-period energy from the 1960 Chilean earthquake even though the ratio of the total seismic moments for the two earthquakes is at least 1000:1.

The results of the empirical Green's function simulations are summarized in Fig. 6. These curves represent a best guess of the average response spectral levels (5% damped) for horizontal ground motions observed at points located about 50 km inland from the

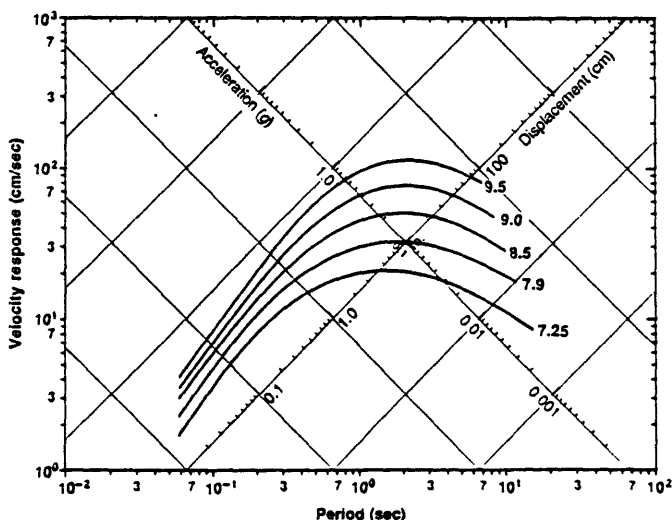


Fig. 6. Estimates of the variation in average horizontal ground motion response spectra (5% damping) as a function of energy magnitude for sites located 50 km inland from the coast. Scatter of actual data about mean values may be similar to that in the data observed in Fig. 4.

coast and for a variety of sizes of subduction earthquakes. Ground motion estimates for earthquakes of  $M_w < 8$  are based on the direct observation of strong motion data, whereas the ground motions for larger earthquakes are estimated by the empirical Green's functions technique. Large scatter about these averages (about a factor of 2) can be expected for suites of actual data. For the very largest earthquakes, motions may be about 25% larger at coastal sites and about 67% as large at sites in the Puget Sound. The duration of strong shaking during such giant earthquakes is expected to exceed 2 minutes. Average peak accelerations may be in the range of 600  $\text{cm/sec}^2$  for coastal sites and 250  $\text{cm/sec}^2$  for Puget Sound sites.

## Tsunami Hazards

All of the regions that we considered to be potential analogs for the Cascadia subduction zone have experienced large local tsunamis. The 1944  $M_w$  8.1 and 1946  $M_w$  8.1 earthquakes in southwestern Japan generated local tsunamis that had maximum run-up heights of 7.5 and 6.0 m, respectively, and the 1707 southwestern Japan earthquake ( $M_w > 8.5$ ) probably generated an even larger tsunami (34). The 1906 Colombian earthquake also generated a large local tsunami that extensively damaged much of the coastal regions of southwestern Colombia and northern Ecuador (34). The 1960 Chilean earthquake generated one of the largest tsunamis in recent times, with heavy damage occurring both locally (35) and also in Hawaii and Japan. Although the maximum local run-up may have exceeded a height of 20 m, it seems likely that most of the coastal regions adjacent to the earthquake experienced run-up heights of less than 10 m. If very large subduction earthquakes do occur in the Pacific Northwest, they will almost certainly be accompanied by tsunamis. It is difficult at this point to reliably estimate the tsunami run-up heights that may follow any large earthquake on the Cascadia subduction zone. However, run-up heights ranging from several meters to several tens of meters have been observed along other subducting boundaries after events of the type that we consider to be feasible for the Cascadia subduction zone.

## Conclusions

Strong evidence exists for active convergence at about 4  $\text{cm/year}$  on the 1200-km Cascadia subduction zone. Furthermore, the physical characteristics of the Cascadia subduction zone resemble those of other subduction zones that have experienced large shallow earthquakes. Even though there have not been large historic subduction earthquakes in the Pacific Northwest for at least 150 years, the Cascadia subduction zone may be storing strain energy to be released in future great earthquakes. If the Cascadia subduction zone

is locked, a sequence of several great earthquakes ( $M_w$  8) or a giant earthquake ( $M_w$  9) would be necessary to fill this gap. If great subduction earthquakes occur, then relatively strong shaking can be expected over a large area of the Pacific Northwest, including Puget Sound and Willamette Valley regions. Large and potentially destructive local tsunamis would be expected if large subduction events do occur. Great earthquakes, such as those in southwestern Japan or southern Chile, have caused great damage over very large regions. The suggestion of similar events in the Pacific Northwest is disturbing.

## REFERENCES AND NOTES

1. J. R. Delaney, H. P. Johnson, L. L. Karsten, *J. Geophys. Res.* **86**, 11747 (1981).
2. C. Nishimura, S. S. Wilson, R. N. Hey, *ibid.* **89**, 10283 (1984).
3. R. D. Hyndman and D. H. Wiechert, *Geophys. J. R. Astron. Soc.* **72**, 59 (1983).
4. K. D. Klingor and J. Mammertick, *J. Geophys. Res.* **87**, 6725 (1982).
5. L. D. Kulm *et al.*, *Atlas 1* (Ocean Margin Drilling Program, Regional Atlas Series: Marine Science International, Woods Hole, MA, 1984).
6. B. Parsons and J. G. Sclater, *J. Geophys. Res.* **82**, 803 (1977).
7. R. S. Crosson, *U.S. Geol. Surv. Open-File Rep.* **83-19** (1983), p. 6. Seismicity within the subducted slab is chiefly limited to the region beneath the Puget Sound.
8. S. Uyeda and H. Kanamori, *J. Geophys. Res.* **84**, 1049 (1979).
9. L. Ruff and H. Kanamori, *Phys. Earth Planets. Inter.* **23**, 252 (1980).
10. T. H. Heaton and H. Kanamori, *Bull. Seismol. Soc. Am.* **74**, 933 (1984).
11. T. H. Heaton and S. H. Hartzell, *ibid.* **76**, 675 (1986).
12. H. Kanamori and L. Asiz, *Earthquake Predict. Res.* **3**, 305 (1985).
13. J. C. Savage, M. Lisowski, W. H. Prescott, *J. Geophys. Res.* **86**, 4929 (1981).
14. M. Lisowski and J. C. Savage, unpublished manuscript. Trench-parallel strain rates were assumed to be 0 for calculating extensional strains along the axis of maximum compression.
15. R. S. Crosson, *J. Geophys. Res.* **91**, 7555 (1986); J. C. Savage, M. Lisowski, W. H. Prescott, *ibid.*, p. 7559.
16. R. E. Reilinger and J. Adams, *Geophys. Res. Lett.* **9**, 401 (1982).
17. G. Plafker and J. Savage, *Geol. Soc. Am. Bull.* **81**, 1001 (1970).
18. G. Plafker, in *The Great Alaskan Earthquakes of 1964*, K. Krautkopf, Ed. (National Academy of Sciences, Washington, DC, 1972).
19. J. Adams, *Tectonics* **3**, 449 (1984).
20. K. R. Lajoie *et al.*, in *Proceedings of the International Symposium on Development of Holocene Shorelines*, Y. Ota, Ed. (Tokyo, Japan 1983); K. R. Lajoie, *U.S. Geol. Surv. Open-File Rep.* **83-90** (1983), p. 136.
21. B. F. Atwater, *U.S. Geol. Surv. Open-File Rep.* **86-383** (1986), p. 130. Atwater, in preparation.
22. J. Adams, paper presented at the Chapman Conference on Vertical Crustal Motion, Harpers Ferry, WV (1984).
23. G. B. Griggs and L. D. Kulm, *Geol. Soc. Am. Bull.* **81**, 1370 (1970).
24. T. H. Heaton and P. D. Snavey, Jr., *Bull. Seismol. Soc. Am.* **75**, 1455 (1985).
25. M. Ando, *Tectonophysics* **24**, 119 (1975).
26. H. Kanamori and K. C. McNally, *Bull. Seismol. Soc. Am.* **72**, 1241 (1982).
27. S. H. Hartzell and T. H. Heaton, *ibid.* **75**, 965 (1985).
28. T. H. Heaton and S. H. Hartzell, *U.S. Geol. Surv. Open-File Rep.* **86-328** (1986).
29. W. B. Joyner and D. M. Boore, *Bull. Seismol. Soc. Am.* **71**, 2011 (1981).
30. ———, *U.S. Geol. Surv. Open-File Rep.* **82-977** (1982).
31. K. Kawashima, K. Aizawa, K. Takahashi, in *Proceedings of the Eighth World Conference on Earthquake Engineering* (Prentice-Hall, Englewood Cliffs, NJ, 1984), vol. 2, p. 257.
32. T. H. Heaton, F. Tajima, A. W. Mori, *Surv. Geophys.* **8**, 25 (1986).
33. H. Kanamori, *J. Geophys. Res.* **82**, 2981 (1977).
34. P. A. Lockeridge and R. H. Smith, *Tsunamis in the Pacific Basin* (map) (National Geophysical Data Center, National Oceanic and Atmospheric Administration, Boulder, CO, 1984).
35. H. A. Sievers, G. Villegas, G. Barros, *Bull. Seismol. Soc. Am.* **53**, 1125 (1963).
36. We particularly thank H. Kanamori for his patience and insight. We also thank W. Thatcher, J. Savage, B. Atwater, and anonymous reviewers for their comments on the manuscript.

APPENDIX A. 2.

Plate Motion and Seismicity

by

Hiroo Kanamori

## PLATE MOTION AND SEISMICITY

Hiroo Kanamori  
Seismological Laboratory  
California Institute of Technology  
Pasadena, California

(Prepared for NEPEC meeting to be held in Seattle, April 2 and 3, 1987. The material presented here is taken mainly from Kanamori and Astiz (Earthquake Prediction Research, 3, 305-317, 1985) and Kanamori (Ann. Rev. Earth. Planet. Sci., 14, 293-322, 1986)).

Since great subduction-zone earthquakes are ultimately caused by strain accumulation due to plate motion, seismicity is expected to correlate with plate parameters such as the absolute velocity, convergence rate, plate age, Benioff-zone dip angle, and the length of the downgoing slab. In order to investigate this problem, it is necessary to quantify the seismicity of each subduction zone. One difficulty is that the instrumental data are available only for roughly the past 80 years.

Ruff and Kanamori (1980) assumed that the level of seismic activity of an individual subduction zone can be represented by the magnitude  $M_w$  of the largest earthquake recorded for that subduction zone. Implicit in this assumption is that at least one large earthquake characteristic of each subduction zone occurred during this period. Ideally, it is best to integrate the seismic energy released during the time period considered and determine the energy release rate per unit time and length of the subduction zone. Unfortunately it is difficult to do this accurately because of the lack of reliable data. In an attempt to do this approximately, Ruff and Kanamori (1980) considered the overall level of seismicity during the pre-instrumental period, and modified  $M_w$ . The modified magnitude,  $M_w'$ , differs only slightly from  $M_w$ , but it represents the overall seismicity of subduction zones better than  $M_w$ .

Peterson and Seno (1984) carefully evaluated the magnitude and the seismic moment values listed in various seismicity catalogs, and estimated the moment release rate (MRR) per unit time and unit length along the arc. Although considerable error is

involved in converting the magnitude to the seismic moment, their estimates of the moment release rate are the best presently available.

Figure 1 compares MRR determined by Peterson and Seno(1984) with  $M_w'$ , determined by Ruff and Kanamori (1980) for various subduction zones. Since the division of subduction zones is slightly different between the two studies, some adjustments are made in this comparison, as explained in the figure caption. In general  $\log(\text{MRR})$  correlates very well with  $M_w'$ , suggesting that  $M_w'$  is a good parameter to represent the level of seismicity in each subduction zone. The regression line shown in Figure 1 gives  $\text{MRR} = 10^{(1.2M_w' + 18.2)}$  dyne-cm/(100 km-100 years). In this sense, it is more appropriate to interpret  $M_w'$  as a parameter that represents the rate of seismic moment release rather than as the magnitude of the characteristic earthquake in the region.

Ruff and Kanamori (1980) correlated  $M_w$  (or  $M_w'$ ) with various plate parameters. For example, Figure 2a shows the relation between  $M_w'$  and the plate convergence rate  $V$ . In general, as the convergence rate increases, one would expect stronger inter-plate interaction and, therefore, higher seismicity. Although Figure 2a shows a generally positive correlation, the scatter is very large, suggesting that other factors are also important in controlling seismicity.

Another important plate parameter is the age of the subducting plate. Since the older plates are more dense, they have a stronger tendency to sink spontaneously, thereby decreasing the strength of mechanical coupling (Molnar and Atwater 1978, Vlaar and Wortel 1976, Wortel and Vlaar 1978). Figure 2b shows the relation between  $M_w'$  and the age of the subducting plate  $T$ . The correlation is negative, as expected, but the scatter is very large suggesting that the plate age is not the sole controlling factor of seismicity.

Figure 2 suggests that the convergence rate,  $V$ , and the plate age,  $T$ , together might be controlling seismicity. Ruff and Kanamori (1980) performed a three-parameter regression analysis in the form,  $M_w' = aT + bV + c$ , where  $a$ ,  $b$ , and  $c$  are constants.

Using the data listed in table 1 of Ruff and Kanamori (1980), they obtained a relation,

$$M_w' = -0.00953T + 0.143V + 8.01 \quad (1)$$

where T is in million years and V is in cm/year.

Figure 3 compares the observed  $M_w'$  with that calculated from T and V through (6), showing a good correlation between the observed and calculated  $M_w'$ . Also note that the subduction zones with active back-arc opening plot in the lower-left corner of Figure 3, showing good correlation between low seismicity and back-arc opening. Ruff and Kanamori (1980) tried similar correlations between  $M_w'$  and other plate parameters. They found that among all the three-parameter combinations considered, the  $M_w'$ -T-V combination yields the best correlation.

It should be noted that (6) is obtained empirically without any particular physical model. It is possible that other parameters are equally important. For example, Uyeda and Kanamori (1979) and Peterson and Seno (1984) suggest that the absolute velocity of the upper plate is important in determining the strength of plate coupling.

In any case, despite the lack of clear physical models, (6) provides a useful scheme which allows interpretation of global seismicity in terms of a simple plate interaction model.

### *Juan de Fuca Subduction Zone*

The Juan de Fuca subduction zone has a relatively slow convergence rate of about 3.5 cm/year and a very young, 15 M years, subducting plate (Figure 4). Empirical relation (1) predicts an  $M'_w$  of about 8.4 for these values of V and T (Heaton and Kanamori, 1984).

The empirical relation between the fault area S and the seismic moment  $M_0$  is given by (Abe, 1975; Kanamori, 1977a),

$$M_0 = \xi S^{3/2} \quad (2)$$

where  $\xi = 1.23 \times 10^7 \text{ dyne} / \text{cm}^2$  is a constant. Combining this with  $M_0 = \mu \bar{D} S$  ( $\mu$ : rigidity,  $\bar{D}$ : average slip) we obtain

$$\bar{D} = (\xi^{2/3} / \mu) M_0^{1/3} \quad (3)$$

Using  $\mu = 5 \times 10^{11} \text{ dyne} / \text{cm}^2$ , a typical value for subduction zone boundaries, we obtain

$$\bar{D} = \xi M_0^{1/3} \quad (4)$$

or, by using the moment-magnitude relation,  $\log M_0 = 1.5 M_w + 16.1$ ,

$$\bar{D} = \xi 10^{0.5 M_w + 5.37} \quad (4')$$

where  $\xi = 1.1 \times 10^{-7} \text{ dyne}^{-1/3} \text{cm}^{2/3}$  is a constant. Equation (4') predicts an average seismic slip of 4.4 m for an  $M'_w=8.4$  earthquake such as suggested for the Juan de Fuca subduction zone. This would indicate a repeat time of 126 years if the slip at the plate boundary is completely seismic, or 420 years if only 30% of the plate motion is taken up by seismic slip.

The empirical relations used above are subject to considerable uncertainty and the predicted values of  $M_w$  and  $\bar{D}$  should not be taken at face value. This is especially true for the Juan de Fuca plate because  $V$  and  $T$  for this region are not within the range of values originally used to establish empirical relation (1).

Since the subduction zones used to determine (1) have a subducting plate older than 10 My, there is some question as to whether (1) applies to the very young Juan de Fuca plate. A recent study by Singh et al. (1985), however, demonstrates that the 1932 Jalisco, Mexico, earthquake ( $M_s = 8.2$ ) occurred on the boundary between the very young (9 My) Rivera plate and the North American plate. This boundary is geometrically similar to that between the Juan de Fuca plate and the North American plate.

#### *The Ratio of Seismic Slip to Plate Motion*

Another important element in the long-term prediction of earthquakes is the repeat time. In principle, if the convergence rate  $V$ , average slip of the characteristic earthquake  $\bar{D}$ , and the ratio of seismic slip to total plate motion  $\eta$  are known, we can calculate the repeat time  $\tau$  by

$$\tau = \bar{D} / \eta V \quad (5)$$



Although  $V$  and  $\bar{D}$  are known reasonably well for various subduction zones, a large uncertainty is involved in  $\eta$ . For some subduction zones, such as South Chile, Kurile, N.E. Japan, Mexico and the Marianas, estimates by different investigators agree reasonably well. Kanamori (1977b) obtains  $\eta = 1.0, 0.25, 0.04$  and  $0.0$  for Chile, Kurile, N.E. Japan and the Marianas respectively. Peterson and Seno's (1984) estimates are  $0.36, 0.24$  and  $0.01$  for the Kuriles, N.E. Japan and the Izu-Bonin-Marianas respectively. Sykes and Quittmeyer (1981) calculate  $\eta$  using Shimazaki and Nakata's (1980) time predictable model, and obtain  $\eta = 0.62$  to  $0.91, 0.30$  to  $1.05, 0.29$  to  $0.38$  and  $0.32$  to  $0.56$  for Chile, Kuriles, N. Japan and Mexico respectively.

However, for some other subduction zones, the estimate of  $\eta$  is very uncertain because of either the lack of reliable historical data or the variable rupture length of large earthquakes at a given subduction zone. The latter problem is best illustrated by earthquake sequences observed along the Nankai Trough (Southwest Japan), the Ecuador-Colombia Coast, and the Aleutian Islands. For the Nankai Trough, as demonstrated by Imamura (1928) and Ando (1975), a long segment broke in a single large earthquake in 1707 and in two large events spaced closely in time in 1854, while the same segment broke in two smaller earthquakes in 1944 and 1946. For the Ecuador-Colombia coast, the rupture zone of the great 1906 earthquake has been ruptured in three smaller earthquakes that occurred in 1942, 1958 and 1979 (Kanamori and McNally, 1982).

In these cases, the estimate of the repeat time  $\tau$  and  $\eta$  is very uncertain. Here we use a simple model described by Kanamori and McNally (1982) and Astiz and Kanamori (1984) to define and estimate  $\eta$ .

We model an interplate boundary at subduction zones by a distribution of discrete stress patches, here called asperities. The area  $S$  of an asperity determines the seismic moment  $M_0$  of the earthquake that occurs as a result of

failure of the asperity. Simple scaling relations similar to (2) suggest a relation  $M_0 \propto S^{3/2}$  if each asperity breaks independently. Several historical sequences of great earthquakes (e.g. Nankai Trough events and Ecuador-Colombia events mentioned earlier) suggest that occasionally more than one asperity break simultaneously and produce an event larger than expected by failure of single asperity. Kanamori and McNally (1982) show that for the Ecuador-Colombia sequence, the seismic moment of the event that involves multiple asperities is significantly larger than the sum of the moments of the event associated with each asperity. They suggest that the effective width of the rupture zone varies from sequence to sequence even at the same location.

In many of the previous studies, the width of the rupture zone is assumed constant both in time and space. In this case the ratio of seismic slip to total plate motion  $\eta$  is defined by

$$\eta = \frac{\sum(M_{oi} / S_i)}{\mu V t} = \frac{\sum(M_{oi} / L_i)}{\mu W V t} \quad (6)$$

where  $t$  is the total length of the time period studied,  $W$  is the constant fault width,  $L_i$  is the fault length and  $M_{oi}$  is the seismic moment of the  $i$ -th event. The summation is taken over all the events during the time period  $t$ .

In contrast, if the effective fault width is not constant, the fault area of the  $i$ -th event can be estimated by (2):

$$S_i = \xi^{-2/3} M_{oi}^{2/3} \quad (7)$$

Substituting this into (6), we obtain

$$\eta = \frac{\xi^{2/3}}{\mu V t} \sum M_{oi}^{1/3} \quad (8)$$

We define the average moment,  $\bar{M}$ , by

$$\bar{M} = \left[ \frac{1}{N} \sum M_i^{1/3} \right]^3 \quad (9)$$

where  $N$  is the number of events during  $t$ . Using the magnitude-moment relation  $\log M_0 = 1.5 M_w + 18.1$ , we rewrite (9) in terms of the magnitude

$$\bar{M}_w = 2 \log \left[ \frac{1}{N} \sum 10^{0.5 M_{wi}} \right] \quad (10)$$

where  $\bar{M}_w$  is the average magnitude and  $M_{wi}$  is the magnitude of the  $i$ -th event. Using (8), (9) and (10), we obtain

$$\eta = \frac{\xi^{2/3}}{\mu V \tau} \bar{M}_0^{1/3} = \frac{\xi^{2/3}}{\mu V \tau} 10^{0.5 \bar{M}_w + 5.37} \quad (11)$$

where  $\tau$  is the average repeat time.

To accurately estimate  $\bar{M}_0$  and  $\tau$ , several sequences of great earthquakes for an individual subduction zone are needed. Unfortunately, for most subduction zones, only two sequences are known; consequently estimates of  $\bar{M}_0$  and  $\tau$  are very uncertain. If the seismic moment of the events is the same from sequence to sequence, (11) is identical to the conventional formula (6). However, if the size of the event is different from one sequence to another, (11) yields a value different from that obtained by the conventional method.

Although the model is obviously oversimplified, we use it to handle the situation where the size of the event is significantly different from sequence to sequence. Table 1 shows the results for various subduction zones. The details of the calculation for the individual events are given in the footnote.

Figure 5 shows the values of  $\eta$  as a function of the age of the subducting plate  $T$ . Although it is quite possible that the value of  $\eta$  depends on various other factors such as the convergence rate, upper plate velocity, roughness of

the oceanic and upper plate, and the thickness of the sediment, Figure 5 shows only the effect of  $T$  on  $\eta$ . Because of the very limited seismicity data, this result should be considered tentative. Nevertheless it is interesting to note that subduction zones with a relatively young subducting plate, ranging from 20 to 60 M years, have a value of  $\eta$  very close to 1, indicating that interplate slip is predominantly seismic. For subduction zones with a very old plate, such as the Marianas and N. Japan  $\eta$  is very small indicating that the plate is almost decoupled. The two largest normal-fault earthquakes, the 1933 Sanriku earthquake (Kanamori, 1971) and the 1977 Sumbawa earthquake (Stewart, 1978; Given and Kanamori, 1980), occurred in plates 120 to 140 M years old indicating that these events may be due to plate decoupling. Here, our main interest is in subduction zones with a very young ( $0 \sim 20$  M years) plate. The Mexican subduction zone is such an example. For Mexico, the results of several investigators, including Sykes and Quittmeyer (1981) and Astiz and Kanamori (1984) all indicate that  $\eta$  is about 0.5.

Since the interplate deformation is most likely to be aseismic as  $T \rightarrow 0$ , one would expect a value of  $\eta$  that is significantly smaller than 1 for  $T$  less than 20 M years. The dotted curve in Figure 5 roughly indicates the trend exhibited by the data. If this trend is applicable to all the subduction zones, the Juan de Fuca subduction zone ( $T \sim 10$  to 15 M years) may have a relatively small value of  $\eta$ , around 0.3.

## References

- Abe, K., Reliable estimation of the seismic moment of large earthquakes, *J. Phys. Earth.*, **23**, 381-390, 1975.
- Ando, M., Source mechanisms and tectonic significance of historical earthquakes along the Nankai Trough, Japan, *Tectonophysics*, **27**, 119-140, 1975.
- Astiz, L., and Kanamori, H., An earthquake doublet in Ometepepec, Guerrero, Mexico, *Phys. Earth Planet. Inter.*, **34**, 24-45, 1984.
- Given, J. W., and Kanamori, H., The depth extent of the 1977 Sumbawa Indonesia earthquake, abstract, *EOS*, **61**, 1044, 1980.
- Heaton, T. H., and Kanamori, H., Seismic potential associated with subduction in the Northwestern United States, *Bull. Seismol. Soc., Am.*, **74**, in press, 1984.
- Imamura, A., On the seismic activity of central Japan, *Japanese J. Astron. Geophys.*, **6**, 119-137, 1928.
- Kanamori, H., Seismological evidence for a lithospheric normal faulting - the Sanriku earthquake of 1933, *Phys. Earth Planet. Inter.*, **4**, 289-300, 1971.
- Kanamori, H., The energy release in great earthquakes, *J. Geophys. Res.*, **82**, 2981-2987, 1977a.

- Kanamori, H., Seismic and aseismic slip along subduction zones and their tectonic implications, in Island Arcs, Deep Sea Trenches and Back-Arc Basins, Maurice Ewing Series, edited by M. Talwani and W. C. Pittman, American Geophysical Union, Washington, D. C., 163-174, 1977b.
- Kanamori, H., Rupture process of subduction-zone earthquakes, *Ann. Rev. Earth Planet. Sci.*, 14, 293-322, 1986.
- Kanamori, H., Astiz, L. 1985. The 1983 Akita-Oki earthquake ( $M_w=7.8$ ) and its implications for systematics of subduction earthquakes. *Earthquake Prediction Research*, 3, 305-317, 1985.
- Kanamori, H., and Given, J. W., Use of long-period surface waves for rapid determination of earthquake-source parameters, *Phys. Earth Planet. Inter.*, 27, 8-31, 1981.
- Kanamori, H., and McNally, K. C., Variable rupture mode of the subduction zone along the Ecuador-Colombia coast, *Bull. Seismol. Soc. Am.*, 72, 1241-1253, 1982.
- Lay, T., Kanamori, H., and Ruff, L., The asperity model and the nature of large subduction zone earthquakes, *Earthquake Prediction Research*, 1, 3-71, 1982.
- Molnar, P., Atwater, T. 1978. Inter-arc spreading and cordilleran tectonics as alternates related to the age of subducted oceanic lithosphere. *Earth Planet. Sci. Lett.* 41:330-40

- Peterson, E.T., and T. Seno, Factors affecting seismic moment release rates in subduction zones, *J. Geophys. Res.*, 89, 10233-10248, 1984.
- Ruff, L., and Kanamori, H., Seismicity and the subduction process, *Phys. Earth Planet. Inter.*, 23, 240-252, 1980.
- Seno, T., and Eguchi, T., Seismotectonics of the Western Pacific, in Geodynamics of the Western Pacific Indonesian Region, edited by T. W. C. Hilde and S. Uyeda, *Geodynamic Ser.*, 11, 5-46, Am. Geophys. Union and Geological Soc. Amer., 1983.
- Shimazaki, K., and Nakata, T., Time-predictable recurrence model for large earthquakes, *Geophys. Res. Lett.*, 7, 229-282, 1980.
- Singh, S. K. Ponce, L., Nishenko, S. P. 1985. The great Jalisco, Mexico, earthquake of 1932 and the Rivera subduction zone, *Seismol. Soc. Am. Bull.* 75, 301-313.
- Stewart, G., Implications for plate tectonics of the August 19, 1977, Indonesia decoupling normal fault earthquake, abstract, *EOS*, 59, 326, 1978.
- Sykes, L. R., and Quittmeyer, R. C., Repeat times of great earthquakes along simple plate boundaries, in Earthquake Prediction, An International Review, Maurice Ewing Series; 4, edited by D. W. Simpson and P. G. Richards, American Geophysical Union, Washington, D. C., 217-247, 1981.
- Uyeda, S., and Kanamori, H., Back-arc opening and the mode of subduction, *J. Geophys. Res.*, 84, 1049-1061, 1979.
- Vlaar, N. J., Wortel, M. J. R. 1976. Lithospheric aging, instability, and subduction. *Tectonophysics.* 32:331-51
- Wortel, M. J. R., Vlaar, N. J. 1978. Age-dependent subduction of oceanic lithosphere beneath western south America. *Phys. Earth Planet. Inter.* 17:201-08

TABLE 1

Rupture Zone	$M_w$	V, cm/year	$\tau$ year	$\eta$	T, My
Chile, 1960	9.5	11.1	123	1.0	20
S.W. Japan	8.4 <sup>(1)</sup>	3.8	119	0.88	25
Aleutian, 1965	8.5 <sup>(2)</sup>	8.5	59 <sup>(2)</sup>	0.89	60
Colombia, 1979	8.6 <sup>(3)</sup>	7.7	73 <sup>(3)</sup>	0.89	20
Kamchatka, 1952	9.0	9.3	215 <sup>(4)</sup> or 111	0.40 0.77	80
Oaxaca (Mexico)	7.75	7.3	51	0.51	10.~15
Tokachi-Oki, 1968	8.2	10.4	100	0.31	120
Tohoku, Japan	7.75	9.7	~ 800 <sup>(5)</sup>	0.033 <sup>(5)</sup>	130
Mariana	7.2	5.0	?	0.008 <sup>(6)</sup>	150

(1)  $M_w = 8.1$  for 1944 and 1946, and  $M_w \sim 8.6$  for 1854 and 1707 are used.

(2)  $M_w = 8.7$  for 1965 and  $M_s = 8.2$  for 1906 are used.

(3)  $M_w = 8.2$  for 1979 and  $M_w = 8.8$  for 1906 are used.

(4) The activity prior to 1952 is uncertain. The events in 1737 and 1841 may be similar to the 1952 event (see Lay et al. (1981) and Sykes and Quittmeyer (1981)).

(5) See Kanamori (1977b).

(6) Estimates by Seno and Eguchi (1983)



## Figure Captions

- Figure 1 The relation between the seismic moment release rate, MRR, (in  $10^{27}$  dyne-cm/(100km-100years) ) and  $M_w'$ . The data are taken from Peterson and Seno (1984) and Ruff and Kanamori (1980). Peterson and Seno's regionalization of the subduction zones is modified as follows (the first and the second names in the parentheses refer to Peterson and Seno's, and Ruff and Kanamori's respectively). (Peru-south, Peru),(average of Central America and Mexico, Central America), (Aleutian-east and Aleutian-west, Aleutian), (Nankai, S.W.Japan), (Japan, N.E.Japan).
- Figure 2 (a) The relation between convergence rate,  $V$ , and  $M_w'$ . The inter-arc spreading is not included in the calculation of  $V$ . (b) The relation between the age of the subducting slab and  $M_w'$ . For both (a) and (b), the data are taken from Ruff and Kanamori (1980), and the closed and open symbols indicate subduction zones with and without active back-arc opening.
- Figure 3 The relation between  $M_w'$  calculated from  $T$  and  $V$  using the relation  $M_w' = -0.00953T + 0.143V + 8.01$  and the observed  $M_w'$ . Closed and open symbols indicate subduction zones with and without active back-arc opening.
- Figure 4 Schematic figure showing the plate geometry of the Juan de Fuca subduction zone. Triangles indicate active volcanoes.
- Figure 5 The ratio of seismic slip to total plate motion, as a function of the age of the subducting plate (after Kanamori and Astiz 1985). Two largest lithospheric normal-fault earthquakes, 1933 Sanriku and 1977 Sumbawa earthquakes, occurred in the lithospheres of 120 and 140 My old.

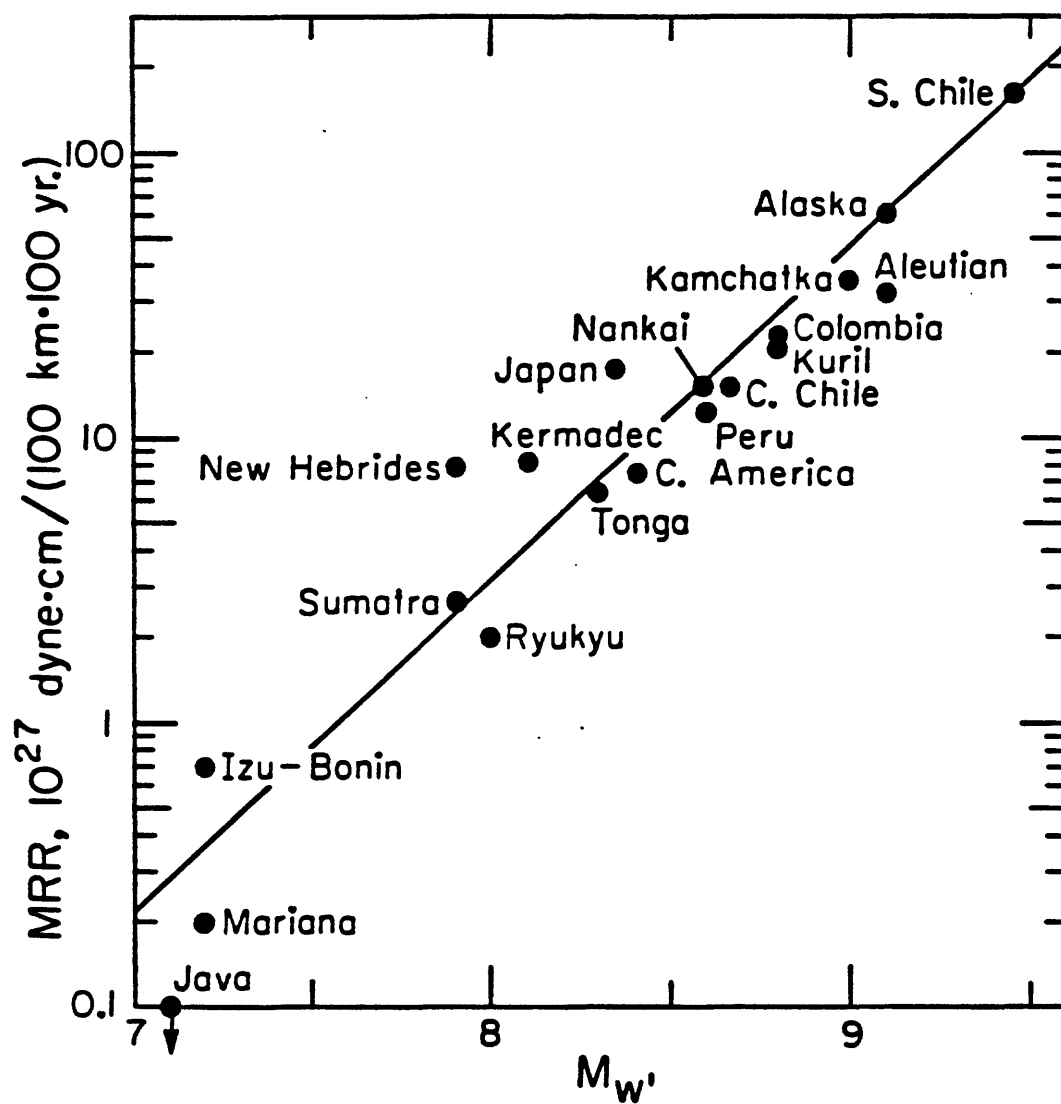


*Fig. 1*

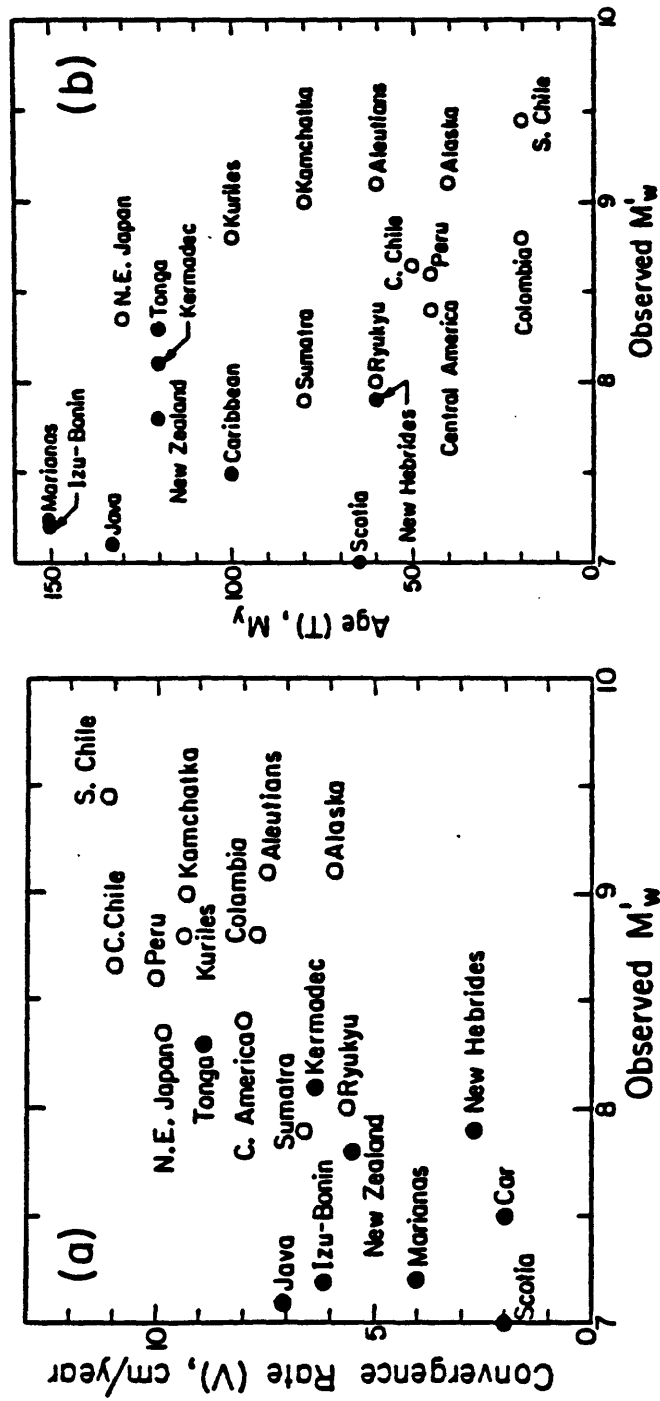
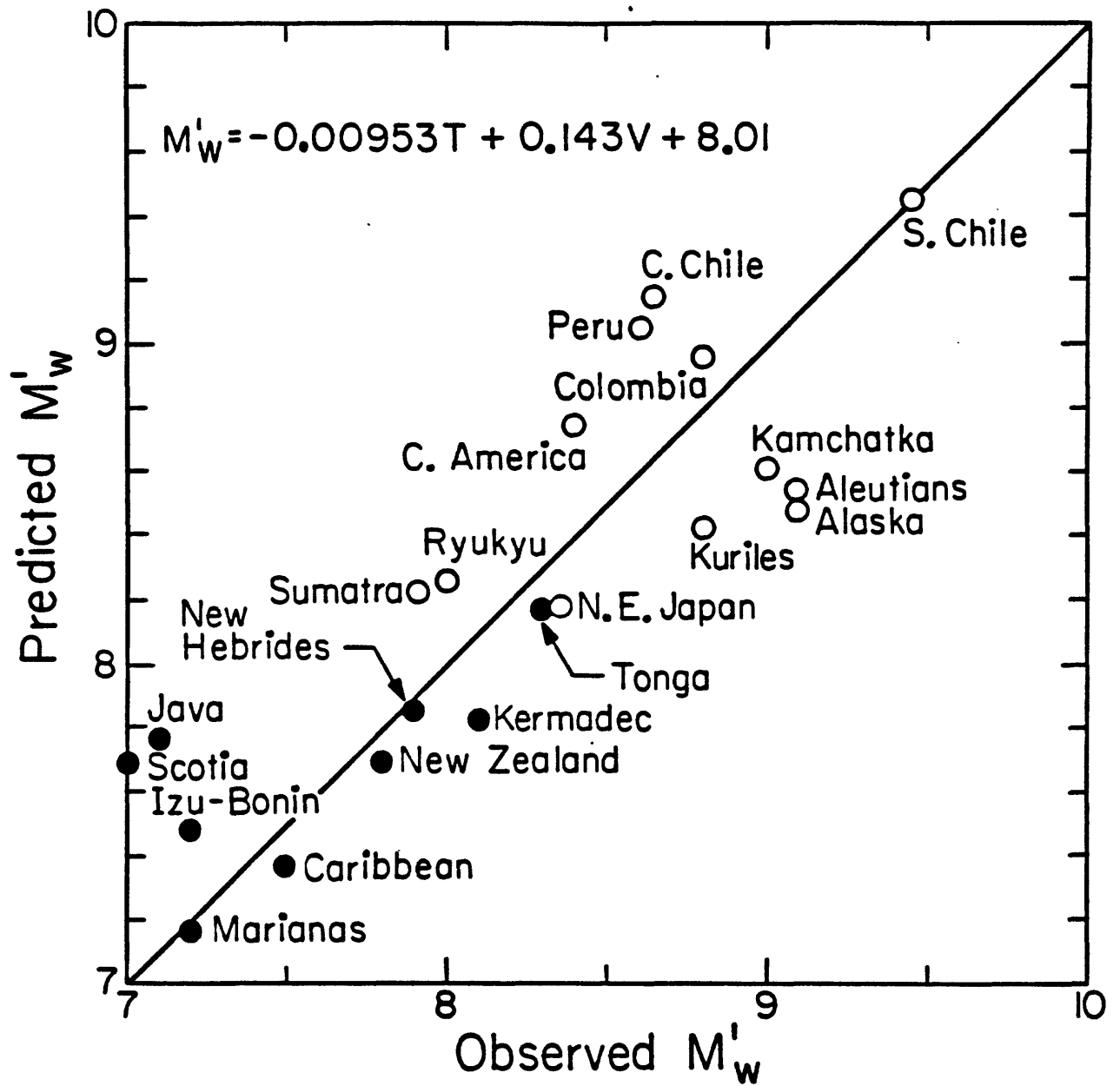
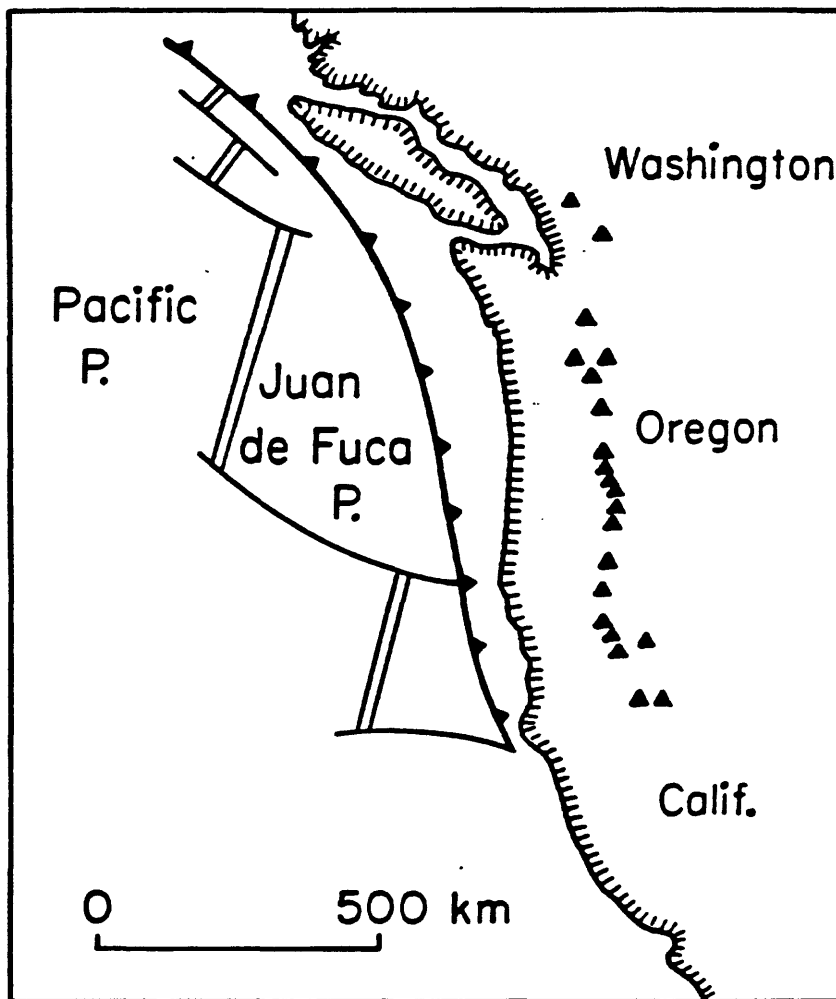


Fig. 2



*Fig. 3*



*Fig. 4*

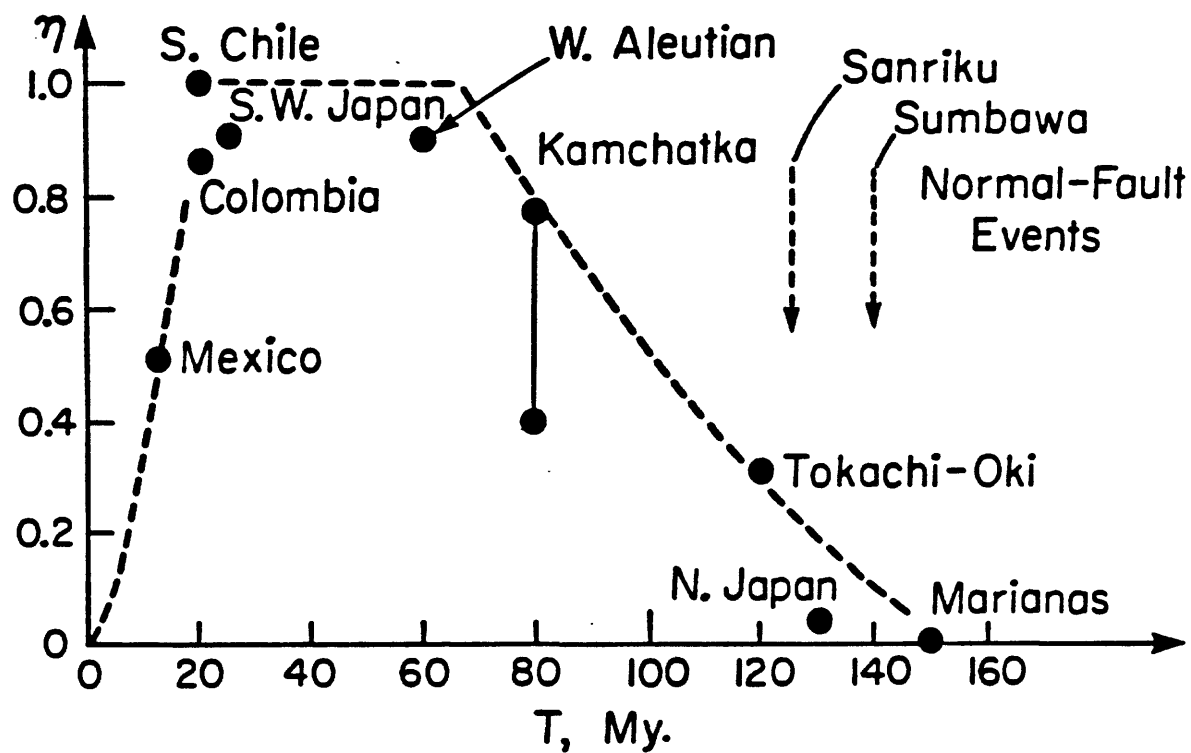


*Fig. 5*

APPENDIX A. 3.

Seismicity and Structure of the Cascadia Subduction Zone

by

R. S. Crosson

## Seismicity and Structure of the Cascadia Subduction Zone

R.S. Crosson  
Geophysics Program AK-50  
University of Washington  
Seattle, WA 98195  
(202) 543-8020

### Introduction

In this summary we will highlight recent developments in understanding the structure and seismicity of the Cascadia subduction zone. High quality hypocenters have been combined with structure interpretation from receiver functions, refining our understanding of the structure of the subducted slab beneath western Washington. Constraints on slab structure from refraction and deep reflection profiles to the north (British Columbia) and south (Oregon) have also been utilized. Supporting evidence is found in an analysis of focal mechanisms. More complete review of the literature as well as detail of our analysis will be found in the published literature or articles in preparation for publication. (Crosson and Owens, 1987; Owens and Crosson, 1987; Owens et al., 1987; Ma et. al., 1987; Crosson et. al., 1987).

### Seismicity and Structure

Seismicity has been an important factor in the analysis of the structure of subduction zones. Mapping out the variations in Benioff zone structure, for example, has been used to determine slab shape. In the case of the Cascadia subduction zone (CSZ), seismicity is only helpful in the vicinity of the Puget Sound region of western Washington where significant slab seismicity is found. Fig. 1 from the NOAA catalog shows the major activity of the Juan de Fuca (JDF) plate and vicinity. At the level of this catalog, the majority of the subduction zone is quiet, having activity in neither the overlying continental plate nor the subducted slab. No topographic trench is evident, but the hingeline of the subducting Juan de Fuca plate parallels the coast of Washington and Vancouver Island. Fig. 1 illustrates the change in direction of the CSZ from nearly NS along the Oregon margin to N30E along Vancouver Island. This feature requires a deformation of the subducting JDF plate merely from geometrical considerations (Rogers, 1983). Such deformation could be accommodated by plate arching (Dickenson, 1970), crinkling (Rogers, 1983), or tearing (Michaelson and Weaver, 1986).

Refraction and deep reflection have revealed the slab configuration at a few places along the CSZ. Fig. 2 is a key refraction profile from Taber, 1983. This profile was obtained on the Washington margin at a point near Grays Harbor. In Taber's interpretation the slab dip is about  $10^\circ$  eastward. However, the actual data (circles at top) suggests a slightly larger dip. An adjusted dip of  $16^\circ$  is required to fit the data exactly, suggesting that the initial slab dip is somewhat steeper than interpreted by Taber (1983). Similarly, Lithoprobe studies (Green et al., 1986) in Vancouver Island and COCORP studies in Oregon (Keach et al., 1986) indicate slab dips in the range of  $15$ - $20^\circ$  normal to the "trench" (note that there is no physiographic trench along the CSZ). To examine what the seismicity tells us about the slab structure beneath Puget Sound, we have selected a subset of the most accurately located hypocenters. These are described in the more detail elsewhere (Crosson and Owens, 1987). Since depth control is critical to our interpretation, we show the depth standard errors computed for the approximately 5,000 selected earthquakes in Fig. 3. Events with standard depth errors greater than 4 km were excluded. The resulting distribution has relative uncertainties small enough to ensure accurate delineation of structure at the regional scale.

Fig. 4 shows epicenters of all selected earthquakes. Active zones in the St. Helens and Mt. Ranier regions are apparent. These are mostly shallow crustal ( $\leq 10$ km depth) events. The scattered clusters in the central Puget Sound region are at both crustal (continental plate) and



subcrustal (subducted JDF slab) depths. Much detail is of course lost at this scale. Fig 5 is an EW cross section showing hypocenters of all earthquakes in the selected set. Clear separation is evident between the continental and slab activity. To the best of our present knowledge, virtually all of this activity is intraplate as opposed to interplate. No earthquakes of any size have been located to date which can be identified with slip on the megathrust separating the North American (NA) and JDF plates. We suggest that the megathrust lies in the quiet zone between the two distinct earthquake zones in Fig. 5.

To gain further insight into the slab earthquake distribution, a series of N-S cross-sections have been constructed. Fig. 6 shows selection corridors and Fig. 7 shows the corresponding cross-sections. All cross-sections are 1:1 vertical exaggeration, and north is to the right. Panels E-E', F-F', and G-G', which pick up the slab earthquakes starting from the eastern side, show clear evidence of a gentle upward arching of the slab. We have constructed paper and metal analog models to explore what shapes the slab might take to minimize surface areal strain while accommodating the change in trench direction. These models indicate that an upward arch qualitatively similar to the model proposed by Dickenson (1970) is reasonable. We believe that the hypocenter data provides direct evidence for this structure.

Strong confirmation of the arch structure comes independently from work we have carried out using broadband stations south of the Olympic Mountains (Owens and Crosson, 1986). An eastward plunging arch in the subducted slab would produce slab dips to the southeast on the south flank of the arch. South of the Olympic Mountains at point A of Fig. 12, we have detected dips to the southeast of magnitudes consistent with the arch hypothesis. Fig. 8 shows the principles used to interpret broadband teleseismic P waveforms recorded on our temporary stations. At the top of Fig. 8, we see the effect of P waves arriving updip versus those from downdip directions for a 20° assumed slab dip. Downdip arrivals are nearly normal to the major velocity discontinuities in the slab (e.g., subducted oceanic Moho) and thus produce little Ps conversion. Updip arrivals, by comparison, efficiently produce Ps conversions which may be detected in source-equalized radial seismograms (i.e. receiver functions; Owens et al., 1987). At the bottom of Fig. 8 theoretical and actual receiver functions illustrate this effect. Fig. 9 is a sensitivity study calculated by Tom Owens for a hypothetical dipping slab. It shows how the Ps phase off of the dipping oceanic Moho is particularly sensitive both in arrival time and amplitude to the direction of wave arrival. Fig 10 shows how this effect was modeled at our initial western Washington site for the two main backazimuths (SE and SW) for which data were obtained. (see Owens and Crosson, 1987; Owens et al, 1987).

To construct contour maps on the dipping slab, we utilized both seismicity and the single broadband datum. We made the assumption that the top of the seismogenic layer was approximately the subducted oceanic Moho. This assumption produced the geometrically most satisfactory results, but if incorrect will not drastically change our results. Fig. 11 shows how the 50 km contour was constructed. Epicenters of earthquakes in the 45-50 km depth range were plotted along with strike and dip of the 37 km deep Moho datum determined from broadband data. Assuming eastward dip of the slab, the eastward edge of the epicenter pattern is contoured smoothly to reflect the arch structure. Fig. 12 shows the result including the broadband datum at point A and the epicenters of two large slab earthquakes, the 1949 magnitude 7.1 and the 1965 magnitude 6.5 Puget Sound earthquakes. The "trench" or slab hingeline location is shown approximately at the left of Fig. 12. This slab configuration reflects the dip results from Lithoprobe to the north and COCORP (central Western Oregon) to the south of Puget Sound.

## Discussion

Both the slab intraplate seismicity and the adjacent continental seismicity are concentrated at the location of the slab arch. This strongly suggests that the structure controls or induces earthquakes near or on the arch but that the "normal" parts of the subduction zone away from the arch are typically quiet or nearly aseismic. A few apparent slab earthquakes have been detected in southern British Columbia, southwest Washington, and western Oregon, but the rate of activity appears to be low for these regions.

Within the subducted slab, the arch may serve to localize seismicity by either concentrating plate bending stress, or by changing pressure and temperature conditions sufficiently in the slab to produce earthquakes. For example, along the axis of the arch, slab material stays cooler at lower pressure for relatively longer periods of time, possibly keeping the slab in the brittle regime. Along the "normal" sections of the CSZ, the slab which is already young and relatively hot before it begins to subduct rapidly reaches the brittle-ductile transition and becomes aseismic. Also, the slab may be subject to less internal deformation along these normal sections.

Concentration of seismicity in the North American plate above the slab arch is more difficult to explain. If the NA plate is in relatively uniform compressional stress along the entire CSZ, then one possibility is that the arch locally reduces the elastic thickness of the lithosphere above the arch, producing a stress concentration. This idea is generally consistent with our study of focal mechanism data (Ma and Ludwin, 1987).

Fig. 13 shows a comparison of P and T axes from continental and slab earthquakes. There is clear evidence of stress decoupling between these two sets of earthquakes. The continental data are consistent with average NS compression (both thrust and normal mechanisms). Slab earthquakes by contrast indicate P axes dominantly vertical (normal mechanisms) with T axes scattered to the NE and SE. Fig. 14 shows a set of directions to slab T axes according to their epicenter locations. There is a suggestion, although not clear, that these axes are oriented sub-normal to the main axis of the arch suggesting direct structural control by the slab geometry.

In summary, we believe that through the combination of several observations a first order picture of an uparched structure in the subducted JDF slab is emerging. This structure appears to be important in controlling slab seismicity, and promises to be of major significance to earthquake hazard estimation both from a purely geometric point of view and from the point of view of understanding the physical conditions and tectonics of the CSZ.

#### Acknowledgements

Ruth Ludwin assisted in preparation of this manuscript, and collaborated with the author and Ma Li in the collection and interpretation of focal mechanisms. Tom Owens collaborated in interpretation of the broadband data. Their contribution is gratefully acknowledged. Numerous individuals deserve acknowledgement for the operation and processing of the regional network data. Network operations are supported by U.S.G.S. Joint Operating Agreement 14-08-0001-A0266, U.S.G.S. Contract 14-08-0001-21978, and U.S. Dept. of Energy Contract DE-AM06-76RL02225. Matthew Hendrickson's assistance was crucial for the installation and operation of the initial broadband stations. The broadband work is being carried out under contract C-20142 with the Washington Public Power Supply. This report was prepared under U.S.G.S. grant 14-08-0001-G1390, for the evaluation of seismic hazards using network data.

## REFERENCES

- Crosson, R.S. and T.J. Owens, (1987). Structure of the subducted Juan de Fuca plate beneath western Washington, *Geophys. Res. Letts.*, in preparation.
- Dickenson, W. R., (1970). Relations of andesites, granites, and derivative sandstones to arc-trench tectonics, *Rev. Geophys.*, **8**, 813-860.
- Green, A.G., R.M. Clowes, C.J. Yorath, C. Spencer, E.R. Kanasewich, M.T. Brandon, and A.S. Brown, (1986). Seismic reflection imaging of the subducting Juan de Fuca plate, *Nature*, **319**, 210-213.
- Keach, R.W., C.J. Potter, J.E. Oliver, and L.D. Brown, (1986). Cenozoic active margin and shallow Cascades structure: COCORP results from western Oregon (abstract), *GSA Annual Meet.*, 652.
- Ma, L. and R.S. Ludwin, (1987). Can focal mechanisms be used to separate subduction zone from intra-plate earthquakes in Washington? (abstract), *EOS*, **68**, 46.
- Ma, L., R.S. Crosson, and R.S. Ludwin, (1987). Focal mechanisms and tectonic implications of western Washington earthquakes, *J. Geophys. Res.*, (in prep.).
- Michaelson, C. A. and C. S. Weaver, (1986). Upper mantle structure from teleseismic P-wave arrivals in Washington and norther Oregon, *J. Geophys. Res.*, **91**, 2077-2094.
- Owens, T.J. and R.S. Crosson, (1986). Teleseismic P-waveform modeling for deep structure in a subduction zone environment (abstract), *EOS*, **67**(44), 1116.
- Owens, T.J., R.S. Crosson, and M.A. Hendrickson, (1987). Constraints on the subduction geometry beneath western Washington from broadband teleseismic waveform modeling, *J. Geophys. Res.*, in preparation.
- Owens, T.J. and R.S. Crosson, (1987). Shallow structure effects on broadband teleseismic P-waveforms, *Bull. Seis. Soc. Am.*, Submitted.
- Rogers, G.C., *Seismotectonics of British Columbia*, Univ. British Columbia, Vancouver, 1983. Ph.D. thesis
- Taber, J.J., *Crustal structure and seismicity of the Washington continental margin*, University of Washington, 1983. Ph.D. Thesis

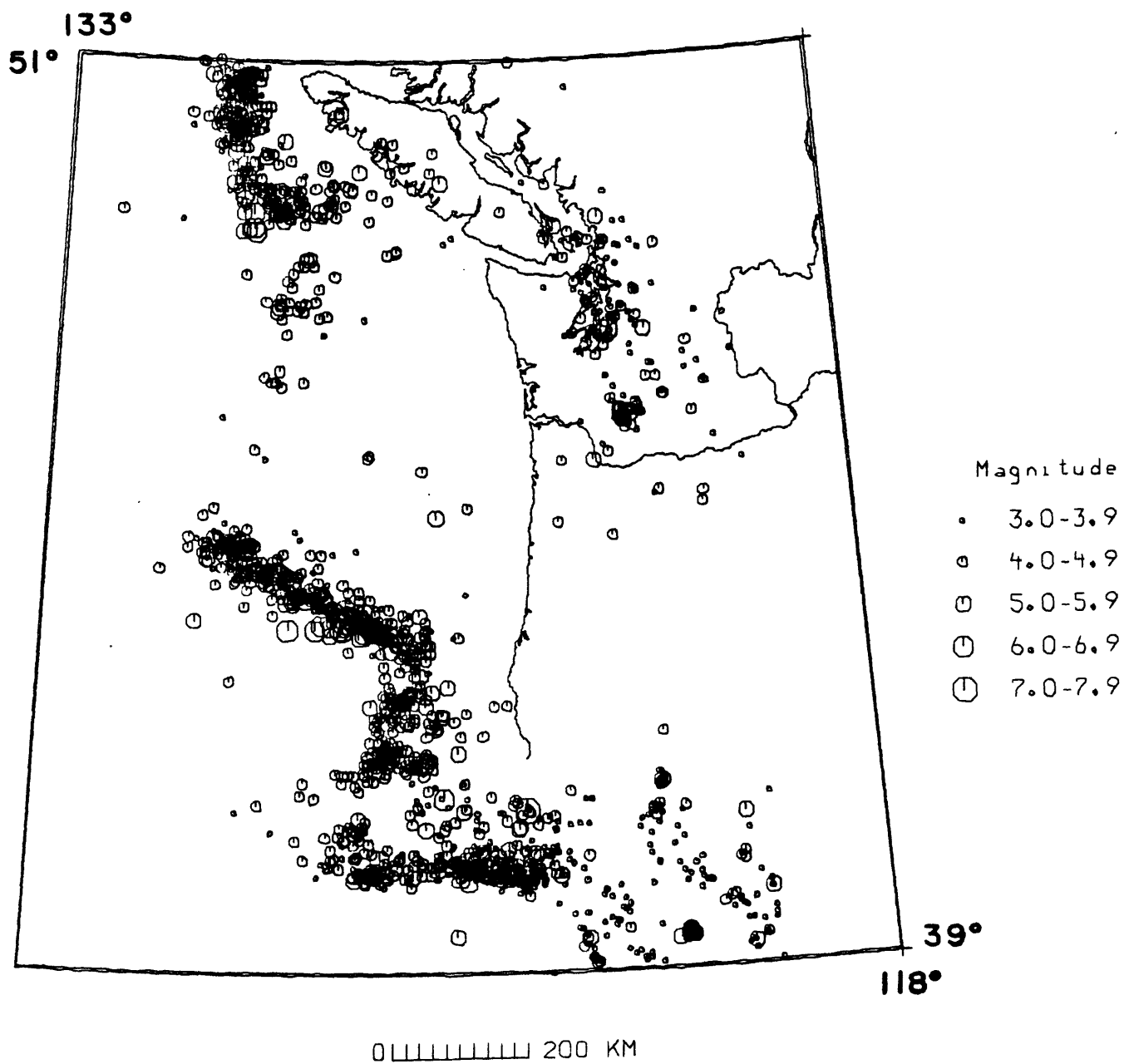


Figure 1. Map view of major seismicity related to the Juan de Fuca plate. Events from the NOAA catalog with magnitudes given as 3.0 or larger are included.

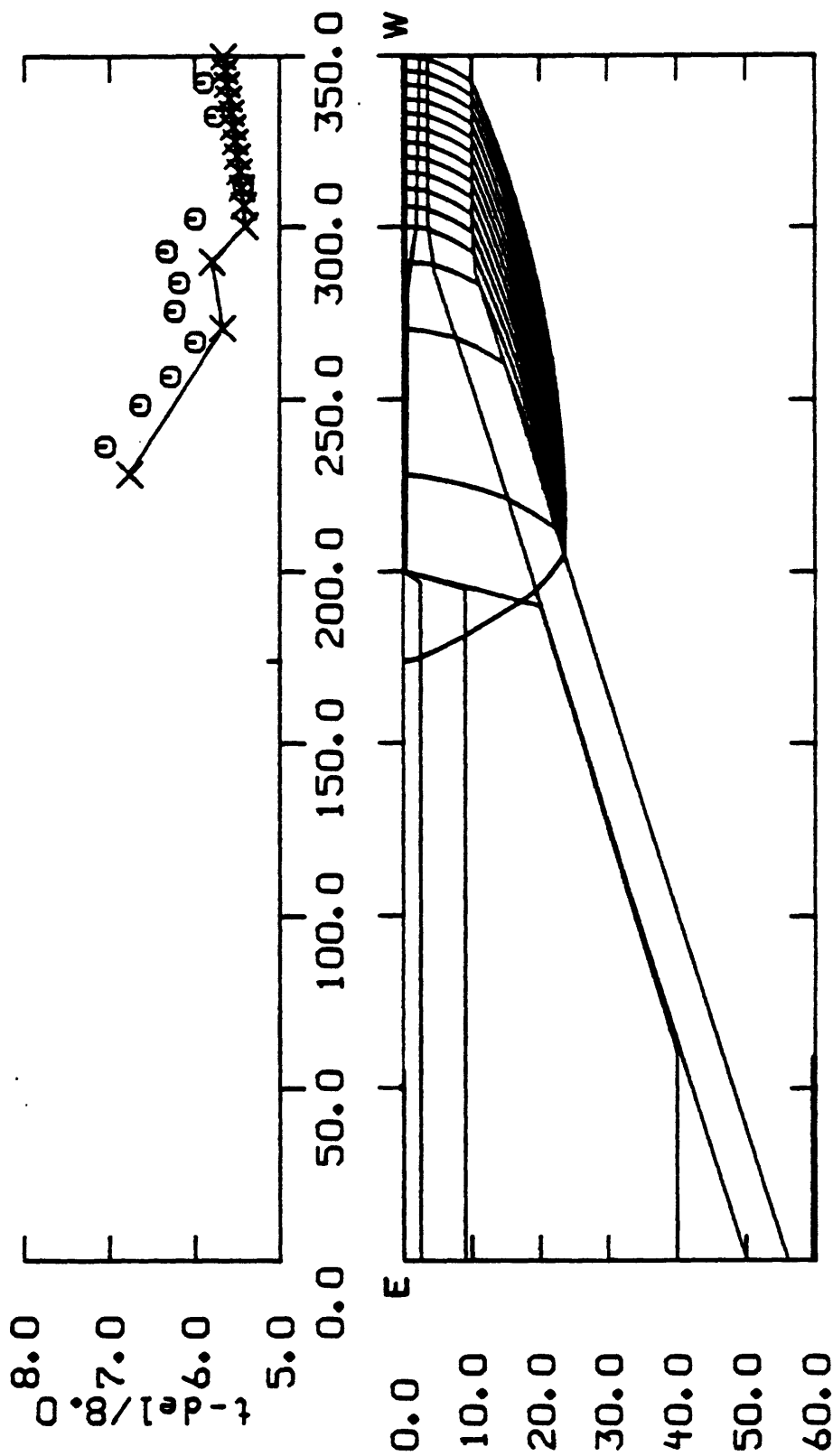


Figure 2. Refraction travel time profile (top) and structure interpretation (bottom) normal to the Washington coast from Taber (1983). The X's are points computed by raytracing and the O's are observations. Note that reduced travel-time is plotted. See Taber (1983) for velocities used in model.

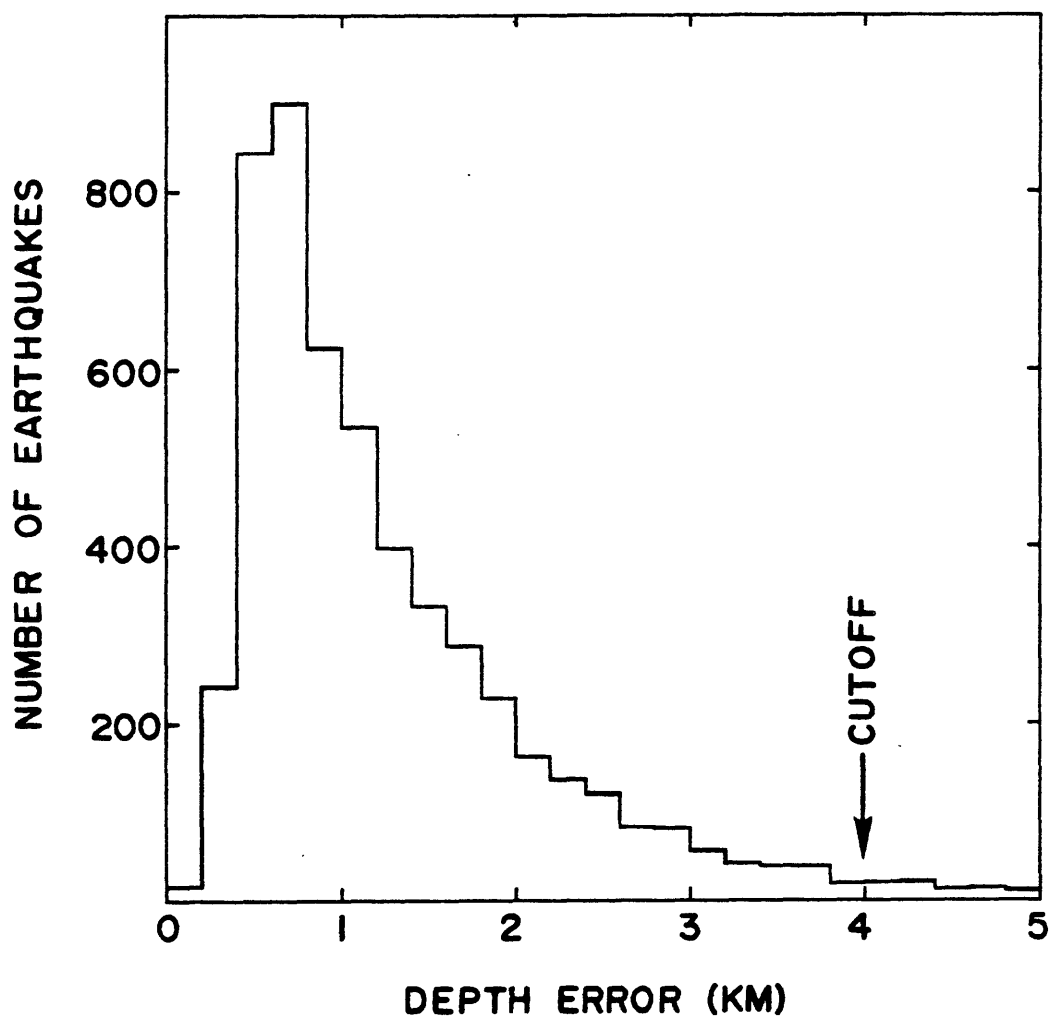


Figure 3. Distribution of standard errors in depth for the earthquakes shown in Figs. 4, 5, and 7.

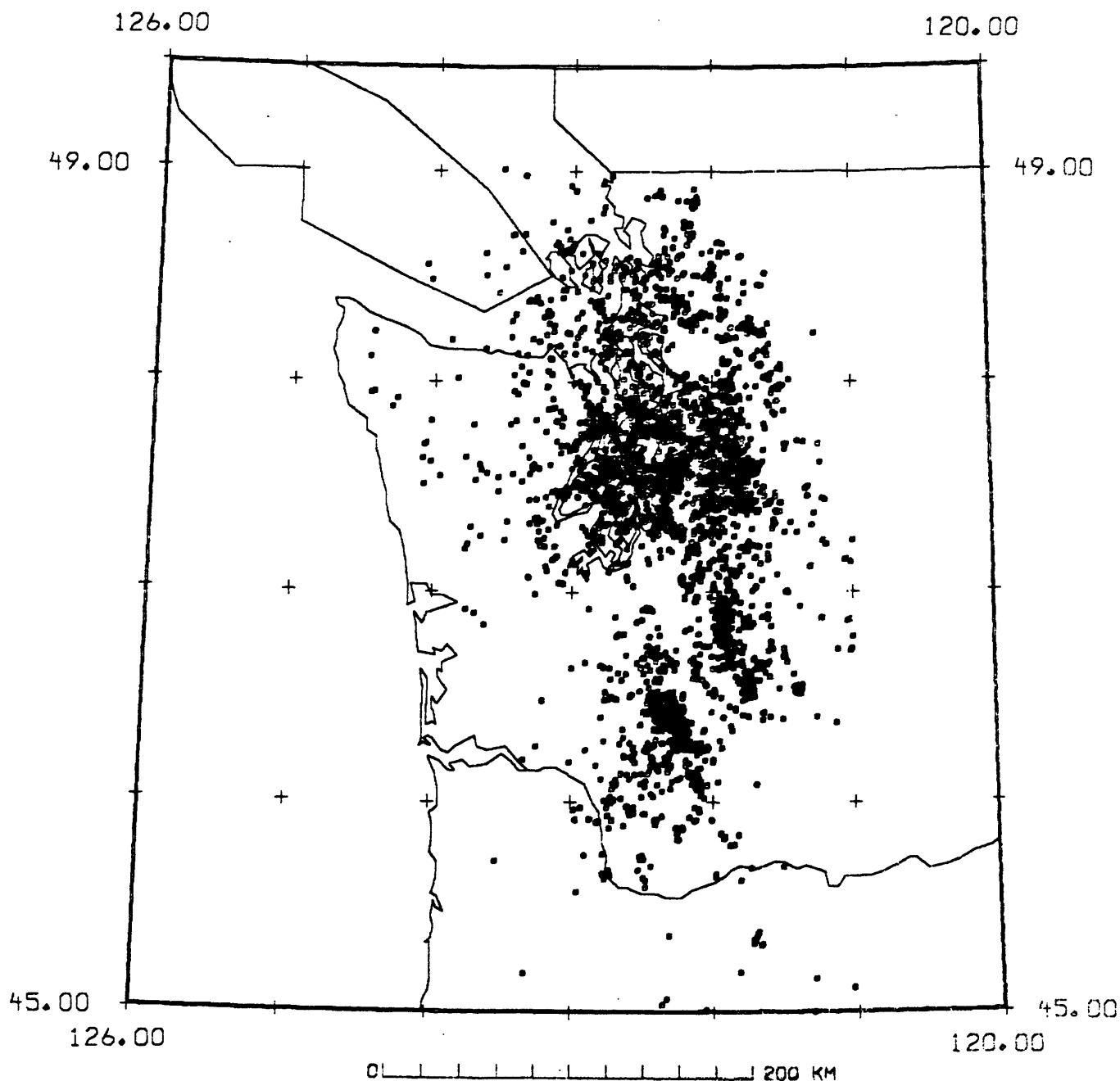


Figure 4. Epicenters of selected earthquakes in western Washington, 1970 - 1986. One symbol size is used for all events, regardless of magnitude. Criteria for selection: no known or suspected blasts, at least six P readings, one or more S readings, RMS residual less than 0.5 seconds, standard error in depth  $\leq 4.0$  km, horizontal standard error  $\leq 5.0$  km, azimuthal gap  $\leq 180^\circ$ , and distance to the nearest station  $\leq 50$  km.

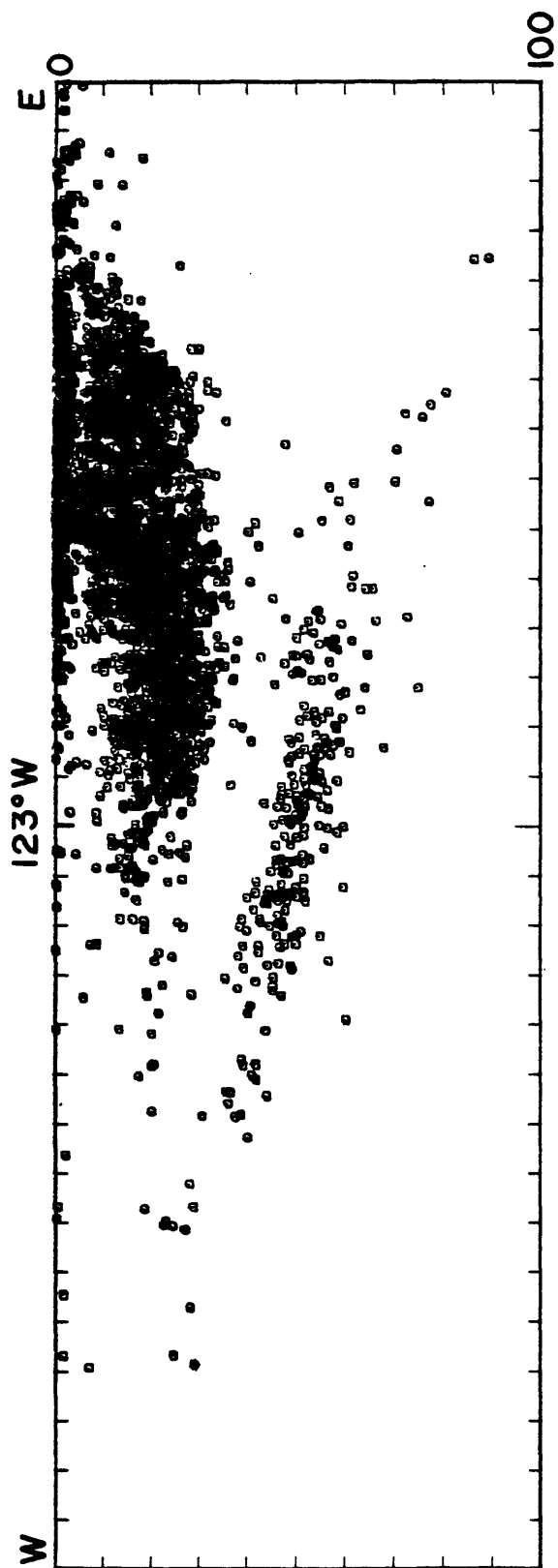


Figure 5. East-West cross-section of all data shown in Fig. 4. Center of plot is at 123°W and scale intervals are 10 km. One symbol size is used for all events. Cross section has no vertical exaggeration.



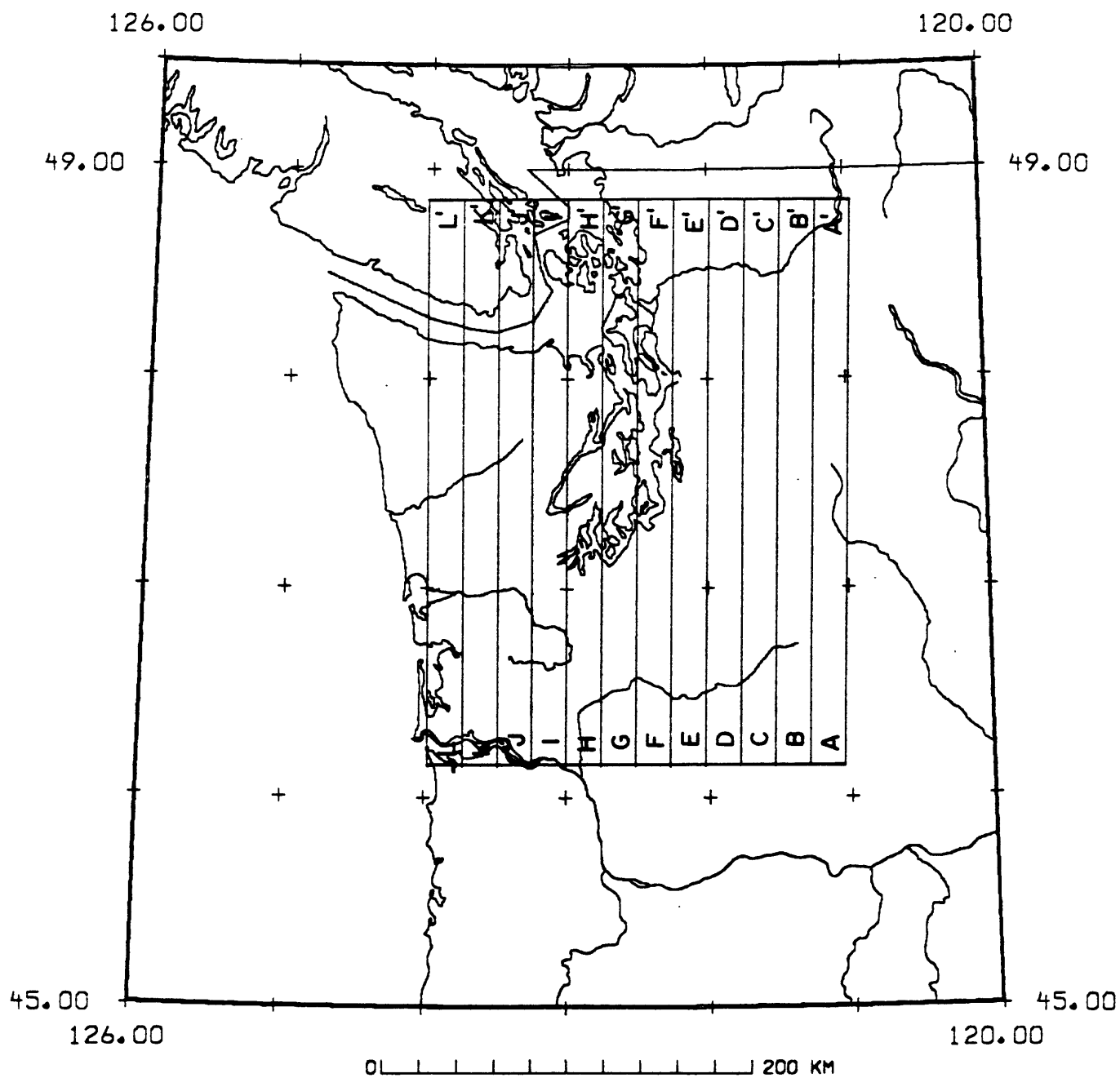
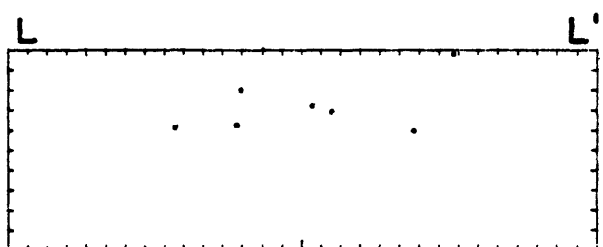
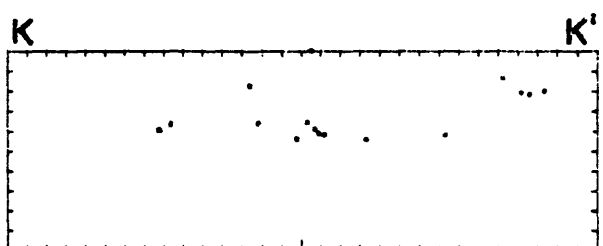
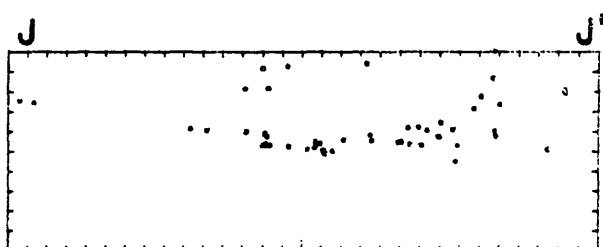
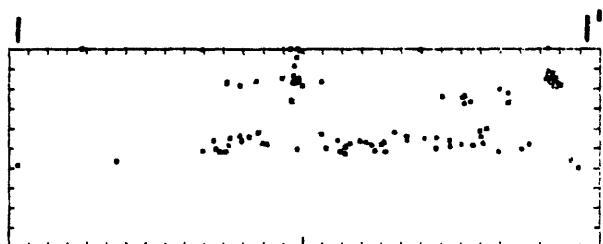
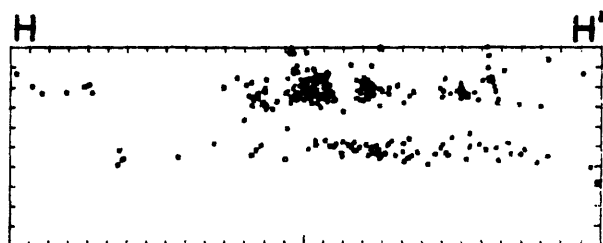
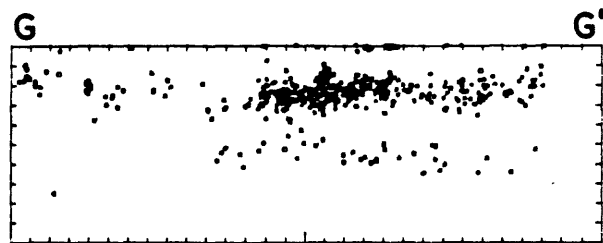
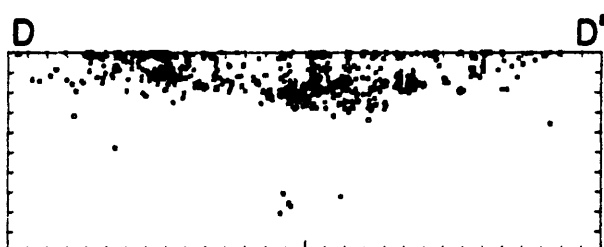
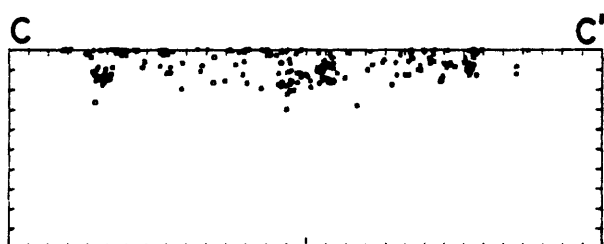
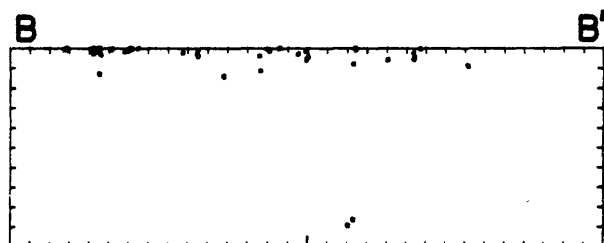
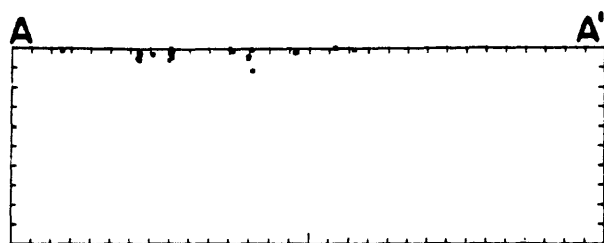


Figure 6. Map view showing selection regions for 12 cross-sections in Fig 7.

Figure 7. South to North cross sections of selected western Washington earthquakes (from Figs. 4 and 5). No vertical exaggeration, looking west; north is to the right.



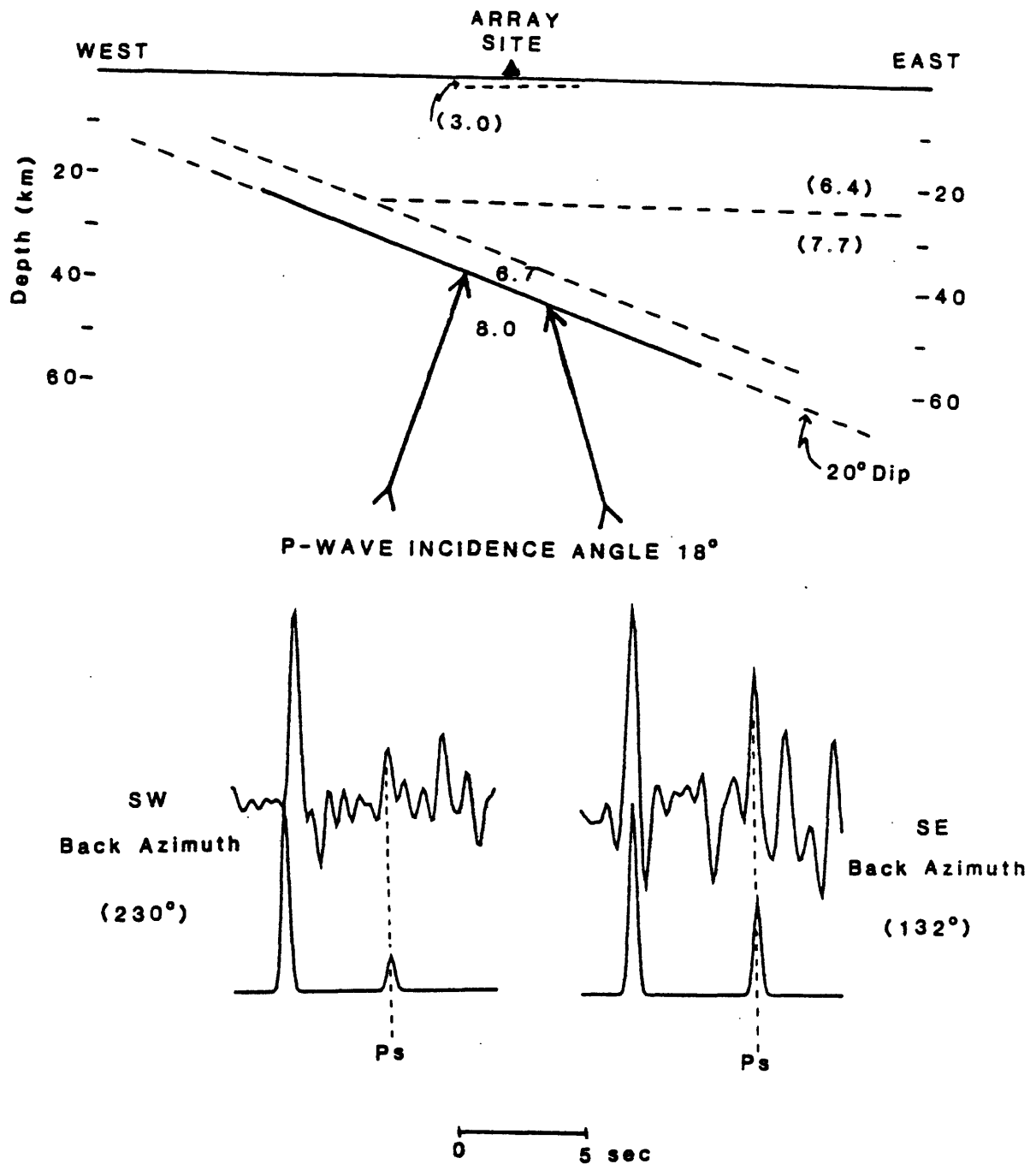


Figure 8. Top: Schematic cross section of a broad-band experiment to record P to S energy conversions arising from teleseismic P waves impinging on a subducting slab. Rays coming from down-dip direction will produce efficient P to S conversion, while rays coming from up-dip will produce less efficient conversion. Bottom: Theoretical and actual examples of receiver functions illustrating the effect described above.

## Ps PHASES FROM AN IDEALIZED SUBDUCTION ZONE

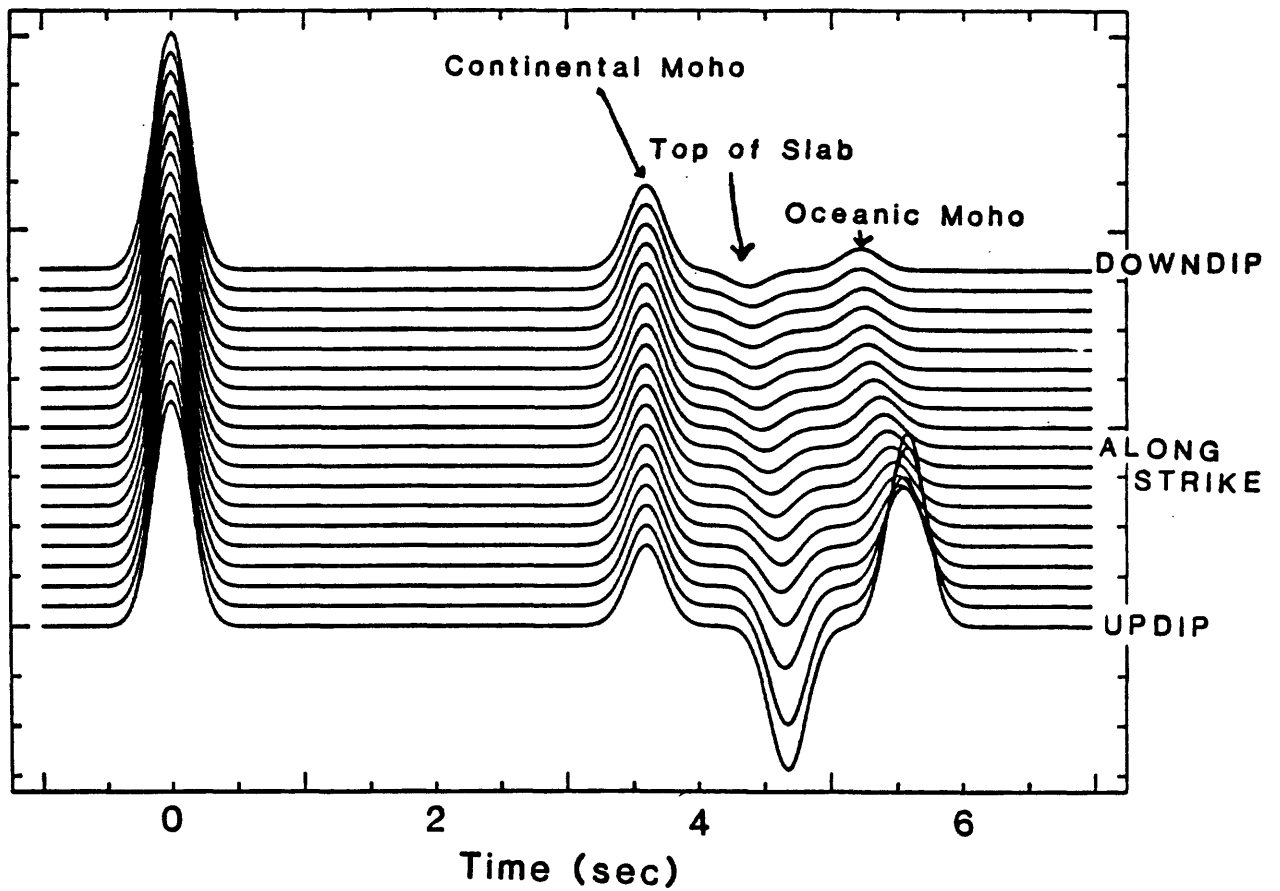


Figure 9. P to S conversions from an idealized subduction zone dipping about  $20^\circ$  illustrating effect of azimuth of teleseismic arrival relative to direction of slab dip.

# MODELED WAVEFORM FITS AT SITE 1 (NW)

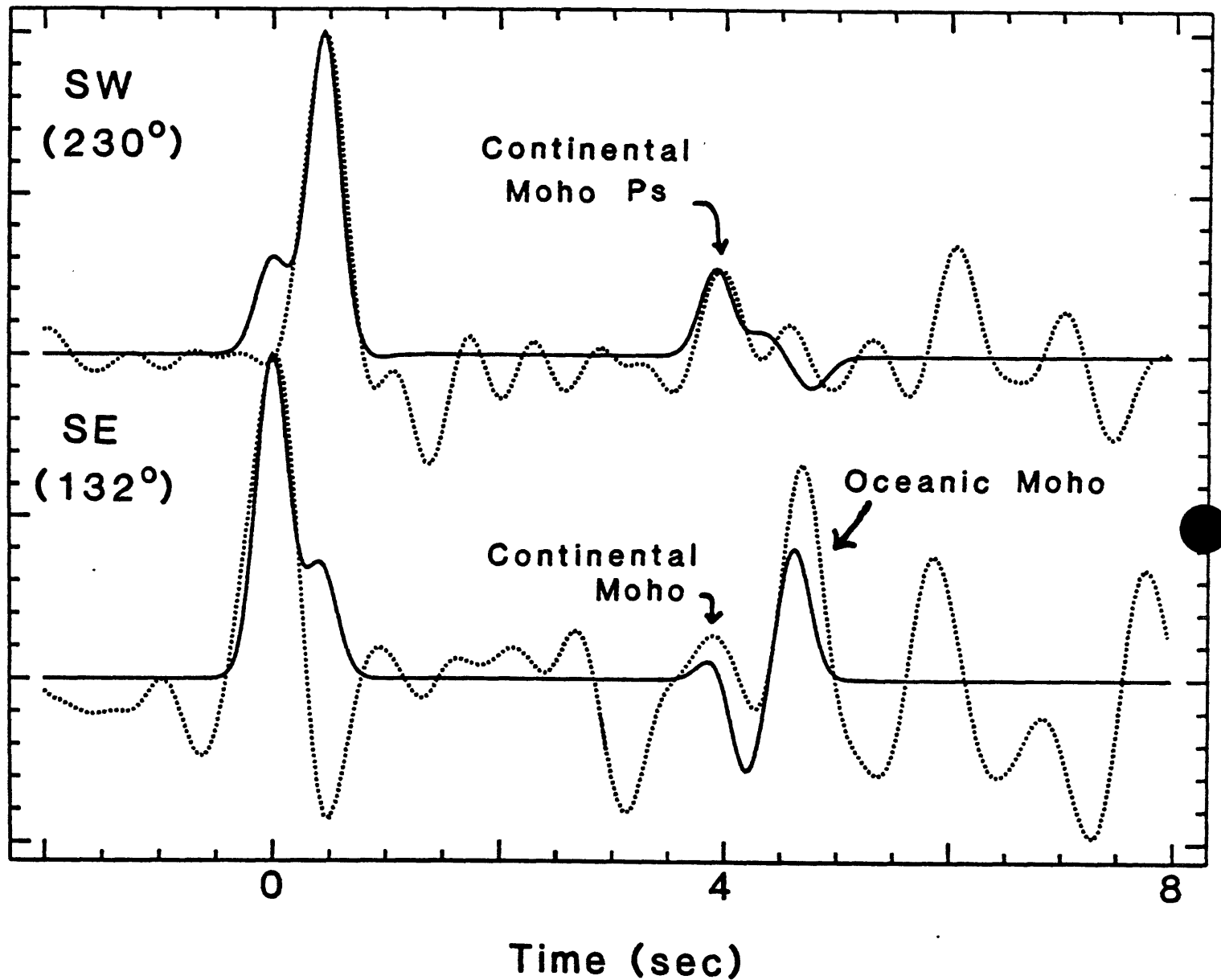


Figure 10. Results of receiver function modeling at one station in the Satsop network. Two back azimuths are shown. Dotted traces represent the average of stacked data, with path and source effects removed by deconvolution. Solid traces represent response to a theoretical slab model at 37 km depth beneath the array dipping at 25° at an azimuth of 125°.

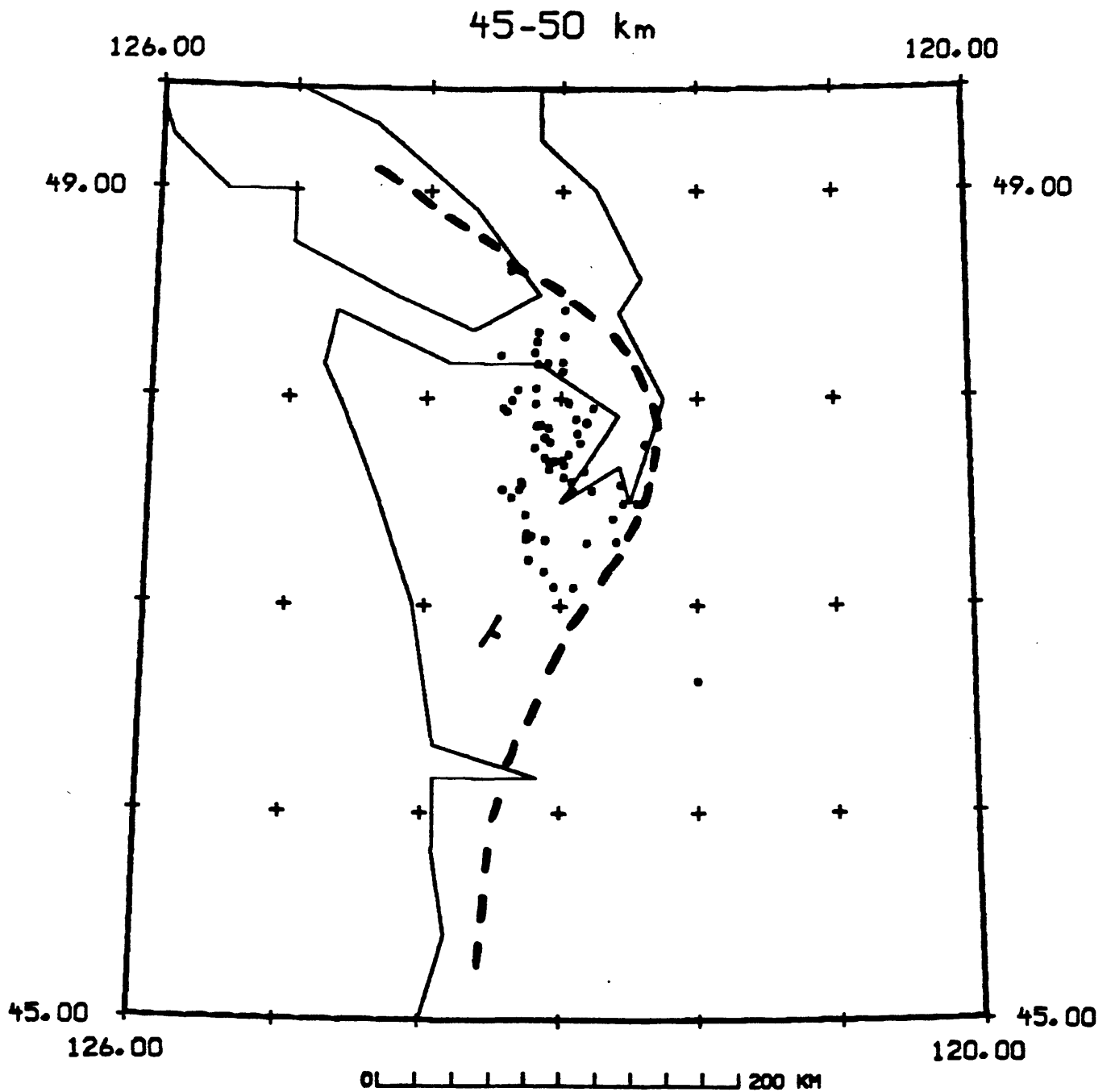


Figure 11. Construction of the 50 km depth contour of the subducted Juan de Fuca plate. Epicenters of earthquakes in the 45-50 km depth range are shown. The strike, dip, and depth (37 km) of the subducted Moho at the southern end of the Olympic Peninsula have been determined from broadband data. The eastward edge of the epicenter pattern is smoothly contoured.

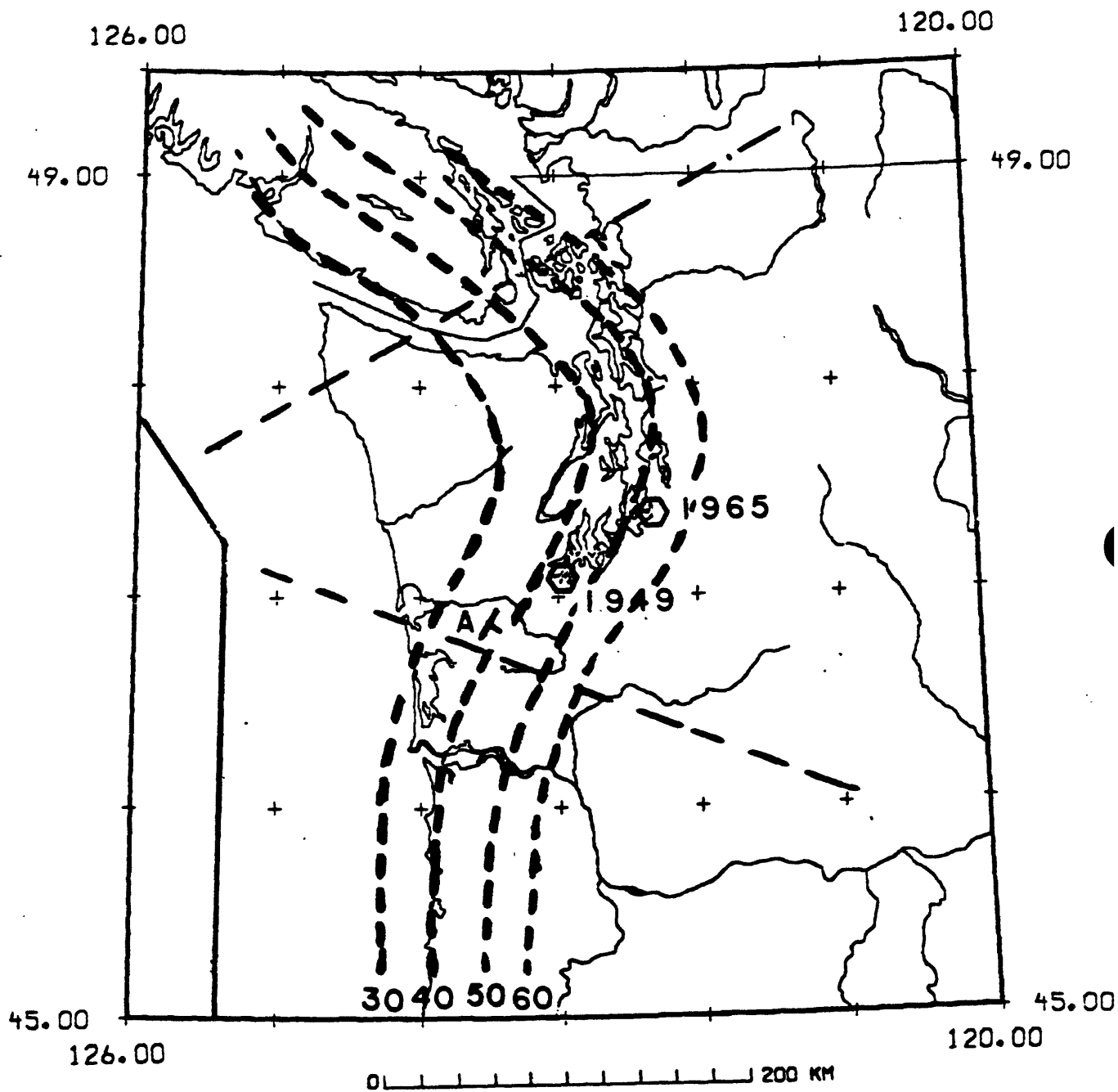


Figure 12. Preliminary depth contour map of the Moho in western Washington. Contour interval is 10 km. Point A is the position of the datum obtained from broadband network experiment. Epicenters of the 1949 and 1965 major slab earthquakes are shown with open hexagons. Langston's (1985) revised location of the 1949 earthquake is used.



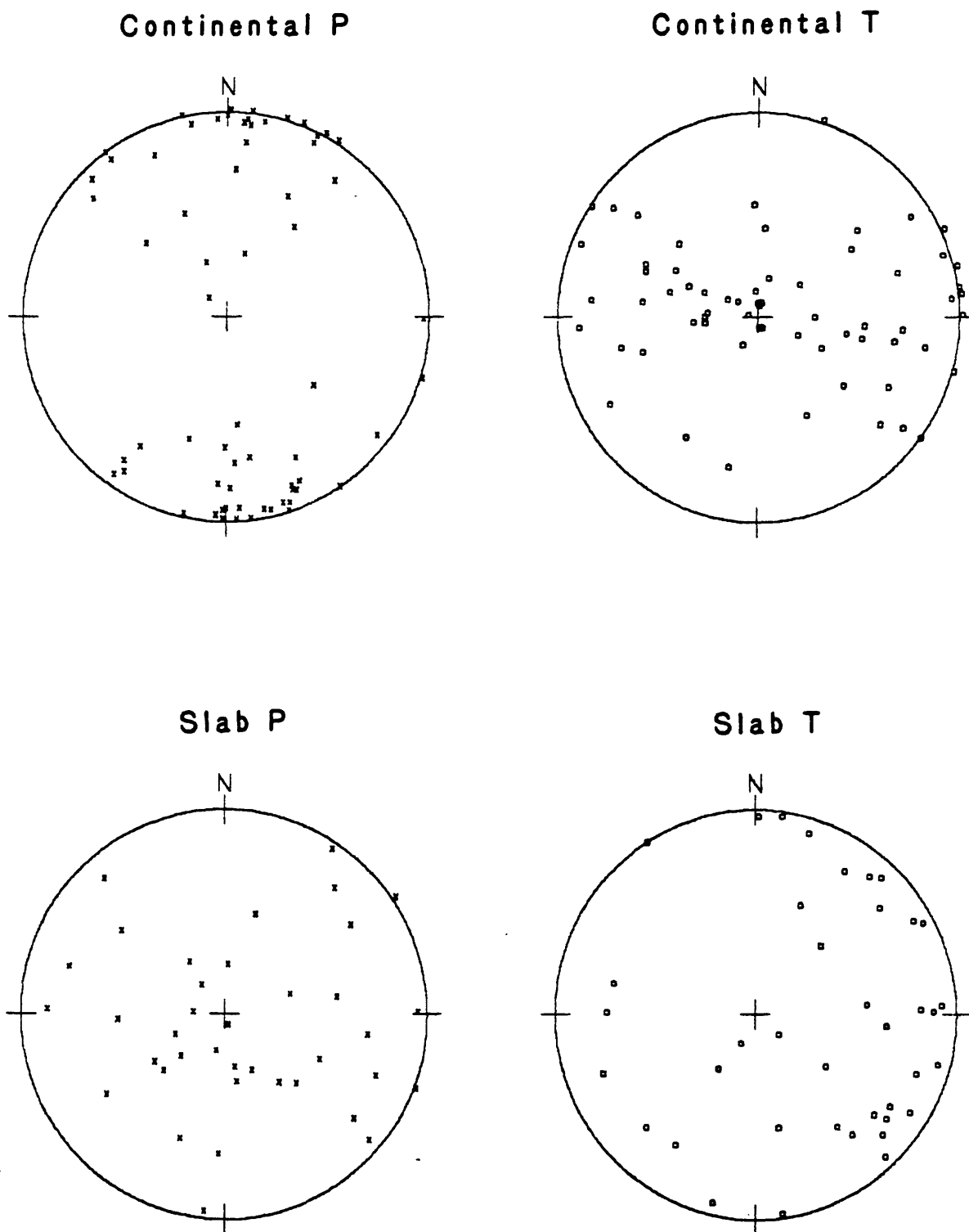


Figure 13. Lower hemisphere equal area stereo projections showing P and T tectonic axes for focal mechanisms of selected earthquakes in western Washington. 'Continental' events are shallower than 35 km, while 'Slab' events are 35 km or deeper. Only events with Quality 'BC' or better which had at least 9 polarities are included.

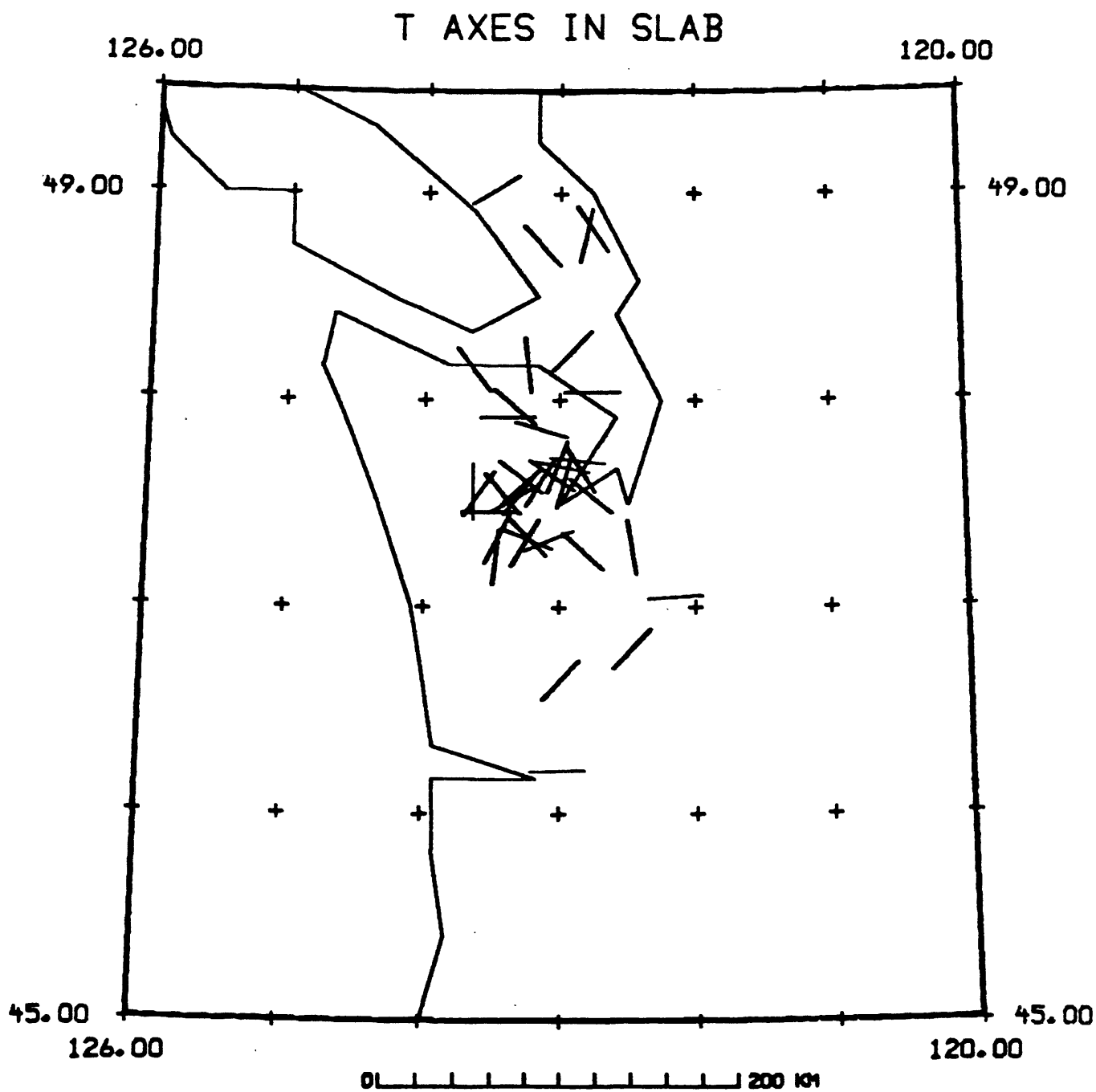


Figure 14. Orientation of T axes for slab earthquakes shown in Fig. 7.

APPENDIX A. 4.

Geometry of the Juan de Fuca Plate from Seismicity and Segmentation  
of the Cascadia Range Based on the Distribution of Volcanic Vents

by

Craig Weaver

# GEOMETRY OF THE JUAN DE FUCA PLATE FROM SEISMICITY AND SEGMENTATION OF THE CASCADE RANGE BASED ON THE DISTRIBUTION OF VOLCANIC VENTS

Presentation Before the National Earthquake Prediction Evaluation  
Council Meeting in Seattle, Washington, April 2, 1987

Craig S. Weaver  
U.S. Geological Survey  
at Geophysics Program AK-50  
University of Washington  
Seattle, Washington 98195  
(206) 442-0627 or 399-0627 FTS

My comments before the meeting were taken from two papers that have been submitted to journals. The first portion of my talk concerned the geometry of the Juan de Fuca plate beneath Washington and northern Oregon and all of these slides are from the paper "Geometry of the Juan de Fuca plate beneath Washington and north Oregon from seismicity" by C. S. Weaver and G. E. Baker (copy attached). This paper has been accepted for publication in the *Bulletin of the Seismological Society of America* subject to final approval of the editor. The second half of the talk concerned the segmentation of the Cascade Range using the pronounced differences in the distribution of late Cenozoic volcanic vents. The slides I showed were from the paper "Distribution of late Cenozoic volcanic vents in the Cascade Range (USA): Volcanic arc segmentation and regional tectonic considerations" by M. Guffanti and C. S. Weaver (copy attached). This paper has been submitted to the *Journal of Geophysical Research*. I concluded my talk by suggesting that the segmentation of the volcanic arc is related to changes in the geometry of the Juan de Fuca plate, and hypothesized that the volcanic arc segments would define the lateral extent of great subduction zone earthquakes on the interface between the Juan de Fuca and North American plates (see Figure 6 of the paper by Guffanti and Weaver).

GEOMETRY OF THE JUAN DE FUCA PLATE BENEATH WASHINGTON  
AND NORTHERN OREGON FROM SEISMICITY

Craig S. Weaver  
Glenn E. Baker

U. S. Geological Survey  
Geophysics Program AK-50  
University of Washington  
Seattle, Washington 98195

October 12, 1986  
Revised May 28, 1987

*Submitted to Bull. Seis Soc Am*

## ABSTRACT

Earthquake hypocenters within the subducting Juan de Fuca plate beneath Washington and northern Oregon are interpreted as showing that the direction of plate dip changes from northeast beneath the Puget Sound region to east-southeast beneath southwestern Washington. The shallowest hypocenters within the Juan de Fuca plate are between 30-40 km depth, and the distribution of these events strikes north-northeast from near the mouth of the Columbia River to the northern Olympic Mountains. The distribution of hypocenters between 40-50 km generally strikes parallel with the shallowest events, but shows a significant broadening beneath the eastern Olympic Mountains and Puget Sound. Events with depths greater than 50 km south of the 1965 Seattle earthquake ( $m_b=6.5$ ) strike north-northeast, approximately parallel with the shallower distributions; however, north of this event the distribution of these deeper hypocenters strikes northwest. This change in the distribution of earthquake hypocenters results in an upward arching of the Juan de Fuca plate beneath Puget Sound compared with the depth of the plate beneath southwestern Washington. The T-axis calculated for the 1949 south Puget Sound earthquake ( $M_S=7.1$ ) is oriented to the southeast, and the  $20^\circ$  plunge of the T-axis is in good agreement with the plate dip angle determined from the earthquake hypocenters. We conclude that the 1949 earthquake resulted at least in part from down-dip tensional forces within the subducting Juan de Fuca plate. One consequence of the change in the direction of plate dip is that volcanic front in Washington is everywhere perpendicular to the dip of the Juan de Fuca plate.

## INTRODUCTION

The geometry of subducting plates is usually inferred from the locations of Benioff zone earthquakes. But in the Pacific Northwest, the geometry of the subducting Juan de Fuca plate has been difficult to resolve because of the limited number of Benioff zone earthquakes and the limited volume over which these events have been located. The most active portion of the Benioff zone is beneath the forearc of northwestern Washington, where several large magnitude earthquakes, including the 1949 south Puget Sound ( $M_s=7.1$ ) and the 1965 Seattle ( $m_b=6.5$ ) earthquakes have occurred (Figure 1). This is an area where the plate geometry is expected to be complex, as the strike of the offshore subduction zone changes from nearly north-south along the Oregon coast to northwest along the Vancouver Island coast (Figure 1). The plate geometry beneath Washington must accommodate this change in strike and the associated lateral shortening when the subducting plate encounters the convex face of the continental plate. Rogers (1983b) commented extensively on possible models of the Juan de Fuca plate in the bend region.

Previous studies of the seismically active volume of the Juan de Fuca plate have shown that the Benioff zone earthquakes are occurring within the oceanic mantle of the subducting plate and not at the interface with the overlying North American plate (Smith and Knapp, 1980; Rogers, 1983a; Taber and Smith, 1985). Most of these earthquakes have been located beneath northwestern Washington, and these intraplate earthquakes show a shallow dip of about  $11^\circ$  landward from the coast to the Puget Sound region (Crosson, 1983; Taber and Smith, 1985).

The installation of additional seismographic stations in 1980 both along the coast and in southwestern Washington and northwestern Oregon has allowed for better detection and location of earthquakes within the Juan de Fuca plate beneath North America. Despite these improvements in the seismic network monitoring capabilities, most detected earthquakes within the Juan de Fuca plate have continued to be concentrated beneath northwestern Washington. However, since 1980, some earthquakes have been

located at depths greater than 30 km beneath southwestern Washington and the northern Oregon Coast Range. In this paper we emphasize these events to the south and show that the dip direction of the Juan de Fuca plate is to the east-southeast beneath southwestern Washington. The east-southeast dip direction begins south of the 1965 Seattle earthquake, whereas to the north of this event the plate dip direction is northeast as previously reported by others (Crosson, 1983; Rogers, 1983b). From the distribution of the earthquake hypocenters we conclude that the change in plate dip direction results in an upward arching of the Juan de Fuca plate beneath central and southern Puget Sound. There is excellent agreement between the dip of the Juan de Fuca plate defined by the hypocenters beneath southwestern Washington and the plate dip inferred from the orientation of the T-axis calculated from the focal mechanism for the 1949 south Puget Sound earthquake (Baker, 1985; Baker and Langston, 1987).

#### SEISMICITY DATA

The seismicity data used in this report consist of well-located earthquake hypocenters, with calculated depths greater than 20 km and coda magnitudes greater than 1.5 for the period January 1, 1980 to December 31, 1986, that were located by the University of Washington. The errors in the locations are less than 3 km, vertical or horizontal. To this set of the recent data we have added three large earthquakes for which focal mechanisms have been calculated: the 1949 south Puget Sound earthquake ( $M_s=7.1$ ) (Baker and Langston, 1987), the 1965 Seattle ( $m_b=6.5$ ) (Isacks and Molnar, 1971; Rogers, 1983a), and the 1976 Pender Island ( $m_b=5.1$ ) (Rogers, 1983a) earthquakes (Figure 1). We have plotted in Figure 2 the earthquakes divided into five depth intervals (20-30, 30-40, 40-50, 50-60, and 60+ km).

The shallowest epicenters (20-30 km) have a bimodal spatial distribution. There are a few epicenters located near the Washington coast (Figure 2a), but most earthquakes within this depth range are within a broad arc from the Willamette Valley to southern Vancouver Island. The events near the coast were interpreted by Taber and



Smith (1985) as occurring within the Juan de Fuca plate, whereas Crosson (1976) noted that events in this depth range in the Puget Sound basin were occurring within the overlying North American plate. We likewise interpret the events between 20-30 km beneath southwestern Washington as occurring within the North American plate. Between 30-40 km, the hypocenters are east of the westerly group of events near the Washington coast in the 20-30 km depth range, and the distribution strikes north-northeast from north of the mouth of the Columbia River to the southeastern end of Vancouver Island (Figure 2b). The few events that locate at depths of 30-40 km to the east in the Puget Sound basin are the deepest extent of the crustal events (Crosson, 1976), and we suggest that the single event near the Columbia River is within the North American plate.

Between 40 and 50 km, the earthquake distribution occurs beneath a wide area from the central Olympic Mountains to the central Puget Sound basin (Figure 2c). With respect to the two shallower depth ranges, these events continue the trend of hypocenters deepening to the east. The most southerly earthquake in the 40-50 km depth range of earthquakes deserves special comment. This event had a coda magnitude of 2.8 and occurred on June 6, 1981 when the U.S. Geological Survey was operating the 32 station Oregon seismic network (Kolman, 1984). Three stations in this network were near the Oregon coast, and 13 stations were operating to the southeast of this event. We have re-read all available data for this event, including the WWSSN station at COR which was the nearest station at an epicentral distance of 54 km. Because of this epicentral distance to COR, this location is more poorly determined than the others in our data set, we have compared individual station residuals, relative arrival times between pairs of stations, and S-P times for this event with similar data for several earthquakes with shallow hypocenters ( $<10$  km) along the Oregon coast and conclude that this is truly a deep earthquake ( $41 \pm 5$  km).

The 50-60 km distribution (Figure 2d) includes the 1949 South Puget Sound earthquake, that has a depth of 54 km based on pP-P travel time differences (Baker and

Langston, 1987). From the Columbia River northward to the 1949 earthquake, the strike of this distribution is approximately parallel with that of the 30-40 km deep events (Figure 2b). This strike changes north of the 1949 event, with the most easterly extent of the 50-60 km deep earthquakes being approximately parallel with the eastern shoreline of Puget Sound (Figure 2d). The change in strike observed for the earthquake distribution between 50-60 km becomes more pronounced for those events below 60 km (Figure 2e). This deepest group of events includes the 1965 and 1976 events, located at 60 and 62 km respectively. North of the location of the 1965 earthquake, events greater than 60 km depth strike north-northwest, cutting across the north-northeast strike of the shallower distributions to the west (e.g., compare Figure 2b with Figure 2e). The deepest events, greater than 70 km, are east of the 1965 event (Figure 2e).

Previous cross sections of the deep seismicity beneath western Washington (eg., Crosson, 1983; Taber and Smith, 1985; Weaver and Michaelson, 1985) have projected nearly all of the available hypocenters in western Washington onto a single plane. However, because of the change in the strike of the distributions of events greater than 50 km depth with respect to shallower distributions, projecting all of the hypocenters onto a single plane obscures details of the seismicity distribution evident in the epicentral maps (Figure 2). As an example of this problem, we have selected earthquakes in an area from the vicinity of the 1965 earthquake southward about 280 km (large clear area in Figure 3), and have oriented the cross section approximately perpendicular to the Washington coast (Figure 3, line A-A'). The earthquakes projected onto the resulting cross section have considerable scatter, particularly below about 50 km (Figure 4a), making it difficult to unambiguously determine the dip of the Benioff zone and the inferred position of the Juan de Fuca plate.

To avoid the problem illustrated in Figure 4a, we have selected four quadrilaterals such that the sides are approximately perpendicular and parallel to the strike of the distributions of earthquakes below 50 km (compare Figure 2 & Figure 3). Physically, we

justify this data selection by the noting that the change in the strike of the deeper earthquake distributions is approximately the same as the change in the strike of the volcanic front defined by the most westward of the large Quaternary stratovolcanoes in Washington (Mount Baker, Glacier Peak, Mount Rainier, and Mount St. Helens), and to a lesser extent, the change in the strike of the trench offshore (Figure 1).

The most southerly of these four quadrilaterals includes earthquakes from the 1981 event on the Oregon coast (Figure 2c) to the location of the 1965 earthquake, where the strike of the 50-60 and 60+ km deep earthquake distributions changes from north-northeast to more north-south (Figure 2 d & e). This selection of events (stippled pattern in Figure 3) plotted onto the plane located at B-B' results in a thin distribution of earthquakes, about 10 km thick, that dips at an approximate angle of  $11^{\circ}$  from the vicinity of the coast to the projected location of the 1949 earthquake (Figure 4b). East of the 1949 event, the dip increases to about  $20^{\circ}$ , but because of the small number of events below 50 km we consider this steeper dip to be preliminary.

Excluding the earthquakes in southwestern Washington from cross sections plotted for events beneath central and southern Puget sound results in tighter distributions of dipping hypocenters than those previously published (e.g., Figure 2 in Weaver and Michaelson, 1985). Beneath central Puget Sound we have plotted two different data selections to emphasize the change in the plate dip direction. The first area (heavy, bold line in Figure 3) is an extension of the southern cross section of Figure 4b. This quadrilateral includes the portion of the deeper event distributions (50-60 and 60+ km) that strike more north-south than those events plotted in Figure 4b, but we have excluded those portions of the deeper distributions that clearly strike to the northwest (compare bold outline in Figure 3 with Figure 2d). The second section is oriented along the direction of convergence (Figure 3, dense line pattern) between the Juan de Fuca and North American plates, and the area was chosen to exclude the northeast striking portion of the 50-60 and 60+ km deep distributions to the south of the 1965 earthquake. In both

sections the earthquakes plot in a thin distribution, about 10 km thick (Figure 4 c&d). From the coast to the 1965 earthquake the dip is about  $11^{\circ}$  to the east, similar to the results of Taber and Smith (1985). East of the 1965 earthquake, the dip of the distribution appears to increase to about  $25^{\circ}$  (Figure 4c). The fact that two areas so differently oriented produce nearly identical dipping distributions results from the broad area over which the change in strike of the deeper (50-60 and 60+ km) distributions occur and the broad area of earthquakes located between 40 and 50 km (Figure 2c).

The final cross section includes events in the northern Puget Sound basin, and the section is aligned approximately along the convergence direction (Figure 4e). This is an area completely removed from the change in the strike of the distribution of 60+ km deep earthquakes. As a consequence, unlike the central Puget Sound area where earthquakes plot in thin distributions that dip both to the northeast and the east-southeast, these northern events dip in a narrow distribution only toward the northeast. This final section is similar to one compiled by Rogers (1983a) for historical earthquakes recorded prior to the installation of the University of Washington seismic network in 1970. Although the section in Figure 4e is truncated at  $49^{\circ}$ , very few earthquakes are well located to the north (Rogers, 1983b).

From the distribution of earthquakes and the cross-section plots, we conclude that the dip direction of the Juan de Fuca plate changes along the strike of the subduction zone. Beneath southwestern Washington, south of the 1965 earthquake, the plate dips to the east-southeast, whereas beneath northwestern Washington the plate dips to the northeast. The available hypocenters indicate that the transition in dip direction is smooth, with no sudden offset in the geometry of the Juan de Fuca plate beneath Puget Sound.

The T-axes calculated from the focal mechanisms for the three larger magnitude earthquakes (1965, 1976, and 1949) show a change in strike consistent with our interpretation of a change in the dip direction of the Juan de Fuca plate inferred from the

seismicity. Generally, earthquakes within the portion of a plate that is subject to gravitational sinking are normal faulting events, and the T-axis calculated from these focal mechanisms is approximately parallel with the dip of the subducting plate (Isacks and Molnar, 1971). A recent study of the 1949 earthquake has indicated that it was a complex event that consisted of four distinct source pulses (Baker, 1985; Baker and Langston, 1987). The focal mechanism (Figure 1), which is similar for each pulse, is based on modeling of long period P, SV, and SH waves; the quality of the data resulted in tightly constrained fault planes. The strike of the T-axis (azimuth of N.  $150^{\circ}$  E. with a plunge of  $20^{\circ}$ ) is significantly different from the T-axis directions calculated for either the 1965 or 1976 earthquakes (Rogers, 1983a). The 1965 Seattle earthquake ( $m_b=6.5$ ) and the 1976 Pender Island earthquake ( $m_b=5.1$ ) were normal faulting events at depths of 60 and 62 km respectively, that had T-axes that dipped  $25-35^{\circ}$  to the northeast (Rogers, 1983a). Because the T-axis calculated for the 1949 event indicates down-dip tension to the southeast with a dip similar to the plate dip inferred from the hypocenters (Figure 4b), we conclude that this earthquake was the result, at least in part, of the gravitational sinking of the Juan de Fuca plate beneath western Washington.

#### IMPLICATIONS FOR PLATE GEOMETRY

The epicenter map plots of the 50-60 km (Figure 2d) and 60+ km depth (Figure 2e) distributions allow us to clearly define the location of the 60 km depth contour of the Juan de Fuca plate beneath all of Washington. In Figure 5 we have sketched the location of the eastern extent of the earthquake hypocenters in the depth intervals 50-60 km. We have also sketched the location of the eastern extent of the 30-40 km depth range (Figure 2b), excluding those events noted beneath Puget Sound and the Willamette Valley. Although the 40 km contour is well-defined by the available hypocenters beneath Washington, the extension of the 40 km contour to the central Oregon coast is very tentative.

It is apparent from Figure 5 that there is a change in the average dip of the Juan de Fuca plate between the trench and the position of the plate at a depth of 60 km. Beneath southwestern Washington, the horizontal distance between the trench and the 60 km depth of the plate is about 200 km, and this distance increases to about 300 km beneath the center of the Olympic Mountains and Puget Sound (Figure 5). Thus, with respect to the plate dip defined in southwestern Washington, the Juan de Fuca plate arches upward beneath Puget Sound. In large part, this arching is reflected in the broadening of the earthquake distribution between 40-50 km (Figure 2c) beneath the eastern Olympic Mountains and Puget Sound.

The definition of the 60 km contour also shows that the direction of plate dip in Washington is approximately perpendicular to the volcanic front. We have indicated the position of the volcanic front, defined as the westernmost occurrence of late Cenozoic volcanism as mapped by Luedke and Smith [1982], on Figure 5. The volcanic front and the 60 km plate depth contour in northwestern Washington are both approximately perpendicular to the direction of convergence between the Juan de Fuca and North American plates. As there is no late Cenozoic volcanism from Glacier Peak to a few vents north of Mount Rainier, the volcanic front is not defined here. From the vicinity of Mount Rainier to the Portland, Oregon area (where late Cenozoic basalts have been erupted, see Luedke and Smith, 1982), both the volcanic front and the 60 km plate depth are parallel and strike to the south-southeast (Figure 5). In southwestern Washington the volcanic front is oblique to the convergence direction.

The plate geometry south of Portland, Oregon cannot be inferred from earthquake data. The volcanic front steps eastward to the axis of the Cascade Range, and continues along the western edge of the range throughout Oregon and northern California. In andesitic arcs studied in subduction zones where Benioff zone earthquakes allow the plate geometry to be inferred beneath the areas of recent volcanism, the subducting plate is usually found to be at a depth near 100 km (Gill, 1981). Thus, the change in

the volcanic front position near Portland may indicate that the geometry of the Juan de Fuca plate to the south may also change.

Finally, in Figure 6 we have summarized the geometry of the Juan de Fuca plate as now available from earthquake hypocenters. To the plate depth contours drawn for Washington and northern Oregon in Figure 5 we have added the corresponding depth contours for northern California (from Cockerham, 1984; Walter, 1986). The average plate dip in northern California is similar to that in southwestern Washington, as the 60 km depth contour is about 200 km from the trench. One further point clear from the contours in Figure 6 is that between the available hypocenters in northern Oregon and the deep events beneath northern California, a large variation in the geometry of the Juan de Fuca plate is expected. Extrapolating the hypocentral contours west of Lassen Peak northward results in an unreasonably shallow depth of the Gorda plate beneath Mount Shasta and the Juan de Fuca plate beneath the southern Cascade Range of Oregon.

## DISCUSSION

The plate geometry outlined by the seismicity is similar to that predicted beneath Washington on the basis of plate motions and the volumetric problem caused by the sharp change of strike of the subduction zone off the Washington and British Columbia coasts (Keen and Hyndmann, 1979; Rogers, 1983 a&b). The data are particularly supportive of Rogers (1983a) suggested undulation of the Juan de Fuca plate, although our data indicates that the undulation (termed arching in this paper) occurs over a broader region than originally suggested by Rogers. The seismicity distribution is also consistent with the suggestion by Weaver and Michaelson (1985) that the Juan de Fuca plate dipped more steeply beneath southwestern Washington than beneath northwestern Washington. Their suggestion was based on a comparison of the distribution of crustal seismicity and volcanism in the Pacific Northwest with similar distributions in the Nazca

subduction zone, where Benioff zone earthquakes allow the position of the subducting plate to be inferred.

The fault planes determined for the 1949 event are not parallel with the convergence direction between the North American and Juan de Fuca plates, indicating that the event did not occur on a tear fault parallel with the convergence direction. However, the strike-slip mechanism indicates that shearing occurs within the Juan de Fuca plate. Consequently, in addition to the down-dip tensional forces, compression within the shallow dipping portion of the Juan de Fuca plate near the 1949 epicenter is significant for earthquake generation. We note that Taber and Smith (1985) found a strike-slip solution similar to that determined by Baker and Langston (1987) for the 1949 earthquake for an event near the Washington coast, additional evidence of compression acting within the shallow dipping portion of the plate beneath southwestern Washington.

The possible effect of the plate position on the occurrence of the deep crustal earthquakes is raised by the spatial relation between the distribution of the deepest (20-30 and a few events below 30 km) crustal events and the Juan de Fuca plate geometry. The westernmost extent of the deep crustal events is approximately coincident with the western edge of earthquakes within the Juan de Fuca plate at depths between 50 and 60 km (compare Figure 2a and 2d, Figure 4b,c,&d). The greatest concentration of deep crustal events is beneath central Puget Sound, where the Juan de Fuca plate arches upward. It may be that the extended proximity of the subducting plate to the overlying crustal plate beneath the eastern Olympic Mountains and Puget Sound results in a more effective transfer of stress into the overriding crustal plate than can occur beneath southwestern Washington where the average dip of the plate is steeper above 60 km depth.

A second possible explanation for the greater concentration of deep crustal earthquakes beneath Puget Sound could be related to the sudden change in plate dip from the shallow dip near the coast to the steeper dip of the plate toward the Cascade Range.



The available hypocentral data indicates that the Juan de Fuca dips steeply ( $25^{\circ}$ ) to the east of the 1965 earthquake and that the change in plate dip from the  $11^{\circ}$  observed beneath Puget Sound occurs suddenly, over a few ten's of kilometers of horizontal distance (Figures 2e & 4c). On the otherhand, in southwestern Washington, the transition in the plate dip from the shallow dip near the coast to the steeper dip toward Mount St. Helens and Mount Rainier appears to be gradual (Figure 4b). Thus, bending stresses associated with the change in plate dip may be more concentrated in Puget Sound than in southwestern Washington, resulting in the greater number of deep crustal earthquakes.

In repeat surveys of a strain network that crosses Puget Sound in the vicinity of the 1965 earthquake, Savage et al. (1981) observed a  $N71^{\circ}E$  direction of principal compressive strain rate and a  $N19^{\circ}W$  direction of principal extensional strain rate. Using a two-dimensional model of a subduction zone thrust interface, Savage et al. (1981) were able to calculate a reasonable fit to the compressional strain rate, but noted that the origin of the extension was unknown. Above we noted that the T-axis direction for the 1949 earthquake is reflecting the geometry of the Juan de Fuca plate and the spatial relation between the deep crustal earthquakes and the Juan de Fuca plate. It seems possible that the extensional strain rate measured by Savage et al. (1981) is the result of the arching structure of the plate beneath Puget Sound, with the extensional strain being transmitted to the crust and superimposed on the east-northeastward compressional strain.

## CONCLUSIONS

The dip direction of the Juan de Fuca plate changes from northeast beneath northwestern Washington to east-southeast beneath southwestern Washington. The plate dips at about  $11^{\circ}$  from the coast to eastern Puget Sound in northwestern Washington, where the dip angle increases to about  $25^{\circ}$ . In southwestern Washington, the dip of

the plate near the coast is about also about  $11^{\circ}$ , and the dip increases to about  $20^{\circ}$  near the epicenter of the 1949 south Puget Sound earthquake. The T-axis calculated from the focal mechanism of this event is oriented to the southeast and has a dip nearly identical to that indicated by the hypocenters, indicating that gravitational sinking of the slab is at least partly responsible for this earthquake. South of the location of the 1965 Seattle earthquake, the horizontal distance between the trench and the plate position at 60 km decreases from about 300 km to 200 km, indicating that the average dip of the shallow Juan de Fuca plate increases to the south. Because the average dip of the plate is greater to the south, the more shallow dip to the north results in an upward arching of the Juan de Fuca plate beneath the Olympic Mountains and Puget Sound.

## ACKNOWLEDGEMENTS

Jim Zollweg, Jim Savage, and Bob Page commented on an earlier version of this paper. We appreciate numerous discussions with Stew Smith concerning the nature of the Juan de Fuca plate. Randy Jacobsen verified earthquake arrival times in Corvallis and Steve Walter checked data in Menlo Park. Pat Muffler suggested the term arch for the geometry of the plate beneath Puget Sound. We thank the University of Washington Geophysics Program for access to their earthquake hypocenter catalogs. This work was funded by the U.S. Geological Survey Earthquake Hazards and Geothermal Research programs.

## REFERENCES

- Baker, G.E. and C.A. Langston (1987). Source parameters of the magnitude 7.1, 1949, South Puget Sound, Washington, earthquake determined from long-period body waves and strong motion, *Bull. Seism. Soc. Am.*, 76, (in press).
- Baker, G.E. (1985). Source parameters of the magnitude 7.1, 1949, south Puget Sound, Washington earthquake determined from long-period body waves, *M.S. Thesis*, University of Washington, Seattle, Washington.
- Cockerham, R.S. (1984). Evidence for a 180-km-long subducted slab beneath northern California, *Bull. Seism. Soc. Am.*, 74, 569-576.
- Crosson, R.S. (1983). Review of seismicity in the Puget Sound region from 1970 through 1978, in *U.S. Geol. Surv., Open-File Rept. 83-19*, 6-10.
- Crosson, R.S. (1976). Crustal structure modeling of earthquake data, 2: Velocity structure of the Puget Sound region, Washington, *J. Geophys. Res.*, 81, 3047-3054.
- Gill, J.B. (1981). *Orogenic Andesites and Plate Tectonics*, Springer-Verlag, Berlin, 390 pp.
- Isacks, B.L. and P. Molnar (1971). Distribution of stresses in the descending lithosphere from a global survey of focal mechanism solutions of mantle earthquakes, *Rev. Geophys.*, 9, 103-174.
- Keen, C.E. and R.D. Hyndman (1979). Geophysical review of the continental margins of eastern and western Canada, *Can. J. Earth Sci.*, 16, 712-745.
- Kollman, A. (1984). Oregon seismicity, August 1980 - October 1982, *U.S. Geol. Surv., Open-File Rept. 84-892*, 33 pp.
- Luedke, R.G. and R.L. Smith (1982). Map showing distribution, composition, and age of Late Cenozoic volcanic centers in Oregon and Washington, *U. S. Geol. Survey Misc. Invest. Series Map I-1091-D*, scale 1:1,000,000.

- Rogers, G.C. (1983a). Some comments on the seismicity of the northern Puget Sound-southern Vancouver Island region, in *U.S. Geol. Surv., Open-File Rept. 83-19*, 19-39.
- Rogers, G.C. (1983b). Seismotectonics of British Columbia, *Ph.D. thesis*, University of British Columbia, Vancouver, British Columbia.
- Savage, J.C., M. Lisowski, and W.H. Prescott (1981). Geodetic strain measurements in Washington, *J. Geophys. Res.* 86, 4929-4940.
- Smith, S.W. and J.S. Knapp (1980). The northern termination of the San Andreas Fault, in *Studies of the San Andreas Fault Zone in Northern California*, R. Streitz and R. Sherburne, Editors, *Calif. Div. Mines Geol. Spec. Rept. 140*, 153-164.
- Taber, J.J. and S.W. Smith (1985). Seismicity and focal mechanisms associated with the subduction of the Juan de Fuca plate beneath the Olympic Peninsula, Washington, *Bull. Seism. Soc. Am.*, 75, 237-249.
- Walter, S.R. (1986). Intermediate-focus earthquakes associated with Gorda Plate subduction in northern California, *Bull. Seism. Soc. Am.*, 76, 583-588.
- Weaver, C.S. and C.A. Michaelson (1985). Seismicity and volcanism in the Pacific Northwest: Evidence for the segmentation of the Juan De Fuca plate, *Geophys. Res. Let.* 12, 215-218.

## FIGURE CAPTIONS

Fig. 1. Geographic place names and earthquake distribution. The earthquakes are all greater than 20 km depth and are from the period 1 January 1980 to 31 August 1986; the 1949, 1965 and 1976 earthquakes discussed in the text have been added to this data set. Earthquake magnitudes indicated by size of symbol, with the smallest symbols representing magnitudes between 1.5 and 3.4, event magnitudes between 3.5 and 5.4 by medium symbols, and magnitudes 5.5 to 7.4 by large symbols. Focal mechanisms for the three events have compressional quadrants darkened, dilatational quadrants white. Sources for the mechanisms are given in the text. Darkened triangles are Quaternary Cascade stratovolcanoes, abbreviated as follows: B, Mount Baker; G, Glacier Peak; R, Mount Rainier; S, Mount St. Helens; A, Mount Adams; H, Mount Hood; J, Mount Jefferson; T, Three Sisters.

Fig. 2. Depth plots for earthquakes. a) Events between 20 and 30 km depth; b) Events between 30 and 40 km depth; c) events between 40 and 50 km depth; d) events between 50 and 60 km depth; e) events greater than 60 km depth with those events darkened are greater than 70 km depth. Same magnitude scaling as in Fig. 1. Vancouver Island is abbreviated as VI.

Fig. 3. Areas plotted in cross section in Fig. 4. All events within each quadrilateral have been projected onto vertical planes oriented along the lines A-A', B-B', C-C', D-D', and E-E'.

Fig. 4. Cross section plots. The orientation of each plane and the area of the projected hypocenters are given in Fig. 3. Earthquake magnitudes are scaled as in Fig. 1. Each section is 220 km wide and there is no vertical exaggeration. In "b" the plunge of the T-axis, taken from Baker and Langston (1987) is indicated by the arrows.

Fig. 5. Summary of plate geometry beneath Washington and northern Oregon. The 40 and 60 km depth contours are taken from the westward extent of the 30-40 km and westward extent of the 50-60 km distributions, shown in Figure 2, respectively. The volcanic front is the westward extent of late Cenozoic volcanism taken from the map by Luedke and Smith (1982). Bold arrow offshore shows the direction of convergence between the Juan de Fuca and North American plates.

Fig. 6. Schematic of the geometry of the Juan de Fuca plate system as inferred from Benioff zone earthquakes. The 40 and 60 km contours are described in the text. The azimuth of the T-axis is indicated for the three larger magnitude earthquakes discussed in text. Volcanoes not identified in Fig. 1 are abbreviated as L for Lassen Peak and SH for Mount Shasta.

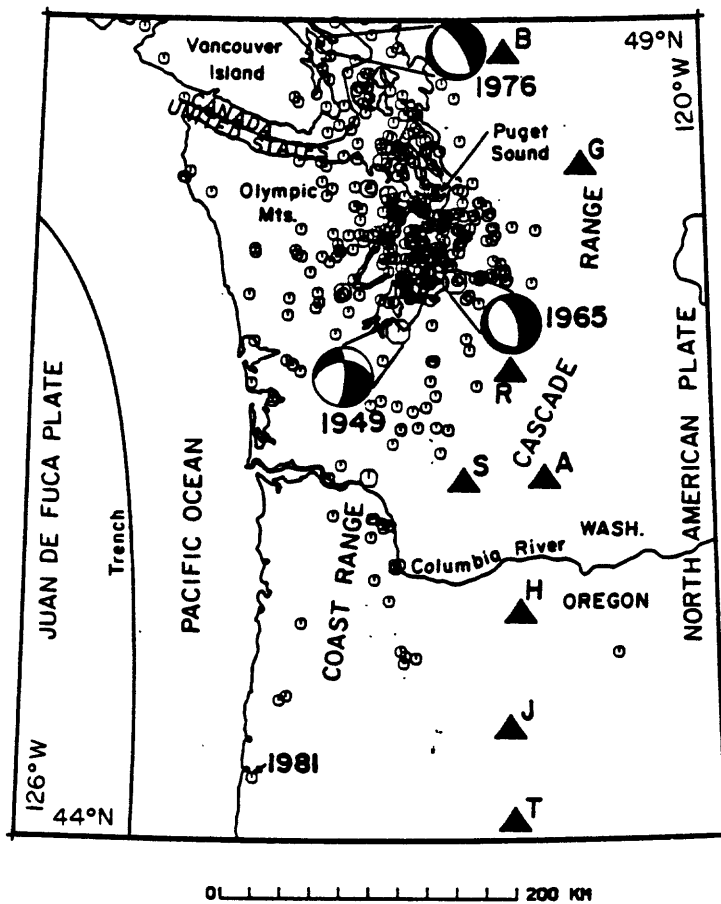


Figure 1



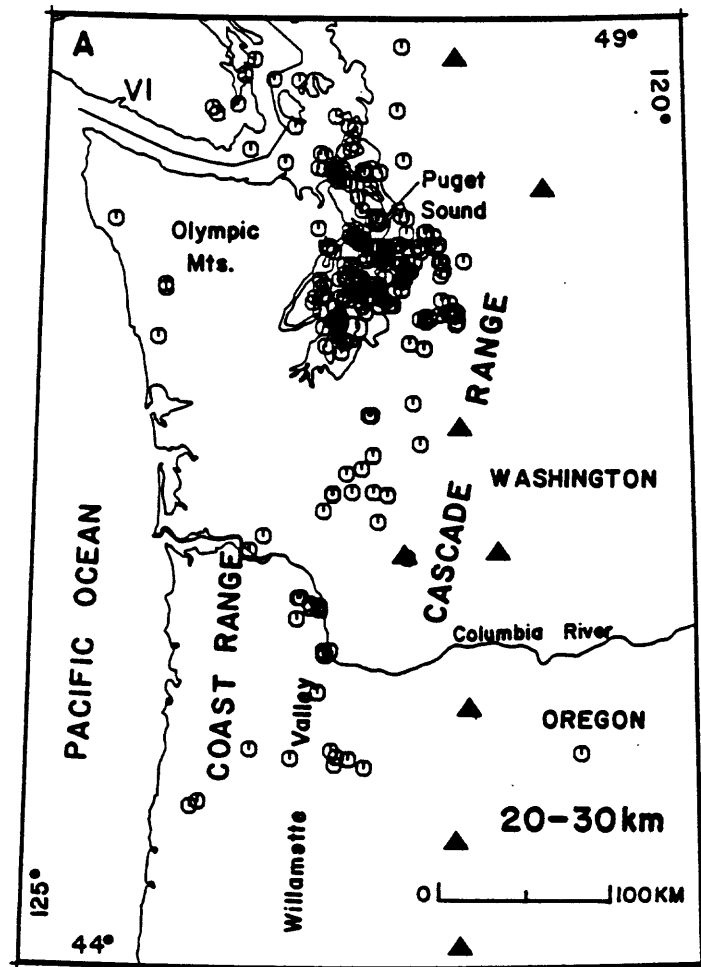


Figure 2a

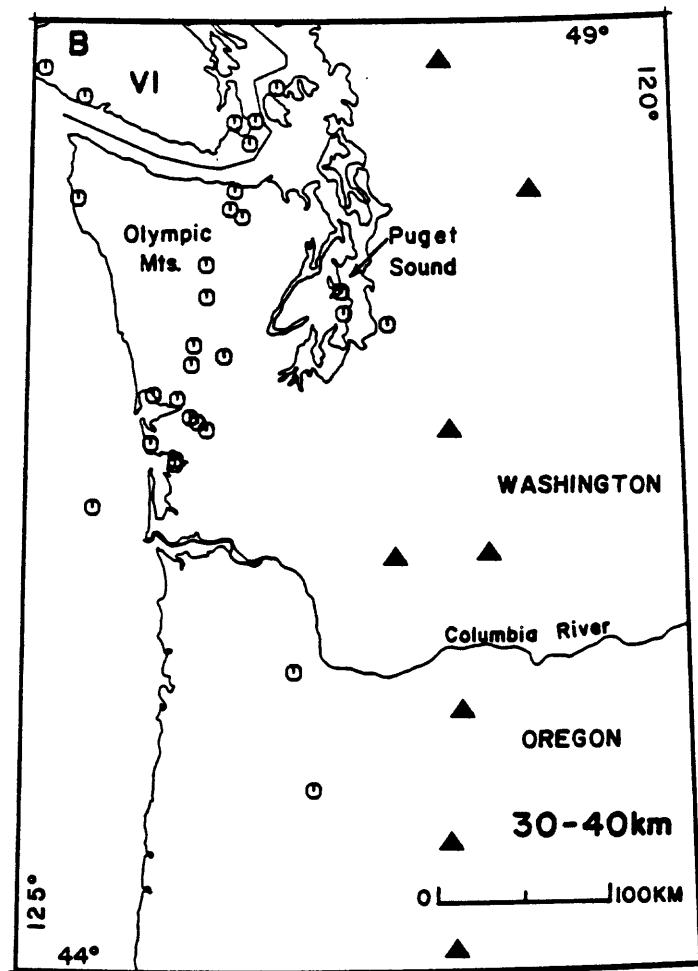


Figure 2b

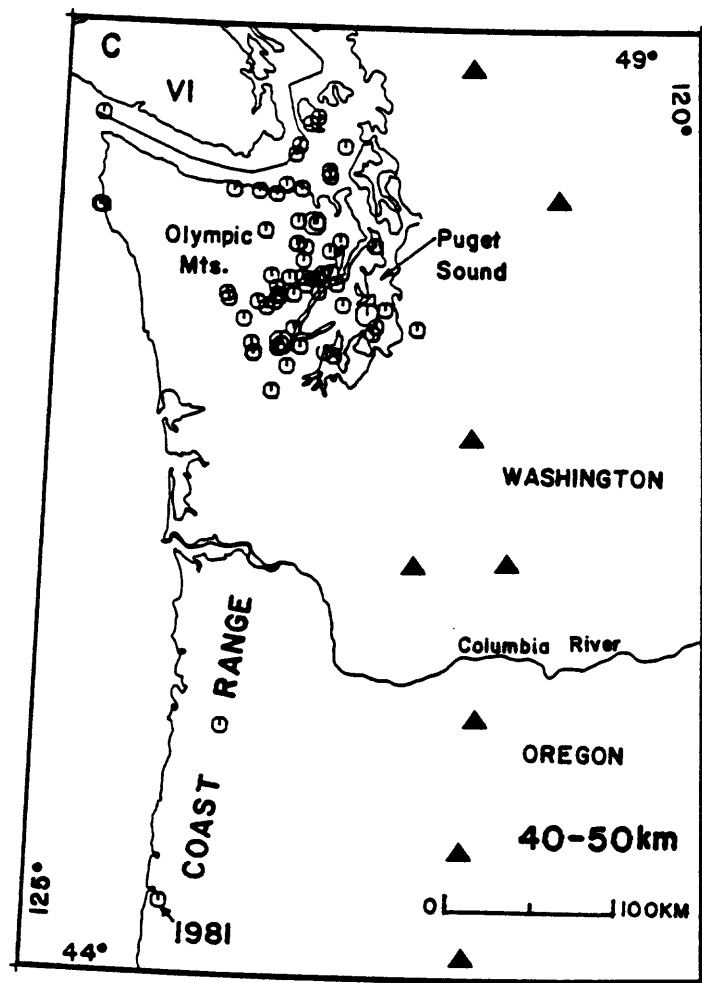


Figure 2c

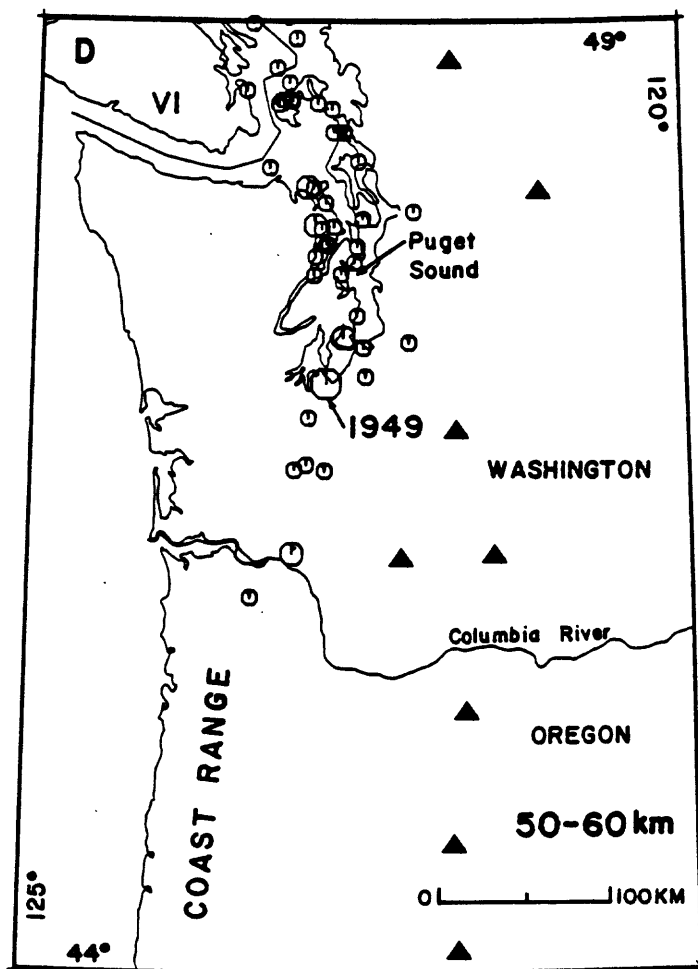


Figure 2d

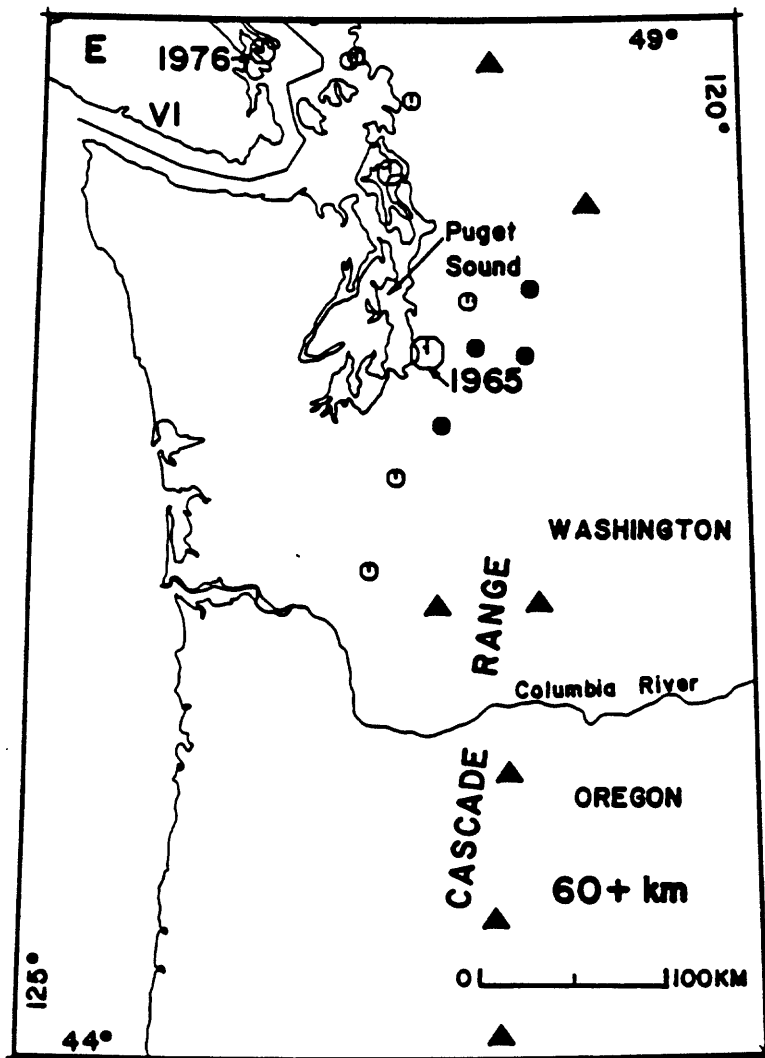


Figure 2e

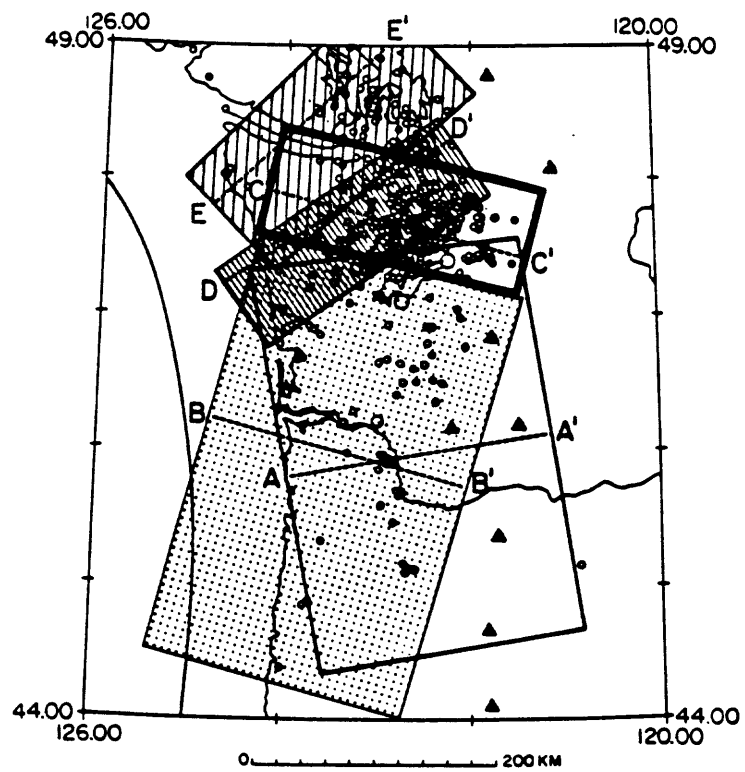


Figure 3

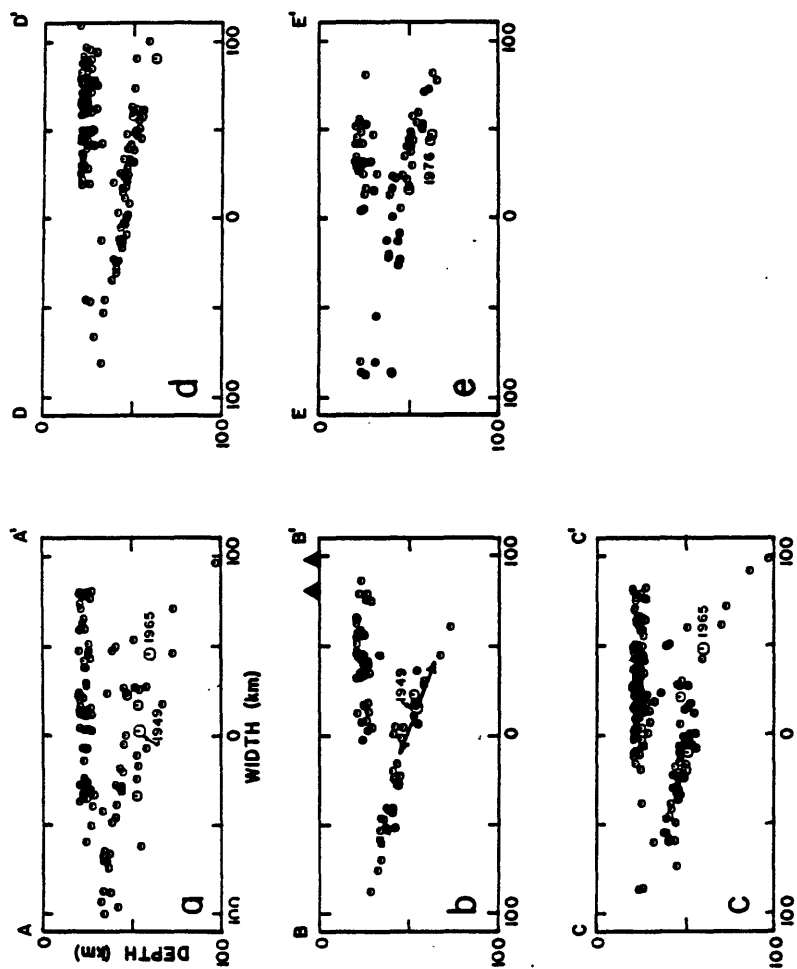


Figure 4

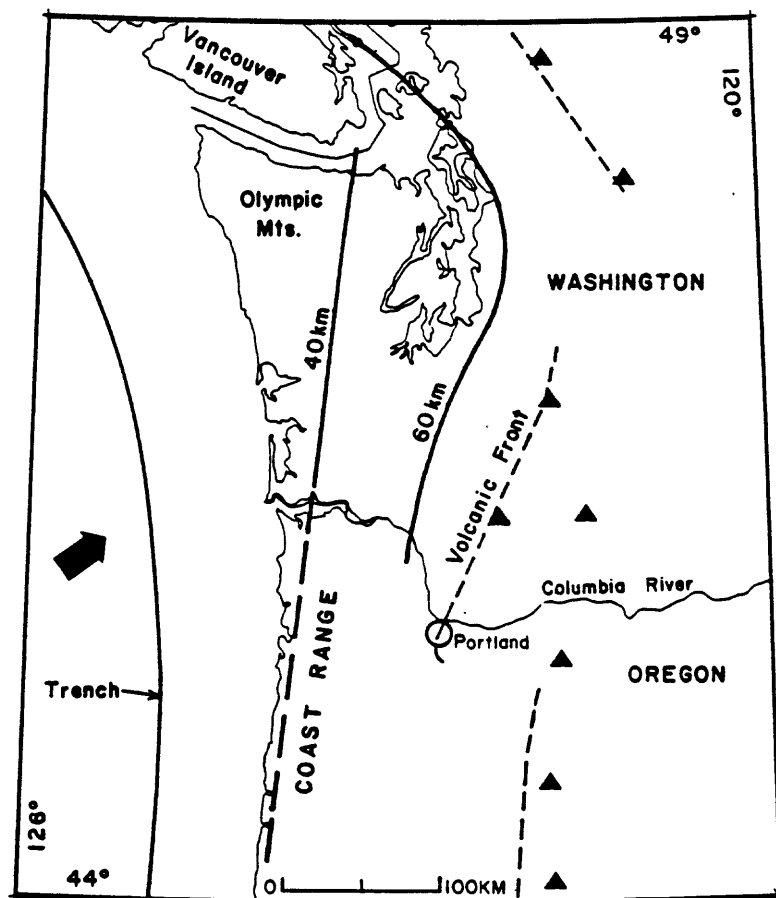
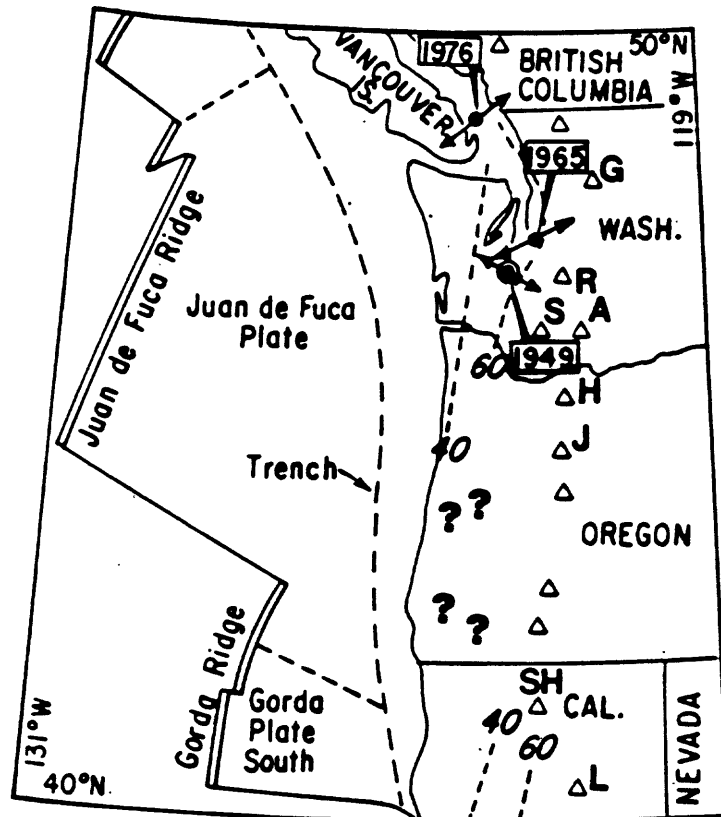


Figure 5





0 200 km

Figure 6

DISTRIBUTION OF LATE CENOZOIC VOLCANIC VENTS IN THE CASCADE RANGE (USA):  
VOLCANIC ARC SEGMENTATION AND REGIONAL TECTONIC CONSIDERATIONS

(1) Marianne Guffanti

(2) Craig S. Weaver

U.S. Geological Survey

(1) Reston, Virginia

(2) Seattle, Washington

May 21, 1987

Submitted to: Journal of Geophysical Research

## ABSTRACT

Spatial, temporal, and compositional distributions of approximately 4000 volcanic vents less than 16 Ma in Washington, Oregon, northern California, and northwestern Nevada illustrate the evolution of two volcano-tectonic regimes: Juan de Fuca subduction and Basin and Range extension. Vent data were obtained from published map compilations and include monogenetic and small polygenetic volcanoes in addition to major stratovolcanoes. Based on the distribution of 2821 vents less than 5 Ma, the Cascade Range can be divided into five segments; vents of the High Lava Plains along the northern margin of the Basin and Range province in Oregon form a sixth group. Some aspects of the Cascade Range segmentation can be related to gross structural features of the subducting Juan de Fuca plate that are inferred from Benioff-zone seismicity. The volcanic front of two segments parallels the strike of the subducting Juan de Fuca plate, which changes from NE beneath southern Washington to NW beneath northern Washington; these two segments are separated by a 90-km volcanic gap between Mount Rainier and Glacier Peak which is landward of the portion of the plate with the least average dip to a depth of 60 km. A narrow, N-S trending, dominantly andesitic belt of vents in Oregon constitutes a third segment which is landward of the seismically quiet portion of the Benioff zone; the narrowness of this segment indicates steep dip of the subducting plate beneath the Cascade arc in Oregon. Paucity of vents between segment four (containing Mount Shasta and Medicine Lake) and segment five (containing Lassen Peak) occurs between the Juan de Fuca and Gorda North plates, which have differing age and Benioff-zone seismicity. From the relation between the plate-depth contours at 60 km in areas of Benioff-zone seismicity and the volcanic front of vents less than 5 Ma, it appears that

variations in the geometry of the Juan de Fuca plate likely occur near boundaries between independently determined volcanic segments in northern Oregon and northern California. East of the Cascade arc in Oregon and northern California, basin-range volcanism migrated into the region directly adjacent to the Cascade Range during the interval 5-10 Ma. This basin-range impingement against the Cascade arc is characterized by cessation of basin-range volcanism in southern Oregon since 5 Ma, continuation of basaltic volcanism during the past 5 Ma in northeastern California where the impingement process may not yet be complete, and contraction of the area of basaltic volcanism during the past 5 Ma around Mount Shasta, Medicine Lake, and Lassen Peak. In central Oregon where the northern margin of basin-range volcanism (the High Lava Plains) intersects the Cascade arc, basin-range impingement roughly coincides in time and space with the development of the High Cascade graben between Three Sisters and Mount Jefferson.

## INTRODUCTION

Late Cenozoic volcanism in the Cascade Range of the Pacific Northwest is widely attributed to subduction of the Juan de Fuca plate system beneath the North American plate. Beyond this first-order relation between volcanism and subduction, volcanic processes vary along the Cascade arc in time and space. For example, the amount and style of Cascade volcanism during the past 5 Ma years is significantly different north and south of Mount Rainier, Washington. Isolated stratovolcanoes in British Columbia and Washington north of Mount Rainier contrast with composite volcanoes surrounded by fields of numerous, monogenetic, mafic volcanoes in the Oregon and northern California section of the range [Luedke and Smith, 1981; 1982].

Recently, attempts have been made to use the distribution of late Cenozoic volcanism to better constrain tectonic models of interaction between the Juan de Fuca and North American plates. These models assume that the differences observed in the amount of volcanism the result of differences in the manner of interaction between the two plates. Such plate models postulate that the paucity of volcanism in much of Washington and British Columbia is the result of compression in the North American crust, whereas the abundant volcanism in Oregon and northern California is thought to indicate crustal extension there [Weaver and Smith, 1983; Rogers, 1985; Weaver and Michaelson, 1985]. Suggestions for the difference in the crustal stress regime within the volcanic arc include areal variations in the convergence velocity between the plates [Rogers, 1985] and variations in the dip of the Juan de Fuca plate [Weaver and Michaelson, 1985; Michaelson and Weaver, 1986]. Also, extension in the Basin and Range province, which lies directly east of the Cascades in southern Oregon and northern California, has been linked to basaltic magmatism

of the Cascade Range [Priest et al., 1983; Smith and Luedke, 1984].

Typically, models that relate the distribution of volcanism to the regional tectonic framework make little distinction with regard to the nature of volcanic products; attention commonly is focused on major stratovolcanoes [e.g., Hughes et al., 1980]. We extend the treatment of volcanism and investigate the distribution of middle Miocene and younger volcanic vents in the Pacific Northwest with respect to time, space, and composition. Our data set includes monogenetic vents, minor stratovolcanoes, and shield volcanoes, in addition to the major, physiographically dominant, volcanic centers. Our intent is to provide a range-wide volcanic framework with a focus on the past 5 Ma. Our analysis accepts the premise of Smith and Luedke [1984] that the distribution of volcanic vents is a better indicator of the area of regional magma generation than the outcrop area of eruptive products. Our investigation of vent patterns allows us to subdivide the Cascade Range into five segments which we correlate with structural elements of the Juan de Fuca and Gorda plates. We also examine westward migration of Basin and Range volcanism into the Cascade region.

#### VENT DATA

The latitude and longitude of approximately 4000 volcanic vents less than 16 Ma in Washington, Oregon, northern California, and northwestern Nevada were digitized from the map compilations of Luedke and Smith [1981, 1982]. In addition to determining these locations, we followed the classifications of Luedke and Smith [1981, 1982] and assigned each vent to one of eight age groups (in years: <100; 100-1000; 1000-10,000; 10,000-100,000; 100,000-1 million; 1-5 million; 5-10 million; 10-16 million), to one of four

compositional categories based on  $\text{SiO}_2$  percentage (basalt, 46-54%; andesite, 54-62%; dacite, 62-70%; rhyolite, >70%), and to one of seven vent types (cinder cone, dome, shield, stratovolcano, neck, maar, dome cluster).

The vent data have some notable limitations. Because of erosion and possible burial of vents by younger rocks, the data provide minimum values for the number and areal extent of any given temporal distribution of vents. The problem of vent loss can be expected to worsen for increasingly older age groups. We do not estimate the volume of rock erupted from each vent, so volcanism at polygenetic volcanoes is under-represented. Luedke and Smith [1981; 1982] used available chemical analyses to assign vents to compositional categories that differ slightly from those defined by some other workers. For example, andesite is defined as 53-63%  $\text{SiO}_2$  in Gill [1981]. In addition, the andesite category in this study does not distinguish basaltic andesite (53-57%  $\text{SiO}_2$ ), a compositional category common in central Oregon (e.g., Sherrod, 1986; Hughes and Taylor, 1986). Errors in digitizing locations of vents on 1:1,000,000 scale maps result in an accuracy of about  $\pm 1$  minute of latitude and longitude. Because we consider vent patterns of such a large region, these uncertainties in location are not significant for this study; however, original sources, listed by Luedke and Smith [1981, 1982], should be consulted for details of vent patterns.

Another limitation of our data set is that it does not include volcanic vents of the Canadian Cascade Range in southern British Columbia. Detailed geological and geochronological information for the Meager Mountain, Mt. Cayley, and Mt. Garibaldi volcanic centers currently is in largely uncompiled and unpublished form [C. Hickson, oral communication, 1987] and not readily available for the kind of temporal and compositional analysis of vents undertaken here.

## DISTRIBUTION OF VOLCANIC VENTS

A pronounced westward to northwestward migration of volcanism has occurred in Oregon, California, and northwestern Nevada during the past 16 Ma [MacLeod et al., 1976; Christiansen and McKee, 1978; Smith and Luedke, 1984]. In Figure 1, we plot vents in the period 5-16 Ma to illustrate this migration, outlining the area of younger vents to indicate where older vents probably are obscured. The oldest observable vents (10-16 Ma) are, with the exception of two groups, distributed east of the Quaternary Cascade arc (Figure 1a). The majority of vents in southeastern Oregon and northwestern Nevada in this time interval are basaltic or rhyolitic and have been interpreted as part of the extensional volcanism of the Basin and Range province [Christiansen and Lipman, 1972; Christiansen and McKee, 1978]. Such volcanism is thought to involve rise of mantle-derived basaltic magma through extensionally thinned and faulted crust, with basaltic intrusions supplying heat for partial melting of crustal rock to produce rhyolitic magma. Other notable features of the 10-16-Ma vent distribution include basalt, andesite, and rhyolite in the Blue Mountains of northeastern Oregon, basaltic vents along the Oregon coast, and a band of 10 andesitic vents roughly between 44° and 45°N that constitute part of the Western Cascades. This last group comprises few vents but a relatively large outcrop area.

The area of volcanism 5-10 Ma (Figure 1b) is west of the 10-16-Ma distribution. Vents 5-10 Ma occur primarily south of 44°N (the approximate latitude of the Quaternary Three Sisters volcanic field). Most of the vents are basaltic shields and cones that form a wide, NNW trending belt east of the position of the younger Cascade arc. Andesitic vents are restricted to the



most northwesterly area of the distribution, southwest of present-day Newberry volcano. The paucity of vents 5-10 Ma in southeastern Oregon and northwestern Nevada is consistent with the model of Christiansen and McKee (1978) that, although extension began 17 to 14 Ma and occurred throughout the northern Basin and Range up to 12 Ma, faulting and volcanism subsequently became progressively concentrated outward along the brittle margins of the province.

The distribution of 2821 vents less than 5 Ma (Figure 2a) is in sharp contrast to that of older vents. The overall pattern depicts the Cascade Range in Washington, Oregon, and California and delineates the northern margin of basin-range volcanism along the WNW trending High Lava Plains. Unlike vent distributions of the two earlier intervals, the well developed N-S trending volcanic arc is a salient feature. Although the vent patterns suggest that there was apparently little volcanism in the Cascade Range prior to 5 Ma, we emphasize that products of the 0-5-Ma volcanism likely cover an indeterminate number of older vents, particularly in central Oregon where late Miocene volcanic rocks that occur west and east of the Quaternary arc are recognized by Sherrod [1986] and Smith et al. [1987] to have vented from the site of the Quaternary arc. In Figure 2b, we have plotted the area of 5-16-Ma outcrops that lie west of the 0-5-Ma vents in Oregon (from Luedke and Smith [1982]) to illustrate that there is geologic evidence of an andesitic arc prior to 5 Ma although the vent data are sparse.

Between Mount Shasta and Mount Hood, the 0-5-Ma arc is a narrow belt approximately 50-km wide except where the High Lava Plains join the arc. On both ends of the narrow belt, the distribution of vents changes. To the north between Mount Hood and Mount Rainier, the zone of vents broadens to about 150 km, with less dense spacing of vents. Further north, a 90-km gap separates Mount Rainier from Glacier Peak, and volcanism in northern Washington is

limited to a few vents in the vicinity of the stratovolcanoes Mount Baker and Glacier Peak. In California, the area of vents widens around Mount Shasta and Lassen Peak compared to the distribution in Oregon, and the Lassen area is spatially separated from the continuous distribution of vents to the north.

Separate plots of andesitic (Figure 3a) and basaltic (Figure 3b) vents emphasize contrasts in the compositional distribution. Within the N-S trending arc in Oregon (excluding vents around Newberry volcano where burial makes vent counts highly uncertain), approximately 60% of the vents are andesitic and 30% are basaltic. Near the Oregon-California border, there is a pronounced change in the ratio of andesitic to basaltic vents. Andesite predominates north of the border, whereas basalts constitute about three-fourths of vents to the south. The southern extent of the andesitic belt in Oregon has shifted northward about 35 km between 5 and 1 Ma (dashed horizontal lines on Figure 3a).

The distribution of basaltic vents less than 5 Ma (Figure 3b) generally is not similar to that of andesitic vents of the same age group (Figure 3a). Between the Three Sisters field and the Oregon-California border and between Mount Jefferson and Mount Hood, there are few basaltic vents, in contrast to the dense distribution of andesitic vents over most of this region. In southern Washington, where the overall width of the zone of vents is about 150 km, nearly 80% of these vents are basaltic. Some of these basaltic vents lie further west than nearby andesitic vents, and others lie east of Mount Adams (note outlined area in Figure 3b). In northern California, a few basaltic vents occur southwest of the main concentration of vents around Lassen Peak. To the east of the Lassen center, basaltic vents occur up to 75 km east of identified andesitic vents.

A similarity between the andesitic and basaltic distributions in Figure 3

is that south of Mt. Hood the western extent of basaltic vents coincides with the western extent of andesitic vents. A second similarity is in northern California where few basaltic or andesitic vents occur between Mount Shasta and Lassen Peak.

Basaltic vents also occur considerably east of the andesitic vents along the High Lava Plains, which in Oregon are characterized by concentration of basaltic and rhyolitic rocks in a zone of WNW trending en echelon normal faults called the Brothers fault zone [Walker, 1977; Walker and Nolf, 1981]. The region between Newberry volcano and Three Sisters volcanoes, where the High Lava Plains intersect the Cascade Range, is distinguished by: increased density of both andesitic and basaltic vents compared to areas to the north and south; widening of the andesitic zone from about 30 to 80 km; and eastward indentation about 20 km of the western limit of andesitic vents near Three Sisters.

Vents less than 1 Ma (Figure 4) constitute about 60% of the identified 0-5-Ma vents and exhibit a spatial pattern similar to that of the 0-5-Ma vents. The andesitic arc predominates in Oregon, basaltic volcanism continues in southeastern Oregon, major volcanic centers occur at Mount Shasta and Lassen Peak, and a less dense zone of vents occurs in southern Washington. Figure 4 indicates the areal extent of volcanism has contracted during the past 5 Ma, as evidenced by: widening of the andesitic gap northward between Mount Shasta and Mount McLoughlin; localization of volcanism around Mount Shasta, Medicine Lake, and Lassen Peak; and narrowing of the zone of vents in southern Washington, although this last evidence may be partly an artifact of insufficient dating. The age of the Simcoe field (2-5 Ma), which lies southeast of Mount Adams, is constrained by only three dates on samples from the southeast part of the field; based on youthful-looking geomorphology,

parts of the field actually may be less than 1 Ma [W. Hildreth, oral communication, 1986].

During the time interval of less than 0.1 Ma (Figure 5), volcanism in the Cascade Range is concentrated around the major composite volcanoes, with only a few vents active elsewhere. Exceptions to this pattern are seen at the Indian Heaven basaltic field between Mount St. Helens and Mount Adams and vents south of Three Sisters (Figure 5a). The area from Three Sisters to Newberry is the most intense focus of venting during the past 0.1 Ma. A more detailed study of vent patterns at South Sister by Bacon [1985] shows that Holocene basaltic vents form a NNW striking en echelon pattern of short N-S vent segments that are aligned with the regional stress field of the Cascades. The South Sister silicic volcanic field occurs where this NNW striking zone intersects the axis of the N-S chain of major Cascade stratovolcanoes.

About 12% of vents less than 0.1 Ma are dacitic and rhyolitic (Figure 5b), and these silicic vents account for about 45% of dacitic and rhyolitic vents in the Cascade Range (west of 121°W) in the interval 0-5 Ma. That nearly half of the silicic vents occur within only 2% of the time interval 0-5 Ma may reflect better preservation of young silicic vents and/or an episode of greater eruptive frequency of silicic volcanism during the past 0.1 Ma compared with basaltic and andesitic volcanism.

#### VOLCANIC-ARC SEGMENTATION

Based on the distribution of 2821 volcanic vents less than 5 Ma, we divide volcanism of the Pacific Northwest into six areal segments; five segments comprise the Cascade Range, and a sixth constitutes the High Lava

Plains (Figure 6). The most northerly segment contains only the isolated stratovolcanoes Glacier Peak and Mount Baker, as well as the Cascade centers in British Columbia (Meager Mountain, Mount Cayley, and Mount Garibaldi) which we include for completeness although detailed vent data currently are not available. From Mount Rainier to Mount Hood, segment two encompasses the wide zone of primarily basaltic volcanism and includes the occurrence of basalts east and west of the poorly defined andesitic arc. A long segment, approximately 370 km, extends from south of Mount Hood to the vicinity of the Oregon-California border and is characterized by a dense distribution of andesitic vents. We define the southern boundary of this third segment by the decrease in the ratio of andesitic to basaltic vents, noted in the previous section. The fourth segment includes Mount Shasta and Medicine Lake volcano in California and the basaltic vents to the north. The Lassen area, spatially isolated from the Cascade Range to the north in terms of the distribution of both andesitic and basaltic vents, constitutes the fifth segment. This six-fold subdivision of 0-5-Ma vents also is applicable to the distribution of 0-1-Ma vents (Figure 4).

Our segmentation model of the Cascade Range is based on different criteria than commonly used by others to segment volcanic arcs. Typically, segmentation of volcanic arcs has been based on assigning active stratovolcanoes to discrete linear segments, such that each linear segment drawn through 2 or more individual stratovolcanoes has a stratovolcano at its ends [e.g., Stoiber and Carr, 1973; Carr et al., 1976; Hughes et al., 1980]. Using such a method, Stoiber and Carr [1973] divided historically active volcanoes of the Central American arc into seven linear segments and characterized boundaries between segments as areas of normal faulting, concentrated shallow seismicity, basaltic cinder cones, and catastrophic large

eruptions. The boundaries between segments were modeled as tear faults that break the subducting Cocos plate into separate blocks of differing strikes and dips; these lower-plate variations were assumed to give rise to the observed volcanic segmentation.

The areal occurrence of volcanism has been related to the distribution of seismicity in the Nazca subduction zone beneath South America. Areas of moderate crustal seismicity and limited Cenozoic volcanism overlie shallow-dipping portions of the Nazca plate, whereas areas with few crustal earthquakes and extensive Cenozoic volcanism overlie more steeply dipping sections of the Nazca plate [Barazangi and Isacks, 1976; Jordan et al., 1983]. In both the Nazca and Cocos subduction zones, the occurrence of Benioff-zone earthquakes along most of the strike of the subduction zone allows the relation between surface volcanism and the configuration of the subducting plate to be established.

Both segmentation models (alignment of stratovolcanoes and the areal distribution of seismicity and volcanism) have been applied to the Cascade Range. Hughes et al. [1980] applied the alignment model to the Cascades and divided the arc into six linear segments, ranging from 110 to 240 km in length: Mount Garibaldi-Glacier Peak, Glacier Peak-Mount St. Helens, Mount Adams-Three Sisters, Three Sisters-Crater Lake, Crater Lake-Mount Shasta, and Mount Shasta-Lassen Peak. They postulated that irregularities and changes in strike of the base of the continental slope indicate segmentation of the convergent margin; however, they cite no independent topographic, structural, or seismic evidence for this segmentation. Hughes et al. [1980] noted that these inferred margin segments, if extrapolated northeastward in the direction of convergence of the Juan de Fuca and North American plates, correlate with boundaries between volcanic segments. Our segments do not coincide with those

of Hughes et al. [1980] mainly because we use the distribution and composition of 2821 vents formed during the past 5 Ma rather than offsets in the alignment of about 20 recently active volcanic centers. Also, we consider vent distributions within segments, in addition to the locations of boundaries between segments.

Weaver and Michaelson [1985] used the earthquake distribution and areal extent of late Cenozoic volcanism to divide the northern Cascade Range into three segments: Mount Baker to Mount Rainier, Mount Rainier to Mount Hood, and Mount Hood south. The two northern segments are similar to those in our model, but the orientation of the boundaries defined by Weaver and Michaelson [1985] is parallel to convergence direction. We do not specify any orientation of boundaries on Figure 6 because we cannot independently confirm them to be linear physical features in the crust or slab.

## REGIONAL TECTONIC CONSIDERATIONS

### Structural Elements of the Juan de Fuca Plate

Some aspects of our segmentation model correlate with inferred structural elements of the Juan de Fuca plate system. At present, the system consists of small remnants of the Farallon plate, which was subducting beneath most of the west coast of North America until about 30 Ma when the San Andreas transform fault system began to form and grow in length northward and southward (Atwater, 1970). The Juan de Fuca plate is bounded by 2 smaller sub-plates, the Explorer on the north and the Gorda on the south (Figure 6). The Juan de Fuca plate is converging obliquely to the northeast relative to the North American plate at the comparatively slow rate of 3-4 cm/yr [Riddihough, 1977; 1984]. The Explorer plate apparently is no longer be subducting beneath North

America and instead is pivoting about a pole of motion different from the rest of the plate system; to the south, the Gorda South plate similarly may be in the process of moving independently relative to the Juan de Fuca and Gorda North plates [Riddihough, 1984].

In most subduction zones, the occurrence of Benioff-zone earthquakes indicates that the subducting plate is about 100-150 km depth below the volcanic arc [e.g., Gill, 1981; Isacks and Barazangi, 1977]; these Benioff-zone earthquakes allow the geometry of the subducting plate to be determined from the trench to the position of the volcanic arc. In the Pacific Northwest, however, Benioff-zone earthquakes occur only west of the volcanic arc beneath western Washington, northern Oregon, and northern California, generally at depths less than 80 km [Weaver and Baker, in press; Walter, 1986; Cockerham, 1984]. Although the position of the plate directly beneath the Cascade arc is conjectural, it is reasonable to assume that the andesitic volcanism of the past 5 Ma is the result of magma genesis associated with the Juan de Fuca plate being at a depth of about 100 km beneath the andesitic arc. Walter [1986], for example, notes that near Lassen Peak continued projection of the Gorda plate at 25° dip (determined from 50 to 80 km by Benioff-zone seismicity) would place the plate at a depth of approximately 100 km beneath the volcanic arc.

In Figure 6 we show the location of the 40- and 60-km contours of plate depth that have been inferred from the known distribution of sub-crustal hypocenters [from Weaver and Baker, in press; Walter, 1986; Cockerham, 1984]. There is no seismic data to constrain the position of the plate beneath most of Oregon. Weaver and Baker [in press] noted that beneath the Puget Sound basin, the Juan de Fuca plate has an upward undulation or arch between a depth of 40 and 60 km with respect to the depth of the plate to the



south; north of the undulation the Juan de Fuca plate dips to the northeast and south of it the plate dips to the east-southeast (dip is approximately perpendicular to plate depth contours in Figure 6). As a result, the horizontal distance from the convergent margin to the 60-km contour is greatest (300 km) where the plate arches upward and decreases to about 200 km elsewhere beneath southwestern Washington, Vancouver Island, and northern California.

Within this context, we are able to relate our segmentation of the Cascade Range to gross structural elements of the Juan de Fuca plate (Figure 6). We cannot unambiguously determine the position of the subducting plate solely from the distribution of volcanism. However, from the spatial relation of the vent distributions and Benioff-zone seismicity, we conclude that volcanic segments reflect the subducting-plate geometry which varies along the entire length of the subduction system.

North of the plate arch, the stratovolcanoes represent a volcanic front (defined here as the most trenchward extent of volcanism less than 5 Ma) that is approximately parallel with the 60-km depth contour of the plate and perpendicular to the direction of relative convergence (N.50°E.) between the Juan de Fuca and North American plates. The volcanic gap between segments one and two is landward of the plate arch, that portion of the subducting plate with the least average dip between the margin and a depth of 60 km (approximately 11°). In segment two, the volcanic front from Mount Rainier to the basaltic vents near Portland, Oregon is approximately parallel with the 60-km plate depth contour to the west, in similar fashion to segment one, but the strike of the volcanic front (and plate-depth contours) is approximately perpendicular to the spreading direction of the Juan de Fuca ridge. The volcanic front of segment one is further east of the 60-km contour than the

volcanic front of segment two, perhaps because the plate dips more steeply beneath segment two at depths greater than 60 km. Segments three and four are landward of the aseismic portion of the subduction system where no plate contours are delineated. The volcanic front of segment five also is parallel with the 60-km plate contour and perpendicular to the ridge-spreading direction, as in segment two.

A prominent feature of Figure 6 is that terminations of the 60-km plate contours in northern Oregon and northern California coincide with boundaries between independently determined volcanic segments. It is evident from the offset of the discontinuous contours that additional variation in the geometry of the Juan de Fuca plate is expected. We infer from the parallel relation of the subducting-plate contour and volcanic front observed in segments one, two, and five that the Juan de Fuca plate should have a similar geometry everywhere beneath segment three and four. Consequently, the expected variations in plate geometry likely occur near the boundaries between volcanic segments two and three and four and five.

The volcanic front of segment three is further east than the volcanic front of segment two, and it is conceivable that the 60-km plate contour likewise is offset to the east beneath northern Oregon. The narrowness of the vent distribution in segment three implies that the zone of magma generation is confined to a small volume of the upper mantle, perhaps because the Juan de Fuca plate dips steeply through the magma-genesis zone.

In the case of segments four and five, Mount Shasta is positioned about 50 km further west toward the convergent margin than the Lassen center which overlies the Gorda North plate. Consequently, northward linear extrapolation of the 60-km contour west of Lassen Peak yields an improbably shallow depth to the Benioff zone beneath Mount Shasta. If the volcanic front of segment four

occurs approximately 40 km east of the 60-km contour, as it does in segment 5, then westward offset of the 60-km contour is suggested between the Shasta and Lassen volcanic centers. If the volcanic front of segment four is closer to the 60-km contour, then the Juan de Fuca plate is dipping more steeply than the Gorda North plate at depths greater than 60 km. In either instance, a change in the configuration of the subducting slab is implied between the Shasta and Lassen centers. Since roughly 4 Ma, the Gorda North plate has been the youngest oceanic crust to subduct, and the presumably hotter and more buoyant crust may have greater resistance to subduction [Riddihough, 1984]. The inferred change in geometry of the Juan de Fuca and Gorda North plates may be related to this difference in subduction.

The spatial congruence between segmentation of a volcanic arc and geometry of a subducting plate is not always observed where the two features are determined independently. Burbank and Frohlich [1986] used hypocenters reported by the International Seismological Center in an effort to systematically examine changes in subduction-zone geometry around the Pacific. They noted that 68% of the probable segment boundaries, defined using earthquake hypocenters as areas where the subduction geometry changed, were associated with noticeable changes in arc volcanism, but that these changes seldom coincided exactly and were often separated by as much as 100 km. Our ability to match more closely the inferred changes in plate geometry and volcanic-arc segmentation in the Pacific Northwest is likely the result of considering longer time intervals and all of the volcanic vents. Furthermore, the congruence of the volcanic segments and subducting-plate geometry implies that the extent of subduction-related magma generation in the mantle is generally well-represented by surface volcanism -- i.e., the crust has sufficient extension to foster the rise of magma to the surface, particularly

in Oregon and northern California.

### Basin and Range Impingement

An interesting aspect of the regional tectonic framework in which subduction takes place is the presence of the extensional Basin and Range province in the North American plate directly adjacent to the subduction zone. The westward migration of basin-range volcanism toward the developing Cascade arc is well depicted in Figures 1 and 2a. We use the term "impingement" for the occurrence of extension-related volcanism adjacent to the Cascade arc. Impingement occurred during the interval 5-10 Ma (Figure 1b), apparently first in the vicinity of the most northwestward group of andesitic and basaltic vents between present-day Crater Lake and Newberry volcanoes. Comparison of Figure 1b with Figure 2a shows that since 5 Ma there is virtually no continuation of volcanic activity in the area of the 5-10 Ma volcanism in south-central Oregon and northeasternmost California; volcanism since 5 Ma in southern Oregon occurs exclusively in the narrow Cascade arc. This cessation of basin-range volcanism is not entirely unexpected, as it is consistent with the trend, as illustrated in Figure 1, of volcanism ceasing behind a migrating zone of vents. However, it is notable that subduction-zone geometry so thoroughly defines the overall volcanic pattern in southern Oregon after 5 Ma.

Basaltic volcanism has continued after 5 Ma east of Medicine Lake and Lassen Peak (Figure 2a), perhaps because the leading edge of the NNW trending belt of basin-range volcanism impinges successively southward against the Cascade arc. If so, basaltic volcanism on the eastern flanks of the Cascade Range in northern California may identify where impingement is not yet complete within the past 5 Ma. Since 5 Ma, volcanism has become more

localized around Mount Shasta, Medicine Lake, and Lassen Peak (Figure 4). In the Lassen area, westward volcanic contraction [Grose and McKee, 1982] has been accompanied by a 90° change in direction of least principal stress as evidenced by fault trends and volcanic alignments [Grose, 1985]. Over a distance of about 50 km, the direction of least principal stress changes from roughly northwest-southeast 10-12 Ma in the Walker Lane of the Basin and Range to roughly southwest-northeast 0-2 Ma directly adjacent to Lassen Peak [Grose, 1985; Grose and McKee, 1986]. The coeval volcanic progression and stress changes in the Lassen vicinity document the migration of basin-range volcanism into the Cascade region.

Juxtaposition of basin-range volcanism and tectonism with the Cascade arc also occurs where faulting and volcanism along the High Lava Plains intersect the arc in the vicinity of Three Sisters and Newberry volcanoes. The High Lava Plains are recognized as the northern transform boundary of maximum extension in the Basin and Range province, separating the Great Basin from the Columbia Plateau province to the north [Christiansen and McKee, 1978]. Discontinuous N-S trending normal faults on both sides of the Quaternary Cascade arc between Three Sisters and Mount Jefferson structurally define what has been called the High Cascades graben. Smith and Taylor [1983] proposed that the graben was formed by regional extension associated with late Miocene mafic volcanism in central Oregon. Smith et al. [1987] concluded that extension-related Cascade volcanism began there about 7 Ma, followed by development of the intra-arc graben, represented by the Green Ridge fault, about 5.3 Ma. Based on linear gravity anomalies, Couch and Foote [1983] extended the graben structure from Crater Lake to the area between Mount Hood and Mount Jefferson. Impingement of basin-range volcanism apparently occurred within the period 5-10 Ma in central Oregon (Figure 1b) and thus is

approximately coincident in time and space with the extensional volcanism that led to the development of the High Cascades graben in central Oregon between Three Sisters and Mount Jefferson.

## DISCUSSION

The fundamental cause of the volcanic migration in the Pacific Northwest is speculative. A model postulated by Christiansen and McKee [1978] is that volcanic migration in the northern Basin and Range province is due to progressive concentration of extension and volcanism in a zone of brittle deformation; this brittle zone has expanded outward along the western and eastern margins of the province owing to decreased rigidity of the initial rift zone in central Nevada. Thus, the rise of basaltic magma generated at the base of the lithosphere may be successively triggered by propagating stress relief.

Extension-related volcanism in the Cascades has been linked to a variety of factors including subduction oblique to the convergent margin [Rogers, 1985; Bacon, 1981], increase in the spreading rate of the Basin and Range [Priest, et al., 1983], and decrease in convergence rate between the Juan de Fuca and North American plates [Walker and Naslund, 1986; Hughes and Taylor, 1986]. While we cannot rule out the effect of some combination of these factors, we emphasize that regional tectonic models also should account for the observed migration of extensional basin-range volcanism adjacent to (and possibly into?) the Cascade Range.

In a plate-tectonic framework, the issue arises as to whether the Basin and Range province effectively acts as a back-arc basin to the Cascade Range. Certainly, the major episode of subduction had ceased along the coast

of California when extension began in Nevada 17 Ma (Atwater, 1970), and thus the entire Basin and Range province is not a back-arc basin in a strict sense (Christiansen and McKee, 1978). Nevertheless, basin-range extension is spatially closely associated with the Cascade Range within the past 10 Ma. Furthermore, petrological investigations indicate that basin-range lavas have geochemical affinities with back-arc basin basalts; in northern California and southeastern Oregon adjacent to the Cascades, low-potassium, low-titanium, high-alumina olivine tholeiites, chemically similar to circum-Pacific back-arc basin basalts, are widespread in the late Miocene to Quaternary [McKee et al., 1983; Hart et al., 1984]. However, it is not yet clear what the stratigraphic relations of this magma type to others is within the Cascade arc.

The vent data do not allow us to deal explicitly with processes of magma generation. However, we wonder if basin-range volcanism and Cascade volcanism involve contrasting mantle magmatic regimes. That is, does basin-range impingement against the Cascade arc juxtapose different source regions of primary magma, one predominantly controlled by extensional tectonism and another deeper zone dominated by subduction-related melting? Although this question is best analyzed by geochemical arguments beyond the scope of this paper the vent data presented here provide a regional context for addressing the issue.

As a final note, we point out that our assumption linking the presence of an andesitic volcanic arc with the presence of a subducting plate at a depth sufficient for melting processes to be sustained is a major departure from the interpretation of the volcanic Cascade Range of McBirney [1978] and McBirney and White [1982]. These authors have suggested that there is little direct evidence to link volcanism in the Pacific Northwest with subduction; in their view, even the spatial relation is ambiguous because the linear belt of

andesitic volcanism observed today has not been a persistent feature of the Cascade Range. In our view, the apparent lack of a persistent volcanic arc throughout the long history of convergence in the Pacific Northwest does not invalidate the commonly acknowledged relation between andesitic volcanism and plate subduction. We are particularly impressed with correlation of volcanic segments with inferred subducting-plate geometry. Furthermore, we suggest that the length of the Cascade arc alone is difficult to explain without invoking causal, plate-scale interactions.

### CONCLUSIONS

Pronounced spatial, temporal, and compositional variations in volcanism in the Cascade Range are exhibited by distributions of 0-16-Ma volcanic vents, and for this reason no single section across the range is representative of volcanism for the entire range. The Cascade Range can be divided into 5 segments, with the High Lava Plains constituting a sixth, based on the spatial distribution of nearly 3000 volcanic vents less than 5 Ma. Some aspects of the segmentation model can be related to inferred structural elements of the Juan de Fuca and Gorda North plates. The relation of plate-depth contours and the volcanic front indicates that the volcanic segments reflect the variable geometry of the subducting slab. The volcanic front is parallel to the strike of the Juan de Fuca plate, being perpendicular to convergence direction in northern Washington but approximately perpendicular to the ridge-spreading direction in southern Washington, northern Oregon and northern California. A volcanic gap between Mount Rainier and Glacier Peak is east of the portion of the subducting plate with the least average dip to a depth of 60 km. A narrow, N-S trending andesite-rich belt in Oregon is landward of the



seismically quiet portion of the subduction zone; the eruption of andesite in a narrow distribution suggests that the Juan de Fuca plate dips steeply beneath the Cascade arc throughout Oregon. Paucity of vents between the Mount Shasta and Lassen centers overlies the boundary between the Juan de Fuca and Gorda North plates, which have differing age and seismicity. Breaks in offset contours of plate depth coincide with independently determined boundaries between volcanic segments in northern Oregon and northern California.

Vent patterns since 16 Ma depict migration of basin-range volcanism toward the Cascade arc. In Oregon, basin-range volcanism migrated adjacent to the Cascade arc (defined here as "impingement") 5-10 Ma, and basin-range volcanism in southern Oregon has ceased since 5 Ma. In contrast, basaltic volcanism east of the Cascade Range continues in the past 5 Ma in northeastern California where the impingement process apparently is not complete in that time period. Contraction of the area of basaltic volcanism during the past 5 Ma around Mount Shasta, Medicine Lake, and Lassen Peak occurs as basin-range volcanism migrates toward the subduction-related volcanism system beneath northern California. In central Oregon, where the High Lava Plains intersect the Cascade arc, impingement roughly coincides in time with commencement of extension-related volcanism and development of the High Cascade graben.

#### ACKNOWLEDGEMENTS

We thank Wes Hildreth and Wendell Duffield for helpful reviews. We also benefited from comments from Charles Bacon, Thomas Bullen, Geoffrey Clayton, Michael Clyne, Robert Luedke, Patrick Muffler, David Sherrod, James Smith, and Robert Smith. We are very grateful to Toni Medlin for use of her digitizing system and to the Reston Seismic Group for computer support and consultation.

## REFERENCES CITED

- Atwater, T., Implications of plate tectonics for the Cenozoic evolution of western North America, Geol. Soc. Am. Bull., 81, 35-13,3536, 1970.
- Bacon, C. R., Geology and geophysics of the Cascade Range, Geophysics, 47, 423-424, 1981.
- Bacon, C. R., Implications of silicic vent patterns for the presence of large crustal magma chambers, J. Geophys. Res., 90, 11243-11252, 1985.
- Barazangi, M., and B. Isacks, Subduction of the Nazca plate beneath Peru: evidence from spatial distribution of earthquakes, Geophys. J. R. Astron. Soc., 57, 537-555, 1976.
- Burbank, G.V., and C. Frolich, Intermediate and deep seismicity and lateral structure of subducted lithosphere in the circum-Pacific region, Reviews of Geophysics, 24, 833-874, 1986.
- Carr, M. J., R. E. Stoiber, and C. L. Drake, The segmented nature of some continental margins, in C. A. Burk and C. L. Drake, ed., The Geology of Continental Margins, Springer-Verlag, 105-114, 1976.
- Christiansen, R. L., and P. W. Lipman, Cenozoic volcanism and plate tectonic evolution of the western United States - Part II, late Cenozoic, R. Soc. London Philos. Trans., ser. A, 272, 249-284, 1972.

- Christiansen, R. L., and E. H. McKee, Late Cenozoic volcanic and tectonic evolution of the Great Basin and Columbia Intermontaine regions, Mem. Geol. Soc. Am. 152, 283-311, 1978.
- Cockerham, R. S., Evidence for a 180-km-long subducted slab beneath northern California, Bull. Seis. Soc. Am., 74, 569-576, 1984.
- Couch, R. W., and R. W. Foote, Graben structures of the Cascade Range in Oregon, Eos Trans. AGU, 64, 887, 1983.
- Gill, J. B., Orogenic andesites and plate tectonics, Springer-Verlag, 390 p., 1981.
- Grose, T. L. T., Volcanotectonic evidence for stress field changes since Late Miocene in Basin and Range-Cascade boundary zone (Walker Lane) of northeastern California (abstract), Eos Trans. AGU, 66, 1091, 1985.
- Grose, T. L. T., and E. H. McKee, Late Cenozoic westward volcanic progression east of Lassen Peak, northeastern California, Eos Trans. AGU, 63, 1149, 1982.
- Grose, T. L. T., and E. H. McKee, Potassium-argon ages of late Miocene to late Quaternary volcanic rocks in the Susanville-Eagle Lake area, Lassen County, California, Isochron/West, 45, 5-11, 1986.
- Hart, W. K., J. L. Aronson, and S. A. Mertzman, Areal distribution and age of low-K, high-alumina olivine tholeiite magmatism in the northwestern Great Basin, Geol. Soc. Am. Bull., 95, 186-195, 1984.

- Hughes, J. M., R. E. Stoiber, and M. J. Carr, Segmentation of the Cascade volcanic chain, Geology, 8, 15-17, 1980.
- Hughes, S. S., and E. M. Taylor, Geochemistry, petrogenesis, and tectonic implications of central High Cascade mafic platform lavas, Geol. Soc. Am. Bull., 97, 1024-1036, 1986.
- Isacks, B. L. and M. Barazangi, Geometry of Benioff zones: Lateral segmentation and downwards bending of the subducting lithosphere, in Island Arcs, Deep Sea Trenches, and Back-Arc Basins, Maurice Ewing Ser., vol. 1, pp. 99-114, 1977.
- Jordan, T. E., B. L. Isacks, R. W. Allmendinger, J. A. Brewer, V. A. Ramos, and C. J. Ando, Andean tectonics related to geometry of subducted Nazca plate, Geol. Soc. Am. Bull., 94, 341-361, 1983.
- Luedke, R.G., and R. L. Smith, Map showing distribution, composition, and age of Late Cenozoic volcanic centers in California and Nevada, U.S. Geol. Survey Misc. Invest. Series Map I-1091-C, scale 1:1,000,000, 1981.
- Luedke, R.G., and R. L. Smith, Map showing distribution, composition, and age of Late Cenozoic volcanic centers in Oregon and Washington, U.S. Geol. Survey Misc. Invest. Series Map I-1091-D, scale 1:1,000,000, 1982.
- MacLeod, N. S., G. W. Walker, and E. H. McKee, Geothermal significance of eastward increase in age of upper Cenozoic rhyolitic domes in southeastern Oregon, Proc. Second UN Symp Develop. Use Geothermal Resources, 1, Washington D.C., U.S. Govt. Printing Office, 465-474, 1976.

- McBirney, A. R., Volcanic evolution of the Cascade Range, Annu. Rev. Earth Planet. Sci., 6, 437-456, 1978.
- McBirney, A. R., and C. M. White, The Cascade Province, in Andesites: Orogenic Andesites and Related Rocks, R. S. Thorpe, editor, John Wiley, New York, 115-135, 1982.
- McKee, E. H., W. A. Duffield, and R. J. Stern, Late Miocene and early Pliocene basaltic rocks and their implications for crustal structure, northeastern California and south-central Oregon, Geol. Soc. Am. Bull., 94, 292-304, 1983.
- Michaelson, C. A., and C. S. Weaver, Upper mantle structure from teleseismic P-wave arrivals in Washington and northern Oregon, J. Geophys. Res., 91, 2077-2094, 1986.
- Priest, G. R., N. M. Woller, G. L. Black, and S. H. Evans, Overview of the geology of the central Oregon Cascade Range, Oregon Dept. Geology Mineral Industries Spec. Paper 15, 3-28, 1983.
- Riddihough, R., A model for recent plate interactions off Canada's west coast, Can. J. Earth Sci., 14, 384-396, 1977.
- Riddihough, R., Recent movements of the Juan de Fuca plate system: J. Geophys. Res., 89, p. 6980-6994, 1984.

- Rogers, G. C., Some comments on the seismicity of the Northern Puget Sound-Southern Vancouver Island region, in U.S. Geol. Survey Open-File Rep. 83-19, J. C. Yount and R. S. Crosson, Editors, 19-39, 1983.
- Rogers, G. C., Variation in Cascade volcanism with margin orientation, Geology, 13, 495-498, 1985.
- Sherrod, D. R., Geology, petrology, and volcanic history of a portion of the Cascade Range between latitudes 43°-44°N, central Oregon, USA, Ph.D dissertation, University of California at Santa Cruz, 320 p., 1986.
- Smith, R. L., and R. G. Luedke, Potentially active volcanic lineaments and loci in western conterminous United States, Explosive Volcanism: Inception, Evolution, Hazards, Nat. Academy Press, Washington, D.C., 47-66, 1984.
- Smith, G. A., and E. M. Taylor, The central Oregon High Cascade graben - what? where? when?, Geothermal Resources Council Trans., 7, 275-279, 1983.
- Smith, G. A., L. W. Snee, and E. M. Taylor, Stratigraphic, sedimentologic, and petrologic record of late Miocene subsidence of the central Oregon High Cascades, Geology, 15, p. 389-392, 1987.
- Stoiber, R. E., and M. J. Carr, Quaternary volcanic and tectonic segmentation of Central America, Bull. Volcanol., 37, 304-325, 1973.
- Walker, G. W., Geologic map of Oregon east of the 121 meridian, U.S. Geol. Surv. Misc. Invest. Map I-902, scale 1:500,000, 1977.

Walker, J. R., and H. R. Naslund, Tectonic significance of mildly alkaline Pliocene lavas in Klamath River Gorge, Cascade Range, Oregon, Geol. Soc. Am. Bull. 97, 206-212, 1986.

Walker, G. W., and B. Nolf, High Lava Plains, Brothers fault zone to Harney basin, Oregon, U.S. Geol. Survey Circ. 838, 105-111, 1981.

Walter, S. R., Intermediate-focus earthquakes associated with Gorda plate subduction in northern California, Bull. Seis. Soc. Am., 76, 583-588, 1986.

Weaver, C. S., and G. E. Baker, Geometry of the Juan de Fuca plate beneath Washington -- evidence from seismicity and the 1949 South Puget Sound earthquake, Bull. Seis. Soc. Am., 1987.

Weaver, C. S., and C. A. Michaelson, Seismicity and volcanism in the Pacific Northwest: evidence for the segmentation of the Juan de Fuca plate, Geophys. Res. Lett., 12, 215-218, 1985.

Weaver, C. S., and S. W. Smith, Regional tectonic and earthquake hazard implications of a crustal fault zone in southwestern Washington, J. Geophys. Res., 88, 10371-10383, 1983.

## FIGURE CAPTIONS

Figure 1. Map of volcanic vents in Washington, Oregon, northeastern California, and northwestern Nevada: (a) 385 vents 10-16 Ma, with outline of area of vents younger than 10 Ma taken from Figures 1b and 2; (b) 881 vents 5-10 Ma, with outline of area of vents younger than 5 Ma taken from Figure 2a. Vent data from Luedke and Smith [1981, 1982]. Pluses: basalt; squares: andesite; triangles: dacite; circles: rhyolite. Large triangles indicate locations of major Quaternary volcanoes for comparison. BAKR: Mt. Baker; GLPK: Glacier Peak; RAIN: Mt. Rainier; STHN: Mt. St. Helens; ADMS: Mt. Adams; HOOD: Mt. Hood; JEFF: Mt. Jefferson; 3SIS: Three Sisters; NEWB: Newberry; CRLK: Crater Lake; MCLN: Mt. McLoughlin; SHTA: Mt. Shasta; MEDL: Medicine Lake; LASN: Lassen Peak; VI: Vancouver Island.

Figure 2. (a) Map of 2821 volcanic vents in the Cascade Range and adjacent areas younger than 5 Ma; (b) area of Cascade volcanic rocks 5-16 Ma that lie directly west of vents younger than 5 Ma. Data from Luedke and Smith [1981, 1982]. Pluses: basalt; squares: andesite; triangles: dacite; circles: rhyolite.

Figure 3. Map of volcanic vents younger than 5 Ma in the Cascade Range and adjacent areas, showing andesitic and basaltic vents separately: (a) 814 andesitic vents (squares), with outline of area of basaltic vents taken from Figure 3b; Horizontal dashed lines show southern extent of andesitic arc in Oregon at 1 and 5 Ma; (b) 1780 basaltic vents (pluses), with outline of area of andesitic vents taken from Figure 3a.



Figure 4. Map of 1711 volcanic vents younger than 1 Ma in the Cascade Range and adjacent areas, with outline of area of vents 1-5 Ma taken from Figure 2. Pluses: basalt; squares: andesite; triangles: dacite; circles: rhyolite.

Figure 5. Map of volcanic vents younger than 0.1 Ma in the Cascade Range and adjacent areas: (a) 837 vents of all compositions (pluses: basalt; squares: andesite; triangles: dacite; circles: rhyolite); (b) 103 dacitic (triangles) and rhyolitic (circles) vents.

Figure 6. Map showing plate tectonic features of the Juan de Fuca - North American subduction system [from Riddihough, 1984] in relation to volcanic segmentation of the Cascade arc based on distribution of vents less than 5 Ma. Open arrows show ridge-spreading directions; closed arrow shows direction of convergence between the Juan de Fuca and North American plates. Numbers refer to volcanic-arc segments discussed in text. The 40- and 60-km contours show depth of seismicity in the upper part of the Juan de Fuca and Gorda plates [from Weaver and Baker, in press]. Pluses: basalt; squares: andesite; triangles: dacite; circles: rhyolite. Bold crosses show generalized Quaternary volcanic centers in British Columbia: (from north to south) Meager Mountain, Mount Cayley, Mount Garibaldi.

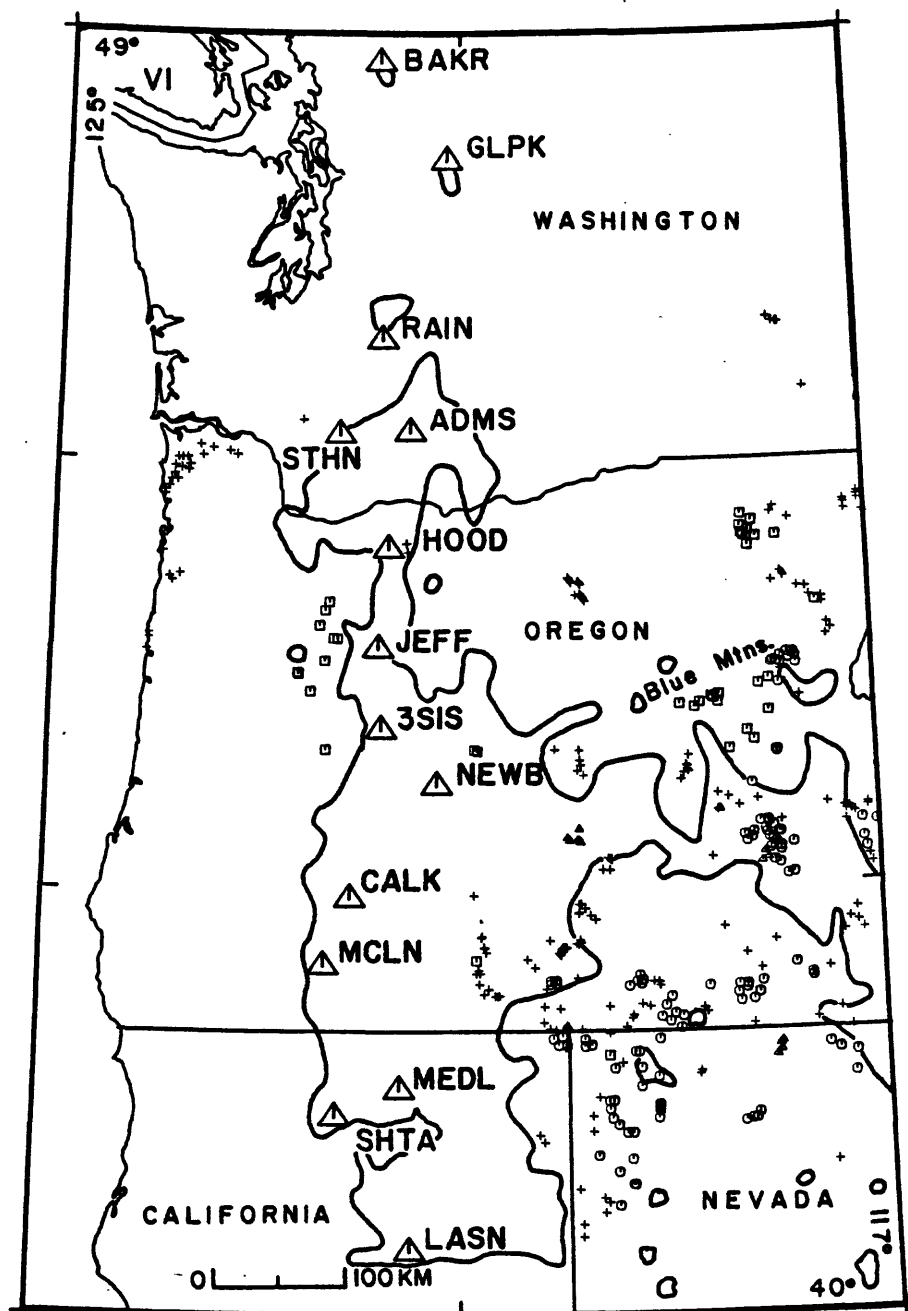


Figure 1a

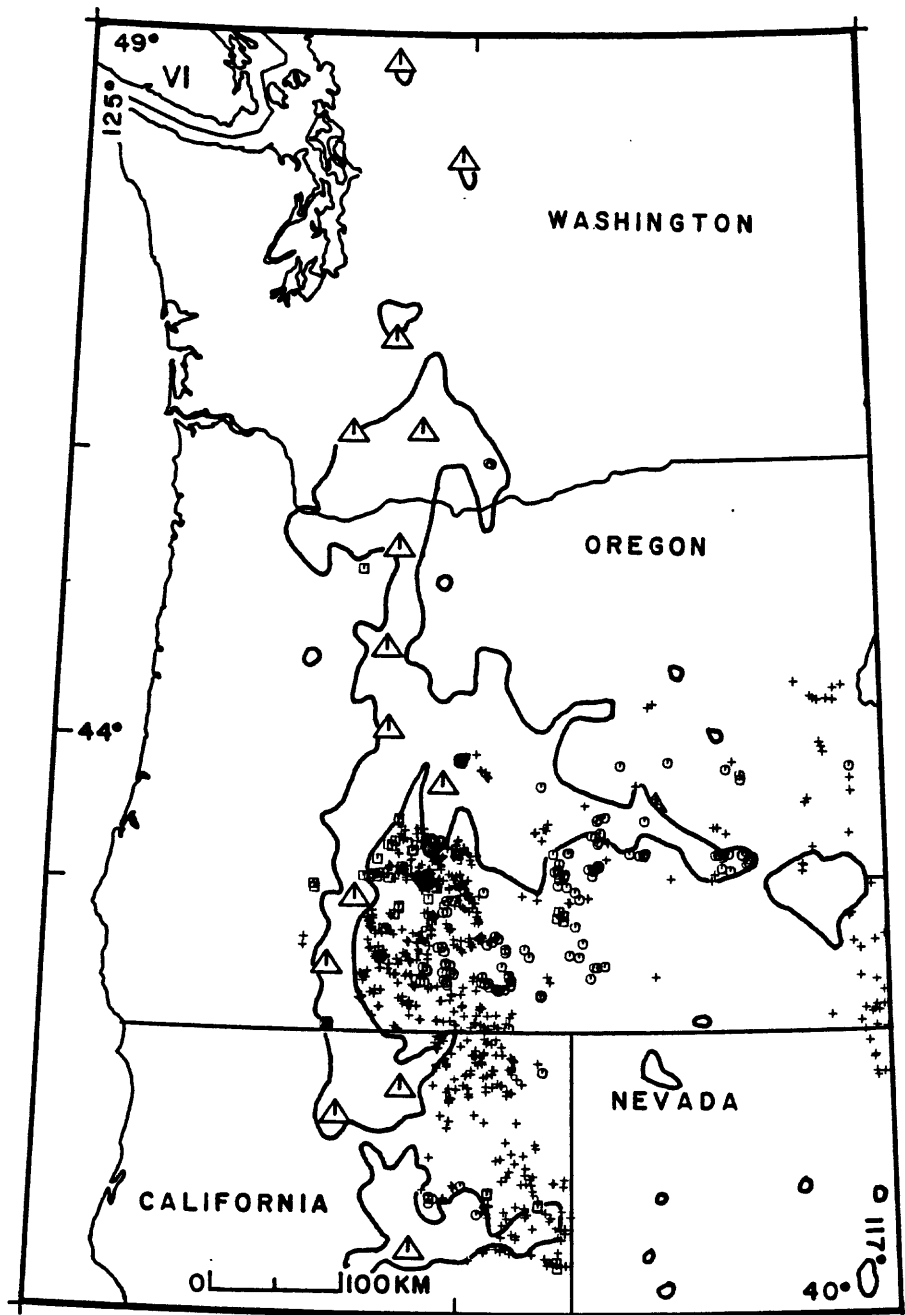


Figure 1b

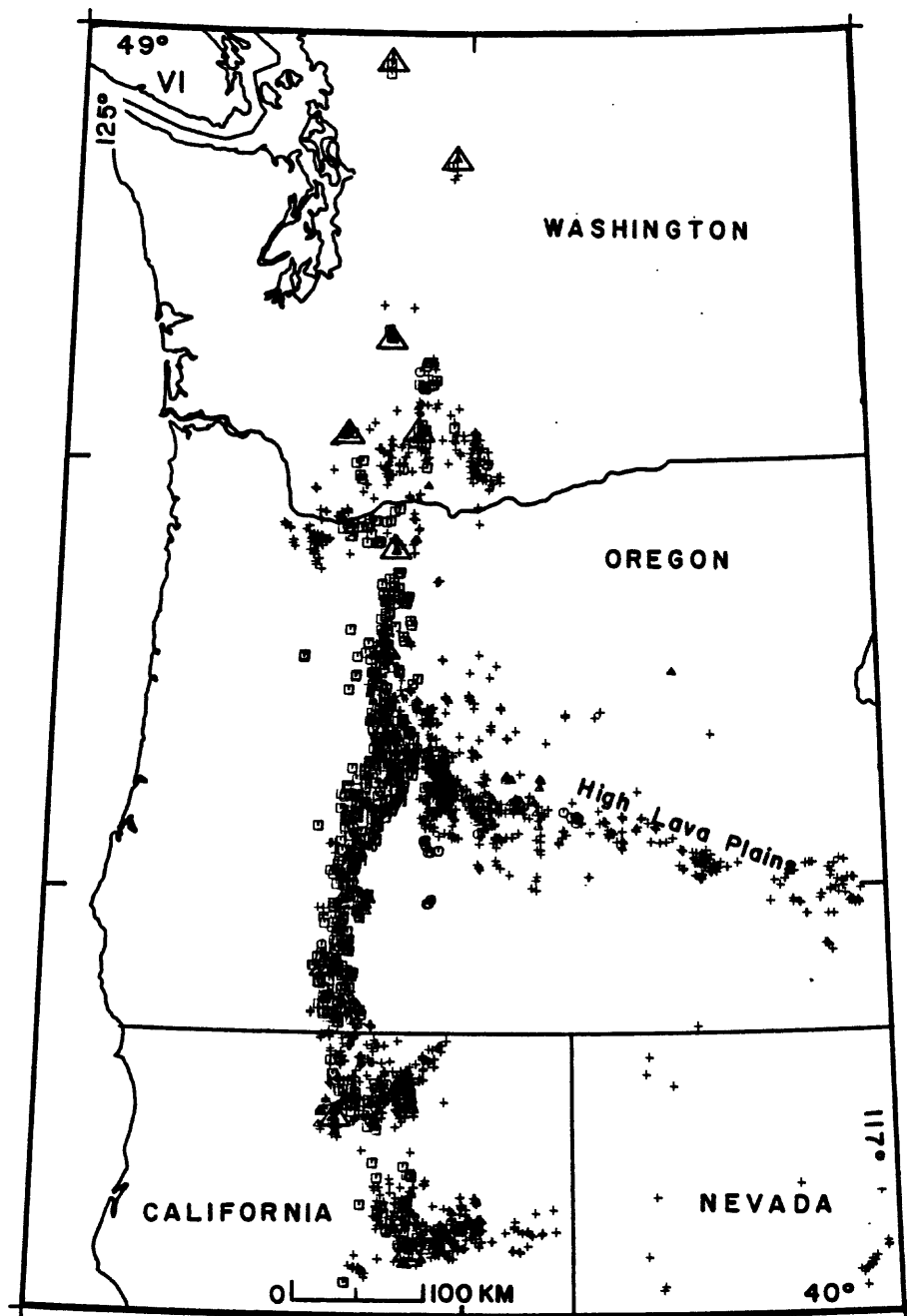


Figure 2a

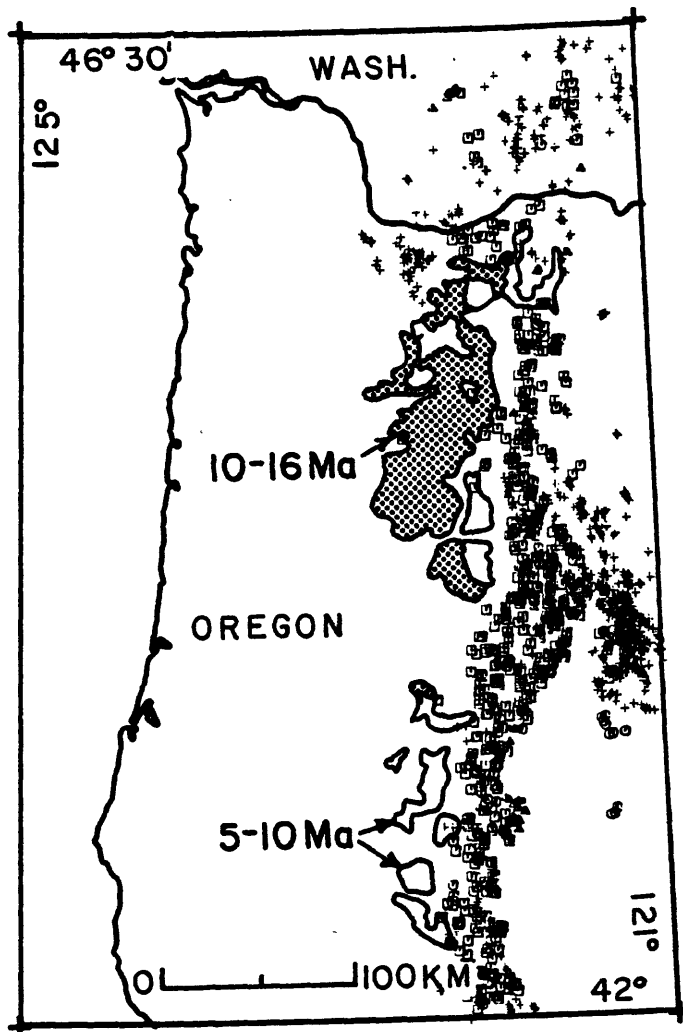


Figure 2b

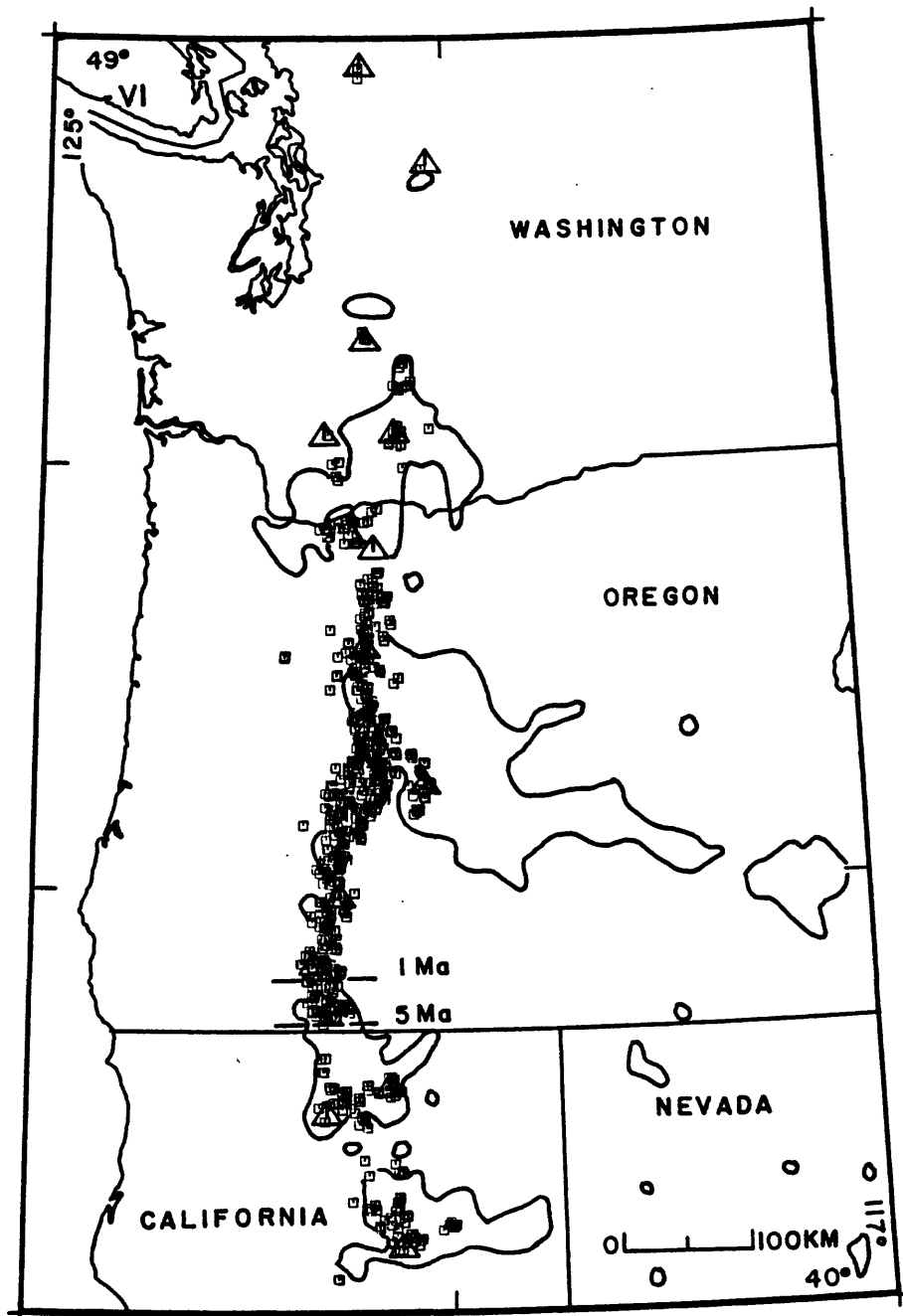


Figure 3a

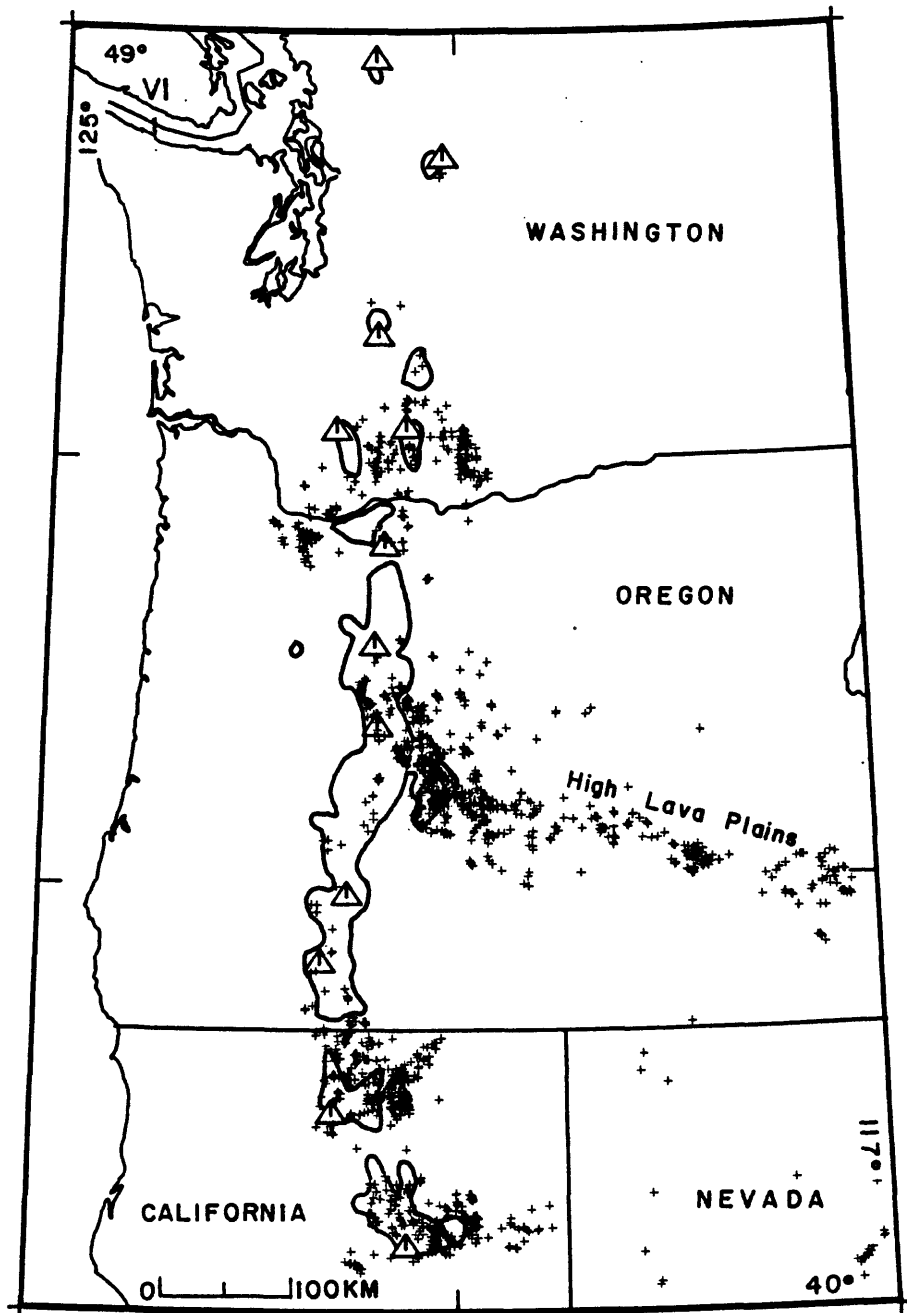


Figure 3b

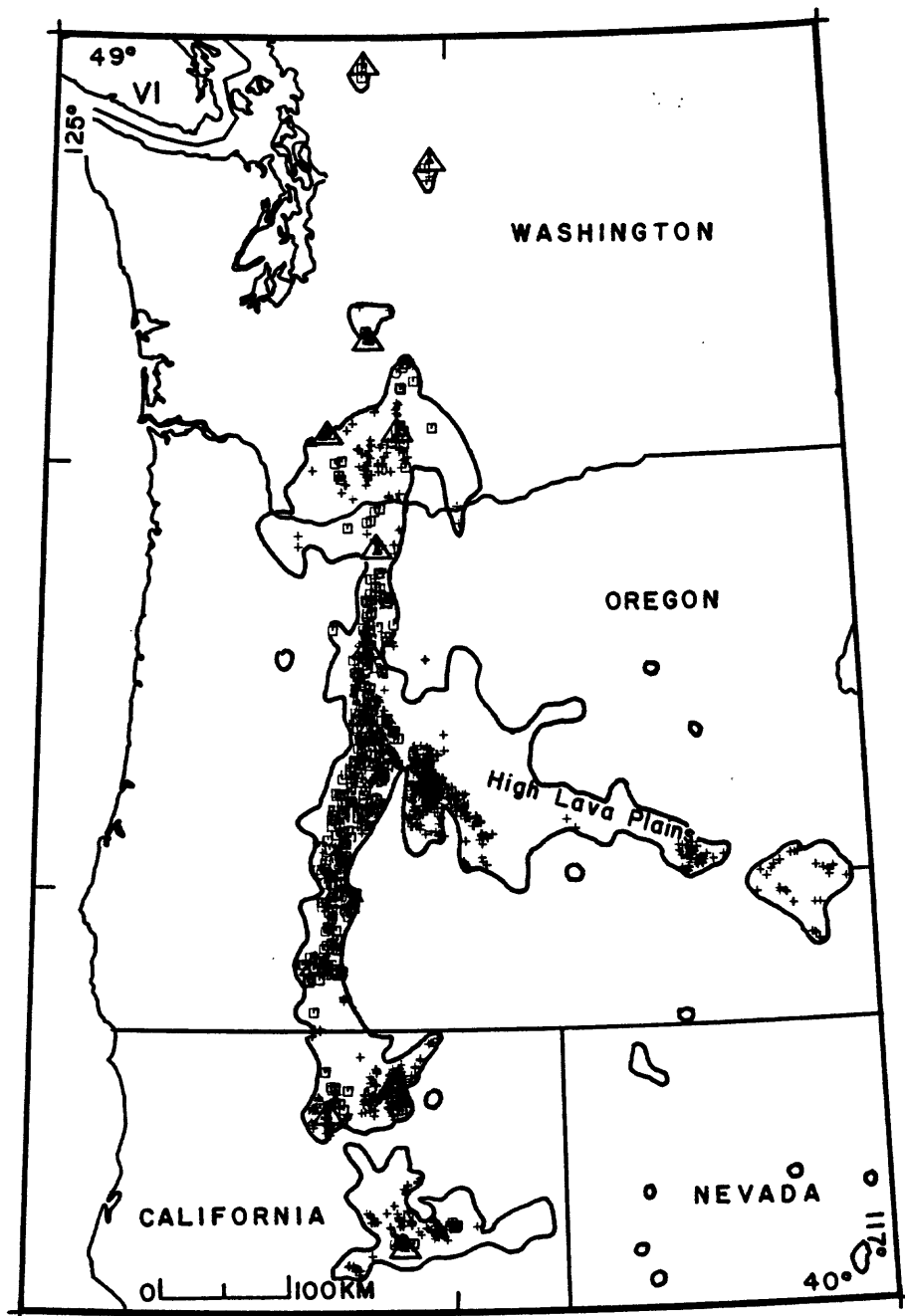


Figure 4



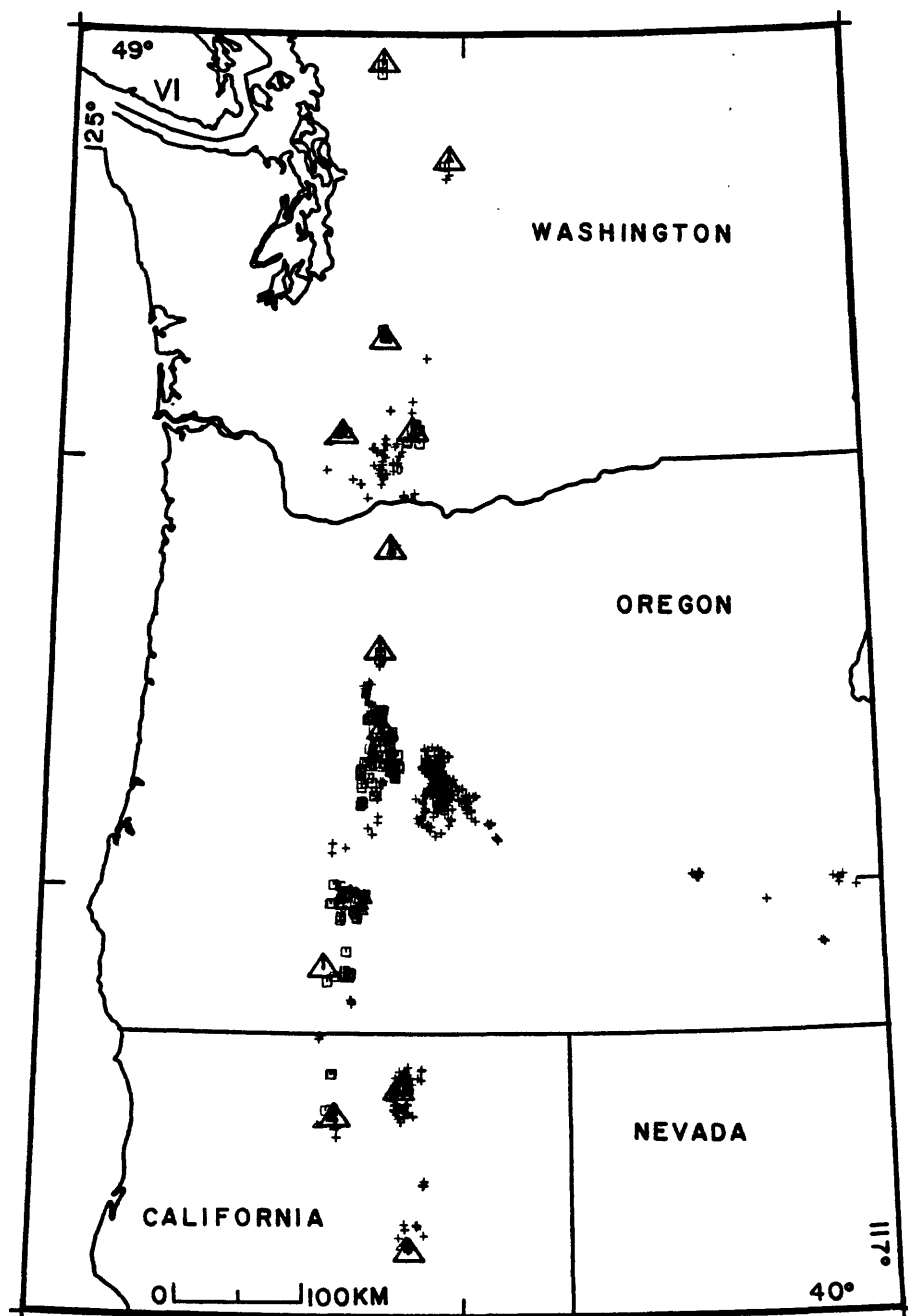


Figure 5a

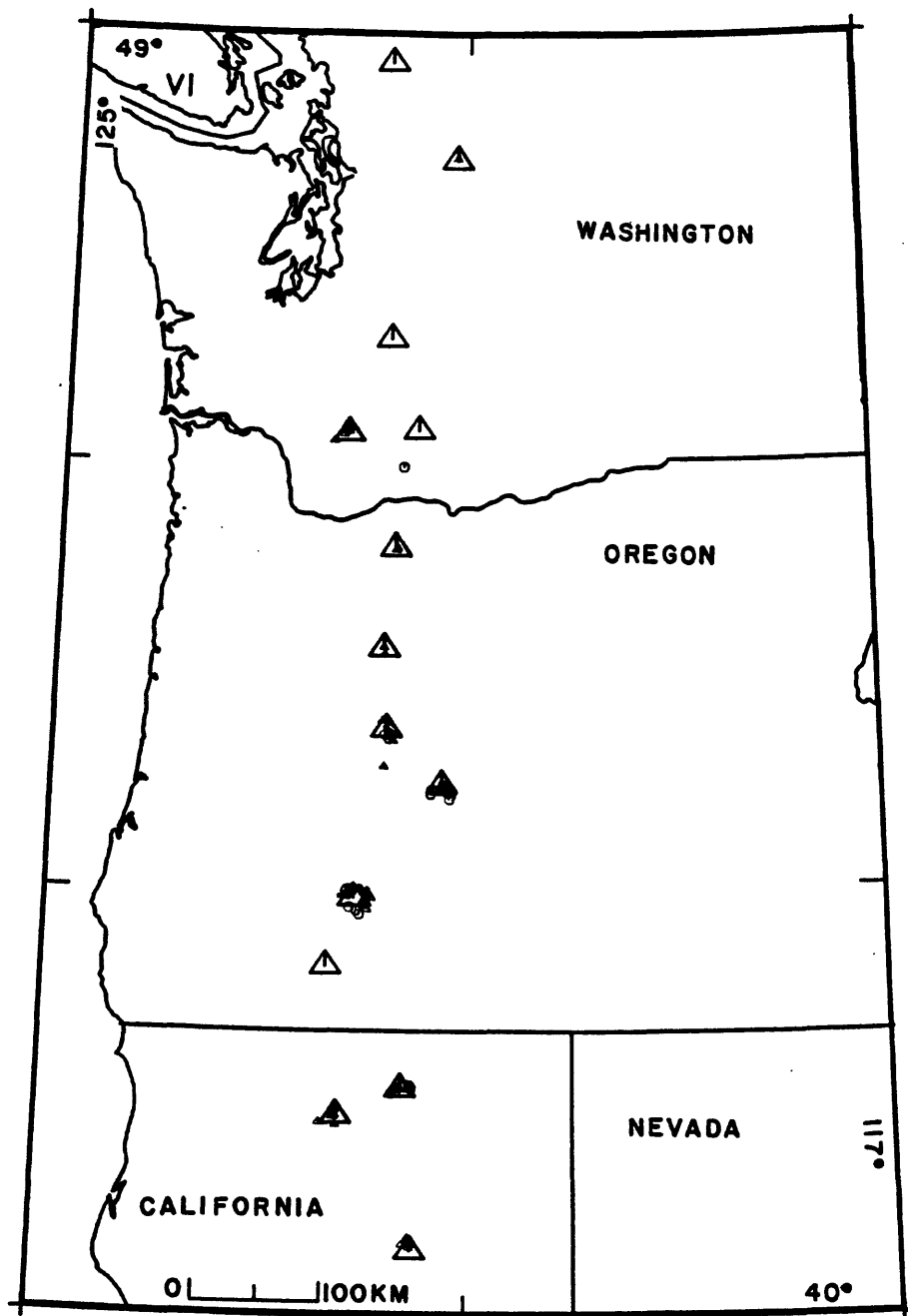


Figure 5b

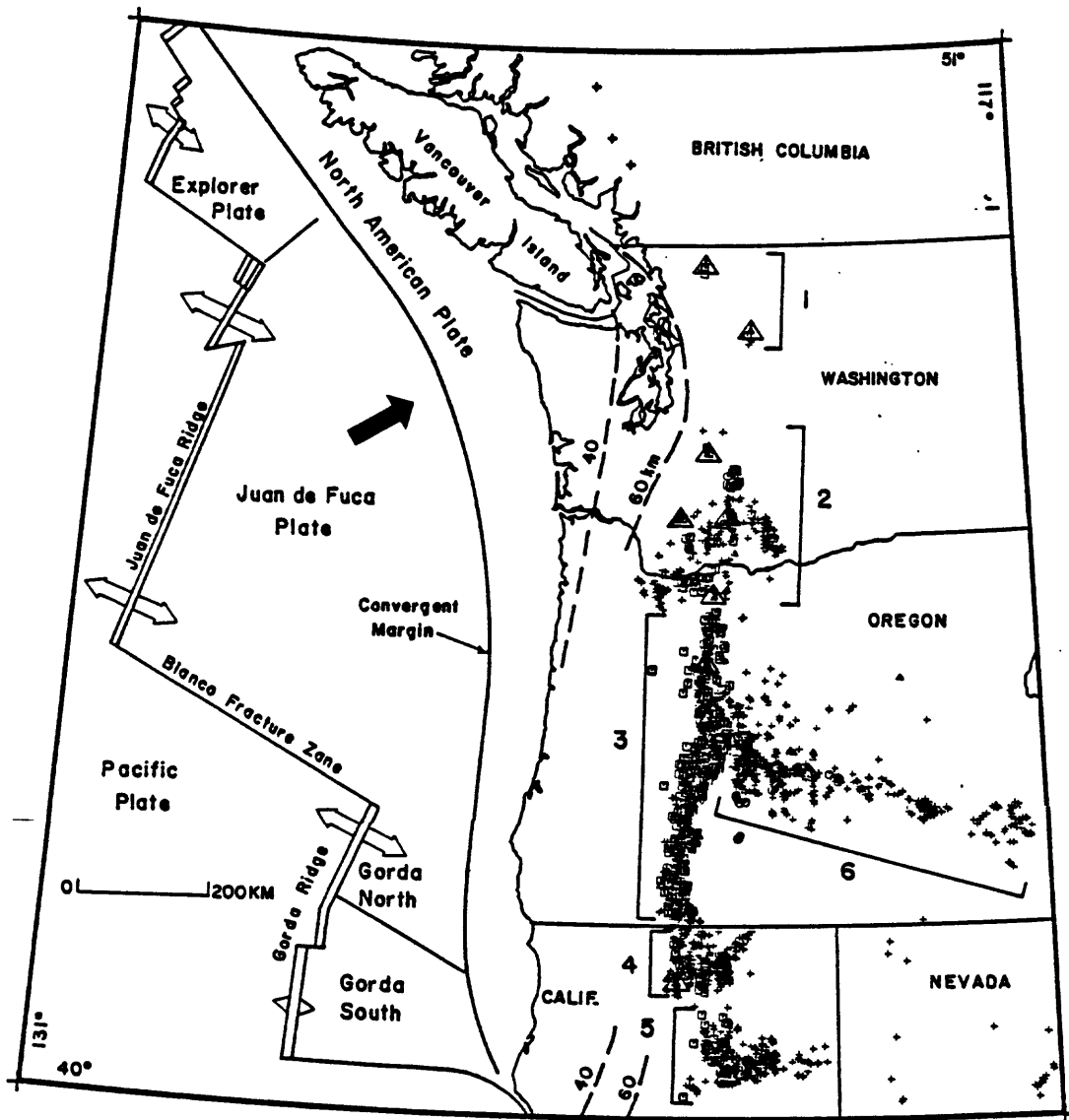


Figure 6

APPENDIX A. 5.

The Initial Deformation Front Along the  
Oregon-Washington Subduction Zone

by

LaVerne Kulm

# **Nature of the Deformation Front along the Oregon-Washington Subduction Zone**

by

LaVerne D. Kulm  
College of Oceanography  
Oregon State University  
Corvallis, OR 97331

and

Robert W. Embley  
NOAA Marine Resource Research Division  
Hatfield Marine Science Center  
Newport, Oregon 97365

## **Introduction**

The subduction of the Juan de Fuca plate beneath North America has produced many structures in the forearc (i.e., continental slope and shelf) that are comparable to those found in other subduction zones of the world where destructive earthquakes have occurred within recorded history. Swath mapping with SeaBeam bathymetry and SeaMARC side scan imagery now allows one to define and map the seafloor expression of fault and fold structures that are evolving on the continental margin and on the subducting oceanic plate off Oregon and Washington. These structures can be correlated with seismic reflection sections and rock outcrop exposures that are either dredged from a surface vessel, or sampled and studied directly with the aid of a submersible. Active fluid venting from these structures was recently observed off

Oregon, expanding our knowledge of the modern deformational processes associated with the Cascadia subduction zone.

### Sedimentation and Structure of the Juan de Fuca Plate

The Juan de Fuca plate (Cascadia Basin) is covered largely with terrigenous abyssal plain sediments consisting of silt turbidites and interbedded muds which are derived from the adjacent North American continental land mass (Fig. 1; Duncan and Kulm, 1970; Kulm, von Huene et al., 1973; Kulm et al., 1984; Peterson et al., 1986). Two intermediate sized submarine fans (Astoria and Nitinat) occur at the foot of the continental slope off Oregon and Washington, respectively, and are comprised of sand turbidites with thin interbedded muds which overlie the abyssal plain sequence. Another thick fan lies at the base of the continental slope in the southern part of the Gorda plate (Gorda Basin). These 2 to 4 km-thick, rapidly deposited sediment bodies have filled the topographic trench, allowing the bottom transported sediments (turbidites) to spill out onto the converging abyssal plain as a time-transgressive sedimentary sequence (Kulm, von Huene et al., 1973; Kulm et al., 1973).

The recurrence intervals of turbidity current deposits (turbidites) in cores from Cascadia Channel in Cascadia Basin (Fig. 1) have been used as a possible indicator of average repeat times of large earthquakes on the Oregon-Washington continental margin (Adams, 1984). The uniform thickness of the hemipelagic clay layers between the graded turbidite units implies that the time intervals between flows were of similar duration in the middle portion of Cascadia Channel and the Mazama ash horizon dated 6,600 years in the cores gives a datum for determining the average flow periodicity of a consistent 410 years (Griggs and Kulm, 1970). Despite these rather unique characteristics, one still cannot correlate these individual turbidites with one another in the middle channel. One channel that is tributary to Cascadia also gives a recurrence interval of 410 years much closer to the margin, but one cannot correlate the turbidites of the middle channel with those of the tributary on any scientific basis.

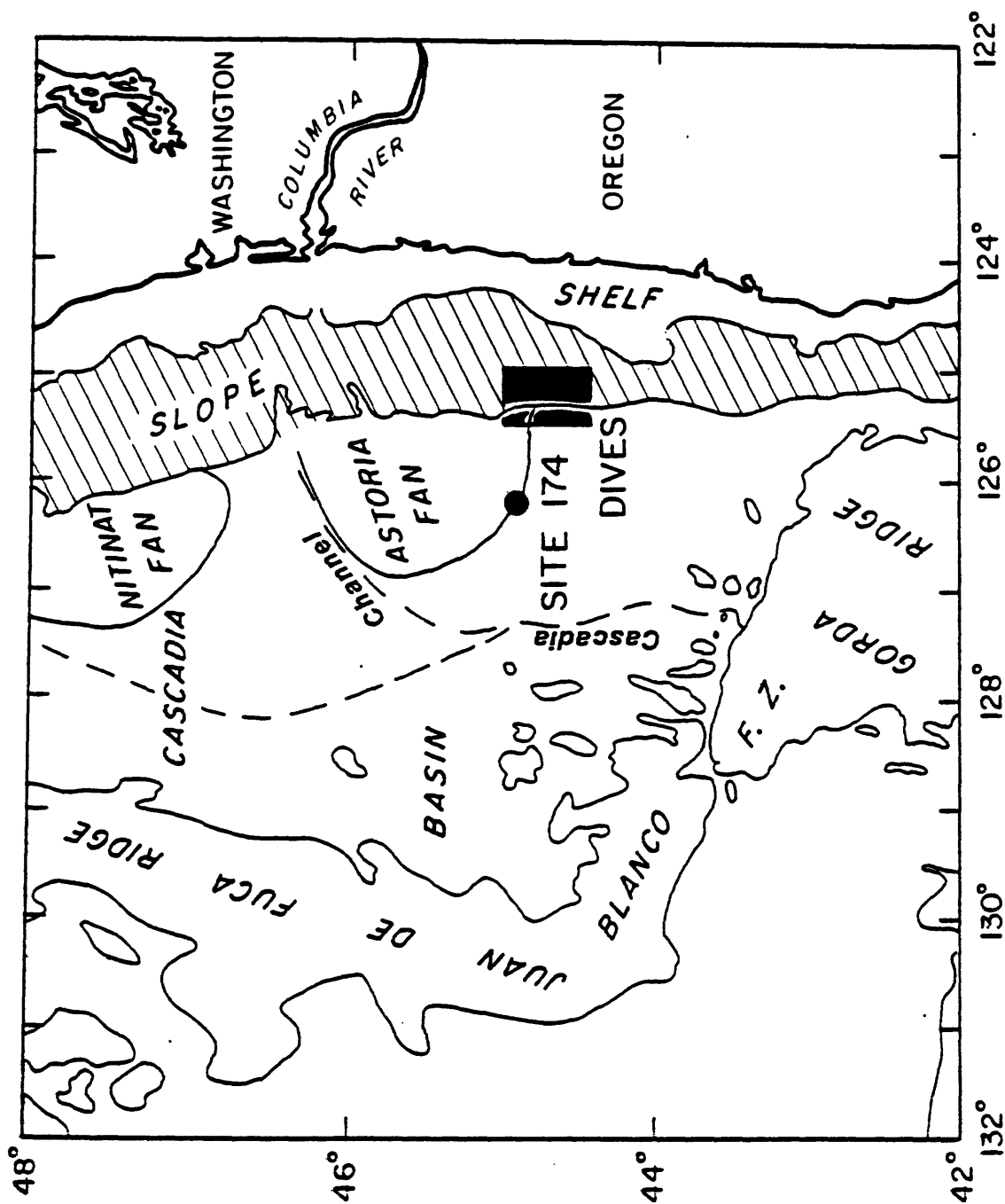


Figure 1. Location map of the Oregon and Washington continental margin (continental shelf and slope). Generalized Cascadia subduction zone indicated by lined pattern. Deep sea drilling site 174 (solid dot) shown on outer portion of Astoria Fan. General area of ALVIN submersible dives off Oregon shown by solid box (see also figure 2).

Whether these recurrence intervals between turbidites represent the repeat times of large earthquakes (Adams, 1984) or merely sediment loading and subsequent slumping from steep slopes of the continental margin (Griggs and Kulm, 1970) is yet to be determined. Generally speaking, the recurrence interval between turbidity current flows is shorter in submarine canyons and proximal environments than it is in the more distal areas because some flows do not have the velocity to travel great distances. Careful study of the turbidity current events in all cores from the submarine canyons, accretionary basins on the lower slope, and adjacent abyssal plain off Oregon and Washington may be rewarding.

Swath mapping with SeaBeam bathymetry and SeaMARC IA side scan imaging and seismic reflection surveys show that the Nitinat Fan sediments contain an 18 km-long landward verging sediment ridge whose thrust plane dips toward the oceanic plate (unpublished research by the authors). Prominent faults, with noticeable seafloor offsets, also cut the layered sedimentary deposits of this fan as well as those of Astoria Fan (Fig. 1). All of these fault and fold structures have a strike perpendicular to the convergence direction of the Juan de Fuca plate and oblique to the initial deformation front of the accretionary prism at the toe of the continental slope. Mud volcanos are associated with these abyssal plain faults off both central Oregon and southern to central Washington. They rise from 75 to 250 m above the surrounding abyssal plain and are located from 2 to 7 km seaward of the initial deformation front. The rapidly deposited fan sediments (370 to 940 m/Ma, Kulm, von Huene et al., 1973), together with the mud volcanos, strongly suggest that the abyssal sediments beneath the fan and, probably the fan sediment themselves, are overpressured.

### Structure of the Accretionary Prism

The Pliocene to Pleistocene portion of the accretionary prism, that forms the lower continental slope off central Oregon to northern Washington, is characterized by both seaward verging (thrust planes dip toward the continent) and landward verging (thrust



planes dip toward the ocean) sedimentary ridges that rise from 400 to 1000 m above the adjacent abyssal plain (Silver, 1972; Barnard, 1978; Kulm and Fowler, 1974; Snively et al., 1980; Duncan and Kulm, 1987). Landward verging sequences are confined to the upper portion of the offscraped deposits and may represent thin skin overthrusting of the sediments onto the existing continental slope, which is promoted by the overpressured abyssal deposits (Seely, 1977). These north-south trending fault-bend anticlines are being uplifted at the rate of 100 to 1000 m/Ma with the highest rates occurring along the initial deformation front (Kulm and Fowler, 1974). Migrated multichannel seismic reflection records made over the lower slope and adjacent plain (Snively et al., 1987) show that about one-half or less of the layered sediments on the subducting oceanic plate are being carried beneath the accretionary prism and the other one-half are being offscraped to form the youngest part of the prism. Seismic refraction studies on the continental slope off Grays Harbor (47° N latitude) show that a 0.5 km thick layer of 4.0 to 4.5 km/sec material is sandwiched between the oceanic basalt layer and lower velocity sedimentary material above (McClain, 1981). This layer has a low porosity and apparently is mechanically consolidated and possibly metamorphosed by heat from the warm oceanic crust.

The accretionary prism is overlain by terrigenous turbidites and hemipelagic muds which are deposited in elongate basins or troughs that are bounded to the east and west by anticlinal folds, faults, or chaotic sediment masses. As the prism sediments continue to deform and dewater across the continental slope in response to subduction-induced compression, the overlying basinal deposits are also faulted and folded. Movement of the boundary features produces angular discordances within the basin deposits, and the depositional centers of the basins migrate either landward or seaward with regard to these tectonic movements. Some of the most recently formed basins exhibit faults whose offset (i.e., several meters) is clearly seen on the seafloor.

Alvin submersible dives off Oregon and Washington in 1984 provided direct observation and study of the active tectonic boundary between the two converging

plates. Off central Oregon the initial deformation front is characterized by a series of low-relief (40 m) structural benches and a more landward marginal ridge that rises about 800 m above the abyssal plain (Fig 2; Kulm et al., 1986). The seaward flank of this ridge is cut by a small submarine canyon which suggests mass movement or slumping of sediments from the ridge onto the adjacent abyssal plain. Unpublished SeaMARC IA side scan work by the authors shows large-scale slumping occurs along other portions of the initial deformation front off northern Oregon. Several dives on the seaward flank of the marginal ridge shows it is characterized by strata with bedding dips of 40 to 60° in a seaward direction interspersed with areas of nearly vertical, 7 to 10 m-high cliffs.

#### Active Fluid Venting from Subduction-Related Structures

Active fluid venting sites were discovered on a Pleistocene marginal ridge and a Pliocene second ridge (Fig. 2) during the Alvin dives off central Oregon (Kulm et al., 1986; Ritger et al., 1987). Unique animal communities, consisting of giant white clams and tube worms, as well as authigenic carbonate deposits (slabs and chimneys) occur along the crest of the marginal ridge at two vent sites of approximately 20 m<sup>2</sup>. Methane concentrations of 180 to 420 nL/L were obtained in the bottom waters one meter above vent site 1428. These concentrations are four to six times higher than the ambient concentrations and indicate that pore fluids are derived from the underlying accretionary complex and expelled onto the seafloor. The animal communities derive their energy metabolism (i.e., carbon for their soft body parts) from the expelled methane by a process called chemosynthesis. The source of carbon for the vent carbonates is the methane and dissolved carbonate-bearing fluids being expelled at the vent sites. These pore fluids apparently migrate up-dip along permeable zones and/or fault zones within the accretionary prism. A temperature anomaly of 0.32°C above the ambient temperature at a vent site suggests that warm fluids may be expelled at the seafloor. Similar animal communities (white clams) were photographed on top of the mud volcano discovered off central Oregon, indicating

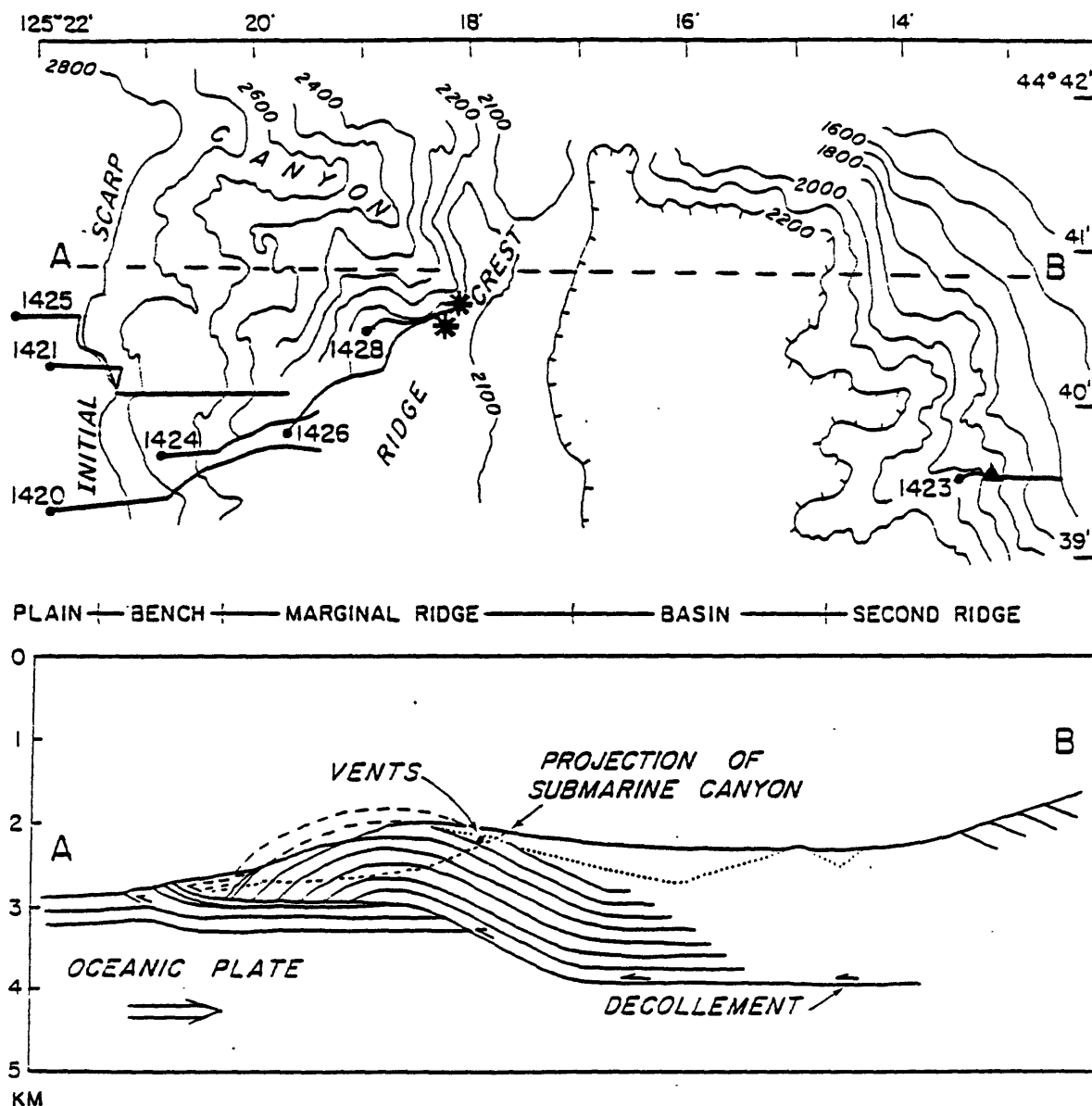


Figure 2. (Top diagram) SeaBeam bathymetry map off central Oregon. ALVIN submersible transects are shown across the lower continental slope (see figure 1). Contours in meters. Numbered dives commence at the solid dots and follow solid lines. Asterisks indicate fluid venting sites and carbonate chimneys; triangle indicates carbonate chimney only. (Bottom diagram) Interpretive structural depth section of the deformation front along profile A-B (dashed line across contour map). (From Kulm, et al., 1986, their figure 2).

active fluid venting through the volcano (unpublished research by the authors). Carbonate chimneys, similar to those observed on the lower continental slope, were recently dragged from the seafloor on the outer continental shelf off Cape Falcon, Oregon (Kulm et al., 1986a). This suggests that fluid venting is occurring in the oldest (Oligocene to Miocene) as well as the youngest (Pleistocene) portions of the accretionary prism on the Oregon margin.

### Structure and Tectonics of the Upper Slope and Shelf

Several sedimentary basins containing several thousand meters of sediment comprise the upper continental slope and continental shelf off Oregon and Washington (Snively et al., 1977; Snively et al., 1980). Broad folds characterize the late Cenozoic deposits in many areas. At least two angular unconformities, Pliocene-Pleistocene and late Miocene, are prominent in the shelf basins. Miocene and Pliocene strata are intruded by shale diapirs especially off Washington or they are tightly folded into steeply dipping anticlines (particularly off Oregon) that are truncated at the seafloor. The youngest sediments (Holocene) of the inner continental shelf are offset on the seafloor about 7 m by a fault seen in a high resolution seismic record made north of Grays Harbor (Snively et al., 1977). Prominent fault and fold structures occur in the exposed Pleistocene to pre-Miocene strata on submarine banks located on the outer continental shelf off Oregon. These banks record some of the most recent tectonic movements along the shelf. The largest amounts of uplift (900 to 1000 m) involves the late Miocene and early Pliocene strata of Heceta Bank off central Oregon (Kulm and Fowler, 1974). Early to middle Pliocene rocks on Nehalem Bank off northern Oregon and Coquille Bank off southern Oregon have been uplifted as much as 500 to 600 m while Pleistocene strata show up to 100 m of uplift. A rather uniform rate of uplift has occurred over much of the shelf during late Cenozoic time with the average rates ranging from about 100 to 160 m at several localities for late Cenozoic time. No studies have been conducted to document the tectonic movements on the Washington shelf.

## Conclusions

The continental margin off Oregon and Washington displays many deformational structures characteristic of margins associated with subductions zones that experience destructive earthquakes (e.g., Japan, southern Chile, Alaska). In fact, the deformation commences on the Juan de Fuca plate (abyssal plain) several kilometers seaward of the accretionary prism. Fault offsets at the seafloor as well as active fluid venting from a mud volcano suggest that at least some of these structures represent recent tectonic movements on the converging oceanic plate.

The accretionary prism appears to be undergoing active deformation because of the continuing development of prominent fault and fold structures. Some faults in the accretionary basins exhibit offsets of several meters at the seafloor. Such tectonic movements have probably enhanced both small- and large-scale slumping along the initial deformation front. One could probably date these slump events by gravity coring the slumped deposits on the abyssal plain.

Active fluid vent sites on the evolving structures of the prism indicate that pore fluids are presently being expelled from the accreted Pleistocene and Pliocene sediments and most likely the older Miocene to Oligocene accreted sediments across the prism. Similar active fluid venting occurs in the accreted sediments of the accretionary prism of the Japan and Kurile trenches and the Nankai Trough (Boulegue et al., 1986).

The Cascadia subduction zone displays many of the subduction-related tectonic features and fluid processes typical of active subduction zones of the circum-Pacific region. However, we have not yet determined how these processes may be related to the coupling or decoupling of the Juan de Fuca and North American plates or how we can utilize them to learn more about the potential of seismic hazards in the region.

## References

- Adams, J., 1984. Active deformation of the Pacific Northwest continental margin, *Tectonics*, v. 3, p. 449-472.
- Boulegue, J., Charlou, J., and De Kersabiec, 1986. Fluids from subduction zones off Japan, Abstract, International Kaiko Conference on Subduction Zones, 10-15 November 1986, Tokyo and Shimizu, Japan, p. 39.
- Barnard, W. D., 1978. The Washington continental slope: Quaternary tectonics and sedimentation, *Marine Geology*, v. 27, p. 79-114.
- Duncan J. R. and Kulm, L. D. 1970. Mineralogy, provenance and dispersal history of late Quaternary deep-sea sands in Cascadia Basin and Blanco Fracture Zone, *Jour. Sedimentary Petrology*, v. 40, p. 874-887.
- Duncan, R. A. and Kulm L. D., 1987. Plate tectonic evolution of the Cascades Arc-subduction complex. *Decade of North American Geology, Eastern Pacific Region*, Geol. Soc. Amer. (in press).
- Griggs, G. B. and Kulm, L. D., 1970. Sedimentation in Cascadia Deep-Sea Channel, *Geol. Soc. Amer. Bull.*, v. 81, p. 1361-1384.
- Kulm, L. D., Suess, E., Moore, J. C., Carson, B., Lewis, B. T., Ritger, S. D., Kadko, D. C., Thornburg, T. M., Embley, R. W., Rugh, W. D., Massoth, G. J., Langseth, M. G., Cochrane, G. R., and Scamman, R. L., 1986. Oregon subduction zone: venting, fauna, and carbonates, v. 231, p. 561-566.
- Kulm, L. D., Suess, E., Snavely, P. D. Jr., Schroeder, N. and Muehlberg, G., 1986a. The role of carbonate chimneys in the fluid venting history of the accretionary complex off Oregon, Abstract, EOS, Transactions Amer. Geophys. Union, v. 67, no. 44, p. 1205.
- Kulm, L.D., and Fowler, G.A., 1974, Oregon continental margin structure and stratigraphy: a test of the imbricate thrust model, In: *The Geology of Continental Margins*, C.A. Burk and C.L. Drake (eds.), Springer-Verlag, N.Y., 261-283.
- Kulm, L. D., Prince, R. A., and Snavely, P. D. Jr., 1973. Site survey of the northern Oregon continental margin and Astoria Fan, In Initial Reports of the Deep Sea Drilling Project, U.S. Government Printing Office, Washington, D.C., v. 18, p. 979-987.
- Kulm, L.D., von Huene, R., and the Scientific Staff of Leg 18, DSDP, Site 174, 1973, In Initial Reports of the Deep Sea Drilling Project, U.S.

Government Printing Office, Washington, D.C., v. 18, 97-167.

McClain, K. J., 1981, A geophysical study of accretionary processes on the Washington continental margin, Ph. D. thesis, Seattle, University of Washington, 141 p.

Peterson, C. P., Kulm, L. D., and Gray J. J., 1986. Geologic map of the ocean floor off Oregon and the adjacent continental margin. State of Oregon Department of Geology and Mineral Industries, Geological Map Series, GMS-42.

Ritger, S., Carson, B., and Suess, E., 1987. Methane-derived authigenic carbonates formed by subduction-induced pore water expulsion along the Oregon/Washington margin, Geological Society of America Bulletin, v. 98, p.147-156.

Seely, D. R., 1977. The significance of landward vergence and oblique structural trends on trench inner slopes, In: Island Arcs, Deep Sea Trenches and Back-arc Basins, Talwani, M. and Pitman III, W. C., (eds), Amer. Geophys. Union Washington D. C., p187-198.

Snavely, P. D., von Huene, R, and Miller, J., 1987. Central Oregon Margin Line WO76-4 and WO76-5, In: von Huene, R (ed.), Seismic images of convergent margin tectonic structures, Amer. Assoc. Petrol. Geologists, Studies in Geology, no. 15, (in press).

Snavely P. D. Jr., Wagner, H. C., and Lander, D. L., 1980. Interpretation of the Cenozoic geologic history, central Oregon continental margin: Cross-section summary, Geol. Soc. Amer. Bull., v. 91, p. 143-146.

## **Oregon Subduction Zone: Venting, Fauna, and Carbonates**

L. D. KULM, E. SUESS, J. C. MOORE, B. CARSON, B. T. LEWIS, S. D. RITGER,  
D. C. KADKO, T. M. THORNBURG, R. W. EMBLEY, W. D. RUGH, G. J. MASSOTH  
M. G. LANGSETH, G. R. COCHRANE, R. L. SCAMMAN



# Oregon Subduction Zone: Venting, Fauna, and Carbonates

L. D. KULM, E. SUESS, J. C. MOORE, B. CARSON, B. T. LEWIS, S. D. RITGER,  
D. C. KADKO, T. M. THORNBURG, R. W. EMBLEY, W. D. RUGH, G. J. MASSOTH,  
M. G. LANGSETH, G. R. COCHRANE, R. L. SCAMMAN

Transects of the submersible *Alvin* across rock outcrops in the Oregon subduction zone have furnished information on the structural and stratigraphic framework of this accretionary complex. Communities of clams and tube worms, and authigenic carbonate mineral precipitates, are associated with venting sites of cool fluids located on a fault-bend anticline at a water depth of 2036 meters. The distribution of animals and carbonates suggests up-dip migration of fluids from both shallow and deep sources along permeable strata or fault zones within these clastic deposits. Methane is enriched in the water column over one vent site, and carbonate minerals and animal tissues are highly enriched in carbon-12. The animals use methane as an energy and food source in symbiosis with microorganisms. Oxidized methane is also the carbon source for the authigenic carbonates that cement the sediments of the accretionary complex. The animal communities and carbonates observed in the Oregon subduction zone occur in strata as old as 2.0 million years and provide criteria for identifying other localities where modern and ancient accreted deposits have vented methane, hydrocarbons, and other nutrient-bearing fluids.

THE JUAN DE FUCA PLATE (CASCADIA BASIN) CONVERGES with the North American plate to produce a subduction complex off Oregon and Washington (Fig. 1). Near the continental margin, abundant clastic sediments load the subducting plate; a portion of these clastics is scraped off and added to the overriding plate as an accretionary sediment complex (1-4). The trench is filled with sediments, and the initial zone of deformation occurs at relatively shallow depths (<2850 m).

During July and August 1984, we made 15 dives with D.S.R.V. *Alvin* on this subduction zone. Six dives define an east-west transect extending from the abyssal plain (Cascadia Basin) across the lower continental slope (Fig. 2). Two additional dives were made approxi-

mately 29 km to the north but are not shown here. The overall objective of this multidisciplinary research program was to investigate the processes of subduction-induced sediment lithification and their relation to the large-scale deformational styles of the accretionary zone. Specifically, we wished to determine how tectonic deformation affects sediment consolidation, sediment microstructure, carbonate cementation, and fluid movement.

## Geologic Setting

The styles of accretion along the Oregon margin include both seaward-verging (thrust faults dipping toward the continental plate) and landward-verging (thrust faults dipping toward the oceanic plate) structures. The surface expression of the accretionary zone at the lower continental slope consists of a series of thrust ridges trending north-south and intervening basins of ponded sediment. The youngest ridges rise from 400 to 1000 m above the adjacent abyssal plain and were formed during the last 2.0 million years (3). The accreted and dewatered material (5) was originally deposited as a terrigenous clastic sequence on the Astoria Fan seaward of the continental slope (Fig. 1) (3, 6).

SeaBeam bathymetry shows that the initial deformation front consists of a series of low-relief (~40 m) structural benches and a more landward marginal ridge that rises more than 800 m above the abyssal plain (Fig. 2). This ridge is incised by a small submarine canyon that locally cuts as much as 500 m into its seaward flank but terminates at the crest of the ridge. A second ridge is situated immediately landward of the marginal ridge and ascends 1800 m above the plain (Fig. 2). The steep base of the second ridge is also cut by small canyons.

The detailed structure of the central Oregon transect across the seaward-verging accretionary complex is compiled from deep-towed seismic records (7) and from measurements and observations obtained during *Alvin* dives shown in Fig. 2. The initial deformation front is characterized by a seaward-facing escarpment that slopes 30° to 40° and rises 30 to 40 m above the abyssal plain (Fig. 2). The scarp exposes largely horizontal to gently landward-dipping strata. Talus accumulates at the base of the scarp. *Alvin* traverses 1421 and 1425 observed thin-bedded mudstone deposits in the outcrops above the talus that are locally broken by microfaults with displacements of several centimeters. The semiconsolidated sediment underlying the scarp crumbled when sampled by the *Alvin* claw. A second set of scarps exposed a few hundred meters landward apparently is the surface manifestation of a décollement that separates the deformed offscraped deposits of the lower continental slope from more gently dipping deposits being underthrust with the converging oceanic plate (Fig. 2).

L. D. Kulm, E. Suess, D. C. Kadko, T. M. Thornburg, and W. D. Rugh are in the College of Oceanography, Oregon State University, Corvallis 97331. J. C. Moore is in the Department of Earth and Marine Sciences, University of California, Santa Cruz 95064. B. Carson and S. D. Ritger are in the Department of Geological Sciences, Lehigh University, Bethlehem, PA 18015. B. T. Lewis and G. R. Cochrane are in the School of Oceanography, University of Washington, Seattle 98195. R. W. Embley is with the National Oceanic and Atmospheric Administration, Marine Resources Research Division, Oregon State University, Hatfield Marine Science Center, Newport 97365. G. J. Massoth is with the National Oceanic and Atmospheric Administration, Pacific Marine Environmental Laboratory, Seattle, WA 98115. M. G. Langseth is at Lamont-Doherty Geological Observatory, Palisades, NY 10964. R. L. Scamman is with Chevron U.S.A., Inc., Box 399, Denver, CO 80201.

The seaward flank of the marginal ridge is characterized by intermittent rock outcrops with localized sharp ridges and precipitous scarps. The walls of the canyon also expose rock outcrops. Bedding measured from *Alvin* dips seaward 40° to 60° on the lower

portion of the ridge (Fig. 2); upslope, bedding dips shallow and becomes approximately horizontal near the crest of the ridge. Near the base of the marginal ridge (dive transect 1420 in Fig. 2), friable, micaceous sandstone beds were encountered in a cliff 7 to 10 m high. These beds are disintegrating to form sandy debris aprons. Laminated turbidites occur higher in the section.

A deep-towed seismic reflection record shows landward-dipping reflectors on the eastern flank of the marginal ridge; they continue beneath a sediment basin lying between this and the second deformational ridge (Fig. 2). *Alvin* outcrop data and these geophysical records show that the marginal ridge is an anticline. By analogy to the known structures of other convergent margins (8) and to fold and thrust belts on land (9), we believe that this anticline is of "fault-bend" origin. The fold formed initially as a sediment package rode up a landward-dipping thrust ramp and then folded over onto a nearly horizontal sea floor.

*Alvin* dive 1423 revealed that the seaward flank of the second ridge (Fig. 2) exposes nearly vertical outcrops of thin to massively bedded strata that appear horizontal to gently landward-dipping. Interbedded sand and mud turbidite beds were observed, as in the marginal ridge. The slope becomes gradually gentler and rock outcrops are less frequent toward the top of the second ridge.

## Venting of Pore Fluids

**Animal communities.** Benthic communities of tube worms and giant clams were observed during *Alvin* dives 1426 and 1428 along the crest of the marginal ridge (Fig. 2). Both sites are located on a

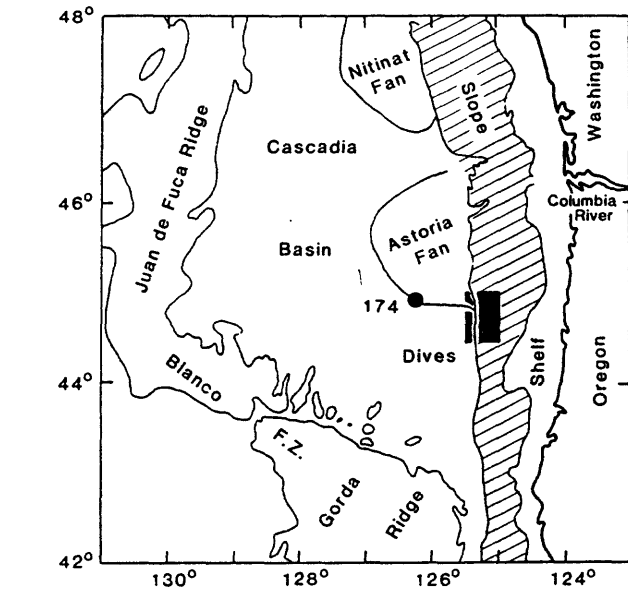


Fig. 1. Oregon subduction zone (lined pattern), Juan de Fuca plate (Cascadia Basin), and Astoria Fan. The dive area is shown by the black box, Deep Sea Drilling Project drill site 174.

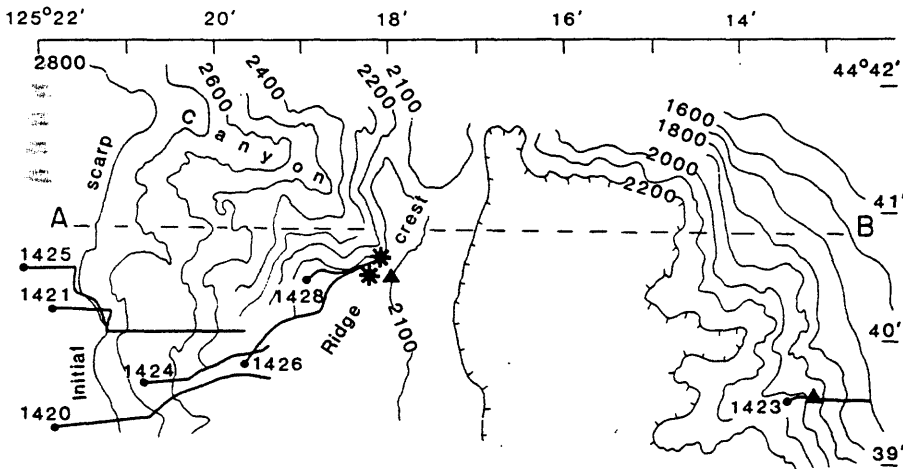
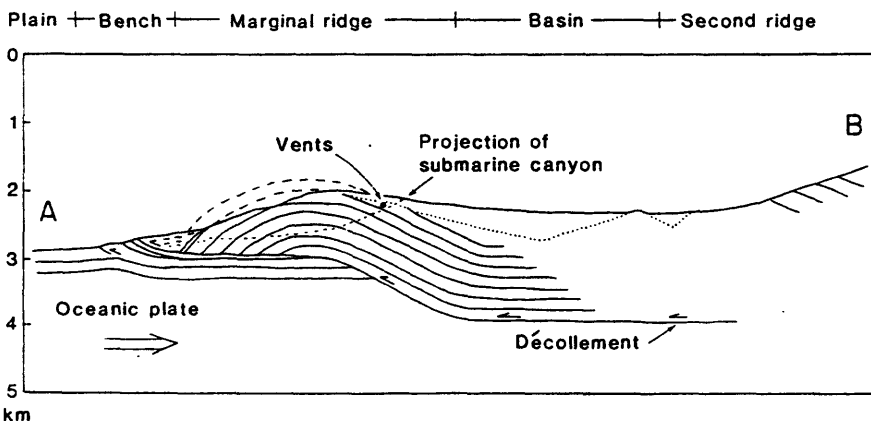


Fig. 2. (Top) *Alvin* dive transects and SeaBeam bathymetry map obtained by the National Oceanic and Atmospheric Administration, National Ocean Survey, aboard the *Surveyor* of the Oregon underthrust region. Contours are in meters; numbered dives commence at the solid dots. Asterisks indicate fluid vent sites (northern site 1428 and southern site 1426); triangles indicate carbonate chimneys at both vent sites and along dive transect 1423. (Bottom) Interpretive structural section of the deformation front along profile A-B (dashed line). This depth section was compiled from seismic refraction and reflection data and bedding dips measured from *Alvin*; oceanic crust here is at 7-km depth.



soft sediment-covered area at 2036 m atop extensive rock exposures with precipitous walls where a canyon breaches the ridge crest (Fig. 3). Colonies of tube worms (phylum Pogonophora, *Lamellibrachia barhami*) were found at both sites (10, 11). The colonies are rooted either in fissures extending beneath rock ledges or in soft sediments overlying a carbonate-cemented crust. A typical colony is 50 to 80 cm in diameter and consists of a tangled mass of six to ten individual tubes.

Both marginal ridge localities are also marked by numerous disarticulated and partially sedimented valves of the giant white clam *Calypptogena* sp. (11, 12). Several clusters of *Calypptogena* sp. were encountered in growth position (Fig. 3) during dive 1428, each cluster consisting of five to six individuals. The clusters of live clams are aligned in rows that may reflect the orientation of pathways of fluid escape in the consolidating rocks underlying the thin sediment blanket. Individual specimens of another clam, *Solemya* sp. (11, 12), were observed and collected during two *Alvin* dives on a small incipient marginal ridge site ~29 km to the north and were also present at vent site 1428 (Fig. 3).

The stable carbon isotope composition of animal soft-tissue parts indicates that these tube worms and giant clams metabolize a unique and extremely  $^{13}\text{C}$ -depleted carbon source, which is usually found only in  $\text{CH}_4$  and other light hydrocarbons (Table 1). A value of  $\delta^{13}\text{C} = -51.6$  per mil relative to the PDB standard, obtained from the gills of *Calypptogena*, is among the lowest yet reported for contemporary marine organic material. The calcareous skeletal parts of the giant clams *Calypptogena* and *Solemya* incorporate carbon from the oceanic bicarbonate reservoir ( $\delta^{13}\text{C} = -1.0$  to  $+1.8$  per mil) with only small variations (Table 1). Their oxygen isotope values (Table 1) indicate that calcification proceeds roughly in equilibrium with ambient bottom water temperatures. The same isotope characteristics and fractionations were observed for the calcareous parts of giant clams from the mid-ocean ridge sites (13–15). The carbon isotope shift toward more  $^{12}\text{C}$ -enriched values in tube worm and giant clam tissue at the margin sites, compared to the mid-ocean ridge sites, apparently reflects a different source of food. There is some indication from the oxygen isotope data (ranging from  $\delta^{18}\text{O} = +4.18$  to  $+3.49$  per mil) that one clam from the Oregon deformation zone recorded higher bottom water temperatures (by about  $4^\circ\text{C}$ ) during its early years of life and incorporated slightly lighter carbon for calcification during that period (Table 1). This may imply episodic venting of warmer and more deeply derived pore fluids enriched in metabolic  $\text{CO}_2$ .

**Bottom water anomalies.** Higher than normal temperatures were detected in the bottom waters overlying the deformation front. In situ recordings made near the bottom during *Alvin* dive 1428, in the vicinity of the clam bed and tube worm colonies, showed a positive anomaly of  $+0.32^\circ\text{C}$  at 2020 m, approximately 14 m above the bottom. During the descent of the submersible through the water column, the temperature dropped gradually from  $2.3^\circ$  to  $1.7^\circ\text{C}$  at depths between 1600 and 2100 m, and two thin isothermal layers with temperatures of  $2.15^\circ$  and  $1.97^\circ\text{C}$  were encountered on both descent and ascent. Near the bottom, however, the variability of temperature recordings increased significantly, and on this dive the relatively large increase was recorded during a 20-minute interval. It apparently reflects the complicated temperature structure near the crest of the nearby marginal ridge. No such anomalies were observed at other sites along the margin and abyssal plain. A similar temperature anomaly ( $0.3^\circ\text{C}$ ) was recently recorded above a *Calypptogena* clam bed at 3830 m along the wall of the Nankai Trough subduction zone by the Franco-Japanese deep diving project "Kaiko" (16).

Water samples were collected in 5-liter bottles held by *Alvin* directly above the animal communities and over other areas of the

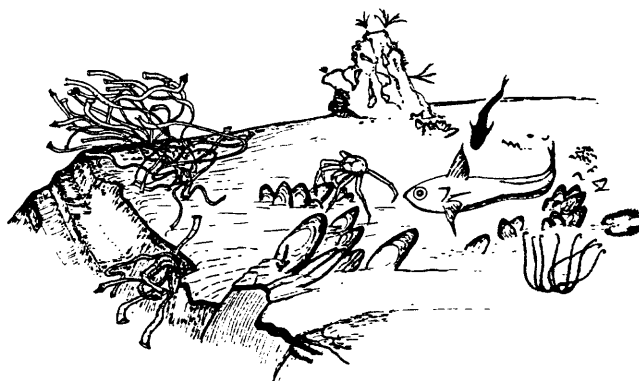


Fig. 3. Composite illustration of vent site 1428 (11). Two colonies of tube worms, *Lamellibrachia barhami*, occur on the ledge above the canyon wall; several clusters of live giant clams, *Calypptogena* sp., are aligned along presumed sites of fluid discharge; an open valve of *Solemya* sp. is seen on the far right; and a cone-shaped chimney structure is shown at the top. Carnivorous fishes and large crabs are attracted to the clam beds. Venting sites are at least  $20\text{ m}^2$  in areal extent. [Courtesy of the Biological Society of Washington]

deformation front to detect the venting of pore waters by anomalous concentrations of dissolved gases. At the clam and tube worm sites of dive 1428, the  $\text{CH}_4$  concentration was 180 to 420 nL/liter at 1 m above the bottom (Table 2, dives). These concentrations are three to six times greater than the  $\text{CH}_4$  concentrations found in the ambient water seaward of the deformation front (Table 2, hydrocasts) and suggest expulsion of pore fluids from the accretionary complex.

Radon-222 was sampled in the bottom waters by *Alvin* in several areas over the deformation front where fluid venting was suspected and by hydrocasts seaward of the front to determine background values. The  $^{222}\text{Rn}$  concentrations in bottom waters at dive sites 1421 and 1426 appear to be anomalously high in comparison to the background sources (Table 2) of this nuclide (17). Site 1426 is the location of a tube worm colony, and site 1421 is situated above the

Table 1. Carbon and oxygen isotope values (per mil relative to PDB) of selected tissue and shell from giant clams and tube worms from the Oregon accretionary complex. We hypothesize that  $\text{CH}_4$ , usually strongly enriched in  $^{12}\text{C}$ , is venting from the accretionary complex and sustains the macrobenthos via microbial symbionts capable of oxidizing  $\text{CH}_4$ . Precision of  $\delta^{13}\text{C}$  is  $\pm 0.10$  per mil and of  $\delta^{18}\text{O}$  is  $\pm 0.07$  per mil based on National Bureau of Standards standard.

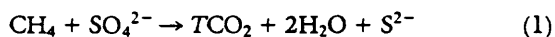
Sample	$\delta^{13}\text{C}$	$\delta^{18}\text{O}$
<i>Dive 1428-04</i>		
<i>Calypptogena</i> sp.*		
Gills†	-51.6	
Periostracum†	-35.7	
Shell†	-0.1	+4.51
Shell, from lip		
5 to 20 mm	+1.5	+4.18
50 to 68 mm	-0.1	+3.92
75 to 85 mm	-1.0	+3.49
<i>Dive 1432-04</i>		
<i>Solemya</i> sp.		
Shell†	+1.8	+4.91
Periostracum†	-31.0	
<i>Dive 1426-01</i>		
<i>Lamellibrachia barhami</i> Webb		
Tissue†	-31.9	
Tube, segment	-26.7	

\*Tentatively identified by R. Turner as *C. magnifica*.

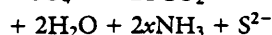
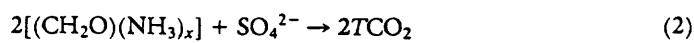
†Composite sample.

incipient escarpments that mark the deformation front (Fig. 2). Both areas are likely locations for fluid venting.

**Pore waters.** Pore waters from sediments of the marginal ridge and the undeformed abyssal plain show dissolved nutrient patterns characteristic of microbial sulfate reduction. This is expected in hemipelagic sediments, but at the marginal ridge the interstitial nutrient pattern is anomalously depleted in dissolved  $\text{NH}_3$  and total  $\text{CO}_2$  ( $\text{TCO}_2$ ). We attribute this to the oxidation of  $\text{CH}_4$  because the utilization of this gas by microbial sulfate reducers generates no dissolved  $\text{NH}_3$  and only half as much  $\text{TCO}_2$  as the utilization of particulate organic carbon (POC). This is shown in reactions 1 and 2, respectively:



$$\Delta\text{TCO}_2 : -\Delta\text{SO}_4^{2-} = 1 : 1$$



$$\Delta\text{TCO}_2 : -\Delta\text{SO}_4^{2-} = 2 : 1$$

$$x = 0.067$$

The contributions of  $\text{CH}_4$  and POC oxidation are illustrated in Fig. 4, which shows the dissolved  $\text{NH}_3$  and  $\text{TCO}_2$  concentrations as a function of sulfate reduction for core 8306-24 from the seaward flank of the marginal ridge and core 8408-4 from the undeformed sediments of the Astoria Fan. The total depletion in  $\text{TCO}_2$  in core 8306-24 is estimated from the measured  $\Delta\text{TCO}_2$  in the pore water above that of bottom water and the loss of dissolved calcium and magnesium. Removal of calcium and magnesium results from interstitial precipitation of carbonate minerals, whereby, for each mol of cations ( $\Delta\text{Ca} + \Delta\text{Mg}$ ), 1 mol of  $\text{TCO}_2$  is used. Accordingly,  $\Sigma(\Delta\text{TCO}_2 + \Delta\text{Ca} + \Delta\text{Mg})$  represents the interstitial  $\text{TCO}_2$  content resulting from sulfate reduction ( $\Delta\text{SO}_4^{2-} = \text{SO}_4^{2-}$  in pore water minus  $\text{SO}_4^{2-}$  in bottom water) and corrected for carbonate mineral

precipitation (Fig. 4). We hypothesize that the difference in yield of  $\text{TCO}_2$  between the two cores (lined area a in Fig. 4) is due to  $\text{CH}_4$  oxidation in core 8306-24. The same explanation holds for the depletion of  $\text{NH}_3$  in core 8306-24 (lined area b in Fig. 4). Therefore, the  $\text{NH}_3$  and  $\text{TCO}_2$  concentrations in pore fluids from the marginal ridge reflect the combined contributions of each of the two substrates undergoing decomposition, that is, POC and  $\text{CH}_4$ . By appropriately partitioning these contributions, we calculate that in the area of the marginal ridge, at a depth of  $\sim 2$  m below the sediment-water interface, as much as  $\sim 30$  percent of the  $\text{TCO}_2$  results from microbial decomposition of  $\text{CH}_4$ . The portion can be independently estimated from the observed  $\text{NH}_3$  and  $\text{TCO}_2$  depletions. The estimates are remarkably consistent (18).

**Methane-derived authigenic carbonates.** Carbonate-cemented sediments, which occur as crusts, concretions, and chimney-like structures, have been recovered repeatedly in dredges and were collected during *Alvin* dives from the deformation zone off Oregon. The carbonate was dominantly magnesian calcite, although dolomite and aragonite were also identified (19). Carbonate cementation occurred preferentially in the coarse-grained deposits of the accretionary complex, particularly in sand-sized turbidite layers. Initial porosities of the sediments suggest that the cementation process begins at shallow burial depths, probably within several meters of the sediment-water interface (19).

The vent areas on dives 1426 and 1428 exhibited the most striking and concentrated occurrences of carbonate deposits in the deformation front (Fig. 2). Slabs of carbonate-cemented mudstone, several centimeters thick, occurred beneath a thin terrigenous sediment cover and were frequently exposed at the sea floor as irregularly shaped, sharp-edged masses. Isolated carbonate chimneys, roughly conical and 1 to 2 m high, occurred above the vent site on dive transect 1428 and atop the crest of a canyon wall on transect 1423. They resemble house-of-cards structures in that they are built of sharp-edged plates fused together in a jagged mass.

Dissolution features include surficial grooves, pits, and holes. The carbonate cements of dredged rocks from the deformation front and the crusts and chimney structures recovered by *Alvin* at the vent sites are highly enriched in  $^{12}\text{C}$  and have positive  $\delta^{18}\text{O}$  values (Table 3) (20). The enrichment of  $^{12}\text{C}$  indicates that the carbonate of the cements, crusts, and chimneys is overwhelmingly derived from  $\text{CH}_4$ ; the  $\delta^{18}\text{O}$  values indicate low temperatures of formation, consistent with precipitation at shallow depths in the sediment column.

## Discussion

**Evidence for venting.** The venting of fluids observed to date in the Oregon subduction zone is more subtle than the highly visible plumes emitted at the "smokers" in vent fields along mid-ocean spreading ridges (21, 22). The mid-ocean ridge vents are characterized by jets of discharging waters with temperatures in excess of  $350^\circ\text{C}$ , by sulfide chimneys, and by large communities of animals. The subduction zone venting sites off Oregon lack visible evidence of concentrated avenues of discharging pore waters, although there is indirect evidence for their diffuse discharge from the temperature,  $\text{CH}_4$ , and radon anomalies in the overlying water column. These venting sites are characterized by inorganic precipitation of calcium and magnesium carbonates; the mid-ocean ridge vents are characterized by sulfide deposits. We observed in the Oregon subduction zone manifestations of a new type of venting process not previously described at a plate tectonic boundary.

One notable similarity between the two types of vents, however, is the presence of large benthic organisms. Most of the organisms discovered at the subduction zone venting sites appear to be either

Table 2. Concentrations of  $^{222}\text{Rn}$ ,  $^{226}\text{Ra}$ , and  $\text{CH}_4$  in bottom waters along the Oregon accretionary complex. Measurements are from separate paired sample bottles. For radon the errors are the  $1\sigma$  counting statistics. For radium the errors are either the  $1\sigma$  counting statistic or the standard deviation of duplicate runs, whichever is greater. Stripping efficiency for  $\text{CH}_4$  is 95 to 99 percent; standard error is  $\pm 0.2$  to  $\pm 1.7$  percent relative to the absolute gas concentration.

Sample	$^{222}\text{Rn}$ (dpm per 100 liters)	$^{226}\text{Ra}$ (dpm per 100 liters)	$\text{CH}_4$ (nl/ liter)
<i>Dives*</i>			
1421	$55.3 \pm 1.4$	$25.3 \pm 7.7$	418 182
1421	$52.9 \pm 2.3$		
1425	$42.3 \pm 4.9$		
1426	$59.4 \pm 3.6$		
1426	$59.2 \pm 6.0$		
1427	$43.6 \pm 1.5$		
1428	$43.7 \pm 2.9$		
1428	$36.8 \pm 2.6$		
1429	$40.1 \pm 1.3$		
<i>Hydrocasts†</i>			
H-1-15	$28.2 \pm 0.5$	$29.9 \pm 1.8$	66
H-1-20	$15.7 \pm 0.4\ddagger$	$25.9 \pm 1.6$	55
H-2-15	$25.7 \pm 0.4$	$22.7 \pm 1.4$	
H-2-20	$11.1 \pm 0.3\ddagger$	$25.0 \pm 1.3$	

\*Samples taken 1 m off bottom by *Alvin*.  
bottom. †Possible leaking gas bottle.

‡Samples taken 15 and 20 m off

the same genera or genera closely related to those found in the hot vents of the spreading centers. The chemosynthesis-based energy metabolism of organisms of the mid-ocean ridge hot vents is thought to be based on their capacity to metabolize, in symbiosis with microbes,  $\text{H}_2\text{S}$  emitted from the vents (23–25). We hypothesize that the clams and tube worms found in the cool vent areas of the Oregon subduction zone have successfully adapted to another type of energy metabolism, that is, the capacity to utilize dissolved  $\text{CH}_4$ . Recently it was shown that a related genus of tube worm, *Siboglinum* sp., is equipped with strands of bacteria capable of uptake of  $^{14}\text{CH}_4$  (26). The waters overlying the vent area on dive transect 1428 on the marginal ridge contain three to six times the amount of dissolved  $\text{CH}_4$  found in oceanic bottom water. There is no evidence of  $\text{H}_2\text{S}$  in this water or in the pore water samples taken in the hemipelagic sediments and accreted semiconsolidated sediments on the marginal ridge along the dive transect. Recent reports (27, 28) associate vestimentiferan worms and giant clams off western Florida and Louisiana with the venting of hypersaline waters. Methane and higher hydrocarbons could be the source of food for these communities as well. Dissolved nutrient patterns in the pore waters of sediments of the Oregon deformation front show evidence of microbial  $\text{CH}_4$  oxidation via reduction of sulfate. Furthermore, tube worms are rooted on or near carbonate chimneys and slabs, and the clams burrow into the thin veneer of sediment that surrounds the carbonate slabs. This close association of  $^{12}\text{C}$ -enriched carbonate cement and  $\text{CH}_4$ -derived carbon in the soft tissue of the animals appears to be almost certainly the result of localized expulsion of  $\text{CH}_4$ -enriched pore fluids.

Recognition of fluid expulsion zones on the lower continental slope of Oregon provides clues on the possible pathways for fluid migration within this accretionary complex (0.44 to 2.0 million years old). On the marginal ridge, fluids are being expelled near the breached crest of the "fault-bend" anticline and apparently have migrated up-dip along permeable zones within its landward flank (Fig. 2). Simple up-dip migration along landward-dipping structures suggests source depths of at least 1.0 km. On the second ridge, pore fluids probably migrate along horizontal to shallow-dipping strata and are expelled at outcrops along steep canyon walls cutting its seaward flank. Living tube worm colonies were also dredged from this ridge to the south of the study area (29).

Methane-enriched pore water entrapped in sediments initially deposited on the abyssal plain (Astoria Fan in Fig. 1) appears to be the primary source of expelled fluids in the <0.3 million-year-old deposits of the marginal ridge. Upper Pleistocene fan deposits consist of 50- to 100-cm-thick, very fine to medium-grained unconsolidated sand turbidites with mud interbeds at Deep Sea Drilling Project drill site 174 (6). These sediments also contain abundant  $\text{CH}_4$ , which is highly enriched in  $^{12}\text{C}$  ( $\delta^{13}\text{C} = -80$  per mil PDB), confirming its microbial origin (6, 30). Pore fluids are expelled from these sediments as they consolidate in response to tectonic stresses induced by subduction accretion (5).

**Fossil record.** The high abundance of clams and tube worms in the vent community spread over several square meters at sites 1426 and 1428 off Oregon argues for similar occurrences of fossil animals in exposed accretionary complexes of ancient convergent margins. Most species of the molluscan genus *Calypptogena* sp., both living and fossil, are found around the Pacific rim from Japan to the Gulf of Alaska to South America (31). They also are found in the Atlantic Ocean off Africa and in the western Caribbean. Thus far ten fossil species have been recognized in sediments dating from Oligocene to Holocene age, and seven living species occur on continental margins in water depths ranging from ~100 to 2600 m. The only species that have been studied in modern environments are the clams *Calypptogena pacifica*, *C. kilmeri*, and *C. magnifica*, whose soft parts

Table 3. Carbon and oxygen isotope values (per mil relative to PDB) of selected magnesian calcite cements and carbonate crusts from the Oregon marginal ridge. Samples span the entire range of  $\delta^{13}\text{C}$  and  $\delta^{18}\text{O}$  values measured on all samples recovered; additional analyses are described (20). Precision of  $\delta^{13}\text{C}$  is  $\pm 0.10$  per mil and of  $\delta^{18}\text{O}$  is  $\pm 0.07$  per mil, based on National Bureau of Standards standard.

Sample	$\delta^{13}\text{C}$	$\delta^{18}\text{O}$
<i>Dredged carbonate cements</i>		
22 to 12	-66.7	4.22
16 to 2	-51.2	4.31
22 to 6	-58.7	4.72
16 to 13	-48.7	3.69
<i>Dive 1428-02, carbonate crusts</i>		
1	-39.1	6.39
8	-38.6	6.79
5	-34.9	6.04

resemble one another and may be adapted to symbiosis with microbes (31). Interestingly, the living specimens of *Calypptogena* (*Calypptogena*) *kilmeri* (Bernard) were found offshore from British Columbia, Canada, to northern California ( $53^\circ$  to  $40^\circ\text{N}$ ) at water depths ranging from 549 to 1464 m. These sites share with Oregon a common tectonic setting—all are situated on the accretionary complex of the northeast Pacific subduction zone.

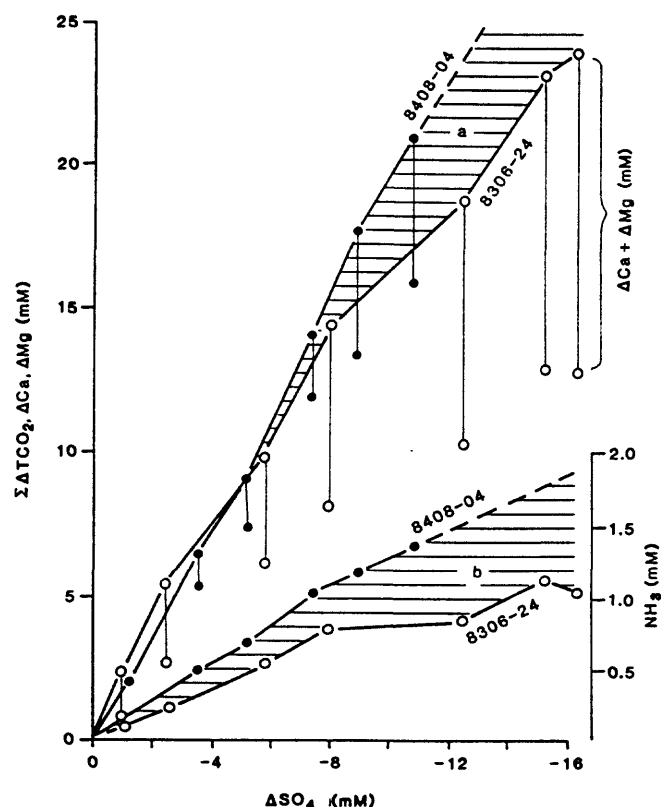


Fig. 4. Changes of concentrations of dissolved metabolites in pore waters of sediments from the subduction zone (core 8306-24) and the undeformed abyssal plain (core 8408-04). Organic matter decomposes by microbial sulfate reduction in both cores, generating  $\text{TCO}_2$  and  $\text{NH}_3$ . Estimating the removal of  $\text{TCO}_2$  by carbonate mineral precipitation and then comparing the metabolite pattern shows that in core 8306-24 a more reduced carbon substrate, such as  $\text{CH}_4$  yielding less  $\text{TCO}_2$  (lined area a) and no  $\text{NH}_3$  (lined area b), is oxidized concurrently with normal sedimentary organic matter. The vertical bars indicate the addition of  $(\Delta\text{Ca} + \Delta\text{Mg})$  to  $\Delta\text{TCO}_2$  with progressive depth in core, thereby correcting for the formation of carbonate minerals.

## Global Implications

Since our discovery of this unique biological community along the Oregon margin in August 1984, four more finds were made in circum-Pacific subduction zones during the summer of 1985. French and Japanese scientists participating in the Kaiko Project discovered giant white clams, tentatively identified as *Calyptogena* sp., with the submersible *Nautilie* in water depths of 3800 m at the northern end of the Nankai Trough and at 5640 m in the Japan Trench. Both sites are located on the landward walls of the trenches opposite the Philippine and Pacific oceanic plates, respectively (16, 32). In addition, the Japanese submersible *Shinkai 2000* discovered similar mollusks and tube worm colonies in 1300 m of water in Sagami Bay, presumably along the Sagami Trough (16). These animals were found where thrust faulting, caused by subduction, apparently expels pore waters along fault planes in the accretionary complexes. The Nankai Trough, the Japan Trench, and the Oregon margin represent subduction zones where thick, organic-rich, terrigenous sediments occupy the trench and are off-scraped to build an accretionary complex. Another, so far unreported discovery of what appear to be species of the mollusk *Calyptogena* was made along the Peru continental margin in April 1985 by Kulm, Suess, and Thornburg. Three living specimens were dredged from a water depth of 3600 to 3900 m in an area of the margin where a large fracture cuts nearly perpendicular to the trend of the Peru continental slope. The Peruvian margin represents a subduction erosion setting where the accretionary complex is relatively small and is apparently retreating landward (33), as opposed to the subduction accretion settings of the northeast and northwest Pacific that are actively building seaward.

Our studies show that compressive tectonic stresses acting along convergent margins are especially effective in expelling  $\text{CH}_4$  and nutrient-rich pore fluids that enable organisms to adapt and evolve in this special ecosystem. Studies of subduction zones with deep submersible technology show that we are on the threshold of numerous global discoveries in convergent margins with different tectonic settings, geologic frameworks, and ages. Such studies may contribute to our understanding of the evolution and history of these dynamic and complicated plate tectonic boundaries.

### REFERENCES AND NOTES

1. E. A. Silver, *Mar. Geol.* 13, 239 (1972).
2. B. Carson, Y. Jennwei, P. B. Myers, Jr., *Geology* 2, 561 (1974).
3. L. D. Kulm and G. A. Fowler, in *The Geology of Continental Margins*, C. A. Burk and C. L. Drake, Eds. (Springer, New York, 1974), pp. 261-283.
4. D. R. Seely, P. R. Vail, G. G. Walton, *ibid.*, pp. 249-260.
5. B. Carson, *Mar. Geol.* 24, 289 (1977).

6. L. D. Kulm et al., Eds., *Init. Rep. Deep Sea Drill. Proj.* 18 (1973).
7. We obtained seismic reflection records (i) by towing from a surface vessel a hydrophone streamer (designed by B. Lewis) about 100 m above the sea floor with a water gun source at surface or (ii) by using a hydrophone streamer mounted on *Alvin* with the source at the surface.
8. D. E. Karig et al., *Nature (London)* 304, 148 (1983).
9. J. Suppe, *Am. J. Sci.* 283, 684 (1983).
10. Taxonomic identification courtesy of M. L. Jones, Smithsonian Institution, Washington, DC.
11. E. Suess et al., in *The Hydrothermal Vents of the Eastern Pacific: An Overview*, M. L. Jones, Ed. [*Bull. Biol. Soc. Washington* No. 6 (1985)], p. 475.
12. Taxonomic identification courtesy of R. Turner, Harvard University.
13. A. J. Southward et al., *Nature (London)* 293, 616 (1981).
14. G. H. Rau, *Science* 213, 338 (1981).
15. J. S. Killingley, W. H. Berger, K. C. MacDonald, W. A. Newman, *Nature (London)* 287, 218 (1980).
16. D. Swinbanks, *ibid.* 316, 475 (1985).
17. In seawater  $^{222}\text{Rn}$  (half-life = 3.85 days), which is produced from  $^{226}\text{Ra}$  (half-life = 1622 years), ordinarily comes from two sources: (i) decay of its parent,  $^{226}\text{Ra}$ , dissolved in the water and (ii) diffusion out of the sediments where it is produced from  $^{226}\text{Ra}$  associated with sediment particles. In the bottom waters, the background level of  $^{226}\text{Ra}$ -supported radon was  $25.8 \pm 3.0$  dpm per 100 liters. Diffusion of  $^{222}\text{Rn}$  from the sediments was estimated to be  $0.27$  dpm/cm<sup>2</sup> from flux =  $\phi \cdot Q \cdot \rho(\tau D)^{1/2}$ , where the porosity ( $\phi$ ) = 0.85 percent (by volume), dry bulk density ( $\rho$ ) =  $0.43$  g/cm<sup>3</sup>, pore water diffusion coefficient ( $D$ ) =  $5 \times 10^{-6}$  cm<sup>2</sup>/sec, and the radon mean life = 5.5 days.  $Q$  is the radon emanation measured at  $0.490$  dpm/g (dry weight) [W. S. Broecker, in *Symposium of Diffusion in Ocean and Fresh Water*, T. Ichige, Ed. (Lamont-Doherty Geological Observatory, Palisades, NY, 1965), pp. 116-145]. The combined near-bottom concentration ( $C_0$ ) from these two sources would be in the range of  $\sim 35$  to  $45$  dpm per 100 liters, depending on the extent of bottom turbulence:

$$C_0 = [0.27(\lambda/k)^{1/2}] \times 10^5 + 25.8 \text{ dpm per 100 liters}$$

where  $\lambda$  is the radon decay constant and  $k$  is the turbulent diffusion coefficient in the water column.

18. The percentages of  $\text{TCO}_2$  generated by  $\text{CH}_4$  oxidation in sediment core 8306-24 were calculated for seven depth intervals based on  $\text{NH}_3$  and  $\text{TCO}_2$  deficiencies, respectively. These independent estimates are in good agreement with each other; their relative errors are large at shallow depths because of low  $\text{TCO}_2$  and  $\text{NH}_3$  concentrations and small  $\text{SO}_4^{2-}$  changes. They are as follows:  $36 \pm 2$  and  $36 \pm 2$  percent at 175 to 180 cm;  $29 \pm 2$  and  $31 \pm 2$  percent at 160 to 165 cm;  $40 \pm 5$  and  $32 \pm 5$  percent at 125 to 130 cm;  $24 \pm 5$  and  $10 \pm 5$  percent at 85 to 90 cm;  $19 \pm 5$  and  $18 \pm 5$  percent at 60 to 65 cm;  $36 \pm 20$  and  $0 \pm 20$  percent at 25 to 30 cm; and  $32 \pm 20$  and  $0 \pm 20$  percent at 5 to 10 cm.
19. R. L. Scamman, thesis, Lehigh University (1981).
20. S. Ritger, B. Carson, E. Suess, *Geol. Soc. Am. Bull.*, in press.
21. J. B. Corliss et al., *Science* 203, 1073 (1979).
22. J. Francheteau, *Nature (London)* 277, 523 (1979).
23. H. Felbeck, *Science* 213, 336 (1981).
24. C. M. Cavanaugh, *Nature (London)* 302, 5861 (1983).
25. H. W. Jannasch, in *Hydrothermal Processes at Seafloor Spreading Centers*, P. A. Rona et al., Eds. (Plenum, New York, 1983), pp. 677-710.
26. H. J. Flügel and R. Schmaljohann, *Sarsia*, in press.
27. C. K. Paull et al., *Science* 226, 965 (1984).
28. J. M. Brooks, M. C. Kennicutt, II, R. R. Bidigare, R. A. Fay, *Eos* 66, 106 (1985).
29. M. Webb, *Bull. Mar. Sci.* 19, 18 (1969).
30. R. D. McIver, *Init. Rep. Deep Sea Drill. Proj.* 18, 1013 (1973).
31. K. J. Boss and R. D. Turner, *Malacologia* 20, 161 (1980).
32. D. Swinbanks, *Nature (London)* 315, 624 (1985).
33. R. von Huene, L. D. Kulm, J. Miller, *J. Geophys. Res.* 90, 5429 (1985).
34. We acknowledge the assistance of the crew members of the R/V *Wecoma* (Oregon State University) and R/V *Atlantis II* (Woods Hole Oceanographic Institute); we appreciate the assistance and advice of *Alvin* pilots and support group. We thank K. Kelly-Hansen and A. Ungerer for carrying out the  $\text{CH}_4$  and pore water chemistry analyses, respectively. R. D. Turner identified the clams and M. L. Jones the tube worms. This project was funded by National Science Foundation grants OCE-82-15147-01, -02, -03 (L.D.K.) and OCE-83-15836 (J.C.M.) and National Oceanic and Atmospheric Administration grant NA-84-ABH00030 (E.S. and D.C.K.).

APPENDIX A. 6.

Holocene Subsidence Deposits in Alaskan Earthquakes

by

Susan Bartsch-Winkle

Summary of  
"Post-earthquake sedimentation in Upper Cook Inlet, Alaska"  
NEPEC Meeting, Seattle, WA, April 2, 1987  
presented by Susan Bartsch-Winkler, Branch of Alaskan Geology,  
U.S. Geological Survey, Reston, VA 22092

The Cook Inlet region experiences frequent earthquakes as a result of subduction near the Aleutian arc. In particular, during the 1964 great earthquake ( $M = 9.2$ ; Kanamori, 1977) of March 27, 1964, two areas of regional uplift and subsidence were produced in two nearly parallel zones trending SW-NE above the gently dipping Aleutian megathrust (Plafker, 1969, fig. 15, p. I-22). Regional uplift and regional and localized subsidence produced by the 1964 earthquake affected intertidal and near-intertidal sediments in south-central Alaska (Plafker and Rubin, 1967; Plafker, 1969; Ovenshine and others, 1976; Bartsch-Winkler and Schmoll, 1984a). Aggradation of intertidal sediment in upper Cook Inlet, especially Turnagain Arm, began because of earthquake-induced subsidence.

In the Portage area at the head of Turnagain Arm, upper intertidal or freshwater marshlands subsided into the lower intertidal zone and were covered with deeper-water sediment (Ovenshine and others, 1976). The postearthquake intertidal deposit, the Placer River Silt of Ovenshine and others (1976), and the underlying unnamed 1964 marsh deposit were described. The subsidence-induced deposition at Portage, which totals as much as 2.5 m in thickness, has been subsequently monitored. Changes in flora and fauna, as well as changes in sedimentological patterns indicate that sediment aggradation has slowed since the initial reporting on the status of postearthquake sedimentation in 1973, and that the region returned to a state of preearthquake equilibrium 17 years after the event (Bartsch-Winkler and Garrow, 1982).

Study of a Late Holocene intertidal deposit exposed near the upper intertidal zone of Upper Cook Inlet, Knik, and Turnagain Arms shows that areas of accumulating organic sediments, particularly marsh areas that have undergone earthquake-induced subsidence and are preserved beneath subsequently deposited sediments, can possibly determine the age of past earthquake events by utilization of radiocarbon methods (Bartsch-Winkler and others, 1983; Bartsch-Winkler and Schmoll, 1984; 1987; Combellick, 1986). The hypothesis that earthquake-related events may have occurred repeatedly throughout Cook Inlet during late Holocene time is currently being tested by radiocarbon dating on over 50 samples collected from measured sections in 1986. As indicated by the sedimentary sequences measured in the 17 sections from the intertidal zone of Upper Cook Inlet, the most reliable area for obtaining earthquake-caused sedimentary couplets is a narrow, middle-intertidal region located near the earthquake-induced region of maximum subsidence.

Besides radiocarbon dating of layered peats, additional sedimentological evidence for earthquakes includes sequences of contorted beds separated by undisturbed beds, anomalous sand layers occurring immediately above peat layers possibly indicating tsunami deposits, sand blows produced during liquefaction, and evidence for repeated, rapid change of base level in the stratigraphic section (e.g., fluctuation between fluvial and tidal settings).



## References cited

- Bartsch-Winkler, Susan, and Garrow, H.C., 1982, Depositional system approaching maturity at Portage Flats, in Coonrad, W.L., ed., the United States Geological Survey in Alaska--Accomplishments during 1980: U.S. Geological Survey Circular 844, p. 115-117.
- Bartsch-Winkler, Susan, Ovenshine, A.T., and Kachadoorian, Reuben, 1983, Holocene history of the estuarine area surrounding Portage, Alaska, as recorded in a 93-m core: Canadian Journal of Earth Science, v. 20, no. 5, p. 802-820.
- Bartsch-Winkler, Susan, and Schmoll, H.R., 1984a, Guide to Late Pleistocene and Holocene deposits of Turnagain Arm, Alaska: Anchorage, Alaska Geological Society, 70 p., 2 maps (Fieldtrip guide for the 80th Cordilleran Section Meeting, Geological Society of America).
- 1984b, Bedding types in Holocene tidal channel sequences, Knik Arm, Upper Cook Inlet, Alaska: Journal of Sedimentary Petrology, v. 54, no. 4, p. 1239-1250.
- 1987, Earthquake-caused sedimentary couplets in the Upper Cook Inlet region, in Hamilton, T.D., and Galloway, J.P., eds., Geologic studies in Alaska by the U.S. Geological Survey during 1986: U.S. Geological Survey Circular 998, p. 92-95.
- Combellick, R.A., 1986 (abs.), Chronology of late Holocene earthquakes in southcentral Alaska--Evidence from buried organic soils in upper Turnagain Arm, in Abstracts with Programs, Geological Society of America, v. 18, no. 6, p. 569.
- Kanamori, Hiroo, 1977, The energy release in great earthquakes: Journal of Geophysical Research, v. 82, p. 2981-2987.
- Ovenshine, A.T., Lawson, D.E., and Bartsch, S.R., 1976, The Placer River Silt--Intertidal sedimentation caused by the Alaska earthquake of March 27, 1964: U.S. Geological Survey Journal of Research, v. 4, no. 2, Mar-Apr 1976, p. 151-162.
- Plafker, George, 1969, Tectonics of the March 27, 1964 Alaska earthquake, in The Alaska Earthquake, March 27, 1964--Regional effects: U.S. Geological Survey Professional Paper 543-I, p. 11-174.
- , 1972, Alaskan earthquake of 1964 and Chilean earthquake of 1960--Implications for arc tectonics: Journal of Geophysical Research, v. 77, no. 5, p. 901-925.
- Plafker, George, and Rubin, Meyer, 1967, Vertical tectonic displacements in south-central Alaska during and prior to the Great 1964 Earthquake: Journal of Geosciences, Osaka City University, v. 10, p. 53-66.

## EARTHQUAKE-CAUSED SEDIMENTARY COUPLETS IN THE UPPER COOK INLET REGION

Susan Bartsch-Winkler and Henry R. Schmoll

The Cook Inlet region experiences frequent earthquakes as a result of subduction near the Aleutian arc. Earthquakes originate beneath and north of Cook Inlet on the steeply dipping Wadati-Benioff zone, which marks the descent of the Pacific plate into the mantle (Stephens and others, 1986). Although many earthquakes of generally low to moderate magnitude are associated with the Wadati-Benioff zone, only the large magnitude earthquakes that occur closer to the Aleutian trench south and east of Cook Inlet are likely to be capable of significantly affecting intertidal sedimentation in the region. In particular, during the 1964 earthquake (moment magnitude 9.2; Kanamori, 1977), two areas of regional uplift and subsidence were produced in two nearly parallel zones trending southwest-northeast above the gently dipping Aleutian megathrust (Plafker, 1969, fig. 15, p. I-22). Upper Cook Inlet, and especially upper Turnagain Arm, lies within the subsidence zone, which is centered over the Kenai-Chugach Mountains (Plafker, 1969).

Regional uplift and regional and localized subsidence produced by the 1964 earthquake affected intertidal and near-intertidal sediments in south-central Alaska (Plafker and Rubin, 1967; Plafker, 1969; Ovenshine and others, 1976; Bartsch-Winkler and Schmoll, 1984a). Relative sea-level changes along the coast are recorded in sedimentary sequences at the affected sites (figs. 1 and 2). Areas of accumulating organic sediments, particularly marsh areas that have undergone earthquake-induced subsidence and are preserved beneath subsequently deposited sediments, can be dated by the radiocarbon method and the age of the earthquake event thus determined (Plafker and Rubin, 1967; Plafker, 1972; Ovenshine, 1976; Bartsch-Winkler and others, 1983; Bartsch-Winkler and Schmoll, 1984b; Atwater and Grant, 1986).

In the Portage area at the head of Turnagain Arm (fig. 1), upper intertidal or freshwater marshlands subsided into the lower intertidal zone and were covered with deeper-water (tidal) sediment at the time of the 1964 earthquake (Ovenshine and others, 1976). The postearthquake intertidal deposit, the Placer River Silt of Ovenshine and others (1976), and the underlying unnamed 1964 marsh deposit were described. The subsidence-induced deposition at Portage, which totals as much as 2.5 m in thickness in some locations, has been subsequently monitored; the sedimentation rate has declined to nearly nil and the surrounding area has attained a state of equilibrium only 20 years after the earthquake

(Bartsch-Winkler and Garrow, 1982). That is, a new marsh and forest have become established in an area where marsh and forest were destroyed by subsidence into the intertidal zone at the time of the 1964 earthquake.

Our data from Upper Cook Inlet support the suppositions of Plafker (1972) and of Ovenshine and others (1976) that older submerged marsh and forest layers would be found in intertidal zones of regions experiencing earthquakes. Such organic horizons beneath intertidal silt form depositional packages termed "earthquake couplets" by A.T. Ovenshine (U.S.G.S., written commun., 1976). When dated by radiocarbon methods, these couplets provide information on the late Holocene earthquake history of the region surrounding Anchorage.

Seventeen sections have been measured in the intertidal zone of the Susitna Lowland, Knik Arm, and Turnagain Arm (figs. 1 and 2). Two sections in the Placer River Silt at Portage (secs. 16, 17) have been described previously (Ovenshine and others, 1976), as have two sections (secs. 5, 6) in convoluted and hummocky beds of the lower intertidal zone at Anchorage and within Knik Arm (Bartsch-Winkler and Schmoll, 1984b). Section 10 was measured in a drainage channel constructed after the earthquake in June 1983, and the remaining 13 sections (secs. 1-4, 7-9, and 11-15) were measured in July 1986.

The bases of most of the sections are at the lower-low tide level or at river level. Tops of the sections vary with the availability of exposure at each site, but most are within the upper intertidal zone. The elevations of the upper, middle, and lower intertidal zones vary throughout Upper Cook Inlet region; maximum tide range is about 11.4 m (35 ft) at the official tide station at Anchorage. Records from the unofficial tide station midway in Turnagain Arm near Hope indicate a larger mean tide range there than at Anchorage. The tide range at the mouth of the Little Susitna River is not documented. Because the tide range is large in this estuary, an effort was made to observe the deposits that had bases at tide level when the tide range was the greatest for the month (spring tide) and at lower-low tide; this enabled measurement during maximum exposure at the base of the sections.

Sections 3 and sections 8-11, located within the upper intertidal zone, contain the most abundant organic material (fig. 2) because of their position near the continuous marsh zone. Conversely, sections 4-6, located within the lower intertidal zone, contain the largest proportion of inorganic silt and sand and are the only sections that contain shell debris. Sections 1-2, 7, 12-15, and 17 are located in a narrow zone in the middle of the intertidal region, here called the middle intertidal zone. Section 16 was measured within the Twentymile River channel, a major fluvial and

Bartsch-Winkler, Susan, and Schmoll, Henry R., 1987, Earthquake-caused sedimentary couplets in the Upper Cook Inlet region, in Hamilton, T.D., and Galloway, J.P., eds., *Geologic studies in Alaska by the U.S. Geological Survey during 1986*: U.S. Geological Survey Circular 998, p. 92-95.

estuarine channel that drains extensive glacial and estuarine areas of the Portage flats. With the exception of section 16, which contains a large amount of sediment carried by this river, the sections measured in the middle intertidal zone have the greatest number of distinct organic layers separated by intertidal silt deposits.

The middle intertidal zone is the most useful region for locating earthquake-induced sedimentary couplets. This zone has numerous distinct peat and wood layers intercalated with silt, a deposit that results from the burial of marsh and forest by intertidal sediment after earthquake-induced subsidence (fig. 3). Earthquake events can be identified by dating radiocarbon samples collected from the top of the organic layers and correlating them with other such radiocarbon-dated layers in the Upper Cook Inlet region (table 1). By dating organic material from the base of organic layers and measuring their thickness, the rate of accretion of the marsh might also be determined.

Table 1.—Radiocarbon dates and laboratory numbers of samples collected from Upper Cook Inlet as of 1983

Radiocarbon date (yr B.P.)	Laboratory No.	Section No.	Reference
180 ± 45	USGS-332	17	Ovenshine and others (1976)
350 ± 80	I-12,027	5	Bartsch-Winkler and Schmolli (1984b)
635 ± 40	USGS-1780	10	This paper
1,000 ± 70	USGS-1781	10	This paper
1,480 ± 50	USGS-1782	10	This paper
1,595 ± 75	I-11,767	5	Bartsch-Winkler and Schmolli (1984b)
1,825 ± 45	USGS-1570	6	Bartsch-Winkler and Schmolli (1984b)
1,840 ± 50	USGS-1117	15	This paper
2,350 ± 125	I-12,008	6	Bartsch-Winkler and Schmolli (1984b)
3,040 ± 50	USGS-1573	6	Bartsch-Winkler and Schmolli (1984b)
3,205 ± 110	I-11,718	6	Bartsch-Winkler and Schmolli (1984b)
3,270 ± 90	I-11,717	5	Bartsch-Winkler and Schmolli (1984b)
3,280 ± 90	I-11,706	6	Bartsch-Winkler and Schmolli (1984b)

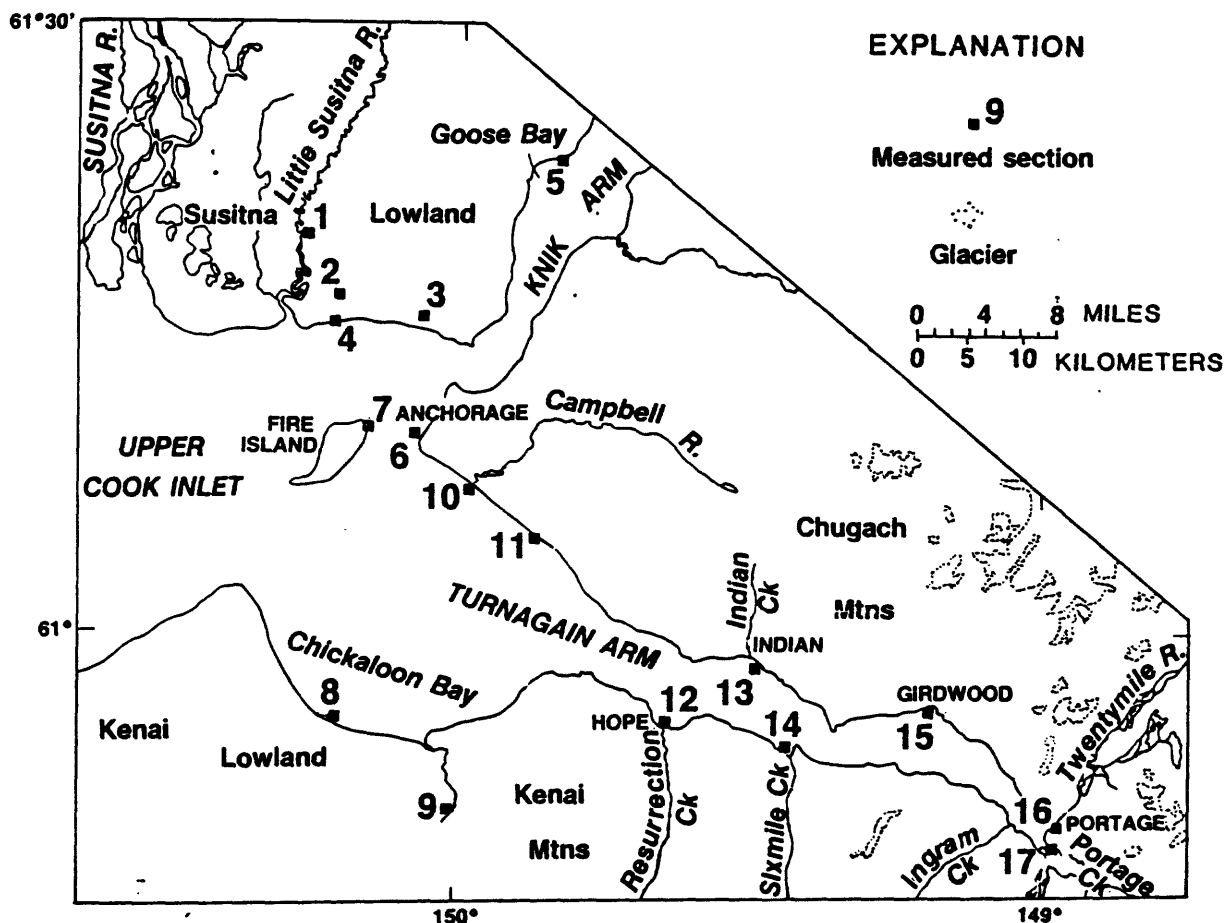


Figure 1.—Upper Cook Inlet showing locations of measured stratigraphic sections in intertidal deposits.

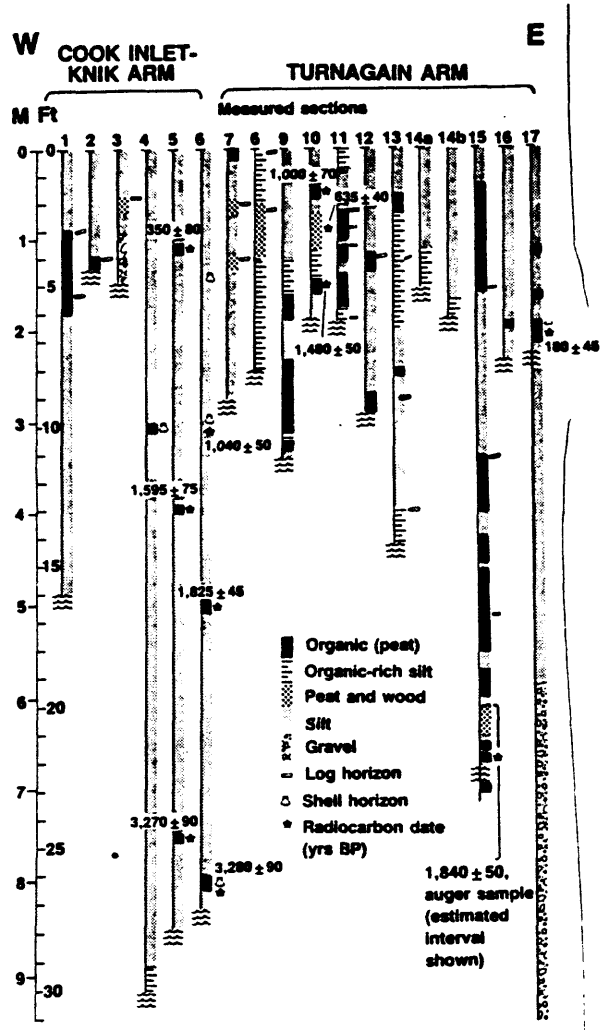


Figure 2.—Stratigraphic sections showing organic layers and lithologies, wood and shell horizons, and radiocarbon-dated samples at 17 sites in Upper Cook Inlet. The tide or stream level is indicated by wave symbol. Table 1 lists pertinent information on radiocarbon dates.

Earthquake recurrence is more difficult to determine from sediment and organic layers deposited above or below the middle intertidal zone. In the upper intertidal zone, pre- and post-earthquake organic layers commonly are deposited directly above each other without intervening intertidal silt layers (fig. 3.). Discrete log layers enclosed in peat are the most likely indicators of an earthquake in this zone, because subsidence of the coastal forest immediately following an earthquake would result in forest kill by saltwater incursion (as occurred in 1964 at Portage). In the lower intertidal zone, in contrast, the absence of in situ organic-rich layers complicates the analysis. In this zone, bedding discontinuities,

such as planar beds that truncate underlying contorted beds, are the best criteria for distinguishing earthquakes (Bartsch-Winkler and Schmoll, 1984b). Because such discontinuities might be caused by sedimentary processes other than those induced by earthquakes (see Bartsch-Winkler and Schmoll, 1984b, p. 1246-1248), they cannot be used alone to date earthquake events in these areas.

As indicated by the sedimentary sequences measured in our 17 sections from the intertidal zone of Upper Cook Inlet, the most reliable area for obtaining earthquake-caused sedimentary couplets from the Upper Cook Inlet intertidal zone is the narrow, middle intertidal region. The 11 radiocarbon dates presently available from 4 of our 17 sections (table 1) suggest that earthquake-related events may have occurred repeatedly throughout Cook Inlet during late Holocene time. This hypothesis is currently being tested by radiocarbon dating that is now in progress on over 50 additional organic samples that we collected from our measured sections in 1986.

#### REFERENCES CITED

- Atwater, B.F., and Grant, W.C., 1986, Holocene subduction earthquakes in coastal Washington (abs.): *Eos (Transactions, American Geophysical Union)*, v. 67, no. 44, p. 906.
- Bartsch-Winkler, Susan and Garrow, H.C., 1982, Depositional system approaching maturity at Portage Flats, in Coonrad, W.L., ed., *The United States Geological Survey in Alaska—Accomplishments during 1980: U.S. Geological Survey Circular 844*, p. 115-117.
- Bartsch-Winkler, Susan, Ovenshine, A.T., and Kachadoorian, Reuben, 1983, Holocene history of the estuarine area surrounding Portage, Alaska, as recorded in a 93-m core: *Canadian Journal of Earth Science*, v. 20, no. 5, p. 802-820.
- Bartsch-Winkler, Susan, and Schmoll, H.R., 1984a, Guide to Late Pleistocene and Holocene deposits of Turnagain Arm, Alaska: Anchorage, Alaska Geological Society, 70 p., 2 maps (Fieldtrip guide for the 80th Cordilleran Section Meeting, Geological Society of America).
- 1984b, Bedding types in Holocene tidal channel sequences, Knik Arm, Upper Cook Inlet, Alaska: *Journal of Sedimentary Petrology*, v. 54, no. 4, p. 1239-1250.
- Kanamori, Hiroo, 1977, The energy release in great earthquakes: *Journal of Geophysical Research*, v. 82, p. 2981-2987.
- Ovenshine, A.T., Lawson, D.E., and Bartsch, S.R., 1976, The Placer River Silt—Intertidal sedimentation caused by the Alaska earthquake of March 27, 1964: *U.S. Geological Survey Journal of Research*, v. 4, no. 2, Mar-Apr 1976, p. 151-162.

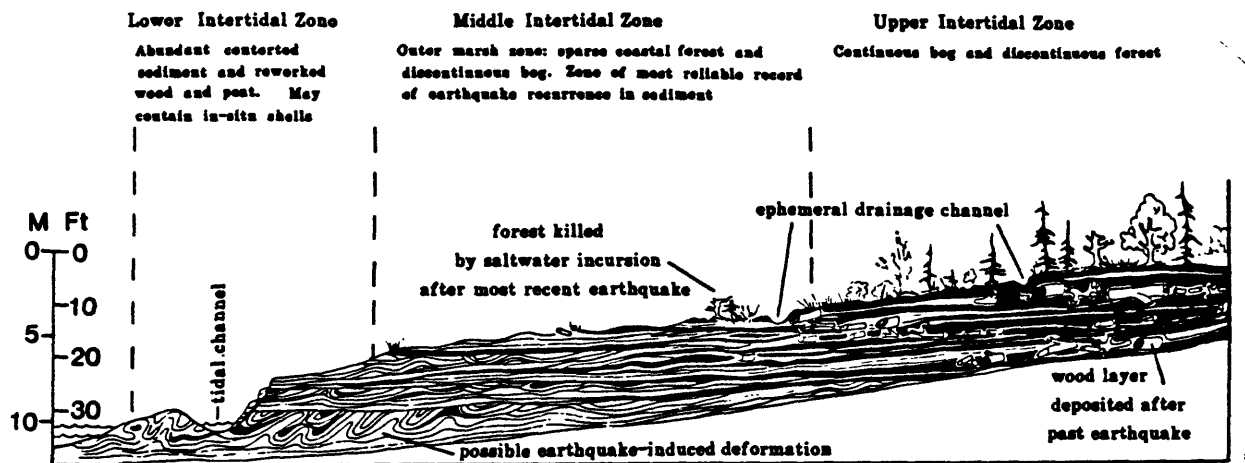


Figure 3.—Diagrammatic section showing characteristics of upper, middle, and lower intertidal zones and sedimentary features indicative of earthquake deformation. Model assumes a constant shoreline position not subject to progradation or regression.

Plafker, George, 1969, Tectonics of the March 27, 1964 Alaska earthquake, in *The Alaska Earthquake, March 27, 1964: Regional effects*: U.S. Geological Survey Professional Paper 543-I, p. 11-174.

Plafker, George, 1972, Alaskan earthquake of 1964 and Chilean earthquake of 1960—Implications for arc tectonics: *Journal of Geophysical Research*, v. 77, no. 5, p. 901-925.

Plafker, George, and Rubin, Meyer, 1967, Vertical tectonic displacements in south-central Alaska during and prior to the Great 1964 Earthquake: *Journal of Geosciences, Osaka City University*, v. 10, p. 53-66.

Stephens, C.D., Fogleman, K.A., Lahr, J.C., and Page, R.A., 1986, Seismicity in southern Alaska, October 1984-September 1985; in *Bartsch-Winkler, Susan, and Reed, K.M., eds., Geologic studies in Alaska by the U.S. Geological Survey during 1985*: U.S. Geological Survey Circular 978, p. 81-85.

Reviewers: A.F. Espinosa and J.R. Riehle

## THE PLACER RIVER SILT—AN INTERTIDAL DEPOSIT CAUSED BY THE 1964 ALASKA EARTHQUAKE

By A. T. OVENSCHINE, DANIEL E. LAWSON,<sup>1</sup> and SUSAN R. BARTSCH-WINKLER,  
Menlo Park, Calif., Urbana, Ill., Menlo Park, Calif.

**Abstract.**—At the head of Turnagain Arm near Anchorage, the major lasting geologic consequence of the Alaska earthquake of 1964 was deposition of the Placer River Silt, an intertidal deposit covering an area of more than 18 km<sup>2</sup> and containing more than  $20 \times 10^6$  m<sup>3</sup> of sediment. This formation, which was derived from erosion of intertidal bars in Turnagain Arm, averages 1.5 m thick seaward of the Seward Highway and 0.9 m thick landward. Its distribution is controlled both by the arrangement of the major streams that enter tidewater and by manmade features such as the highway and railroad embankments. The Placer River Silt is still being deposited. The contemporary lowland sedimentation system of the Portage area includes a number of depositional settings: (1) In the Placer River Silt—upper tidal flats, levees, and channelway fans, (2) elsewhere in the intertidal zone—tidal stream channels, lower tidal flats, and saltwater marsh, and (3) in the supratidal zone—gravel levees, freshwater marsh, bogs, and lakes. Since 1964, the critical environmental results of the earthquake-caused deposition have been abandonment of the settlement of Portage, formation of an unsightly blanket of silt, destruction of natural plant communities, localized erosion, and creation of quicksand hazards.

The Alaska earthquake of March 27, 1964, caused land subsidence in the Portage area (fig. 1) amounting to at least 2.4 m. Of this, slightly more than 1.6 m resulted from regional tectonic subsidence and 0.8 m was from local subsidence (McCulloch and Bonilla, 1970, p. D128 and fig. 114), probably related to seismically induced compaction in the 300 m (Dennis Kalpacoff, oral commun., 1973) of unconsolidated sediment that underlies the area. The subsidence allowed high tides to inundate approximately 18 km<sup>2</sup> of land that had been above sea level, resulting in deposition of more than  $20 \times 10^6$  m<sup>3</sup> of fine-grained intertidal sediment. This report describes this sediment and the contemporary sedimentation system at Portage and notes some of the environmental consequences of its deposition.

The Portage area, about 77 km southeast of Anchorage, was within the area of maximum damage and

shaking related to the Alaska earthquake of 1964. The small roadside settlement of Portage was abandoned after the earthquake; present habitation is limited to one house and several mobile homes associated with a service station. The area is crossed by the Seward Highway and contains the junction of the Whittier and Seward spurs of The Alaska Railroad.

Portage is situated at the mouths of three broad, alluviated valleys—Twentymile, Portage, and Placer—separated by steep bedrock ridges that rise 900–1,200 m above the valley floors. Bedrock in the region is Jurassic(?) and Cretaceous graywacke, siltite, and argillite assigned to the Valdez(?) Group (Clark, 1972). The valleys in the Portage area, 1.5–2.5 km wide and within 10 m of sea level, are underlain by Holocene sands and gravels that interfinger with tidal silts and sands about 1 km landward of the present shoreline. The water table is within 1.5 m of the ground surface throughout most of the area. Large fast-flowing braided streams near the midlines of each of the three valleys typically are flanked by well-drained natural levees underlain by sand and gravel. Much of the water in the streams originates in snowfields of the Chugach Mountains and in glaciers that descend to low altitudes at the heads of the valleys. Between the levees and the bedrock valley walls is grassy or sparsely forested freshwater marsh and bog.

The streams reach tidewater at the head of Turnagain Arm, a southeast-trending, 72-km-long marine embayment at the northeast end of Cook Inlet. Turnagain Arm is noteworthy for its high tidal range (10 m), frequent occurrence of bore tides, and extensive development of intertidal sand bars. No data on tide characteristics are available for the Portage area, but our observations during the summer of 1973 suggest a tidal range of 8 m or more and lag in the start of flooding of 4 hours or more relative to Anchorage.

<sup>1</sup> University of Illinois.

## THE PLACER RIVER SILT, ALASKA

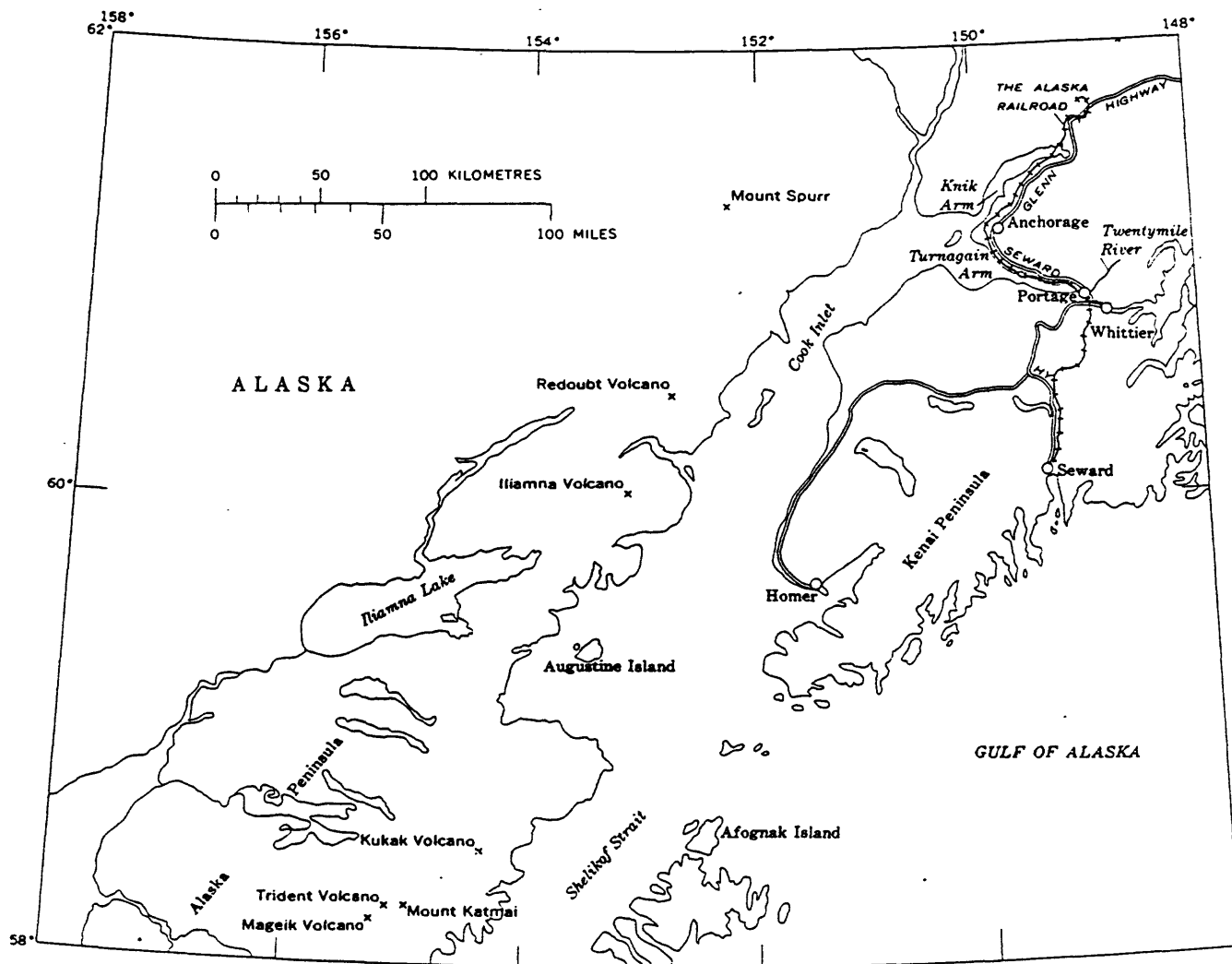


FIGURE 1.—Location of the Portage area in Alaska. Active volcanoes on the west side of Cook Inlet indicated by X.

### THE PLACER RIVER SILT

The deposits of intertidal origin that resulted from the Alaska earthquake make up a recognizable geologic unit that has been mapped throughout the Portage area (fig. 2). This unit, here named the Placer River Silt for its occurrence on Placer River, commonly overlies a soil horizon rich in organic material. In 1973 the Placer River Silt was still being deposited.

The best exposures of the formation are in the steep banks of Portage Creek and Placer and Twentymile Rivers. The exposure in the north bank of the north fork of Portage Creek west of the Seward Highway is designated the type section (fig. 3D). Excellent exposures occur in many of the small channels that cross the tidal flats seaward of the Seward Highway.

Sections of the Placer River Silt have been measured at five localities shown in figure 3: Ingram Creek (A), Placer River (B and C), Portage Creek (D), and Twentymile River (E).

### Base of the Placer River Silt

As shown in the measured sections (fig. 3), the Placer River Silt overlies a buried soil and vegetation horizon developed on an older unit of intertidal silts. These older silts, in contrast to the post-1964 silts, are relatively firmly compacted and contain abundant yellowish-orange and yellowish-brown oxidized zones that encapsulate rootlets, twigs, or other buried plant debris.

The soil horizon developed at the top of the older silt ranges in thickness from a few centimetres to more

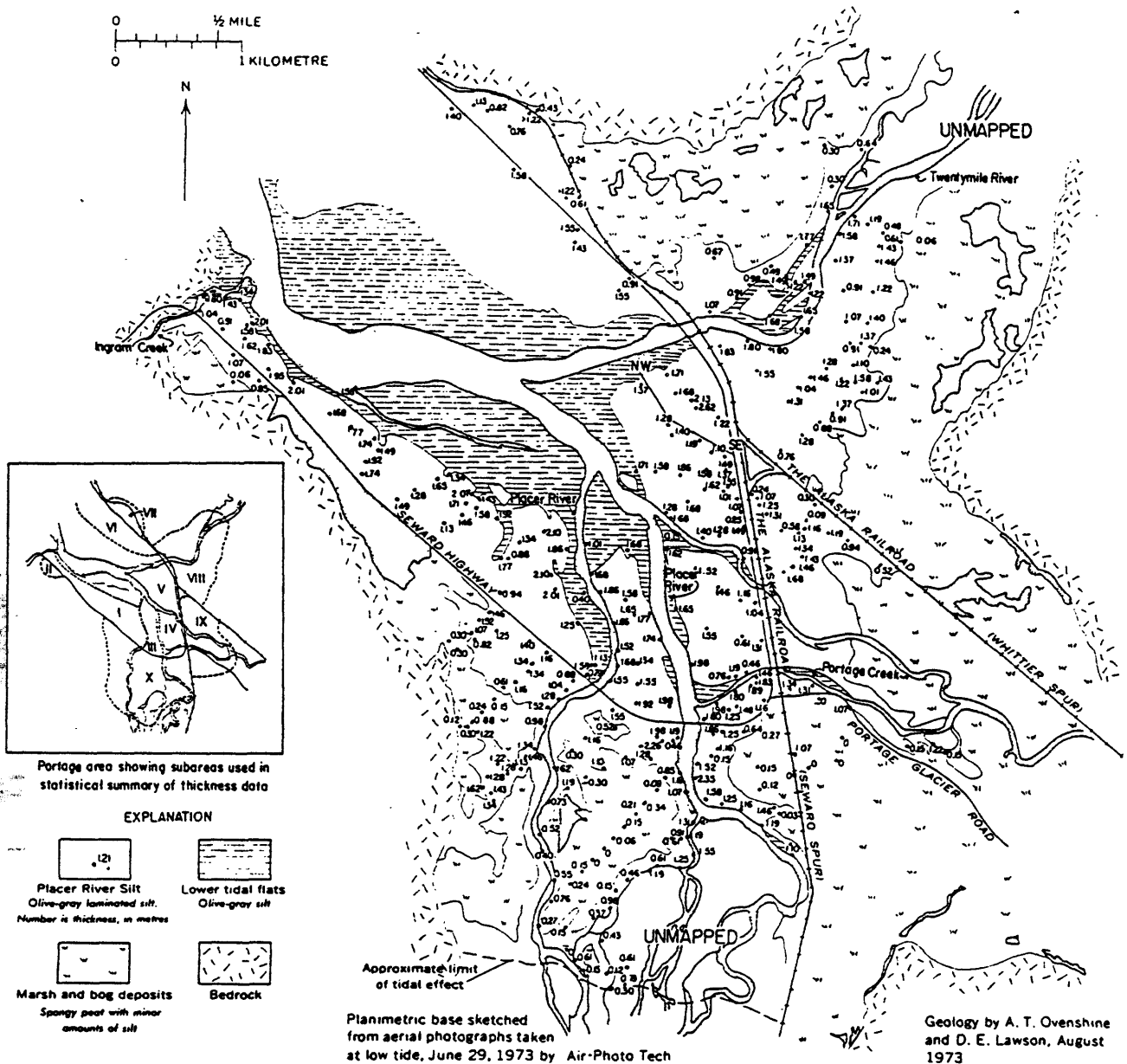


FIGURE 2.—Geologic sketch map showing distribution of the Placer River Silt and depositional framework of the Portage area.

than several tens of centimetres and is recognized mainly by a high proportion of nearly undecayed vegetable matter. The nature of the soil varies according to the plant community that lived on it at the time of the earthquake: in areas that were forest or alder thicket, the soil is a centimetre or more of black leaf duff overlying 1–10 cm of brown rootlet-bearing silt; in areas that were bog or marsh, from 1 to 5 cm of spongy black malodorous peat composed of partly decayed grass blades, sphagnum moss, and rootlets; in areas that were

grassland, as much as 30 cm of compacted silt bound together by a lacework of grass roots. The grassland soil is well exposed in the shoreline bluffs of Turnagain Arm between Placer and Ingram Creeks. During storm high tides, blocks of this rootbound silt as much as 1 m<sup>2</sup> in area and 0.3 m in thickness are eroded and transported hundreds of metres across the tidal flats.

Before the Alaska earthquake, the Portage area had a variety of plant communities including spruce and cottonwood forest, willow and alder thickets, well-



# THE PLACER RIVER SILT, ALASKA

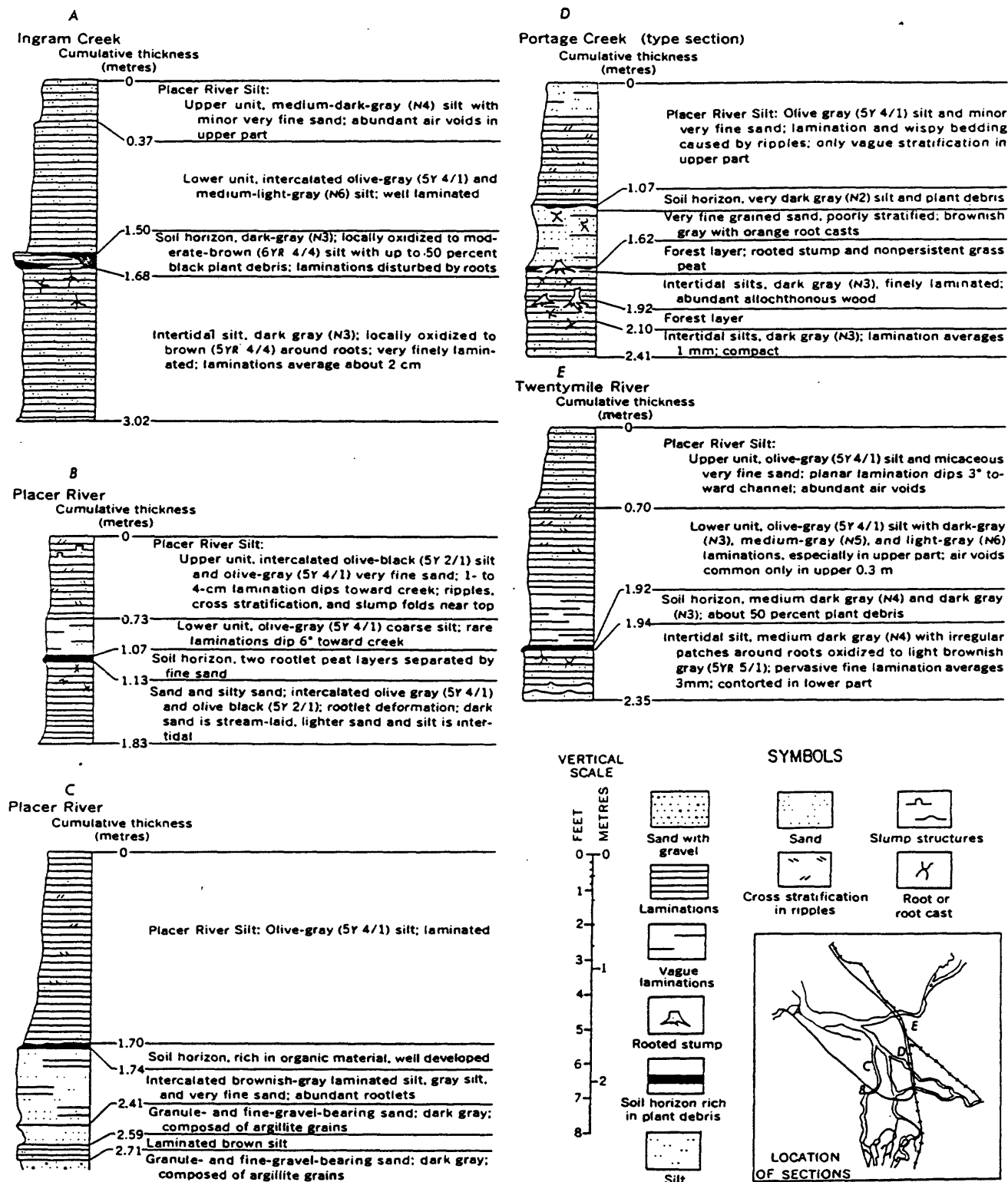


FIGURE 3.—Measured sections of the Placer River Silt.

drained and marshy grasslands, and sphagnum bogs. After the earthquake, these communities were killed by the change to a saltwater environment, but sedimentation was so rapid that nearly all trees and shrubs were buried intact, in upright position (figs. 4 and 5). Ten years after the earthquake, the parts of the plants that project above the silt were desiccated and brittle and were being broken off in increasingly large numbers with each passing year. The buried parts of the plants, however, were little decayed and retained their

bark, fresh wood color, and much of the strength of living plant tissue. One of the principal future characteristics of the Placer River Silt will be its extensive preservation of upright rooted stumps in a peat-bearing soil layer.

### LITHOLOGY

The Placer River Silt is a thin-bedded to laminated micaceous silt that locally contains thin intercalations of silty clay or very fine grained sand. The predominant color is olive gray (5Y 4/1), darkening when wet; individual clay or very fine sand laminations range from medium dark gray (N4) to medium light gray (N6).

Under the hand lens, the sediment is uniform in composition, appears well sorted, and consists of medium and coarse silt-size grains of quartz and feldspar (60 percent), green and black rock fragments (25 percent), and mica (15 percent). The quartz and feldspar grains are angular and equant, whereas the lithic fragments are angular to subround and range from equant to rod or plate shaped. Muscovite, biotite, and chlorite occur in cleavage flakes and elongate shreds as much as 1 mm in length.

Examination of samples taken along the profile from Twentymile River to the highway indicates that the silt consists of quartz (30 percent), quartzose lithic fragments (25 percent), feldspar (20 percent), hornblende (15 percent), and chlorite plus mica (15 percent). Trace constituents are glauconite(?), opaque minerals, garnet, apatite, colorless and brown volcanic glass, and diatoms. All the grains are angular, and except for iron staining of some of the lithic fragments, all are fresh and unaltered.

Plant debris is the only constituent of organic origin that is at all common in the Placer River Silt. In most sections, material such as twigs, limbs and logs, bark fragments, willow and cottonwood leaves, and spruce needles are dispersed rather than concentrated in layers and make up less than 3 percent of the sediment volume. At no place in the Portage area was evidence of sediment infauna found, although centimetre-size valves of *Macoma* sp. are transported from Turnagain Arm and, rarely, incorporated in the formation.

In figure 6 are the results of pipet grain-size analysis of eight surface samples from the locations shown on the profile of figure 7. Attempts to draw separate curves on the same plot for each of the eight samples analyzed were unsuccessful, because many of the data points were coincident or nearly so. Shown in figure 6 are "average" curves drawn through points that represent the means at each phi class boundary of percentage

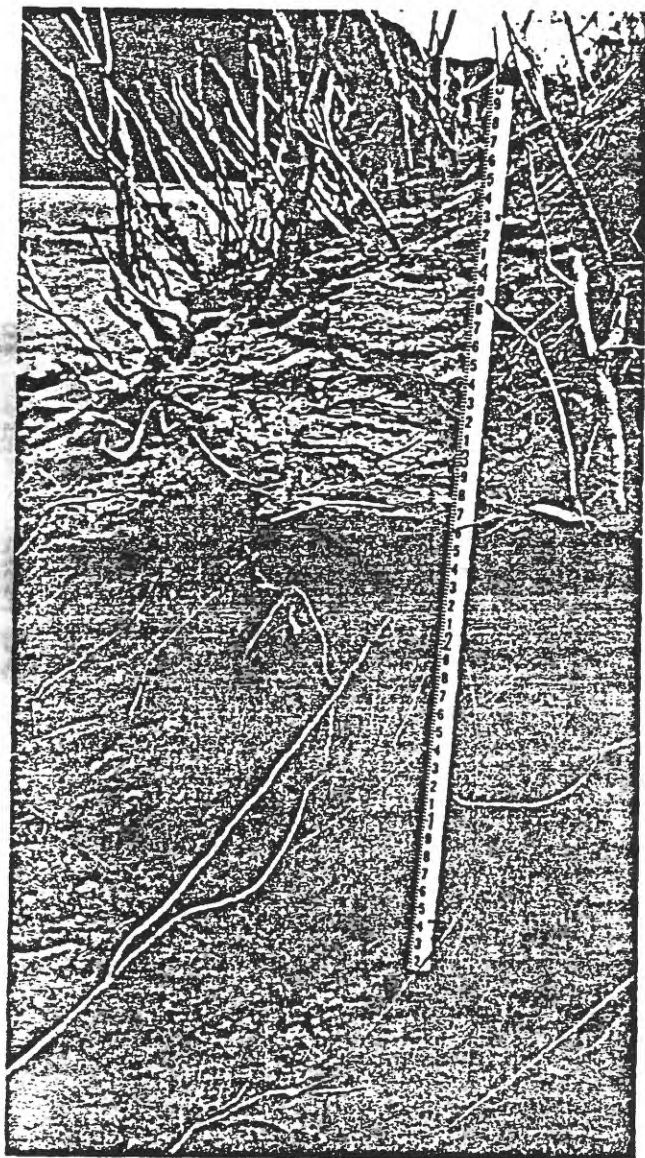


FIGURE 4.—Tidal stream cutbank exposing alder thicket killed and buried by deposition of the Placer River Silt. The pre-Placer River soil horizon is at 1.6 ft on the measuring rod. Bank of Portage Creek, seaward of the Seward Highway.



FIGURE 5.—Spruce forest buried by the Placer River Silt, Portage Creek tidal flats. Augering in the tidal channel (foreground) showed that 1.83 m of silt had accumulated between 1964 and 1973.

values obtained by analysis of the eight samples. Standard deviations for the means used in constructing the frequency percent curve are also shown on the figure and indicate that the variations in percentages are generally small.

Slightly less than 97 percent of the sediment is silt size, and most (91 percent) is medium and coarse silt. The median diameter is  $37\mu\text{m}$  and the Folk graphic mean diameter is  $35\mu\text{m}$ . The grain-size distribution is moderately well sorted (Folk inclusive graphic standard deviation = 0.64 phi units) and moderately fine skewed (Folk inclusive graphic skewness = 0.43 phi units).

The samples analyzed show no systematic grain-size trends that can be correlated with distance along the profile. Field observations suggest that although the silt may become finer grained in the marsh areas near the zero edge, the grain-size distribution depicted in

figure 6 is probably representative of most of the formation.

The most common sedimentary structures are planar lamination and small-scale cross stratification within ripple marks. The planar lamination, which ranges in thickness from 0.5 to 4 cm and averages about 1 cm, is caused by burial of thin layers of fine silt or clayey silt that are darker in color and less erodable than the medium and coarse silt that makes up an estimated 91 percent of the formation. The planar lamination commonly is laterally persistent for 2 m or more. In channel-bank exposures, it dips  $3^\circ$  to  $15^\circ$  toward the channel axis.

Small-scale cross stratification resulting from the migration and eventual burial of ripple marks is common in most exposures but generally is clearly visible only on outcrop faces that have been cleared of slope-wash. Sets of ripples have amplitudes of approximate-

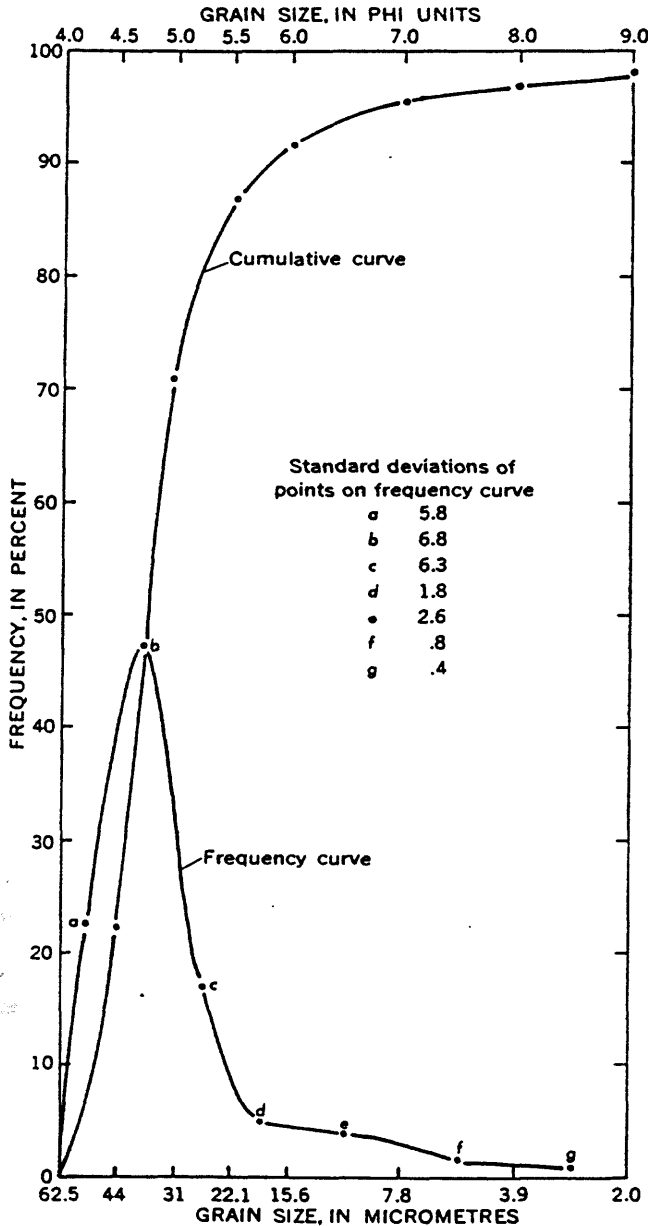


FIGURE 6.—“Average” grain-size frequency and cumulative frequency per phi unit class for eight samples of the Placer River Silt. Sample localities shown in figure 7.

ly 2 cm and wave lengths of 10–15 cm. Commonly, both ebb and flood directions are observed in a single outcrop. Less than 5 percent of the ripples and cross strata observed show oversteepened, convoluted, or folded forms caused by syn- or post-depositional processes.

#### Thickness and distribution

The distribution of the Placer River Silt is determined to a large extent by the geometry of the three valleys and five streams that intersect at tidewater in the Portage area. The thickness of the formation reflects not only the influences of these elements but also the effects of the highway and railroad embankments, structures that existed before and were rebuilt after the Alaska earthquake.

Thickness measurements of the Placer River Silt (figs. 2 and 7; table 1) were obtained either by hand augering to the vegetation-rich soil layer underlying the formation or hand leveling to the “general sediment surface” from exposures of the buried soil layer in the banks of tidal channels.

For purposes of discussion and statistical summary, the thickness data are grouped into the 10 subareas shown on figure 2 inset. Subareas I, III, IV, V, and VI are tidal flats separated by the major stream channels entering Turnagain Arm and situated inside, or sea-

TABLE 1.—Thickness and volume of the Placer River Silt by subarea

Subarea	Number of thickness observations	Average thickness* (m)	Area (m <sup>2</sup> × 10 <sup>6</sup> )	Sediment volume (m <sup>3</sup> × 10 <sup>6</sup> )
I	42	1.57	2.01	3.16
II	3	.66	.26	.17
III	16	1.65	.75	1.24
IV	23	1.35	.89	1.20
V	27	1.44	1.11	1.60
VI	6	1.41	1.72	2.43
VII	6	.66	.58	.38
VIII	53	1.21	2.95	3.57
IX	24	.92	1.44	1.33
X	101	.90	6.28	5.65
Totals	301	---	17.99	20.73

\* Average thickness:  
 All subareas ..... 1.18  
 Subareas I, III, IV, V, VI ..... 1.48  
 Subareas II, VII, VIII, IX, X ..... .87

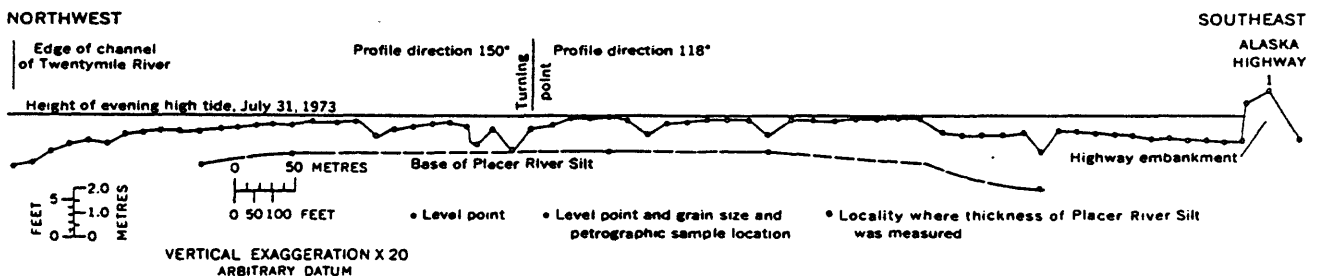


FIGURE 7.—Cross section of the Placer River Silt from the edge of the Twentymile River tidal channel to Alaska Highway 1. Section location shown in figure 2.

ward, of the curve of the Seward Highway as it goes around the head of Turnagain Arm. Subareas II, VIII, IX and X are "outside" the highway and most include the landward or zero edge of the formation. The thickness data grouped in subarea VII are, with two exceptions, from a tidal flat situated between the highway and railroad embankments and connected to Turnagain Arm by only a single culvert 2 ft in diameter.

Seaward of the Seward Highway, the Placer River Silt averages about 1.5 m in thickness; landward of the highway, it averages about 0.9 m. Although factors such as proximity to the sediment source and greater subsidence could cause more accumulation inside the highway, doubtless the single most important factor is the containment effect imposed on the flood tide by the gravel highway embankment. Flow through the embankment can occur only at the culvert connecting subareas VI and VII, at the bridges across the Twentymile and Placer Rivers, and at the two forks of Portage Creek.

In subareas I, III, IV, V and VI, deposition has produced tabular sediment bodies of relatively even thickness. Levees are not typically present along the banks of the major channels, and in the few localities in which they are observed, levees show an estimated relief above the sediment surface of less than 0.3 m. Tidal channels as much as 2 m deep and 25 m wide are present but are less numerous and more widely spaced than in the intricate channelway fan systems that occur landward of the highway in the Placer River area.

Landward of the Seward Highway, the thickness and distribution of the Placer River Silt presents a more complicated pattern controlled largely by the geometry of the major stream channels and to an unknown extent by differential subsidence. In this area, the active depositional elements are levees and channelway fans, both of which are prograding into marshland surrounding freshwater bogs and lakes. In figure 2, the narrow bands of the formation mapped along the main forks of the Placer River are levees 60–250 m wide with relief of as much as 1 m.

The term "channelway fan" is used here to designate areas of active deposition that are lobate to irregular in outline and crossed by numerous small tidal channels. Channelway fans form where one or more tidal channels breach the levees and allow silt-laden flood waters to extend hundreds of metres into the marsh. In the Portage area, channelway fans occur in two places west of the west fork of the Placer River, between the north fork of Portage Creek and the embankment of the Whittier spur of The Alaska Railroad, and on the north side of the Twentymile River.

The thickness data from the south side of the Twentymile River are contoured in figure 8 in order to show the geometry of the sediment body that has formed between 1964 and 1973. The deposit is thickest adjacent to the river and is shown by relatively wide-spaced contours over most of the area. At the distal edge of the deposit, however, the contours are closely spaced, indicating abrupt thinning toward the zero edge. Possibly this almost tabular deposit has formed by the coalescing of a series of channelway fans whose outlines are still partly discernible in the lobate form of the distal edge of the formation.

In the years since 1964 the marshlands beyond the levees and channelway fans have received only minor amounts of silt—generally less than 0.3 m (fig. 2). The grass-dominated plant community seems to be flourishing and keeping pace with the slow buildup of parts of the marsh surface.

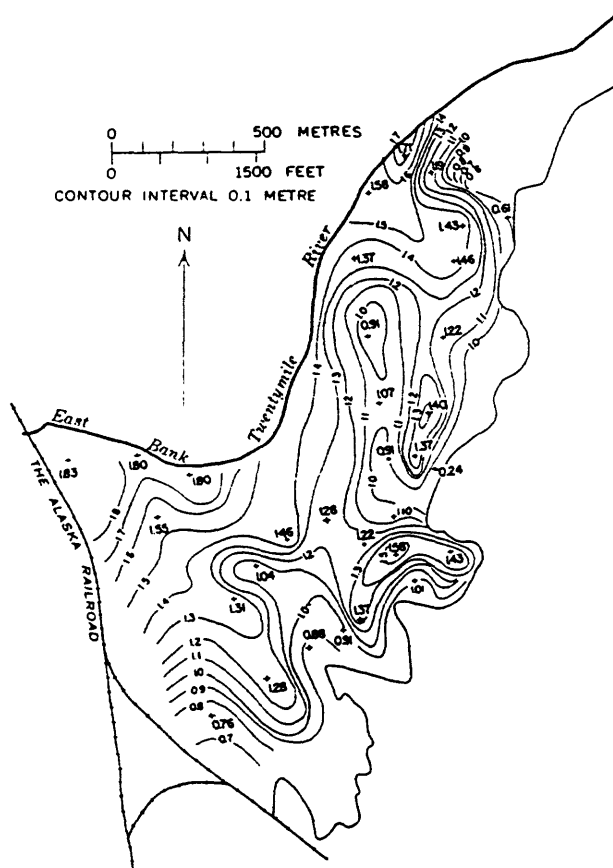


FIGURE 8.—Isopach map of the Placer River Silt on the south side of Twentymile River. Contours are closely spaced near the edge of the deposit and more widely spaced elsewhere.



## Source

Source is considered at two levels as follows: The original source is the bedrock terrane from which the sediment was eroded; the immediate source is the location of the sediment prior to movement into the Portage area from 1964 to 1973.

At least three bedrock sources appear to be represented in the Placer River Silt. The quartzose lithic fragments, the chlorite, and much of the quartz are consistent with derivation from the weakly metamorphosed graywacke and argillite that make up the Chugach Mountains surrounding Turnagain Arm. The volcanic glass and the unaltered hornblende associated with it, however, do not occur in the bedrock of the Turnagain watershed and probably were derived from one or more of the active volcanoes on the northwest side of Cook Inlet (fig. 1). They could have reached their present locations through combinations of wind and water currents. There is no major local source for the biotite and plagioclase feldspar that make up a significant part of the sediment. These constituents were probably derived from the batholithic terrane of the Talkeetna Mountains and transported to Knik Arm through the Susitna or Matanuska Rivers. This suggests the existence of currents that sweep sediment from the Knik area into Turnagain Arm.

Prior to the investigations reported here, we believe that the immediate source of all the silt was the alluvium in the valleys of the major streams that meet in tidewater at Portage. However, the inferred bedrock sources far to the north and west and the thickness pattern of the formation are clear indications that the immediate source of the formation is seaward of Portage rather than landward. Probably this immediate source is the extensive intertidal bars of sandy silt that occur throughout Turnagain Arm.

## THE SEDIMENTATION SYSTEM OF THE PORTAGE AREA

The Placer River Silt is only one of the recognizable sedimentary elements in the environment of the Portage area. In this section we list and describe briefly some of the intertidal and supratidal settings that occur in this environment of contemporary sedimentation. The characteristics and interrelations of the various settings are the subject of continuing study.

A diagrammatic portrayal of the arrangement of the recognized subdivisions of the intertidal and fluvial environments, figure 9, points up the importance of zones of maximum sedimentation in the formation of the lowland physiography. The most rapid sedimentation occurs on the tidal flats and on the levees of the

supratidal rivers. As these regions build up, drainage from the peripheral areas is impeded and a zone of marshes, bogs, and lakes develops in the vicinity of the valley walls. The distribution of this zone is clearly shown in figure 2.

## Intertidal settings

In the intertidal environment, 3 km wide at some places, we now recognize six subdivisions, discussed here in order of decreasing proportion of time covered by the tide.

**Tidal stream channels.**—The discharge of the streams that flow through the valleys and into Turnagain Arm is sufficient to maintain swift currents in the channels during times of low tide. Surface-water velocities in the channels are in the range from 50 to 150 cm/s on the basis of a single series of observations on the Twentymile River at the start of ebb flow. Standing waves and antidunes are typical features of the water surface. The channel deposits cannot be directly observed, but from study of midchannel bars and channel banks, the streams appear to be moving coarse sand and fine gravel. Large ripples with wave lengths of approximately 1 m and amplitudes of 7 cm are exposed on some bars during low water.

**Lower tidal flats.**—These flat constructional terraces are graded to the average low-tide water level. The landward juncture of the lower tidal flats with the upper tidal flats is typically an erosional scarp 1–2 m

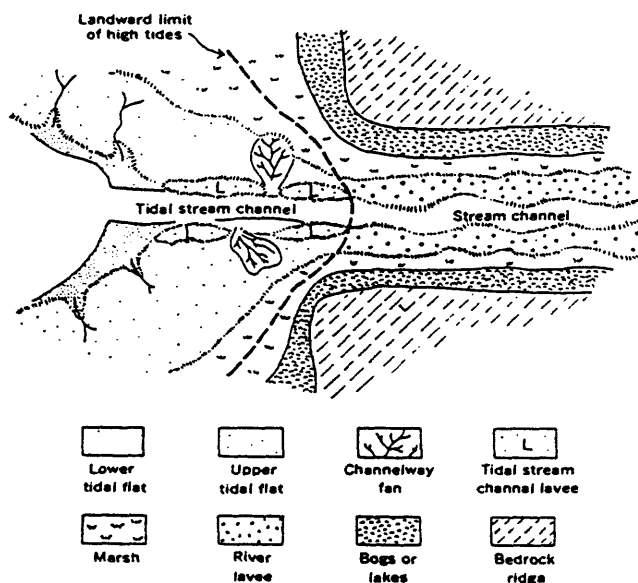


FIGURE 9.—Idealized diagram depicting the major elements in the lowland depositional system of the Portage area.

high and rarely a smooth constructional slope dipping about 35° toward the channel. Rippled silt and very fine sand accumulate on the lower tidal flats. As the water table is nearly at the surface, the sediment is saturated, readily liquefiable, and hazardous to traverse.

*Channelway fans.*—Channelway fans occur behind the leveed parts of tidal streams where one or more tidal channels breach the levee system. In the Portage area, the channelway fans are flooded during about half of the high tides and appear to be actively prograding into the saltwater marshes. The sediment surface is extremely irregular because of the close spacing of numerous small channels 0.5–1.5 m wide and 0.3–0.5 m deep. Many of the channels are constructional in origin because laminations in their banks dip toward the channel axis at the same angle as the bank face. Interchannel areas support a sparse to abundant flora of salt-tolerant grasses. As deposition continues, channelway fans may coalesce and evolve into upper tidal flats.

*Upper tidal flats.*—The upper tidal flats are nearly horizontal constructional terraces that are building toward the level of the highest tides that reach the Portage area (fig. 7). The deposits of the upper tidal flats are laminated and rippled silts, commonly exhibiting small voids that originate from air entrapment during rapid flooding. The more landward parts support a sparse flora consisting of two or three types of salt-tolerant grasses.

*Levees.*—Levees are common only in the upper reaches of the tidal streams, where they probably originate through the formation of current nulls caused by the meeting of seaward-directed streamflow and shoreward-directed tidal flow. Levees do not generally occur at the junction between the lower and upper tidal flats, probably because the boundary is erosional. Levee deposits show air-entrapment voids, laminations, and ripples and are indistinguishable from the sediments of the upper tidal flats.

*Saltwater marsh.*—The saltwater marsh zone supports a dense growth of several species of salt-tolerant grass and had received less than 0.3 m of sediment from 1964 to 1973. Deposits are fetid fine silt and mud that may exhibit millimetre-scale lamination.

#### Supratidal settings

Stream gravels and organic deposits are forming beyond the influence of the tide in the Portage area. We recognize three supratidal zones.

*Braided streams.*—Deposits of pebble and cobble gravel and variable amounts of coarse, poorly sorted

sand occur in and near the present stream courses. The deposits are linear in shape and parallel to the stream axis.

*Freshwater marsh.*—Between the stream gravels and the bogs and lakes that border the valley walls is a densely vegetated freshwater marsh. Growth of vegetation is apparently much more rapid than sedimentation because samples obtained by augering consist of slightly muddy plant debris in various states of decay.

*Bogs and lakes.*—Little or no sediment reaches the bog area between the marsh and valley wall, and auger samples consist almost entirely of water-saturated spongy peat. Sphagnum moss, several varieties of grass, and prostrate shrubs are the dominant vegetation. Deposits in the lakes are finely comminuted plant debris.

### ENVIRONMENTAL CONSEQUENCES OF INUNDATION AND SEDIMENTATION

The direct effects of the earthquake in the Portage area included destruction of bridges (Kachadoorian, 1968), subsidence of railroad and highway embankments (McCulloch and Bonilla, 1970; Kachadoorian, 1968), and damage to buildings (Plafker and others, 1969). Although railroad and highway damage was quickly repaired, there are longer lasting effects on the environment of the Portage area that resulted from the inundation and sedimentation. These effects include abandonment of the area, destruction of flora, esthetic deterioration, localized erosion, and development of "quicksand" hazards.

The Portage area has been all but abandoned by man because of the high tides and the blanket of silt that now covers the lowlands. The sole house and the service station currently maintained were constructed on thick gravel pads after the earthquake. Although the house is safely located, the service station is on the seaward side of the highway where it is threatened by the spring and storm high tides.

Having to abandon the Portage area was a hardship to the residents for many reasons, perhaps mainly because it thwarted development that might reasonably have been expected. The area is one of the very few roadside parcels of fee simple land excluded from the Chugach National Forest. It is situated on the heavily traveled Seward Highway at the junction of the road to Portage Glacier, one of the major tourist attractions of the Anchorage area; it is approximately midway between Anchorage and the popular recreation areas around Kenai Lake; and it is at the vehicle-loading point for The Alaska Railroad where, during the summer months, thousands of touring cars and buses are

shuttled to the Alaska Ferry System at the deepwater port of Whittier. The Portage area, before its inundation and siltation, was ideally situated for commercial development based on tourist and roadside services.

Special construction techniques, though adding to costs, might still facilitate development of Portage were it not for the esthetic deterioration of the area. The abandoned, partly buried and vandalized buildings (fig. 10), the uniform mantle of gray silt, and the stands of dead spruce and cottonwood are depressing sights. A measure of the deterioration of the area is that tourist buses now use it as the main stopping point at which to discuss effects of the Alaska earthquake.

Contributing to the esthetic deterioration is the widespread destruction of preearthquake plant communities. Forest at least 250 years old, well-drained and marshy grassland, and alder thicket have been killed over an area of more than 18 km<sup>2</sup>. Salt-tolerant grasses and reeds and a few willows that have sprouted roots from branches at levels as much as 2 m above the former root zones constitute the only vegetation of the active tidal flats. The dead forest and thicket at Portage are the sources of extensive layers of plant debris that accumulate on intertidal bars elsewhere in Turnagain Arm and of the huge limbs and whole trees that are transported seaward to become hazards to boating in Cook Inlet.

Although many of the environmental effects result from sedimentation, currents generated during the ebb and flood locally focus to produce erosion that forms, enlarges, and extends tidal channels. A major consequence of headward erosion of channels is providing tidal access to the low-lying marsh, bog, and lake areas that rim the active intertidal zones. The result is con-

tinued progradation of intertidal sediment into the freshwater marsh, leading to further destruction of plant communities. A channelway fan system is developing in a marsh on the northwest side of the Twentymile River (fig. 11). Access to the marsh and a pathway for sediment influx is provided by a 150-m-long channel that is being eroded in the trench fill of the Anchorage-Whittier refined products pipeline. As much as 0.7 m of silt has entered the marsh by this developing tidal channel. A similar channel is developing along the axis of an old wooden waterline between Portage Creek and the junction of the Seward and Whittier spurs of the railroad.

Another group of environmental effects are quicksand hazards resulting from the properties of the Placer River Silt. The uncompacted nature and predominance of silt-size sediment results in ready liquefaction if the sediment is saturated (as it is in the tidal channels at all times and over the entire area immediately following high tide). The instability of the sediment is well known to local sportsmen, who shun foot travel in the region. In our experience, the lower tidal flats, tidal channel bottoms, point bars, and mid-channel bars are extremely dangerous to traverse because it is possible to sink instantly to midhigh depths.



FIGURE 10.—Roadside business abandoned after the 1964 Alaska earthquake. As much as 2 m of silt has accumulated in this area. Photograph taken during high tide.

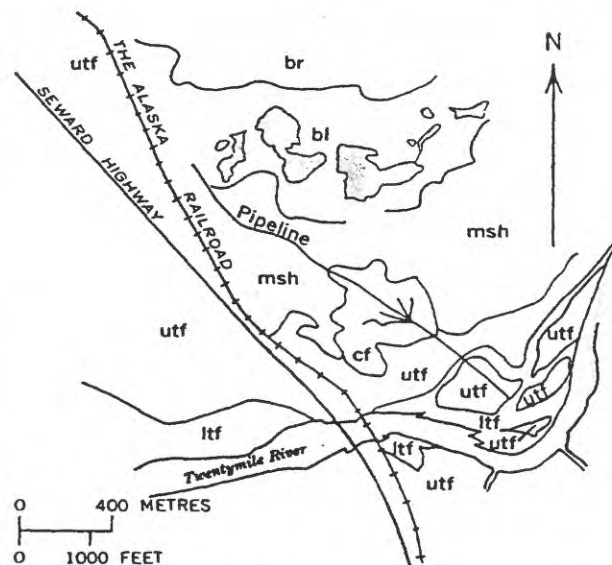


FIGURE 11.—Sketch map of north side of Twentymile River showing depositional environments and a channelway fan prograding into marsh deposits where tidal access is provided through erosion along the pipeline trench. Symbols: lrf, lower tidal flat; utf, upper tidal flat; cf, channelway fan; msh, marsh; bl, bog or lake; br, bedrock ridge.



## THE FUTURE OF THE PORTAGE AREA

The effects on the environment of the Portage area brought about by intertidal deposition—the destruction of natural plant communities, erosion, and creation of quicksand hazards—are severe and lasting results of the Alaska earthquake of March 27, 1964. But they are not necessarily permanent consequences. As shown in figures 3 and 4, beneath the buried soil horizon that records the earthquake is a unit of older intertidal silts resembling the Placer River Silt in many ways. From this, and from the evident buildup of the Placer River Silt toward the level of the highest tides (fig. 7), we can expect that the surface will eventually reach a level at which saltwater incursion is exceedingly rare. As this level is approached, the former plant communities will recolonize, ultimately prosper, and play an important role in stabilizing the courses of the tidal streams and channels. The area will then much resemble Portage as it was before the earthquake.

The circumstances that developed the Placer River Silt—earthquake, subsidence, and a gradation leading to natural “repair” of the landscape—may have occurred many times during Holocene deposition in the Portage area. The older intertidal silts may record one comparable episode of subsidence and sedimentation that occurred more than 250 years ago, as judged by the age of an old spruce rooted in the silts, and possi-

bly less than 723 years ago on the basis of tenuous correlation with a carbon-dated section in the Girdwood area, 18 km west of Portage (Karlstrom, 1964, pl. 7). As the area is underlain by at least 300 m of silt (McCulloch and Bonilla, 1970, p. D131; Dennis Kalpachoff, oral commun., 1973), it is possible that many episodes of earthquake-caused sedimentation are preserved in the geologic record. Deciphering this record may have a critical bearing on the future of Portage and of the greater Anchorage area.

## REFERENCES CITED

- Clark, S. H. B., 1972, Reconnaissance bedrock geologic map of the Chugach Mountains near Anchorage, Alaska: U.S. Geol. Survey Misc. Field Studies Map MF-350, scale 1:250,000.
- Kachadoorian, Reuben, 1968, Effects of the earthquake of March 27, 1964, on the Alaskan Highway system: U.S. Geol. Survey Prof. Paper 545-C, 66 p.
- Karlstrom, T. N. V., 1964, Quaternary geology of the Kenai Lowland and glacial history of the Cook Inlet region, Alaska: U.S. Geol. Survey Prof. Paper 443, 69 p.
- McCulloch, D. S., and Bonilla, M. G., 1970, Effects of the earthquake of March 27, 1964 on The Alaska Railroad: U.S. Geol. Survey Prof. Paper 545-D, 161 p.
- Plafker, George, Kachadoorian, Reuben, Eckel, E. B., and Mayo, L. R., 1969, Effects of the earthquake of March 27, 1964, on various communities: U.S. Geol. Survey Prof. Paper 542-G, 50 p.

APPENDIX A. 7.

Coastal Lowland Evidence of Great Holocene Earthquakes  
in the Cascadia Subduction Zone

by

Brian Atwater

# Evidence for Great Holocene Earthquakes Along the Outer Coast of Washington State

BRIAN F. ATWATER

Intertidal mud has buried extensive, well-vegetated lowlands in westernmost Washington at least six times in the past 7000 years. Each burial was probably occasioned by rapid tectonic subsidence in the range of 0.5 to 2.0 meters. Anomalous sheets of sand atop at least three of the buried lowlands suggest that tsunamis resulted from the same events that caused the subsidence. These events may have been great earthquakes from the subduction zone between the Juan de Fuca and North America plates.

GEOLOGIC HISTORY COULD OFFER valuable constraints on the probability of a great (magnitude about 8 or 9) earthquake in the Pacific Northwest. Analogies with other subduction zones suggest that great earthquakes could emanate from the Cascadia subduction zone (Fig. 1), in which the Juan de Fuca plate has slipped beneath the North America plate at an average Quaternary rate of 3 to 4 cm per year (1). But no earthquake of the past 150 to 200 years in the states of Washington or Oregon has exceeded magnitude 7.5 (2), and Indian legends seem too ambiguous to indicate whether great Northwest earthquakes occurred before that time (1). Only geologic evidence is likely to reveal whether great earthquakes from the Cascadia subduction zone have occurred and, if they did, whether enough time has elapsed since the last event for another to be expected soon.

In this report I consider Cascadia's seismic potential in light of geologic evidence for recurrent coastal subsidence. This approach, new to the Pacific Northwest and seldom used elsewhere, yields strong evidence that great earthquakes have occurred in the Cascadia subduction zone during the past 10,000 years (the Holocene) (3, 4).

Coastal subsidence commonly accompanies a great subduction earthquake. The coseismic subsidence, in a chiefly onshore belt flanked by a mostly offshore zone of coseismic uplift, apparently results from elastic extension within and behind the seaward-lurching part of the continental plate (5, 6). Washington's outer coast conceivably could undergo either uplift or subsidence during a great Cascadia earthquake (Fig. 2). But westernmost Washington apparently lacks Holocene marine terraces indicative of coseismic uplift (7). Therefore, any great

Cascadia earthquake of Holocene age most likely entailed coseismic subsidence in the present vicinity of Washington's outer coast.

Subsidence during great subduction earthquakes in Chile (1960) and in Alaska (1964) changed vegetated coastal lowlands into barren estuarine flats, particularly where the subsidence was augmented by shaking-induced settlement (8, 9). At the head of Cook Inlet near Portage (Fig. 2), estuarine silt buried 18 km<sup>2</sup> of preearthquake lowland that had subsided 1.6 m and ~~then~~ settled an additional 0.8 m in 1964 (10). Aggradation [1 to 2 m (10)] and uplift [0.2 to 0.3 m (11)] after 1964 have allowed lowland shrubs and trees to become reestablished in this area (12). A bed of estuarine mud that abruptly overlies a lowland soil and passes gradually upward into another lowland soil may thus indicate a cycle of coseismic submergence and postseismic shoaling. This cycle was recognized in Chile and Alaska, where rhythmic alternation between estuarine mud and buried lowland soils has been cited as evidence of ancient subduction earthquakes (10, 13, 14).

Similar rhythmic bedding abounds in estuarine deposits of late Holocene age near Washington's outer coast. Peaty layers representing well-vegetated lowlands alternate rhythmically with muddy intertidal deposits at all of the estuaries that I studied, both large (Columbia River, Willapa Bay, and Grays Harbor) and small (Copalis River and Waatch River). The minimum number of buried lowlands per estuary ranges from one to six (Fig. 1), increasing with the depth to which Holocene intertidal deposits extend. Typically, the peaty layers are 0.05 to 0.20 m thick and the intervening intertidal deposits are 0.5 to 1.0 m thick. As exemplified at Willapa Bay (Fig. 3), the typical peaty layer

consists of peaty mud that resembles the A or O horizon of the soil on broad, rarely inundated parts of modern tidal marshes in the area. Conifer stumps rooted in buried peaty layers near uplands and streams confirm that the peaty layers represent nearly supratidal conditions. The bed above a typical peaty layer at Willapa Bay has an abrupt base but grades upward, from soft gray mud through firm mottled mud, into the succeeding peaty layer. The soft gray mud contains injected rhizomes (below-ground plant stems) of only *Triglochin maritima*. At modern Willapa Bay this shallowly rooted plant is dominant only in salt-affected intertidal settings that are 0.5 to 2.0 m lower than the high-marsh surface represented by the typical peaty layer (Fig. 3C). The superposition of *T. maritima* mud over a peaty layer consequently indicates at least 0.5 m of submergence, and the sharpness of that contact indicates that the submergence was rapid. Conversely, the upward gradation from mud into a succeeding peaty layer implies at least 0.5 m of relatively gradual shoaling and the consequent building of a new high-level tidal marsh. Thus Washington's outer coast has undergone submergence and shoaling in cycles that resemble, at least superficially, the known and inferred cycles of coseismic submergence and postseismic shoaling in great-earthquake regions of Alaska and Chile.

Three points tend to confirm that great subduction earthquakes triggered the cycles of submergence and shoaling in Washington.

1) Nothing other than rapid tectonic subsidence readily explains the burial of the peaty layers. Deposition during floods and storms should promote emergence of a coastal lowland, not submergence to the level of *T. maritima* salt marshes. Filled tidal creeks commonly produce bodies of sediment that are thicker and less conformable than the mud beds that buried the lowlands (Fig. 3C). Shaking-induced settlement, although consistent with the sagging of peaty layers and thickening of intertidal mud over the soft Holocene fill of a Pleistocene valley, does not explain why intertidal mud buries the peaty layers where they lap onto stiff Pleistocene deposits of the valley's sides (Fig. 3 B and C). Purely isostatic and eustatic submergence during the late Holocene should have been sufficiently gradual to

permit the high parts of tidal marshes to build apace with rising relative sea level, thereby producing homogeneous high marsh peat many meters thick. Such peat is present on many mid-latitude coasts (15), Puget Sound included (16), but not at the sites that I studied within 20 km of Washington's outer coast. Late Holocene submergence along Washington's outer coast was punctuated by jerks of tectonic subsidence that prevented the continuous maintenance of high marsh surfaces.

2) Tsunamis probably coincided with at least three of the episodes of rapid tectonic subsidence. A great subduction earthquake usually produces a great tsunami (17). The tsunami from the great 1960 Chile earthquake deposited sheets of sand on two or more Chilean lowlands in the belt of coseismic subsidence (13). Similarly at Willapa Bay, a thin sandy interval mantles each of at least three buried lowlands among otherwise sand-free deposits. The most accessible of these sandy intervals forms a sheet (maximum thickness, 7 cm) that extends 3 km up the valley from the seaward edge of the buried marsh surface that it covers. This sheet disappears landward (Fig. 3B) and also becomes generally thinner and finer grained in that direction—a sign of a bayward source (Fig. 3A). Found almost exclusively on buried lowlands, the sandy intervals do not imply great storms or exotic tsunamis, for these events need not coincide with rapid tectonic subsidence at Willapa Bay. However, coincidence with Willapa Bay subsidence should be expected of tsunamis from great earthquakes in nearby parts of the Cascadia subduction zone.

3) Tectonic subsidence during great subduction earthquakes could reconcile rates of short-term uplift with rates of long-term uplift in westernmost Washington. The uplift measured at tide gages and bench marks (2 to 3 mm per year average during the past 50 years) is much faster than that inferred from Pleistocene marine terraces (<0.5 mm per year average during the past ~100,000 years) (18). But these rates need not conflict if, as part of cyclic earthquake-related deformation (19), coseismic subsidence (like that inferred from the buried lowlands) has nearly negated cumulative interseismic uplift (of which tide-gage and bench-mark uplift would be a modern sample).

Jerky Holocene submergence at Washington estuaries thus strengthens the hypothesis that a future great earthquake could emanate from the Cascadia subduction zone. The number and shallow depth of buried lowlands at Willapa Bay (Fig. 3C) may mean that at least six such earthquakes have occurred since sea level approached its present position on mid-latitude coasts, that is, since 7000 years ago (20). The earthquake ruptures, if really from events of magnitude 8 or greater, should have extended coastwise for at least 100 km (21). This corollary can be tested by determining the coastwise extent of individual episodes of coseismic subsidence. Another testable corollary is that shaking during the postulated earthquakes should have caused the liquefaction of Holocene coastal lowland sand (22). If buried lowlands prove coeval for coastwise distances greater than 100 km, and if sand proves to have vented onto some of these lowlands at the start of burial, then the chronology of jerky submergence could be used to constrain the current probability of a great subduction earthquake in the Pacific Northwest.

#### REFERENCES AND NOTES

1. T. H. Heaton and S. H. Hartzell, *Science* 236, 600 (1987).
2. M. G. Hopper *et al.*, *U.S. Geol. Surv. Open-File Rep.* 75-375 (1975).
3. Episodic Quaternary thrusting in the Cascadia subduction zone is implied by faults, folds, and unconformities in the overlying North America plate. Unless accomplished by episodic creep, such thrusting would suggest that great Cascadia earthquakes have occurred in the Quaternary [P. D. Snavely, Jr., *Am. Assoc. Petrol. Geol. Mem.*, in press].
4. Great interplate earthquakes could account for uniform numbers of Holocene turbidites off the mouth of the Columbia River, but so could large intraplate earthquakes [T. H. Heaton and S. H. Hartzell, *Bull. Seismol. Soc. Am.* 76, 675 (1986)] or the self-induced failure of persistently accumulating sediment [J. Adams, *Tectonophysics* 29, 141 (1975)].
5. G. Plafker, *J. Geophys. Res.* 77, 901 (1972), 3, 949.
6. — and M. Rubin, *U.S. Geol. Surv. Open-File Rep.* 78-943 (1978), p. 687.
7. D. O. West and D. R. McCrumb, *Geol. Soc. Am. Abstr. Programs* 18, 197 (1986).
8. G. Plafker, *U.S. Geol. Surv. Prof. Pap.* 543-I (1969).
9. — and J. C. Savage, *Geol. Soc. Am. Bull.* 81, 1001 (1970).
10. A. T. Owenshine, D. E. Lawson, S. R. Bartsch-Winkler, *J. Res. U.S. Geol. Surv.* 4, 151 (1976).
11. L. D. Brown *et al.*, *J. Geophys. Res.* 82, 3369 (1977).
12. S. R. Bartsch-Winkler and H. C. Garrow, in *U.S. Geol. Surv. Circ.* 844 (1982) p. 115.
13. C. Wright and A. Mella, *Bull. Seismol. Soc. Am.* 53, 1367 (1963).
14. R. A. Combellick, *Geol. Soc. Am. Abstr. Programs* 18, 569 (1986); S. R. Bartsch-Winkler and H. R. Schmoll, *U.S. Geol. Surv. Circ.*, in press.
15. For example, A. C. Redfield, *Ecol. Monogr.* 42, 201 (1972).
16. M. Eronen, T. Kankainen, M. Tsukada, *Quat. Res. (NT)* 27, 147 (1987).
17. K. Abe, *J. Geophys. Res.* 84, 1561 (1979).
18. K. R. Lajoie, in *Active Tectonics* (National Academy Press, Washington, DC, 1986), pp. 95–124.
19. W. Thatcher, *J. Geophys. Res.* 89, 3087 (1984).
20. J. A. Clark, W. E. Farrell, W. R. Peltier, *Quat. Res. (NT)* 9, 265 (1978).
21. Assumptions:  $M = \log A + 4.15$ , where  $M$  is magnitude and  $A$  is rupture area [M. Wyss, *Geology* 7, 336 (1979)]; rupture width of about 100 km, inferred from the occurrence of coseismic subsidence 130 to 140 km from the foot of the continental slope.
22. For example, E. Reimnitz and N. F. Marshall, *J. Geophys. Res.* 70, 2363 (1965).
23. H. Kanamori, *ibid.* 82, 2981 (1977).
24. H. E. Clifton, *J. Sediment. Petrol.* 53, 353 (1983).
25. I thank S. R. Bartsch-Winkler, S. M. Colman, A. R. Nelson, and R. B. Waitt for reviewing the manuscript; and W. C. Grant and R. T. Versical for field assistance. Access to the Waatch River was permitted by the Makah Tribal Council.

23 December 1986; accepted 11 March 1987

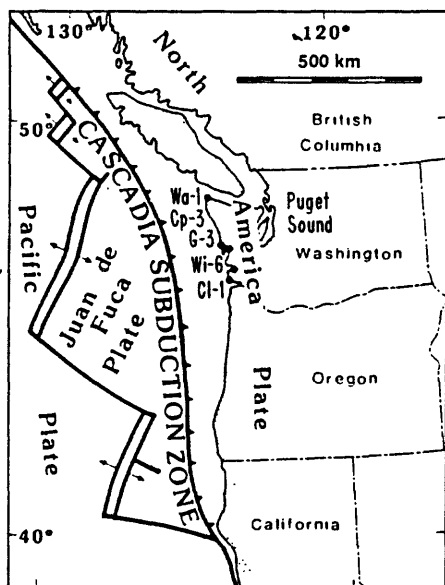


**Fig. 1.** Index map. Alphanumeric symbols give minimum numbers of widely buried coastal lowland surfaces of Holocene age. Cl, Columbia River (study area at  $46^{\circ}18'6''\text{N}$ ,  $124^{\circ}57'88''\text{W}$ ); Cp, Copalis River ( $47^{\circ}07'1''\text{N}$ ,  $124^{\circ}09'9''\text{W}$ ); G, Grays Harbor ( $47^{\circ}01'78''\text{N}$ ,  $124^{\circ}01'47''\text{W}$ ); Wa, Waatch River ( $48^{\circ}21'41''\text{N}$ ,  $124^{\circ}37'96''\text{W}$ ); Wi, Willapa Bay (Fig. 3). Spreading ridge (—), transform fault (—), and subduction zone (—); barbs show direction of dip.

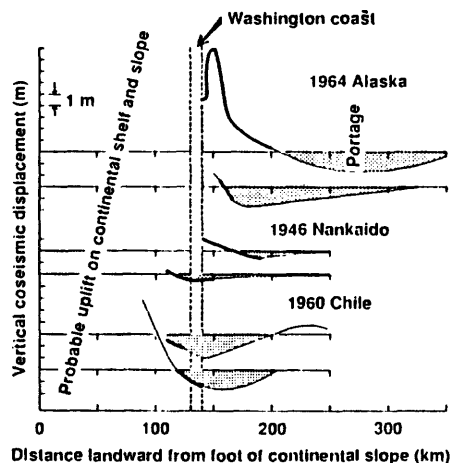


**Fig. 2.** Profiles of vertical coseismic displacement in south-central Alaska (8), southwest Japan (Nankaido) (19), and south-central Chile (9). Two profiles are shown for each earthquake. Subsidence is highlighted by shading; displacement equals zero where profile line intersects horizontal line. Thickened part of profile line shows location of outermost coast (small offshore islands excluded) in vicinity of profile. The moment magnitude ( $M_w$ ) from Kanamori (23) and the length of belt of coseismic subsidence ( $L$ ) are as follows: Alaska ( $M_w$ , 9.2;  $L$ , 950 km), Nankaido ( $M_w$ , 8.1;  $L$ , 300 km), and Chile ( $M_w$ , 9.5;  $L$ ,  $>800$  km). The arrow indicates the projected position of estuarine marshes near the outer coast of Washington State. Inferred uplift on shelf and slope pertains to all profiles. The distance represented between adjoining pairs of tick marks on the vertical axis is 1 m.

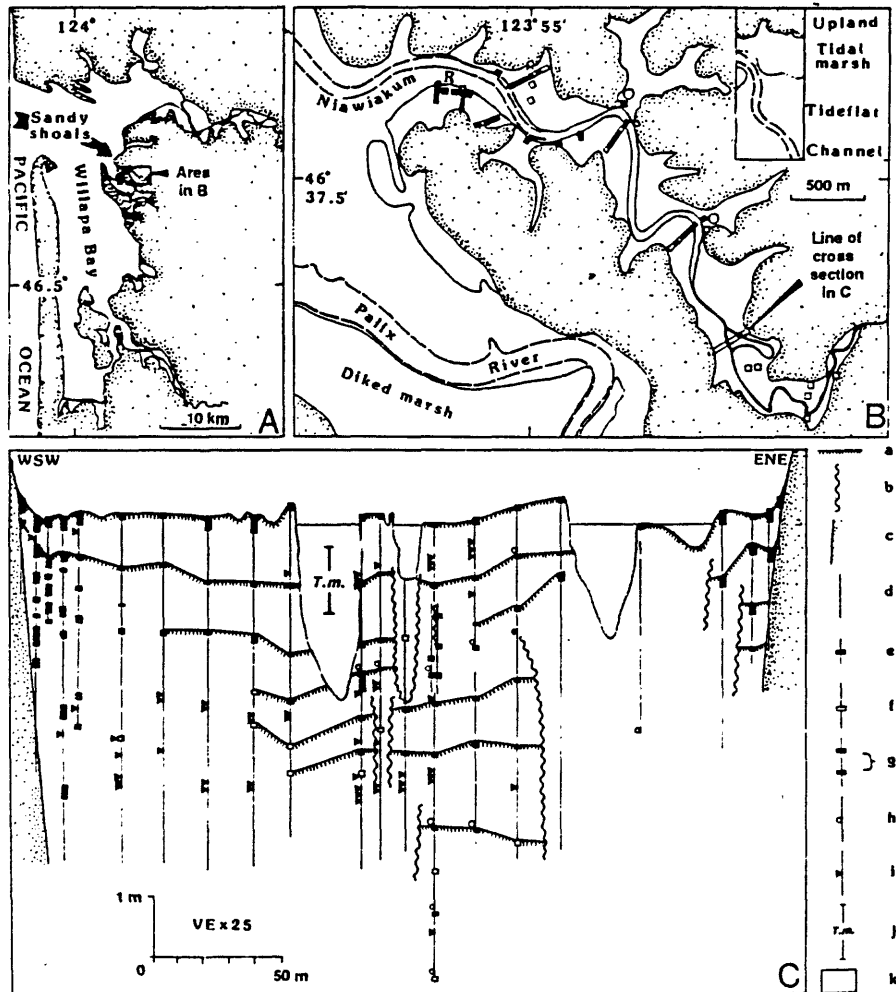


**Fig. 3.** Willapa Bay. (A) Index map. Arrow shows a path of the tsunamis that are inferred from sandy intervals atop buried lowlands in (B) and (C). Location of sandy shoals from Clifton (24). (B) Study area. O, outcrop showing onlap of stiff Pleistocene deposits by buried peaty layers. Sandy interval atop uppermost buried peaty layer in cores and outcrops: present (solid square, single site; or rectangle, multiple sites); absent (open square or rectangle). (C) Cross section from correlated cores. Abbreviations: VE, vertical exaggeration; a, well-vegetated lowland—shape of modern surface determined by leveling; buried lowlands shown only where soils can be correlated with confidence on the combined bases of depth, serial order, position with respect to sandy intervals, and presumption of the same lateral continuity that is evident in low-ride outcrops; b, former margin of tidal creek that bounds body of soft mud; c, side of Pleistocene valley (line denotes top of Pleistocene deposits); d, borehole made with half-cylinder corer 1 m long and 2 cm in diameter; e, peaty layer, woody where thick near upland; f, contact akin to top of peaty layer, soft mud over firm mud; g, intertidal mud, typically stiffens upward between peaty layers; h, sandy interval, contains very fine sand and coarse silt in planar layers mutually separated by mud; i, fossil rhizome of *T. maritima*; j, zone in which *T. maritima* is the dominant living plant; k, water, top approximates mean higher high water; floor of deepest channel is near mean lower low water; ENE, east-northeast; WSW, west-southwest.

Summary, as of 2 April 1987, of Radiocarbon Ages on Episodes of Rapid  
Coastal Subsidence in Westernmost Washington State

Brian F. Atwater  
U. S. Geological Survey at Department of Geological Sciences  
University of Washington AJ-20  
Seattle, Washington 98195

Plant remains from buried lowlands yield radiocarbon ages for four episodes of rapid coastal subsidence in southwestern Washington. Corrected for variations in atmospheric  $^{14}\text{C}$ , these dates indicate that rapid subsidence occurred about 300, 1700, 2700, and 3000-3400 years ago. The ages of about 300 sidereal years (17th century A.D.) come from roots and sticks along both the Niawiakum River (Willapa Bay) and the Copalis River--sites that are 60 km apart along the strike of the Cascadia subduction zone. Synchrony between the Niawiakum and Copalis sites, if exact, would suggest some of the regionality that one should expect of coseismic subsidence from a great subduction earthquake. The earlier episodes were dated only at the Niawiakum River. More work is needed to determine whether these episodes had great coastwise extent and, if they did, whether they represent the only four great earthquakes in southwestern Washington during the past 3000-3400 years.

As for northwestern Washington, new ages confirm an date of about 1100 years ago for what appears to be the most recent episode of rapid coastal subsidence along the Waatch River, near Neah Bay. The ages from the Niawiakum River suggest that this subsidence did not extend to Willapa Bay; conversely, the most recent episode of rapid coastal subsidence in southwestern Washington does not appear to be represented at Neah Bay. Such asynchrony may signify division of the Cascadia subduction zone into patches that are capable, at least sometimes, of independent rupture.



APPENDIX A. 8.

Geodetic Deformation Measured in Washington and British Columbia

by

J. C. Savage

GEODETIC DEFORMATION MEASURED  
IN WASHINGTON AND BRITISH COLUMBIA

J. C. Savage and M. Lisowski

U.S. Geological Survey  
Menlo Park, California 94025

Measurements of strain accumulation in the Puget Sound area and on Vancouver Island provide strong evidence that major megathrust earthquakes should be expected in the Cascadia subduction zone. The strain accumulation was first identified in trilateration measurements spanning Puget Sound at the latitude of Seattle in the interval 1971-1979, and the interpretation that the deformation was due to strain building up across the Cascadia subduction zone was proposed by Savage et al. [1981]. This interpretation was tested at several sites on the Olympic peninsula and Vancouver Island in subsequent years, and in each case the direction of greatest compression was found to be directed ENE and the magnitude of the compression to be on the order of  $0.1 \mu\text{strain/yr}$  (Figure 1). The observations are therefore consistent with the interpretation that the measured strain accumulation is caused by locking of the main thrust zone beneath the continental shelf.

Although the observations in Figure 1 establish that the axis of greatest compression along the North American-Juan de Fuca plate margin is directed ENE, actual compression in that direction has not been proved. That is, the deviatoric strain rates are determined unambiguously, but the absolute strain rates are not significant at the level of two standard deviations. The observations then could be explained by a NNW extension rather than ENE compression. However, ENE compression is preferred because there is an obvious tectonic explanation.

The vertical deformation observed in the Puget Sound-Vancouver Island region has generally been described as 2 mm/yr uplift along the coast and perhaps 1 mm/yr subsidence in Puget Sound and Georgia Strait [Ando and Balazs, 1979]. This picture is based mainly on tide gauge recordings along the Pacific coast and inland in Puget Sound and Georgia Strait. Some leveling data have also been used to support this interpretation. Generalized contours representing this uplift pattern are shown in Figure 1. The most recent compilation of tide gauge and leveling data [Holdhal et al., 1987] (Figure 2) suggests that the uplift pattern may be somewhat more complicated. In particular, the trend in coastal uplift appears to be interrupted on the Pacific coast of central Vancouver Island and central Washington. These interruptions may coincide with segmentation in the subducted plate.

The deformation predicted by a simple dislocation model that represents locking of the main thrust zone in an otherwise active subduction zone is shown in Figure 3. As can be seen in the figure uplift is expected along the coastline and significant compressional strain (negative  $\epsilon_{xx}$ ) should accumulate as far inland as Puget Sound. Thus, the observations are at least roughly in accord with the model.

At the NEPEC presentation an objection to the dislocation model of Figure 3 was raised. It was argued that the model did not properly represent a subduction zone because the locked main thrust zone extended all the way to the trench whereas it should extend only to the accretionary prism. In the dislocation model the locked main thrust is represented by two edge dislocations, one at the down-dip end of the main thrust zone and the other at the up-dip end. If the up-dip dislocation is somewhere beneath the low-strength accretionary prism, not at the fault trace near the trench, would it not have an affect on the arcward deformation? The answer appears to be that it would not: the postulated absence of strength in the accretionary prism would require that the deformation from the up-dip dislocation be absorbed locally and not propagated elastically back into the more-competent portion of the overthrust wedge. Thus, the model of Figure 3 would be approximately correct even if a very weak accretionary prism extends appreciably arcward from the trench.

We regard the measured strain rates (Figure 1) as too large to be attributed to plastic deformation associated with aseismic subduction. Recall that plate motion is accommodated in aseismic subduction by continuous slip (fault creep) on the plate interface; plastic deformation within the plates, if it occurs at all, is a secondary effect. The observed strain rates are consistent with a locked main thrust and are much too large to be attributed to a secondary effect. Moreover, we have found no significant strain accumulation in a strain network at another subduction zone (Shumagin Islands in Alaska). We have tentatively identified that segment of the Alaskan subduction zone as aseismic, and, if that identification is correct, the absence of strain accumulation there would indicate that the plastic deformation in aseismic subduction is below our measurement resolution.

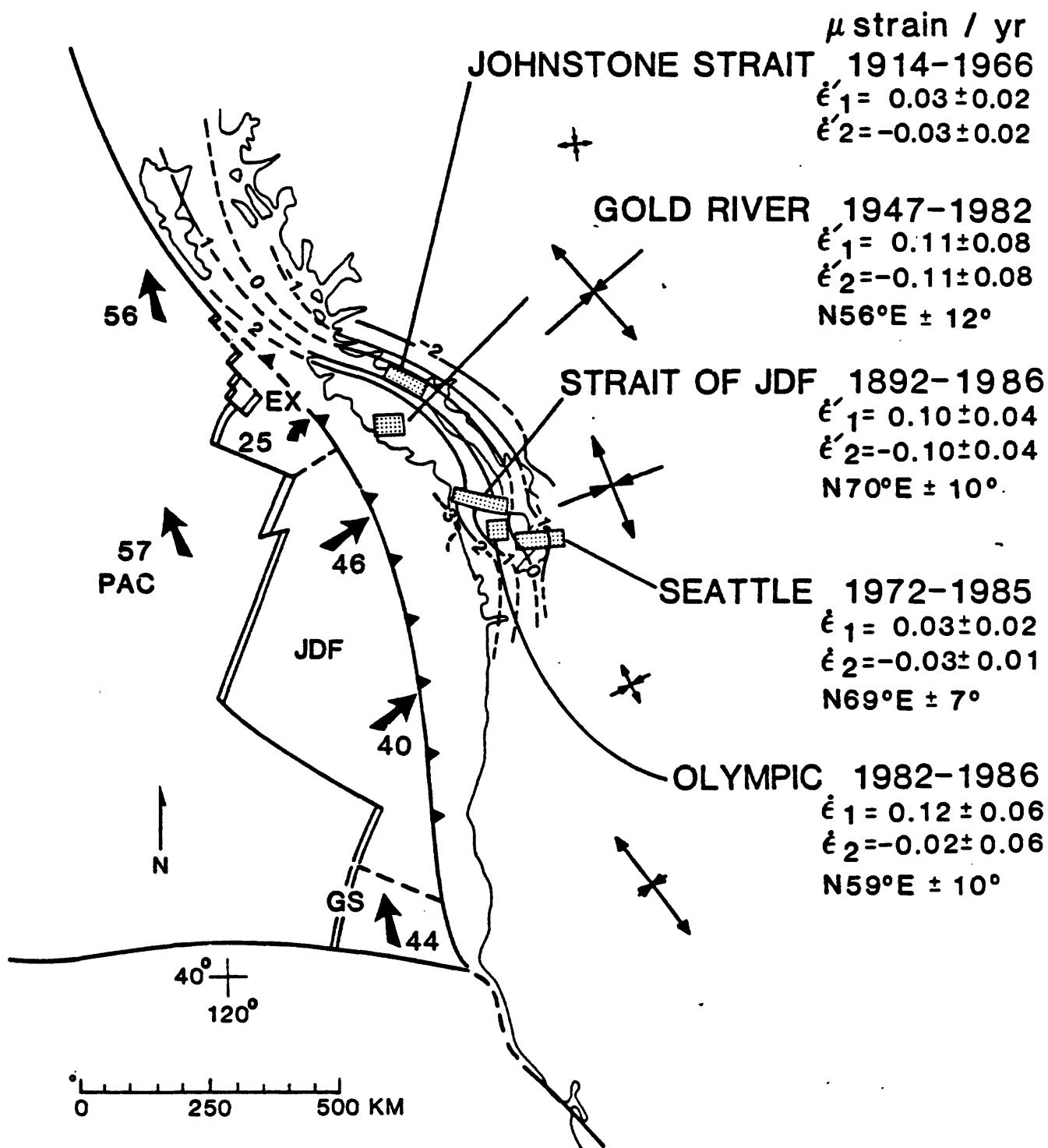
We believe that the measurements of strain accumulation in Washington and British Columbia imply a loading that must eventually be released in a major thrust event along the Cascadia subduction zone. We admit there are other possibilities. For example, the strain that appears to have accumulated since the 1890's in the Straits of Juan de Fuca could be released in a "silent" earthquake. Or, perhaps, the long-term deviatoric stresses measured in Figure 1 are due to a NNW extension rather than an ENE compression. We regard these alternatives as rather unlikely. The straightforward explanation of the observed deformation involves elastic strain accumulation.

## REFERENCES

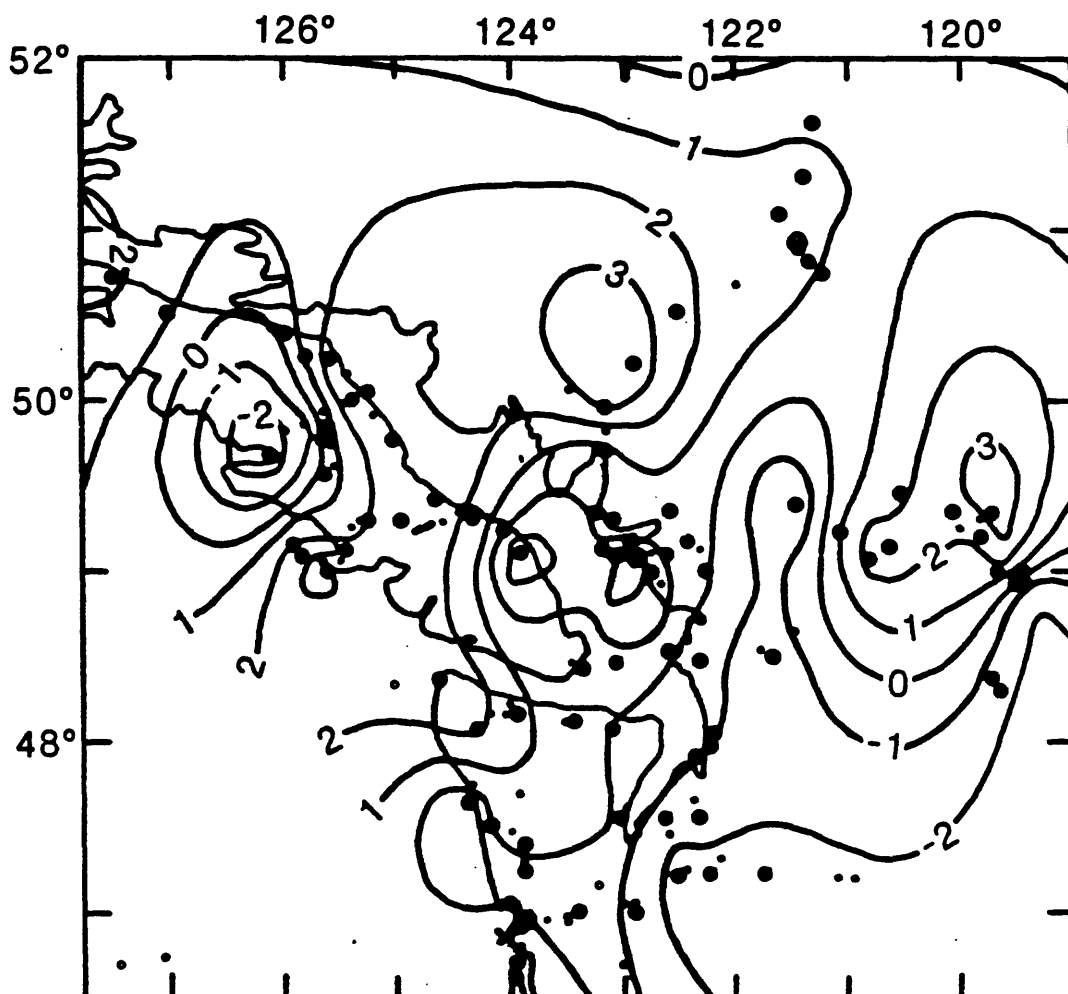
- Ando, M., and E. I. Balazs, Geodetic evidence for aseismic subduction of the Juan de Fuca plate, J. Geophys. Res., 84, 3023-3028, 1979.
- Holdahl, S. R., D. R. Martin, and W. M. Stoney, Methods for combination of water level and leveling measurements to determine vertical crustal motions, (manuscript in preparation), 1987.
- Savage, J. C., M. Lisowski, and W. H. Prescott, Geodetic strain measurements in Washington, J. Geophys. Res., 86, 4929-4940, 1981.

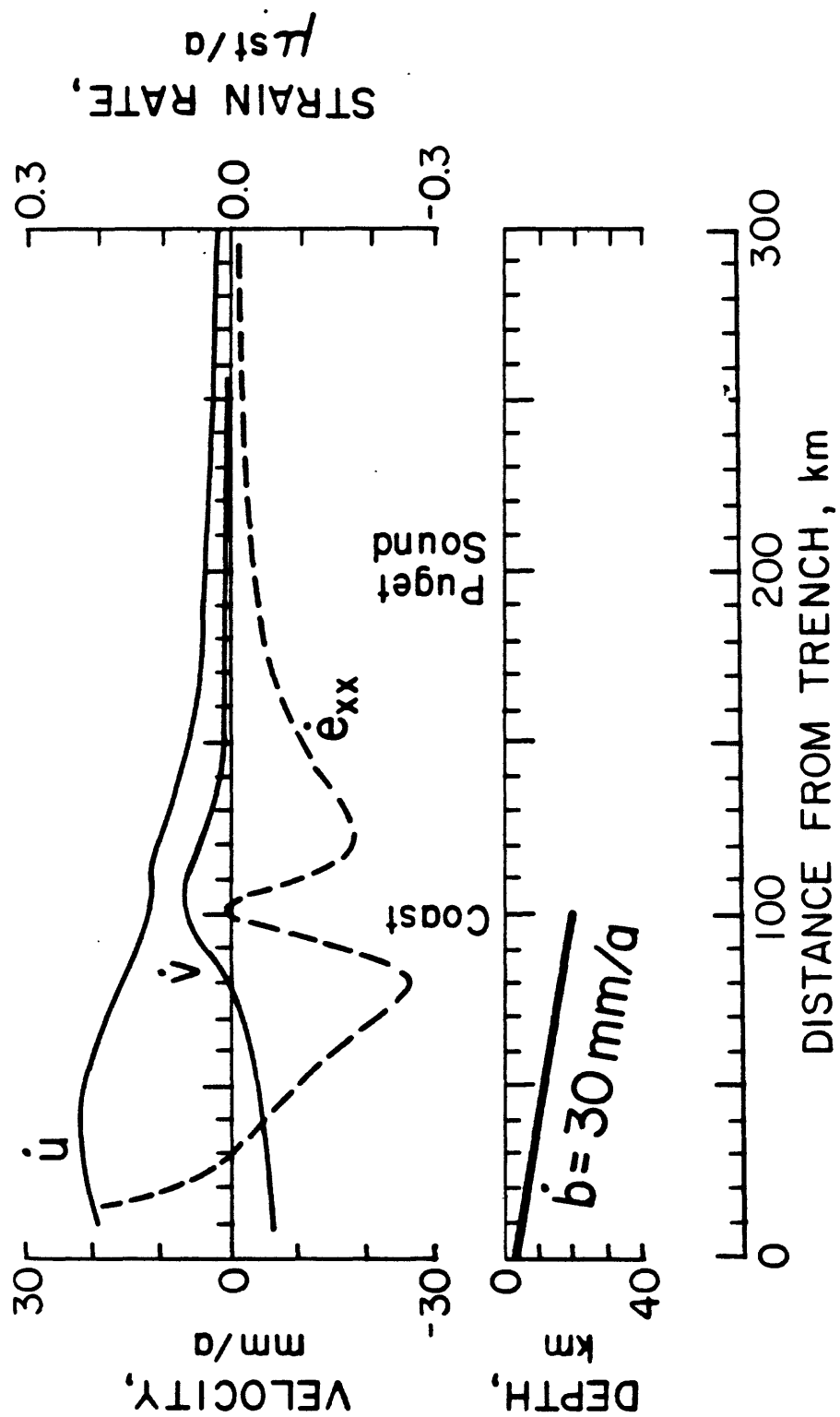
## FIGURE CAPTIONS

- Fig. 1. Measurements of strain accumulation in  $\mu\text{strain/yr}$  in Washington and British Columbia. The Canadian measurements were made by the Geological Survey of Canada and the U.S. measurements by U.S. Geological Survey. Each strain measurement is labeled by the network name, the interval over which the measurements were made, the principal strain rates (indicated by  $\epsilon'$  if only the strain deviator was measured), and the direction of greatest compression where defined. The plate boundaries (EX = Explorer, JDF = Juan de Fuca, GS = Gorda South, PAC = Pacific) and plate velocities relative to North America are shown offshore. Uplift contours in  $\text{mm/yr}$  are shown along the coast.
- Fig. 2. Average uplift rates in  $\text{mm/yr}$  inferred from leveling and tide gauges in Washington and British Columbia for the interval 1915 to 1986. (from Holdahl et al., [1987]).
- Fig. 3. Simple model of subduction with predicted uplift rate ( $\dot{V}$ ), strain rate  $\dot{\epsilon}_{xx}$ , and horizontal velocity ( $\dot{U}$ ) relative to the interior of the North American plate. The lower diagram represents the geometry of the main thrust zone (heavy sloping line). Horizontal distances are measured in an ENE direction. There is no vertical exaggeration. The rate of plate convergence has been taken as  $30 \text{ mm/yr}$ .









APPENDIX A. 9.

Pleistocene Raised Marine Terraces Along the Washington-Oregon  
Coastline and Implications to Cascadia Subduction Zone Tectonics

by

Donald West

PLEISTOCENE RAISED MARINE TERRACES ALONG  
THE WASHINGTON-OREGON COASTLINE AND IMPLICATIONS  
TO CASCADIA SUBDUCTION ZONE TECTONICS

by

Donald O. West  
Golder Associates, Inc.  
4104 148th Avenue N.E.  
Redmond, Washington 98052

**INTRODUCTION**

Underthrusting along the shallow portions of subduction zones is commonly accompanied by large magnitude ( $M_w$  8+) earthquakes that result in significant coseismic and permanent vertical deformation of the coastline of the overriding plate. The long-term deformation, in particular uplift, is recorded in the geomorphology of the coastline as raised marine terraces, wave-cut platforms and strandlines. The geologic characteristics of such uplift (nature, amount, rate, recurrence) can provide information regarding the paleoseismicity of a subduction zone and, therefore, information about the nature of future seismicity.

The ability to examine geologic evidence and evaluate the paleoseismic characteristics is particularly important for the Cascadia subduction zone which, in marked contrast to other subduction zones, has been aseismic with respect to large magnitude shallow thrust earthquakes for at least the past 200 years (Heaton and Snavely, 1985). This lack of historic events (along with geodetic evidence) has led some researchers to suggest that underthrusting along the Cascadia zone is occurring aseismically with plastic slip or has a high component of aseismic slip (Ando and Balazs, 1979; Reilinger and Adams, 1982; Taber and Smith, 1985), while to others it suggests that the plates are locked, and a large shallow thrust earthquake is possible (Savage et al, 1981; Heaton and Kanamori, 1984; Heaton and Hartzell, 1987). In the absence of definitive seismological data, the geologic record of

vertical deformation (specifically uplift) along the Cascadia subduction zone coastline, when compared to the characteristics of coseismic and long-term deformation along seismically active subduction zones, may be used to help constrain the possible interpretations.

#### **CHARACTERISTICS OF COASTLINE DEFORMATION ADJACENT TO SEISMICALLY ACTIVE SUBDUCTION ZONES**

The occurrence of large magnitude, shallow thrust earthquakes along subduction zones is accompanied by significant vertical deformation of several hundred to one thousand kilometers of coastline of the overriding plate adjacent and parallel to the subduction zone trench. Such coseismic deformation has been documented from 14 earthquakes along nine subduction zones, including Alaska, southern Chile, Nankai, Colombia, Mexico, Sagami, Kuriles, Makran, and New Hebrides (Plafker, 1969; Plafker, 1972; Plafker and Savage, 1972; Kaizuka et al, 1973; Herd et al, 1981; Ando, 1975; Fitch and Scholz, 1971; Matsuda et al, 1978; Fujita et al, 1975; Page et al, 1979; Taylor et al, 1980; Bodin and Klinger, 1986).

Typically, coseismic deformation of the overriding plate (including the accretionary wedge) is characterized by linear zones of uplift and subsidence that are parallel to and arcward of the trench. The 1960 Mw 9.5 Chile earthquake, the 1964 Mw 9.2 Alaska earthquake, and the 1707 Mw 8.6 Nankai earthquake created zones of coseismic deformation that were 1000 x 250 km, 1000 x 450 km, and >600 x >200 km, respectively (Plafker, 1969; Plafker and Savage, 1970; Ando, 1975). Uplift occurs closest to the trench. Subsidence is more distant and is bounded by a zero uplift line adjacent to the zone of uplift. Depending on the distance of the coastline to the trench, it may experience either coseismic uplift or subsidence.

Coseismic uplift of the coastline is characterized by emerged marine, rocky wave-cut platforms, a few tens to a few hundred meters wide, emerged wave-cut notches in rocky headlands, emerged coral platforms and uplifted strandlines (Plafker, 1969; Plafker and Savage, 1970; Kaizuka et al, 1973; Taylor et al, 1980). Coseismic subsidence is characterized by submerged topography and vegetation along coastal plains and bays (Plafker, 1969; Plafker and Savage, 1970; Herd et al, 1981).

A review of the data regarding the pattern, nature and amounts of coseismic deformation reveals that as the earthquake magnitude increases so does the length of the zone of deformation (Figure 1). It is apparent from Figure 1 that shallow thrust subduction zone earthquakes of magnitude  $>8.5$  should generate zones of deformation with lengths  $>400$  km. In addition, the apparent linear relationship of earthquake magnitude to length of the zone of deformation suggests a magnitude threshold of about  $M 7.0$  below which coseismic deformation of the overriding plate may not occur or be too small to be observable.

A comparison of earthquake magnitude versus the amount of coseismic vertical deformation at the coastline suggests a weak relationship of increasing uplift and subsidence with increasing magnitude (Figure 2). In addition, for any given earthquake, the amount of coseismic coastline uplift generally exceeds that of subsidence. Also evident from Figure 2 is that some earthquakes may result in only uplift or only subsidence of the coast. For example, only subsidence was observed resulting from the 1979  $M_s 7.9$  Tumaco earthquake off Colombia (Herd et al, 1981) and only uplift of the coastline was recorded from the 1985  $M_s 7.5/8.1$  Mexico earthquake (Bodin and Klinger, 1986).

The distance from the trench, at which either coseismic uplift or subsidence of the coastline occurs, appears to be only roughly related to earthquake magnitude (Figure 3). Figure 3 is a plot of earthquake magnitude versus the distance from the trench that coseismic uplift and subsidence of the coastline has occurred. For each specific earthquake, the range in distances that only uplift and only subsidence of the coastline was observed are shown; the area between these ranges indicates the zone of coastline for which both coseismic uplift or subsidence were observed. These data suggest that for magnitudes greater than 8, coseismic uplift of the coastline generally occurs exclusively to 110-120 km from the trench, and the zone in which either uplift or subsidence may occur is narrow ( $<20$  km).

Studies of the characteristics of coseismic uplift with respect to long-term evidence of episodic uplift in Alaska, southern Chile, New Hebrides, Sagami and Makran indicate that the recurrence for such uplift events ranges from 300 to 2000 years and averages about 980 years (Plafker, 1969; Kaizuka et al, 1973; Taylor et al, 1980; Matsuda et al,

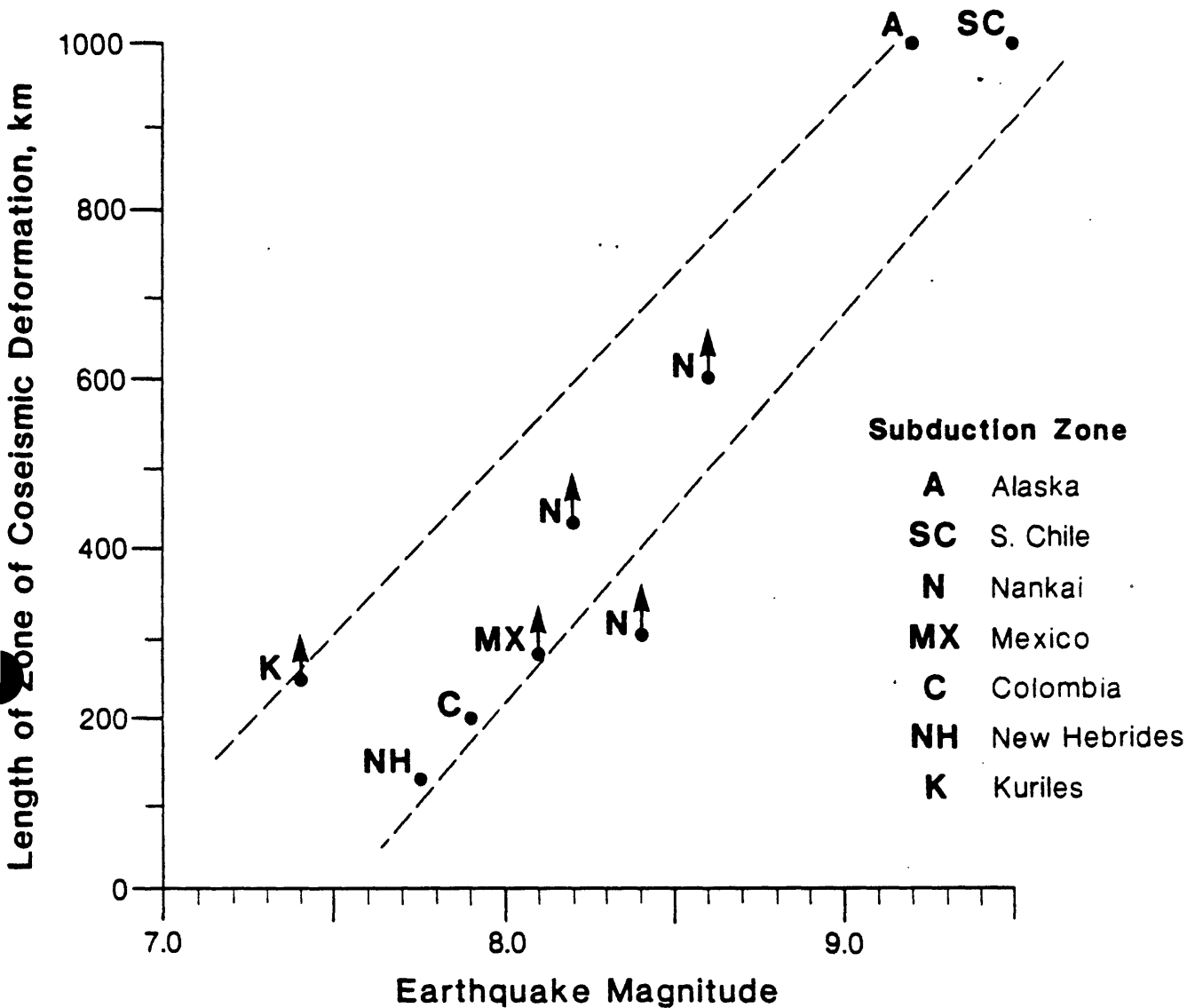
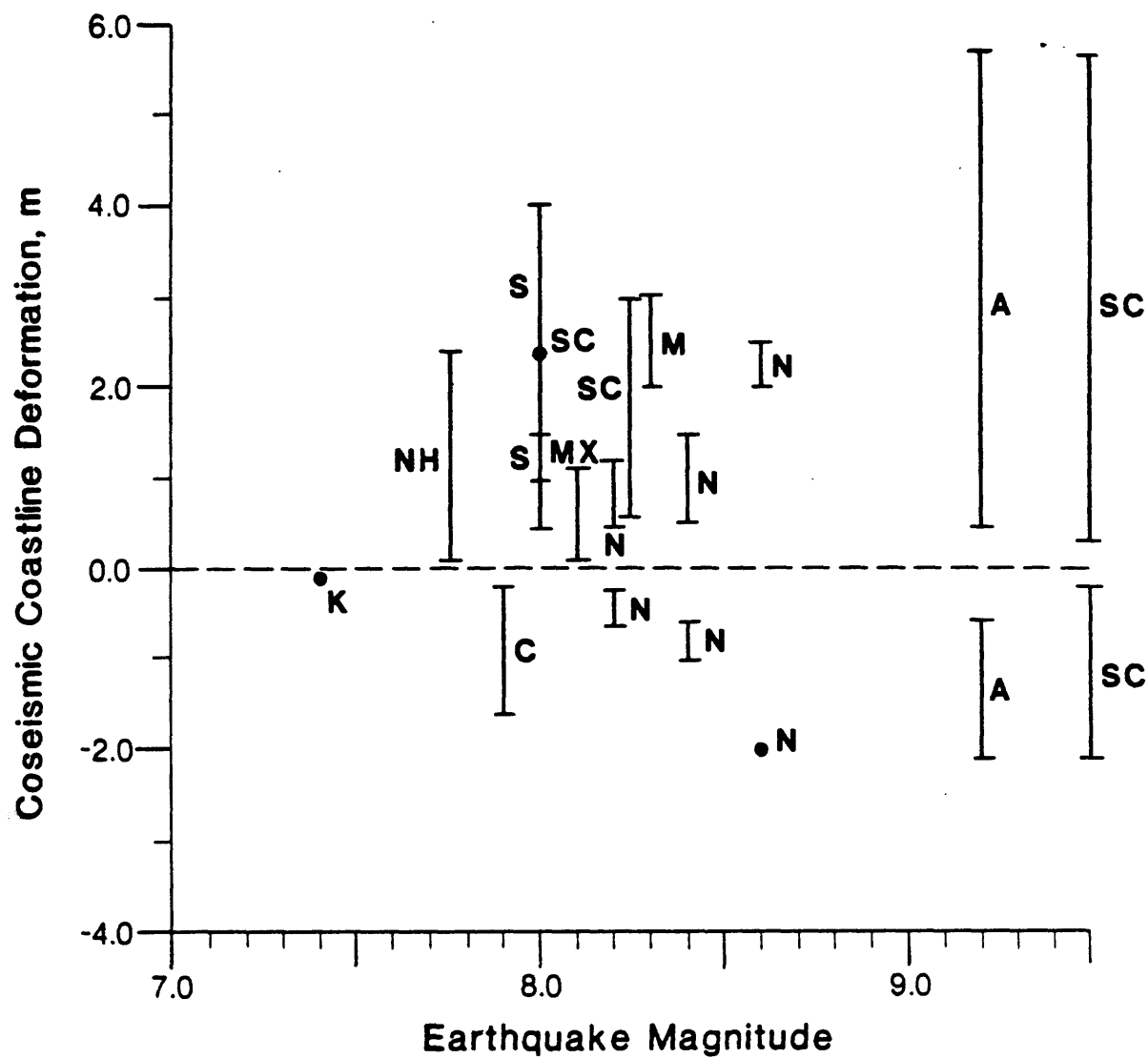


Figure 1. Plot of Earthquake Magnitude of Shallow Subduction Zone Thrust Events Versus the Length of the Zone of Coseismic Deformation. The Subparallel Curves Roughly Envelope the Data.

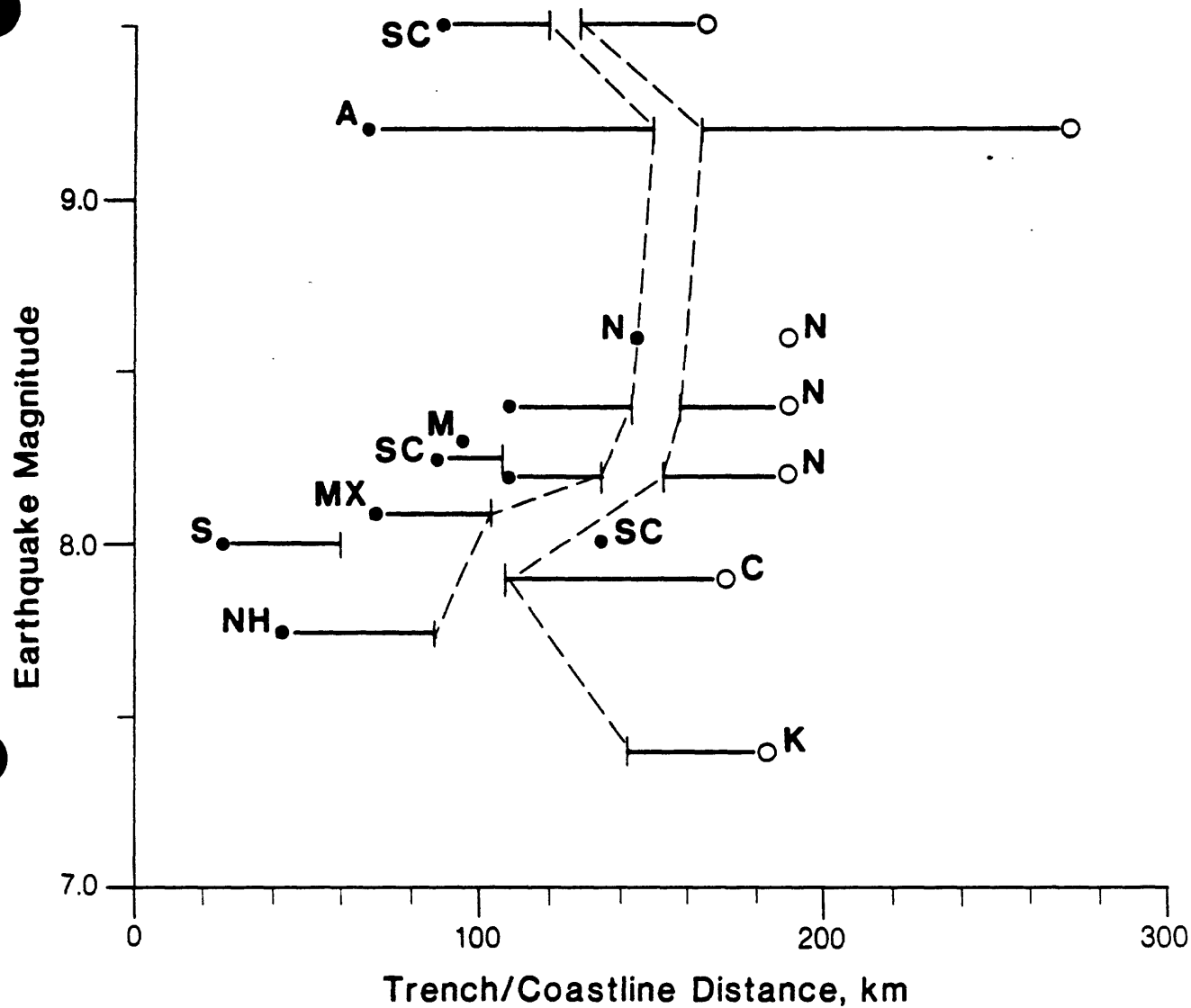


#### Subduction Zone

- |                    |                        |
|--------------------|------------------------|
| <b>A</b> Alaska    | <b>MX</b> Mexico       |
| <b>SC</b> S. Chile | <b>C</b> Colombia      |
| <b>N</b> Nankai    | <b>NH</b> New Hebrides |
| <b>M</b> Makran    | <b>K</b> Kuriles       |
|                    | <b>S</b> Sagami        |

Figure 2. Plot of Earthquake Magnitude of Shallow Subduction Zone Thrust Events Versus the Amount of Coseismic Coastline Deformation.





Subduction Zone			
●—	Coseismic uplift	SC	S. Chile
—○	Coseismic subsidence	A	Alaska
		N	Nankai
		M	Makran
		MX	Mexico
		S	Sagami
		NH	New Hebrides
		K	Kuriles
		C	Colombia

Figure 3. Plot of Earthquake Magnitude of Shallow Subduction Zone Thrust Events Versus the Distance From the Trench That the Coastline was Coseismically Uplifted and/or Subsided.

1978; Page et al, 1979). These geologic data likely reflect the maximum recurrence intervals for large magnitude, shallow thrust earthquakes. In contrast, the historic record of large subduction zone earthquakes in southern Chile (last 412 years) and Nankai (last 1300 years) suggests that the recurrence interval for shallow thrust events along the same segment is about 130 and 160 years, respectively (Kaizuka et al, 1973; Ando, 1975). In addition, the last two events in southern Chile (1837, 1960) and the last three in Nankai (1707, 1854, 1944-46) produced preserved evidence of coseismic uplift.

It is common for the subduction zone coastlines along which coseismic deformation has occurred to also exhibit evidence of long-term (Holocene and Pleistocene) uplift. This evidence is in the form of raised marine wave-cut platforms, raised marine terraces and raised strandlines. Multiple uplifted Holocene shoreline features are common to 30 meters elevation, and locally to over 50 meters, above coseismically uplifted shoreline features (Figure 4). In Alaska, for example, six raised marine wave-cut terraces (<4500 years old) occur above the 1964 coseismic terrace at Middleton Island and nine strandlines (<7700 years old) occur at Katalla above the 1964 coseismic uplift (Plafker, 1969). These localities are 69 and 105 km, respectively, from the trench axis. In southern Chile at least three Holocene wave-cut terraces (<4000 years old) lie above the coseismic terraces created during the 1835 and 1960 earthquakes at Isla Mocha, 90 km from the trench (Kaizuka et al, 1973). The highest elevations of the Holocene terraces are within the zone of expected coseismic uplift; i.e., about 30-120 km from the trench (Figure 4).

It is important to note that the Holocene terraces are not rare, isolated features but appear to be common along the coastlines experiencing large magnitude, shallow thrust earthquakes. In New Zealand they occur along over 200 km of coastline at distances of 85 to 180 km from the trench (Singh, 1971; Wellman, 1971 and 1962). Holocene terraces are common along more than 200 km of the Makran coast at distances of 95 to 160 km from the trench, and in Peru they occur along at least 100 km of coastline at 70 to 93 km from the trench (Woodward-Clyde Consultants, 1975; Lemon and Churcher, 1961; Richards and Broecker, 1963).

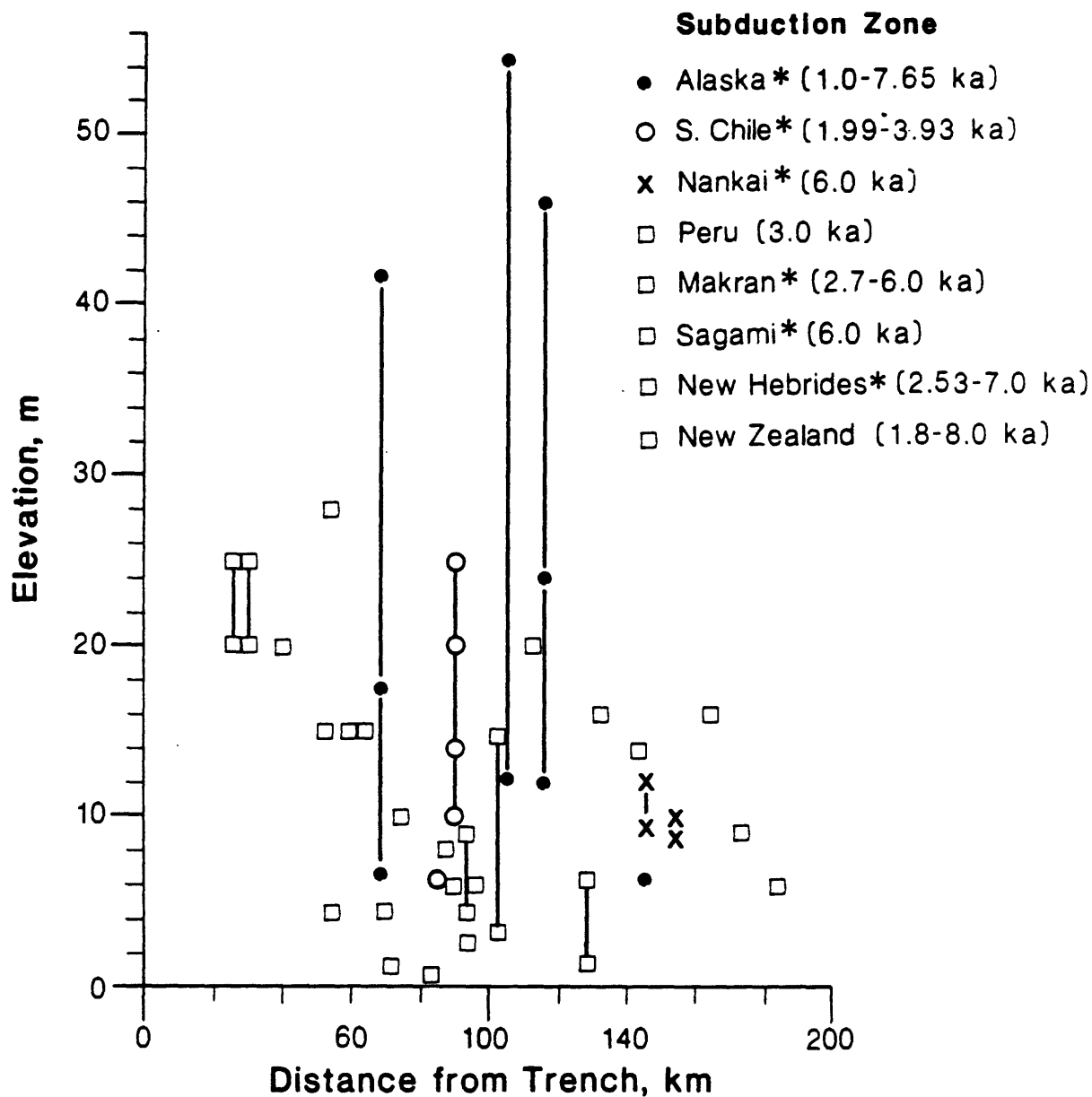


Figure 4. Plot of Height of Holocene Terraces, Wave-Cut Platforms or Beach Berms Along Coastlines Adjacent to Seismically Active Subduction Zones Versus Distance From the Trench. Asterisks Indicate Those Coastlines Where a Coseismic Terrace(s) is the Lowest in the Sequence of Raised Terraces. The Numbers in Parentheses Indicate the Range, in Thousands of Years, of the Age of the Holocene Features.

Multiple uplifted, late Pleistocene, high sea level stand marine terraces are common along overriding plate coastlines adjacent to seismically active subduction zones and occur above raised Holocene terraces. The late Pleistocene terraces may be greater than 300 meters elevation and lie at 40 to 180 km from the trench axis. In southern Chile, for example, a 103,000-year-old terrace (the youngest of three Pleistocene terraces) is 390 m above sea level at 90 km from the trench axis, and in Nankai, a 125,000-year-old terrace is 190 m elevation at 145 km from the trench (Kaizuka et al, 1973; Ota and Yoshikawa, 1978). Rates of uplift, calculated from Pleistocene terraces along seven subduction zones (Figure 5), indicate that, for distances of 40 to 180 km from the trench, uplift is generally 0.2 - 3.0 mm/yr and commonly >0.5 mm/yr, and that the highest rates are generally in the zone of expected coseismic uplift; i.e., about 30 - 120 km from the trench.

#### **CHARACTERISTICS OF RAISED MARINE TERRACES ALONG THE WASHINGTON-OREGON COASTLINE**

A sequence of at least five uplifted, late Pleistocene, high sea level stand marine terraces, varying from 42,000 - 220,000 years old, occurs along about 600 km of the Washington-Oregon coastline, from La Push on the north, to Cape Blanco on the south (Figure 6). The sequence is most well preserved along the south and central part of the Oregon coast between Cape Blanco and Newport. The youngest terrace, the 42,000- year-old Cape Blanco terrace, occurs only at Cape Blanco. Based on field reconnaissance mapping, photogeologic interpretation, radiocarbon dating at three localities, and previous uranium series, amino acid racemization and palynology age determinations at five localities (Kennedy, 1978; Heusser, 1972), the most well preserved, continuous, and persistent terrace is the 82,000-year-old Whiskey Run.

The Whiskey Run terrace is persistent either as a fairly continuous and broad terrace surface (several tens of kilometers long and a few hundred to several thousand meters wide) or as remnants of terrace surfaces, exhumed wave-cut platforms and wave-cut notches in headlands. At some localities the paleoshoreline angle of the terrace could be directly observed and its elevation recorded. However, in general, data on the amount, and rate of uplift are derived from elevations recorded

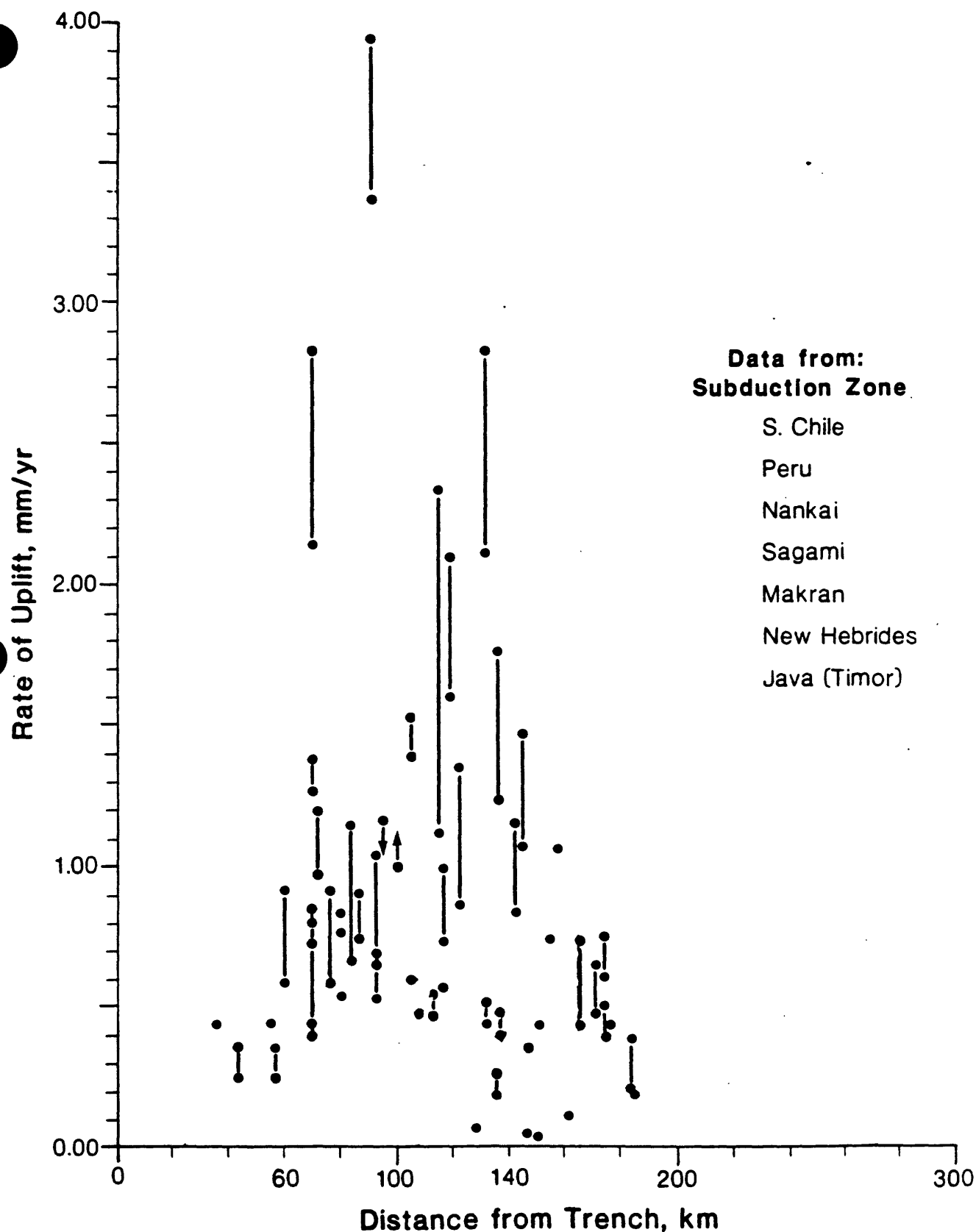


Figure 5. Plot of the Rate of Uplift Derived From Raised Pleistocene Terraces Along Coastlines Adjacent to Seismically Active Subduction Zones Versus Distance From the Trench.

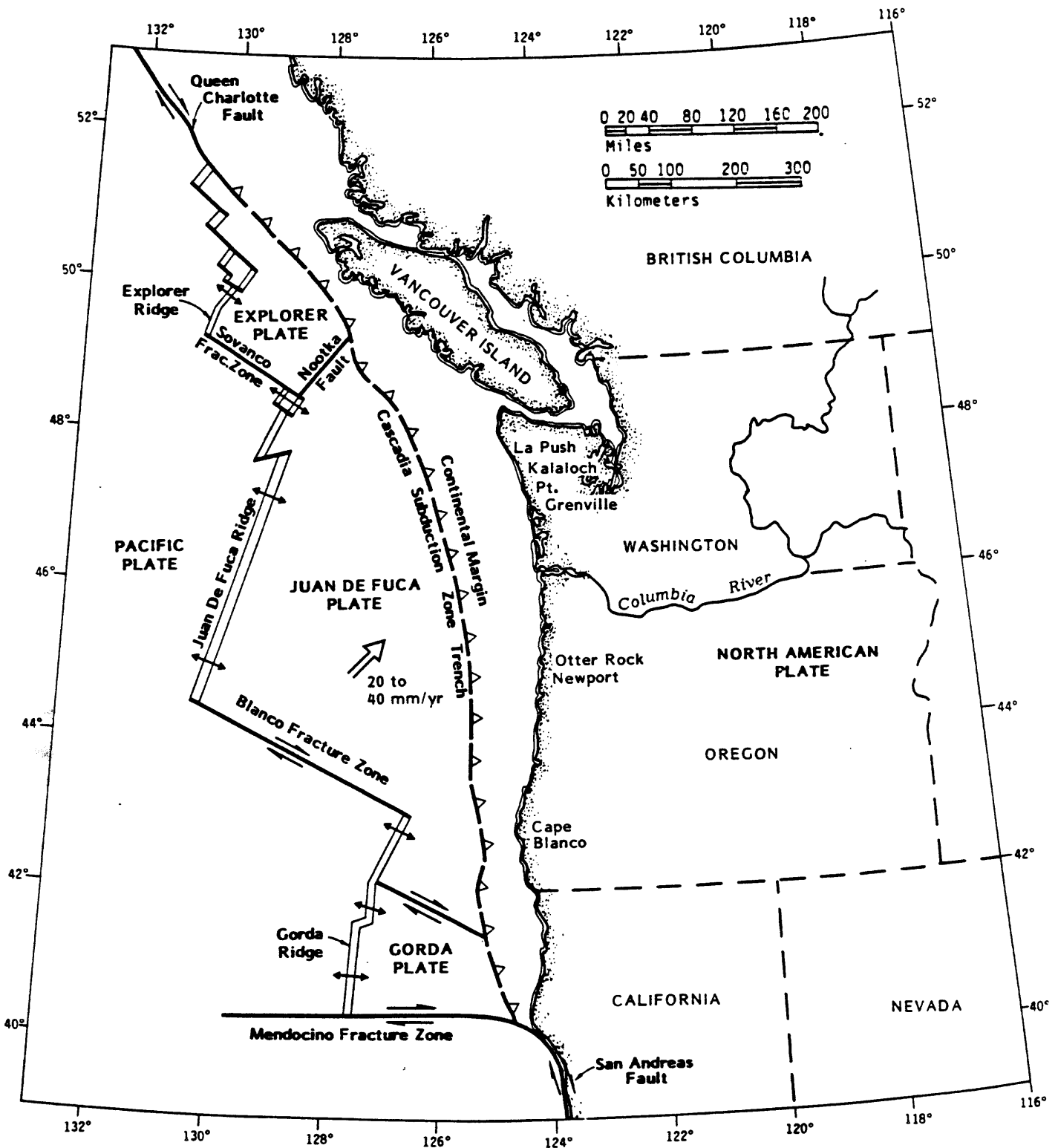


Figure 6. Tectonic Setting of the Cascadia Subduction Zone That Comprises the Convergence and Subduction of the Juan de Fuca, Explorer and Gorda Oceanic Plates Beneath the North American Plate.

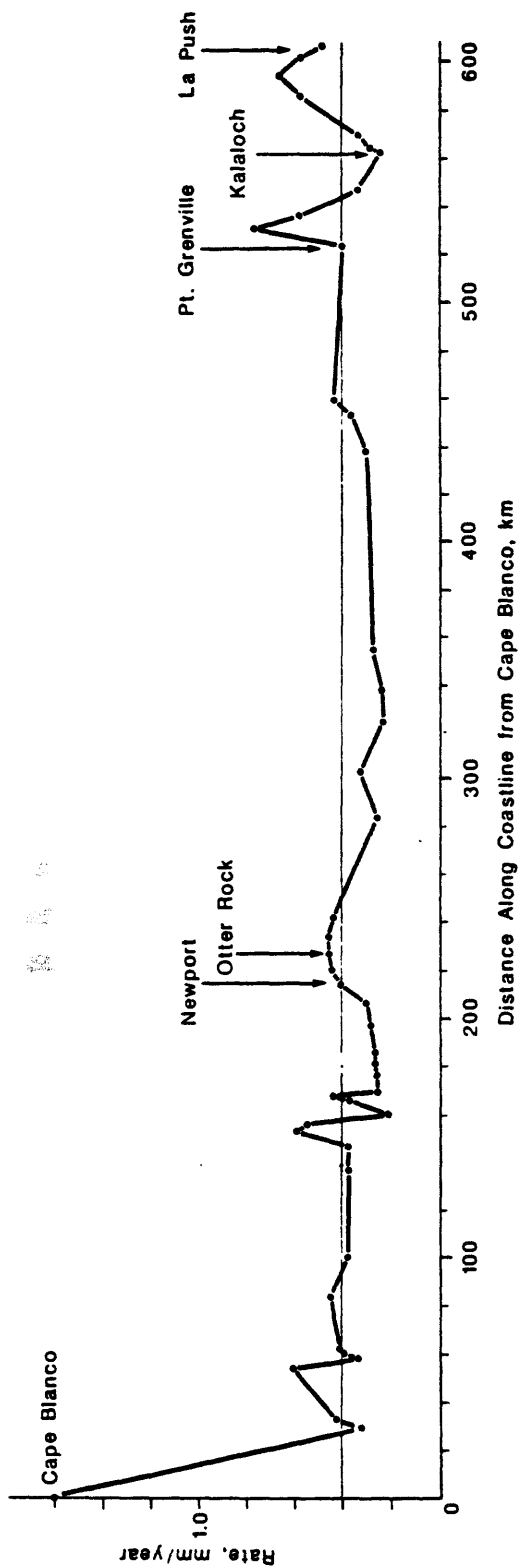
in close proximity (generally <1 km) to the interpreted paleoshoreline angle. Because of its continuity along the coast, evaluations regarding the pattern, amount and rate of late Quaternary uplift are based on the Whiskey Run terrace.

Except at Cape Blanco, where it is 121 m above sea level, the Whiskey Run terrace varies only from about 5-50 m elevation and averages about 20 m elevation for the entire 600 km of coastline. Uplift rates derived from the Whiskey Run terrace, along with a plot of the distance to the trench, are shown on Figure 7 for the coastline from Cape Blanco to La Push. The highest rate is at Cape Blanco, 1.62 mm/yr (60 km from the trench), yet this decreases rapidly to 0.33 mm/yr 29 km north of the cape (65 km from the trench). From this point northward, and with the exception of two anomalies at the north end of the coast, the uplift rate appears to be uniform; it varies from only about 0.2 - 0.6 mm/yr and averages about 0.4 mm/yr while the distance to the trench increases from 65 km to 140 km.

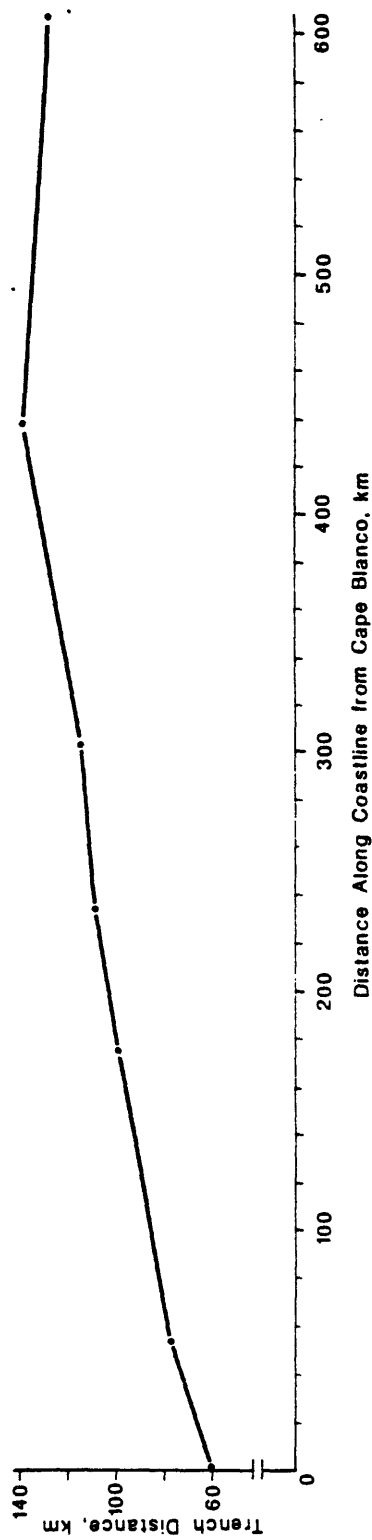
No uplifted marine terraces, wave-cut platforms or beach berms younger than the Cape Blanco terrace at Cape Blanco or Whiskey Run terrace north of the cape were observed. Geomorphically, the youngest Pleistocene terraces sit directly above modern wave-cut platforms without uplifted Holocene features between. This is the case whether the coastline is 60 km from the trench (Cape Blanco), 110 km from the trench (Otter Rock), or 138 km from the trench (Pt. Grenville and Kalaloch) (Figure 6). The modern wave-cut platform, observed at low tide, is well developed in Tertiary sedimentary and volcanic rock, is often broad (several tens to a few hundred meters wide) and terminates landward with a well developed shoreline angle in the sea cliff below the Pleistocene terrace.

## DISCUSSION

A review of the characteristics of coseismic and long-term vertical deformation of overriding plate coastlines in seismically active convergent margins provides information on what might be expected to be seen in the geologic record along the Cascadia subduction zone coastline if large magnitude, shallow thrust earthquakes have occurred frequently in the past similar to the other zones. It is evident that if a large



(a) Late Pleistocene Uplift Rate



(b) Trench/Coastline Distance

Figure 7. (a) Plot of Late Pleistocene Rate of Uplift Along Washington-Oregon Coastline Derived from Whiskey Run Terrace (82,000 Years Old). (b) Plot of the Variation in Distance to the Trench Along the Washington-Oregon Coastline.



magnitude ( $> M_w 8.5$ ) earthquake were to occur it should: 1) affect more than 400 km of the coastline (Figure 1), 2) result in 0.5 - 4.0+ m of uplift or 0.2 - 2.0 m of subsidence of the coastline (Figure 2), and 3) cause only coseismic uplift to occur at least to about 110 - 120 km from the trench, both uplift or subsidence may occur from about 110 to 150 km, and only coseismic subsidence should occur beyond about 150 m (Figure 3). It is also evident that multiple past historic earthquakes have resulted in multiple uplifted coseismic terraces (e.g., southern Chile, Nankai) and that multiple uplifted Holocene shoreline features (interpreted to represent past large magnitude thrust events) are common in other subduction zone coastlines in the area of expected coseismic uplift (out to 110 - 120 km from the trench (Figure 4)). Recurrence intervals for such shallow thrust events along the same subduction zone segment may be 130 - 150 years, based on historic seismicity, or from 300 - 2000 years (980 years average), based on the geologic record. In addition, uplift rates based on raised late Pleistocene marine terraces should commonly exceed 0.5 mm/yr at distances out to 140 km from the trench (Figure 5).

The coastline of the Cascadia subduction zone lies from 60 - 140 km from the trench; the Washington coast is about 120 - 140 km, while the Oregon coast is 60 - 120 km. This means that essentially all of the Oregon coastline is situated in the zone of expected coseismic and long-term (Holocene and Pleistocene) uplift, given a large magnitude, shallow thrust event on the subduction zone, while the coastline of Washington could experience either uplift or subsidence. If large magnitude thrust events have occurred in the past on the Cascadia subduction zone with the characteristics of other zones, the effects of uplift should be particularly evident along the Oregon coast.

The Oregon and Washington coasts do have uplifted, late Pleistocene, marine terraces similar to other subduction zone coastlines. However, the characteristics of the uplifted terraces and the present coastal geomorphology appear to be different in two significant respects from other subduction zone coastlines:

1. There are no uplifted Holocene, wave-cut platforms, terraces or multiple beach berms that would indicate repeated large magnitude, thrust-type paleoseismicity on the Cascadia subduction zone interface.

This is especially significant for the Oregon coast, which occurs well within the zone of expected coseismic uplift and zone of multiple uplifted Holocene terraces. The present coastline configuration with locally broad, modern wave-cut platforms situated directly below the uplifted Pleistocene terraces without intervening Holocene terraces suggests that relative tectonic stability (without episodic uplift) has been in effect during the late Holocene. Coseismic uplift with the amounts (several meters) and frequencies (a few hundred to two thousand years), apparently typical of other subduction zones, should result in the preservation of uplifted Holocene terraces and not the observed broad, modern platform.

2. The amount and rate of uplift of the Cascadia subduction zone coastline, derived from the Pleistocene terraces, is low when compared to other subduction zones. Other subduction zone coastlines, at distances of 60 - 140 km from the trench, have rates consistently  $>0.5$  mm/yr, and many are  $>1.0$  mm/yr. In contrast, the Cascadia coastline varies from 0.2 - 0.6 mm/yr and averages 0.4 mm/yr. In addition, the rate is relatively uniform along the coast and appears to be essentially the same, whether close to the trench, as in Oregon, or farther, as in Washington. This uniformity suggests that, over the long term, the tectonic mechanism resulting in uplift of the coast may be similar along the entire coastline.

The apparent differences with other subduction zones provide insight into the nature of the underthrusting along the Cascadia subduction zone and the characteristics of potential shallow thrust earthquakes. The lack of uplifted Holocene shoreline features, the presence of broad modern wave-cut platforms, and the low overall rate of late Quaternary uplift suggests that there may be a significantly longer recurrence for large magnitude thrust events on the Cascadia zone such that the evidence for episodic uplift (Holocene platforms) is eroded by eustatic sea level rise, and the longer recurrence results in a lower overall rate of uplift. The differences may also suggest that smaller magnitude thrust earthquakes occur that may be below a threshold level to produce coseismic uplift of the coast that would be preserved in Holocene terraces or higher uplift rates. It is possible that the tectonic mechanism contributing to vertical deformation of the Cascadia coastline

behaves differently from other subduction zones, such that large magnitude earthquakes occur as frequently, but without uplift in the zone of expected coseismic uplift (the Oregon coast). It is also possible that subduction along the Cascadia zone may be occurring aseismically.

## REFERENCES

- Ando, M., 1975. Source Mechanisms and Tectonic Significance of Historical Earthquakes Along the Nankai Trough, Japan: *Tectonophysics*, v. 27, p. 119-140.
- Ando, M. and Balazs, E.J., 1979. Geodetic Evidence for Aseismic Subduction of the Juan de Fuca Plate: *Journal of Geophysical Research*, v. 84, p. 3023-3027.
- Bodin, P. and Klinger, T., 1986. Coastal Uplift and Mortality of Intertidal Organisms by the September 1985 Mexico Earthquakes: *Science*, v. 233, p. 1071-1073.
- Fitch, T.J. and Scholz, C.H., 1971. Mechanism of Underthrusting in Southwest Japan: A Model of Convergent Plate Interactions: *Journal of Geophysical Research*, v. 76, n. 29, p. 7260-7292.
- Fujita, N., Fujii, Y. and Tada, T., 1975. Crustal Effects of a Heavy Offshore Earthquake in Eastern Hokkaido, Japan: *Tectonophysics*, v. 29, p. 523-528.
- Heaton, T.H. and Hartzell, S.H., 1987. Earthquake Hazards on the Cascadia Subduction Zone: *Science*, v. 236, p. 162-168.
- Heaton, T.H. and Kanamori, H., 1984. Seismic Potential Associated with Subduction in the Northwestern United States: *Bulletin of the Seismological Society of America*, v. 74, p. 933-941.
- Heaton, T.H. and Snavely, P.D., Jr., 1985. Possible Tsunami along the Northwestern Coast of the United States Inferred from Indian Traditions: *Bulletin of the Seismological Society of America*, v. 75, n. 5, p. 1455-1460.
- Herd, D.G., Youd, T.L., Meyer, H., Arango, C., J.L., Person, W.J. and Mendoza, C., 1981. The Great Tumaco, Colombia Earthquake of 12 December 1979: *Science*, v. 211, p. 441-445.

- Heusser, C.J., 1972. Palynology and Phytogeographical Significance of a Late Pleistocene Refugium Near Kalaloch, Washington: *Quaternary Research*, v. 2, p. 189-201.
- Kaizuka, S., Matsuda, T., Nogami, M. and Yonekura, N., 1973. Quaternary Tectonic and Recent Seismic Crustal Movements in the Arauco Peninsula and Its Environs, Central Chile: *Geographical Reports of Tokyo Metropolitan University*, n. 8, 38 p.
- Kennedy, G.L., 1978. Pleistocene Paleoecology, Zoogeography and Geochronology of Marine Invertebrate Faunas of the Pacific Northwest Coast (San Francisco Bay to Puget Sound): PhD Thesis, University of California, Davis, 824 p.
- Lemon, R.R.H. and Churcher, C.S., 1961. Pleistocene Geology and Paleontology of the Talara Region, Northwest Peru: *American Journal of Science*, v. 259, p. 410-429.
- Matsuda, T., Ota, Y., Ando, M. and Yonekura, N., 1978. Fault Mechanism and Recurrence Time of Major Earthquakes in Southern Kanto District, Japan as Deduced from Coastal Terrace Data: *Geological Society of America Bulletin*, v. 89, p. 1610-1618.
- Ota, Y. and Yoshikawa, T., 1978. Regional Characteristics and Their Geodynamic Implications of Late Quaternary Tectonic Movement Deduced from Deformed Former Shorelines in Japan: *Geodynamics of the Western Pacific*, S. Uyeda et. al. (eds.), Center for Academic Publications Japan, Japan Scientific Societies Press, Tokyo, p. 379-389.
- Page, W.D., Alt, J.N., Cluff, L.S. and Plafker, G., 1979. Evidence for the Recurrence of Large-Magnitude Earthquakes Along the Makran Coast of Iran and Pakistan: *Tectonophysics*, v. 52, p. 533-547.
- Plafker, G., 1969. Tectonics of the March 27, 1964 Alaska Earthquake: *U.S. Geological Survey Professional Paper* 543-I, 74 p.
- Plafker, G., 1972. Alaskan Earthquake of 1964 and Chilean Earthquake of 1960: Implications for Arc Tectonics: *Journal of Geophysical Research*, v. 77, n. 5, p. 901-925.
- Plafker, G. and Savage, J.C., 1970. Mechanism of the Chilean Earthquakes of May 21 and May 22, 1960: *Geological Society of America Bulletin*, v. 81, p. 1001-1030.

- Reilinger, R.E. and Adams, J., 1982. Geodetic Evidence for Active Landward Tilting of the Oregon and Washington Coastal Ranges: *Geophysical Research Letters*, v. 9, p. 401-403.
- Richards, H.G. and Broecker, W., 1963. Emerged Holocene South American Shorelines: *Science*, v. 141, p. 1044-1045.
- Savage, J.C., Lisowski, M. and Prescott, W.H., 1981. Geodetic Strain Measurements in Washington: *Journal of Geophysical Research*, v. 86, n. B6, p. 4929-4940.
- Singh, L.J., 1971. Uplift and Tilting of the Oterei Coast, Wairarapa, New Zealand, During the Last Ten Thousand Years: Recent Crustal Movements, *Royal Society of New Zealand Bulletin* 9, p. 217-219.
- Taber, J.J. and Smith, S.W., 1985. Seismicity and Focal Mechanisms Associated with the Subduction of the Juan de Fuca Plate Beneath the Olympic Peninsula, Washington: *Bulletin of the Seismological Society of America*, v. 75, n. 1, p. 237-249.
- Taylor, F.W., Isacks, B.L., Jouannic, C., Bloom, A.L. and Dubois, J., 1980. Coseismic and Quaternary Vertical Tectonic Movements, Santo, and Malekula Islands, New Hebrides Island Arc: *Journal of Geophysical Research*, v. 85, n. B10, p. 5367-5381.
- Wellman, H.W., 1962. Holocene of the North Island of New Zealand: A Coastal Reconnaissance: *Transactions of the Royal Society of New Zealand, Geology*, v. 1, n. 5, p. 29-99.
- Wellman, H.W., 1971. Holocene Tilting and Uplift on the Glenburn Coast, Wairarapa, New Zealand: Recent Crustal Movements, *Royal Society of New Zealand Bulletin* 9, p. 221-223.
- Woodward-Clyde Consultants, 1975. Site Safety Analysis, Bandar Abbas Region, Iran, Phase 1 Site Confirmation Studies, Appendix A, Raised Beach Study: prepared for Atomic Energy Organization of Iran.

## **APPENDIX B**

### **Additional Papers**

APPENDIX B. 1.

Estimating Seismic Potential of Subduction Zones Using the  
Seismic Front and Forearc Morphology

by

D. E. Byrne, L. R. Sykes, and D. M. Davis

## ESTIMATING SEISMIC POTENTIAL OF SUBDUCTION ZONES USING THE SEISMIC FRONT AND FOREARC MORPHOLOGY

Daniel E. Byrne, Lynn R. Sykes, Lamont-Doherty Geo. Obs. and Dept. of Geo. Sci., Columbia Univ., Palisades, NY 10964, USA, and Dan M. Davis, Dept. of Earth and Space Sci., SUNY Stony Brook, Stony Brook, NY 11794.

Large variation is observed between subduction zones in the maximum sized earthquake each experiences (its seismic potential) and in the repeat time of these events. A part of this variation is successfully ascribed to differences in some key parameters that govern the coupling. Because the size of an earthquake is proportional to the area it ruptures, a more direct way of assessing seismic potential would be to estimate potential rupture area. We describe a forearc model that helps delimit this area by estimating the shallow or trenchward limit to rupture, the seismic front. Using estimates of the location of the seismic front we can assess the seismic potential, and, combined with estimates of convergence velocity, the repeat times of large thrust earthquakes at convergent margins.

Seismicity does not extend seaward all the way to the trench in most subduction zones. Instead motion along the shallowest part of the plate boundary, beneath the accretionary wedge, is aseismic. It thus appears that the seismic front is related to forearc structure. We use a mechanical analysis to examine outer-arc highs and forearc basins, features whose formation has not previously been well explained. We find that their development depends on an abrupt arcward increase in shear strength within the forearc. Such lateral strength contrasts are not generally observed along the seafloor, and so we postulate that it occurs at depth beneath the outer-arc high. This stronger material is called the backstop. Recent observations of trenchward dipping reflectors in MCS lines from several margins have been interpreted as backstops. We also use laboratory scale modeling to investigate the effect that backstops have on forearc morphology. Experiments with sand and a stronger material representing a backstop simulate the morphology observed at several forearcs. It appears that because the stronger material supports most of the compressive force, a morphologic high occurs over the trenchward tip of the backstop, arcward of which a passive basin may form.

The location of the seismic front appears to coincide with the most trenchward extent of the backstop. We think it is understandable that earthquakes are not observed in the weak sediments of the accretionary wedge but are within the backstop, because one of the necessary conditions for earthquakes to occur is that the material must be able to accumulate sufficient levels of shear stress. The backstop also affects forearc morphology and thus at several margins we observe a correlation between the seismic front and the morphologic inflections. We can use this relationship to estimate the location of the seismic front in the absence of a direct seismic determination. The identification of the seaward limit of thrust earthquakes is important in estimating the down dip width,  $W$ , of rupture area.  $W$  is crucial in seismic potential calculations because scalar seismic moment of thrust events is proportional to  $W^n$  where  $2 \leq n \leq 3$ . We can thus estimate  $W$  combining estimates of the depth of the lower limit of rupture with the seismic front, and from  $W$  and convergence velocities, assess the seismic potential and repeat time for a number of subduction zones.



## FIGURE CAPTIONS

Figure 1

Schematic cross-section of the shallow part of a subduction zone (the uppermost 50 km). This illustrates the hypothesis that a backstop of stronger material extends trenchward at depth. The backstop controls the surface morphology, causing the development of a relatively undisturbed forearc basin and a break in the accretionary wedge slope, here an outer-arc high. Interplate thrust earthquakes, T, do not occur along the entire interface, but stop at a point that we define as the seismic front. Earthquakes within the upper plate occur mainly arcward of this point. The seismic front occurs at approximately the same distance from the trench as the outer-arc high suggesting that the backstop is controlling the location of both features. Interplate earthquakes do not occur below the brittle-ductile transition where higher temperatures favor stable sliding. The depth of this transition and the seismic front together determine the width of the seismogenic zone,  $W$ , the down dip length that ruptures in large thrust earthquakes.  $a$  is the ratio of seismic slip to total slip. The term trench is used to indicate the deepest part of the trench throughout this paper.

Figure 2

Bathymetric profile and earthquake hypocenters along a cross-section perpendicular to the central Aleutian Trench near Adak Island at  $176^\circ$  W longitude. The upper figure shows bathymetry vertically exaggerated by a factor of 3, there is no vertical exaggeration in the lower figure. The hypocenters have been relocated by Engdahl and Gubbins [1986]. The earthquakes are of magnitude 4.8 and greater, and are observed by the local network on Adak Island as well as teleseismically. Note the proximity between the outer-arc high and the seismic front, and the absence of seismicity in the region between the trench and the seismic front.

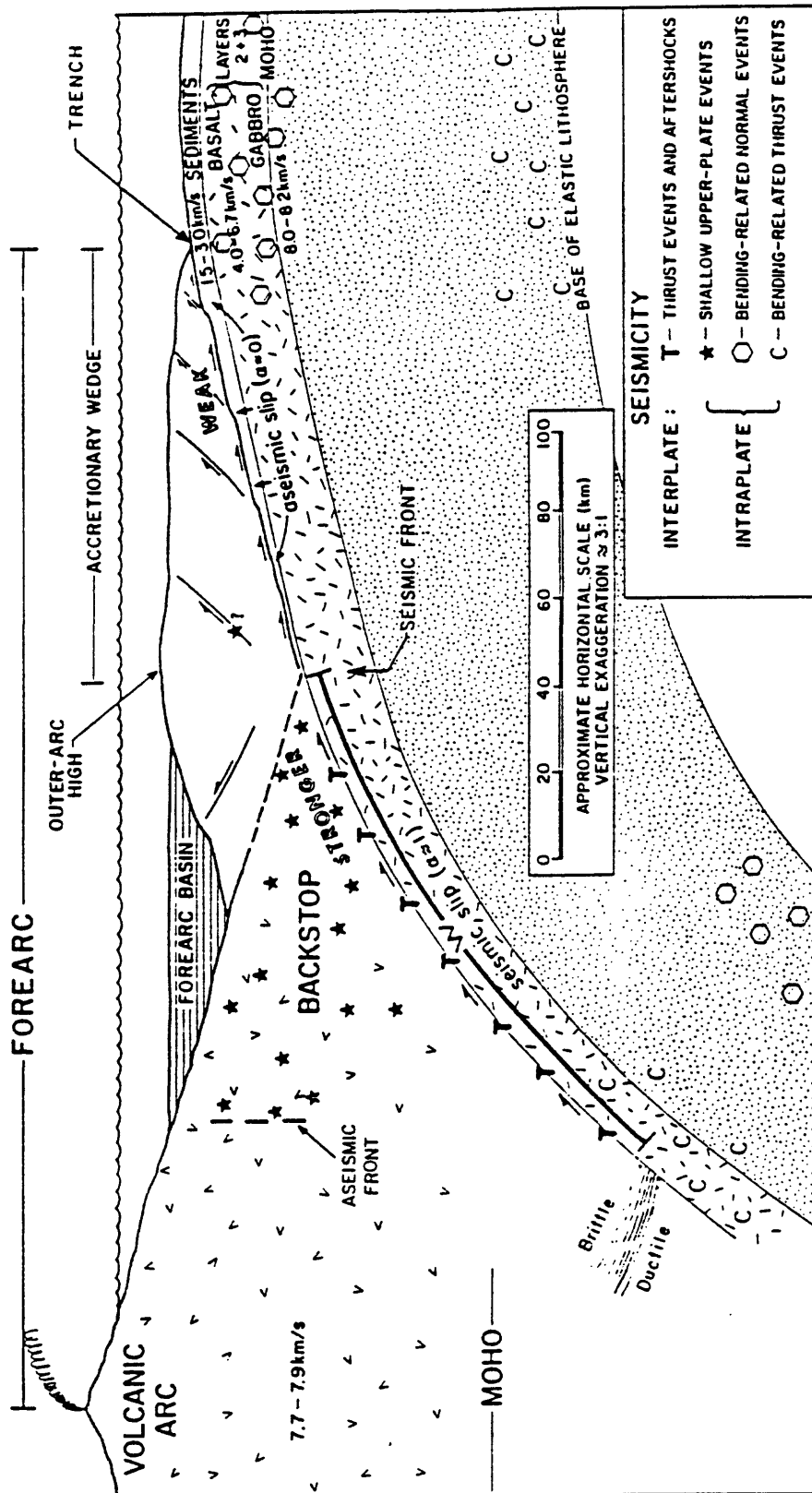
Figure 3

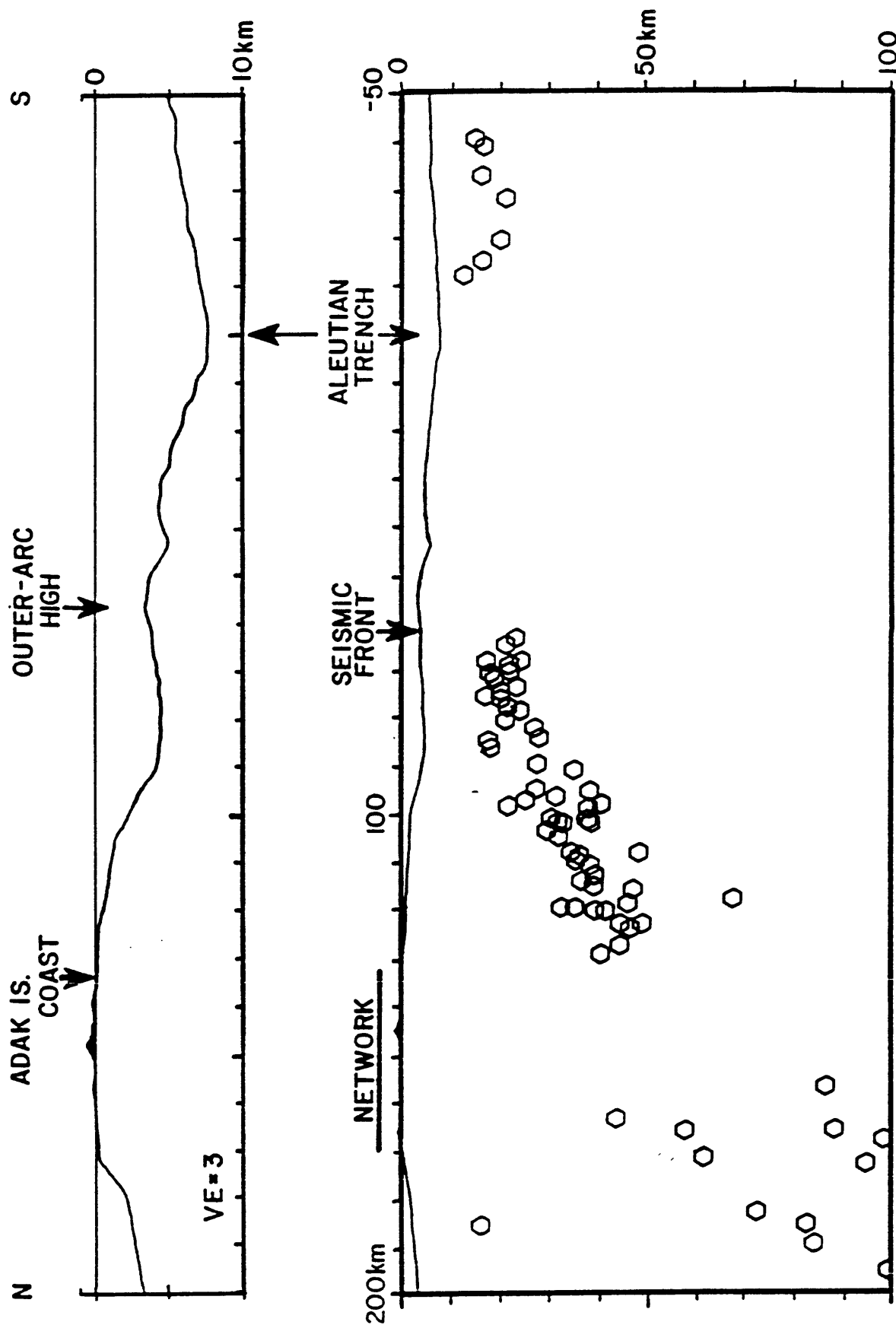
Cross-section of earthquake hypocenters located by two ocean-bottom seismometer (OBS) arrays parallel to Figure 3. The triangles on the ocean floor indicate OBS locations projected into the section. The solid triangles and circles are OBS and earthquake locations from a 1978 survey, and the open symbols are from a 1979 survey. Both surveys supplemented their observations with those of the Adak network. The figure is modified from Frolich et al., 1982. S.F. is the

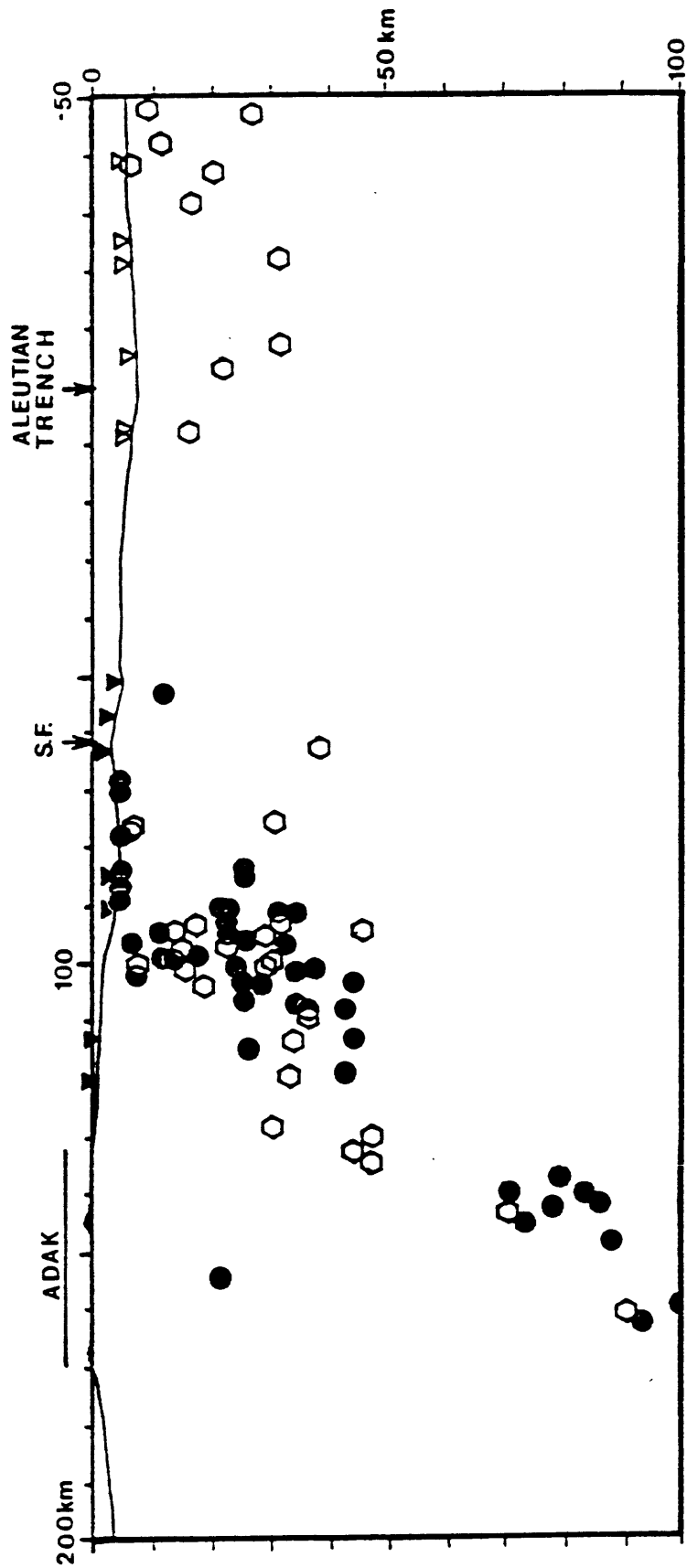
seismic front identified in Figure 5. The seismic front is not as sharply defined with this data set. Note that the region of little or no seismicity between the trench and the seismic front is also observed in this data set. These surveys were able to detect earthquakes down to very small magnitudes, thus if events were occurring in the quiet region they would have been observed. This indicates that for earthquakes of all magnitudes we observe a relatively aseismic region near the trench.

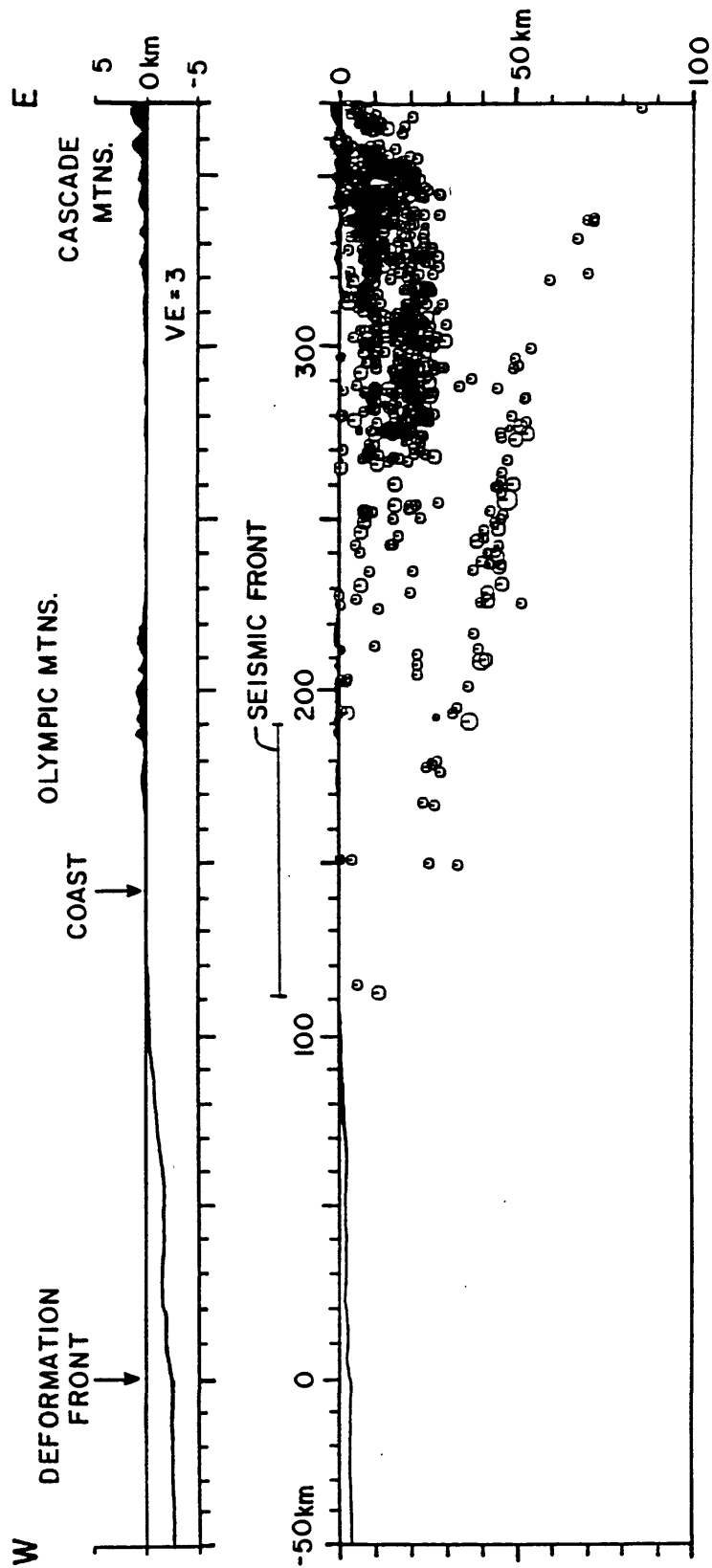
Figure 4

Seismicity, bathymetry, and topography of the Cascadia subduction zone along an east-west cross-section at 47.5° N. The upper figure shows bathymetry vertically exaggerated by a factor of 3, there is no vertical exaggeration in the lower figure. Earthquake hypocenters are from Taber and Smith [1985]. The deeper earthquakes that form an eastward dipping trend are within the lower plate and hence do not define the plate interface or the seismic front. The location of the seismic front is not well determined, but clearly lies at least 110 km landward of the deformation front.









APPENDIX B. 2.

Algorithm of Long-Term Earthquakes' Prediction

by

A. M. Gabrielor, et al.

XERO X - 10 copies  
p 1, 2-13, 18-22, 1  
42-44, 51-52,  
H2. 6. E. P. C.  
number

## Algorithm of Long-Term Earthquakes' Prediction

A.M. GABRIELOV, O.E. DMITRIEVA, V.I. KEILIS-BOROK,  
V.G. KOSOBOKOV, I.V. KUZNETSOV, T.A. LEVSHINA,  
K.M. MIRZDEV, G.M. MOLCHAN, S.Kh. NEGMATULLAEV,  
V.F. PISARENKO, A.G. PROZOROFF, W. RINEHART,  
I.M. ROTVAIN, P.N. SHEBALIN, M.G. SHNIRMAN, S.Yu. SHREIDER.

International School for Research Oriented to Earthquake Prediction-Algorithms,  
Software and Data Handling.  
Curso Internacional Sobre Investigación Orientada a la Predicción de Terremotos-  
Algoritmos, Programática (software) y Procesamiento de Datos.



ACADEMY OF SCIENCES OF THE USSR

O.Yu. SCHMIDT INSTITUTE OF THE PHYSICS OF THE EARTH

COUNCIL FOR SEISMOLOGY AND SEISMORESISTANT BUILDINGS

ALGORITHMS  
OF LONG-TERM EARTHQUAKES' PREDICTION

A.M. GABRIELOV, O.E. DMITRIEVA, V.I. KEILIS-BOROK,  
V.G. KOSOBOKOV, I.V. KUZNETSOV, T.A. LEVSHINA,  
K.M. MIRZOEV, G.M. MOLCHAN, S.Kh. NEGMATULLAEV,  
V.F. PISARENKO, A.G. PROZOROFF, M. RINEHART,  
I.M. ROTVAIN, P.M. SHEBALIN, M.G. SHNIRMAN, S.Yu. SHREIDER.

Editor - Academician M.A. SADOVSKY

PREPRINT

MOSCOW 1986

# CONTENTS

Foreword of the editor (Academician M.A. Sadovsky)	3
Introduction	4
CHAPTER I. DIAGNOSIS OF THE TIME OF INCREASED PROBABILITY OF A STRONG EARTHQUAKE (V.I. Keilis-Borok, V.G. Kosobokov, I.M. Rotvain)	8
CHAPTER II. THE TEST OF ALGORITHM CM	23
Caucasus (I.V. Kuznetsov)	33
East of Central Asia (Pamir and Tien-Shan) (K.M. Mirzoev, S.Kh. Megmatullaev, I.M. Rotvain)	28
Western Turkmenia (O.E. Dmitrieva, T.A. Levshina)	32
Baikal and adjacent regions (I.M. Rotvain)	34
Kamchatka and Kuril arc (S.Yu. Shreider)	35
Vrancea (O.E. Dmitrieva)	38
Central America and Mexico (I.M. Rotvain, W. Rinehart)	39
CHAPTER III. THE TEST OF ALGORITHM MB	42
Caucasus (V.G. Kosobokov)	44
East of Central Asia (Pamir and Tien-Shan) (V.G. Kosobokov, K.M. Mirzoev, S.Kh. Megmatullaev)	44
Western Turkmenia and adjacent territories (V. G. Kosobokov)	46
Baikal and adjacent territories (V.G. Kosobokov)	47
Kamchatka and Kuril arc (V.G. Kosobokov)	47
Vrancea (V.G. Kosobokov)	49
Central America and Mexico (V.G. Kosobokov, W. Rinehart)	49
Western US (V.I. Keilis-Borok, V.G. Kosobokov, W. Rinehart)	51
Conclusion	52
Appendix A. STRONG EARTHQUAKES AND TIPS	53
Appendix B. EARTHQUAKES' CATALOGS USED FOR DIAGNOSIS (P. N. Shebalin)	58
Appendix C. SOFTWARE (I.V. Kuznetsov)	59
References	60

## FOREWORD OF THE EDITOR

The problem of earthquakes' prediction can be posed as a consecutive reduction of space-time domain within which a strong earthquake should be expected. This problem becomes more and more acute, since the potential damage from the earthquakes is rapidly growing due to the growth of the cities and proliferation of high-risk objects. According to UNESCO data, the damage inflicted by the earthquakes averages per decade tens of thousands of casualties and tens of billions of US dollars. A single earthquakes in a heavily populated region may take more than a half a million of human lives, while the damage to economy may run into \$ 100 billion.

Cautious estimates made by Soviet scientists demonstrated that by the end of the century from 20 to 60 million people in the largest cities of the world will experience a catastrophic earthquake.

Along with the increase of seismic risk the arsenal of protective measures designed to reduce it has been expanded. Our country invests more than 1 billion roubles per year in seismoresistant building only.

Earthquakes' prediction is necessary to provide for wider range of protective measures and to increase their cost/benefit ratio. Important discoveries have been made in recent years, but the real performance remains unsatisfactory: failures to predict the time of earthquakes occur too often; successful predictions are not always reproducible; rate of false alarms is too large, though they are not registered regularly.

The algorithms presented here are directly designed to solve rather limited problem: a long-term prediction of the strongest earthquakes of a region, using a part of relevant data. Their advantage is the possibility to start immediately, using only the routine data, i.e. catalogs of earthquakes which are regularly compiled (or ought to be compiled) by existing seismological networks.

At first, this prediction will be experimental, since the algorithms have been tested but retrospectively. The results of this testing yield a promise that the experiment will be successful. Then, predictions by these algorithms will offer a possibility to prevent a considerable damage (though far not the entire one) by way of relatively economical protective measures. Also, such prediction may be useful as a background for subsequent stages of prediction.

This study presents a know-how in exploratory data analysis for earthquakes' prediction with intense attention to the reliability of results. This know-how may help utilize other data. Contrary to natural apprehensions, this approach helps not only to escape unreliable conclusions but to extract more reliable results out of available data.

Finally, presented algorithms may be useful as an insight into the nature of earthquakes' occurrence; they reflect the theoretical concepts of the pseudostochastic nature of seismicity intrinsically related to the problem of earthquake prediction.

In conclusion, let us remind that the release of earthquakes' predictions is a responsible procedure, which requires the strictest regulation and should be executed only by competent scientific institutes. Violation of the procedure may cause the damage of the same scale as the earthquake itself.

Academician M.A.Sadovsky

## INTRODUCTION

1. This paper suggests a methodology for an experiment on long-term prediction of the strong earthquakes on the territory of the USSR and some other countries. "Long-term" means the prediction within 3-5 years and the territory of hundreds of kilometers in linear dimension. This prediction (if the experiment is successful) may be used in the following ways:

(a) To prevent part of the damage, which may be caused by earthquakes. In spite of low precision, long-term prediction is sufficient to undertake series of important and economical protective measures.

(b) To increase the reliability of medium- and short-term predictions\*).

Besides, the algorithms of prediction are of independent interest for theoretical modeling of the dynamics of the lithosphere, since they reflect the regularities in the occurrence of the strong earthquakes, through which a considerable part of the relative motion of lithospheric blocks is realized.

2. The algorithms considered are designed to diagnose the Time of Increased Probability (abbreviated as TIP), utilizing a set of the following traits of the earthquakes' flow:

- The level of seismic activity.
- Temporal variation of activity.
- Space-time clustering.
- Concentration in space.
- Long-range interaction.

The routine catalogs of earthquakes are sufficient to monitor these traits in the most regions of the world. Obviously, we are far from using all the information potentially relevant to prediction.

Two algorithms for the diagnosis of TIPs are considered here; both are based on the traits indicated above. The first was described in [1,2], where the problem of predicting earthquakes with magnitude  $M \geq 6.4$  in California and Nevada was considered. The second was presented in [3,4] where the problem of prediction of the strongest earthquakes,  $M \geq 8.0$ , of the world was considered. These algorithms are denoted as CM and MB respectively.

3. Both algorithms were intended to be applicable in the regions with different seismic activity and different maximal magnitude of earthquakes. Therefore, all the patterns are normalized and a priori rules of transition from one region to another are built in into the algorithms.

---

\* Let us remind that the problem of earthquake prediction is posed, as the consecutive, stage-by-stage, narrowing of the space-time domain, within which a strong earthquake has to be expected. Several stages are distinguished [22,23]; one of them is the long-term prediction, considered here. The division into such stages is partly a drawback of the methods, but partly it may reflect the discrete nature of the process which generates the earthquakes.

In this paper we test the applicability of the indicated algorithms to the following regions:

Caucasus	Kamchatka and Kuril arc
East of Central Asia	Vrancea
Western Turkmenia	Central America and Mexico
Baikal and adjacent regions	Western US

Though the reliability of the algorithms can not be strictly estimated yet, the results of the testing yield hope and provide a base for the decisive test - prediction of the future.

These results support the hypothesis of M.A. Sadovsky on the global selfsimilarity in the occurrence of earthquakes.

4. Such tests are necessary due to the absence of adequate theoretical model, which is the major stumbling block for the present research in earthquake prediction. In lieu of adequate model, the algorithms are based mainly on phenomenological retrospective analysis of seismicity patterns that preceded strong earthquakes in the past. Therefore, the algorithms are formulated and the free numerical parameters are adjusted so as to minimize the number of retrospective errors. This engenders the danger of self-deception, illustrated by figure 1.

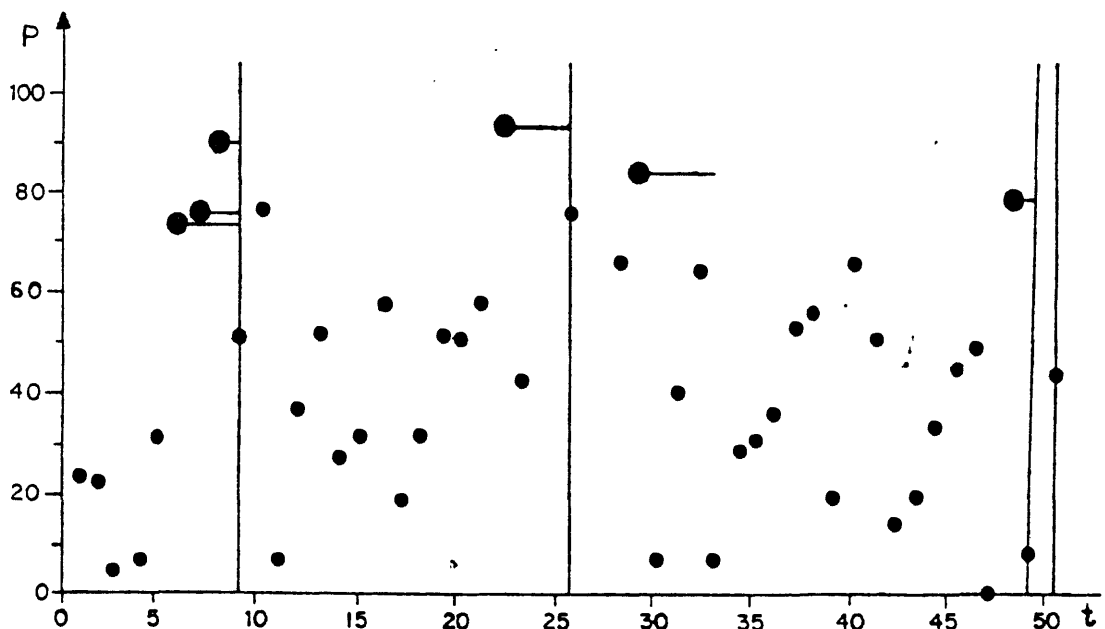


Fig. 1. Illustration of the danger of retrospective data-fitting. The points represent a sample of random integers  $P$  from 0 to 99. Vertical lines correspond to integer 9 in an independent sample of random integers from 0 to 9.  $t$  is the sequence number of an integer in a sample. When  $P \geq \bar{P}$  (large dots), an alarm is declared for time - interval  $\tau$  (horizontal lines). A "satisfactory prediction" of the random integer 9 by independent integers  $P$  is obtained by retrospective data-fitting of two parameters:  $\bar{P} = 70$ ,  $\tau = 5$ .

In order to avoid it we need independent data that had not been used in the design of the algorithms. Few such data are available, since the strong earthquakes occur but rarely and the necessary earthquake catalogs are sufficiently complete for a relatively short time (in the major part of the world - since 60-ies, somewhere - since the 30-ies of this century). In order to expand our data base we have to use jointly the data on many regions. This is possible if we can establish the similarity of the flow of earthquakes in different regions. Practically, we have to establish how to readjust the parameters of the algorithms to a new region.

5. This paper is focused on formulation and test of the abovementioned algorithms, CN and MB. The test consists of retrospective diagnosis of TIPs on independent data. The available ("routine") catalogs of earthquakes are sufficient for this purpose. If the number of failures-to-predict and the total space-time domain occupied by TIPs are both not larger than in retrospection, the test will be successful. Then, the prediction by these algorithms will allow to prevent part of the damage from future earthquakes and will provide a basis for designing better algorithms. The latter is important, since the presented algorithms have essential shortcomings: not all potentially relevant data are used; only long-term prediction and only of strongest earthquakes of a region is ventured. The algorithms are not claimed to be optimal; some modifications are now in progress.

6. From the practical point of view, the territorial uncertainty of prediction is the main weakness of the diagnostics considered here. It might be reduced at the cost of acceptance of some additional hypothesis, limiting the places where strong earthquakes may occur. These places are being identified at present in different ways;

(a) By pattern recognition based on stationary data (geomorphology, gravity anomalies, etc.)

(b) By preliminary stage of the prediction, i.e. identification of the zones, where such earthquakes are due first (e.g. seismic gaps, long-range aftershocks, etc.)

Seismic zoning may serve the same purpose, unless high macroseismic intensity say VIII, is possible in too many places.

7. Different sections of this paper were written by different groups of authors (see Contents). However, each author has taken some part in preparation of each section; this volume presents the results of close collaboration of all the authors.

8. A warning. The concrete prediction of a strong earthquake has to be released only by a qualified scientific body to the proper authorities (see for example the code, established under the auspices of UNESCO and IUGG). The methods, presented here, are insufficiently tested so far and are suggested for the research in earthquake prediction.

The actual forward prediction by these methods can be made so far only on experimental basis and the readers are advised to disclaim any liability for the consequences of the actions, based on their predictions. Accordingly the authors disclaim the liability for any consequences of the use of this paper.

9. The authors will be grateful for any criticism, especially because the methods described are in the stage of further development. We would appreciate also editorial corrections.

#### ACKNOWLEDGEMENTS

The authors are grateful to the colleagues, which provided the significant part of the data used: Drs. Kondorskaya M.V. and Starovoi O.E. (Seismological network of the USSR); Dr. J.Dewey (USGS); Dr. M.Chinnery (US National Geophysical Data Center).

This work was to a large extent facilitated by joint research with University of California, Los Angeles, California Institute of Technology and United States Geological Survey. Significant part of this research was conducted under the auspices of Soviet-American intergovernmental agreement on cooperation in environment protection studies.

We are especially indebted to Academician M.A. Sadovsky: without his permanent support this work could not have been done.

## CHAPTER 1

### DIAGNOSIS OF THE TIME OF INCREASED PROBABILITY OF A STRONG EARTHQUAKE

We assume that the earthquakes' flow includes a large stochastic or pseudostochastic component, so that the symptoms of an incipient strong earthquake may be different each time. Accordingly, our algorithms use a set of premonitory phenomena, while each of them per se may be insufficiently informative; also each phenomenon and the whole set of them are given a rather broad definition.

Both algorithms considered here use the same traits of the earthquakes' flow, but they were designed on different data (see section 2 of the Introduction). The general idea of the diagnosis is illustrated by fig. 2. Each trait listed in fig. 2 is represented by some functions of time defined on the sequence of the main shocks in the territory within a sliding time window. Different functions may correspond to different traits or to the same trait but with different values of numerical parameters (range of magnitudes, length of time interval, etc.). At each moment of time the sequence of earthquakes is represented by the vector of values of these functions.

Our problem is the following: this vector is given at the time  $t$ ; determine whether the time interval  $(t, t + \tau)$  belongs to a TIP;  $\tau$  is a numerical parameter. Similar approach was used in [6] for the study of origin of earthquakes.

#### DEFINITION OF BASIC FUNCTIONS [2]

The sequence of main shocks of a certain territory (region, area) is considered. Let  $t(i)$  and  $M(i)$  be time and magnitude of a main shock numbered  $i$ . Different traits of the earthquakes' flow are represented by the following functions:

Level of seismic activity:

$$N(t; \underline{M}, s) \quad (1)$$

the number of main shocks with magnitudes  $M(i) \geq \underline{M}$  in the sliding time window  $(t-s, t)$ . (Here and in the text below  $P(t; A, B, C, \dots)$  is a function of time  $t$  and numerical parameters  $A, B, C, \dots$ . For example, lower magnitude threshold  $\underline{M}$  and duration  $s$  of a sliding time interval  $(t-s, t)$  are numerical parameters of  $N(t; \underline{M}, s)$ .)

$$\Sigma(t; \underline{M}, s, \alpha, \beta) = \sum_{\{i\}} 10^{\beta(M(i) - \alpha)} \quad (2)$$

the number of main shocks weighted according to  $M(i)$ . The summation is made on the main shocks with magnitude  $M \geq \underline{M}$  from time-interval  $(t-s, t)$ . The value of  $\beta$  is determined by one of two conditions: that each term under summation is roughly proportional to the area of the source or to its linear dimension. If the energy of earthquake depends on magnitude as  $\lg E = A + BM$ , these conditions imply  $\beta = 2B/3$  or  $\beta = B/3$  respectively.



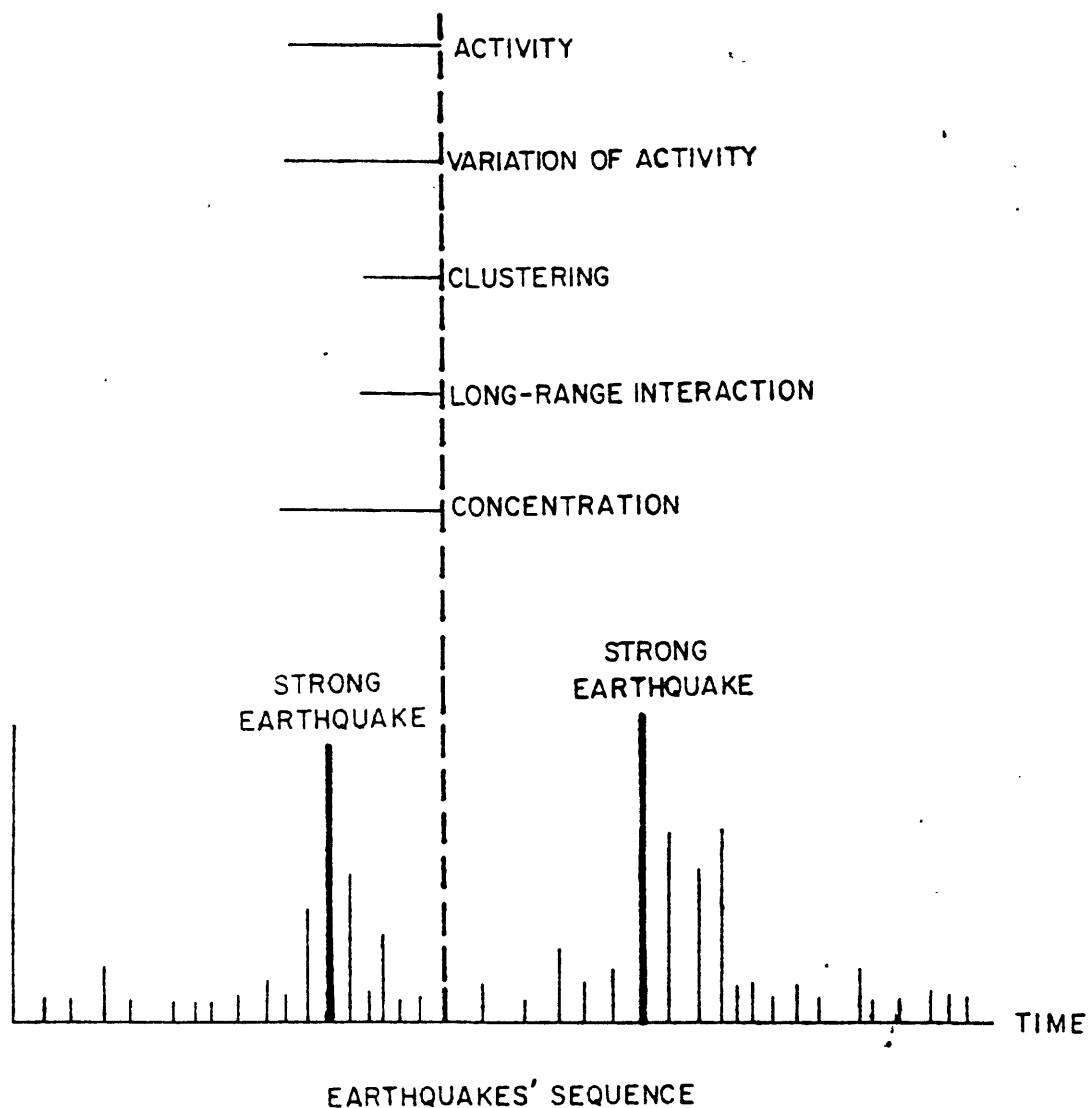


Fig. 2. Scheme of description of earthquakes' sequence for diagnosis of TTPs.

Earthquakes' sequence is described by several integral traits. Horizontal lines show the sliding time windows, on which different traits are defined. All windows end at the common moment of time, shown by dashed vertical line. The traits are attributed to this moment.

$$G(t; \underline{M}_1, \underline{M}_2, s) = 1 - \frac{N(t; \underline{M}_2, s)}{N(t; \underline{M}_1, s)}, \quad \underline{M}_1 < \underline{M}_2 \quad (3)$$

- the ratio of the numbers of main shocks in two magnitude ranges,  $(\underline{M}_1, \underline{M}_2)$  and  $M \geq \underline{M}_1$ .

#### Seismic quiescence:

$$q(t; \underline{M}, s) = \int_{t-s}^t [a(\underline{M})s - N(t; \underline{M}, s)] dt \quad (4)$$

- deficiency of the activity.  $a(\underline{M})$  is the average yearly number of main shocks with  $M \geq \underline{M}$ ,  $f_+(t) = f(t)$ , when  $f(t) \geq 0$ , and  $f_+(t) = 0$ , when  $f(t) < 0$ .

$$Q(t; \underline{M}, s) = \text{Var} \left| \begin{matrix} t \\ t' \end{matrix} N(t; \underline{M}, s) \right. \quad (5)$$

- variation of the number of main shocks  $N(t; \underline{M}, s)$  between  $t$  and its previous maximum  $t'$ . Common definition is meant here:

$$\text{Var} \left| \begin{matrix} b \\ a \end{matrix} f \right. = \sup \sum_{k=1}^{n-1} |f(t_k) - f(t_{k+1})|$$

where sup is taken on all finite sets  $a = t_1 < \dots < t_n = b$  at the interval  $[a, b]$ .

#### Variation of seismicity:

$$L(t; \underline{M}, s) = N(t; \underline{M}, t-t_0) - N(t; \underline{M}, t-t_0-s) \cdot (t-t_0) \cdot (t-t_0-s)^{-1} \quad (6)$$

- deviation from the long-term trend ( $t$  beginning of the catalog).

$$K(t; \underline{M}, s) = N(t; \underline{M}, s) - N(t-s; \underline{M}, s) \quad (7)$$

- difference between the number of main shocks at two successive time-intervals  $(t-s, t)$  and  $(t-2s, t-s)$ .

$$V(t; \underline{M}, s, u) = \text{Var} \left| \begin{matrix} t \\ t-u \end{matrix} N(t; \underline{M}, s) \right. \quad (8)$$

- variation of the number of main shocks  $N(t; \underline{M}, s)$  at the interval  $(t-u, t)$ .

Spatial concentration:

$$S(t; \underline{M}, \bar{M}, s, \alpha, \beta) = \sum (t; \underline{M}, \bar{M}, s, \alpha, \beta) / (N(t; \underline{M}, s) - N(t; \bar{M}, s)) \quad (9)$$

- average area of the fracture surfaces ( $\beta = 2B/3$ )

$$Z(t; \underline{M}, \bar{M}, s, \alpha, \beta) = \sum (t; \underline{M}, \bar{M}, s, \alpha, \beta) \cdot (N(t; \underline{M}, s) - N(t; \bar{M}, s))^{-2/3} \quad \beta = B/3$$

- the ratio of average radius of the fracture surface to average distance between fractures. This function is in inverse proportion to concentration criterion of overall rupture [7].

Along with functions (9), (10) their maxima were considered:

$$S(t; \underline{M}, \bar{M}, s, u, \alpha, \beta) = \max_{[t-u, t]} S(t; \underline{M}, \bar{M}, s, \alpha, \beta) \quad (9a)$$

$$Z(t; \underline{M}, \bar{M}, s, u, \alpha, \beta) = \max_{[t-u, t]} Z(t; \underline{M}, \bar{M}, s, \alpha, \beta) \quad (10a)$$

Clustering in time and space:

$$b(t; \underline{M}, \bar{M}, s, M_a, e) = \max_{\{i\}} b(M_a, e) \quad (11)$$

- maximal number of aftershocks. Here  $b_i(M_a, e)$  is the number of aftershocks with  $M_a \leq M$  of the  $i$ -th main shock at the time interval  $(t(i), t(i) + e)$ ; maximum is taken on the main shocks with  $\bar{M} > M(i) \geq \underline{M}$  in the time interval  $(t-s, t)$ .

Contrast of activity in adjacent areas:

We considered a territory as being in the state of quiescence, if  $N(t; \underline{M}, s) < N_q$  and in the state of activity, if  $N(t; \underline{M}, s) > N_a$ . The thresholds  $N_q$  and  $N_a$  are computed from conditions that p% of time  $N(t; \underline{M}, s) < N_q$  and p% of time  $N(t; \underline{M}, s) > N_a$  in other words, these are the p% and (100-p)% quantiles of  $N(t; \underline{M}, s)$ . Spatial contrast of activity is measured as

$$T(t; \underline{M}, s, p) \quad (12)$$

- the time since the area under study and some adjacent area were in different states for more than a year.

Long-range interaction.

It is characterized by two phenomena. One is suggested by A. Prozoroff: a strong earthquake activates the places where one of the next strong earthquakes is due. A main shock that had occurred within  $u$  years after an earthquake with

$M \geq M_0$ , is called a long-range aftershock. As before, only the main shocks of certain territory are considered. Maximal (during  $s$  years) magnitude of long-range aftershock is the measure of interaction:

$$M(t; s, M_0, u) = \max_{i \in \{i\}} M(i) \quad (13)$$

where maximum is taken on long-range aftershocks in the time interval  $(t-s, t)$ .

Another measure of long-range interaction is the simultaneous activation of several interrelated territories. It was measured as

$$N(t; M, s) \quad (14)$$

R

- the value of  $N(t; M, s)$  in the territory of higher rank, which includes the territory under consideration.

#### NORMALIZATION OF THE FUNCTIONS

We define the magnitude thresholds  $\bar{M}$ ,  $\bar{M}'$  in such a way as to normalize the values of the functions considered. Normalization is necessary to apply the algorithms to territories different in seismic activity and in the maximal possible magnitude, without returning to data-fitting of the numerical parameters.

The normalization to seismic activity was made by the choice of the magnitude threshold from the condition  $a_u(M') = a$ , where  $a_u(M')$  is the yearly average number of main shocks with  $M \geq M'$  in the territory  $U$ ,  $a$  is a numerical parameter, common for all territories.

The normalization to  $M_0$  was made by the magnitude thresholds  $(M_0 - c)$ , where  $c$  is a numerical parameter common for all territories.

As a rule,  $\bar{M}$  was defined in the first way and  $\bar{M}'$ ,  $M_0$  were defined in the second way.

#### ALGORITHM CN [1,2]

##### Reduction to Pattern Recognition.

Let us consider several regions divided into smaller areas. The flow of earthquakes in each territory (a region or an area) is represented by the vector  $P_u(t) = (P_{u1}(t), \dots, P_{um}(t))$

where  $P_{ui}(t)$  is one of the functions introduced earlier.

Our problem, again, is the following: knowing  $P_u(t)$ , determine whether the probability of a strong ( $M \geq M_0$ ) earthquake in the territory  $U$  and in the time interval  $(t, t+T)$  has increased.

In pattern recognition parlance, the combination of time and territory ( $u, t$ ) represented by vector  $P_u(t)$  is the object of recognition. The objects of two classes are distinguished.

- class D includes the territories where a strong earthquake will occur within  $\tau$  years;

- class N includes the territory in all the other time-intervals.

The examples of objects D and N (learning material) are also given. By analysis of these examples (learning) we have to formulate a rule of recognition, which allows to determine by the known  $P_u(t)$  whether the time interval  $(t, t+\tau)$  belongs to D or N.

#### Data analysis [2]

The territory of California and adjacent parts of Nevada was divided into Northern and Southern regions; each of them in turn was divided into three areas. We assumed  $M_0 = 6.4$ . The problem was solved in two stages: TIP was diagnosed first for the regions, next for the areas.

At the first stage we used functions and the numerical parameters indicated in table 1.

In order to represent the vector  $P_u(t)$  in a binary code, the range of the values of each function was divided into 2 or 3 intervals, each interval containing equal number of objects D and N. For this discretization the last moments before each strong earthquake were taken; the moments within 3 years after each strong earthquake were eliminated from class N. The thresholds of discretization computed in that way are shown in table 1. By definition, single threshold coincides with the median of the corresponding function; two thresholds coincide with the quantiles of the levels 1/3 and 2/3.

The features of the classes D and N found by the algorithm "Subclasses" are shown in table 2.

No.	$M, s=6$	K	$\Sigma$	$z_{max}$	$M(t-6)$	L	$M_f$	$\theta$	$M_R$
				Features N					
1.				S or L	M, L				S, M
2.				M, L	M, L				S, M
3.			S, M		M, L				S, M
4.		M, L			M, L				S, M
5.	S, M						M, L	S, M	
6.	S, M					S, M		S, M	
7.			S, M		M, L			S, M	
8.	S, M			S or L				S, M	
9.				S or L	M, L		S, M		
10.			S, M		M, L		S, M		
11.			S	S, M	M, L				
12.				S or L	M, L				
13.	S, M				M, L				

NOTE: Notations as in Table 2.

#### ALGORITHM MB [3,4]

Formulation of the problem is similar to the one formulated earlier. The vicinities of the places, where earthquakes with  $M \geq 8.0$  may occur, were considered. The distribution of earthquakes in each vicinity U is represented by the vector  $P_U(t)$ , its components are some of the functions indicated above. Our problem is to find the rule by which one can decide whether the time interval  $(t, t + \tau)$ , belongs or does not belong to a TIP for an earthquake with  $M \geq 8.0$ .

The vicinities U were chosen as the rectangles on the geographical grid

$$U(\varphi_0, \lambda_0) = \{(\varphi, \lambda) : |\varphi - \varphi_0| \leq 6^\circ, |\lambda - \lambda_0| \leq 6^\circ / \cos \varphi_0\}$$

132 epicenters of all earthquakes with  $M \geq 8.0$  in 1885-1982, according to [11], were taken as the centers of the rectangles; added were 2 epicenters of the strongest earthquakes in XIX century in California and 9 points near which the earthquakes with  $M \geq 8.0$  are possible, though yet unknown, according to [19]. The components of vector  $P_U(t)$  were the functions (1), (2), (6)-(11). Components representing the same function with different values of numerical parameters compose a "group".

Vector  $P_U(t)$  was computed for the catalog of earthquakes [11] at discrete moments of time  $\{t_j\}$ , with half-a-year step.

We hypothesize an anomalous activation of the earthquakes' flow before a earthquake. Accordingly, the algorithm was adjusted in the following way [3].

1. We selected p% of largest values of each component of vector  $P_U(t)$ . The selection was made in the time interval from 1965 to the end of the catalog or to the moment of the earthquake which determined the center of U. Such values are called "abnormally large". We assumed p=10 % for all the functions except b and p=25 % for b.

2. For each vicinity U the following 2 numbers were defined on a sliding time-interval  $(t-3 \text{ years}, t) = \Delta t$ :

$h_U(t)$  - shows how many components of  $P_U(t)$  became abnormally large within  $\Delta t$ ;

$g_U(t)$  - shows how many groups of components of  $P_U(t)$  had at least one abnormally large member within  $\Delta t$ .

3. If  $h_U(t)$  and  $g_U(t)$  are sufficiently large at two successive moments  $t_{k-1}$  and  $t_k$ , TIP is declared for the time-interval  $(t, t_k + \tau)$  in the territory U.

Unlike [3], in our test TIP is not terminated by a strong earthquake. However, in the description of the results, we will indicate the time-space domain of "expectation" of strong earthquakes; it includes the part of each TIP from its beginning to the moment of strong earthquake or to the end of the TIP, whichever comes first.

According to [11], in 1965-1982 9 earthquakes with  $M \geq 8.0$  had occurred in the world. In the vicinities of 3 of them the catalog [11] shows very few earthquakes with  $M \geq 4$  ( $a_U(4.0) < 4$ ), so that these territories were excluded from consideration.

Acceptable results are obtained in [4] for 6 modifications of the algorithm. They differ in the choice of the functions and the values of the parameters. The sum of the TIPs in each modification was less than 7.5% of the total time-space domain; and the TIPs covered 4 out of 6 earthquakes with  $M \geq 8$ .

These 6 modifications are mutually dependent. We used one of them which is considered in [4] as the main one. It will be called algorithm MB.

#### FORMULATION OF ALGORITHM MB

1. Vector  $P(t)$  is composed by the following functions:

$$\begin{aligned} M(t; M(10), 6), \\ M(t; M(20), 6), \\ L(t; M(10), 6), \\ L(t; M(20), 6), \\ Z(t; M(10), M_0 = 0.2, 6, 5, 0.91), \\ Z(t; M(20), M_0 = 0.2, 6, 5, 0.91), \\ b(t; M = 2, M_0 = 0.2, 1, M_0 = -4, 30 \text{ days}) \end{aligned}$$

(time constants are given in years, except the value of e in function b).

2. TIP is declared in U for the interval  $(t_k, t_k + 5 \text{ years})$  if at two successive moments  $t_{k-1}, t_k$  we have:

$$h_U(t) \geq 6, g_U(t) = 4.$$

# TEST OF THE ALGORITHMS ON INDEPENDENT DATA

It is clear from the preceding description that algorithm CN requires less representative catalogs, i.e. it uses the earthquakes with higher magnitudes. Algorithm MB is simpler. In algorithm CN seismicity and morphostructures are taken into account, though not in a formalized way, to choose the territories for diagnosis. In algorithm MB this choice is more formal; this has some advantages and some disadvantages. In some regions algorithm CN allowed to diagnose the TIPs before more frequent earthquakes (i.e. for smaller values of  $M_0$ ). Algorithm MB is less resolving in time, since larger  $\tau$  is assumed. Both algorithms are not claimed to be optimal; we hope that they reflect the same general regularity in the occurrence of strong earthquakes.

Exact assertion about each algorithm is the following: "Within the territories and during the years considered most of the strong earthquakes were preceded by the situation diagnosed as TIPs; and most of such situations were followed by strong earthquakes within  $\tau$  years".

However, since the algorithms were constructed retrospectively, the question remains open, whether they really diagnose the TIPs, thus reflecting real regularities in the occurrence of strong earthquakes.

In order to answer this question, it is necessary to test the algorithms on independent data. Sufficient data may be collected in a reasonable time only if we assume the similarity of earthquakes' flow in different territories, as is implied by the concept by Academician M.A. Sadovsky on the self-similarity of the process which generates the seismic activity.

We describe in the next chapters the retrospective test of both algorithms on the territories indicated in the Introduction. All these territories together produce one or two earthquakes with  $M \geq M_0$  each year.

The following general ground rules were assumed.

1. Seismic territories are considered within generally accepted boundaries (see, for instance, [9]). In the algorithm MB each territory was scanned by intersecting rectangles, each rectangle is formed by some meridians  $\lambda_1, \lambda_2$  and parallels  $\varphi_1, \varphi_2$ . Its size depends on  $M_0$  as

$$l = (\exp(M_0 - c) + 2\epsilon)^0$$

where  $c$ ,  $2\epsilon$  are numerical parameters. This dependence on  $M_0$  is about the same as suggested in [9]:  $lgR = 0.43 M$ , where  $R$  is the maximal distance within which precursors of earthquakes with magnitude  $M$  were reported. We calculated  $c$  from the condition:

$$l = 12^0 \text{ for } M_0 = 8$$

(as in [3,4] where the algorithm was designed). Assuming  $2\epsilon = 1^0$  we obtain

$$l = (\exp(M_0 - 5.6) + 1)^0.$$



2. In the algorithm CN in all the regions, except Kuril arc and Kamchatka,  $M_0 = 6.4$  was assumed - the same as in [1,2]. In algorithm MB the size of the scanning rectangle is determined by the value of  $M_0$ , according to the last relation.

3. The catalog of main shocks is obtained by the algorithm of identification of aftershocks described in [5]. Exceptions will be specially indicated. The identification of aftershocks is intentionally robust. The number of aftershocks  $b_k$  was counted for  $M \geq 2.75$  unless otherwise indicated; for "the energy class"  $k$  given in [9,10] this corresponds to  $K \geq 9$ .

4. The magnitude thresholds are defined by the rules of normalization of the functions indicated above.

5. Time-scale and, therefore, numerical parameters measured in the units of time were not changed.

6. Discretization of the functions. In the algorithm CN "large", "medium" and "small" values of a function were separated by the quantiles of 1/3 and 2/3 level; "large" and "small" - by median. In the algorithm MB an "abnormally large" value of a function was separated by the quantile of 0.9 level except 0.75 level for  $b(t)$ . Thus, the thresholds were defined by an apriori rule; actually, they normalize the functions.

7. In the algorithm MB the value of  $B = 1.37$  was assumed as in [3,4].

In general, these rules provide for practically unambiguous change of all parameters for transition to a new territory.

However, the experiment is not strict due to some freedom in several decisions, such as the following: the choice of  $M_0$ ; the choice of boundaries of regions and areas in algorithm CN (the boundaries were drawn according to seismotectonics; we tried to minimize, but could not avoid, the intersection of boundaries with major lineaments and hence with clouds of epicenters); a posteriori change of the threshold  $\bar{\Delta}$  in few cases, which will be indicated. Let us note, that a change of  $\bar{\Delta}$  does not nullify the success of a test completely: it shows that the approach of a strong earthquake is still characterized by the same seismicity patterns.

Additional tests were necessary due to retrospective nature of our analysis. Following the suggestions of G.M. Molchan and M.G. Shnirman we evaluated some dangers of artificial improvement of results due to the use of information about strong earthquakes.

(i) The thresholds of discretization of the functions in algorithm CN were determined on a sample of objects D and N; their identification is based on the known times of strong earthquakes. To avoid this, one may try to use the thresholds obtained for California and Nevada [1,2].

(ii) In algorithm MB the thresholds of discretization of the functions were determined on the interval before a strong earthquake. It is not much longer than the accepted duration of alarm ( $T = 5$  years) since the diagnosis in the algorithm was made on the interval 10-12 years. Hence, the danger to succeed by chance increased. In order to reduce it, the possibility of determination of thresholds of discretization on a larger period of time is to be explored.

(iii) In [3] the threshold  $M$  was the same for the whole period of time. However after a strong earthquake a seismic activation is possible, which may be not completely suppressed by the exclusion of aftershocks. If that is the case, then the main shocks before a strong earthquake may be more irregular than after it. This increases the probability to meet abnormally large functions, to diagnose a TIP and to "succeed" by chance.

In order to eliminate this danger,  $M$  also ought to be determined on the interval, preceding strong earthquake.

\* \* \* \*

The retrospective test of algorithm CN on independent data is described in Chapter II; that of algorithm MB - in Chapter III. The results are summarized in the beginning of each chapter.

We eliminated from English version numerous statistics of main shocks; they are available at request.

# CHAPTER III

## THE TEST OF ALGORITHM M8

Algorithm M8 was applied to the following territories: Caucasus, East of Central Asia (Pamir and Tien-Shan), Western Turkmenia and adjacent territories, Baikal and adjacent territories, Kamchatka and Kuril arc, Vrančea, Central America and Mexico, Western US.

The rules of the test are formulated above in Chapter 1. The earthquakes' catalogs available are sufficiently complete since 1962 for most of the regions within USSR and for Vrančea and since 1964 for most of other regions. This allows to diagnose TIPs since 1975 and 1977 respectively. Numerical parameters of the algorithm are the same as in (3); exceptions will be pointed out.

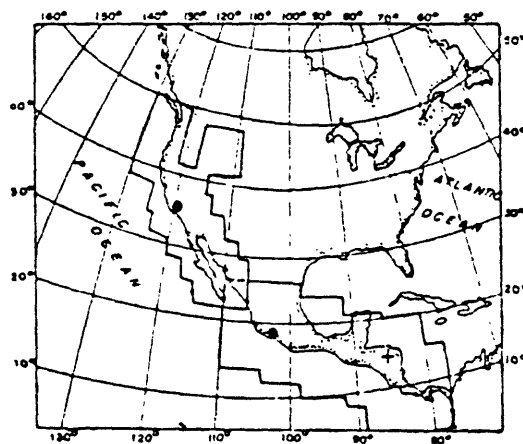
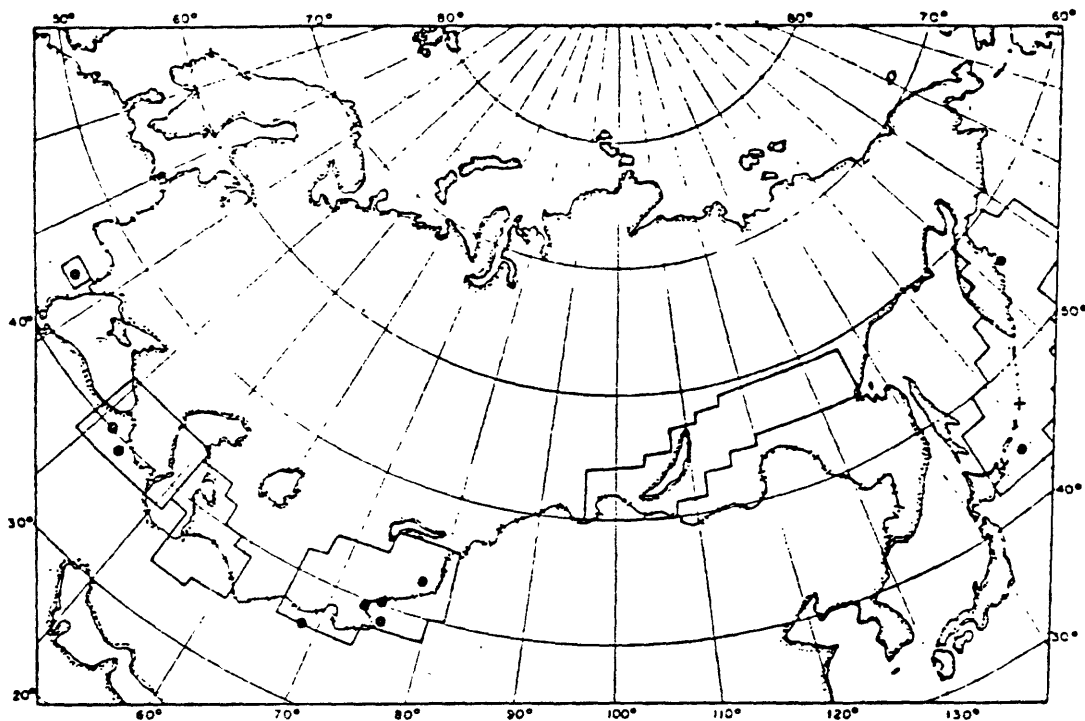
The results are summarized in Table 12 and fig. 19. TIPs and strong earthquakes are also given in Appendix A.

TABLE 12

Test of algorithm M8; summary of results.

Territory	M <sub>0</sub>	Period of diagnosis	Strong earthquakes <sup>1)</sup>		Space-time volume, 10 <sup>6</sup> km <sup>2</sup>		
			Total	Within TIPs	TIPs	Expectations <sup>2)</sup>	Total (100%)
Caucasus	6.5	1975-1983	2	1	1.1 (16%)	0.6 (9%)	6.8
East of Central Asia	6.5	1975-1983	4(1)	4(0)	3.2 (28%)	1.5 (14%)	11.2
W. Turkmenia and adjacent territories	6.5	1975-1983 <sup>3)</sup>	-	-	0	0	1.7
Baikal and adjacent territories	6.7	1975-1983 <sup>4)</sup>	-	-	0	0	8.6
Kamchatka and Kuril arc	7.5	1975-1983	1(1)	1(1)	4.7 (25%)	1.8 (10%)	18.6
Vrančea <sup>5)</sup>	6.5	1975-1983	1	1	0.67(56%)	0.26 (2%)	1.2
Central America and Mexico	8.0	1977-1983	-(1)	-(1)	12.0 (20%)	12.0 (20%)	59.0
Western US	7.5	1977-1984	-	-	1.3 (4%)	1.3 (4%)	33.1
Southern California	7.5	1947-1985.6	1	1	3.2 (13%)	0.3 (1%)	24.9
All territories together:			9(3)	8 (2)	26.17(16%)	17.76(11%)	165.1

Notes: 1) Strong earthquakes, which occurred after the end of catalog, are



— 1      ● 3  
● 2      + 4

Fig. 19. Test of algorithm M3.  
a - Eurasia, b - North America.

- 1 - Boundaries of territories considered.
- 2 and 3 - Epicenters of strong earthquakes preceded and not preceded by TTPs.
- 4 - Centers of the windows where false alarms were diagnosed.

indicated in brackets.

- 2) Expectation means the part of a TIP up to the strong earthquake.
- 3) Since the beginning of catalog [9] is insufficiently complete, only years 1981-1983 are included in space-time volume.
- 4) For eastern Sayan the period starts from 1979; for Stanovoi ridge - since 1980.
- 5) Due to incompleteness of catalog  $M$  (10) and  $M$  (20) are replaced by  $M$  (3).

## CAUCASUS

The territory considered is shown in fig. 20. It is scanned by 10 overlapping rectangular windows  $4^\circ \times 4^\circ$  (their centers are shown in fig. 20).

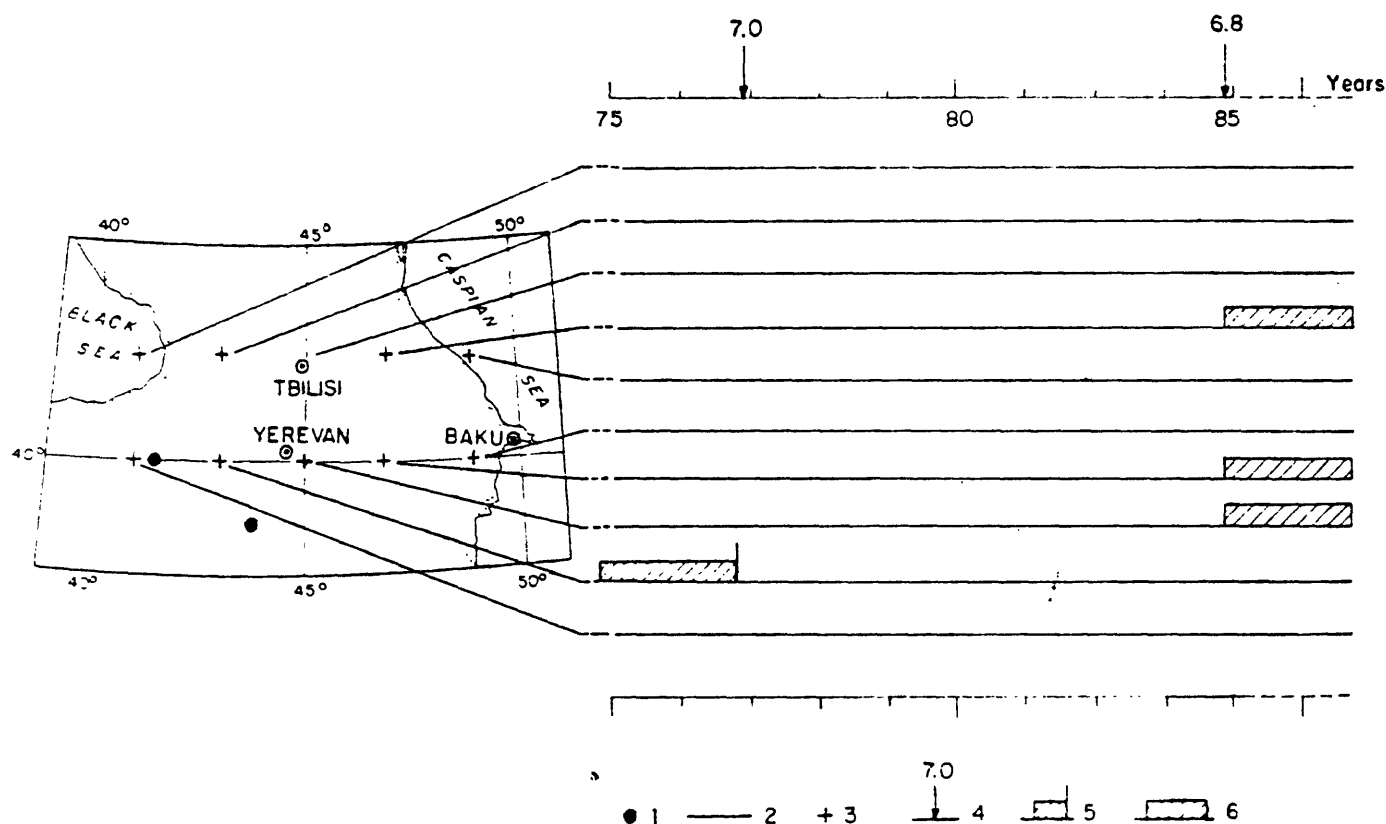


Fig. 20. Strong earthquakes and TIPs diagnosed by algorithm M8 in Caucasus.  
 $M_0 = 6.5$ .

- 1 - Epicenters of strong earthquakes, 1975 - 1985.
- 2 - Boundary of territory
- 3 - Centers of windows for diagnosis.
- 4 - Moment and magnitude of strong earthquake.
- 5 and 6 - TIP interrupted and not interrupted by strong earthquake.

# WESTERN US

The territory, considered is shown in fig. 25. It includes California and Nevada, which provided the data for the design of algorithm CN.

The territory was scanned by 8 overlapping rectangular windows 7° in latitude and 9° in longitude; their centers are shown in fig. 25. This size, allowing for the width of seismic belt here, roughly corresponds to  $M_0 = 7.5$ , which we assumed. No strong earthquakes occurred here during the time considered. We used catalog [11]. It seems complete for  $M \geq 4$ . The average annual number of main shocks  $\mu(4.0)$  in a window varies from 10 to 40. It is below 20 (the minimum, required by algorithm) in three windows: two in the Gulf of California and one in the Rocky Mountains within Idaho. The lower magnitude thresholds  $M(20)$  lie between 4 and 4.25.

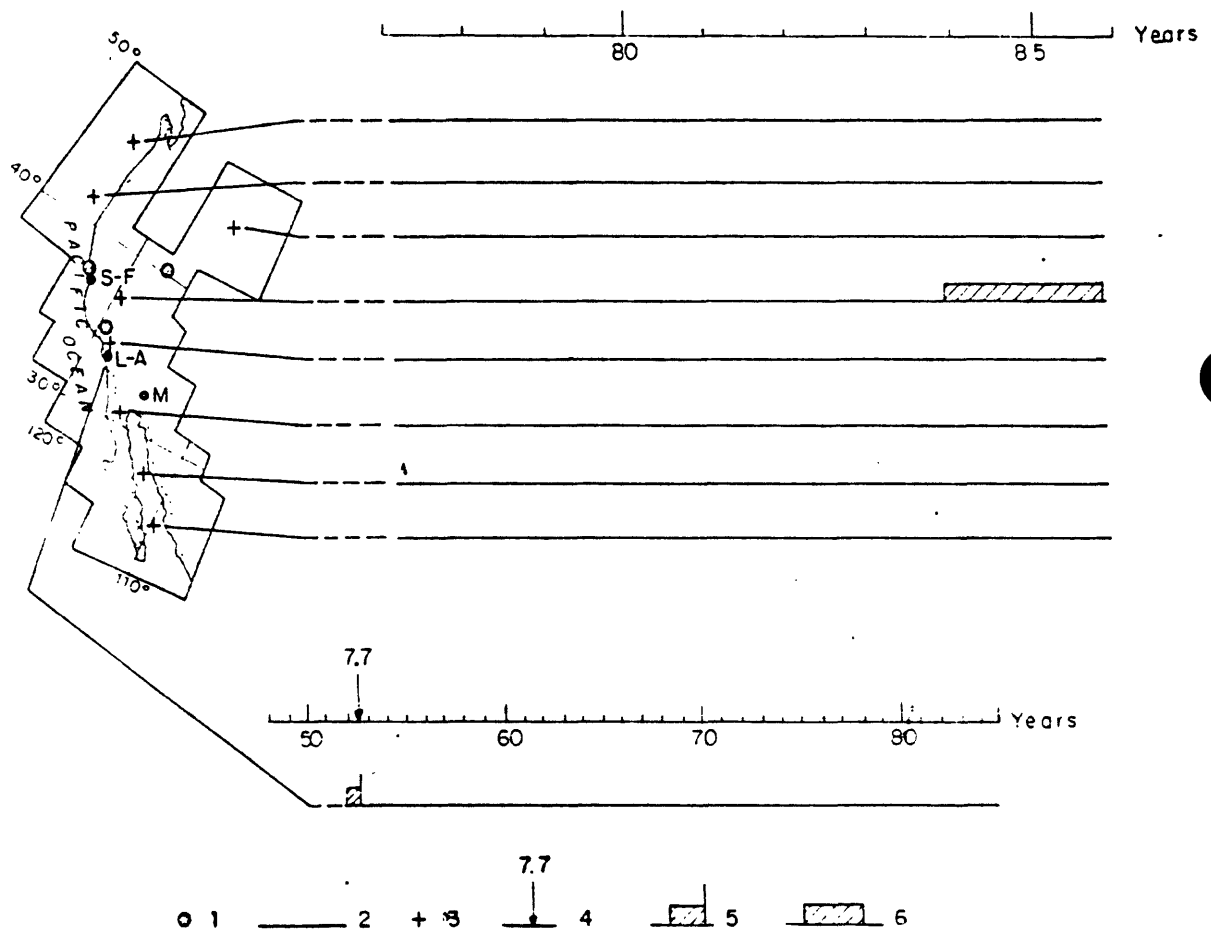


Fig. 25. Strong earthquakes and TIPs diagnosed by algorithm MB in Western US.  
 $M_0 = 7.5$

- 1 - Epicenters of strong earthquakes 1900-1983 (none occurred after 1977).
  - 2 - Boundary of territory.
  - 3 - Centers of windows for diagnosis.
  - 4 - Kern County earthquake: moment and magnitude.
  - 5 and 6 - TIP interrupted and not interrupted by strong earthquake.
- Cities from North to South: San Francisco, Los Angeles, Mexicali.

TIF diagnosed is shown in fig. 25. The rough integral estimate is the following:

- total volume considered is  $33.1 \times 10^6 \text{ km}^2 \times \text{year}^{-1}$
- TIF occupies  $1.3 \times 10^6 \text{ km}^2 \times \text{year}^{-1}$  (4%)

This suggests the small volume of alarms, but does not answer the question, whether TIFs could be expected here before strong earthquakes.

To get some indication, we considered the window, centered around Kern County earthquake of 1952,  $M = 7.7$ . For this window a much longer catalog [12] is available. Main shocks were separated exactly as for the regions, considered above. The estimate of lower magnitude threshold  $M(20) = 4.25$ .

TIF diagnosed in this window for 1948 - 1985 is shown in the lower line of fig. 25.

The rough integral estimates are the following:

- volume considered is  $24.19 \times 10^6 \text{ km}^2 \times \text{year}$
- TIF occupies  $3.2 \times 10^6 \text{ km}^2 \times \text{year}$  (13%).
- expectation occupies  $3 \times 10^6 \text{ km}^2 \times \text{year}$  (1.3%).

This TIF precedes the only strong earthquake - Kern County, 1952.

\*\*\*

The test for  $M \geq 7.5$  in the Western US seems satisfactory. The current TIF should be studied in details.

#### CONCLUSION

The test of algorithms CM and MB on independent data seems, as a whole, encouraging. The set of seismicity patterns involved in diagnosis is obviously relevant to the approach of strong earthquakes. The diagnosis is consequential both for the search of new methods for more definite prediction and directly for some damage prevention.

At the same time the methods used are open for improvement: only a part of relevant and available data was used; the description of seismicity is hardly complete, nor defined in an optimal way; space, time and energy scaling remains a problem; the possibility of diagnosis for different ranges of magnitude in the same region is not explored; etc.

In spite of limitations, forward monitoring of the Time of Increased Probability of strong earthquakes by the algorithms CM and MB seems to be justified indeed, though each prediction should be handled with necessary precautions.

Table 14 (continuation)

TIPs			Strong earthquakes ( $M \geq M_0$ )		Time of expectation, months
Center of window		Time	date	M	
$\varphi^\circ$	$\lambda^\circ$				

Central America and Mexico,  $M_0 = 8$ ;  $12^\circ \times 12^\circ$ ; 1977-1983

14	-86	1980.07.01-1985.07.01	-	-	60
20	-104	1984.01.01-1989.01.01	1985.09.19	8.2	21

Western US;  $M_0 = 7.5$ ;  $7^\circ \times 9^\circ$ ; 1977-1985.02  
(Southern California, 1948-1985.02)

34.5	-118.5	1952.01.01-1956.01.01	1952.07.21	7.7	7
37.5	-119.5	1984.01.01-1988.01.01			24

NOTES: \*) Diagnosis starts in 1979 for Eastern Sayan mts and in 1980 for Stanovov ridge.

\*\*)  $M(10)$  and  $M(20)$  are replaced by  $M(3)$ .

Time of expectation is estimated up to 1986.01.01.



APPENDIX B. 3.

Summary of Parkfield Alerts, June 1985 to March 1987

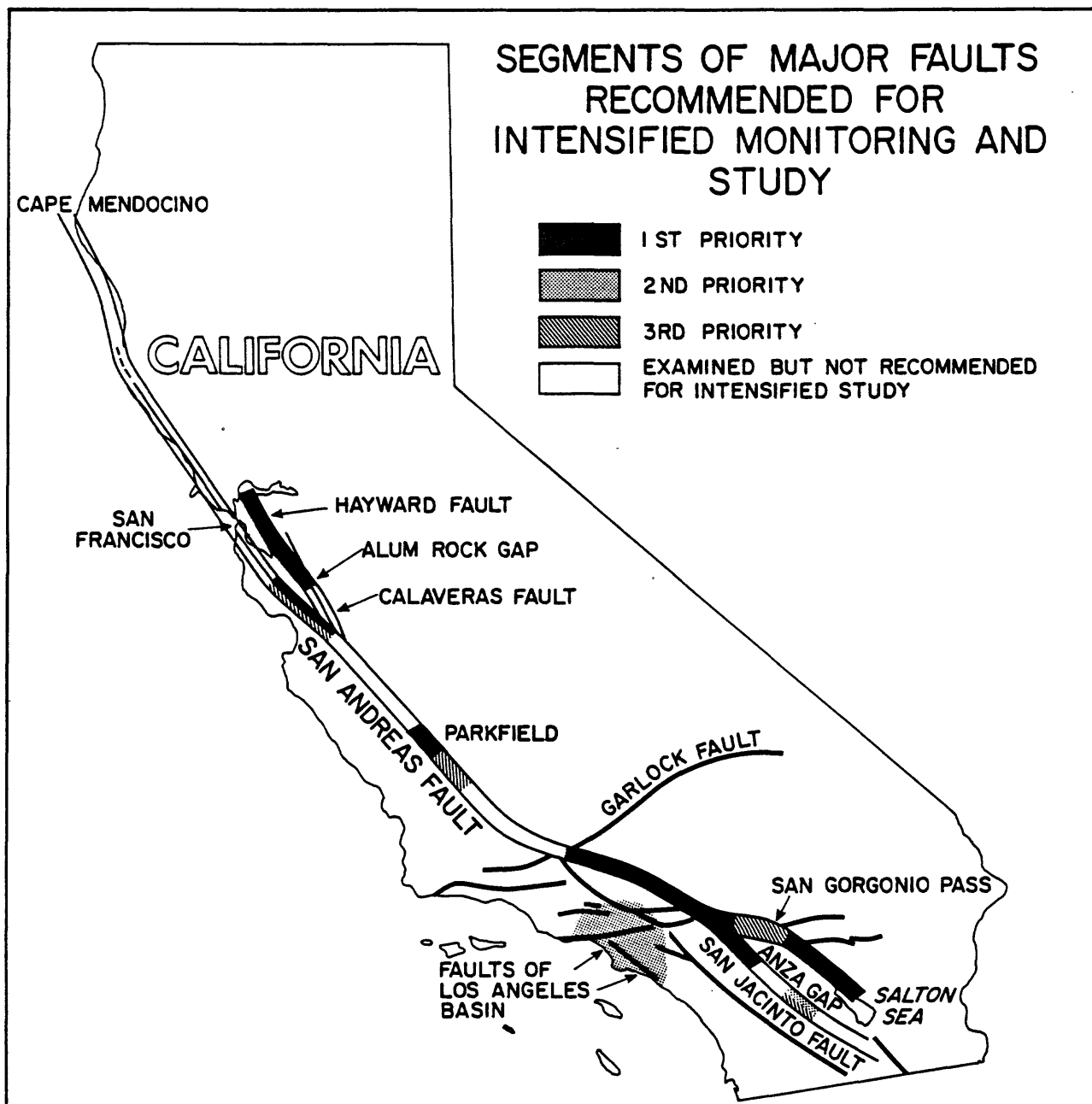
Summary of Parkfield Alerts  
June 1985 - Mar 1987

<u>Date</u>	<u>Source Network</u>	<u>Observed Data</u>	<u>Alert Level</u>	
06/08/85	Earthquake (Middle Mountain)	M = 1.5	d	
07/12/85	Earthquake (Parkfield)	M = 3.0	d	
08/06/85	Two-Color Laser	Co- and Post-seismic changes from Kettleman Hills earthquake	d	
10/10/85 -11/10/85	Creep (XPK1)	1.5 mm Creep Surge	d	
12/14/85	Earthquake (Parkfield)	M = 3.1	d	combine to
12/17/85	Creep (CRR1)	1mm creep surge	d	c-level alert
12/29/85	Creep (CRR1)	2mm creep surge	d	combine to
12/30/85	Earthquake (Parkfield)	M = 2.9	d	c-level alert
01/01/86	Creep (XMM1)	0.4mm creep event	d	
01/15/86	Earthquake (Parkfield)	M = 2.6	d	
01/28/86	Earthquake (Middle Mountain)	M = 2.2	d	combine to
01/30/86	Water Well (Turkey Flat)	0.05 PPM	d	c-level alert
03/04/86	Earthquake (Parkfield)	M = 2.5	d	
04/02/86	Earthquake (Middle Mountain)	M = 2.1	d	
04/08/86	Two-color laser	deep slip event?	d	
04/18/86 -04/26/86	Creep (XPK1)	0.8mm Creep Surge	d	
04/26/86	Earthquake (Parkfield)	M = 2.5	d	
06/08/86	Earthquake Middle Mountain	M = 1.3, 1.2	d	
06/07/86 -06/19/86	Creep (XTA1)	1.1 mm Creep Surge	d	
06/15/86	Water Well (Turkey Flat)	0.06 PPM	c	
06/12/86 -07/01/86	Creep (CRR1)	1.2 mm Creep Surge (left lateral)	d	

08/04/86	Earthquake (Middle Mountain)	M = 1.7	d
8/17/86	Creep (XGH1)	1.5 mm Creep Event	d
8/29/86	Earthquake (Parkfield)	M = 3.5+	c
09/01/86	Earthquake (Parkfield)	M = 2.8	d
09/03/86	Creep (XMM1)	3.5 mm Creep Event (ampl. affected by site visic)	c
09/16/86 -09/26/86	Creep (CRR1)	0.6 mm Creep Surge	d
09/19/86 -10/10/86	Creep (XPK1)	0.5 mm Creep Surge	d
10/10/86	Earthquake (Middle Mtn)	M = 1.6	d
10/25/86 -12/04/86	Creep (CRR1)	4.0 mm Creep Surge	d
12/24/86	Earthquake (Middle Mtn)	M = 1.1, 1.1	d
01/02/87	Earthquake (Middle Mtn)	M = 1.2, 1.2	d
02/01/87	Water Well (Middle Mtn)	0.2 PPM	d
02/02/87	Earthquake (Middle Mtn)	M = 2.7	c
02/03/87	Earthquake (Middle Mtn)	M = 1.7	d
02/13/87 -02/27/87	Creep (WK R1)	1 mm Creep Surge	d
02/21/87	Creep (XMM1)	0.7 mm Creep Event	d
03/14/87	Earthquake (Middle Mountain)	M = 1.6	d

APPENDIX B. 4.

Map - Segments of Major Faults Recommended for  
Intensified Monitoring and Study, NEPEC



**APPENDIX C**

**Council Correspondence**

APPENDIX C. 1.

General



# United States Department of the Interior

GEOLOGICAL SURVEY  
RESTON, VA. 22092

In Reply Refer To:  
Mail Stop 905

MAR 30 1987

Dr. Lynn R. Sykes, Chairman  
National Earthquake Prediction  
Evaluation Council  
Lamont-Doherty Geological Observatory  
Palisades, New York 10964

Dear Lynn:

I am writing in response to your letter of March 11, 1987, in which you report on the November 1986 meeting of the National Earthquake Prediction Evaluation Council (NEPEC). I also want to give the Council some specific instructions regarding the assessment of earthquake hazards in California.

I am pleased that the workshop on intermediate-term precursors went well; making the distinction between tectonic precursors and those that might be associated with a specific fault break should be an important one in analyzing precursor patterns.

On the Parkfield experiment, we hope to have a revised decision procedure and response plan available soon; the Council's comments on this revision would be welcome. A small group has been working on the problem of the Parkfield earthquake extending south of Cholame and a short report on the group's progress will be made at your April meeting.

I appreciate the Council's dealing with the Adak and central California predictions. It is important to note that the Council's role in evaluating these predictions allowed the scientists involved to come forth with their results to a group of their peers and without undue publicity and public confusion. I believe this is in the scientists' and the public's best interests.

Finally, I have a specific charge for the Council regarding the evaluation of the earthquake threat to southern California. Considerable work has been done during the past few years in this region, and it is appropriate that earlier estimates of the earthquake potential in the region be revised and refined in the light of this work. Specifically, I would appreciate your assessment by the end of the year on the likelihood of a great earthquake in southern California during the next few decades.

Please accept my continuing appreciation for your help in this important work.

Sincerely yours,

Dallas L. Peck  
Director



Lamont-Doherty Geological Observatory  
of Columbia University

Palisades, N.Y. 10964

Cable: LAMONTGEO  
Palisades New York State  
TWX-710-576-2653

Telephone: Code 914, 359-2900

23 April 1987

Dr. Dallas Peck  
Director  
U.S. Geological Survey  
National Center, MS106  
12201 Sunrise Valley Drive  
Reston, VA 22092

Dear Dallas,

I am writing to report to you the results of the meeting of the National Earthquake Prediction Evaluation Council (NEPEC) in Seattle on April 3, 1987. The meeting was preceded by a one-day workshop on April 2 on subduction earthquakes in the Pacific Northwest and by a field trip on April 1.

Cascadia Subduction Zone

At the NEPEC meeting in Seattle on April 3, 1987 the Council considered the question of the earthquake potential of the Cascadia subduction zone, an area that extends from southern B.C. to northern California. There was consensus that several lines of evidence would suggest that large earthquakes in this zone are plausible. Among these lines of evidence are (1) seismicity data that show a Wadati-Benioff zone beneath the Puget Sound region; (2) new geologic evidence for episodic subsidence of several locations along the Washington and Oregon coast; (3) geologic evidence from offshore that convergence and subduction are occurring; and (4) geodetic data from several networks in Washington that strain is accumulating that is consistent with the direction and magnitude of plate convergence.

However, there remain many unresolved issues which are important to the question of the level of seismic potential of this region. These issues include: (1) a sense that the Cascadia zone is unique in many ways and that it is difficult to extrapolate from other regions, (2) the young age of the Juan de Fuca plate and high sediment cover might yield mechanical coupling conditions that would result in aseismic subduction or might limit the maximum size earthquake; (3) the possibility that slow earthquakes might explain the strain data and the geologic data; (4) the

significance of the low level of seismic activity along the thrust zone (plate interface); and (5) the possibility that the geologic evidence for subsidence might be explained in some way that does not require large subduction earthquakes.

Despite these unresolved issues, the Council believes that the possibility of a large subduction zone event must be taken seriously although the evidence is not yet compelling. Basic research and further investigations are urgently needed to resolve these uncertainties. Important problems include: (1) further geologic work on the Washington and Oregon coastal regions to improve our understanding of the mechanisms of uplift and subsidence in reference to eustatic sea level changes, particularly the significance of the rapid subsidence events and their spatial extent; (2) further theoretical, experimental and observational work is needed on the question of mechanical coupling at subduction plate boundaries especially for areas that include very young subducted plates; (3) geodetic work is needed in southwestern Washington and all of western Oregon; (4) seismicity data are needed in Oregon to understand the geometry and possible segmentation of the plate boundary in that area; and (5) a major experiment like the Trans Alaska Lithospheric Investigation and the Canadian LITHOPROBE effort could provide important new data to improve our understanding of the structure of the subducted lithosphere.

#### Parkfield Prediction Scenarios and Possibility of a Parkfield Earthquake Breaking into Segment Southeast of Cholame

The latest version of the USGS Parkfield response plan (open-file report) was distributed to NEPEC members. USGS and State of California officials stated that the document has been valuable. A summary of Parkfield alerts from June 1985 to March 1987 was distributed. Filson summarized the sequence of changes on February 1, 1987 that may have been premonitory to the February 2 earthquake that took place in the Middle Mountain preparation zone.

A copy of a memorandum dated March 24, 1987 about the segment of the San Andreas fault to the southeast of Cholame was distributed and the document was discussed. NEPEC had previously recommended that a working group examine that fault segment in terms of repeat times and characteristic displacements. The memo summarizes the conclusion of nine geologists who made a field trip to that area from February 18 to 20, 1987. NEPEC urges that trenching be carried out along that segment of the San Andreas fault and urges participation by scientists from USGS, universities and the State of California.

#### Earthquakes in Southern California

NEPEC will devote its next meeting, probably in October 1987, to earthquakes in southern California. Sykes distributed a map "Segments of Major Faults Recommended for Intensified Monitoring and Study" that he prepared for briefings in conjunction with the letter he sent on behalf of NEPEC to you dated May 9, 1986. Sykes distributed copies of your letter of March 30, 1986 about the last NEPEC meeting and about the evaluation of the earthquake threat to southern California.

### Soviet Predictions of Great Earthquakes Using Pattern Recognition

Professor Leon Knopoff of UCLA wrote to Sykes on December 16, 1986 about a prediction that Dr. V. Keilis-Borok and his colleagues in the USSR have made for California. His letter will be published shortly in the open-file report of the November 1986 NEPEC meeting. Sykes distributed copies of Knopoff's letter to all NEPEC members in January 1987 and distributed relevant portions of the document *Algorithms of Long-Term Earthquake Prediction* by Gabrielov et al. that was published by the Regional Center of Seismology for South America in Lima in September 1986. The paper includes several long-term predictions called Times of Increased Probabilities for events of about magnitude 8 on a worldwide basis including one for California. An analysis for a broad area centered on latitude 37.5°N and longitude 119.5°W is prognosticated to have a magnitude 7.5 or greater event between January 1, 1984 and January 1, 1988.

NEPEC concluded that the paper by Gabrielov et al. did not provide sufficient discussion of methodology, etc., to warrant a formal review. The Council also noted that the uncertainty in the location of the predicted earthquake includes a very large area of California and that the document states that the forecasts contained therein should be regarded as experimental in nature. Filson stated that a joint US-USSR meeting on earthquake prediction is scheduled to be held in the United States in October 1987. NEPEC recommends that the above prediction be discussed in more detail at that meeting. NEPEC does not take the material submitted to it thus far to require more urgent action prior to the US-USSR meeting in October.

Sincerely yours,

Lynn R. Sykes  
Chairman, National Earthquake  
Prediction Evaluation Council

LRS/llm

cc: J. Filson  
C. Shearer

**APPENDIX C. 2.**

**Soviet Prediction**

Lamont-Doherty Geological Observatory  
of Columbia University

*Palisades, N.Y. 10964*

Cable: LAMONTGEO  
Palisades New York State  
TWX-710-576-2653

Telephone: Code 914, 359-2900

23 April 1987

Professor Leon Knopoff  
Selwyn College  
Cambridge University  
Cambridge CB3-9DQ  
United Kingdom

Dear Leon,

I distributed your letter of December 16, 1986 on the Soviet prediction of a great earthquake in California to members of the National Earthquake Prediction Evaluation Council in January 1987. I also distributed relevant portions of the Gabrielov et al. document to the Council prior to its recent meeting on April 3, 1987. I am enclosing a copy of my report as Chairman of NEPEC to Dr. Dallas Peck, the Director of the U.S. Geological Survey which includes our assessment thus far of the prediction.

As mentioned in the letter to Peck the Council hopes that the prediction can be discussed in more detail at an upcoming meeting of U.S. and Soviet scientists working on earthquake prediction in the United States in the Fall of 1987. Our hope is that Dr. Keilis-Borok will be able to attend that meeting.

I understand from a message relayed to me by your secretary at UCLA that you are preparing a write-up on the Soviet prediction. I hope you will send it to me in the near future. I will be happy to distribute it to the members of NEPEC.

Sincerely yours,

Lynn R. Sykes  
Chairman, National Earthquake Prediction  
Evaluation Council

LRS/llm  
Encls.

cc: J. Filson  
C. Shearer

Copy also sent to Professor Leon Knopoff, Institute of Geophysics and Planetary Physics,  
University of California at Los Angeles, Los Angeles, CA 90024

Lamont-Doherty Geological Observatory  
of Columbia University

Palisades, N.Y. 10964

Cable: LAMONTGEO

Palisades New York State

TWX-710-576-2653

Telephone: Code 914, 359-2900

2 November 1987

Dr. V.I. Keilis-Borok  
Geophysical Committee  
Molodezhnaya 3  
Moscow 117296  
U.S.S.R.

Dear Volodya,

Thank you for your recent letter that arrived yesterday asking me for my opinion about directions for the International Union of Geodesy and Geophysics and relaying an update of predictions you and your group have made for earthquakes in California. Congratulations on your election as President of the IUGG; I can see already from your letter that you are determined to try and inject some vigor and life into the IUGG. I will send you my comments on the IUGG in about two weeks.

The main purpose of this letter is to follow up on the prediction that you and other members of your group have made for a large earthquake in either California or western Nevada. In this regard I am writing to you as Chairman of the U.S. National Earthquake Prediction Evaluation Council (NEPEC). My understanding is that that prediction was relayed from Secretary General Gorbachev to President Reagan at their meeting in Reykjavik, Iceland. NEPEC is very anxious to receive more details on that prediction both in writing and at a meeting, if such can be arranged, in which you and some of your colleagues would present the prediction and the data supporting it.

Dr. John Filson, Chief, Office of Earthquakes, Volcanos and Engineering of the U.S. Geological Survey has been corresponding with the Academy of Sciences of the USSR trying to set up a meeting in the United States for discussion of various aspects of earthquake prediction under the bi-lateral program in earthquake studies between our two countries. The members of NEPEC had originally hoped that your prediction could have been presented at that meeting, which was originally proposed for this Fall. Filson is now proposing to hold that meeting in March 1988 or soon thereafter. I would like to propose that NEPEC meet to hear the California prediction by you and your colleagues right after the joint Soviet-American meeting on the earthquake program. If it is not possible to have the two meetings one after the other or if the joint meeting on earthquake studies cannot take place next Spring, the members of NEPEC still want to hear a formal presentation on the California prediction. Thus, in any case, we very much hope that you and some of your colleagues would be able to present that prediction to us at a NEPEC meeting. Dr. Filson's Office would make arrangements for the travel, living and other expenses for you and your colleagues while you are in the United States. I will make sure as Chairman that there will be enough time for you and your colleagues to make a detailed presentation of your methods and of your California prediction.

Let me give you some information about NEPEC. NEPEC advises the Director of the U.S. Geological Survey about the scientific validity of predictions made for earthquakes in the United States. The Council makes recommendations to the Director of USGS but does not issue formal predictions itself. It consists of 15 members, of which half must be from outside the U.S. Geological Survey. I have been the Chairman for the past 3 years. Dr. Filson is the Vice-Chairman. We have found it very helpful to ask each person or group who makes a presentation

or presents a formal prediction to NEPEC to put the prediction in writing including a summary of a few pages and copies of figures of all relevant data. We hope that you and your colleagues will send us such a write-up well in advance of the NEPEC meeting we are proposing. The minutes of that NEPEC meeting along with written material submitted will then be published as a U.S. Geological Survey Open-File Report. From past experience we have found that predictions NEPEC has considered have been changed by their authors over time. Thus we feel it is important to have a written record of the actual prediction presented to the Council and of the scientific basis for it.

Professor Leon Knopoff wrote to me in December 1986 stating his concern about the prediction that you and your colleagues had made for a large earthquake in California. I sent his letter along with the Gabrielov et al. article, Algorithms of Long-Term Earthquakes' Prediction that was published by Ceresis (Lima, Peru) in September 1986. The Council discussed Knopoff's letter and the prediction contained in the Ceresis article at our last meeting on April 1, 1987. The Council concluded that we needed more information on the prediction. Those two documents indicated that the period of the prediction would end January 1, 1988. Knopoff's letter indicated, however, that the occurrence of moderate-size earthquakes in California in 1986 might extend the prediction. In August 1987 Knopoff sent me a write-up on the prediction dated November 1986. I sent that write-up to members of NEPEC along with your latest letter. I note from it that the prediction (TIP) ends on December 31, 1988 rather than January 1.

I hope that Leon Knopoff will be able to attend a NEPEC meeting at which we propose to hear your prediction. Prior to that meeting I would like to send all of the written materials to several reviewers who are experts on pattern recognition. I hope the two of you can send me the names of experts in that field and others who would be in a position to make a wise evaluation of the methodology and scientific basis for the California prediction. Dr. Filson has asked one of his colleagues in USGS to send you an updated listing of moderate-size earthquakes in California, I hope it will be possible for you and your colleagues to use that information to update your predictions.

There are several topics related to the California prediction about which we would like to have additional information. Are there any ways in which you or others can reduce the size of the area for which the prediction is made? It is obviously of concern to us that the area is now very large and includes all of California and parts of western Nevada. How applicable is the methodology to major strike-slip or transform faults? What is the probability that the predicted event will occur in the time window specified and what is the probability that it would happen by random occurrence?

I and other members of NEPEC hope that you and your colleagues will be able to join us in the United States in the Spring of 1988 to learn about the details of your prediction of a large earthquake in California.

Sincerely yours,



Lynn R. Sykes  
Chairman, National Earthquake Prediction Evaluation Council

cc: Dr. John Filson Chief, Office of Earthquakes, Volcanos and Engineering  
Professor Leon Knopoff  
Dr. James Davis Chairman, California Earthquake Prediction Evaluation Council  
Other NEPEC Members

LRS/lis

Received by L. Sykes  
Wed Oct 28  
1988

UNION GÉODÉSIQUE ET GÉOPHYSIQUE INTERNATIONALE  
INTERNATIONAL UNION OF GEODESY AND GEOPHISICS  
Président President

V. I. Keilis-Borok

Geophysical Committee, Molodezhnaya 3, Moscow 117296, USSR  
tel 1107795, tx 411478 SGC SU

Prof. L. R. Sykes  
Lamont-Doherty Geological  
Observatory, Columbia University,  
Palisades, New York, 10964  
USA

Dear Lynn:

1. It was nice to talk to you in Vancouver. I enclose the sales pitch on the IUGG business. I would be grateful for any response from you personally and from Lamont community.

What do you think of IUGG if anything?

2. For the purpose of evaluating the IUGG activities - could you recommend a list of 5 to 15 youngsters under 33, from within or outside US, who to your personal opinion are really promising in IUGG scope.

3. Following our discussion I looked through the papers prepared for the Geneva meeting and can reproduce the conclusion precisely:  $M > 7.5$  in the whole California and adjacent Nevada, and also  $M > 6.5$  in Southern California as defined in my paper with Clarence Allen et. al.

Second one already materialized (21. 1. 1986; lat. = 37. 65N; long. = 118. 44 W;  $M = 6.6$ ) for the big one - the TIP ends on December 31, 1988 (year 1987 indicated in the subsequent preprint which you have is an obvious misprint; it can be easily verified since diagnosis is reproducible. L. Knopoff has programs, if you are interested to repeat the diagnosis yourself).

What would be essential is to launch forward diagnosis. Uncertainty in place can now be hopefully reduced to one or two source-dimensions, using Mandocino scenario. This may expand the possible disaster prevention measures.

Sincerely yours

V. I. Keilis-Borok

/V. I. Keilis-Borok/



UNIVERSITY OF CAMBRIDGE  
DEPARTMENT OF PHYSICS

Telephone: 0223 - 337733  
Telex: 81292

CAVENDISH LABORATORY  
MADINGLEY ROAD  
CAMBRIDGE CB3 0HE

August 6, 1987

Professor Lynn R. Sykes  
Chair, National Earthquake Prediction  
Evaluation Council

Dear Lynn,

Last mid-April I indicated that I was unable to locate a copy of the report I drafted last November of my observations and reflections on the Soviet prediction of a great earthquake in California, and that it was buried somewhere in this great mass of paper on my desk here. It has finally diffused to the near-surface and I am pleased, if only many months late, to send you a copy. Despite the fact that your request for a copy was dated April 23rd, I hope that there is still some interest in my report.

In your letter of April 23rd, you expressed the hope that the prediction could be discussed at a fall meeting of US and USSR experts I hope so too. I have not heard anything more about this meeting. Have you?

With best regards,



Leon Knopoff

Received by  
Library  
1987

UNIVERSITY OF CAMBRIDGE  
DEPARTMENT OF PHYSICS

Telephone: 0223 - 337733  
Telex: 81292

CAVENDISH LABORATORY  
MADINGLEY ROAD  
CAMBRIDGE CB3 0HH

This is a report on my discussions with V.G. Kosobokov and V.I. Keilis-Borok on the Soviet prediction of a very large earthquake in California and/or Nevada in the interval 1984-1988. This report has appeared in the preprint Algorithms of Long -Term Earthquakes' Prediction, by 15 Soviet and one U.S. authors; the first author is A.M. Gabrielov; in alphabetical order of authorship. The preprint, 61 pages in length, has been distributed widely in the form issued by CERESIS in Lima, in September, 1986. At the time of my visit to the USSR, 14-21 October, 1986, I was informed that the paper has been submitted for publication; I assume, without direct information, that publication will be in Russian.

The prediction for California is to be found on pages 51 and 57 of the preprint. This section, written by V.I. Keilis-Borok, V.G. Kosobokov and W. Rinehart<sup>2</sup> indicates that an alarm exists for an earthquake with  $M \geq 7.5$  in a roughly square region of dimensions  $70 \times 90$ , centered at  $37.50^\circ\text{N}$  and  $119.50^\circ\text{W}$ , and extending from January 1, 1984 to January 1, 1988. For reference, the center of the rectangle is just south of Yosemite National Park. The window spans both San Francisco and the northern part of Los Angeles.

The method of prediction is derivative from the better known method of pattern recognition. By way of aside, the method of pattern recognition first burst upon the western geophysical scene in a paper by Gelfand, Guberman, Keilis-Borok, Knopoff, Press, Ranzman, Rotwain and Sadovsky, (Phys. Earth and Planet Interiors, 11; 227-283, 1976); the Gelfand, et al. paper was concerned with the identification of potential epicenters of future great earthquakes in California, without regard to the times at which these events were likely to occur. This more traditional method has been recently applied to temporal recognition of times at which large earthquakes are likely to occur, without regard to their epicenters, in California and Nevada. This paper, Prediction of Times of Occurrence of Strong Earthquakes in California and Nevada, by V.I. Keilis-Borok, L. Knopoff, I.M. Rotwain and C.R. Allen<sup>3</sup> is in the last stages of preparation for publication.

I indicate how the new technique differs from the old by reviewing the older version. In the "classical" pattern recognition procedure, a three stage process was followed. The first, called learning, involved writing down all the possible environmental attributes that one could think of that might be associated with the pattern of rare events that we are trying to predict. So, for example, in the case of temporal recognition (see paper Prediction of times...), one cites swarms, gaps, foreshocks, remoteness in time of the last preceding large earthquake, etc., as a list. One then breaks up the time history into two parts, that corresponding to the times immediately before large events in the region, and that that does not. If an attribute from the list, or combination of these attributes is observed

to occur frequently in one of the two groups of time intervals and infrequently in the other, then it is accepted as a pattern for future study. The second stage is called voting. In this stage, the patterns that have been accepted are counted to see how frequently they are successful or unsuccessful in each of the two time interval-groups. If the voting has a majority of one sign for one type of region and conversely for the other, then the procedure is deemed operative. The final stage involves testing the list of successful patterns by a variety of means. Perhaps the most critical of these tests, is the direct application of the pattern recognition procedure derived for one region, to a second region without further adjustment of parameters. This has been done both in the spatial predictions of Gelfand, et al.<sup>3</sup>, and in the temporal predictions of Keilis-Borok, et al.<sup>4</sup>, and with significant success in both cases.

However the success of the predictions for California and Nevada by Keilis-Borok, et al.<sup>4</sup> is restricted to earthquakes in the  $M=6.5$  range and depends on the availability of a significant catalog of historical seismicity of reasonably high quality; in this case, the catalog spans more than 50 years. Although the "learning" episode was performed on only 14 earthquakes in California, a direct application of the procedure to earthquakes in Central Asia and the Caucasus, give an admirably high success rate of temporal prediction.

The methodology for California is not directly applicable for extension to prediction of larger earthquakes for several reasons. The principal reason is the obvious one: if one were to raise the magnitude threshold for prediction to, let us say, 7.5 for California, then there would only be one earthquake in the past 50 years to practice on, namely the Kern County Earthquake, instead of 14 or so. Therefore, one must consider very large earthquakes worldwide as a data set for learning and the other subactivities of pattern recognition. In this case, the program must be made robust, sufficiently so that its success (or failure) will not be locally or region-dependent on the choice of parameters. Robustness significantly reduces the number of parameters in the procedure. The new procedure is called M8; the older one, specific to California<sup>4</sup>, is called CN. In the M8 program, most of the learning phases of the procedure are skipped. Instead, guided by program CN<sup>3</sup>, they have fixed on 4 traits extracted wholly from program CN. These have now been made robust so that they can be applied to any region of the world with an adequate catalog. For example, several of the magnitude cutoffs for counting main earthquakes are set so that the average seismicity of main shocks above the threshold is the same number for all regions. Other thresholds are fixed at a given number of magnitude units below the threshold for definition of strong earthquakes.

3

The parameters in the algorithm were data-fitted to the precursory, main-shock seismicity of 6 earthquakes in the years 1965-1982 with magnitudes greater than 8.0. The time interval 1965-1982 spans that part of the NOAA catalog for which magnitudes are reported. In all of the work described, surface-wave magnitudes are used. (Three additional earthquakes in the above time interval with magnitudes greater than 8 were not used in the data fitting because they were not preceded by significant predecessor seismicity).

Main shocks are identified by removing aftershocks from the catalog according to a certain algorithm<sup>5</sup>; the details of the aftershock filter are not crucial to the procedure. For three of the four criterion traits, two magnitude-normalized thresholds are set so that two different measures of seismicity are obtained. For the fourth criterion, which is a measure of the number of aftershocks of predecessor earthquakes, only one threshold is set. When any of the first three criterion traits- with two different thresholds for the definition of mainshocks- exceeds the 90th percentile in a three-year sliding window, it is declared to be "abnormally large". In the fourth case, the aftershock seismicity is "abnormally large" if it exceeds the 75th percentile.

An alarm is sounded if

- a) "abnormally large" signatures appear in 6 or 7 of the 7 components.
- b) If these signatures appear in only 6 components, it must appear in all four traits. (If it appears in all 7 components, by definition it appears in all four traits).
- c) a) and b) must be satisfied on two successive evaluations taken 6 months apart.

The alarm window is 5 years from the date of the second of the two consecutive 6 month evaluations.

Following the initial exploration for parameter adjustment, the algorithm was applied to seismicity in 9 different areas of the world, for which good documentation is available, but this time catalogs were used mainly in the interval 1975 to 1983. (In the case of California/Nevada, the catalog spanned 1947 to 1985+). The 9 regions have threshold magnitudes for the definition of large earthquakes that range from 6.5 to 8.0; earthquakes larger than threshold are targets for prediction; the method is constructed so that it depends on seismicity relative to the threshold magnitude and not to the level of absolute seismicity.

Results:

- a. For three of the 9 regions, no strong earthquakes were predicted and none occurred.
- b. For the remaining 6 regions, 9 earthquakes took place within the time span of the catalogs with magnitudes greater than the threshold, and 8 of these occurred within the time-space windows of the predictions.

In other words there was one failure-to-predict.

- c. Three earthquakes occurred after the ends of the catalogs, and two of these were predicted. Thus there was one failure to predict an earthquake beyond the end of the catalog.
- d. There were two false alarms.
- e. There is one alarm in progress, for the Western United States.

Footnotes: Two of the earthquakes with magnitudes greater than or equal to 8 were used in the original data fit, and are also included among the 8 successes. Of the other 7 earthquakes (see b above), none had a magnitude greater than 8, although each was above threshold.

The total space-time reduction for the alarms is about a factor of 6. This means that there is a narrowing of the available space-time so that in  $5/6$  of the time and space, there are no alarms. If the earthquakes that occurred were imagined to terminate the alarms, then the improvement is about a factor of 9.

One of the 8 successes in b. above, was accomplished by a modification of the parameters in the algorithm since there were too few main shock earthquakes in the region annually to fit the normalized definition of mainshocks. The earthquake in question is a Romanian event, with larger depth of focus than the other cases. In the other cases, the algorithm was applied literally, i.e. without a posteriori adjustment of parameters.

Comments: The pattern recognition procedure is the systematization of all empirical procedures that have been developed and applied that have no or a not very significant theoretical basis. Examples in which such empiricism has been applied in postulated predictors taken singly in the last decade or two include searches for fluctuations in  $v_p/v_s$ , heights of well water, radon concentration, tilts, etc. The list is well-known. Such phenomenologies have been deemed promising or not in a series of case history studies; there is unfortunately an annoying paucity of tests of these procedures to be able to derive statistical tests of their validity, or lack thereof.

Because of its inherent, non-theoretically based phenomenology, the pattern recognition procedure is logically no better than any of the above methods taken singly. What the pattern recognition procedure does, is a) systematize the application of phenomenological searches, b) remove personal bias from the evaluation of the hypothesis under assessment, c) sort out relevant from irrelevant proposals hypothesized to be precursors, and d) take into account the possibility that a given method may not always work in every instance of a future strong earthquake. As long as we do not apply a theory of earthquakes to find out why these phenomenological methods fail on occasion, and as long as we do not have adequate numbers of case histories to provide a statistical evaluation of their success, we are restricted in our ability to assess the performance of pattern recognition, or indeed any other empirical/phenomenological procedure.

Despite the obvious advantages pattern recognition procedures have over the competing single-trait proposals, which latter may or may not be relevant, the pattern recognition procedures are strongly data-fitted. That is, they are highly parameterized and as such give the impression of being a model that is strongly tailored to the data (or catalog) at hand. Thus it should come as no surprise that the quality of the fit to the precursors of the events that were involved in the selection of the parameters has been good; to repeat, the number of successes on the fit earthquakes is expected to be high. Not very many earthquakes were used in this fitting process.

The decisive test of this method (or indeed of any method) is whether the scheme, data-fitted to one set of earthquakes, can be transferred boldly and without readjustment of the parameters to another set of earthquakes that may be set in a totally different tectonic environment. This has been done in the present case with the remarkable success scores noted above. I know of no other empirical procedure that can make this claim of success for large earthquakes.

The pattern recognition procedure raises many questions about physical mechanism as well as it does about the robustness of the procedure. The same comment can be made about any of the other, less-successful empirical procedures that also have negligible basis in theory, including those listed above. I have a long list of such questions.

Recommendation: Despite the reservations that I have attempted to summarize here, I believe that the phenomenal success rate of Pattern Recognition Procedure M8 is so outstanding on earthquakes not used in the data fitting that any prediction made under its umbrella must be taken very seriously. Clearly research must be done on why the method works and on reduction of the number of parameters in the model, but these comments must not and should not detract from the clearcut success that the Soviet scientists have had.

Leon Knopoff

Cambridge, England  
November, 1986

## References:

1. A.M. Gabrielov, O.E. Dmitrieva, V.I. Keilis-Borok, V.G. Kosobokov, I.V. Kuznetsov, T.A. Levshina, K.M. Mirzdev, G.M. Molchan, S. Kh. Negmatullaev, V.F. Pisarenko, A.G. Prozoroff, W. Rinehart, I.M. Rotwain, P.N. Shebalin, M.G. Shnirman and S. Yu. Schreider, Algorithm of long-term earthquake prediction, submitted, Nauka Press, Moscow (In Russian).  
  
English language preprint available from Centro Regional de Sismologia para America del Sur, Lima.
2. V.I. Keilis-Borok, V.G. Kosobokov and W. Rinehart, op. cit., pp. 51, 57. .
3. I.M. Gelfand, Sh. A. Guberman, V.I. Keilis-Borok, L. Knopoff, F. Press, E. Ja. Ranzman, I.M. Rotwain and A.M. Sadovsky, Pattern Recognition Applied to Earthquake Epicenters in California, Physics Earth and Planetary Interiors, 11, 227-283, 1976.
4. V.I. Keilis-Borok, L. Knopoff, I.M. Rotwain and C.R. Allen, Prediction of Times of Occurrence of Strong Earthquakes in California and Nevada, submitted, Nature.

INSTITUTE OF GEOPHYSICS AND PLANETARY PHYSICS  
LOS ANGELES, CALIFORNIA 90024

December 16, 1986

Professor Lynn Sykes  
Lamont-Doherty Geophysical Observatory  
Columbia University  
Palisades, N.Y. 10964

Dear Lynn,

I have recently returned from Moscow where I visited Volodya Keilis-Borok. He is extremely anxious to get a prediction he and his team have made into the machinery for evaluation of earthquake predictions. I understand that you are now the chair of the committee for such evaluations.

The prediction of his team is that an earthquake with magnitude  $M > 7.5$  in a  $7^\circ$  (lat.) by  $9^\circ$  (long.) rectangle with center at  $37.5^\circ\text{N}$  and  $119.5^\circ\text{W}$ . The earthquake is predicted to occur in the 4-year window January 1, 1984 to January 1, 1988. The documentation is to be found in a booklet entitled Algorithms of Long-Term Earthquake Prediction by Gabrielov, Dmitrieva, Keilis-Borok, and 13 other authors, and published by CERESIS (The Regional Center of Seismology for South America) at Lima, September, 1986. The prediction is to be found on page 57 of the booklet with details on pages 51-52. If you do not have a copy, I will send you mine.

Information regarding this prediction reached the U.S. last winter/spring and part of the purpose of my trip was to assess the prediction. As indicated in the booklet, the method used in the prediction was pattern recognition of seismic histories. The pattern recognition method uses parameters that are data-fit to a small number of events. The parameterized system is then applied without further adjustment of parameters to other recent large earthquakes with huge success. It is then further applied to recent seismic histories worldwide, geographically systematically. The event in the Western U.S. then showed up. I haven't gone through the analysis in detail, but it is my guess that the Chalfont Valley earthquake (July 21, 1986) will keep the window open somewhat longer than 1-1-88.



-2-

I am writing a more detailed report of my discussions and exchanges in Moscow. If you want a copy I will be happy to send it to you when it is finished.

I reiterate, that K-B wants his prediction entered into the lists for consideration by your committee.

With very best regards,

*Joyce Martin-Somers for*  
Leon Knopoff

jms/  
dictated but not read

APPENDIX C. 3.

Central California



# United States Department of the Interior

## GEOLOGICAL SURVEY

OFFICE OF EARTHQUAKES, VOLCANOES, AND ENGINEERING  
BRANCH OF ENGINEERING SEISMOLOGY AND GEOLOGY  
345 Middlefield Road, MS 977  
Menlo Park, California 94025

### MEMORANDUM

March 24, 1987

To: John R. Filson, Chief  
Office of Earthquakes, Volcanoes, and Engineering

From:

*James J. Lienkaemper* *Tom Hanks* *P.E. Wallace*  
*Dave Schwartz* *Bob Sharp*  
*John Sims* *Malcolm Clark* *Eikichi Tsukuda*

Subject: Field trip to the Cholame segment, San Andreas fault,  
February 18, 19, and 20, 1987

Herewith a report of the trip that eight of us took to the Cholame segment of the San Andreas fault, the 20 km stretch south of Highway 46. The Cholame Eight are Malcolm Clark, Tom Hanks, Jim Lienkaemper, Dave Schwartz, Bob Sharp, John Sims, Eikichi Tsukuda (visiting us from Japan), and Bob Wallace. Bill Bakun spent all of February 19 with us, in between other jobs. At issue are the 1857-earthquake displacements along this reach, inasmuch as a slip deficit is postulated for it on the basis of 1857 displacements in the Carrizo Plain and an 1857  $t=0$  datum. All of us felt that a written summary of our three days here was in order, in view of the great interest focussed on these slip estimates, although this report will necessarily be brief and preliminary. This report began as a group consensus of all the scientists above reached on the evening of February 19 in Room 318, Black Oak Inn. Hanks served as recording secretary. We used Friday morning to look again at KS #11, returning to Menlo Park after lunch. Hanks wrote the first draft of this report over the weekend, and the eight of us spent three hours reworking it on February 24.

This document was ready in "final" form on February 25, by which time both Jim Lienkaemper and Bob Wallace had spoken to Kerry. Kerry expressed his own interest in this document, and we all agreed to go over it with Kerry, with an eye toward Kerry signing this report as well. This meeting occurred on March 11 in Menlo Park and this document is its outcome, the consensus of the Cholame Nine.

Horizontal displacements inferred for the 1857 earthquake on this stretch of the San Andreas fault, whether by Kerry, us, or anybody else, come almost entirely from fault-crossing drainages, many ephemeral. There are several implicit, but important assumptions built into this methodology. First, one

assumes that the original drainage configuration can be reconstructed where it crossed the fault prior to the offsetting earthquake and, second, that the material underlying the entire channel can be evaluated with respect to erosion processes. In fact, these conditions are rarely met. The fault itself can provide a material and a topographic irregularity that can produce deflection, whether or not an historic earthquake occurred.

An even more difficult problem in this region, where erosion rates are clearly rapid, is the unknown amount of post-1857 incision and modification of any marker channel offset. For example, as a channel deepens, it also broadens, so surface traces of the two channel walls separate. If both above and below the fault, this broadening is symmetric with respect to the pre-1857 stream bottom, no uncertainty arises. But if either above or below the fault, or both, a channel widens at the expense of only one wall (and we don't know it) a substantial uncertainty exists in the apparent offset; this can be as large as the channel width, several meters or more for the ones we saw. That channel offsets tend to straighten out with time guarantees that asymmetric erosion is general and important near the fault trace.

It is also worth noting that even an apparently well-defined drainage offset (whatever its cause may be) can rarely be measured with an uncertainty of less than 1 m along this stretch, depending on who thinks what is sort of straight. In the Carrizo Plain, offsets are large relative to this uncertainty: on the Cholame segment, this intrinsic noise is more comparable to signal.

To conclude these general introductory remarks, a few more words about the rapid erosion rates. Landform markers in this region commonly are offset 50 to 70 meters, which means (at 3-1/2 cm/yr) much if not most of the faulting-controlled topography is less than 2,000 years old. In the past century, probably due to animal husbandry practices in the region, erosion rates in a number of channels are astonishing. We saw a barbed-wire fence hanging about 30 feet above a channel that eroded beneath it in just the last 50 years. We saw fence posts nearly buried by fan aggradation at the mouth of another rapidly eroding channel (KS #11), and knick points in two minor drainages at this site suggest approximately two meters of incision that is most likely post-1857. To a major extent, differing interpretations of fault slip among various investigators, including among ourselves, are a function of differing evaluations of the rates and amounts of erosion.

To get started on the specifics, refer to Sieh, *BSSA*, p. 1421-1448, 1978, Table 1, Sites 1-15. The relevant part of Table 1 is attached. Jim Lienkaemper from our Office has revisited these sites, and our trip was to see what Jim found *vis a vis* Kerry. Numbered sites prefixed by KS are Kerry's site, revisited by Jim and then by us. Jim, in addition, has explored several additional sites, labeled JL with following numbers. We did not, however, go to all of Kerry's and Jim's sites, but we did see most of the better ones.

KS #1 (see Fig. 13 of Sieh, 1978), attached  
KS measured a 3.5 m offset on the fault trace, as indicated in Fig. 13. JL measures 1-2 m of "channel offset" across the fault trace by extrapolating more distant trends inward. One's preference for one alternative or the other depends on various assumptions, some of which can be checked with trenching.

- KS #2 KS measures 7.2 m, JL 6.3. Sensible agreement on 6-7 m here, but channel is very short. 1857 contribution unknown.
- KS #5 We do not regard this site to be a reliable offset indicator and don't know what to do to make it one. The fault here is on the head-wall of an unstable, steep, headwardly retreating gully, bifurcating just before reaching the fault. The fault trace here is poorly defined. JL has suggested a second fault trace approximately 50 m downslope (to SW); apparent offset at crossing of two gullies, but trace is poorly defined.
- KS #6 In a deep channel, with young downcutting and slumping. Perhaps measurements of long-term offset are possible, but hard to demonstrate 1857 offsets. Uncertain as to what KS measured.
- KS #7 Uncertain as to what KS measured. We did not see certain 1857 offsets.
- KS #8 KS  $6.7 \pm 2.1$  m, JL  $5.4 \pm 0.5$  m. Knocker of silica-carbonate at NW (effluent) end of the gully may influence measured offset. These values in sensible agreement, but both may be biased high. 1857 contribution unknown.
- KS #9 Not sure we're looking at the same thing as KS. We measured 9-12 m apparent channel offset on one fault trace. KS,  $7.0 \pm 0.6$  m. Sinuosity of channel (hairpin turn just above fault and apparent left-lateral offset!) and multiple fault traces make any offset here hard to pin down. 1857 contribution unknown.
- KS #10 KS identifies three strands, and we see possibly one more SW of the strand that KS measures. Altogether, the fault zone is approximately 65 m wide here, and the channel bends significantly (approx. 25 m, in a right lateral sense) across it. While KS value may be minimum 1857 value (subject to all the general uncertainties), we doubt that the full 1857 story can be told here on the basis of channel-offset geomorphology.
- KS #11 See Fig 12 of Sieh (1978), attached  
KS measures  $4.1 \pm 0.9$  on right leg of Y configuration of gullies. We prefer 2-4 m of offset here. Possible post-1857 downcutting in both legs of the Y raises questions as to whether present gully configuration bears any resemblance to pre-1857 configuration. Notable erosion/deposition in major channel into which below-fault gully empties. Headward erosion of this below-fault gully, probably due to downcutting of major channel. JL identifies splay fault SW of main trace, with possible offset at major channel.
- KS #12 See Fig. 11 of Sieh (1978), attached  
This gently deflected gully, with much post-1857 incision, does not lend itself to accurate offset measurements. Slump into channel from SE, upstream from fault. KS measures  $3.2 + 0.2, -0.5$  m., which we see as minimum value. Perhaps 6 m maximum value.

- KS #13 See Fig. 7 of Sieh (1978), attached  
There are questions about the fault trace location as shown in Fig. 7. Extrapolating from points approximately 30 m to the NW and SE places the most active trace at an elevation above the man's white hat, rendering the apparent offset entirely non-tectonic. In any event, the landslide sidewall "offset" is highly susceptible to modification. We have reservations that 1857 offsets can be recovered from this site on the basis of geomorphology alone.
- KS #15 On the ground in 1987, we see the offset here pretty much as Kerry did ( $3.4 \pm 1$  m). JL has 1966 photos, however, that plainly suggest a larger offset ( $5.5 \pm 0.7$  m). The culprit here seems to be 21 years of disking of this terrain by the Bob Grant folks since 1966. The fault trace here cannot be defined except by the offset.
- JL #1 (5.6 km SE of KS #15), attached  
This offset ( $6.7 \pm 0.4$  m) is so clear in the 1966 photos that it shows up on a xerox copy (attached). One can hardly see this feature today, and an offset would be hard to measure reliably. Again landform modifications due to disking.
- JL #2 (approximately 300 m SE of JL #1)  
Here a well-defined channel offset of approx. 12 m. 1857 contribution unknown. No clear evidence of multiple events, but certainly possible.
- JL #3 (1/2 mile SE of KS #13)  
Here a gully sidewall is offset 4 to 6 m in a pronounced swale. Work here is needed to locate the active traces precisely.
- JL #22-A (1.2 km N of Highway 46)  
Here offset of a gully is between 3 and 6 m, but Parkfield earthquakes and creep since 1857 have probably contributed 1.2 m to this figure. 1857 contribution is unknown, although all of the remaining offset could be the 1857 earthquake.

Where does this leave us with respect to displacements along the Cholame segment, especially those that occurred in 1857? We think a tectonic signal is expressed by stream offsets that lie between 3 and 7 meters at some of the sites described above. We could not determine whether all of this slip occurred in 1857 or is cumulative slip from two or more events. We did not see convincing field evidence for a 3-1/2 m slip "plateau." Relative to the Carrizo Plain segment, there does appear to have been less slip along the Cholame segment in 1857. We should also note that the number of "good" sites for measuring offsets represents a frustratingly small sample of the more than 100 intersections of drainage channels and fault strands along the Cholame segment. There are, of course, any number of landforms on the Cholame segment offset by 10, 20, ... 50, 60, 70 meters, but we don't know anything about their age.

What, then, can be done to improve this highly uncertain situation, which will probably please nobody? It is worth remembering that all work to date is based solely on what can be seen on the Earth's surface, either on the ground or on aerial photographs, and virtually all of this work has been directed to

the matter of 1857 displacements. First, then, a couple of long-term slip rates in this area would provide a valuable context, since it is a long way from Wallace Creek to the fully creeping section of the San Andreas fault. Sims has identified some promising sites, and we saw a couple more on our trip. Second, to our knowledge very little subsurface work has been done on the Cholame segment, and trenching half a dozen of the better sites almost certainly will improve accuracy of the 1857 offset measurements and hopefully will provide dates as well. Finally, there are several other promising gully offsets along the Cholame segment that have not been studied by either Kerry or Jim. Indeed, this work promises to be far more interesting than arguing about what can or cannot be seen on the ground and on aerial photographs and arguing about what it does or does not mean in a region where surface processes and modification are so active and rapid.

It is not our field of expertise to translate these uncertainties about 1857 earthquake displacements along the Cholame segment into a probability-of-occurrence of a  $M \approx 7$  (or any other size) earthquake. We encourage those who do such work, however, to take note of these and other geologic uncertainties.

TCH:cr





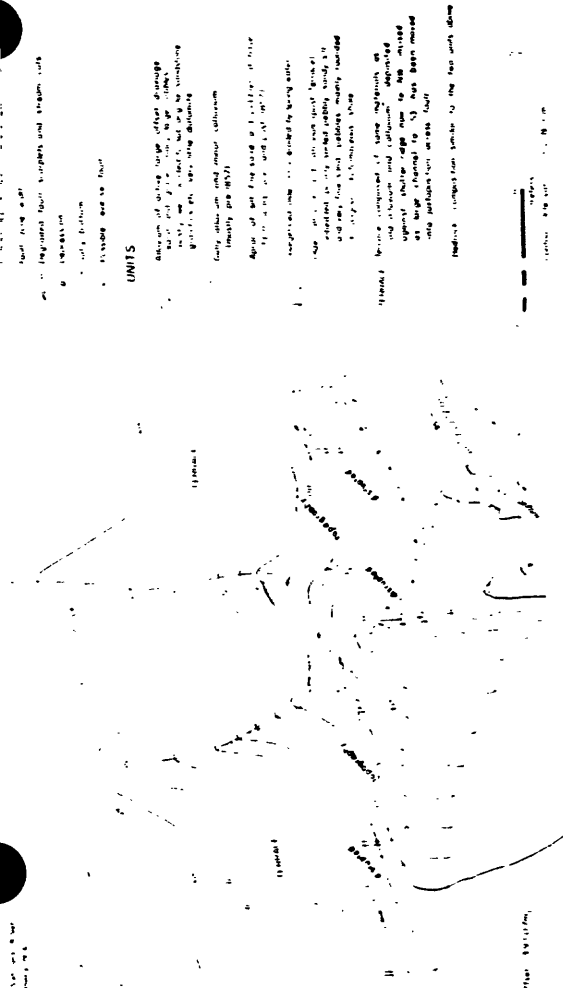


FIG. 12. Gully offset about 3.9 m along the San Andreas fault, Bitterwater Valley (site 11). The recent trace of the fault traverses the base of an alluvial terrace, which is cut by two small gullies. A small segment of a large channel which is offset about 70 m appears in the lower right corner. The more southeasterly of the two small gullies cutting the terrace probably was offset about 3.9 m from its downstream segment in 1857.



FIG. 7. The two photographs provide a stereoscopic view of the offset edge of a landslide scar (site 14). Amount of offset (about 14 m) is indicated by positions of the two individuals. View is northeastward.

- Youngest alluvium (mostly or wholly post-1857)
- Youngest slump deposits (mostly or wholly post-1857)
- Young spring deposits - thin, unvegetated lag of diatomite and sandstone pebbles, silt, and sand
- Post-older alluvium colluvium
- Older (late Holocene) alluvium

- Contact (approximate, ? where questionable)
- Scarp (vertical or near-vertical)
- Scarp (non-vertical)
- Gully bottom
- Fault zone width
- Landslide

FIG. 11. Gully offset about 3.2 m along the San Andreas fault, Bitterwater Valley (site 12). Erosion within the gully since the 1857 earthquake has removed any obvious evidence of the offset, but a subtle right lateral separation of the channel segments upstream and downstream from the fault zone remains. A beheaded channel (stipple pattern) is offset about 20 m from the upstream segment of the modern gully. Several meters of incision of the modern gully have occurred since the beheaded gully was offset.

In Reply Refer To:  
Mail Stop 905

March 24, 1987

Dr. Carl Kisslinger  
Lamont-Doherty Geological Observatory  
at Columbia University  
Palisades, New York 10964

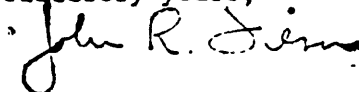
Dear Carl:

At its November 1986 meeting, the National Earthquake Prediction Evaluation Council reviewed the seismological data rising from the May 7, 1986, magnitude 7.7 earthquake in the central Aleutian Islands. You presented a prediction of an event in this region before the Council in September 1985. In your abstract to the Council you stated "An earthquake with surface-wave magnitude 7 or greater will occur in the Adak seismic zone in the near future. If the single observed case of a 3-year precursory quiescence is characteristic, the most likely time is before the end of October 1985. A likely place for the initiation of rupture is at the asperity in the subregion SW2, with the main break occurring either immediately or soon after under Adak Canyon."

The Council's review noted that the rupture zone of the May 1986 event included the area of the earthquake predicted; however, the time, 6 months later, the epicenter, 150 kilometers to the east, and the size of the 1986 event were significantly different from the "likely" event described by you. Therefore, the Council concluded that, although your prediction was not borne out, the seismic quiescence pattern you reported might well be related to the stress accumulation process associated with the 1986 earthquake.

The Council commends your sustained study of Aleutian seismicity and the application of this work to the difficult problem of earthquake prediction. The Council recognizes the importance of the data collected by the Adak Network for earthquake prediction research and encourages further analysis of data from this region.

Sincerely yours,



cc: ✓ Lynn Sykes  
Chron 905  
File  
Filson

John R. Filson  
Vice Chairman, National Earthquake  
Prediction Evaluation Council

JRFILSON:jac

# NATIONAL RESEARCH COUNCIL

COMMISSION ON PHYSICAL SCIENCES, MATHEMATICS, AND RESOURCES

2101 Constitution Avenue Washington, D. C. 20418

BOARD ON EARTH SCIENCES

(202) 334-2160

February 24, 1987

Dr. Robert M. Hamilton  
Chief Geologist  
U.S. Geological Survey  
911 National Center  
Reston, VA 22092

Dear Bob:

During the meetings of July 1-2, 1986 and January 26-27, 1987, the Subcommittee on Earthquake Research considered the implications of some recent findings of the National Earthquake Prediction Evaluation Council (NEPEC) for earthquake hazards reduction efforts in California. On December 18, 1986, Dr. Lynn Sykes, Chairman of NEPEC, and I were given the opportunity to review these findings for Dr. Frank Press, President of the National Academy of Sciences. The Subcommittee discussed the substance of the meeting of December 18, 1986, on January 26 and 27, 1987, and recommended that this matter be brought to your attention for action.

Statements have been widely circulated during the past few years that there is a 50% probability of a great earthquake in southern California within the next 30 years. Statements have appeared in summary documents on earthquake hazards and in the public press, but few scientific papers presenting a formal long-term prediction or forecast for this area have been published. However, Sieh (1984) and Sieh and Jahns (1984) published forecasts for large earthquakes in California with the probability range of 7% to 60% for an event at Palmett Creek by the year 2000 and with the probability range of 26% to 98% in the next 50 years for an event on the San Andreas Fault. The ranges of probability are dependent on the assumptions used for the models. If applicable forecasts are scientifically valid, the implications for the nation are obviously serious in terms of lives and property at risk, and a great threat to our industrial and defense capabilities.

The Subcommittee, therefore, urges that you suggest to Dr. Dallas Peck, Director of the U. S. Geological Survey, that he make a formal request to NEPEC for an evaluation of current estimates of the likelihood of a great earthquake in southern California within the next few decades. Although NEPEC has reviewed the earthquake situation in selected parts of southern California during the past two years, the suggested evaluation is timely because NEPEC has not addressed this particular issue. Recently acquired data can be taken into account, and improved knowledge of earthquake generating processes gained in recent years can be applied. The results of previous NEPEC workshops on scientific fault zones provide a good basis for starting the evaluation process.

Dr. Joseph Berg  
2/24/87  
3:54 p.m.

Handled on  
at meeting  
with Peck  
on Feb  
1987

Without trying to anticipate the outcome of the evaluation, the Subcommittee feels that it will be an important element in decisions regarding the scope and urgency of appropriate measures to mitigate earthquake hazards. Even with all the expected uncertainties, which must be faced, the evaluation should be available to federal, state, and local government agencies and to private citizens.

Sincerely yours,



Carl Kisslinger  
Chairman, Subcommittee on  
Earthquake Research of the  
Committee Advisory to the  
U.S. Geological Survey

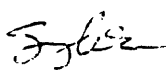
# State of California

## GOVERNOR'S OFFICE OF EMERGENCY SERVICES

2800 MEADOWVIEW ROAD  
SACRAMENTO, CA 95833

REGION I  
107 South Broadway  
Room 19-B  
Los Angeles, CA 90012

  
GEORGE DEUKMEJIAN  
GOVERNOR

  
WILLIAM M. MEDICOVICH  
DIRECTOR

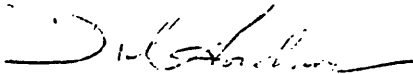
February 19, 1987


Dr. William L. Ellsworth  
Chief, Branch of Seismology  
US Geological Survey  
345 Middlefield Rd., MS 977  
Menlo Park, CA 94025

Dear Bill:

During the past two days, Bill Bakun assisted OES in the conduct of a tabletop exercise which discussed government response to a Parkfield Alert, and the attendant policy issues that need to be resolved. He also provided participants a Parkfield area field trip. The thirty that attended the trip were vocal as to their appreciation for the chance to see the project at work. The (over one hundred) participants in the exercise were even more appreciative.

Throughout the course of the Parkfield discussions and negotiations between our agencies, I have always found Bill very considerate of our concerns, and dilligent in mutual phases of the project. His work with us during the past two days has been particularly commendable. Everyone in attendance gave Bill the highest compliments. Please stress my appreciation for his work, and the assistance of Carl Mortenson and Tom Burdette. Each is a credit to the survey.

  
RICHARD ANDREWS  
Assistant Director

cc:   
USGS Reston



# United States Department of the Interior

GEOLOGICAL SURVEY  
OFFICE OF EARTHQUAKES, VOLCANOES AND ENGINEERING

Branch of Seismology  
345 Middlefield Road - Mail Stop 977  
Menlo Park, California 94025

February 17, 1987

## MEMORANDUM

To: John Filson, Chief, OEVE  
From: Bill Bakun, Parkfield Coordinator  
Subject: Parkfield Alerts of February 1 - 6, 1987

### Summary

A sequence of anomalous signals were observed near and within the Parkfield preparation zone that constituted d-, c-, and d-level alerts. The correlation of the signals suggests that a tectonic event did occur, and that unambiguous strain changes clearly preceded the M=2.7 shock that constituted the C-level alert.

### Jan 25-29, 1987

The first unusual signals observed were changes on Jan. 25-29 in the lengths of 2-color geodimeter lines CAN, GOLD, CREEK, LAND, and POMO. While these changes do not constitute an alert under the current alert level criteria, they would constitute a d- level geodetic alert under the provisional revisions of the alert level criteria.

### February 1, 1987

At 0559GMT, an M=1.2 shock (shock #1 on Fig. 1) occurred at 8.45 km depth to the northwest of the MM3 alert zone.

At 0800-1300GMT, there was a 10 centimeter drop in the 772'-810' monitor level of the Middle Mountain water well, constituting a d- level alert. The change corresponds to ~ 0.20  $\mu$ strain dilatation, well above the 0.05  $\mu$ strain threshold for d-level water well alerts.

→ At 0950-1000GMT, a 0.22 mm right-lateral creep event began at XMM1.

At 1125GMT, an M=2.0 shock (#2 on Fig. 1) occurred at 5.1 km depth above the MM3 alert zone. A right-lateral coseismic creep event with 0.01 mm amplitude was recorded on the XMD1 creepmeter.

At 1143GMT, an M=1.1 shock (#3 on Fig. 1) occurred at 0.5 km depth above the MM3 alert zone.

### February 2, 1987

At 0445GMT, an M=2.7 shock (#4 on Fig. 1) occurred at 10.0 km depth in MM3, constituting a c-level alert. Right-lateral coseismic steps were recorded on the XMM1 (0.5 mm), XMD1 (0.14 mm), and XPK1 (0.06 mm) creepmeters.

At 0909GMT, an M=1.3 shock (#5 on Fig. 1) occurred at 6.5 km depth northwest of MM3.

February 3, 1987

At 0250-0300GMT, a 0.02mm right lateral creep event occurred at XMM1.

At 1252GMT a magnitude 1.5 shock (#6 on Fig. 1) occurred at 6.0 km depth northwest of MM3.

At 1449GMT a magnitude 1.7 shock (#7 on Fig. 1) occurred at 9.7 km depth in MM3, constituting a d-level seismic alert that lasted until 1449GMT on February 6, 1987.

cc: Ellsworth  
Thatcher

